INSTITUT NATIONAL POLYTECHNIQUE DE LORRAINE
ENSIC – NANCY

THESE

Présentée à l'INPL
Ecole Doctorale RP2E : Ressources, Procédés, Produits, Environnement
Laboratoire Réactions et Génie des Procédés – UPR 3349 CNRS – INPL

Pour l'obtention du grade de

DOCTEUR de l'INPL
Spécialité : Génie des Procédés et des Produits

Par

Junwei QIAN
Ingénieur ENSIC

Développement du modèle *E*-PPR78 pour prédire les équilibres de phases et les grandeurs de mélange de systèmes complexes d'intérêt pétrolier sur de larges gammes de températures et de pressions

Soutenue publiquement le 12 décembre 2011 devant la commission d'examen :

Rapporteurs :	M.	Jean-Charles DE HEMPTINNE
	M.	Jérôme PAULY
Examinateurs :	M.	Laurent AVAULLEE
	M.	Pierre DUCHET-SUCHAUX
	M.	Jean-Noël JAUBERT (directeur de thèse)
	M.	Abderrazak LATIFI
	M.	Romain PRIVAT (co-directeur de thèse)
	M.	Roland SOLIMANDO
Invité :	M.	François MONTEL

Remerciements

Cette étude a été réalisée au Laboratoire Réactions et Génie des Procédés (LRGP-UPR 3349 CNRS) à Nancy. Je remercie donc tout d'abord Monsieur Gabriel WILD, Directeur de Recherche au CNRS, de m'avoir accueilli au sein de l'unité qu'il dirige.

Je tiens à exprimer mes sincères remerciements à mes directeurs de thèse : Monsieur Jean-Noël JAUBERT, Professeur à l'INPL/LRGP et Monsieur Romain PRIVAT, Maître de Conférences à l'INPL/LRGP, qui, tout au long de ces trois années, m'ont soutenu. Je les remercie pour leur sympathie, leur confiance, leur disponibilité, leurs précieux conseils et toutes les discussions enrichissantes. C'est en bénéficiant de leur savoir que ma formation de chercheur a progressé !

Je souhaite exprimer ma reconnaissance à Monsieur Jean-Charles DE HEMPTINNE, Professeur à l'IFP Energies nouvelles et à Monsieur Jérôme PAULY, Maître de Conférences à l'Université de Pau et des Pays de l'Adour, pour leur lecture attentive et pour leur participation à mon jury de thèse en qualité de rapporteurs.

Je tiens également à remercier Monsieur le Président du jury, Roland SOLIMANDO, Professeur à l'INPL/LRGP, ainsi que les membres du jury, Monsieur Abderrazak LATIFI, Professeur à l'INPL/LRGP, Monsieur Laurent AVAULLEE, Docteur et Ingénieur TOTAL, Monsieur Pierre DUCHET-SUCHAUX, Responsable simulation procédés TOTAL et Monsieur François MONTEL, Docteur et Expert TOTAL pour m'avoir fait l'honneur de participer au jury de cette thèse.

Un grand merci à tous les membres du laboratoire : Dominique ALONSO, Marie BLANCHET-HARDOUIN, Mohammed BOUROUKBA, Michel DIRAND, Ludivine FRANCK-LACAZE, Nathalie HUBERT, Jean-Charles MOÏSE, Fabrice MUTELET, Dominique PETITJEAN, Viviane RENAUDIN, Hervé SIMONAIRE…

Je voudrais aussi remercier tous les stagiaires, thésards, ex-thésards et post-doc qui ont su faire de ces trois ans une expérience agréable et enrichissante, pour leur sympathie, leur générosité et le partage de leur savoir : Afef ATTIA, Daniela BELTRAN, Yushu CHEN, Pablo FERNANDEZ, Sonia GARCIA REDONDO, Yingying GU, Rafik HAFID, Niramol JUNTARACHAT, Karolina KEDRA-KROLIK, Halima NOUBLI, Roberto OLCESE, Anne-Laure REVELLI, Virginia ORTEGA-VILLA…

Merci à mes grands-parents, mes parents, mes sœurs, mes beaux-frères et mes amis pour leur soutien, affectueux et moral. Enfin, le meilleur pour la fin, merci à Jie ZHANG, qui est toujours là, pour son soutien au quotidien, et pour bien d'autres…

Nancy, le 21 décembre 2011
Junwei QIAN

Table des matières

Liste des symboles

Alphabet latin

Symbole	Signification	Unité
a	Paramètre a d’une équation d’état cubique	$\mathrm{kg \cdot m^{5} \cdot s^{-2} \cdot mol^{-2}}$
a_i	Paramètre a d’une équation d’état cubique du corps pur i	$\mathrm{kg \cdot m^{5} \cdot s^{-2} \cdot mol^{-2}}$
a_m	Paramètre a d’une équation d’état cubique d’un mélange	$\mathrm{kg \cdot m^{5} \cdot s^{-2} \cdot mol^{-2}}$
$\mathbf{a}$	Energie de Helmholtz molaire totale	$\mathrm{J \cdot mol^{-1}}$
$\mathbf{a}_m$	Energie de Helmholtz molaire totale de mélange	$\mathrm{J \cdot mol^{-1}}$
$\mathbf{a}_i^*$	Energie de Helmholtz molaire du constituant i pur	$\mathrm{J \cdot mol^{-1}}$
$\mathbf{a}^\bullet$	Energie de Helmholtz molaire totale de gaz parfait	$\mathrm{J \cdot mol^{-1}}$
$\mathbf{a}_m^\bullet$	Energie de Helmholtz molaire totale de mélange de gaz parfait	$\mathrm{J \cdot mol^{-1}}$
$\mathbf{a}_i^\bullet$	Energie de Helmholtz molaire du constituant i pur de gaz parfait	$\mathrm{J \cdot mol^{-1}}$
$\mathbf{a}^{E,V}$	Energie de Helmholtz molaire d’excès à volume constant	$\mathrm{J \cdot mol^{-1}}$
$\mathbf{a}^{E,P}$	Energie de Helmholtz molaire d’excès à pression constante	$\mathrm{J \cdot mol^{-1}}$
A_{kl}	Paramètre d’interaction entre groupes du modèle PPR78	$\mathrm{J \cdot m^{-3}}$
b	Covolume	$\mathrm{m^{3} \cdot mol^{-1}}$
b_i	Covolume du corps pur i	$\mathrm{m^{3} \cdot mol^{-1}}$
b_m	Covolume d’un mélange	$\mathrm{m^{3} \cdot mol^{-1}}$
B_{kl}	Paramètre d’interaction entre groupes du modèle PPR78	$\mathrm{J \cdot m^{-3}}$
c_P	Capacité calorifique molaire totale à pression constante	$\mathrm{J \cdot mol^{-1} \cdot K^{-1}}$
$c_{P,i}^*$	Capacité calorifique molaire du constituant i pur à pression constante	$\mathrm{J \cdot mol^{-1} \cdot K^{-1}}$
c_P^E	Capacité calorifique molaire d’excès à pression constante	$\mathrm{J \cdot mol^{-1} \cdot K^{-1}}$
c_v	Capacité calorifique molaire totale à volume constant	$\mathrm{J \cdot mol^{-1} \cdot K^{-1}}$
E_{ij}	Paramètre intervenant dans la fonction d’excès de type Van Laar	$\mathrm{J \cdot mol^{-1}}$
ELV	Equilibre liquide-vapeur	–
ELL	Equilibre liquide-liquide	–
ELLV	Equilibre liquide-liquide-vapeur	–
g	Energie de Gibbs molaire totale	$\mathrm{J \cdot mol^{-1}}$
g_m	Energie de Gibbs molaire totale de mélange	$\mathrm{J \cdot mol^{-1}}$
g_i^*	Energie de Gibbs molaire du constituant i pur	$\mathrm{J \cdot mol^{-1}}$
$g_i^\bullet$	Energie de Gibbs molaire du constituant i pur de gaz parfait	$\mathrm{J \cdot mol^{-1}}$
$\bar{g}_i$	Potentiel chimique du constituant i dans un mélange	$\mathrm{J \cdot mol^{-1}}$
$\bar{g}_{i,liq}$	Potentiel chimique du constituant i dans la phase liquide	$\mathrm{J \cdot mol^{-1}}$
$\bar{g}_{i,liq}^{\alpha}$	Potentiel chimique du constituant i dans la phase liquide α	$\mathrm{J \cdot mol^{-1}}$
$\bar{g}_{i,liq}^{\beta}$	Potentiel chimique du constituant i dans la phase liquide β	$\mathrm{J \cdot mol^{-1}}$
$\bar{g}_{i,vap}$	Potentiel chimique du constituant i dans la phase vapeur	$\mathrm{J \cdot mol^{-1}}$

Suite du tableau page suivante.

Symbole	**Signification**	**Unité**
g^E	Energie de Gibbs molaire d'excès	$J \cdot mol^{-1}$
$g^{E,P}$	Energie de Gibbs molaire d'excès à pression constante	$J \cdot mol^{-1}$
g^E_{EoS}	Energie de Gibbs molaire d'excès à partir d'une équation d'état	$J \cdot mol^{-1}$
g^E_γ	Energie de Gibbs molaire d'excès à partir d'un modèle d'énergie de Gibbs d'excès	$J \cdot mol^{-1}$
h	Enthalpie molaire totale	$J \cdot mol^{-1}$
h_i^*	Enthalpie molaire du constituant i pur	$J \cdot mol^{-1}$
h^E	Enthalpie molaire d'excès	$J \cdot mol^{-1}$
k_{ij}	Coefficient d'interactions binaires entre les molécules i et j	–
m	Paramètre de l'équation d'état de Soave-Redlich-Kwong ou de Peng-Robinson qui tient compte de la taille de la molécule	–
n_c	Nombre de constituants dans un mélange	–
n_g	Nombre de groupes définis par le modèle PPR78	–
P	Pression d'un fluide	Pa
P_c	Pression critique	Pa
R	Constante des gaz parfaits	$J \cdot mol^{-1} \cdot K^{-1}$
s	Entropie molaire totale	$J \cdot mol^{-1} \cdot K^{-1}$
T	Température d'un fluide	K
T_c	Température critique	K
u	Energie interne molaire totale	$J \cdot mol^{-1}$
v	Volume molaire total	$m^3 \cdot mol^{-1}$
v_c	Volume molaire critique	$m^3 \cdot mol^{-1}$
v_i	Volume molaire d'un constituant i pur dans l'état de référence, avant mélange à compacité constante	$m^3 \cdot mol^{-1}$
v_i^*	Volume molaire d'un constituant i pur	$m^3 \cdot mol^{-1}$
$\mathbf{x}$	Vecteur des fractions molaires des constituants d'un mélange ou vecteur des fractions molaires des constituants dans la phase liquide	–
$\mathbf{x}^\alpha$	Vecteur des fractions molaires des constituants dans la phase liquide α	–
$\mathbf{x}^\beta$	Vecteur des fractions molaires des constituants dans la phase liquide β	–
x_i	Fraction molaire globale du constituant i ou fraction molaire du constituant i dans la phase liquide	–
x_i^α	Fraction molaire du constituant i dans la phase liquide α	–
x_i^β	Fraction molaire du constituant i dans la phase liquide β	–
$\mathbf{y}$	Vecteur des fractions molaires des constituants dans la phase vapeur	–
y_i	Fraction molaire du constituant i dans la phase vapeur	–
$\mathbf{z}$	Vecteur des fractions molaires des constituants d'un mélange	–
z_i	Fraction molaire globale du constituant i	–
z	Facteur de compressibilité molaire $\left(z = \dfrac{P \cdot v}{R \cdot T}\right)$	–

Alphabet grec

Symbole	Signification	Unité
α	Fonction de Soave dans le paramètre a d'une équation d'état cubique	–
γ	Coefficient d'activité	–
δ_i	Paramètre de l'équation d'état : $\delta_i = \sqrt{a_i} / b_i$	$J^{1/2} \cdot m^{-3/2}$
η	Compacité	–
κ_T	Coefficient de compressibilité isotherme	Pa^{-1}
φ_i	Coefficient de fugacité	–
$\varphi_{i,liq}$	Coefficient de fugacité du constituant i dans la phase liquide	–
$\varphi_{i,vap}$	Coefficient de fugacité du constituant i dans la phase vapeur	–
ω	Facteur acentrique du corps pur	–
Ω_a	Constante intervenant dans le paramètre a d'une équation d'état cubique	–
Ω_b	Constante intervenant dans le paramètre b d'une équation d'état cubique	–

Indices et exposants

Symbole	Signification
$\bullet$	Gaz parfait
$*$	Fluide pur
ath	Athermique
c	critique
E	Grandeur d'excès
éc	Grandeur d'écart au gaz parfait de même température et même volume molaire que la grandeur réelle
rés	Résiduel (écart à l'athermicité)

Introduction

A notre époque, la conception et l'optimisation des installations et des procédés chimiques s'appuient nécessairement sur la connaissance précise des propriétés thermodynamiques, comme par exemple, les équilibres entre phases, l'enthalpie et la capacité calorifique du mélange. Ces propriétés peuvent être mesurées par différentes méthodes. Même si posséder des données expérimentales est toujours souhaitable, les mesures restent longues et coûteuses à effectuer et il n'est pas concevable d'acquérir l'ensemble des données nécessaires à la recherche des conditions opératoires optimales des procédés. Il est donc essentiel de disposer d'un modèle puissant, permettant de prédire avec la plus grande précision possible les propriétés thermodynamiques.

Depuis 2004, l'équipe ThermE du LRGP développe le modèle PPR78 (Predictive Peng-Robinson equation of state 1978) qui repose sur une méthode de contributions de groupes permettant de prédire le coefficient d'interaction binaire $k_{ij}(T)$ de l'équation d'état cubique de Peng et Robinson. En 2008, quinze groupes étaient définis et il était donc possible d'estimer les k_{ij} pour n'importe quel mélange renfermant des alcanes, des aromatiques, des naphtènes, du CO_2, du N_2, du H_2S et des mercaptans. La même année, ce modèle a été incorporé à la base thermodynamique des logiciels de simulation SIMULIS THERMODYNAMICS et PROSIMPLUS commercialisés par la société PROSIM. L'objet de ce travail s'inscrit dans un cadre très précis, destiné à étendre, par l'ajout de six groupes supplémentaires qui viennent compléter les groupes déjà existants, le modèle PPR78 et ainsi permettre l'étude complète des fluides pétroliers. Les six nouveaux groupes incluent la molécule d'eau (H_2O), la molécule d'hydrogène (H_2) ainsi que quatre groupes pour modéliser les alcènes. Une étude approfondie de la capacité du modèle PPR78 pour prédire les enthalpies et les capacités calorifiques d'excès a également été menée.

Dans le chapitre I, nous nous intéresserons en premier lieu aux bases théoriques de l'étude des mélanges de fluides. Une fois ce travail préliminaire effectué, nous préciserons la théorie qui sous-tend le modèle PPR78, les groupes inclus dans ce modèle et le mode opératoire employé pour l'ajustement des paramètres.

L'eau intervient dans de nombreuses applications industrielles. Du fait qu'elle est fortement polaire, les équations d'état cubiques sont en général incapables de bien décrire ses propriétés thermodynamiques. La prédiction des équilibres entre phases de systèmes contenant des hydrocarbures, des gaz (N_2, H_2S, CO_2) et de l'eau devient alors plus délicate. Les modèles qui sont capables de décrire de tels mélanges sont habituellement de type hétérogène (coefficient d'activité pour décrire la phase liquide). Cependant, ces modèles de g^E ne sont pas applicables aux mélanges sur de larges gammes de températures, de pressions et de compositions. Le chapitre II comportera les résultats obtenus suite à l'ajout du nouveau groupe H_2O au modèle de contribution de groupes PPR78.

Au cours des années passées, l'utilisation des alcènes comme des réactifs, des intermédiaires, ou des produits finis a énormément augmentée dans l'industrie chimique, pétrochimique et polymérique. Par conséquent, la connaissance précise des équilibres entre phases de systèmes contenant des alcènes est essentielle pour la conception et l'optimisation des procédés. Le chapitre III montrera la précision de notre modèle quant à la description des équilibres liquide-vapeur et du lieu des points critiques de mélanges binaires contenants des alcènes.

L'hydrogène est fréquemment rencontré dans le domaine pétrolier, notamment dans les procédés d'hydrodésalkylation, d'hydrodésulfuration, d'hydrocracking, etc. De plus, depuis quelques années, la pollution et l'effet de serre sont devenus de sérieux problèmes sociétaux, c'est pourquoi la transition de l'énergie 'fossile' à l'énergie propre utilisant H_2 semble inévitable. Le groupe H_2 sera inclus au modèle PPR78 dans le chapitre IV et nous présenterons les résultats concernant la prédiction du comportement de mélanges asymétriques.

Notons que l'enthalpie d'excès et la capacité calorifique d'excès sont des propriétés importantes pour l'analyse énergétique et exergétique des procédés. De plus, jusqu'à présent, très peu de travaux ont été réalisés sur la restitution de ces propriétés par un modèle thermodynamique sur un large intervalle de température et de pression. Dans le chapitre V, nous nous intéresserons au problème de la prédiction des propriétés thermodynamiques telles que l'équilibre entre phases, l'enthalpie d'excès et la capacité calorifique d'excès, en définissant le nouveau modèle *E*-PPR78 (enhanced PPR78).

Chapitre I. Bibliographie et description du modèle PPR78

Dans ce chapitre, nous aborderons les différentes notions théoriques liées au calcul des propriétés thermodynamiques par des équations d'état cubiques. Après la description de ces équations d'état cubiques et des règles de mélange les plus largement utilisées, nous présenterons le modèle développé durant cette thèse : le modèle PPR78 (Predictive Peng-Robinson equation of state 1978). Il s'agira évidement de rappeler l'équation d'état ainsi que les règles de mélange choisies. Ce modèle est rendu prédictif par le calcul du coefficient d'interaction binaire k_{ij} à partir d'une méthode de contributions de groupes qui sera ensuite détaillée. Enfin, nous présenterons le mode de calcul de l'enthalpie molaire d'excès h^E et celui de la capacité calorifique molaire d'excès à pression constante c_P^E par le modèle PPR78.

I.1 La relation d’équilibre entre phases

Soit un système à n_c constituants, à la température T et sous la pression P. A l’équilibre entre phases (équilibre liquide-vapeur noté ELV, équilibre liquide-liquide noté ELL et équilibre liquide-liquide-vapeur noté ELLV), la température T, la pression P et le potentiel chimique $\bar{g}_i$ de chacun des constituants sont uniformes dans tout le système polyphasique. On pourra donc écrire :

$$\forall i \in 1;n_c \ , \begin{cases} \bar{g}_{i,liq}(T,P,\mathbf{x}) = \bar{g}_{i,vap}(T,P,\mathbf{y}) & \text{(cas de l'ELV)} \\ \bar{g}_{i,liq\ \alpha}(T,P,\mathbf{x}^{\alpha}) = \bar{g}_{i,liq\ \beta}(T,P,\mathbf{x}^{\beta}) & \text{(cas de l'ELL)} \\ \bar{g}_{i,liq\ \alpha}(T,P,\mathbf{x}^{\alpha}) = \bar{g}_{i,liq\ \beta}(T,P,\mathbf{x}^{\beta}) = \bar{g}_{i,vap}(T,P,\mathbf{y}) & \text{(cas de l'ELLV)} \end{cases} \qquad (I-1)$$

$$\text{avec } \mathbf{x} = \left(x_1,...,x_{n_c}\right), \mathbf{x}^{\alpha} = \left(x_1^{\alpha},...,x_{n_c}^{\alpha}\right), \mathbf{x}^{\beta} = \left(x_1^{\beta},...,x_{n_c}^{\beta}\right) \text{ et } \mathbf{y} = \left(y_1,...,y_{n_c}\right)$$

où x_i est la fraction molaire du constituant i dans la phase liquide, x_i^{α} la fraction molaire du constituant i dans la phase liquide α, x_i^{β} la fraction molaire du constituant i dans la phase liquide β et y_i la fraction molaire du constituant i dans la phase vapeur.

Il existe deux grandes approches pour expliciter la relation (I−1) :

- l’approche φ − φ (approche homogène ou symétrique),
- l’approche γ − φ (approche hétérogène ou dissymétrique).

L’approche utilisée au cours de ce travail de thèse est l’approche homogène ou symétrique (φ − φ). Pour l’illustrer, nous prenons l’exemple d’une solution diphasique liquide-vapeur. Dans cette approche, le potentiel chimique de chaque constituant dans chaque phase est exprimé en prenant comme référence le gaz parfait pur à la même température et sous la même pression que le mélange. Les constituants liquide et gazeux étant traités mathématiquement de la même manière (même référence), on qualifie une telle approche symétrique. On peut donc écrire :

$$\begin{cases} \bar{g}_{i,liq}(T,P,\mathbf{x}) = g_i^{\bullet}(T,P) + R \cdot T \cdot \ln\left[x_i \cdot \varphi_{i,liq}(T,P,\mathbf{x})\right] \\ \bar{g}_{i,vap}(T,P,\mathbf{y}) = g_i^{\bullet}(T,P) + R \cdot T \cdot \ln\left[y_i \cdot \varphi_{i,vap}(T,P,\mathbf{y})\right] \end{cases} \qquad (I-2)$$

A l’équilibre liquide-vapeur :

$$x_i \cdot \varphi_{i,liq}(T,P,\mathbf{x}) = y_i \cdot \varphi_{i,vap}(T,P,\mathbf{y}) \quad \forall i \in 1;n_c \qquad (I-3)$$

Cette équation est la condition d'ELV pour la méthode $\varphi - \varphi$. Elle relie la température, la pression et la composition des phases liquide et vapeur en équilibre. Cette approche présente le net avantage d'être applicable à haute pression et de permettre le calcul d'autres propriétés du mélange. Les coefficients de fugacité φ_i doivent être calculés par une équation d'état cubique par exemple, après avoir défini des règles de mélange.

I.2 Equations d'état cubiques

Les équations d'état cubiques sont très utilisées dans le domaine de la thermodynamique des fluides. Depuis les premiers développements datant du $19^{\text{ème}}$ siècle, nombreuses créations et améliorations des équations existent dans la littérature. Parmi les plus connues, nous allons tout d'abord citer celles de Van der Waals, de Redlich-Kwong, de Soave-Redlich-Kwong et de Peng-Robinson.

I.2.1 L'équation d'état de Van der Waals

En 1873, Van der Waals[1] a proposé la première équation d'état cubique capable de prédire et représenter aussi bien les phases liquides que gazeuses. Son expression pour un corps pur s'écrit :

$$P = \frac{R \cdot T}{v-b} - \frac{a}{v^2} = P_{\text{rép}} + P_{\text{att}} \quad \text{avec} \quad \begin{cases} b = \dfrac{1}{8}\dfrac{R \cdot T_c}{P_c} \\ a = \dfrac{27}{64}\dfrac{R^2 \cdot T_c^2}{P_c} \end{cases} \qquad (I-4)$$

Elle représente la pression par la somme de deux termes, l'un répulsif contenant le paramètre b, relatif aux interactions répulsives, l'autre attractif contenant le paramètre a, relatif aux interactions attractives entre sphère dures. Les valeurs de ces paramètres a et b peuvent être déterminées par application des contraintes critiques :

$$\begin{aligned} &P_c - P(T_c, v_c) = 0 \\ &\left(\partial P/\partial v\right)_T \Big|_{T=T_c, v=v_c} = 0 \\ &\left(\partial^2 P/\partial v^2\right)_T \Big|_{T=T_c, v=v_c} = 0 \end{aligned} \qquad (I-5)$$

L'équation de VdW est d'une précision insuffisante, ce qui a conduit à de nombreuses modifications, donnant lieu à des équations améliorées.

I.2.2 L'équation d'état de Redlich-Kwong

En 1949, Redlich et Kwong[2] ont proposé une équation d'état dans laquelle ils modifient la partie attractive de l'équation de VdW ainsi que le paramètre a qu'ils expriment en fonction de la température T. Pour un corps pur, elle possède la forme :

$$P = \frac{R \cdot T}{v - b} - \frac{a(T)}{v \cdot (v + b)} \text{ avec } \begin{cases} b = \Omega_b \dfrac{R \cdot T_c}{P_c} \text{ et } \Omega_b \approx 0,08664 \\ a(T) = \Omega_a \dfrac{R^2 \cdot T_c^2}{P_c} \alpha(T) \text{ et } \Omega_a \approx 0,42748 \\ \alpha(T) = \sqrt{T_c/T} \end{cases} \qquad (I-6)$$

I.2.3 L'équation d'état de Soave-Redlich-Kwong

En 1972, Soave[3] a modifié l'expression du terme attractif a(T) dans l'équation originale de Redlich et Kwong, en faisant dépendre la fonction α(T) de la température T et du facteur acentrique ω :

$$\begin{aligned} &a(T) = \Omega_a \frac{R^2 \cdot T_c^2}{P_c} \alpha(T) \text{ et } \Omega_a \approx 0{,}42748 \text{(inchangé)} \\ &\alpha(T) = \left[1 + m\left(1 - \sqrt{T/T_c}\right)\right]^2 \\ &m = 0,480 + 1,574\omega - 0,176\omega^2 \end{aligned} \qquad (I-7)$$

Le paramètre m est spécifique du constituant considéré puisqu'il dépend du facteur acentrique du corps pur. L'introduction du facteur acentrique par Soave ajoute donc un troisième paramètre (ω) aux deux premiers (T_c et P_c) qui intervenaient tant dans l'équation d'état de VdW que dans l'équation originale de Redlich-Kwong. Cette équation portant le nom d'équation Soave-Redlich-Kwong (SRK) permet une nette amélioration du calcul des équilibres liquide-vapeur.

I.2.4 L'équation d'état de Peng-Robinson (1976)

En 1976, Peng et Robinson[4] ont proposé une nouvelle équation en utilisant la fonction α(T) de Soave et en améliorant le terme attractif pour mieux représenter les propriétés volumétriques en phase liquide. Pour un corps pur, elle s'écrit de la manière suivante :

$$P=\frac{R\cdot T}{v-b}-\frac{a(T)}{v\cdot(v+b)+b\cdot(v-b)} \quad \text{avec} \begin{cases} b=\Omega_b\dfrac{R\cdot T_c}{P_c} \text{ et } \Omega_b\approx 0.0777960739 \\ a(T)=\Omega_a\dfrac{R^2\cdot T_c^2}{P_c}\alpha(T) \text{ et } \Omega_a\approx 0,457235529 \\ \alpha(T)=\left[1+m\left(1-\sqrt{T/T_c}\right)\right]^2 \\ m=0,37464+1,54226\omega-0,26992\omega^2 \end{cases} \qquad (I-8)$$

I.2.5 L'équation d'état de Peng-Robinson (1978)

En 1978, les même Peng et Robinson[5] ont proposé une extension du modèle de 1976, afin d'améliorer la précision de leur équation pour les constituants lourds. Une seconde expression du paramètre m en fonction du facteur acentrique du corps pur a été rajoutée par les auteurs :

$$\begin{cases} \text{si } \omega\le 0,491 \;\; m=0,37464+1,54226\omega-0,26992\omega^2 \\ \text{si } \omega> 0,491 \;\; m=0,379642+1,48503\omega-0,164423\omega^2+0,016666\omega^3 \end{cases} \qquad (I-9)$$

Ils recommandent l'utilisation de la première expression pour des corps purs dont le facteur acentrique est inférieur ou égal au facteur acentrique du décane et la seconde pour les constituants dont le facteur acentrique est supérieur à celui du décane. Cette équation désignée par l'abréviation PR78 est largement utilisée pour les hydrocarbures et les fluides pétroliers.

I.2.6 Autres développements des équations d'état cubiques

Après les travaux de Redlich et Kwong, de Soave et de Peng et Robinson, le développement des équations d'état cubiques a suivi trois grandes voies. La première consiste à modifier à nouveau le terme d'attraction des équations d'état, notamment la fonction a(T) ou le dénominateur du terme d'attraction. La deuxième est d'améliorer le terme de répulsion. Les nombreux travaux issus de ces deux voies peuvent être trouvés dans l'article de Wei et Sadus[6]. La troisième grande voie consiste à appliquer une translation de volume au terme répulsif ainsi qu'au terme attractif.

I.2.6.1 Modification du terme d'attraction

On présente brièvement ci-après quelques-unes des modifications du terme d'attraction et on notera que Valderrama[7] fait, entre autre, le point dans son article de revue sur la plupart des améliorations du terme attractif des équations d'état. De plus, on remarquera que la détermination de l'enthalpie par une équation d'état cubique fait intervenir la dérivée première de la fonction a(T) par rapport à la température T, alors que la dérivée seconde intervient pour la détermination des capacités calorifiques. D'après Trebble et Bishnoi[8], la qualité des résultats de tels calculs est un moyen d'évaluer la validité de nouvelles équations d'état cubiques.

Les fonctions a(T) utilisées dans les équations d'état cubiques s'expriment en fonction de a_c (valeur de a calculée au point critique) et de la fonction α(T) :

$$a(T) = a_c \cdot \alpha(T) \qquad (I-10)$$

La fonction α (T) intervient dans le terme attractif et joue un grand rôle dans la précision du calcul des équilibres liquide-vapeur. Après la fonction α(T) de Soave, de nombreux auteurs ont proposé de nouvelles fonctions α(T) pour améliorer les équations d'état cubiques. Parmi les plus connues, on peut citer les fonctions suivantes :

♣ En 1983, Mathias et Copeman[9] ont établi une fonction α(T), avec trois paramètres ajustables sur des données expérimentales :

$$\begin{cases} \alpha(T) = \left[1 + c_1\left(1 - \sqrt{T/T_c}\right) + c_2\left(1 - \sqrt{T/T_c}\right)^2 + c_3\left(1 - \sqrt{T/T_c}\right)^3\right]^2 & \text{si } T < T_c \\ \alpha(T) = \left[1 + c_1\left(1 - \sqrt{T/T_c}\right)\right]^2 & \text{si } T \geq T_c \end{cases} \qquad (I-11)$$

Où c_1, c_2 et c_3 sont tabulés dans la banque de données D.D.B. (Dortmund Data Bank) pour de nombreux constituants purs.

♣ En 1986, Stryjek et Vera[10] ont proposé une modification de l'équation de Peng-Robinson. Cette modification porte sur le facteur m qui n'est pas seulement fonction du facteur acentrique, mais dépend de la température et d'une constante m_1 qui est spécifique à chaque fluide. Le paramètre m est de la forme :

$$m = m_0 + m_1\left(1+\sqrt{T/T_c}\right)\left(0,7 - T/T_c\right) \quad \text{avec : } m_0 = 0,378893 + 1,4897153\omega - 0,1713184\omega^2 + 0,0196554\omega^3 \qquad (I-12)$$

Les valeurs numériques de m_1 ont été ajustées pour de nombreux corps purs d'intérêt industriel. Les auteurs recommandent que m_1 soit considéré comme nul à température supercritique. La fonction alpha s'exprime alors par :

$$\begin{cases} \alpha(T) = \left[1 + m_0\left(1-\sqrt{T/T_c}\right) + m_1\left(1 - T/T_c\right)\left(0,7 - T/T_c\right)\right]^2 & \text{si } T \le T_c \\ \alpha(T) = \left[1 + m_0\left(1-\sqrt{T/T_c}\right)\right]^2 & \text{si } T > T_c \end{cases} \qquad (I-13)$$

♣ En 1991, Twu et al.[11] ont développé une fonction alpha faisant intervenir une forme logarithmique :

$$\alpha(T) = \left(T/T_c\right)^{N(M-1)} \exp\left\{L\left[1-\left(T/T_c\right)^{N\cdot M}\right]\right\} \qquad (I-14)$$

qui permet de bien représenter la pression de vapeur et la capacité calorifique du liquide pour plus de 1000 molécules.

En 1995, Twu et al.[12-13] ont proposé une fonction alpha basée sur une approche différente. Ils ont considéré une fonction linéaire par rapport au facteur acentrique de la forme :

$$\alpha(T) = \alpha^{(0)} + \omega\left(\alpha^{(1)} - \alpha^{(0)}\right) \text{ avec } \begin{cases} \alpha^{(0)} = \left(T/T_c\right)^{a_0} \exp\left\{a_1\left[1-\left(T/T_c\right)^{a_2}\right]\right\} \\ \alpha^{(1)} = \left(T/T_c\right)^{b_0} \exp\left\{b_1\left[1-\left(T/T_c\right)^{b_2}\right]\right\} \end{cases} \qquad (I-15)$$

Les paramètres L, M, N, a_0, a_1, a_2, b_0, b_1 et b_2 dépendent des équations d'état choisies et leurs valeurs sont données par les auteurs.

En ce qui concerne le dénominateur du terme d'attraction, Patel et Teja[14] ont établi une équation à trois paramètres qui s'exprime par :

$$P = \frac{R \cdot T}{v - b} - \frac{a(T)}{v \cdot (v + b) + c \cdot (v - b)} \quad \text{avec} \begin{cases} a(T) = \Omega_a \dfrac{R^2 \cdot T_c^2}{P_c} \alpha(T) \\ b = \Omega_b \dfrac{R \cdot T_c}{P_c} \\ c = \Omega_c \dfrac{R \cdot T_c}{P_c} \end{cases} \qquad (I-16)$$

Le facteur de compressibilité critique correspondant à cette équation d'état est relié au facteur acentrique par la relation :

$$z_c = 0,329032 - 0,076799\omega + 0,0211947\omega^2 \qquad (I-17)$$

Ω_b est la plus petite racine positive de l'équation :

$$\Omega_b^3 + (2 - 3z_c)\Omega_b^2 + 3z_c^2\Omega_b - z_c^3 = 0 \qquad (I-18)$$

Ω_a et Ω_c se calculent par les relations :

$$\begin{cases} \Omega_a = 3z_c^2 + 3(1 - 2z_c)\Omega_b + \Omega_b^2 + 1 - 3z_c \\ \Omega_c = 1 - 3z_c \end{cases} \qquad (I-19)$$

Ils ont pris la fonction alpha de Soave :

$$\begin{aligned} &\alpha(T) = \left[1 + m\left(1 - \sqrt{T/T_c}\right)\right]^2 \\ &\text{avec : } m = 0,452413 + 1,30982\omega - 0,295937\omega^2 \end{aligned} \qquad (I-20)$$

Les résultats obtenus à l'aide de cette méthode présentent une amélioration, en particulier pour le calcul des volumes, par rapport aux équations à deux paramètres.

I.2.6.2 Translation de volume

Du constat que les volumes molaires calculés sont toujours plus grands que les valeurs expérimentales et que, pour un composé donné et une équation d'état donnée, l'erreur commise est plus ou moins constante en fonction de la température, Péneloux et al.[15] ont proposé le concept de translation de volume qui permet d'améliorer la prédiction des propriétés volumiques sans modifier les conditions d'équilibre liquide-vapeur (ELV). Leur correction consiste à utiliser un volume translaté $\tilde{v} = v + c$ également appelé pseudo volume. L'équation d'état cubique générale corrigée proposée par Péneloux s'écrit :

$$P = \frac{R \cdot T}{\tilde{v} - \tilde{b}} - \frac{a(T)}{\tilde{v}\left(\tilde{v} + \gamma\tilde{b}\right)} \text{ avec } \begin{cases} \tilde{v} = v + c \\ \tilde{b} = \tilde{\Omega}_b \dfrac{R \cdot T_c}{P_c} \end{cases} \qquad (I-21)$$

Où γ est le paramètre caractéristique de l'équation d'état et c un facteur de correction volumique dépendant du constituant pur étudié qui peut être calé sur des valeurs expérimentales ou estimé à partir de la corrélation suivante : $c = \theta \cdot R \cdot T_c / P_c$, où θ est une fonction du facteur de compressibilité de Rackett (z_{RA}). Les valeurs des constantes γ et $\tilde{\Omega}_b$, et les expressions de θ pour quelques équations sont données par les auteurs. Cette méthode de translation de volume pour équations d'état cubiques est recommandée dans le calcul des propriétés volumiques des corps purs et des mélanges.

I.2.7 Les équations d'état cubiques de l'ensemble principal

Pour un corps pur, les équations d'état cubiques de l'ensemble principal peuvent être écrites sous la forme :

$$P = \frac{R \cdot T}{v - b} - \frac{a}{\left(v - b \cdot r_1\right)\left(v - b \cdot r_2\right)} \text{ avec } \begin{cases} \left(r_1, r_2\right) \in \mathbb{R}^2 \text{ et } \left(a, b\right) \in \mathbb{R}_+^2 \\ |r_1| \geq |r_2| \end{cases} \qquad (I-22)$$

Les valeurs des constantes r_1 et r_2 de quelques équations d'état cubiques sont données dans le tableau suivant :

Tableau I–1. Valeurs des paramètres r_1 et r_2 pour quelques équations cubiques.

Equation	r_1	r_2
Van der Waals (VdW)	0	0
Soave-Redlich-Kwong (SRK)	-1	0
Peng-Robinson (PR)	$-1-\sqrt{2}$	$-1+\sqrt{2}$

Les équations d'état explicites en pression permettent de calculer les grandeurs d'écart au gaz parfait définies par :

$$x^{éc}(T, v) = x^{*}(T, v) - x^{\bullet}(T, v) \qquad (I-23)$$

où $x^{*}(T,v)$ est une grandeur d'état du fluide réel de température T, de volume molaire v et de pression P(T,v). $x^{\bullet}(T,v)$ est une grandeur d'état du gaz parfait de même température T et volume molaire v que le fluide réel. La pression du gaz parfait est alors $P^{\bullet}=R\cdot T/v\neq P(T,v)$. Et $x\in\{h,\ u,\ s,\ g,\ \mathbf{a},\ c_P,\ c_V\ ...\}$.

I.2.7.1 Calcul des fonctions d'écart lorsque $r_1 \neq r_2$

On commence toujours par déterminer l'énergie de Helmholtz d'écart car **a** est fonction caractéristique dans les variables T et v. Les autres grandeurs molaires d'écart s'en déduisent simplement, comme illustré ci-après.

♣ Energie de Helmholtz molaire d'écart :

Par définition :

$$\mathbf{a}^{\text{éc}}(T,v)=-\int_{+\infty}^{v}\left[P(T,v)-\frac{R\cdot T}{v}\right]\cdot dv \qquad (I-24)$$

En insérant l'équation (I–22) dans l'équation (I–24), il vient :

$$\mathbf{a}^{\text{éc}}(T,v)=R\cdot T\ln\left(\frac{v}{v-b}\right)+\frac{a(T)}{b\cdot(r_1-r_2)}\ln\left(\frac{v-b\cdot r_1}{v-b\cdot r_2}\right) \qquad (I-25)$$

♣ Energie de Gibbs molaire d'écart :

On a : $g^{\text{éc}}=\mathbf{a}^{\text{éc}}+(P\cdot v)^{\text{éc}}=\mathbf{a}^{\text{éc}}+P\cdot v-P\cdot v^{\bullet}=\mathbf{a}^{\text{éc}}+P\cdot v-R\cdot T$ et par conséquent :

$$g^{\text{éc}}(T,v)=R\cdot T\cdot\ln\left(\frac{v}{v-b}\right)+\frac{a(T)}{b\cdot(r_1-r_2)}\ln\left(\frac{v-b\cdot r_1}{v-b\cdot r_2}\right)+\frac{R\cdot T\cdot b}{v-b}-\frac{a(T)\cdot v}{(v-b\cdot r_1)(v-b\cdot r_2)} \qquad (I-26)$$

♣ Entropie molaire d'écart :

Elle s'obtient par la formule : $s^{\text{éc}}=-\left(\frac{\partial\mathbf{a}^{\text{éc}}}{\partial T}\right)_v$. L'entropie molaire d'écart s'écrit dans le cas des équations d'état cubiques de l'ensemble principal :

$$s^{\text{éc}}(T,v) = R\cdot\ln\left(\frac{v-b}{v}\right) - \frac{1}{b\cdot(r_1-r_2)}\cdot\frac{da}{dT}\cdot\ln\left(\frac{v-b\cdot r_1}{v-b\cdot r_2}\right) \qquad (I-27)$$

♣ Energie interne molaire d'écart :

On a : $u^{\text{éc}} = \mathbf{a}^{\text{éc}} + T\cdot s^{\text{éc}}$ et par conséquent :

$$u^{\text{éc}}(T,v) = \frac{1}{b\cdot(r_1-r_2)}\cdot\left(a - T\cdot\frac{da}{dT}\right)\cdot\ln\left(\frac{v-b\cdot r_1}{v-b\cdot r_2}\right) \qquad (I-28)$$

♣ Enthalpie molaire d'écart :

De $h^{\text{éc}} = u^{\text{éc}} + (P\cdot v)^{\text{éc}} = u^{\text{éc}} + P\cdot v - R\cdot T$, on déduit :

$$h^{\text{éc}}(T,v) = \frac{R\cdot T\cdot b}{v-b} - \frac{a(T)\cdot v}{(v-b\cdot r_1)(v-b\cdot r_2)} + \frac{1}{b\cdot(r_1-r_2)}\cdot\left(a - T\cdot\frac{da}{dT}\right)\cdot\ln\left(\frac{v-b\cdot r_1}{v-b\cdot r_2}\right) \qquad (I-29)$$

♣ Capacité calorifique molaire d'écart à volume constant :

Elle est définie par la relation : $c_v^{\text{éc}} = \left(\frac{\partial u^{\text{éc}}}{\partial T}\right)_v$. Ainsi :

$$c_v^{\text{éc}}(T,v) = \frac{-T}{b\cdot(r_1-r_2)}\cdot\frac{d^2a}{dT^2}\cdot\ln\left(\frac{v-b\cdot r_1}{v-b\cdot r_2}\right) \qquad (I-30)$$

♣ Capacité calorifique molaire d'écart à pression constante :

Elle s'obtient par la formule :

$$c_P^{\text{éc}}(T,v) = c_v^{\text{éc}}(T,v) - R + T\cdot(\kappa_T\cdot v)\cdot(\beta\cdot P)^2 \qquad (I-31)$$

avec :

$$\begin{cases} \kappa_T\cdot v = -\left(\frac{\partial v}{\partial P}\right)_T = -\left[\left(\frac{\partial P}{\partial v}\right)_T\right]^{-1} = \left[\frac{R\cdot T}{(v-b)^2} - \frac{a(T)\cdot\left[2v - b\cdot(r_1+r_2)\right]}{(v-b\cdot r_1)^2(v-b\cdot r_2)^2}\right]^{-1} \\ \beta\cdot P = \left(\frac{\partial P}{\partial T}\right)_v = \frac{R}{v-b} - \frac{da}{dT}\cdot\frac{1}{(v-b\cdot r_1)(v-b\cdot r_2)} \end{cases} \qquad (I-32)$$

I.2.7.2 Calcul des fonctions d'écart des équations d'état cubiques de l'ensemble principal lorsque $r_1 = r_2$

On note $r = r_1 = r_2$. L'équation (I–22) s'écrit donc à présent :

$$P(T,v) = \frac{R\cdot T}{v-b} - \frac{a(T)}{(v-b\cdot r)^2} \qquad (I-33)$$

Il vient alors:

♣ **Energie de Helmholtz molaire d'écart :**

$$\mathbf{a}^{\text{éc}}(T,v) = RT\ln\left(\frac{v}{v-b}\right) - \frac{a(T)}{v-r} \qquad (I-34)$$

♣ **Energie de Gibbs molaire d'écart :**

$$g^{\text{éc}}(T,v) = RT\ln\left(\frac{v}{v-b}\right) - \frac{a(T)}{v-r} + \frac{R\cdot T\cdot b}{v-b} - \frac{a(T)\cdot v}{(v-b\cdot r)^2} \qquad (I-35)$$

♣ **Entropie molaire d'écart :**

$$s^{\text{éc}}(T,v) = R\cdot\ln\left(\frac{v-b}{v}\right) - \frac{1}{v-r}\cdot\frac{da}{dT} \qquad (I-36)$$

♣ **Energie interne molaire d'écart :**

$$u^{\text{éc}}(T,v) = \frac{\left(a - T\cdot\frac{da}{dT}\right)}{v-r} \qquad (I-37)$$

♣ **Enthalpie molaire d'écart :**

$$h^{\text{éc}}(T,v) = \frac{R\cdot T\cdot b}{v-b} - \frac{a(T)\cdot v}{(v-b\cdot r)^2} - \frac{1}{v-r}\cdot\left(a - T\cdot\frac{da}{dT}\right) \qquad (I-38)$$

♣ **Capacité calorifique molaire d'écart à volume constant :**

$$c_v^{\text{éc}}(T,v) = \frac{T}{(v-r)^2}\cdot\frac{d^2a}{dT^2} \qquad (I-39)$$

♣ Capacité calorifique molaire d'écart à pression constante :

$$c_P^{éc}(T,v) = c_V^{éc}(T,v) - R + T \cdot (\kappa_T \cdot v) \cdot (\beta \cdot P)^2 \qquad (I-40)$$

avec :

$$\begin{cases} \kappa_T \cdot v = \left[\dfrac{RT}{(v-b)^2} - \dfrac{2a(T)}{(v-r)^3} \right]^{-1} \\ \beta \cdot P = \dfrac{R}{v-b} - \dfrac{da}{dT} \cdot \dfrac{1}{(v-r)^2} \end{cases} \qquad (I-41)$$

I.3 Application des équations d'état aux mélanges

Les équations d'état pour les corps purs peuvent être appliquées à des mélanges en considérant l'influence mutuelle des différents composés sur les paramètres des équations d'état, qui nécessite l'utilisation de règles de mélange. On notera qu'un article de revue assez complet a été écrit sur ce sujet par Ghosh[16] en 1999.

I.3.1 Règles de mélange classique

Les règles de mélange les plus répandues sont sans doute celles de type Van der Waals. Ces règles de mélange sont souvent appelées règles de mélange classiques ou règles de mélange quadratiques. Si l'on considère un mélange à n_c constituants, elles s'écrivent de la façon suivante :

$$\begin{cases} a_m = \sum_{i=1}^{n_c}\sum_{j=1}^{n_c} x_i \cdot x_j \cdot a_{ij} \ \text{ avec : } a_{ij} = \sqrt{a_i a_j}\left(1-k_{ij}\right) \text{ et } k_{ij} = k_{ji} \\ b_m = \sum_{i=1}^{n_c}\sum_{j=1}^{n_c} x_i \cdot x_j \cdot b_{ij} \ \text{ avec : } b_{ij} = \frac{1}{2}\left(b_i + b_j\right)\left(1-l_{ij}\right) \text{ et } l_{ij} = l_{ji} \end{cases} \qquad (I-42)$$

Où a_{ij} et b_{ij} représentent les paramètres d'interactions correspondant à deux espèces différentes. k_{ij} et l_{ij} sont appelés coefficients d'interactions binaires, l'un associé au paramètre a_m, l'autre associé au paramètre b_m, qui sont ajustables sur des données expérimentales. Un cas particulier fréquemment rencontré est le cas où le paramètre l_{ij} est posé égal à zéro et une règle de mélange linéaire sur le covolume est obtenue, ce qui amène :

$$\begin{cases} a_m = \sum_{i=1}^{n_c}\sum_{j=1}^{n_c} x_i \cdot x_j \sqrt{a_i \cdot a_j}\left(1-k_{ij}\right) \\ b_m = \sum_{i=1}^{n_c} x_i \cdot b_i \end{cases} \qquad (I-43)$$

Remarque : Lorsque l'équation d'état est utilisée pour représenter un système multi-constituant, nous notons a_m et b_m, les paramètres a et b du mélange.

I.3.2 Règles de mélange non conventionnelles

Du fait que les règles de mélange classiques sont utilisées avec succès uniquement pour les mélanges apolaires ou faiblement polaires, plusieurs autres règles de mélange ont été développées dans le but de représenter les mélanges asymétriques et/ou polaires. Les règles de mélange s'agissant d'introduire une dépendance des règles de mélange par rapport à la densité[9, 17-18] ne sont pas discutés ici, car ils détruisent la nature de l'équation d'état cubique sans présenter des nettes améliorations. En outre, de nombreux travaux reposent sur une variation du paramètre d'interaction avec la composition[10, 19-22]. A titre d'exemple, Panagiotopoilos et Reid[19] ont présenté la fonction $a_m(T,\mathbf{x})$ sous la forme :

$$a_m = \sum_{i=1}^{n_c}\sum_{j=1}^{n_c} x_i \cdot x_j \sqrt{a_i \cdot a_j}\left[1 - k_{ij} + \left(k_{ij} - k_{ji}\right)x_i\right] \text{ avec } k_{ij} \neq k_{ji} \qquad (I-44)$$

Signalons que ces modifications rendent ces règles de mélange flexibles et capables de représenter le comportement de mélanges multiconstituants contenant des molécules telles que l'eau, l'acétone ou le méthanol, Elles ne sont cependant pas applicables à des mélanges complexes tels que les fluides pétroliers[23-24]. L'autre inconvénient est le non respect de la dépendance quadratique du second coefficient du viriel pour ces règles de mélange.

I.3.3 Règles de mélange de types EoS/g^E

Une autre approche consiste à intégrer dans les règles de mélange des équations d'état (EoS) les modèles d'énergie de Gibbs d'excès (g^E), conduisant à l'apparition de nouvelles règles de mélange. De nombreux auteurs ont suivi ce chemin qui consiste à égaler l'expression de g^E déterminée pour une EoS à l'expression de g^E issue d'un modèle de coefficients d'activité. Ce dernier ne dépend pas de la pression. Certains auteurs proposent pour raccorder les modèles, de faire tendre la pression vers l'infini (c'est le cas de Huron et Vidal[25] par exemple). D'autres proposent de faire tendre la pression vers zéro (c'est par exemple, le cas de Michelsen[26] puis de Dahl et Michelsen[27] qui ont mis au point les règles de mélange MHV-1 et MHV-2). En 1992, Wong et Sandler [28] ont proposé des règles de mélange similaires où g^E a été remplacée par l'énergie de Helmholz d'excès $\mathbf{a}^E$, et qui respectent la variation quadratique en composition du second coefficient du viriel. Dans ce qui suit, on commence par présenter très succinctement les règles de mélange de Huron-Vidal puis, on aborde les règles de mélange à compacité constante qui ont été choisies pour mettre au point le modèle PPR78.

I.3.3.1 Règle de mélange de Huron-Vidal

L'expression de g^E obtenue à partir d'une équation d'état cubique de l'ensemble principal est donnée par :

$$\frac{g^E_{EoS}(T,v,\mathbf{x})}{R\cdot T}=\frac{g^E_1(T,v,\mathbf{x})}{R\cdot T}+\frac{g^E_2(T,v,\mathbf{x})}{R\cdot T}+\frac{g^E_3(T,v,\mathbf{x})}{R\cdot T}$$

$$\begin{cases}\dfrac{g^E_1(T,v,\mathbf{x})}{R\cdot T}=\displaystyle\sum_{i=1}^{n_c}x_i\cdot\ln\left(v_i^*-b_i\right)-\ln\left(v-b_m\right)\\ \dfrac{g^E_2(T,v,\mathbf{x})}{R\cdot T}=\dfrac{1}{r_1-r_2}\left[\displaystyle\sum_{i=1}^{n_c}\frac{x_i\cdot a_i}{b_i\cdot R\cdot T}\ln\left(\frac{v_i^*-b_i\cdot r_2}{v_i^*-b_i\cdot r_1}\right)-\frac{a_m}{b_m\cdot R\cdot T}\ln\left(\frac{v-b_m\cdot r_2}{v-b_m\cdot r_1}\right)\right]\\ \dfrac{g^E_3(T,v,\mathbf{x})}{R\cdot T}=\dfrac{P(T,v,\mathbf{x})}{R\cdot T}\cdot\left(v-\displaystyle\sum_{i=1}^{n_c}x_i\cdot v_i^*\right)\end{cases}\qquad (I-45)$$

En 1979, Huron et Vidal[25] ont d'abord développé une règle dont l'état de référence est l'état à pression infinie.

Lorsque $P\to\infty$, $v\to b_m$, $v_i^*\to b_i$, $g^E_{EoS}=g^E_\gamma$, où g^E_γ est l'énergie de Gibbs d'excès issue d'un modèle de coefficients d'activité, l'énergie de Gibbs sous pression infinie s'écrit :

$$\lim_{P\to+\infty}\frac{g^E_{EoS}(T,v,\mathbf{x})}{R\cdot T}=\frac{1}{r_1-r_2}\ln\left(\frac{1-r_2}{1-r_1}\right)\left[\left(\sum_{i=1}^{n_c}x_i\frac{a_i}{b_i\cdot R\cdot T}\right)-\frac{a_m}{b_m\cdot R\cdot T}\right]\qquad (I-46)$$

qui se réarrange en :

$$\frac{a_m}{b_m}=\sum_{i=1}^{n_c}x_i\frac{a_i}{b_i}-\frac{g^E_\gamma(T,P\to\infty,\mathbf{x})}{C}\ ;\ C=\frac{1}{r_1-r_2}\ln\left(\frac{1-r_2}{1-r_1}\right)\qquad (I-47)$$

L'approche de Huron-Vidal permet d'intégrer les modèles de g^E dans les règles de mélange des équations d'état. Cependant, les modèles de g^E sont établis pour représenter correctement les basses pressions, et comme ces règles de mélange sont proposées à pression infinie, il n'est pas possible d'utiliser les paramètres des modèles de g^E directement dans l'équation d'état.

1.3.3.2 Règles de mélange à compacité constante

Le but de cette partie est de dresser une approche qui consiste à intégrer dans les règles de mélange à compacité constante des équations d'état cubiques les modèles d'énergie de Gibbs d'excès (g^E). Cette approche est basée sur l'approximation d'ordre zéro du modèle quasi-réticulaire de Guggenheim[29], initialement proposé par Péneloux et al.[30]. La validité du modèle quasi-réticulaire repose sur l'hypothèse que le réseau sur lequel sont placées les molécules ne subit pas de déformation pendant le processus de mélange, qui s'effectue alors à compacité constante :

$$\eta = \frac{b_m}{v} = \frac{b_i}{v_i} \qquad (I-48)$$

On notera que le volume v_i est ici le volume molaire du constituant i pur dans l'état de référence, avant mélange à compacité constante. Il ne doit pas être confondu avec le volume molaire v_i^* du constituant i pur à la même température et la même pression que le mélange.

Le but de ce qui suit est de déterminer une expression des règles de mélange à compacité constante. Pour davantage de clarté, la démonstration est divisée en quatre sous-parties.

(a) Théorie de Guggenheim

Dans l'approximation d'ordre zéro du modèle quasi-réticulaire, l'énergie de Helmholtz molaire d'excès à volume constant $\mathbf{a}^{E,V}$ (où l'exposant V indique volume constant) peut s'écrire comme la somme de deux contributions :

$$\mathbf{a}^{E,V} = \mathbf{a}_{ath}^{E,V} + \mathbf{a}_{rés}^{E,V} \qquad (I-49)$$

Afin d'éviter la confusion avec le paramètre a dans les équations d'état cubiques, nous noterons par la suite **a** (en gras), l'énergie de Helmholtz molaire. Dans l'expression (I−49), le premier terme est appelé terme athermique (ou combinatoire). Il tient compte des effets dus aux différences de taille et de forme des molécules. Ce terme peut lui-même être décomposé en deux termes selon la théorie de Guggenheim :

$$\mathbf{a}_{\text{ath}}^{\text{E,V}} = \mathbf{a}_{\text{Flory}}^{\text{E,V}} + \mathbf{a}_{\text{Forme}}^{\text{E,V}} \quad \text{avec :} \begin{cases} \mathbf{a}_{\text{Flory}}^{\text{E,V}} = R \cdot T \sum_{i=1}^{n_c} x_i \ln\left(\dfrac{v_i}{v}\right) \\ \mathbf{a}_{\text{Forme}}^{\text{E,V}} = R \cdot T \cdot \dfrac{z}{2} \sum_{i=1}^{n_c} q_i x_i \ln\left(\dfrac{\theta_i}{\varphi_i}\right) \end{cases} \tag{I – 50}$$

- φ_i est la fraction volumique du constituant i : $\varphi_i = x_i \cdot v_i \Big/ \sum_{j=1}^{n_c} x_j \cdot v_j$.

- θ_i est la fraction de surface du constituant i : $\theta_i = x_i \cdot q_i \Big/ \sum_{j=1}^{n_c} x_j \cdot q_j$.

- v_i est une mesure du volume de la molécule i. C'est un nombre sans dimension car les volumes sont exprimés par rapport du méthane.

- q_i est une mesure de la surface de la molécule i (nombre sans dimension car rapporté à la surface du méthane).

- z est l'indice de coordination du quasi-réseau sur lequel sont supposées réparties les molécules.

Le second terme est appelé terme résiduel. Il représente les effets des interactions moléculaires et prend la forme de la fonction d'excès de Van Laar :

$$\mathbf{a}_{\text{rés}}^{\text{E,V}} = \frac{1}{2} \frac{\sum_{i=1}^{n_c} \sum_{j=1}^{n_c} q_i \cdot q_j \cdot x_i \cdot x_j \cdot \Phi_{ij}}{\sum_{j=1}^{n_c} q_j \cdot x_j} \tag{I – 51}$$

q_i est une mesure de la surface de la molécule i et Φ_{ij} représente une énergie dite d'interéchange.

(b) Ecriture d'une équation d'état généralisée en fonction de $\mathbf{a}^{\text{E,V}}$

Se basant sur la thermodynamique classique, l'énergie de Helmholtz molaire d'excès à pression constante $\mathbf{a}^{\text{E,P}}$, peut être écrite sous la forme :

$$\mathbf{a}^{\text{E,P}}(T, P, \mathbf{x}) = \mathbf{a}_m(T, P, \mathbf{x}) - \sum_{i=1}^{n_c} x_i \mathbf{a}_i^*(T, P) - RT \sum_{i=1}^{n_c} x_i \ln x_i \tag{I – 52}$$

où $\mathbf{a}_i^*$ est l’énergie de Helmholtz molaire du constituant i pur.

Cependant :
$$\underbrace{\mathbf{a}_i^*(T,P)}_{\substack{\text{le volume molaire}\\ \text{est } v_i^*(T,P)}} = \underbrace{\mathbf{a}_i^*(T,v_i)}_{\substack{\text{la pression est } P_i\\ \text{(pression du constituant}\\ \text{i avant mélange à}\\ \text{volume constant)}}} - \int_{v_i}^{v_i^*(T,P)} P\cdot dv \qquad (I-53)$$

En négligeant l’influence de la pression entre P et P$_i$ sur l’énergie de Helmholtz molaire des constituants purs, on peut écrire : $\mathbf{a}_i^*(T,P) = \mathbf{a}_i^*(T,v_i)$

L’énergie de Helmholtz molaire d’excès à volume constant $\mathbf{a}^{E,V}$ s’écrit alors :

$$\mathbf{a}^{E,V}(T,v,\mathbf{x}) = \mathbf{a}_m(T,v,\mathbf{x}) - \sum_{i=1}^{n_c} x_i\mathbf{a}_i^*(T,v_i) - RT\sum_{i=1}^{n_c} x_i \ln x_i \quad \text{avec : } v = \sum_{i=1}^{n_c} x_i \cdot v_i \qquad (I-54)$$

Comme expliqué précédemment, les équations d’état explicites en pression : P(T,v,**x**) ou z(T,η,**x**) permettent de calculer l’énergie de Helmholtz molaire d’écart au gaz parfait :

$$\mathbf{a}_m(T,v,\mathbf{x}) = \mathbf{a}_m^\bullet(T,v,\mathbf{x}) + \left[\mathbf{a}_m(T,v,\mathbf{x}) - \mathbf{a}_m^\bullet(T,v,\mathbf{x})\right] \qquad (I-55)$$

$$\text{avec : } \mathbf{a}_m(T,v,\mathbf{x}) - \mathbf{a}_m^\bullet(T,v,\mathbf{x}) = -\int_{\infty}^{v}\left[P(T,v,\mathbf{x}) - \frac{RT}{v}\right]dv = RT\int_0^{\eta}\frac{z(T,\eta,\mathbf{x})-1}{\eta}d\eta \qquad (I-56)$$

De même, dans le cas d’un constituant i pur :

$$\mathbf{a}_i^*(T,v_i) = \mathbf{a}_i^\bullet(T,v_i) + \left[\mathbf{a}_i^*(T,v_i) - \mathbf{a}_i^\bullet(T,v_i)\right] = \mathbf{a}_i^\bullet(T,v_i) + RT\int_0^{\eta_i}\frac{z_i(T,\eta_i)-1}{\eta_i}d\eta_i \qquad (I-57)$$

En utilisant les équations (I−55) et (I−57), l’équation (I−54) devient :

$$\mathbf{a}^{E,V} = \left[\mathbf{a}_m^\bullet - \sum_{i=1}^{n_c} x_i\mathbf{a}_i^\bullet\right] + \left[\mathbf{a}_m - \mathbf{a}_m^\bullet\right] - \sum_{i=1}^{n_c} x_i\left[\mathbf{a}_i^* - \mathbf{a}_i^\bullet\right] - RT\sum_{i=1}^{n_c} x_i \ln x_i \qquad (I-58)$$

En introduisant la grandeur molaire partielle $\bar{\mathbf{a}}_i^\bullet$, le contenu de la première parenthèse dans l’équation (I−58) peut être écrit :

$$\mathbf{a}_m^{\bullet}(T,v,\mathbf{x})-\sum_{i=1}^{n_c}x_i\mathbf{a}_i^{\bullet}(T,v_i)=\sum_{i=1}^{n_c}x_i\,[\underbrace{\bar{\mathbf{a}}_i^{\bullet}(T,v,\mathbf{x})}_{\substack{\text{la pression est}\\ P^{\bullet}=RT/v}}-\underbrace{\mathbf{a}_i^{\bullet}(T,v_i)}_{\substack{\text{la pression est}\\ P_i^{\bullet}=RT/v_i}}]\qquad(I-59)$$

L’énergie de Helmholtz molaire partielle du constituant i dans un mélange de gaz parfaits vaut :

$$\bar{\mathbf{a}}_i^{\bullet}(T,P,\mathbf{x})=\mathbf{a}_i^{\bullet}(T,P)+RT\ln x_i\qquad(I-60)$$

On peut ainsi écrire :

$$\bar{\mathbf{a}}_i^{\bullet}(T,v,\mathbf{x})=\mathbf{a}_i^{\bullet}(T,P^{\bullet})+RT\ln x_i\qquad(I-61)$$

La variation isotherme de l’énergie de Helmholtz molaire d’un constituant i pur peut être écrite :

$$\Delta\mathbf{a}_i^{\bullet}=RT\ln\frac{v_1}{v_2}=RT\ln\frac{P_2}{P_1}\ \text{(T constante)}\qquad(I-62)$$

L’équation (I−61) devient alors :

$$\bar{\mathbf{a}}_i^{\bullet}(T,v,\mathbf{x})=\mathbf{a}_i^{\bullet}(T,P_i^{\bullet})+RT\ln\frac{P^{\bullet}}{P_i^{\bullet}}+RT\ln x_i=\mathbf{a}_i^{\bullet}(T,v_i)+RT\ln\frac{v_i\cdot x_i}{v}\qquad(I-63)$$

L’équation (I−59) s’écrit :

$$\mathbf{a}_m^{\bullet}(T,v,\mathbf{x})-\sum_{i=1}^{n_c}x_i\mathbf{a}_i^{\bullet}(T,v_i)=-RT\ln\left(\frac{v}{x_i\cdot v_i}\right)\qquad(I-64)$$

Finalement, l’équation (I−58) devient :

$$\mathbf{a}^{E,V}(T,v,\mathbf{x})=\left[\mathbf{a}_m(T,v,\mathbf{x})-\mathbf{a}_m^{\bullet}(T,v,\mathbf{x})\right]-\sum_{i=1}^{n_c}x_i\left[\mathbf{a}_i^{*}(T,v_i)-\mathbf{a}_i^{\bullet}(T,v_i)\right]+\underbrace{RT\sum_{i=1}^{n_c}x_i\ln\left(\frac{v_i}{v}\right)}_{\mathbf{a}_{\text{Flory}}^{E,V}}\qquad(I-65)$$

En remplaçant le terme de Flory $\mathbf{a}_{\text{Flory}}^{E,V}$ par l’expression (I−50), on peut écrire :

$$\mathbf{a}_{\mathrm{m}}(T,v,\mathbf{x})-\mathbf{a}_{\mathrm{m}}^{\bullet}(T,v,\mathbf{x})=\sum_{i=1}^{n_c}x_i\left[\mathbf{a}_i^{*}(T,v_i)-\mathbf{a}_i^{\bullet}(T,v_i)\right]+\mathbf{a}_{\text{rés}}^{E,V}+\mathbf{a}_{\text{Forme}}^{E,V} \qquad (I-66)$$

En dérivant l'équation (I−56) par rapport à η puis en réarrangeant cette équation, on obtient l'expression suivante de l'équation d'état :

$$z(T,\eta,\mathbf{x})=\frac{\eta}{RT}\left(\frac{\partial\left(\mathbf{a}_{\mathrm{m}}(T,v,\mathbf{x})-\mathbf{a}_{\mathrm{m}}^{\bullet}(T,v,\mathbf{x})\right)}{\partial\eta}\right)_{T,\mathbf{x}}+1 \qquad (I-67)$$

En combinant les équations (I−66) et (I−67), il vient l'expression générale d'une équation d'état en fonction de $\mathbf{a}^{E,V}$:

$$\boxed{z(T,\eta,\mathbf{x})=\frac{\eta}{RT}\left[\sum_{i=1}^{n_c}x_i\left[\frac{\partial\left(\mathbf{a}_i^{*}(T,v_i)-\mathbf{a}_i^{\bullet}(T,v_i)\right)}{\partial\eta}\right]_T+\left[\frac{\partial\left(\mathbf{a}_{\text{rés}}^{E,V}+\mathbf{a}_{\text{Forme}}^{E,V}\right)}{\partial\eta}\right]_{T,\mathbf{x}}\right]+1} \qquad (I-68)$$

(c) Application de l'équation d'état généralisée aux équations d'état cubiques de l'ensemble principal

Les équations d'état cubiques de l'ensemble principal pour un mélange peuvent être écrites sous la forme suivante :

$$P(T,v,\mathbf{x})=\frac{RT}{v-b_m}-\frac{a_m}{(v-b_m r_1)(v-b_m r_2)} \qquad (I-69)$$

Les valeurs des constantes r_1 et r_2 de quelques équations d'état cubiques sont données dans le tableau (I−1). De manière équivalente :

$$z(T,v,\mathbf{x})=\frac{P(T,v,\mathbf{x})\cdot v}{RT}=\frac{v}{v-b_m}-\frac{a_m v}{RT(v-b_m r_1)(v-b_m r_2)} \qquad (I-70)$$

En introduisant la compacité (v = b/η), l'équation (I−70) devient :

$$z(T,\eta,\mathbf{x})=\frac{1}{1-\eta}-\frac{a_m\eta}{RTb_m(1-\eta r_1)(1-\eta r_2)}=\frac{1}{1-\eta}-\alpha\cdot Q'(\eta)\ \text{avec}\ \begin{cases}\alpha=\dfrac{a_m}{b_m RT}\\ Q'(\eta)=\dfrac{\eta}{(1-\eta r_1)(1-\eta r_2)}\end{cases} \qquad (I-71)$$

En égalisant les équations (I−68) et (I−71), on obtient :

$$\frac{\eta}{\mathrm{RT}}\left[\sum_{i=1}^{n_c} x_i \left[\frac{\partial\left(\mathbf{a}_i^{*}(\mathrm{T},v_i)-\mathbf{a}_i^{\bullet}(\mathrm{T},v_i)\right)}{\partial\eta}\right]_{\mathrm{T}} + \left[\frac{\partial\left(\mathbf{a}_{\text{rés}}^{\mathrm{E,V}}+\mathbf{a}_{\text{Forme}}^{\mathrm{E,V}}\right)}{\partial\eta}\right]_{\mathrm{T},\mathbf{x}}\right]+1=\frac{1}{1-\eta}-\alpha\cdot \mathrm{Q}'(\eta) \qquad (\mathrm{I}-72)$$

Cependant, comme expliqué par Péneloux et al.[30], les équations d'état cubiques de type Van der Waals ne contiennent pas de paramètres liés à la forme des molécules dans le terme répulsif. En effet, $z_{\text{rép}}=1/(1-\eta)$ est une fonction qui ne dépend que de la compacité η. Il s'ensuit alors : $\mathbf{a}_{\text{Forme}}^{\mathrm{E,V}}=0$. L'équation (I−72) s'écrit donc :

$$\mathrm{RT}\alpha\cdot \mathrm{Q}'(\eta)=\frac{\mathrm{RT}}{1-\eta}-\eta\left[\sum_{i=1}^{n_c} x_i \left(\frac{\partial\left(\mathbf{a}_i^{*}(\mathrm{T},v_i)-\mathbf{a}_i^{\bullet}(\mathrm{T},v_i)\right)}{\partial\eta}\right)_{\mathrm{T}} + \left(\frac{\partial \mathbf{a}_{\text{rés}}^{\mathrm{E,V}}}{\partial\eta}\right)_{\mathrm{T},\mathbf{x}}\right]-\mathrm{RT} \qquad (\mathrm{I}-73)$$

En appliquant l'équation (I−67) au constituant i pur, on obtient :

$$\left[\frac{\partial\left(\mathbf{a}_i^{*}(\mathrm{T},v_i)-\mathbf{a}_i^{\bullet}(\mathrm{T},v_i)\right)}{\partial\eta_i}\right]_{\mathrm{T}}=\frac{\mathrm{RT}}{\eta_i}\left[z_i(\mathrm{T},\eta_i)-1\right] \qquad (\mathrm{I}-74)$$

De même, en appliquant l'équation (I−71) au constituant i pur :

$$z_i(\mathrm{T},\eta_i)=\frac{1}{1-\eta_i}-\alpha_i\cdot \mathrm{Q}'(\eta_i) \qquad (\mathrm{I}-75)$$

En combinant les équations (I−74) et (I−75) et en tenant compte que la compacité est constante ($\eta_i = \eta$), il vient :

$$\left[\frac{\partial\left(\mathbf{a}_i^{*}(\mathrm{T},v_i)-\mathbf{a}_i^{\bullet}(\mathrm{T},v_i)\right)}{\partial\eta}\right]_{\mathrm{T}}=\frac{\mathrm{RT}}{\eta}\left[\frac{1}{1-\eta}-\alpha_i\cdot \mathrm{Q}'(\eta)-1\right] \qquad (\mathrm{I}-76)$$

A ce stade, l'équation (I−73) devient :

$$\begin{aligned}\mathrm{RT}\alpha\cdot \mathrm{Q}'(\eta)&=\frac{\mathrm{RT}}{1-\eta}-\left[\sum_{i=1}^{n_c} x_i \left(\frac{\mathrm{RT}}{1-\eta}-\mathrm{RT}\alpha_i\cdot \mathrm{Q}'(\eta)-\mathrm{RT}\right)\right]-\eta\left(\frac{\partial \mathbf{a}_{\text{rés}}^{\mathrm{E,V}}}{\partial\eta}\right)_{\mathrm{T},\mathbf{x}}-\mathrm{RT}\\&=\sum_{i=1}^{n_c} x_i\left[\mathrm{RT}\alpha_i\cdot \mathrm{Q}'(\eta)\right]-\eta\left(\frac{\partial \mathbf{a}_{\text{rés}}^{\mathrm{E,V}}}{\partial\eta}\right)_{\mathrm{T},\mathbf{x}}\end{aligned} \qquad (\mathrm{I}-77)$$

En se rappelant que $RT\alpha = a_m / b_m$ [voir l'équation (I−71)], on obtient :

$$\frac{a_m(T,\mathbf{x})}{b_m(\mathbf{x})} = \sum_{i=1}^{n_c} x_i \frac{a_i(T)}{b_i} - \frac{\eta}{Q'(\eta)} \left(\frac{\partial \mathbf{a}_{\text{rés}}^{E,V}}{\partial \eta} \right)_{T,\mathbf{x}} \qquad (I-78)$$

Le second terme de la partie droite de l'égalité ne dépend alors nécessairement que de T et **x**, on note donc :

$$E(T,\mathbf{x}) = \frac{\eta}{Q'(\eta)} \left(\frac{\partial \mathbf{a}_{\text{rés}}^{E,V}}{\partial \eta} \right)_{T,\mathbf{x}} \qquad (I-79)$$

L'équation (I−78) devient :

$$\boxed{\frac{a_m(T,\mathbf{x})}{b_m(\mathbf{x})} = \sum_{i=1}^{n_c} x_i \frac{a_i(T)}{b_i} - E(T,\mathbf{x})} \qquad (I-80)$$

Cette équation est une première expression des règles de mélange à compacité constante. Il suffit ensuite de choisir une fonction d'excès appropriée pour le terme E(T,**x**).

(d) Expression de la fonction d'excès E(T,x)

En intégrant la relation (I−79) entre η = 0 pour lequel $\mathbf{a}_{\text{rés}}^{E,V} = 0$ (le mélange se comporte comme un mélange de gaz parfaits, c'est-à-dire, une solution idéale) et η, il est possible de trouver la relation liant la fonction E(T,**x**) et $\mathbf{a}_{\text{rés}}^{E,V}$:

$$\mathbf{a}_{\text{rés}}^{E,V}(T,\eta,\mathbf{x}) = \int_0^{\eta} \frac{E(T,\mathbf{x}) \cdot Q'(\eta)}{\eta} d\eta = E(T,\mathbf{x}) \times \int_0^{\eta} \frac{Q'(\eta)}{\eta} d\eta \qquad (I-81)$$

En notant $Q(\eta) = \int_0^{\eta} \frac{Q'(\eta)}{\eta} d\eta$, l'équation (I−81) devient :

$$\boxed{\mathbf{a}_{\text{rés}}^{E,V}(T,\eta,\mathbf{x}) = E(T,\mathbf{x}) \times Q(\eta)} \qquad (I-82)$$

En utilisant l'équation (I−71), on a :

$$Q(\eta) = \int_0^\eta \frac{Q'(\eta)}{\eta} d\eta = \frac{1}{r_1 - r_2} \cdot \ln\left(\frac{1-\eta \cdot r_2}{1-\eta \cdot r_1}\right) \qquad (I-83)$$

De plus, il est possible de montrer que pour un liquide incompressible ($\eta \to 1$) :

$$g^{E,P} = \mathbf{a}^{E,V} \qquad (I-84)$$

Cette expression peut être démontrée par les équations de (I−85) à (I−88).

Par définition : $g^{E,P}(T,P,\mathbf{x}) = g_m - \sum_{i=1}^{n_c} x_i g_i^*(T,P) - RT \sum_{i=1}^{n_c} x_i \ln x_i$ (I − 85)

En rappelant l'équation (I−54) puis en remplaçant **a** par ($g - P \cdot v$), on a :

$$\mathbf{a}^{E,V}(T,v,\mathbf{x}) = g_m - P \cdot v - \sum_{i=1}^{n_c} x_i \left[g_i^*(T,P_i) - P_i \cdot v_i \right] - RT \sum_{i=1}^{n_c} x_i \ln x_i \qquad (I-86)$$

En soustrayant les équations (I−85) et (I−86), il vient :

$$\begin{aligned} g^{E,P} - \mathbf{a}^{E,V} &= P \cdot v + \sum_{i=1}^{n_c} x_i \left[g_i^*(T,P_i) - g_i^*(T,P) - P_i \cdot v_i \right] \\ &= P \cdot \sum_{i=1}^{n_c} x_i \cdot v_i + \sum_{i=1}^{n_c} x_i \cdot \int_P^{P_i} v_i \cdot dP - \sum_{i=1}^{n_c} x_i \cdot P_i \cdot v_i \end{aligned} \qquad (I-87)$$

En supposant que les volumes molaires ne dépendent pas de la pression (fluides incompressibles), l'équation (I−87) devient :

$$g^{E,P} - \mathbf{a}^{E,V} = P \cdot \sum_{i=1}^{n_c} x_i \cdot v_i + \sum_{i=1}^{n_c} x_i \cdot v_i \cdot (P_i - P) - \sum_{i=1}^{n_c} x_i \cdot P_i \cdot v_i = 0 \qquad (I-88)$$

A partir de l'équation (I−84), on peut écrire :

$$\mathbf{a}_{\text{rés}}^{E,V}(T, \eta \to 1, \mathbf{x}) = g_{\text{rés}}^{E}(T, \eta \to 1, \mathbf{x}) \qquad (I-89)$$

L'équation (I−82) est toujours vérifiée, y compris lorsque η tend vers 1. On déduit donc :

$$E(T,\mathbf{x})=\frac{g^E_{\text{rés}}(T,\eta\to 1,\mathbf{x})}{Q(1)}=\frac{g^E_{\infty,\text{rés}}}{C}\quad \text{avec : } C=Q(1)=\frac{1}{r_1-r_2}\cdot\ln\left(\frac{1-r_2}{1-r_1}\right)\qquad (I-90)$$

Les modèles de g^E classiques (Redlich-Kister, Margules, Wilson, Van Laar, NRTL, UNIQUAC, UNIFAC, …) ne dépendent pas de la pression. On peut conclure que $E(T,\mathbf{x})=g^E_{\text{rés}}/C$ est proportionnel à la partie résiduelle de n'importe quel modèle de g^E.

En suivant l'équation (I−80), les règles de mélange à compacité constante s'écrivent :

$$\boxed{\begin{cases}\dfrac{a_m(T,\mathbf{x})}{b_m(\mathbf{x})}=\displaystyle\sum_{i=1}^{n_c}x_i\frac{a_i(T)}{b_i}-\frac{g^E_{\text{rés}}}{C}\\ b_m(\mathbf{x})=\displaystyle\sum_{i=1}^{n_c}x_ib_i\end{cases}}\qquad (I-91)$$

Compatibilité des règles de mélange de Van der Waals avec les règles de mélange à compacité constante

Les règles de mélange de Van der Waals s'écrivent :

$$\begin{cases}a_m=\displaystyle\sum_{i=1}^{n_c}\sum_{j=1}^{n_c}x_i\cdot x_j\sqrt{a_i\cdot a_j}\left(1-k_{ij}\right)\\ b_m=\displaystyle\sum_{i=1}^{n_c}x_i\cdot b_i\end{cases}\qquad (I-92)$$

Ces règles de mélange sont compatibles avec la règle de mélange à compacité constante [équation (I−80)]. Pour le prouver, il suffit de remplacer les paramètres a_m et b_m dans l'expression (I−80) par les expressions de la règle de mélange de Van der Waals.

On commence donc par exprimer le terme d'excès E(T,**x**) dans le cas où a_m et b_m suivent les règles de mélange de Van der Waals.

$$
\begin{aligned}
E(T,\mathbf{x}) &= \sum_{i=1}^{n_c} x_i \frac{a_i}{b_i} - \frac{a_m}{b_m} \\
&= \sum_{i=1}^{n_c} x_i \cdot \frac{a_i}{b_i} - \frac{\sum_{i=1}^{n_c}\sum_{j=1}^{n_c} x_i \cdot x_j \sqrt{a_i \cdot a_j}\,(1-k_{ij})}{\sum_{j=1}^{n_c} x_j \cdot b_j} \\
&= \frac{\sum_{i=1}^{n_c} x_i \cdot \frac{a_i}{b_i} \times \sum_{j=1}^{n_c} x_j \cdot b_j - \sum_{i=1}^{n_c}\sum_{j=1}^{n_c} x_i \cdot x_j \sqrt{a_i \cdot a_j} \cdot (1-k_{ij})}{\sum_{j=1}^{n_c} x_j \cdot b_j}
\end{aligned}
\qquad (I-93)
$$

A ce stade, on utilise une petite astuce de calcul qui permet d’obtenir une expression finale de k_{ij} plus élégante :

$$
\begin{aligned}
\sum_{i=1}^{n_c} x_i \cdot \frac{a_i}{b_i} \times \sum_{j=1}^{n_c} x_j \cdot b_j &= \sum_{i=1}^{n_c}\sum_{j=1}^{n_c} x_i \cdot x_j \frac{a_i \cdot b_j}{b_i} \\
&= \frac{1}{2}\sum_{i=1}^{n_c}\sum_{j=1}^{n_c} x_i \cdot x_j \frac{a_i \cdot b_j}{b_i} + \frac{1}{2}\sum_{i=1}^{n_c}\sum_{j=1}^{n_c} x_i \cdot x_j \frac{a_j \cdot b_i}{b_j}
\end{aligned}
\qquad (I-94)
$$

On revient à l’expression de E(T,**x**) :

$$
\begin{aligned}
E(T,\mathbf{x}) &= \frac{\sum_{i=1}^{n_c}\sum_{j=1}^{n_c} x_i \cdot x_j \left[\frac{1}{2}\frac{a_i \cdot b_j}{b_i} + \frac{1}{2}\frac{a_j \cdot b_i}{b_j} - \sqrt{a_i \cdot a_j} \cdot (1-k_{ij})\right]}{\sum_{j=1}^{n_c} x_j \cdot b_j} \\
&= \frac{\sum_{i=1}^{n_c}\sum_{j=1}^{n_c} x_i \cdot x_j \cdot b_i \cdot b_j \left[\frac{1}{2}\frac{a_i}{b_i^2} + \frac{1}{2}\frac{a_j}{b_j^2} - \frac{\sqrt{a_i}}{b_i} \cdot \frac{\sqrt{a_j}}{b_j} \cdot (1-k_{ij})\right]}{\sum_{j=1}^{n_c} x_j \cdot b_j}
\end{aligned}
\qquad (I-95)
$$

On introduit à présent les paramètres δ_i définis par :

$$\delta_i = \frac{\sqrt{a_i}}{b_i} \qquad (I-96)$$

On définit le paramètre E_{ij} par :

$$E_{ij} = \delta_i^2 + \delta_j^2 - 2\delta_i\delta_j\left(1-k_{ij}\right) \qquad (I-97)$$

Il vient finalement :

$$E(T,\mathbf{x}) = \frac{1}{2}\cdot\frac{\sum_{i=1}^{n_c}\sum_{j=1}^{n_c} x_i \cdot x_j \cdot b_i \cdot b_j \cdot E_{ij}}{\sum_{j=1}^{n_c} x_j \cdot b_j} \qquad (I-98)$$

En comparant les équations (I−51) et (I−98), il apparaît clairement que la fonction E(T,**x**) est une fonction d'excès de type Van Laar. En utilisant l'équation (I−97), il est à présent possible d'exprimer le paramètre k_{ij} des règles de mélange de Van der Waals :

$$k_{ij} = \frac{E_{ij} - (\delta_i - \delta_j)^2}{2\delta_i\delta_j} \qquad (I-99)$$

I.4 Le modèle PPR78

I.4.1 L'équation d'état et les règles de mélange dans le modèle

Le modèle PPR78 (Predictive Peng-Robinson equation of state 1978)[31-37] utilise l'équation d'état de Peng et Robinson dans sa version de 1978[5] désignée par l'abréviation PR78. Les règles de mélange que nous associons à PR78 pour le traitement des systèmes multi-constituants peuvent s'exprimer de deux manières qui sont compatibles : règles de mélange à compacité constante où une fonction d'excès de type Van Laar est choisie, et règles de mélange de type Van der Waals. Ce modèle est rendu prédictif par le calcul de paramètre E_{ij} qui intervient dans la fonction d'excès de type Van Laar ou du coefficient d'interaction binaire k_{ij} qui intervient dans les règles de mélange classique, à partir d'une méthode de contributions de groupes.

Pour un corps pur, l'équation d'état PR78 s'écrit :

$$P=\frac{R\cdot T}{v-b_i}-\frac{a_i(T)}{v\cdot\left(v+b_i\right)+b_i\cdot\left(v-b_i\right)} \quad \text{avec}$$

$$\begin{cases} R=8,314472\ \mathrm{J\cdot mol^{-1}\cdot K^{-1}} \\ X=\dfrac{-1+\sqrt[3]{6\sqrt{2}+8}-\sqrt[3]{6\sqrt{2}-8}}{3}\approx 0.253076587 \\ b_i=\Omega_b\dfrac{R\cdot T_{c,i}}{P_{c,i}} \text{ et } \Omega_b=\dfrac{X}{X+3}\approx 0.0777960739 \\ a_i(T)=\Omega_a\dfrac{R^2\cdot T_{c,i}^2}{P_{c,i}}\left[1+m_i\left(1-\sqrt{\dfrac{T}{T_{c,i}}}\right)\right]^2 \text{ et } \Omega_a=\dfrac{8\left(5X+1\right)}{49-37X}\approx 0,457235529 \\ \text{si } \omega_i\le 0,491 \;\; m_i=0,37464+1,54226\omega_i-0,26992\omega_i^2 \\ \text{si } \omega_i>0,491 \;\; m_i=0,379642+1,48503\omega_i-0,164423\omega_i^2+0,016666\omega_i^3 \end{cases} \qquad (I-100)$$

P est la pression, T la température, R la constante des gaz parfaits et v le volume molaire. $T_{c,i}$, $P_{c,i}$ et ω_i sont respectivement la température critique, la pression critique et la facteur acentrique du corps pur i.

L'application de cette équation PR78 à un mélange nécessite l'utilisation de règles de mélange. Le modèle PPR78 peut être vu comme la combinaison à compacité constante de l'équation PR78 et d'un modèle de g^E de type Van Laar, dans le cadre de l'approximation d'ordre zéro de la théorie de Guggenheim (modèle quasi-réticulaire)[29], initialement proposée par Péneloux et al.[30] Le modèle PPR78 est donc une approche de type équation d'état/énergie de Gibbs d'excès (EoS/g^E)[25] dont les règles de mélange s'écrivent :

$$\begin{cases} \dfrac{a_m(T,\mathbf{z})}{b_m(\mathbf{z})} = \displaystyle\sum_{i=1}^{n_c} z_i \frac{a_i(T)}{b_i} - \frac{g_{res}^E}{C} \\ b_m(\mathbf{z}) = \displaystyle\sum_{i=1}^{n_c} z_i b_i \end{cases} \qquad (I-101)$$

avec $\dfrac{g_{res}^E}{C} = \dfrac{1}{2} \dfrac{\displaystyle\sum_{i=1}^{n_c}\sum_{j=1}^{n_c} z_i z_j b_i b_j E_{ij}(T)}{\displaystyle\sum_{j=1}^{n_c} z_j b_j}$ et $C = \dfrac{\sqrt{2}}{2} \ln\left(1+\sqrt{2}\right) \approx 0,6232$

z_i est la fraction molaire du constituant i dans le mélange et n_c le nombre de constituants du mélange. g^E_{res} est la partie résiduelle (non athermique) de l'énergie de Gibbs d'excès.

Pour définir complètement le modèle PPR78 et le rendre prédictif, il est nécessaire d'estimer le paramètre E_{ij} qui intervient dans la fonction d'excès de type Van Laar. A ce titre, nous avons développé une méthode de contributions de groupes dont l'expression littérale est issue des travaux antérieurs de Kehiaian et al.[38] et Abdoul et al.[39]. L'expression de E_{ij} s'écrit alors :

$$E_{ij} = -\frac{1}{2} \sum_{k=1}^{n_g} \sum_{l=1}^{n_g} \left(\alpha_{ik} - \alpha_{jk}\right)\left(\alpha_{il} - \alpha_{jl}\right) A_{kl} \left(\frac{298,15}{T/K}\right)^{\left(\frac{B_{kl}}{A_{kl}} - 1\right)} \qquad (I-102)$$

n_g est le nombre de groupes définis par la méthode (à l'heure actuelle, vingt et un groupes sont définis pour le modèle PPR78 et $n_g = 21$). α_{ik} représente la fraction de la molécule i occupée par le groupe k, c'est-à-dire l'occurrence de présence du groupe k dans la molécule i divisée par le nombre de groupes présents dans la molécule. $A_{kl} = A_{lk}$ et $B_{kl} = B_{lk}$ sont des paramètres qui quantifient les interactions entre les groupes k et l ($A_{kk} = B_{kk} = 0$).

Le modèle PPR78, basé sur l'équation d'état de PR78, peut également être vu comme une méthode de contributions de groupes pour le calcul du coefficient d'interaction binaire k_{ij}

intervenant dans les règles de mélange de type Van der Waals (linéaire sur b et quadratique sur a) :

$$\begin{cases} a_m(T,\mathbf{z}) = \sum_{i=1}^{n_c}\sum_{j=1}^{n_c} z_i z_j \sqrt{a_i a_j}\left(1-k_{ij}(T)\right) \\ b_m(\mathbf{z}) = \sum_{i=1}^{n_c} z_i b_i \end{cases} \qquad (I-103)$$

Le paramètre d'interaction binaire k_{ij} intervenant dans l'équation précédente est calculé à partir de la formule suivante :

$$k_{ij}(T) = \frac{-\frac{1}{2}\sum_{k=1}^{n_g}\sum_{l=1}^{n_g}(\alpha_{ik}-\alpha_{jk})(\alpha_{il}-\alpha_{jl})A_{kl}\cdot\left(\frac{298.15}{T}\right)^{\left(\frac{B_{kl}}{A_{kl}}-1\right)} - \left(\frac{\sqrt{a_i(T)}}{b_i} - \frac{\sqrt{a_j(T)}}{b_j}\right)^2}{2\frac{\sqrt{a_i(T)\cdot a_j(T)}}{b_i\cdot b_j}} \qquad (I-104)$$

Les valeurs des paramètres d'interactions entre groupes A_{kl} et B_{kl} pour les différents groupes définis par la méthode sont donnés dans le tableau (I−2).

I.4.2 Groupes définis par le modèle

♣ Groupe 1 : CH_3

C'est le groupement méthyle. Il est présent deux fois dans tous les alcanes linéaires. On le trouve dans les alcanes ramifiés. Il peut également être présent chez les cycloalcanes ou les molécules aromatiques.

Par exemple, le groupe 1 est présent deux fois dans la molécule de propane, trois fois dans celle d'isobutane et une fois dans celle de méthylcyclohexane :

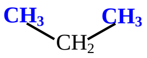
Propane

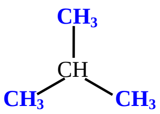
Isobutane

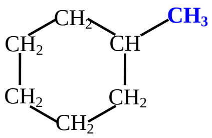
Méthylcyclohexane

♣ Groupe 2 : CH_2

C'est le groupement méthylène. Il est présent dans les alcanes linéaires, ramifiés. Il n'est jamais impliqué dans une insaturation (cycle ou liaison double). Il ne figure donc que dans les groupements alkyles des cycloalcanes et des molécules aromatiques. A titre d'exemple, il est présent trois fois dans la molécule de 3-éthylpentane et une seule fois dans la molécule d'éthylbenzène :

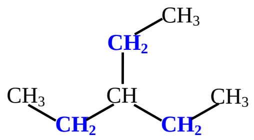

3-éthylpentane

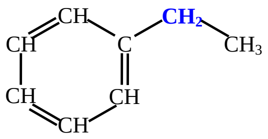

Ethylbenzène

N.B. : A partir des groupes 1 et 2, on peut construire, entre autre, toute la série des alcanes linéaires.

♣ Groupe 3 : CH

C'est le groupement méthyne. Comme le précédent, ce groupe est rencontré chez les alcanes ramifiés (mais pas linéaires) ou dans les groupements alkyles des molécules. Il n'est jamais impliqué dans une insaturation. Par exemple, il est présent une fois dans la molécule de 3-éthylpentane ainsi que dans la molécule d'isopropylbenzène :

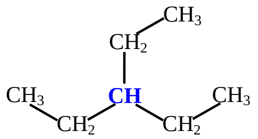

3-éthylpentane

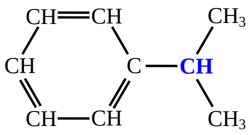

Isopropylbenzène

♣ Groupe 4 : C

Comme les deux précédents groupes, le groupe 4 figure dans les alcanes ramifiés (mais pas linéaires) et les groupements alkyles. Il n'est pas mis en jeu dans une insaturation. On utilise ci-après ce groupe 4 par les molécules de 3-éthyl-3-méthylpentane et de tertiobutylbenzène qui le contiennent chacune une fois.

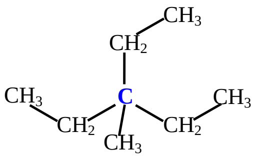

3-éthyl-3-méthylpentane

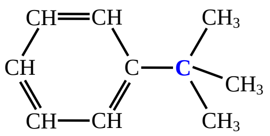

Isopropylbenzène

N.B. : A partir des groupes 1, 2, 3 et 4, on peut construire, entre autres, toute la série des alcanes ramifiés.

♣ Groupe 5 : CH_4

Le groupe méthane est particulier. C'est une molécule qui a été exclue de la série homologue des alcanes linéaires (représentables à partir des groupes 1 et 2) car elle possède un comportement atypique et n'est pas représentée correctement lorsqu'elle est incluse avec les autres molécules de la même série. Cette spécificité est bien connue : les premières molécules d'une série homologue doivent souvent faire l'objet d'un traitement spécifique dans la mis en œuvre des méthodes de contributions de groupes.

♣ Groupe 6 : C_2H_6

Le cas de la molécule d'éthane est complètement identique à celui de la molécule de méthane. Sa représentation par deux groupes 1 n'étant pas convaincante en termes de contributions de groupes, elle constitue un groupe à elle seule.

♣ Groupe 7 : CH_{aro}

Le groupe 7 décrit tous les groupes CH impliqués dans un cycle aromatique (à la différence du groupe 3, où les groupements CH sont impliqués dans des chaînes alkyles mais pas dans des cycles ou noyaux aromatiques). On utilise ce groupe par la molécule de benzène qui le contient six fois et la molécule de toluène qui le contient cinq fois :

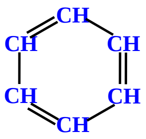

Benzène

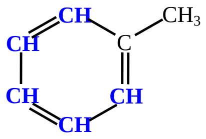

Toluène

♣ Groupe 8 : C_{aro}

De même que le groupe 7, ce groupe C n'est présent que dans les noyaux aromatiques. A titre d'exemple, on le retrouve deux fois dans la molécule de 1,4-xylène et une fois dans la molécule d'éthylbenzène :

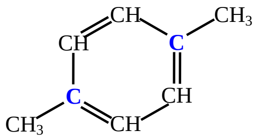

1,4-xylène

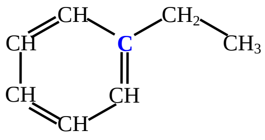

Ethylbenzène

♣ Groupe 9 : $C_{poly\ aro}$

Ce groupe matérialise les atomes de carbone impliqués simultanément dans deux cycles aromatiques. Dans la plupart des cas, les contributions du groupe 9 sont identiques à celles du groupe 8. Dans certains cas particuliers, on peut être amené à différencier ces deux groupes. Pour illustrer ce groupe, on représente la molécule de naphtalène et celle de 1-méthylnaphthalène qui contiennent ce carbone poly aromatique (i.e. imbriqués dans deux noyaux aromatiques) chacune deux fois :

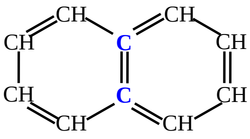

Naphthalène

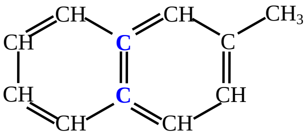

1-methylnaphthalène

N.B. : On notera que les groupes 7, 8 et 9 conjugués aux groupes 1 à 4 permettent de décrire toutes les molécules aromatiques.

♣ Groupe 10 : $CH_{2,\ cycl}$

Ce groupe CH_2 n'est présent qu'à l'intérieur du cycle d'un cycloalcane. Il ne doit pas être confondu avec le groupe 2. Il est par exemple présent six fois dans la molécule de cyclohexane et cinq fois dans la molécule de méthylcyclohexane.

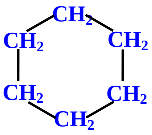

Cyclohexane

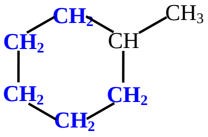

Méthylcyclohexane

♣ Groupe 11 : CH_{cycl}/C_{cycl}

A l'instar du précédent, ce groupe n'est présent que dans les cycles des cycloalcanes. On notera que le modèle PPR78 ne fait pas la distinction entre le groupe CH et le groupe C lorsque ceux-ci sont impliqués dans un cycle. Il convient bien entendu de ne pas le confondre avec les groupes 3, 4, 7, 8 et 9.

La molécule de 1,1,4-triméthylcyclohexane ci-dessous contient un atome de carbone C et un groupement CH imbriqués dans le cycle. Le groupe 11 y est donc présent deux fois. De même, dans la molécule de décaline, le groupe 11 est présent deux fois.

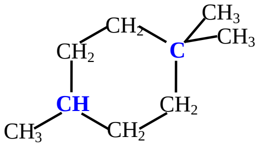

1,1,4-triméthylcyclohexane

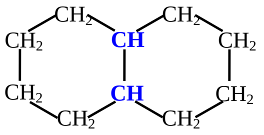

Décaline

N.B. : A partir des groupes 10 et 11 ainsi que des groupes 1 à 4, il est possible de représenter tous les cycloalcanes.

♣ Groupe 12 : CO_2

Comme les groupes 5 et 6, ce groupe est une molécule à lui seul : le dioxyde de carbone.

♣ Groupe 13 : N_2

Le Groupe 13 est la molécule de diazote (ou simplement azote).

♣ Groupe 14 : H_2S

Il décrit la molécule de sulfure d’hydrogène.

♣ Groupe 15 : SH

Ce groupe sulfhydrile caractérise la fonction chimique thiol (équivalent de la fonction alcool dans laquelle l’atome d’oxygène est remplacé par le soufre). Il est impliqué dans toutes les molécules de mercaptans (R−SH, où R désigne un groupement alkyle quelconque).

A titre d’illustration, on représente la molécule d’éthylmercaptan qui contient une fois le groupe 15 :

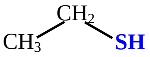

Ethylmercaptan

♣ Groupe 16 : H_2O

Le Groupe 16 est la molécule d’eau.

♣ Groupe 17 : C_2H_4

Le cas de la molécule d’éthylène est identique à celui de la molécule d’éthane. Le groupe 17 décrit la molécule d’éthylène.

♣ Groupe 18 : $CH_{2,\,alc}/CH_{alc}$

Le groupe 18 décrit tous les groupes CH_2 et CH impliqués dans les alcènes linéaires, ramifiés ou dans les groupements alkyles des molécules (mais jamais des carbones impliqués dans un noyau aromatique ou un cycle). Il ne doit pas être confondu avec les groupes 2, 3, 7, 10 et 11. La molécule de propène ci-dessous contient un groupement CH_2 et un groupement CH donc le groupe 18 est présent deux fois. De même, ce groupe est présent quatre fois dans la molécule de 1,3-butadiène et deux fois dans celle du styrène.

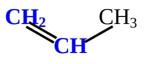

Propène

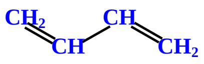

1,3-butadiène

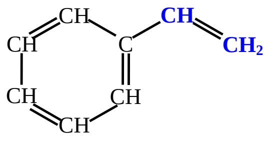

Styrène

♣ Groupe 19 : C_{alc}

A l'instar du précédent, ce groupe n'est présent que dans les alcènes linéaires, ramifiés ou dans les groupements alkyles des molécules. A titre d'exemple, on illustre ci-après ce groupe 19 par les molécules de 2-méthyl-1-butène, de 2-méthyl-1,3-butadiène et de beta-pinène qui le contiennent toutes une fois.

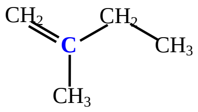

2-méthyl-1-butène

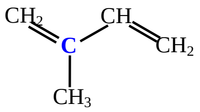

2-méthyl-1,3-butadiène

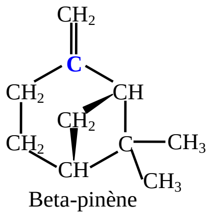

Beta-pinène

♣ Groupe 20 : $CH_{cyclalc}/C_{cyclalc}$

Ce groupe n'est présent que dans les cycles des cycloalcènes, mais pas dans un noyau aromatique ou dans un naphtène. Il ne doit pas être confondu avec les groupes 3, 4, 7, 8, 9, 11, 18 et 19. Par exemple, le groupe 20 est présent deux fois dans la molécule de cyclohexène. Pour la molécule de limonène et celle d'alpha-pinène ci-après, un carbone C et un groupement CH sont imbriqués dans le cycle des cycloalcènes donc le groupe 20 y est présent deux fois.

N.B. : On notera qu'avec les groupes 17, 18, 19 et 20 conjugués aux groupes 1 à 4 ainsi qu'aux groupes 7 à 11, il est possible de représenter tous les alcènes.

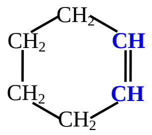

Cyclohexène

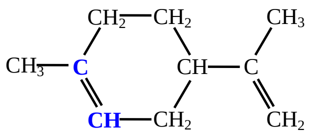

Limonène

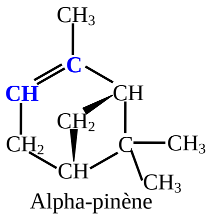

Alpha-pinène

♣ Groupe 21 : H_2

Le Groupe 21 est la molécule d'hydrogène.

I.4.3 La fonction objectif

Les valeurs des paramètres d'interaction A_{kl} et B_{kl} entre groupes ont été ajustés sur des données d'ELV expérimentales. Les paramètres dans le tableau (I−2) sont ceux qui minimisent la fonction objectif suivante :

$$F_{obj}=\frac{F_{obj,bulle}+F_{obj,rosée}+F_{obj,comp.crit}+F_{obj,press.crit}}{n_{bulle}+n_{rosée}+2n_{crit}} \quad \text{avec}$$

$$\begin{cases} F_{obj,bulle}=100\sum_{i=1}^{n_{bulle}}0,5\left(\frac{|\Delta x|}{x_{1,exp}}+\frac{|\Delta x|}{x_{2,exp}}\right)_i \;;\; |\Delta x|=|x_{1,exp}-x_{1,cal}|=|x_{2,exp}-x_{2,cal}| \\ F_{obj,rosée}=100\sum_{i=1}^{n_{rosée}}0,5\left(\frac{|\Delta y|}{y_{1,exp}}+\frac{|\Delta y|}{y_{2,exp}}\right)_i \;;\; |\Delta y|=|y_{1,exp}-y_{1,cal}|=|y_{2,exp}-y_{2,cal}| \\ F_{obj,comp.crit}=100\sum_{i=1}^{n_{crit}}0,5\left(\frac{|\Delta x_c|}{x_{c1,exp}}+\frac{|\Delta x_c|}{x_{c2,exp}}\right)_i \;;\; |\Delta x_c|=|x_{c1,exp}-x_{c1,cal}|=|x_{c2,exp}-x_{c2,cal}| \\ F_{obj,press.crit}=100\sum_{i=1}^{n_{crit}}\left(\frac{|P_{cm,exp}-P_{cm,cal}|}{P_{cm,exp}}\right)_i \end{cases} \quad (I-105)$$

n_{bulle}, $n_{rosée}$ et n_{crit} sont respectivement le nombre de points de bulle, le nombre de points de rosée et le nombre de points critiques. x_1 et y_1 sont respectivement la fraction molaire du constituant le plus volatil dans la phase liquide et la fraction molaire du même constituant dans la phase gazeuse. Evidemment, $x_2 = 1-x_1$ et $y_2 = 1-y_1$. P_{cm} est la pression critique du mélange binaire et x_{c1} est la fraction molaire critique en constituant le plus volatil.

Les points critiques de mélange ont une influence deux fois plus grande qu'un point de bulle ou de rosée sur la fonction objectif car deux écarts interviennent pour un point critique : l'écart à la composition critique et l'écart à la pression critique. Il est à noter que les écarts en composition sont moyennés sur les deux constituants du mélange de manière à éviter un impact trop important des points expérimentaux dont la composition est très faible ou très élevée sur les paramètres ajustés. Prenons l'exemple d'un point de bulle expérimental dont la composition serait $x_{1,exp} = 0{,}001$. Si celui-ci donne $x_{1,cal} = 0{,}002$, l'écart concernant le constituant 2 sera très faible ($\Delta x_2 = 0{,}1\%$) tandis que l'écart concernant le constituant 1 sera très grand ($\Delta x_1 = 100{,}0\%$). Dans ce cas, la fonction objectif que nous avons retenue vaut 50,05%.

Malgré cela, certains binaires contenant de l'eau continuent de présenter des difficultés lors de l'ajustement des paramètres. En effet, pour ce genre de systèmes, à température faible et modérée, les points de bulle expérimentaux ont des compositions très faibles ($x_1 < 0{,}01$) et les points de rosée expérimentaux ont des compositions très élevées ($y_1 > 0{,}99$). Si ces points sont majoritaires dans une base de données, la fonction objectif peut alors être assez élevée. Dans ce cas, l'ajustement des paramètres ne se fait, en réalité, que sur ce genre de points puisque l'écart dû aux autres points d'ELV est négligeable. Ce phénomène peut donc entraîner une mauvaise représentation des ELV où $0{,}01 < x_1(y_1) < 0{,}99$, et une mauvaise restitution du lieu des points critiques. Pour limiter ce problème, un point de bulle ou de rosée dont la composition est inférieure à 0,01 ou supérieure à 0,99 [$x_1(y_1) < 0{,}01$ et $x_1(y_1) > 0{,}99$], et qui présente un écart supérieur à 45% est automatiquement exclu du calcul de la fonction objectif globale (F_{obj}).

Dans la plupart des cas, l'ajustement des paramètres a été réalisé par la méthode de quasi-Newton de Broyden, Fletcher, Goldfard et Shanno (BFGS). Cependant, il est à noter que pour certains groupes, nous avons eu recours à une méthode beaucoup plus basique, de type essai-erreur, pour effectuer l'ajustement car il apparaissait clairement que la méthode BFGS ne conduisait pas au minimum de la fonction objectif. Ce phénomène peut peut-être s'expliquer par l'existence de nombreux minima locaux.

Tableau I−2. Matrice des paramètres d'interactions entre groupes A_{kl} et B_{kl} (en MPa) du modèle PPR78. ND = Non Déterminé.

	CH_3 (G 1)	CH_2 (G 2)	CH (G 3)	C (G 4)	CH_4 (G 5)	C_2H_6 (G 6)	CH_{aro} (G 7)	C_{aro} (G 8)	$C_{poly\ aro}$ (G 9)	$CH_{2,cycl}$ (G 10)	CH_{cycl}/C_{cycl} (G 11)	CO_2 (G 12)	N_2 (G 13)	H_2S (G 14)	SH (G 15)	H_2O (G 16)	C_2H_4 (G 17)	$CH_{2,alc}$ /CH_{alc} (G18)	C_{alc} (G 19)	$CH_{cyclalc}$ /$C_{cyclalc}$ (G 20)	H_2 (G 21)
CH_3 (G 1)	0	-	-	-	-	-	-	-	-	-	-	-	-	-	-	-	-	-	-	-	-
CH_2 (G 2)	$A_{12} = 74.81$ $B_{12} = 165.7$	0	-	-	-	-	-	-	-	-	-	-	-	-	-	-	-	-	-	-	-
CH (G 3)	$A_{13} = 261.5$ $B_{13} = 388.8$	$A_{23} = 51.47$ $B_{23} = 79.61$	0	-	-	-	-	-	-	-	-	-	-	-	-	-	-	-	-	-	-
C (G 4)	$A_{14} = 396.7$ $B_{14} = 804.3$	$A_{24} = 88.53$ $B_{24} = 315.0$	$A_{34} = -305.7$ $B_{34} = -250.8$	0	-	-	-	-	-	-	-	-	-	-	-	-	-	-	-	-	-
CH_4 (G 5)	$A_{15} = 32.94$ $B_{15} = -35.00$	$A_{25} = 36.72$ $B_{25} = 108.4$	$A_{35} = 145.2$ $B_{35} = 301.6$	$A_{45} = 263.9$ $B_{45} = 531.5$	0	-	-	-	-	-	-	-	-	-	-	-	-	-	-	-	-
C_2H_6 (G 6)	$A_{16} = 8.579$ $B_{16} = -29.51$	$A_{26} = 31.23$ $B_{26} = 84.76$	$A_{36} = 174.3$ $B_{36} = 352.1$	$A_{46} = 333.2$ $B_{46} = 203.8$	$A_{56} = 13.04$ $B_{56} = 6.863$	0	-	-	-	-	-	-	-	-	-	-	-	-	-	-	-
CH_{aro} (G 7)	$A_{17} = 90.25$ $B_{17} = 146.1$	$A_{27} = 29.78$ $B_{27} = 58.17$	$A_{37} = 103.3$ $B_{37} = 191.8$	$A_{47} = 158.9$ $B_{47} = 613.2$	$A_{57} = 67.26$ $B_{57} = 167.5$	$A_{67} = 41.18$ $B_{67} = 50.79$	0	-	-	-	-	-	-	-	-	-	-	-	-	-	-
C_{aro} (G 8)	$A_{18} = 62.80$ $B_{18} = 41.86$	$A_{28} = 3.775$ $B_{28} = 144.8$	$A_{38} = 6.177$ $B_{38} = -33.97$	$A_{48} = 79.61$ $B_{48} = -326.0$	$A_{58} = 139.3$ $B_{58} = 464.3$	$A_{68} = -3.088$ $B_{68} = 13.04$	$A_{78} = -13.38$ $B_{78} = 20.25$	0	-	-	-	-	-	-	-	-	-	-	-	-	-
$C_{poly\ aro}$ (G 9)	$A_{19} = 62.80$ $B_{19} = 41.86$	$A_{29} = 3.775$ $B_{29} = 144.8$	$A_{39} = 6.177$ $B_{39} = -33.97$	$A_{49} = 79.61$ $B_{49} = -326.0$	$A_{59} = 139.3$ $B_{59} = 464.3$	$A_{69} = -3.088$ $B_{69} = 13.04$	$A_{79} = -13.38$ $B_{79} = 20.25$	$A_{89} = 0.000$ $B_{89} = 0.000$	0	-	-	-	-	-	-	-	-	-	-	-	-
$CH_{2,cycl}$ (G 10)	$A_{1-10} = 40.38$ $B_{1-10} = 95.90$	$A_{2-10} = 12.78$ $B_{2-10} = 28.37$	$A_{3-10} = 101.9$ $B_{3-10} = -90.93$	$A_{4-10} = 177.1$ $B_{4-10} = 601.9$	$A_{5-10} = 36.37$ $B_{5-10} = 26.42$	$A_{6-10} = 8.579$ $B_{6-10} = 76.86$	$A_{7-10} = 29.17$ $B_{7-10} = 69.32$	$A_{8-10} = 34.31$ $B_{8-10} = 95.39$	$A_{9-10} = 34.31$ $B_{9-10} = 95.39$	0	-	-	-	-	-	-	-	-	-	-	-
CH_{cycl}/C_{cycl} (G 11)	$A_{1-11} = 98.48$ $B_{1-11} = 231.6$	$A_{2-11} = -54.90$ $B_{2-11} = -319.5$	$A_{3-11} = -226.5$ $B_{3-11} = -51.47$	$A_{4-11} = 17.84$ $B_{4-11} = -109.5$	$A_{5-11} = 40.15$ $B_{5-11} = 255.3$	$A_{6-11} = 10.29$ $B_{6-11} = -52.84$	$A_{7-11} = -26.42$ $B_{7-11} = -789.2$	$A_{8-11} = -105.7$ $B_{8-11} = -286.5$	$A_{9-11} = -105.7$ $B_{9-11} = -286.5$	$A_{10-11} = -50.10$ $B_{10-11} = -891.1$	0	-	-	-	-	-	-	-	-	-	-
CO_2 (G 12)	$A_{1-12} = 164.0$ $B_{1-12} = 269.0$	$A_{2-12} = 136.9$ $B_{2-12} = 254.6$	$A_{3-12} = 184.3$ $B_{3-12} = 762.1$	$A_{4-12} = 287.9$ $B_{4-12} = 346.2$	$A_{5-12} = 137.3$ $B_{5-12} = 194.2$	$A_{6-12} = 135.5$ $B_{6-12} = 239.5$	$A_{7-12} = 102.6$ $B_{7-12} = 161.3$	$A_{8-12} = 110.1$ $B_{8-12} = 637.6$	$A_{9-12} = 267.3$ $B_{9-12} = 444.4$	$A_{10-12} = 130.1$ $B_{10-12} = 225.8$	$A_{11-12} = 91.28$ $B_{11-12} = 82.01$	0	-	-	-	-	-	-	-	-	-
N_2 (G 13)	$A_{1-13} = 52.74$ $B_{1-13} = 87.19$	$A_{2-13} = 82.28$ $B_{2-13} = 202.8$	$A_{3-13} = 365.4$ $B_{3-13} = 521.9$	$A_{4-13} = 263.9$ $B_{4-13} = 772.6$	$A_{5-13} = 37.90$ $B_{5-13} = 37.20$	$A_{6-13} = 61.59$ $B_{6-13} = 84.92$	$A_{7-13} = 185.2$ $B_{7-13} = 490.6$	$A_{8-13} = 284.0$ $B_{8-13} = 1892$	$A_{9-13} = 718.1$ $B_{9-13} = 1892$	$A_{10-13} = 179.5$ $B_{10-13} = 546.6$	$A_{11-13} = 100.9$ $B_{11-13} = 249.8$	$A_{12-13} = 98.42$ $B_{12-13} = 221.4$	0	-	-	-	-	-	-	-	-
H_2S (G 14)	$A_{1-14} = 158.4$ $B_{1-14} = 241.2$	$A_{2-14} = 134.6$ $B_{2-14} = 138.3$	$A_{3-14} = 193.9$ $B_{3-14} = 307.8$	$A_{4-14} = 305.1$ $B_{4-14} = -143.1$	$A_{5-14} = 181.2$ $B_{5-14} = 288.9$	$A_{6-14} = 157.2$ $B_{6-14} = 217.1$	$A_{7-14} = 21.96$ $B_{7-14} = 13.04$	$A_{8-14} = 1.029$ $B_{8-14} = -8.579$	$A_{9-14} = 1.029$ $B_{9-14} = -8.579$	$A_{10-14} = 120.8$ $B_{10-14} = 163.0$	$A_{11-14} = -16.13$ $B_{11-14} = -147.6$	$A_{12-14} = 134.9$ $B_{12-14} = 201.4$	$A_{13-14} = 319.5$ $B_{13-14} = 550.1$	0	-	-	-	-	-	-	-
SH (G 15)	$A_{1-15} = 799.9$ $B_{1-15} = 2109$	$A_{2-15} = 459.5$ $B_{2-15} = 627.3$	$A_{3-15} = 425.5$ $B_{3-15} = 514.7$	$A_{4-15} = 682.9$ $B_{4-15} = 1544$	$A_{5-15} = 706.0$ $B_{5-15} = 1483$	ND	$A_{7-15} = 285.5$ $B_{7-15} = 392.0$	$A_{8-15} = 1072$ $B_{8-15} = 1094$	$A_{9-15} = 1072$ $B_{9-15} = 1094$	$A_{10-15} = 446.1$ $B_{10-15} = 549.0$	$A_{11-15} = 411.8$ $B_{11-15} = -308.8$	ND	ND	$A_{14-15} = -77.21$ $B_{14-15} = 156.1$	0	-	-	-	-	-	-
H_2O (G 16)	$A_{1-16} = 3557$ $B_{1-16} = 11195$	$A_{2-16} = 4324$ $B_{2-16} = 12126$	$A_{3-16} = 971.4$ $B_{3-16} = 567.6$	ND	$A_{5-16} = 2265$ $B_{5-16} = 4722$	$A_{6-16} = 2333$ $B_{6-16} = 5147$	$A_{7-16} = 2268$ $B_{7-16} = 6218$	$A_{8-16} = 543.5$ $B_{8-16} = 411.8$	$A_{9-16} = 1340$ $B_{9-16} = -65.88$	$A_{10-16} = 4211$ $B_{10-16} = 13031$	$A_{11-16} = 244.0$ $B_{11-16} = -60.39$	$A_{12-16} = 559.3$ $B_{12-16} = 277.9$	$A_{13-16} = 2574$ $B_{13-16} = 5490$	$A_{14-16} = 603.9$ $B_{14-16} = 599.1$	$A_{15-16} = 30.88$ $B_{15-16} = -113.6$	0	-	-	-	-	-
C_2H_4 (G 17)	$A_{1-17} = 7.206$ $B_{1-17} = 39.12$	$A_{2-17} = 59.71$ $B_{2-17} = 78.58$	$A_{3-17} = 176.7$ $B_{3-17} = 118.0$	$A_{4-17} = 319.5$ $B_{4-17} = -248.1$	$A_{5-17} = 14.69$ $B_{5-17} = 30.20$	$A_{6-17} = 7.549$ $B_{6-17} = 19.22$	$A_{7-17} = 20.25$ $B_{7-17} = 94.02$	$A_{8-17} = 65.20$ $B_{8-17} = 125.2$	$A_{9-17} = 199.0$ $B_{9-17} = 3820$	$A_{10-17} = 35.34$ $B_{10-17} = 52.50$	$A_{11-17} = -38.43$ $B_{11-17} = -688.4$	$A_{12-17} = 73.09$ $B_{12-17} = 115.3$	$A_{13-17} = 88.53$ $B_{13-17} = 109.1$	ND	ND	$A_{16-17} = 1632$ $B_{16-17} = 1612$	0	-	-	-	-
$CH_{2,alc}/CH_{alc}$ (G 18)	$A_{1-18} = 54.22$ $B_{1-18} = 142.4$	$A_{2-18} = 11.67$ $B_{2-18} = 29.51$	$A_{3-18} = 118.4$ $B_{3-18} = 158.9$	$A_{4-18} = 50.79$ $B_{4-18} = -284.5$	$A_{5-18} = 52.84$ $B_{5-18} = 110.5$	$A_{6-18} = 26.42$ $B_{6-18} = 50.44$	$A_{7-18} = 8.579$ $B_{7-18} = -7.549$	$A_{8-18} = -70.69$ $B_{8-18} = 36.72$	ND	$A_{10-18} = 27.11$ $B_{10-18} = 454.7$	ND	$A_{12-18} = 59.71$ $B_{12-18} = 210.3$	$A_{13-18} = 125.2$ $B_{13-18} = 285.5$	ND	ND	$A_{16-18} = 2243$ $B_{16-18} = 5199$	$A_{17-18} = 17.16$ $B_{17-18} = 36.72$	0	-	-	-
C_{alc} (G 19)	$A_{1-19} = 115.6$ $B_{1-19} = 118.4$	$A_{2-19} = 60.39$ $B_{2-19} = 272.8$	$A_{3-19} = 103.6$ $B_{3-19} = 430.6$	ND	ND	ND	$A_{7-19} = 1.029$ $B_{7-19} = -16.81$	$A_{8-19} = 217.6$ $B_{8-19} = -170.2$	ND	$A_{10-19} = -29.85$ $B_{10-19} = -149.3$	ND	$A_{12-19} = 23.68$ $B_{12-19} = -186.0$	$A_{13-19} = 455.7$ $B_{13-19} = 30.54$	ND	ND	ND	$A_{17-19} = -13.04$ $B_{17-19} = 65.20$	$A_{18-19} = 21.62$ $B_{18-19} = 134.9$	0	-	-
$CH_{cyclalc}/C_{cyclalc}$ (G 20)	$A_{1-20} = 177.1$ $B_{1-20} = 358.9$	$A_{2-20} = 0.000$ $B_{2-20} = -7.206$	$A_{3-20} = 39.12$ $B_{3-20} = 1038$	ND	ND	ND	$A_{7-20} = 6.177$ $B_{7-20} = 5.490$	$A_{8-20} = 3.431$ $B_{8-20} = -37.75$	ND	$A_{10-20} = 51.47$ $B_{10-20} = 254.6$	$A_{11-20} = -29.17$ $B_{11-20} = -145.8$	$A_{12-20} = 87.85$ $B_{12-20} = 94.37$	ND	ND	ND	ND	$A_{17-20} = -44.95$ $B_{17-20} = 224.8$	$A_{18-20} = 119.8$ $B_{18-20} = -72.06$	$A_{19-20} = -392.9$ $B_{19-20} = -197.3$	0	-
H_2 (G 21)	$A_{1-21} = 202.8$ $B_{1-21} = 317.4$	$A_{2-21} = 132.5$ $B_{2-21} = 147.2$	$A_{3-21} = 415.2$ $B_{3-21} = 726.4$	$A_{4-21} = 226.5$ $B_{4-21} = 1812$	$A_{5-21} = 156.1$ $B_{5-21} = 92.99$	$A_{6-21} = 137.6$ $B_{6-21} = 150.0$	$A_{7-21} = 284.8$ $B_{7-21} = 175.0$	$A_{8-21} = 377.5$ $B_{8-21} = 1201$	$A_{9-21} = 549.0$ $B_{9-21} = 1476$	$A_{10-21} = 232.0$ $B_{10-21} = 167.5$	$A_{11-21} = -314.0$ $B_{11-21} = -225.8$	$A_{12-21} = 265.9$ $B_{12-21} = 268.3$	$A_{13-21} = 65.20$ $B_{13-21} = 70.10$	$A_{14-21} = 145.8$ $B_{14-21} = 823.5$	ND	$A_{16-21} = 830.8$ $B_{16-21} = -137.9$	$A_{17-21} = 151.3$ $B_{17-21} = 165.1$	$A_{18-21} = 163.0$ $B_{18-21} = 322.2$	$A_{19-21} = 630.0$ $B_{19-21} = 573.1$	$A_{20-21} = 483.1$ $B_{20-21} = 2417$	0

I.4.4 Calcul de l'enthalpie molaire d'excès h^E par le modèle PPR78

L'enthalpie molaire d'excès h^E est définie par l'équation :

$$h^E(T,P,\mathbf{z}) = h(T,P,\mathbf{z}) - \sum_{i=1}^{n_c} z_i h_i^*(T,P) \tag{I−106}$$

Pour calculer aisément l'enthalpie molaire h (T,P,**z**) totale du mélange et l'enthalpie molaire du constituant i pur $h_i^*(T,P)$, on introduit les grandeurs d'écart :

$$\begin{cases} h(T,P,\mathbf{z}) = h^{\bullet}(T,\mathbf{z}) + h^{\text{éc}}(T,P,\mathbf{z}) = \sum_{i=1}^{n_c} z_i h_i^{\bullet}(T) + h^{\text{éc}}(T,P,\mathbf{z}) \\ h_i^*(T,P) = h_i^{\bullet}(T) + h_i^{\text{éc}}(T,P) \end{cases} \tag{I−107}$$

En injectant l'équation (I−107) dans l'équation (I−106), l'enthalpie molaire d'excès s'écrit alors:

$$h^E(T,P,\mathbf{z}) = h^{\text{éc}}(T,P,\mathbf{z}) - \sum_{i=1}^{n_c} z_i h_i^{\text{éc}}(T,P) \tag{I−108}$$

Puisque les équations d'état cubiques sont exprimées dans le jeu de variables (T, v, **z**), on peut écrire :

$$h^E(T,P,\mathbf{z}) = h^E(T,v,\mathbf{z}) = h^{\text{éc}}(T,v,\mathbf{z}) - \sum_{i=1}^{n_c} z_i h_i^{\text{éc}}\left(T, v_i^*(T,P)\right) \tag{I−109}$$

Où v est le volume molaire total stable du mélange à la température T et sous la pression P ; v_i^* est le volume molaire stable du constituant i pur à la température T et sous la pression P.

N.B. : Si le mélange se trouve dans le domaine diphasique : liquide-vapeur (LV), l'enthalpie molaire d'écart $h^{\text{éc}}$ peut être écrite :

$$h^{\text{éc}}(T,v,\mathbf{z}) = \tau_L \cdot h_{\text{liq}}^{\text{éc}}(T,v,\mathbf{x}) + (1-\tau_L)\cdot h_{\text{vap}}^{\text{éc}}(T,v,\mathbf{y}) \text{ avec : } \tau_L = \frac{y_i - z_i}{y_i - x_i} \tag{I−110}$$

où $\mathbf{x}=\left(x_1,...,x_{n_c}\right)$ est le vecteur des fractions molaires dans la phase liquide, $\mathbf{y}=\left(y_1,...,y_{n_c}\right)$ est le vecteur des fractions molaires dans la phase vapeur, τ_L est la proportion molaire de la phase liquide, $h_{liq}^{éc}(T,v,\mathbf{x})$ est l'enthalpie molaire d'écart de la phase liquide de composition **x**, et $h_{vap}^{éc}(T,v,\mathbf{y})$ est l'enthalpie molaire d'écart de la phase vapeur de composition **y**.

On a déjà établi précédemment l'expression de l'enthalpie molaire d'écart avec les équations d'état cubiques de l'ensemble principal [voir l'équation (I–29)]. En prenant $r_1=-1-\sqrt{2}$ et $r_2=-1+\sqrt{2}$, on obtient les expressions suivantes pour le modèle PPR78 :

$$\begin{aligned} h^{éc}(T,v,\mathbf{z}) &= \frac{R\cdot T\cdot b_m(\mathbf{z})}{v-b_m(\mathbf{z})}-\frac{a_m(T,\mathbf{z})\cdot v}{v\left[v+b_m(\mathbf{z})\right]+b_m(\mathbf{z})\left[v-b_m(\mathbf{z})\right]} \\ &\quad -\frac{1}{2\sqrt{2}\cdot b_m(\mathbf{z})}\cdot\left(a_m(T,\mathbf{z})-T\cdot\frac{da_m(T,\mathbf{z})}{dT}\right)\cdot\ln\left[\frac{v+\left(1+\sqrt{2}\right)b_m(\mathbf{z})}{v+\left(1-\sqrt{2}\right)b_m(\mathbf{z})}\right] \qquad \text{(I–111)} \\ h^{éc}(T,v_i^*) &= h^{éc}(T,v,z_i=1) \end{aligned}$$

Sachant que $a_m(T,\mathbf{z})=\sum_{i=1}^{n_c}\sum_{j=1}^{n_c}z_i z_j\sqrt{a_i a_j}\left(1-k_{ij}(T)\right)$ (règles de mélange de Van der Waals), l'expression de la dérivée première de $a_m(T,\mathbf{z})$ par rapport à la température s'écrit :

$$\left(\frac{da_m(T,\mathbf{z})}{dT}\right)_{\mathbf{z}}=\sum_{i=1}^{n_c}\sum_{j=1}^{n_c}z_i z_j\left[\left(1-k_{ij}(T)\right)\frac{a_j\frac{da_i}{dT}+a_i\frac{da_j}{dT}}{2\sqrt{a_i a_j}}-\sqrt{a_i a_j}\,\frac{dk_{ij}(T)}{dT}\right] \qquad \text{(I–112)}$$

A ce stade, il est maintenant nécessaire de déterminer l'expression de la dérivée première de $k_{ij}(T)$ par rapport à la température. Pour davantage de clarté, la formule du coefficient d'interaction binaire $k_{ij}(T)$ est divisée en trois parties :

$$k_{ij}(T)=\frac{f(T)-g(T)}{h(T)} \text{ avec } \begin{cases} f(T)=-\dfrac{1}{2}\displaystyle\sum_{k=1}^{n_g}\sum_{k=1}^{n_g}\left(\alpha_{ik}-\alpha_{jk}\right)\left(\alpha_{il}-\alpha_{jl}\right)A_{kl}\cdot\left(\frac{298.15}{T}\right)^{\left(\frac{B_{kl}}{A_{kl}}-1\right)} \\ g(T)=\left(\dfrac{\sqrt{a_i(T)}}{b_i}-\dfrac{\sqrt{a_j(T)}}{b_j}\right)^2=\left(\delta_i-\delta_j\right)^2 \\ h(T)=2\dfrac{\sqrt{a_i(T)\cdot a_j(T)}}{b_i\cdot b_j}=2\delta_i\delta_j \end{cases} \qquad (I-113)$$

Finalement :

$$\frac{dk_{ij}(T)}{dT}=\frac{h(T)\left[f^{'}(T)-g^{'}(T)\right]-h^{'}(T)\left[f(T)-g(T)\right]}{\left[h(T)\right]^2}$$

$$\text{avec } \begin{cases} f^{'}(T)=\dfrac{1}{2}\displaystyle\sum_{k=1}^{n_g}\sum_{l=1}^{n_g}\left(\alpha_{ik}-\alpha_{jk}\right)\left(\alpha_{il}-\alpha_{jl}\right)\frac{A_{kl}}{T}\cdot\left(\frac{B_{kl}}{A_{kl}}-1\right)\left(\frac{298.15}{T}\right)^{\left(\frac{B_{kl}}{A_{kl}}-1\right)} \\ g^{'}(T)=2\left(\delta_1-\delta_2\right)\left(\delta_1^{'}-\delta_2^{'}\right)\ ;\ \delta_i^{'}=\dfrac{da_i/dT}{2b_i\cdot a_i^{1/2}} \\ h^{'}(T)=2\left(\delta_1^{'}\cdot\delta_2+\delta_2^{'}\cdot\delta_1\right) \end{cases} \qquad (I-114)$$

I.4.5 Calcul de la capacité calorifique molaire d’excès à pression constante $c_P{}^E$ par le modèle PPR78

Similairement au cas de l’enthalpie molaire d’excès h^E, la capacité calorifique molaire d’excès à pression constant $c_P{}^E$ peut être exprimée en fonction de la capacité calorifique à pression constant molaire d’écart $c_P{}^{éc}$ dans le jeu de variable (T, v, **z**).

Par définition :

$$c_P^E(T,P,\mathbf{z})=c_P(T,P,\mathbf{z})-\sum_{i=1}^{n_c}z_i c_{P,i}^{*}(T,P) \qquad (I-115)$$

On fait ensuite apparaître les grandeurs d’écart au gaz parfait :

$$\begin{cases} c_P(T,P,\mathbf{z}) = c_P^{\bullet}(T,\mathbf{z}) + c_P^{éc}(T,P,\mathbf{z}) = \sum_{i=1}^{n_c} z_i c_{P,i}^{\bullet}(T,P) + c_P^{éc}(T,P,\mathbf{z}) \\ c_{P,i}^{*}(T,P) = c_{P,i}^{\bullet}(T) + c_{P,i}^{éc}(T,P) \end{cases} \qquad (I-116)$$

En insérant l'équation (I−116) dans l'équation (I−115), On obtient :

$$c_P^E(T,P,\mathbf{z}) = c_P^{éc}(T,P,\mathbf{z}) - \sum_{i=1}^{n_c} z_i c_{P,i}^{éc}(T,P) \qquad (I-117)$$

Pour les équations d'état explicites en pression, on préfère :

$$c_P^E(T,P,\mathbf{z}) = c_P^E(T,v,\mathbf{z}) = c_P^{éc}(T,v,\mathbf{z}) - \sum_{i=1}^{n_c} z_i c_{P,i}^{éc}\left(T, v_i^{*}(T,P)\right) \qquad (I-118)$$

Où v est le volume molaire total stable du mélange à la température T et sous la pression P ; v_i^* est le volume molaire stable du constituant i pur à la température T et sous la pression P.

N.B. : Si le mélange se trouve dans le domaine diphasique : liquide-vapeur (LV), la capacité calorifique molaire d'écart $c_P^{éc}$ peut être écrite :

$$c_P^{éc}(T,v,\mathbf{z}) = \tau_L \cdot c_{P,liq}^{éc}(T,v,\mathbf{x}) + (1-\tau_L) \cdot c_{P,vap}^{éc}(T,v,\mathbf{y}) \text{ avec : } \tau_L = \frac{y_i - z_i}{y_i - x_i} \qquad (I-119)$$

où $\mathbf{x} = \left(x_1,...,x_{n_c}\right)$ est le vecteur des fractions molaires dans la phase liquide, $\mathbf{y} = \left(y_1,...,y_{n_c}\right)$ est le vecteur des fractions molaires dans la phase vapeur, τ_L est la proportion molaire de la phase liquide, $c_{P,liq}^{éc}(T,v,\mathbf{x})$ est la capacité calorifique molaire d'écart de la phase liquide de composition **x**, et $c_{P,vap}^{éc}(T,v,\mathbf{y})$ est la capacité calorifique molaire d'écart de la phase vapeur de composition **y**.

En prenant les équations (I−31,32), $r_1 = -1-\sqrt{2}$ et $r_2 = -1+\sqrt{2}$, les expressions de la capacité calorifique molaire d'écart à pression constante issues du modèle PPR78 s'écrivent :

$$c_P^{\text{éc}}(T,v,\mathbf{z}) = c_V^{\text{éc}}(T,v,\mathbf{z}) - R + T\left(\kappa_T \cdot v\right)\left(\beta \cdot P\right)^2$$

$$\text{avec}\begin{cases} \kappa_T \cdot v = \left\{ \dfrac{RT}{\left[v - b_m(\mathbf{z})\right]^2} - \dfrac{2 \cdot a_m(T,\mathbf{z})\left[v + b_m(\mathbf{z})\right]}{\left[v\left(v + b_m(\mathbf{z})\right) + b_m(\mathbf{z})\left(v - b_m(\mathbf{z})\right)\right]^2} \right\}^{-1} \\ \beta \cdot P = \dfrac{R}{v - b_m(\mathbf{z})} - \dfrac{da_m(T,\mathbf{z})}{dT} \cdot \dfrac{1}{v\left[v + b_m(\mathbf{z})\right] + b_m(\mathbf{z})\left[v - b_m(\mathbf{z})\right]} \\ c_V^{\text{res}} = \dfrac{T}{2\sqrt{2} \cdot b_m(\mathbf{z})} \cdot \dfrac{d^2 a_m(T,\mathbf{z})}{dT^2} \cdot \ln\left[\dfrac{v + \left(1+\sqrt{2}\right) b_m(\mathbf{z})}{v + \left(1-\sqrt{2}\right) b_m(\mathbf{z})}\right] \end{cases} \qquad (\text{I}-120)$$

$$c_{P,i}^{\text{éc}}(T, v_i^*) = c_P^{\text{éc}}(T, v, z_i = 1)$$

La dérivée seconde de $a_m(T,\mathbf{z})$ par rapport à la température suivante les règles de mélange de Van der Waals s'écrit sous la forme:

$$\left(\frac{d^2 a_m(T,\mathbf{z})}{dT^2}\right)_{\mathbf{z}} = \sum_{i=1}^{n_c}\sum_{j=1}^{n_c} z_i z_j \left[\left(1 - k_{ij}(T)\right) \frac{a_i a_j \left(a_j \dfrac{d^2 a_i}{dT^2} + 2\dfrac{da_i}{dT}\dfrac{da_j}{dT} + a_i \dfrac{d^2 a_j}{dT^2}\right)}{2\left(a_i a_j\right)^{3/2}} - \frac{dk_{ij}(T)}{dT} \frac{a_j \dfrac{da_i}{dT} + a_i \dfrac{da_j}{dT}}{\sqrt{a_i a_j}} - \sqrt{a_i a_j}\frac{d^2 k_{ij}(T)}{dT^2}\right] \qquad (\text{I}-121)$$

La dérivée seconde de $k_{ij}(T)$ par rapport à la température s'écrit, en vertu de l'équation suivante :

$$\frac{d^2 k_{ij}(T)}{dT^2} = \frac{h(T)\left\{h(T)\left[f''(T) - g''(T)\right] - h''(T)\left[f(T) - g(T)\right]\right\} - 2h'(T)\left\{h(T)\left[f'(T) - g'(T)\right] - h'(T)\left[f(T) - g(T)\right]\right\}}{\left[h(T)\right]^3}$$

$$\text{avec :}\begin{cases} f''(T) = -\dfrac{1}{2}\displaystyle\sum_{k=1}^{n_g}\sum_{l=1}^{n_g}\left(\alpha_{ik} - \alpha_{jk}\right)\left(\alpha_{il} - \alpha_{jl}\right)\dfrac{B_{kl}}{A_{kl}}\left(\dfrac{B_{kl}}{A_{kl}} - 1\right) \cdot 298.15^{\left(\frac{B_{kl}}{A_{kl}} - 1\right)} \cdot \left(\dfrac{1}{T}\right)^{\left(\frac{B_{kl}}{A_{kl}} + 1\right)} \\ g''(T) = 2\left[\left(\delta_1' - \delta_2'\right)^2 + \left(\delta_1 - \delta_2\right)\left(\delta_1'' - \delta_2''\right)\right] \; ; \; \delta_i' = \dfrac{da_i/dT}{2b_i \cdot a_i^{1/2}} \\ h''(T) = 2\left(\delta_1''\delta_2 + 2\delta_1'\delta_2' + \delta_2''\delta_1\right) \; ; \; \delta_i'' = \dfrac{1}{2b_i}\left[\dfrac{d^2 a_i/dT^2}{a_i^{1/2}} - \dfrac{1}{2}\dfrac{\left(da_i/dT\right)^2}{a_i^{3/2}}\right] \end{cases} \qquad (\text{I}-122)$$

où $f'(T)$, $g'(T)$ et $h'(T)$ sont décrites par l'équation (I−114).

Références bibliographiques

(1) Van der Waals, J. D. On the continuity of the gaseous and liquid states (Over de continuiteit van den gas- en vloeistoftoestand). *Ph.D. thesis, Leiden* 1873.
(2) Redlich, O.; Kwong, J. N. S. On the thermodynamics of solutions; an equation of state; fugacities of gaseous solutions. *Chem. Rev.* 1949, *44* (1), 233-244.
(3) Soave, G. Equilibrium constants from a modified Redlich-Kwong equation of state. *Chem. Eng. Sci.* 1972, *27* (6), 1197-1203.
(4) Peng, D.-Y.; Robinson, D. B. A new two-constant equation of state. *Ind. Eng. Chem., Fundam.* 1976, *15* (1), 59-64.
(5) Robinson, D. B.; Peng, D. Y. The characterization of the heptanes and heavier fractions for the GPA Peng-Robinson programs. *GPA Research Report* 1978, *RR-28*, 28.
(6) Wei, Y. S.; Sadus, R. J. Equations of state for the calculation of fluid-phase equilibria. *AIChE J.* 2000, *46* (1), 169-196.
(7) Valderrama, J. O. The State of the Cubic Equations of State. *Ind. Eng. Chem. Res.* 2003, *42* (8), 1603-1618.
(8) Trebble, M. A.; Bishnoi, P. R. Accuracy and consistency comparisons of ten cubic equations of state for polar and nonpolar compounds. *Fluid Phase Equilib.* 1986, *29*, 465-474.
(9) Mathias, P. M.; Copeman, T. W. Extension of the Peng-Robinson equation of state to complex mixtures: evaluation of the various forms of the local composition concept. *Fluid Phase Equilib.* 1983, *13*, 91-108.
(10) Stryjek, R.; Vera, J. H. PRSV - an improved Peng-Robinson equation of state with new mixing rules for strongly nonideal mixtures. *Can. J. Chem. Eng.* 1986, *64* (2), 334-340.
(11) Twu, C. H.; Bluck, D.; Cunningham, J. R.; Coon, J. E. A cubic equation of state with a new alpha function and a new mixing rule. *Fluid Phase Equilib.* 1991, *69*, 33-50.
(12) Twu, C. H.; Coon, J. E.; Cunningham, J. R. A new generalized alpha function for a cubic equation of state Part 1. Peng-Robinson equation. *Fluid Phase Equilib.* 1995, *105* (1), 49-59.
(13) Twu, C. H.; Coon, J. E.; Cunningham, J. R. A new generalized alpha function for a cubic equation of state Part 2. Redlich-Kwong equation. *Fluid Phase Equilib.* 1995, *105* (1), 61-69.
(14) Patel, N. C.; Teja, A. S. A new cubic equation of state for fluids and fluid mixtures. *Chem. Eng. Sci.* 1982, *37* (3), 463-473.
(15) Peneloux, A.; Rauzy, E.; Freze, R. A consistent correction for Redlich-Kwong-Soave volumes. *Fluid Phase Equilib.* 1982, *8* (1), 7-23.
(16) Ghosh, P. Prediction of vapor-liquid equilibria using Peng-Robinson and Soave-Redlich-Kwong equations of state. *Chem. Eng. Technol.* 1999, *22* (5), 379-399.
(17) Mollerup, J. A note on excess Gibbs energy models, equations of state and the local composition concept. *Fluid Phase Equilib.* 1981, *7* (2), 121-138.
(18) Whiting, W. B.; Prausnitz, J. M. Equations of state for strongly nonideal fluid mixtures: application of local compositions toward density-dependent mixing rules. *Fluid Phase Equilib.* 1982, *9* (2), 119-147.
(19) Panagiotopoulos, A. Z.; Reid, R. C. New mixing rule for cubic equations of state for highly polar, asymmetric systems. *ACS Symp. Ser.* 1986, *300*, 571-582.
(20) Adachi, Y.; Sugie, H. A new mixing rule - Modified conventional mixing rule. *Fluid Phase Equilib.* 1986, *28* (2), 103-118.
(21) Sandoval, R.; Wilczek-Vera, G.; Vera, J. H. Prediction of ternary vapor-liquid equilibria with the PRSV equation of state. *Fluid Phase Equilib.* 1989, *52*, 119-126.
(22) Schwartzentruber, J.; Renon, H.; Watanasiri, S. Development of a new cubic equation of state for phase equilibrium calculations. *Fluid Phase Equilib.* 1989, *52*, 127-134.
(23) Michelsen, M. L.; Kistenmacher, H. On composition-dependent interaction coefficients. *Fluid Phase Equilib.* 1990, *58* (1-2), 229-230.
(24) Mathias, P. M.; Klotz, H. C.; Prausnitz, J. M. Equation-of-state mixing rules for multicomponent mixtures: the problem of invariance. *Fluid Phase Equilib.* 1991, *67*, 31-44.
(25) Huron, M. J.; Vidal, J. New mixing rules in simple equations of state for representing vapor-liquid equilibriums of strongly non-ideal mixtures. *Fluid Phase Equilib.* 1979, *3* (4), 255-271.
(26) Michelsen, M. L. A modified Huron-Vidal mixing rule for cubic equations of state. *Fluid Phase Equilib.* 1990, *60* (1-2), 213-219.
(27) Dahl, S.; Michelsen, M. L. High-pressure vapor-liquid equilibrium with a UNIFAC-based equation of state. *AIChE J.* 1990, *36* (12), 1829-1836.
(28) Wong, D. S. H.; Sandler, S. I. A theoretically correct mixing rule for cubic equations of state. *AIChE J.* 1992, *38* (5), 671-680.

(29) Guggenheim, E. A., *Mixtures. The Theory of the Equilibrium Properties of Some Simple Cases of Mixtures, Solutions and Alloys*. Oxford University Press: Oxford, 1952.
(30) Peneloux, A.; Abdoul, W.; Rauzy, E. Excess functions and equations of state. *Fluid Phase Equilib.* 1989, *47* (2-3), 115-132.
(31) Jaubert, J.-N.; Mutelet, F. VLE predictions with the Peng-Robinson equation of state and temperature dependent kij calculated through a group contribution method. *Fluid Phase Equilib.* 2004, *224* (2), 285-304.
(32) Jaubert, J.-N.; Vitu, S.; Mutelet, F.; Corriou, J.-P. Extension of the PPR78 model (predictive 1978, Peng-Robinson EOS with temperature dependent kij calculated through a group contribution method) to systems containing aromatic compounds. *Fluid Phase Equilib.* 2005, *237* (1-2), 193-211.
(33) Vitu, S.; Jaubert, J.-N.; Mutelet, F. Extension of the PPR78 model (Predictive 1978, Peng-Robinson EOS with temperature dependent kij calculated through a group contribution method) to systems containing naphtenic compounds. *Fluid Phase Equilib.* 2006, *243* (1-2), 9-28.
(34) Vitu, S.; Privat, R.; Jaubert, J. N.; Mutelet, F. Predicting the phase equilibria of CO2 + hydrocarbon systems with the PPR78 model (PR EOS and kij calculated through a group contribution method). *Journal of Supercritical Fluids* 2008, *45* (1), 1-26.
(35) Privat, R.; Jaubert, J. N.; Mutelet, F. Addition of the nitrogen group to the PPR78 model (predictive 1978, Peng Robinson EOS with temperature-dependent kij calculated through a group contribution method. *Ind. Eng. Chem. Res.* 2008, *47* (6), 2033-2048.
(36) Privat, R.; Jaubert, J. N.; Mutelet, F. Addition of the sulfhydryl group (-SH) to the PPR78 model (predictive 1978, Peng-Robinson EOS with temperature dependent kij calculated through a group contribution method). *Journal of Chemical Thermodynamics* 2008, *40* (9), 1331-1341.
(37) Privat, R.; Mutelet, F.; Jaubert, J. N. Addition of the hydrogen sulfide group to the PPR 78, Model (Predictive 1978, Peng-Robinson equation of state with temperature dependent kij- calculated through a group contribution method). *Ind. Eng. Chem. Res.* 2008, *47* (24), 10041-10052.
(38) Kehiaian, H. V.; Sosnkowska-Kehiaian, K.; Hryniewicz, R. Enthalpy of mixing of ethers with hydrocarbons at 25.deg. and its analysis in terms of molecular surface interactions. *J. Chim. Phys. Physicochim. Biol.* 1971, *68* (6), 922-934.
(39) Abdoul, W.; Rauzy, E.; Peneloux, A. Group-contribution equation of state for correlating and predicting thermodynamic properties of weakly polar and nonassociating mixtures. Binary and multicomponent systems. *Fluid Phase Equilib.* 1991, *68*, 47-102.

Chapitre II. Extension du modèle PPR78 aux systèmes contenant de l’eau

L’eau intervient dans de nombreuses applications industrielles. Lors de la production du pétrole ou dans les conduites de transport, la présence d’eau dans les hydrocarbures peut produire des condensats et/ou des hydrates de gaz. La connaissance de la solubilité des hydrocarbures dans l’eau est aussi importante, car les nouvelles politiques environnementales imposent aux industries émettrices de gaz acides tels que CO_2 et H_2S de limiter les rejets atmosphériques. Dans les gisements, en cours de production de pétrole et de réinjection de gaz (H_2S, CO_2), des fluides hydrocarbonés se trouvent fréquemment au contact d'une phase aqueuse. Les conditions sont telles que les pressions peuvent atteindre de très hautes valeurs dans une large gamme de températures. De même, la prédiction des équilibres de phases des systèmes « eau-hydrocarbures » sur de larges gammes de températures, de pressions est nécessaire dans plusieurs procédés industriels.

L’objectif de ce chapitre est d’utiliser le modèle PPR78 pour prédire et décrire les équilibres entre phases de ces systèmes en présentant des phénomènes complexes :

- formation d’équilibres liquide-vapeur, liquide-liquide et liquide-liquide-vapeur.
- comportement de Type III d’après la classification de Van Konynenburg et Scott[1] pour la plupart des systèmes binaires.

II.1 Introduction

The phase equilibrium behavior of systems containing water is important in a wide variety of engineering[2-4] and geological[5-6] applications. However, such systems show extreme non-ideality that produces unusual and complex thermodynamic behavior. Thus, development of a phase equilibrium model for such systems over wide ranges of temperature and pressure is a difficult and challenging task.

Cubic equations of state (EoSs) developed originally for hydrocarbon mixtures with kinds of mixing rules are most commonly used for phase equilibrium computations because of their simplicity and accuracy. For the (water + hydrocarbon) mixtures, cubic EoS with classical mixing rules can not correlate fairly the mutual solubility. To overcome this deficiency, unconventional mixing rules were developed by several authors, e.g. local composition mixing rules by Tsonopoulos and Heidman[7] and by Economou and Donohue.[8], density-dependent mixing rules by Mathias and Copeman[9] and empirical mixing rules by Michel et al.[10], while most of such models require the use of at least one additional interaction parameter. The results of liquid-liquid equilibrium prediction obtained by some of these methods are reasonable, but the critical locus predictions have not been examined.

New mixing rules that combine cubic EoS with excess free-energy models have been developed over the last decade, e.g. Wong-Sander (WS)[11], the modified Huron-Vidal first-order (MHV-1)[12] and the modified Huron-Vidal second-order (MHV2)[13] mixing rules. Several authors presented the critical locus calculations using these mixing rules that include several water + hydrocarbon systems, such as Kolar and Kojima[14], Alvarado et al.[15], Polishuk et al.[16] and Castier and Sandler.[17] Recently, Wang and Wong[18] examined simultaneously liquid-liquid equilibrium and critical behavior by using both WS and MHV2 mixing rules. They found that the correlation of mutual solubility was satisfactory, but results in spurious branches of critical locus and phase behavior that have no experimental support. It was demonstrated that local-fitted models must be used with extreme caution when applied for predicting phase behavior over wide ranges of temperature and pressure.

In the last 20 years, numerous investigations have been carried out towards the development of other EoS for associating fluids based on statistical mechanical consideration. Galindo et al.[19] have used the statistical associating fluid theory-hard sphere (SAFT-HS) to describe the phase behavior of some systems containing water with an excellent description of the critical lines and coexisting phases. Associated perturbed anisotropic chain theory (APACT) and statistical associating fluid theory (SAFT) were studied by Economou and Tsonopoulos[20] for the calculation of LLE of (water + hydrocarbon) systems. Nevertheless, the increased complexity of APACT and SAFT and the explicit calculation of hydrogen bonding do not improve the fits of water solubility nor does it provide a quantitative description of the hydrocarbon solubility. Voutsas et al.[21] used the cubic-plus-association (CPA) EoS to model the phase equilibria of water-containing systems with accurate hydrocarbon solubility in the water-rich phase. A study of phase equilibria for (water + hydrocarbon) mixtures using the CPA, SAFT and PC-SAFT (perturbed-chain SAFT) with a monoparametric mixing rule was presented by Aparicio-Martínez and Hall.[22] These three models predicted the general shape of the global phase diagrams qualitatively, however, the simultaneous prediction in a quantitative way of critical locus, three-phase equilibria and equilibrium composition is only possible with the PC-SAFT model. Despite their complexities over a simple cubic EoS, investigations of the abilities of these approaches to produce consistent phase behavior for many kinds of such systems over wide ranges of temperature and pressure have hardly been examined.

In this work, the H_2O group is added to the PPR78 model (predictive 1978, Peng-Robinson EoS) so as to predict the mutual solubility and critical loci of (water + hydrocarbon) systems. Such a model combines the widely used Peng-Robinson equation of state (EoS) with a group contribution method aimed at estimating the temperature-dependent binary interaction parameters ($k_{ij}(T)$). In our previous papers[23-29], fifteen groups were defined: CH_3, CH_2, CH, C, CH_4 (methane), C_2H_6 (ethane), CH_{aro}, C_{aro}, $C_{\text{fused aromatic rings}}$, $CH_{2,\text{cyclic}}$, $CH_{\text{cyclic}} = C_{\text{cyclic}}$, CO_2, N_2, H_2S and -SH. In this paper, the interactions between this new group (H_2O) and the fifteen ones previously defined are determined. It is thus possible to estimate, at any temperature, the k_{ij} between two components in any mixture containing paraffins, naphthenes, aromatics, CO_2, N_2, H_2S, mercaptan and water.

II.2 Database and reduction procedure

Table II−1. List of the 56 pure components used in this study

Component	Short name	Component	Short name
methane	1	1,2-dimethylbenzene(o-xylene)	12mB
ethane	2	ethylbenzene	eB
propane	3	1,3,5-trimethylbenzene(mesitylene)	135mB
n-butane	4	1,2,4-trimethylbenzene	124mB
n-pentane	5	1-metylethylbenzene(cumene)	iprB
n-hexane	6	propylbenzene	prB
n-heptane	7	naphthalene	BB
n-octane	8	1-methylnaphthalene	1mBB
n-nonane	9	1,1'-biphenyl	Bph
n-decane	10	phenanthrene	Phe
n-undecane	11	cyclopropane	C3
n-dodecane	12	cyclopentane	C5
n-tetradecane	14	methylcyclopentane	mC5
n-hexadecane	16	cyclohexane	C6
n-octadecane	18	methylcyclohexane	mC6
n-eicosane	20	cycloheptane	C7
2-methylpropane(isobutane)	2m3	ethylcyclohexane	eC6
2-methylbutane	2m4	cyclooctane	C8
2,2-dimethylpropane(neopentane)	22m3	1,2,3,4-tetrahydronaphthalene(tetralin)	tet
2-methylpentane	2m5	cis-decalin	cCC6
3-methylpentane	3m5	trans-decalin	tCC6
2,2-dimethylbutane	22m4	carbon dioxide	CO_2
2,4-dimethylpentane	24m5	nitrogen	N_2
2,2,4-trimethylpentane(isooctane)	224m5	hydrogen sulfide	H_2S
2,2,5-trimethylhexane	225m6	water	H_2O
benzene	B	methyl mercaptan	1sh
methylbenzene(toluene)	mB	ethyl mercaptan	2sh
1,3-dimethylbenzene(m-xylene)	13mB	propyl mercaptan	3sh

Table (II−1) presents the list of the 56 pure components involved in this study. The pure fluid physical properties (T_c, P_c and ω) used originate from two sources. We have used Poling et al.[30] for alkanes, cyclo alkanes, aromatic compounds, CO_2, N_2, H_2S and H_2O. As some mercaptans were missing in this book, the DIPPR database was chosen for these pure components met in our study. Table (II−2) details the sources of the binary experimental data used in our evaluations[31-186] along with the temperature, pressure and composition range for each binary system. Most of the data available in the open literature (4437 bubble points + 3194 dew points + 151 mixture critical points) have been collected. Our database includes VLE data on 46 binary systems. The 30 parameters (15 A_{kl} and 15 B_{kl}) determined in this study [see table (I−2)], are those which minimize the objective function defined in equation (I−105).

Table II−2. Binary systems database

Binary system (1st compound-2nd compound)	Temperature range (K)	Pressure range (bar)	x_1 range (1st compound liquid mole fraction)	y_1 range (1st compound gas mole fraction)	Number of bubble points (T,P,x)	Number of dew points (T,P,y)	Number of binary critical points (T_{cm}, P_{cm}, x_c)	References
3-H_2O	256.21-663.20	0.10-3300.00	0.000001-0.999310	0.031000-0.999480	437	416	17	31-39
4-H_2O	298.15-707.00	1.04-3101.00	0.000002-0.999500	0.040000-0.999500	203	189	17	40-46
5-H_2O	273.20-646.70	0.24-769.00	0.000010-0.115000	0.018000-0.115000	9	0	10	47-48
6-H_2O	373.11-699.00	3.43-2467.00	0.004249-0.998000	0.015000-0.977000	37	146	14	45, 49-52
H_2O-7	298.15-629.60	0.08-324.00	0.001000-0.999000	0.322000-0.971000	12	12	3	47, 53-54
H_2O-8	422.04-552.76	6.55-88.60	0.012000-0.999960	0.086000-0.736000	19	17	0	55-57
H_2O-9	473.15-553.15	20.10-88.26	0.100000-0.575000	0.575000-0.840000	5	5	1	54
H_2O-10	423.15-613.20	4.90-303.00	0.006700-0.999500	0.029000-0.989000	70	139	4	50, 58-60
H_2O-12	473.15-633.00	18.63-219.40	0.073000-0.997700	0.367000-0.985300	28	28	4	54, 61
H_2O-16	413.50-638.15	2.68-294.20	0.018000-0.999500	0.667500-0.999500	163	139	6	62-63
H_2O-20	523.15-625.35	41.38-181.42	0.240000-0.923000	0.923000-0.995000	6	6	1	54
2m3-H_2O	278.15-649.00	1.01-1070.00	0.000010-0.999910	0.070000-0.200000	6	0	8	46, 64-66
2m4-H_2O	298.15-298.15	1.01-1.01	0.000012-0.000012	-	1	0	0	65
22m3-H_2O	278.15-318.15	1.01-1.01	0.000006-0.000017	-	4	0	0	65-66
2m5-H_2O	298.15-628.15	1.01-709.27	0.000003-0.055585	0.044049-0.124928	31	8	0	65, 67
3m5-H_2O	298.15-298.15	1.01-1.01	0.000003-0.000003	-	1	0	0	65
22m4-H_2O	298.15-298.15	1.01-1.01	0.000004-0.000004	-	1	0	0	65
H_2O-24m5	298.15-298.15	1.01-1.01	0.999999-0.999999	-	1	0	0	65
H_2O-224m5	298.15-353.15	1.01-5.01	0.999999-1.000000	-	5	0	0	65, 68
H_2O-225m6	298.15-298.15	1.01-1.01	1.000000-1.000000	-	1	0	0	65
1-H_2O	273.10-649.20	0.97-2500.00	0.000026-0.295000	0.062000-0.999910	665	434	13	69-103
2-H_2O	259.10-673.15	0.63-3700.00	0.000008-0.340000	0.135000-0.999970	257	242	8	75-76, 84, 88, 90, 97-98, 104-112
H_2O-B	293.15-613.15	0.04-2976.68	0.000100-0.999981	0.201465-0.938909	225	162	2	52, 65, 67, 113-122
H_2O-mB	298.15-641.33	1.01-607.95	0.019230-0.999899	0.483000-0.971300	51	16	0	58, 65, 67, 114, 123
H_2O-13mB	398.15-473.35	2.74-20.04	0.027850-0.999800	-	10	0	0	114
H_2O-12mB	298.15-373.50	0.53-1.29	0.218700-0.999970	-	12	0	0	65, 124
H_2O-eB	298.15-568.10	0.09-106.80	0.004300-0.999974	0.691000-0.778000	18	11	1	55, 65, 125
H_2O-124mB	298.15-298.15	1.01-1.01	0.999991-0.999991	-	1	0	0	65
H_2O-iprB	298.15-298.15	1.01-1.01	0.999993-0.999993	-	1	0	0	65
H_2O-1mBB	533.54-673.15	17.23-174.50	0.040000-0.996900	0.393000-0.960000	41	45	3	55, 126
H_2O-Phe	419.80-542.00	3.61-10.55	0.061000-0.072700	-	26	0	0	62
C3-H_2O	294.26-377.59	1.17-42.74	0.000072-0.002400	-	45	0	0	127
C5-H_2O	298.15-298.15	1.01-1.01	0.000040-0.000040	-	1	0	0	65
H_2O-mC5	298.15-298.15	1.01-1.01	0.999991-0.999991	-	1	0	0	65
H_2O-C6	298.10-683.15	0.32-1546.69	0.001130-0.999988	0.203940-0.994094	68	88	2	52, 65, 68, 120, 128
H_2O-mC6	298.15-298.15	1.01-1.01	0.999997-0.999997	-	1	0	0	65
H_2O-C7	298.15-298.15	1.01-1.01	0.999995-0.999995	-	1	0	0	65
H_2O-eC6	310.90-561.40	0.10-99.30	0.000810-0.999998	0.603000-0.755000	19	14	1	55, 125
H_2O-C8	298.15-298.15	1.01-1.01	0.999999-0.999999	-	1	0	0	65
H_2O-tet	573.15-672.85	10.44-179.00	0.026000-0.997000	0.251000-0.956000	55	56	3	126
CO_2-H_2O	273.15-633.15	0.49-3600.00	0.000030-0.998100	0.055000-0.999300	1068	543	23	79, 82, 106, 129-164
N_2-H_2O	257.44-659.00	3.40-2710.00	0.000023-0.480000	0.034000-1.000000	265	261	9	32, 91, 97, 150, 165-178
H_2S-H_2O	283.15-603.15	1.55-206.85	0.000320-0.987000	0.008500-0.996970	522	196	1	82, 168, 179-184
1sh-H_2O	310.93-588.70	0.77-206.84	0.002400-0.265000	0.138000-0.975700	19	16	0	185-186
2sh-H_2O	323.12-588.70	0.39-206.84	0.000589-0.022700	0.122000-0.644000	13	6	0	185-186
3sh-H_2O	323.07-372.97	0.18-1.63	0.000109-0.000567	-	11	0	0	186
Total number of points:					**4437**	**3194**	**151**	

II.3 Difficulties in predicting the phase behavior of binary systems containing water

II.3.1 Type III phase behavior

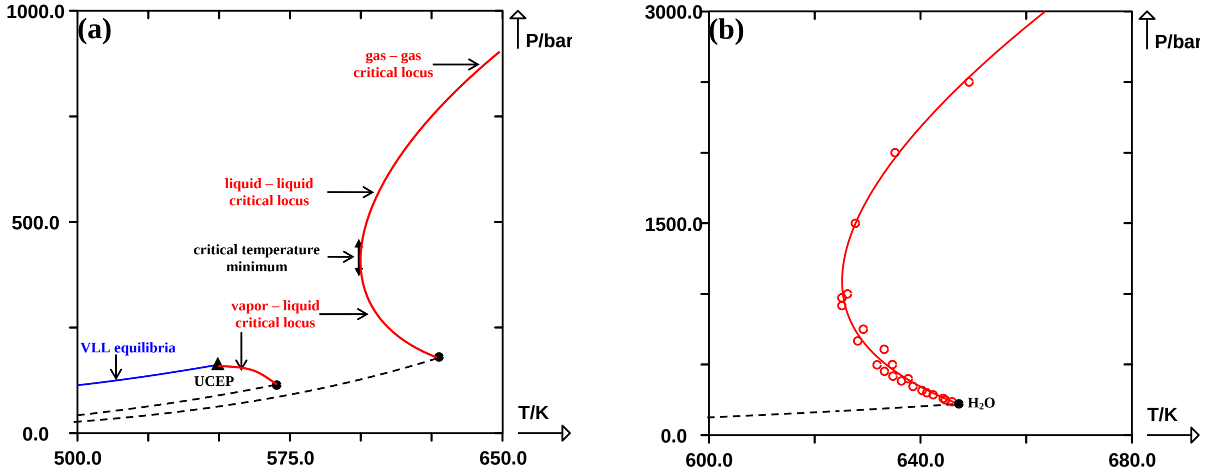

Figure II−1. **(a)** Schematic representation of Type III phase behavior in the pressure-temperature (P-T) projection. (●) critical points of the pure compounds, (▲) upper critical endpoint, UCEP. Red solid line: critical locus. Blue solid line: vapor-liquid-liquid three-phase line. Dashed line: vaporization curves of the pure compounds. **(b)** Prediction of the critical locus for the binary system: (methane(1) + H_2O(2)), optimized on mixture critical points, using the PPR78 model. (●) critical point of the pure compound, (○) experimental critical points. Solid line: calculated critical curve. Dashed line: vaporization curve of the pure compound (water).

Most of the water containing systems exhibit a phase behavior of Type III in the classification scheme of Van Konynenburg[1], as shown in figure (II−1a). Critical lines of Type III systems consist of two branches. One connects the upper critical end point (UCEP) of the liquid–liquid–gas three-phase line with the critical point of the more volatile substance, while the other starts at the critical point of the less volatile substance and goes to high pressures. Furthermore, this critical branch in figure (II−1a) exhibits a critical temperature minimum which is the case for most of the binary mixtures containing water. The high pressure part going above the water critical temperature is called gas-gas immiscibility, but at these high pressures the phases in equilibrium are highly compressed fluids with liquid densities and the term fluid-fluid equilibrium might be more appropriate.

Such phase behaviors are known to be extremely difficult to predict with a cubic EoS. In order to address this problem, we have calculated the critical line optimized on mixture critical points for the system (methane(1) + water(2)) by using temperature-dependent BIP (k_{ij}(T)). Figure (II−1b) indicates that the model is capable of predicting the P-T projection of this system quantitatively using two group interaction parameters ($A_{5\text{-}16}$, $B_{5\text{-}16}$), showing a fair agreement with experimental data, including the critical temperature minimum. However, BIP ($k_{ij}(T)$) values calculated from these two parameters ($A_{5\text{-}16}$, $B_{5\text{-}16}$) at low and intermediate temperatures are not competent to correlate the experimental data. Hence, the parameters fitted on critical points could not describe very well the entire phase space in a wide range of temperature and pressure. Furthermore, by varying the two parameters ($A_{5\text{-}16}$, $B_{5\text{-}16}$), it was found that the more accurate the predicted critical locus is, the worse the objective function defined by equation (I−105) would be. As a consequence, we decided to define a compromise between the accuracy of the predicted critical curves and the minimization of the objective function, so as to the other systems with such kind of problem.

II.3.2 Atypical Type III phase behavior

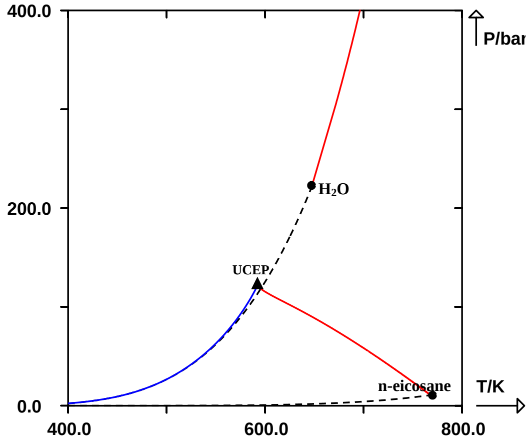

Figure II−2. Prediction of the critical locus for the binary system: (H_2O(1) + n-eicosane(2)) using the PPR78 model. (●) critical points of the pure compounds, (▲) upper critical endpoint, UCEP. Red solid line: critical curves. Blue solid line: vapor-liquid-liquid three-phase line.

For water containing systems, typical Type III phase behaviors are observed for (water + hydrocarbon) mixtures when the hydrocarbon has a relatively low molecular weight, with its critical temperature below that of water, as could be seen in figure (II−1a). When the carbon number increases, the critical temperature of the hydrocarbon becomes higher than that of water, and the critical locus under low pressures appears to be more significant. Figure (II−2) shows the prediction of critical locus for system (water(1) + n-eicosane(2)), the high-pressure branch starts at the critical point of the more volatile substance (water) and goes to high pressures as the temperatures rise. While the low-pressure branch sweeps a large temperature range, reaching an extraordinary value of $\triangle T = 176$ K. That is why it is called atypical Type III phase behavior in this study. This phase behavior is in qualitative accordance with the observation of Brunner[187]. Nevertheless, it is really difficult for our model to predict simultaneously the two critical branches.

II.3.3 Difficulties of temperature-dependent BIP ($k_{ij}(T)$) optimization

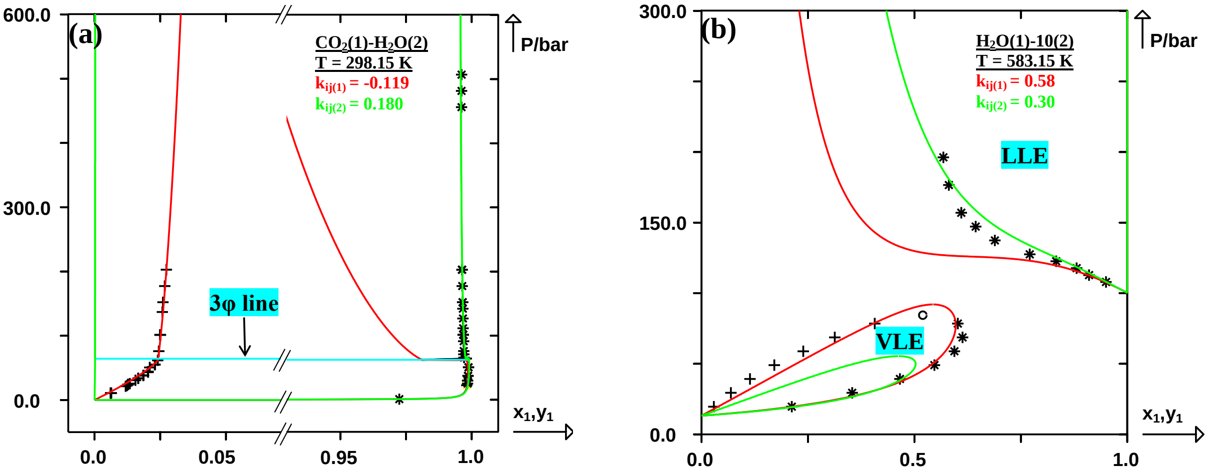

Figure II−3. Isothermal curves for the two binary systems: $CO_2(1)$ + $H_2O(2)$ and $H_2O(1)$ + n-decane(2) calculated with Peng-Robinson equation of state (EoS) with different k_{ij} values. (+) experimental bubble points, (✳) experimental dew points, (○) experimental critical points. Solid line: calculated curves. **(a)** system $CO_2(1)$ + $H_2O(2)$ at T = 298.15 K with two different k_{ij} values: $k_{ij(1)} = -0.119$ and $k_{ij(2)} = 0.180$. **(b)** system $H_2O(1)$ + n-decane(2) at T = 583.15 K with two different k_{ij} values: $k_{ij(1)} = 0.58$ and $k_{ij(2)} = 0.30$.

As outlined in the introduction, cubic EoS with classical mixing rules can not give a fair correlation of mutual solubility for the (water + hydrocarbon) mixtures. However, both the two liquid phases could be well predicted by using different BIP (k_{ij}). Taking ($CO_2(1)$ + water(2)) for example [see figure (II−3a)], the major difficulty is that at T = 298.15 K, the k_{ij} required for the water-rich liquid ($k_{ij} = -0.119$) is strongly different from the one required for the CO_2-rich liquid ($k_{ij} = 0.180$), while CO_2 contents in the gaseous phase have little k_{ij} dependence. Therefore, the choice of k_{ij} becomes an issue. Considering that we have to minimize the objective function defined by equation (I−105), the water-rich liquid curves are better reproduced for the binary mixture ($CO_2(1)$ + water(2)), because there are more experimental data points concerning CO_2 solubility in water.

Another difficulty of temperature-dependent BIP ($k_{ij}(T)$) optimization appears when at a given temperature, we simultaneously observe a VLE region and a LLE region without the existence of a three-phase line. Indeed a single k_{ij} seems to be insufficient to properly correlate the experimental data in these two regions. Such a behavior appears in the temperature range where the low-pressure critical line is present. Figure (II−3b) illustrates the example of (water(1) + n-decane(2)) system for which we could not correlate simultaneously the LLE (appropriate $k_{ij} = 0.30$) in the high-pressure region, and the VLE with a VLE critical point (appropriate $k_{ij} = 0.58$) in the low-pressure region, at T = 583.15 K, by using the same k_{ij} value.

II.4 Results and discussion

For all the data points included in our database, the objective function defined by equation (I−105) is: $F_{obj} = 17.09\,\%$.

The average overall deviation on the liquid phase composition is:

$$\overline{\Delta x_1} = \frac{\sum_{i=1}^{n_{bubble}} \left(\left|x_{1,exp} - x_{1,cal}\right|\right)_i}{n_{bubble}} = 0.016 \text{. Moreover } \frac{F_{obj,bubble}}{n_{bubble}} = 18.33\ \%$$

The average overall deviation on the gas phase composition is:

$$\overline{\Delta y_1} = \frac{\sum_{i=1}^{n_{dew}} \left(\left|y_{1,exp} - y_{1,cal}\right|\right)_i}{n_{dew}} = 0.031 \text{. Moreover } \frac{F_{obj,dew}}{n_{dew}} = 15.67\ \%$$

The average overall deviation on the critical composition is:

$$\overline{\Delta x_{c1}} = \frac{\sum_{i=1}^{n_{crit}} \left(\left|x_{c1,exp} - x_{c1,cal}\right|\right)_i}{n_{crit}} = 0.061 \text{. Moreover } \frac{F_{obj,crit.\ comp}}{n_{crit}} = 22.29\ \%$$

The average overall deviation on the binary critical pressure is:

$$\overline{\Delta P_c}\,\% = \frac{F_{obj,crit.\ pressure}}{n_{crit}} = \frac{100\sum_{i=1}^{n_{crit}} \left(\frac{\left|P_{cm,exp} - P_{cm,cal}\right|}{P_{cm,exp}}\right)_i}{n_{crit}} = 19.97\%$$

The value of the objective function for systems involving water is the largest one in comparison to those obtained in our previous studies[23-29]. Besides the explanations presented in section II.3, this high objective function value can also be explained by the following reasons: (1) Some experimental data reported in the literature are generally inconsistent and there are obvious scatters among them. (2) The immiscibility of water and hydrocarbons at low and moderate temperatures inevitably increases the objective function. In order to illustrate the accuracy and the limitations of our model, it was decided to define several families of binary systems which could give a good representation of the whole database.

II.4.1 Results for mixtures of (water + n-alkane)

In this work, all the (water + n-alkane) mixtures investigated exhibit Type III phase behavior, with the BIP ($k_{ij}(T)$) decreasing remarkably with temperature.

Figure (II−4a) shows the isothermal phase diagrams for (methane (1) + water (2)) at six different temperatures. At the lowest temperature (T = 298.15 K), the region of liquid-liquid immiscibility dominates the phase behavior. The mutual solubility increases with temperature. At the highest temperature (T = 633.15 K), there is a small liquid-vapor region at low pressures extending from the pure water and ending at the liquid-vapor critical point, and another coexistence region appears in the high pressure region. Satisfactory results are obtained at low and intermediate temperatures [see figure (II−4a)]. Regarding the P-xy envelope at T = 625.15 K, the experimental data points exhibit two coexistence regions: VLE and LLE, while the calculated curves present only LLE. It is because the temperature minimum is overestimated, as shown in the corresponding critical locus in an enlarged scale plotted in figure (II−4b). We can also observe that the slope of the critical curve is not very accurate at high pressures. This is due to the compromise that we have defined, as previously discussed in section II.3.1. The isothermal phase diagrams for system (ethane(1) + water(2)) at seven different temperatures are shown in figures (II−4c,4d). Similar phase behaviors are observed except for the VLL three-phase line at T = 298.15 K, below which two LV regions exist, as shown in figure (II−4c). On the other hand, the compositions of ethane-rich liquid curves at intermediate and high temperatures are underestimated [see figure (II−4d)].

Figures (II−5,6,7,8,9) present the P-xy diagrams and P-T projections for other systems consisting of water and an n-alkane (from propane to n-hexadecane). In figures (II−5a,5b,6a,6b,6c,7a,7d,8a,8d,9a,9b,9c,9d), heteroazeotropes at low and intermediate temperatures are accurately predicted by the PPR78 model, including the LLE region at high pressures and the two VLE regions below the VLL three-phase line. We have to notice that the predicted VLE under the VLL three-phase line for (H_2O(1) + n-hexadecane(2)) are not very accurate [see figures (II−9a,9c,9d)]. As previously discussed in section II.3.3, in the temperature range where both the LLE and VLE are presented, without the VLL three-phase line, it is really difficult to predict simultaneously the LLE and VLE. As a result, the correlations of VLE at low pressures are not good for the systems containing a normal or long chain alkane, which are plotted in figures (II−7b,7e,8b,8e,9e). However, in general most of the liquid-vapor and liquid-liquid coexistence regions over a wide temperature and pressure range are predicted with an acceptable accuracy.

Considering the P-T projections of the binary mixtures containing water and an n-alkane, reasonable results are obtained for methane, ethane, propane and n-butane as shown in figures (II−4b,4e,5f,6e). It is interesting to notice that as the chain length of the n-alkane increases, the critical curve at lower pressures appears to be more significant. Unfortunately, the quality of the predicted critical locus decreases with the chain length of the n-alkane, for both the low-pressure branch and the high-pressure branch. Regarding the systems containing an n-alkane heavier than n-hexane [see figures (II−7f,8c,8f,9f)], the high-pressure critical locus evolves directly from the water critical point to higher pressures without a critical temperature minimum and the pressures of the low-pressure critical locus are underestimated. Moreover, atypical Type III phase behavior could be observed for the system (H_2O(1) + hexadecane(2)) in figure (II−9f). We notice here that some of the experimental critical points published by Brunner[187] for (water + an n-alkane) mixtures plotted in the P-T projections, do not appear in table (II−2), and therefore they were not used to fit the parameters of our model because the critical composition is generally unknown.

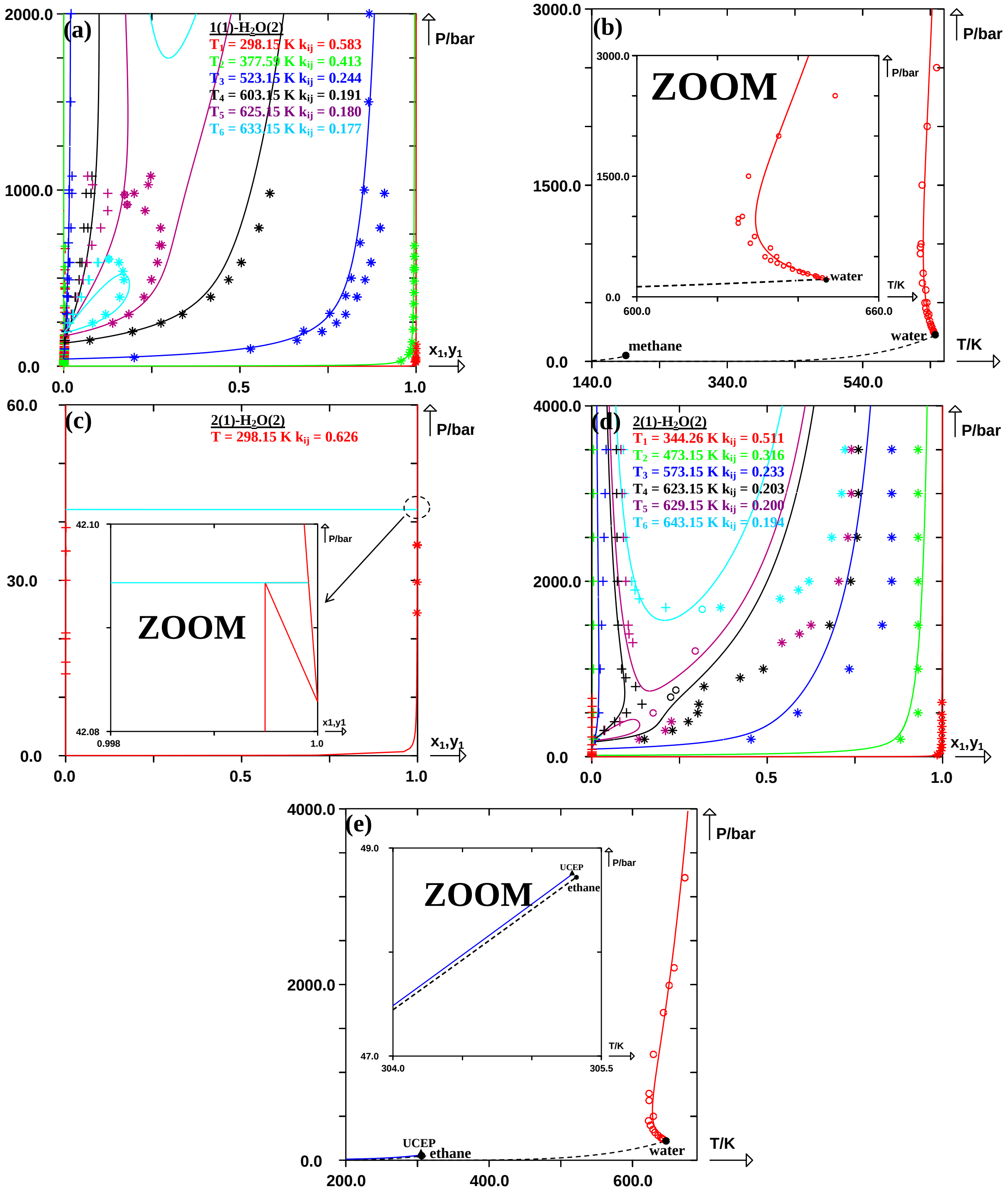

Figure II−4. Prediction of isothermal curves and prediction of the critical locus for the two binary systems: (methane(1) + water(2)) and (ethane(1) + water(2)) using the PPR78 model. (+) experimental bubble points, (✳) experimental dew points, (○) experimental critical points, (●) critical points of the pure compounds, (▲) upper critical endpoint, UCEP. Solid line: predicted curves with the PPR78 model. Dashed line: vaporization curves of the pure compounds. **(a)** System (methane(1) + water(2)) at six different temperatures: T_1 = 298.15 K (k_{ij} = 0.583), T_2 = 377.59 K (k_{ij} = 0.413), T_3 = 523.15 K (k_{ij} = 0.244), T_4 = 603.15 K (k_{ij} = 0.191), T_5 = 625.15 K (k_{ij} = 0.180), T_6 = 633.15 K (k_{ij} = 0.177). **(b)** Critical locus of the system (methane(1) + water(2)). **(c)** System (ethane(1) + water(2)) at T = 298.15 K (k_{ij} = 0.626). **(d)** System (ethane(1) + water(2)) at six different temperatures: T_1 = 344.26 K (k_{ij} = 0.511), T_2 = 473.15 K (k_{ij} = 0.316), T_3 = 573.15 K (k_{ij} = 0.233), T_4 = 623.15 K (k_{ij} = 0.203), T_5 = 629.15 K (k_{ij} = 0.200), T_6 = 643.15 K (k_{ij} = 0.194). **(e)** Critical locus of the system (ethane(1) + water(2)).

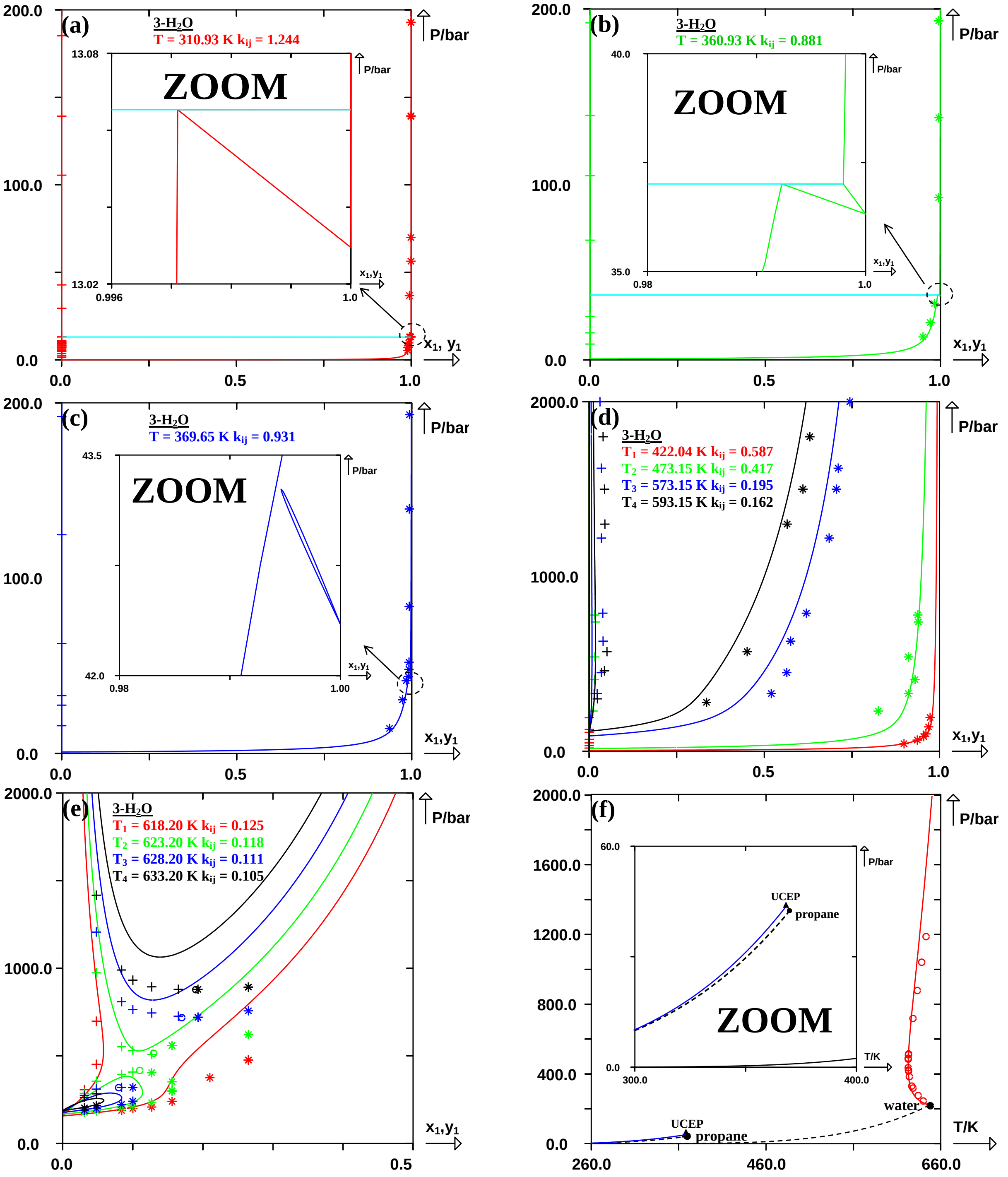

Figure II−5. Prediction of isothermal curves and prediction of the critical locus for the binary system: (propane(1) + water(2)) using the PPR78 model. (+) experimental bubble points, (✳) experimental dew points, (○) experimental critical points, (●) critical points of the pure compounds, (▲) upper critical endpoint, UCEP. Solid line: predicted curves with the PPR78 model. Dashed line: vaporization curves of the pure compounds. **(a)** System (propane(1) + water(2)) at T = 310.93 K (k_{ij} = 1.244). **(b)** System (propane(1) + water(2)) at T = 360.93 K (k_{ij} = 0.881). **(c)** System (propane(1) + water(2)) at T = 369.65 K (k_{ij} = 0.831). **(d)** System (propane(1) + water(2)) at four different temperatures: T_1 = 422.04 K (k_{ij} = 0.587), T_2 = 473.15 K (k_{ij} = 0.417), T_3 = 573.15 K (k_{ij} = 0.195), T_4 = 593.15 K (k_{ij} = 0.162). **(e)** System (propane(1) + water(2)) at four different temperatures: T_1 = 618.20 K (k_{ij} = 0.125), T_2 = 623.20 K (k_{ij} = 0.118), T_3 = 628.20 K (k_{ij} = 0.111), T_4 = 633.20 K (k_{ij} = 0.105). **(f)** Critical locus of the system (propane(1) + water(2)).

]

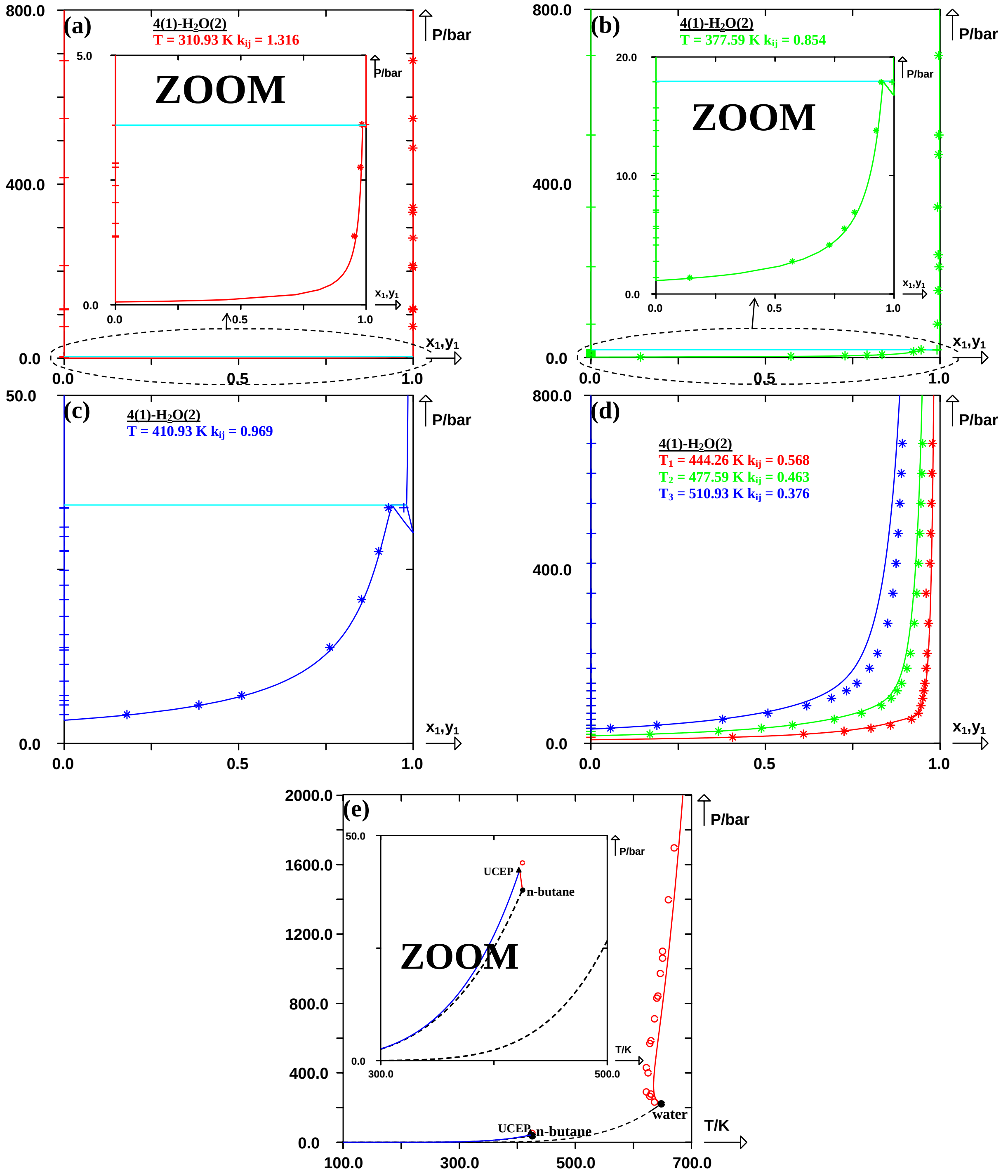

Figure II−6. Prediction of isothermal curves and prediction of the critical locus for the binary system: (n-butane(1) + water(2)) using the PPR78 model. (+) experimental bubble points, (✳) experimental dew points, (○) experimental critical points, (●) critical points of the pure compounds, (▲) upper critical endpoint, UCEP. Solid line: predicted curves with the PPR78 model. Dashed line: vaporization curves of the pure compounds. **(a)** System (n-butane(1) + water(2)) at $T = 310.93$ K ($k_{ij} = 1.316$). **(b)** System (n-butane(1) + water(2)) at $T = 377.59$ K ($k_{ij} = 0.854$). **(c)** System (n-butane(1) + water(2)) at $T = 410.93$ K ($k_{ij} = 0.696$). **(d)** System (n-butane(1) + water(2)) at three different temperatures: $T_1 = 444.26$ K ($k_{ij} = 0.568$), $T_2 = 477.59$ K ($k_{ij} = 0.463$), $T_3 = 510.93$ K ($k_{ij} = 0.376$). **(e)** Critical locus of the system (n-butane(1) + water(2)).

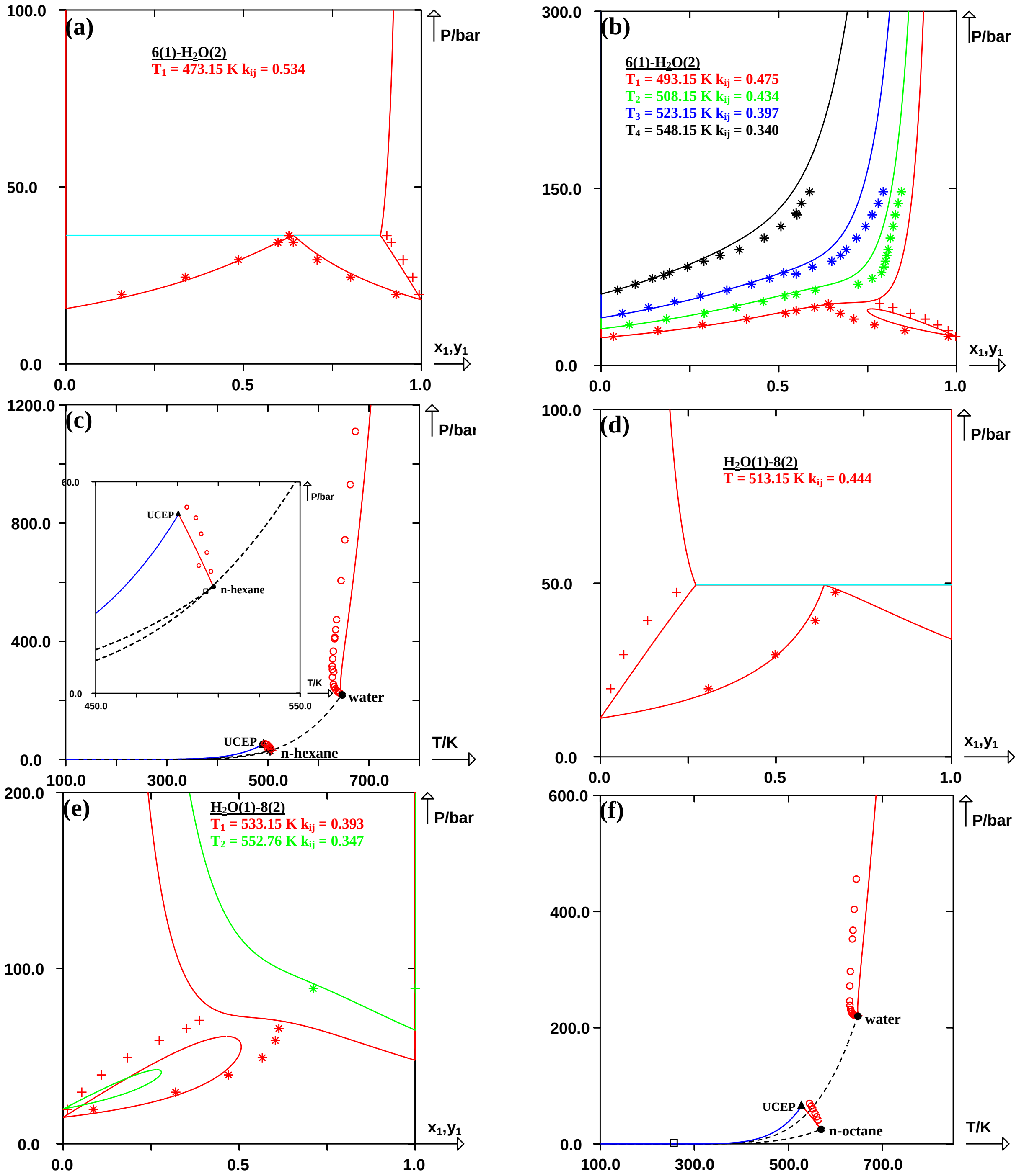

Figure II‒7. Prediction of isothermal curves and prediction of the critical locus for the two binary systems: (n-hexane(1) + water(2)) and (water(1) + n-octane(2)) using the PPR78 model. (+) experimental bubble points, (✳) experimental dew points, (○) experimental critical points, (☐) Bancroft point, (●) critical points of the pure compounds, (▲) upper critical endpoint, UCEP. Solid line: predicted curves with the PPR78 model. Dashed line: vaporization curves of the pure compounds. **(a)** System (n-hexane(1) + water(2)) at $T = 473.15$ K ($k_{ij} = 0.534$). **(b)** System (n-hexane(1) + water(2)) at four different temperatures: $T_1 = 493.15$ K ($k_{ij} = 0.475$), $T_2 = 508.15$ K ($k_{ij} = 0.434$), $T_3 = 523.15$ K ($k_{ij} = 0.397$), $T_4 = 548.15$ K ($k_{ij} = 0.340$). **(c)** Critical locus of the system (n-hexane(1) + water(2)). **(d)** System (water(1) + n-octane(2)) at $T = 513.15$ K ($k_{ij} = 0.444$). **(e)** System (water(1) + n-octane(2)) at two different temperatures: $T_1 = 533.15$ K ($k_{ij} = 0.393$), $T_2 = 552.76$ K ($k_{ij} = 0.347$). **(f)** Critical locus of the system (water(1) + n-octane(2)).

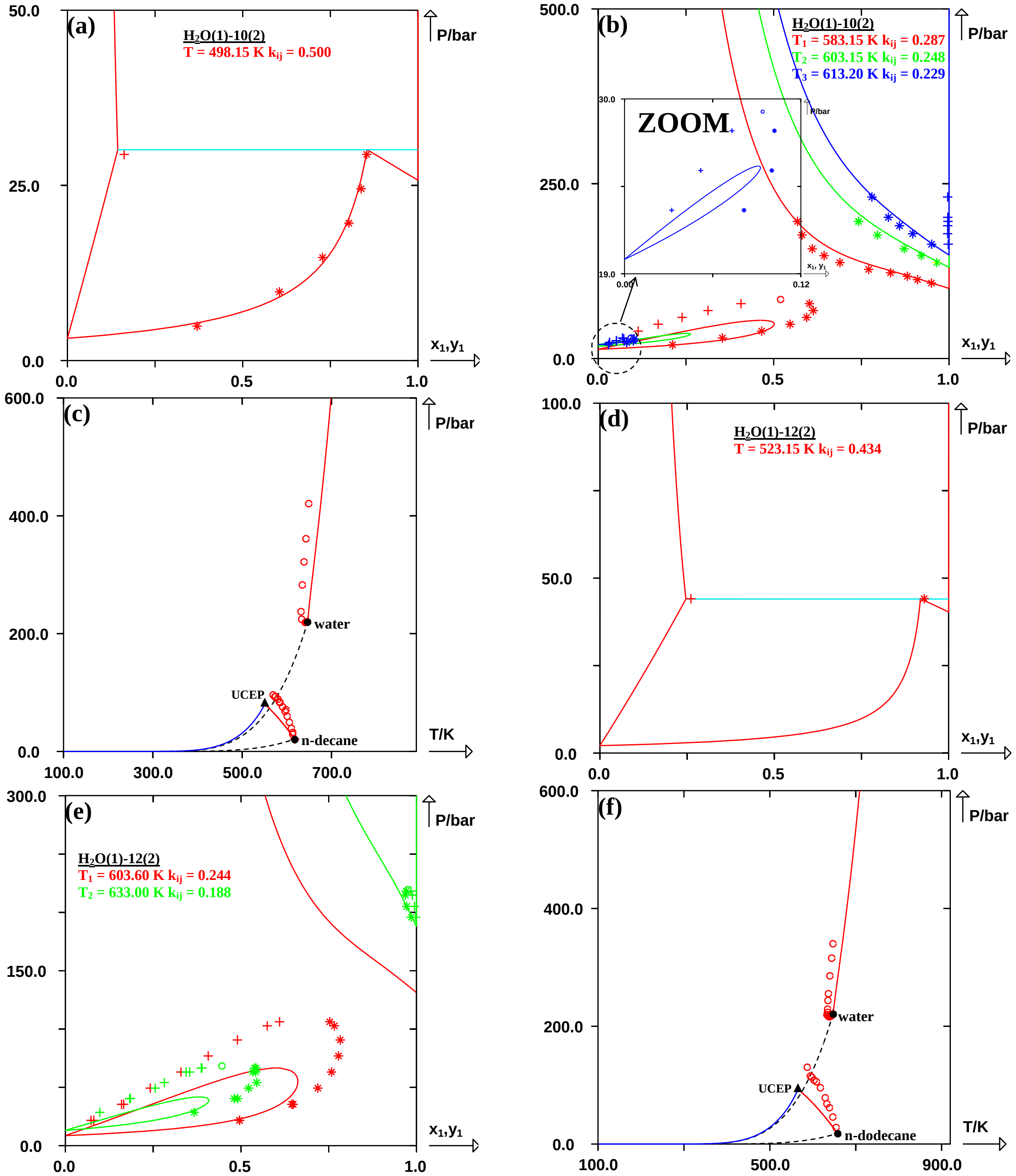

Figure II−8. Prediction of isothermal curves and prediction of the critical locus for the two binary systems: (water(1) + n-decane(2)) and (water(1) + n-dodecane(2)) using the PPR78 model. (+) experimental bubble points, (✳) experimental dew points, (○) experimental critical points, (●) critical points of the pure compounds, (▲) upper critical endpoint, UCEP. Solid line: predicted curves with the PPR78 model. Dashed line: vaporization curves of the pure compounds. **(a)** System (water(1) + n-decane(2)) at T = 498.15 K (k_{ij} = 0.500). **(b)** System (water(1) + n-decane(2)) at three different temperatures: T_1 = 583.15 K (k_{ij} = 0.287), T_2 = 603.15 K (k_{ij} = 0.248), T_3 = 613.20 K (k_{ij} = 0.229). **(c)** Critical locus of the system (water(1) + n-decane(2)). **(d)** System (water(1) + n-dodecane(2)) at T = 523.15 K (k_{ij} = 0.434). **(e)** System (water(1) + n-dodecane(2)) at two different temperatures: T_1 = 603.60 K (k_{ij} = 0.244), T_2 = 633.00 K (k_{ij} = 0.188). **(f)** Critical locus of the system (water(1) + n-dodecane(2)).

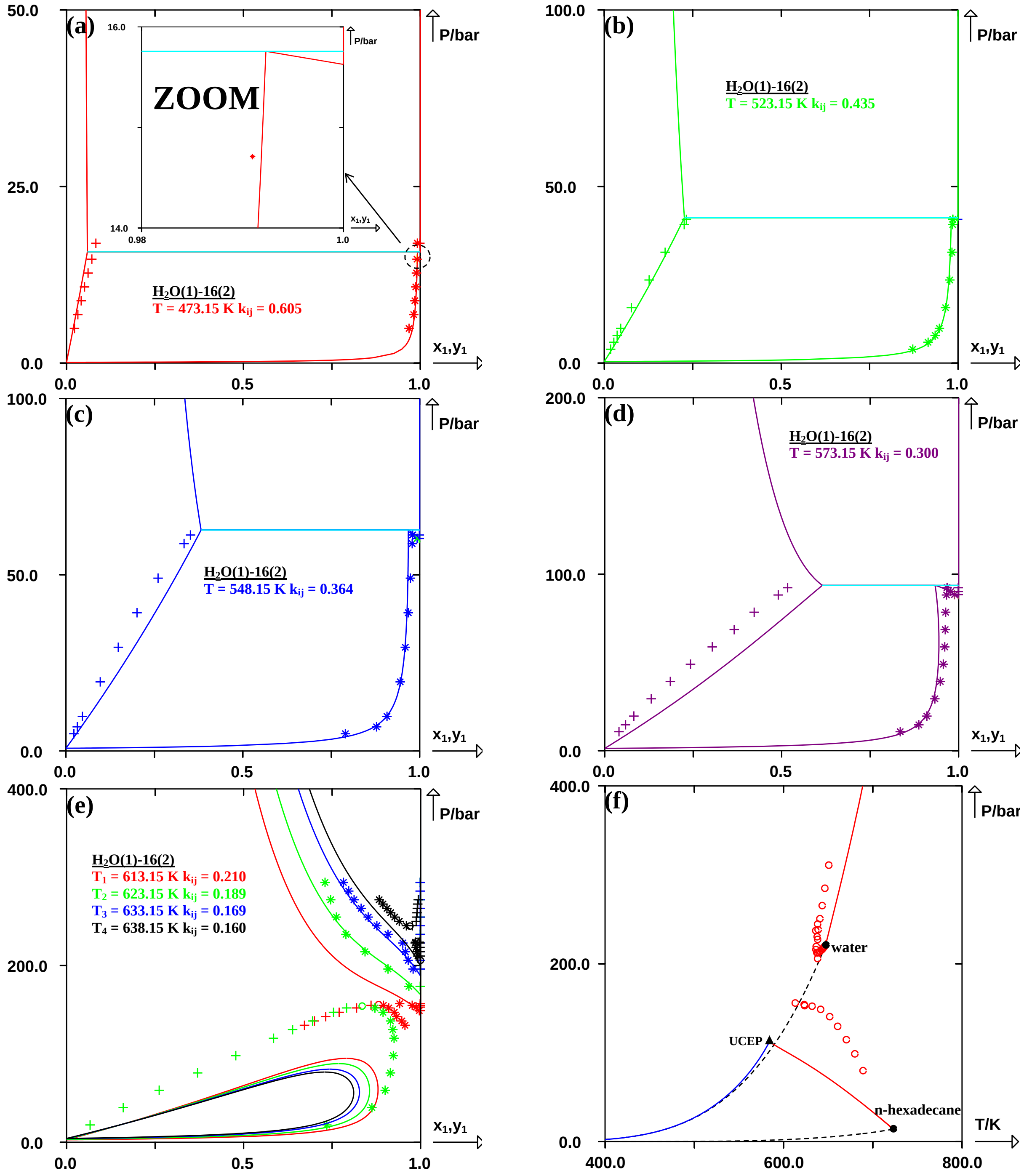

Figure II‒9. Prediction of isothermal curves and prediction of the critical locus for the binary system: (water(1) + n-hexadecane(2)) using the PPR78 model. (+) experimental bubble points, (✳) experimental dew points, (○) experimental critical points, (●) critical points of the pure compounds, (▲) upper critical endpoint, UCEP. Solid line: predicted curves with the PPR78 model. Dashed line: vaporization curves of the pure compounds. **(a)** System (water(1) + n-hexadecane(2)) at T = 473.15 K (k_{ij} = 0.605). **(b)** System (water(1) + n-hexadecane(2)) at T = 523.15 K (k_{ij} = 0.435). **(c)** System (water(1) + n-hexadecane(2)) at T = 548.15 K (k_{ij} = 0.364). **(d)** System (water(1) + n-hexadecane(2)) at T = 573.15 K (k_{ij} = 0.300). **(e)** System (water(1) + n-hexadecane(2)) at four different temperatures: T_1 = 613.15 K (k_{ij} = 0.210), T_2 = 623.15 K (k_{ij} = 0.189), T_3 = 633.15 K (k_{ij} = 0.169), T_4 = 638.15 K (k_{ij} = 0.160). **(f)** Critical locus of the system (water(1) + n-hexadecane(2)).

II.4.2 Results for mixtures of (water + branched alkane)

According to our data base, only a few experimental data are available for (water + branched alkane) mixtures [see table (II−2)] : 51 bubble points, 8 dew points and 8 critical points, among which none is reliable to fit the parameters of group 4 as defined by our group decomposition. The two parameters ($A_{16\text{-}4}$ and $B_{16\text{-}4}$) are thus set to zero. Moreover, most of these experimental data describe the mutual solubility at low temperature and atmospheric pressure which are not very useful for our data-fitting (the mole fractions are all zero or one). As a result, the two parameters ($A_{16\text{-}3}$ and $B_{16\text{-}3}$) are basically fitted on critical points. The prediction of critical locus of (2-methylpropane(1) + H_2O(2)) and that of (2-methylpentane(1) + H_2O(2)) are shown in figure (II−10). Similar to the (water + n-alkane) mixtures, the prediction accuracy decreases with the chain length of the branched alkane.

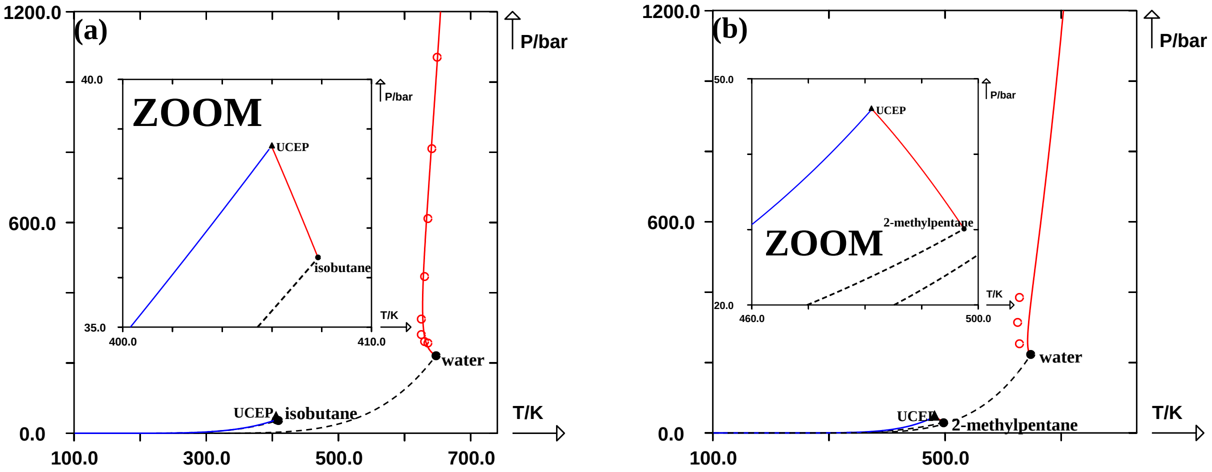

Figure II−10. Prediction of the critical locus for the two binary systems: (isobutane(1) + water(2)) and (2-methylpentane(1) + water(2)) using the PPR78 model. (○) experimental critical points, (●) critical points of the pure compounds, (▲) upper critical endpoint, UCEP. Solid line: predicted curves with the PPR78 model. Dashed line: vaporization curves of the pure compounds. **(a)** Critical locus of the system (isobutane(1) + water(2)). **(b)** Critical locus of the system (2-methylpentane(1) + water(2)).

II.4.3 Results for mixtures of (water + aromatic compound)

For the binary mixtures which consist of water and an aromatic compound, BIP ($k_{ij}(T)$) is a decreasing function of temperature, with an exception of (water(1) + 1-methylnaphthalene(2)). As can be seen in figure (II−11), the system (water(1) + benzene(2)) exhibits Type III phase behavior. In general, the VLE, VLLE and LLE are fairly reproduced, whereas the temperature minimum in the critical locus [figure (II−11f)] is slightly overestimated ($\Delta T \approx 10K$) but the slope of the evolution to higher pressures seems to be correct. We have to indicate that the shape of the critical locus for such system is difficult to well reproduce with a cubic EoS even by using temperature-dependent BIP ($k_{ij}(T)$) because the phase behavior switches to another kind (Type II), which is not reasonable, if we try to improve the accuracy of the critical temperature minimum. Figure (II−12) clearly presents the qualitative predictions of critical locus for some other binary systems containing water and an aromatic compound (toluene, o-xylene, ethylbenzene and n-propylbenzene), exhibiting Type III phase behavior. Figures (II−13a,13b,13c) are the plots of the isothermal phase diagram and critical locus for system (water(1) + 1,3,5-trimethylbenzene(2)). Qualitative representation can be observed owing to the fact that the solubility of water in 1,3,5-trimethylbenzne at high pressures are not accurate. On the other hand, reasonable results are obtained for (water(1) + 1-methylnaphthalene(2)), as shown in figures (II−13d,13e,13f). This system exhibits atypical Type III phase behavior and the high-pressure critical locus goes directly from the water critical point to higher pressures without a temperature minimum [figures (II−13f)]. Furthermore, BIP ($k_{ij}(T)$) of this system is a monotonous increasing function of temperature. Once again, we indicate here that most of the experimental critical points for (water + aromatic compound) mixtures are obtained from the work of Alwani and Schneider[113, 188] without the critical composition.

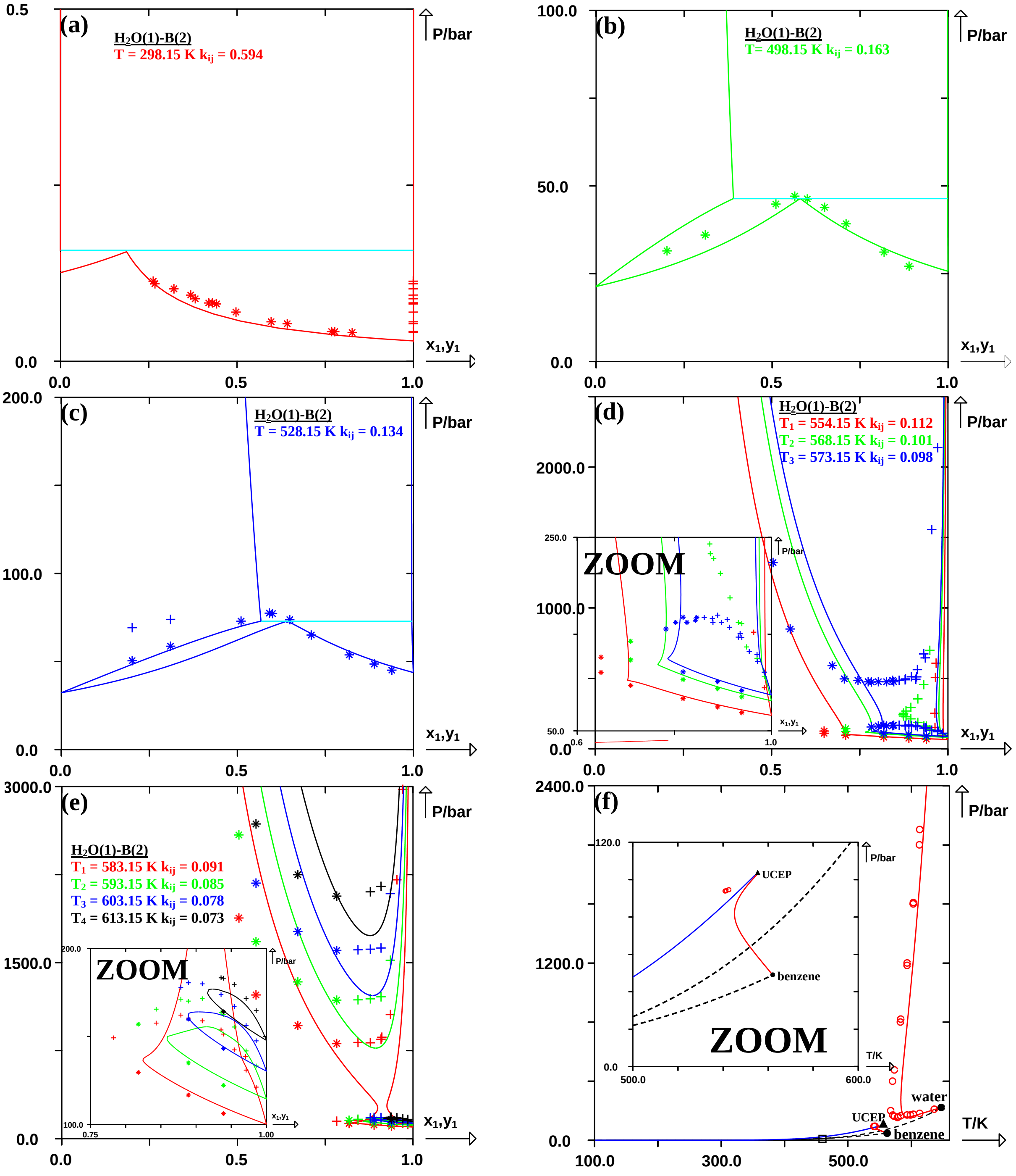

Figure II‒11. Prediction of isothermal curves and prediction of the critical locus for the binary system: (water(1) + benzene(2)) using the PPR78 model. (+) experimental bubble points, (✳) experimental dew points, (○) experimental critical points, (●) critical points of the pure compounds, (▲) upper critical endpoint, UCEP. Solid line: predicted curves with the PPR78 model. Dashed line: vaporization curves of the pure compounds. **(a)** System (water(1) + benzene(2)) at T = 298.15 K (k_{ij} = 0.594). **(b)** System (water(1) + benzene(2)) at T = 498.15 K (k_{ij} = 0.163). **(c)** System (water(1) + benzene(2)) at T = 528.15 K (k_{ij} = 0.134). **(d)** System (water(1) + benzene(2)) at three different temperatures: T_1 = 554.15 K (k_{ij} = 0.112), T_2 = 568.15 K (k_{ij} = 0.101), T_3 = 573.15 K (k_{ij} = 0.098). **(e)** System (water(1) + benzene(2)) at four different temperatures: T_1 = 583.15 K (k_{ij} = 0.091), T_2 = 593.15 K (k_{ij} = 0.085), T_3 = 603.15 K (k_{ij} = 0.078), T_4 = 613.15 K (k_{ij} = 0.073). **(f)** Critical locus of the system (water(1) + benzene(2)).

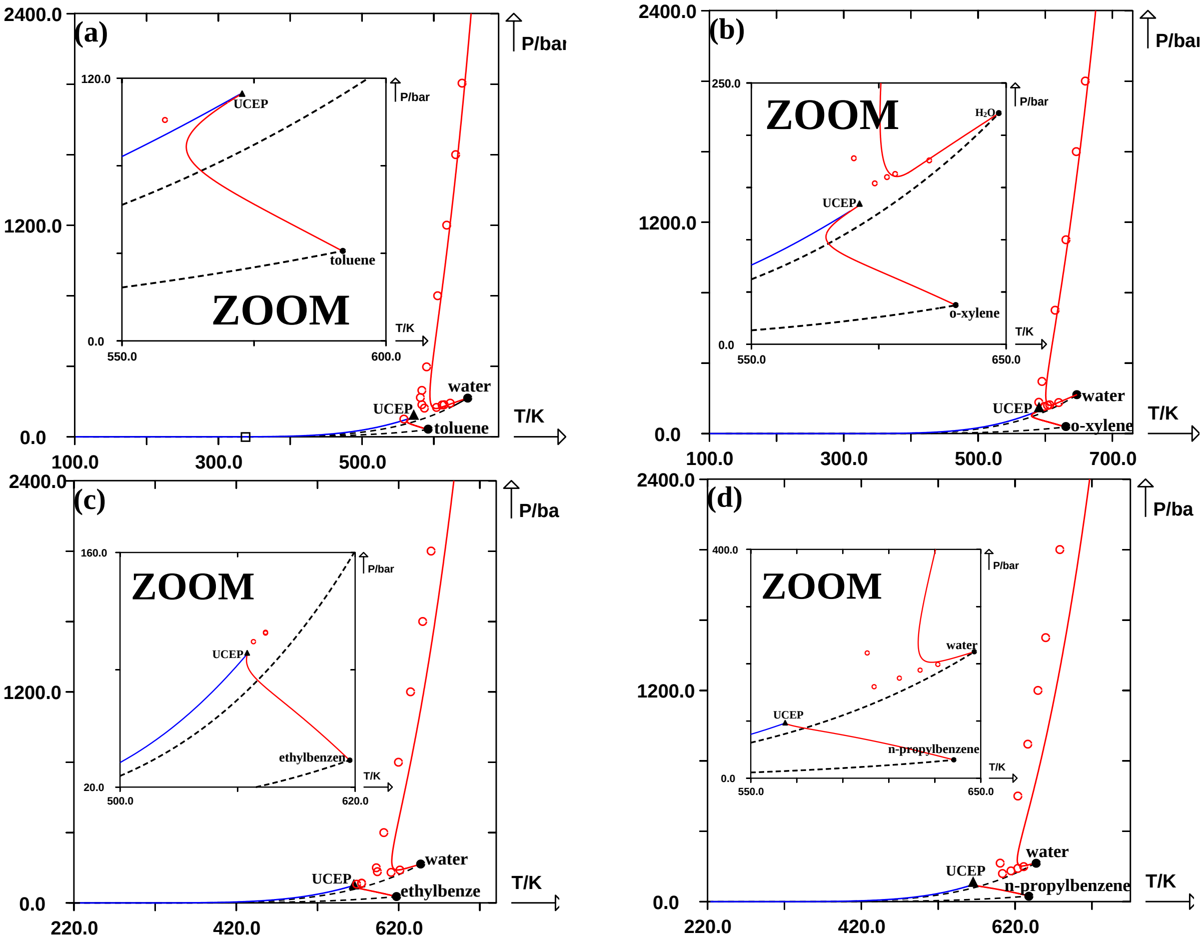

Figure II‒12. Prediction of the critical locus for the four binary systems: (water(1) + toluene(2)), (water(1) + o-xylene(2)), (water(1) + ethylbenzene(2)) and (water(1) + n-propylbenzene(2)) using the PPR78 model. (○) experimental critical points, (●) critical points of the pure compounds, (▲) upper critical endpoint, UCEP. Solid line: predicted curves with the PPR78 model. Dashed line: vaporization curves of the pure compounds. **(a)** Critical locus of the system (water(1) + toluene(2)). **(b)** Critical locus of the system (water(1) + o-xylene(2)). **(c)** Critical locus of the system (water(1) + ethylbenzene(2)). **(d)** Critical locus of the system (water(1) + n-propylbenzene(2)).

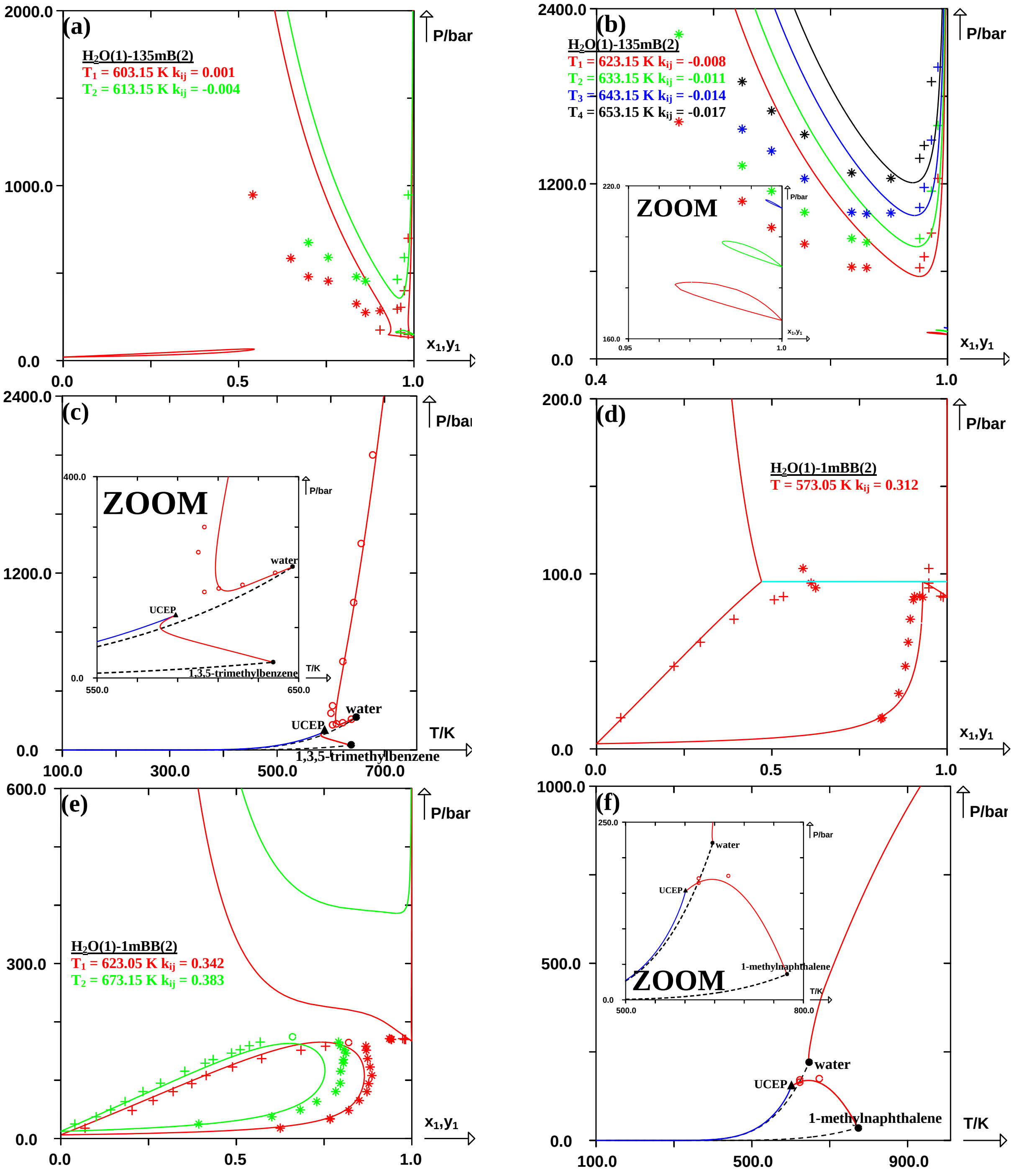

Figure II−13. Prediction of isothermal curves and prediction of the critical locus for the two binary systems: (water(1) + 1,3,5-trimethylbenzene(2)) and (water(1) + 1-methylnaphthalene(2)) using the PPR78 model. (+) experimental bubble points, (✳) experimental dew points, (○) experimental critical points, (●) critical points of the pure compounds, (▲) upper critical endpoint, UCEP. Solid line: predicted curves with the PPR78 model. Dashed line: vaporization curves of the pure compounds. **(a)** System (water(1) + 1,3,5-trimethylbenzene(2)) at two different temperatures: T_1 = 603.15 K (k_{ij} = 0.001), T_2 = 613.15 K (k_{ij} = -0.004). **(b)** System (water(1) + 1,3,5-trimethylbenzene(2)) at four different temperatures: T_1 = 623.15 K (k_{ij} = -0.008), T_2 = 633.15 K (k_{ij} = -0.011), T_3 = 643.15 K (k_{ij} = -0.014), T_4 = 653.15 K (k_{ij} = -0.017). **(c)** Critical locus of the system (water(1) + 1,3,5-trimethylbenzene(2)). **(d)** System (water(1) + 1-methylnaphthalene(2)) at T = 573.05 K (k_{ij} = 0.312). **(e)** System (water(1) + 1-methylnaphthalene(2)) at two different temperatures: T_1 = 623.05 K (k_{ij} = 0.342), T_2 = 673.15 K (k_{ij} = 0.383). **(f)** Critical locus of the system (water(1) + 1-methylnaphthalene(2)).

II.4.4 Results for mixtures of (water + naphthenic compound)

Although our data base involves eleven binary systems which consist of water and a naphthenic compound, only 192 bubble points, 158 dew points and 6 critical points are available in the open literature [see table (II−2)]. Furthermore, no experimental data point has been found at low temperatures where the prediction of our model could be uncertain. The experimental critical points without the critical composition are taken from the work of Broellos et al.[128] and Jockers et al.[189]. By looking at the results obtained by our model, the predicted isothermal curves and critical locus of (water(1) + cyclohexane(2)) are shown in figure (II−14), and those of (water(1) + tetralin(2)) and (water(1) + cis-decalin(2)) are presented in figure (II−15). Although the compositions of the hydrocarbon-rich liquid curves are not in close agreement with experimental data [see figures (II−14c, 15a,15e)] and the correlations of VLE are not very accurate in the vicinity of low-pressure critical branch [see figures (II−15b,15c)], all VLE, LLE and the VLL three-phase lines at moderate and high temperatures are generally predicted with an acceptable accuracy, as well as the critical loci. Type III phase behavior can be observed and BIP ($k_{ij}(T)$) is a monotonous decreasing function of temperature for these three binary systems.

II.4.5 Results for mixtures of (water + carbon dioxide)

Mixtures of (CO_2 + water) have been measured extensively [see table (II−2)] and there is a vast amount of reliable experimental phase equilibrium and critical data. As can be seen in figure (II−16f), the critical line starting from the critical point of water, goes through a temperature minimum and rises steeply to higher pressures. This Type III phase behavior is well reproduced by our model although the prediction in the low pressure region do not have perfect quality. At T = 298.15 K [see figure (II−16a)], the water-rich liquid is better reproduced than CO_2-rich liquid because of our objective function minimization, as outlined in section II.3.3. In general, the phase behavior of this family over a wide range of temperature and pressure is fairly predicted by using the PPR78 model. Moreover, in figure (II−16c.16d), we could observe that the experimental data measured by different authors are generally inconsistent, which increases the objective function and makes our parameters-fitting more difficult.

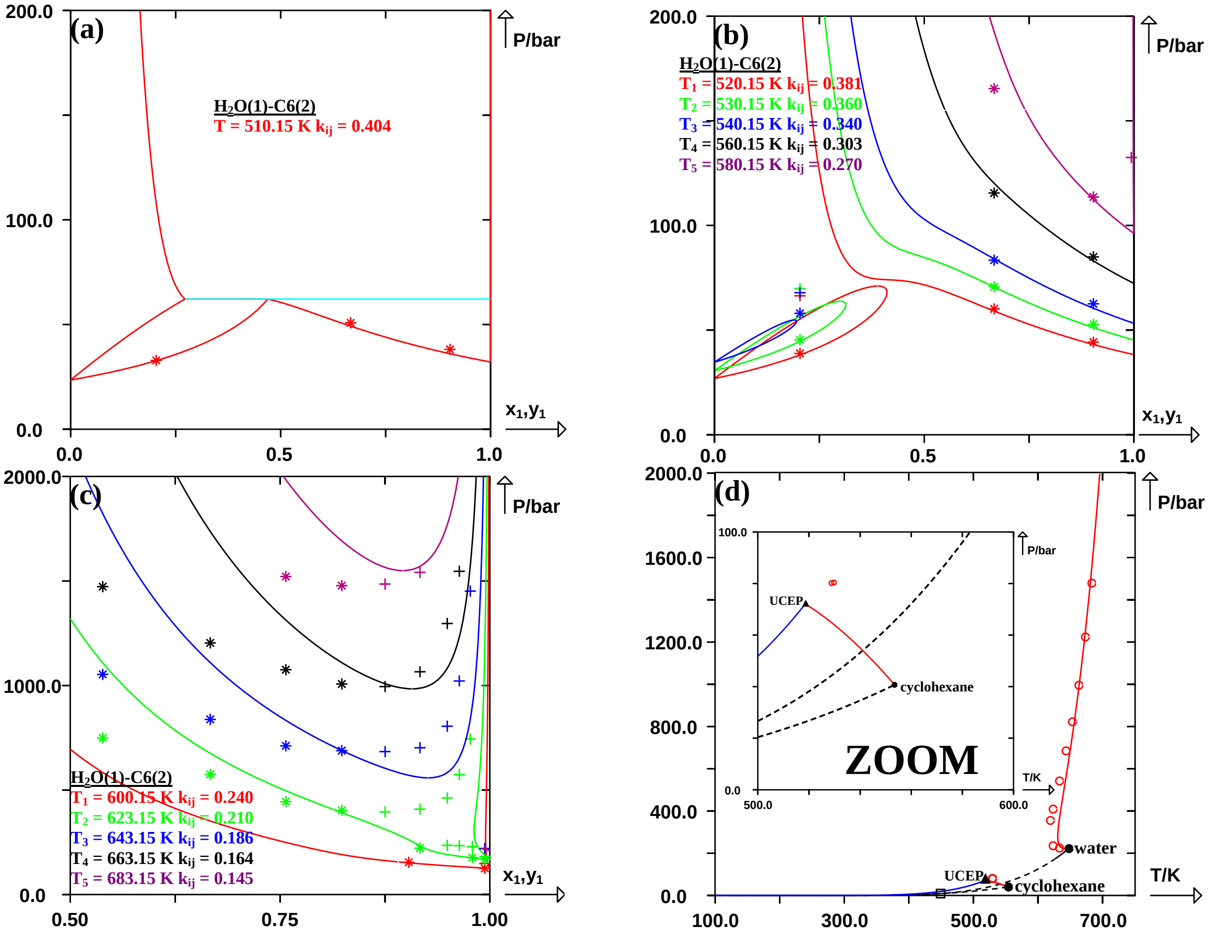

Figure II−14. Prediction of isothermal curves and prediction of the critical locus for the binary system: (water(1) + cyclohexane(2)) using the PPR78 model. (+) experimental bubble points, (✳) experimental dew points, (○) experimental critical points, (●) critical points of the pure compounds, (▲) upper critical endpoint, UCEP. Solid line: predicted curves with the PPR78 model. Dashed line: vaporization curves of the pure compounds. **(a)** System (water(1) + cyclohexane(2)) at T = 510.15 K (k_{ij} = 0.404). **(b)** System (water(1) + cyclohexane(2)) at five different temperatures: T_1 = 520.15 K (k_{ij} = 0.381), T_2 = 530.15 K (k_{ij} = 0.360), T_3 = 540.15 K (k_{ij} = 0.340), T_4 = 560.15 K (k_{ij} = 0.303), T_5 = 580.15 K (k_{ij} = 0.270). **(c)** System (water(1) + cyclohexane(2)) at five different temperatures: T_1 = 600.15 K (k_{ij} = 0.240), T_2 = 623.15 K (k_{ij} = 0.210), T_3 = 643.15 K (k_{ij} = 0.186), T_4 = 663.15 K (k_{ij} = 0.164), T_5 = 683.15 K (k_{ij} = 0.145). **(d)** Critical locus of the system (water(1) + cyclohexane(2)).

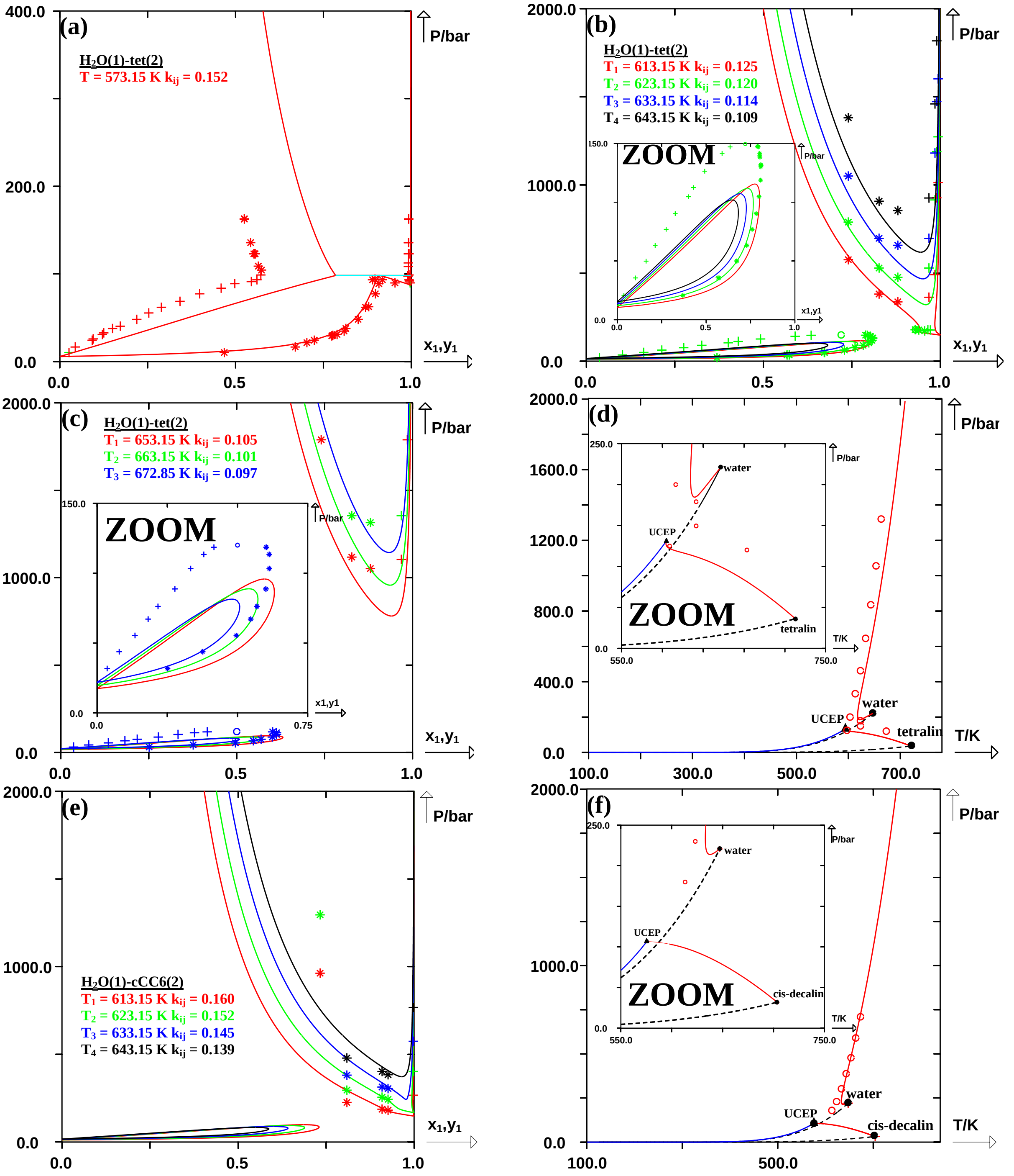

Figure II‒15. Prediction of isothermal curves and prediction of the critical locus for the two binary systems: (water(1) + tetralin(2)) and (water(1) + cis-decalin(1)) using the PPR78 model. (+) experimental bubble points, (✳) experimental dew points, (○) experimental critical points, (●) critical points of the pure compounds, (▲) upper critical endpoint, UCEP. Solid line: predicted curves with the PPR78 model. Dashed line: vaporization curves of the pure compounds. **(a)** System (water(1) + tetralin(2)) at T = 573.15 K (k_{ij} = 0.152). **(b)** System (water(1) + tetralin(2)) at four different temperatures: T_1 = 613.15 K (k_{ij} = 0.125), T_2 = 623.15 K (k_{ij} = 0.120), T_3 = 633.15 K (k_{ij} = 0.114), T_4 = 643.15 K (k_{ij} = 0.109). **(c)** System (water(1) + tetralin(2)) at three different temperatures: T_1 = 653.15 K (k_{ij} = 0.105), T_2 = 663.15 K (k_{ij} = 0.101), T_3 = 672.85 K (k_{ij} = 0.097). **(d)** Critical locus of the system (water(1) + tetralin(2)). **(e)** System (water(1) + cis-decalin(2)) at four different temperatures: T_1 = 613.15 K (k_{ij} = 0.160), T_2 = 623.15 K (k_{ij} = 0.152), T_3 = 633.15 K (k_{ij} = 0.145), T_4 = 643.15 K (k_{ij} = 0.139). **(f)** Critical locus of the system (water(1) + cis-decalin(2)).

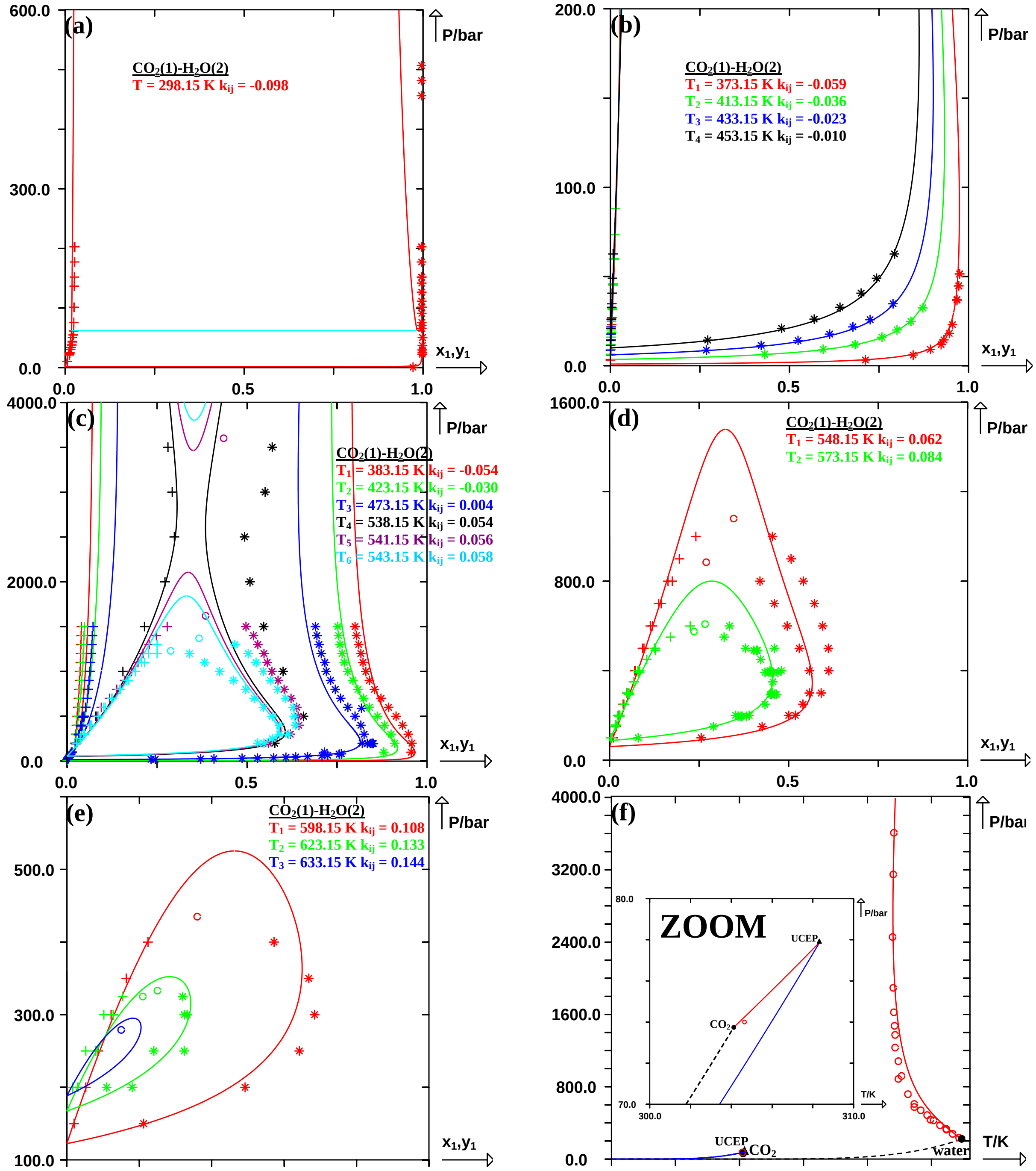

Figure II−16. Prediction of isothermal curves and prediction of the critical locus for the binary system: (CO_2(1) + H_2O(2)) using the PPR78 model. (+) experimental bubble points, (✳) experimental dew points, (○) experimental critical points, (●) critical points of the pure compounds, (▲) upper critical endpoint, UCEP. Solid line: predicted curves with the PPR78 model. Dashed line: vaporization curve of the pure compounds. **(a)** System (CO_2(1) + H_2O(2)) at T = 298.15 K (k_{ij} = -0.098). **(b)** System (CO_2(1) + H_2O(2)) at four different temperatures: T_1 = 373.15 K (k_{ij} = -0.059), T_2 = 413.15 K (k_{ij} = -0.036), T_3 = 433.15 K (k_{ij} = -0.023), T_4 = 453.15 K (k_{ij} = -0.010). **(c)** System (CO_2(1) + H_2O(2)) at six different temperatures: T_1 = 383.15 K (k_{ij} = -0.054), T_2 = 423.15 K (k_{ij} = -0.030), T_3 = 473.15 K (k_{ij} = 0.004), T_4 = 538.15 K (k_{ij} = 0.054), T_5 = 541.15 K (k_{ij} = 0.056), T_6 = 543.15 K (k_{ij} = 0.058). **(d)** System (CO_2(1) + H_2O(2)) at two different temperatures: T_1 = 548.15 K (k_{ij} = 0.062), T_2 = 573.15 K (k_{ij} = 0.084). **(e)** System (CO_2(1) + H_2O(2)) at three different temperatures: T_1 = 598.15 K (k_{ij} = 0.108), T_2 = 623.15 K (k_{ij} = 0.133), T_3 = 633.15 K (k_{ij} = 0.144). **(f)** Critical locus of the system (CO_2(1) + H_2O(2)).

II.4.6 Results for mixtures of (water + nitrogen)

Figure (II−17) presents the predicted P-xy diagrams at twelve different temperatures and the predicted P-T diagram for (N_2(1) + water(2)). The phase behavior of this family is very similar to that of (methane(1) + water(2)). But the BIP (k_{ij}(T)) decrease more remarkably with temperature here, varying from 0.717 to -0.114, showing negative values at high temperatures.

II.4.7 Results for mixtures of (water + hydrogen sulfide)

The P-xy and P-T diagrams of (H_2S(1) + water(2)) are plotted in figure (II−18). The VLE and LLE phase behaviors are predicted with reasonable accuracy except that the correlation of the H_2S-rich liquid phase at high pressures is not very satisfactory [see figure (II−18b)] which is the similar drawback as (CO_2(1) + water(2)). According to our data base, the 719 experimental data points unfortunately do not contain any critical point in the critical locus starting from the critical point of water. Thus, the prediction of the critical locus in this high-pressure region has not been verified.

II.4.8 Results for mixtures of (water + mercaptans)

The study of these systems has been limited by the lack of experimental data. We found only 43 bubble points, 22 dew points and 0 critical point in the open literature. The PPR78 is able to represent the few experimental data for the binary systems: (methyl mercaptan(1) + water(2)) and (ethyl mercaptan(1) + water(2)), shown in figure (II−19). Once again, the performance of our model in the critical region has not been verified.

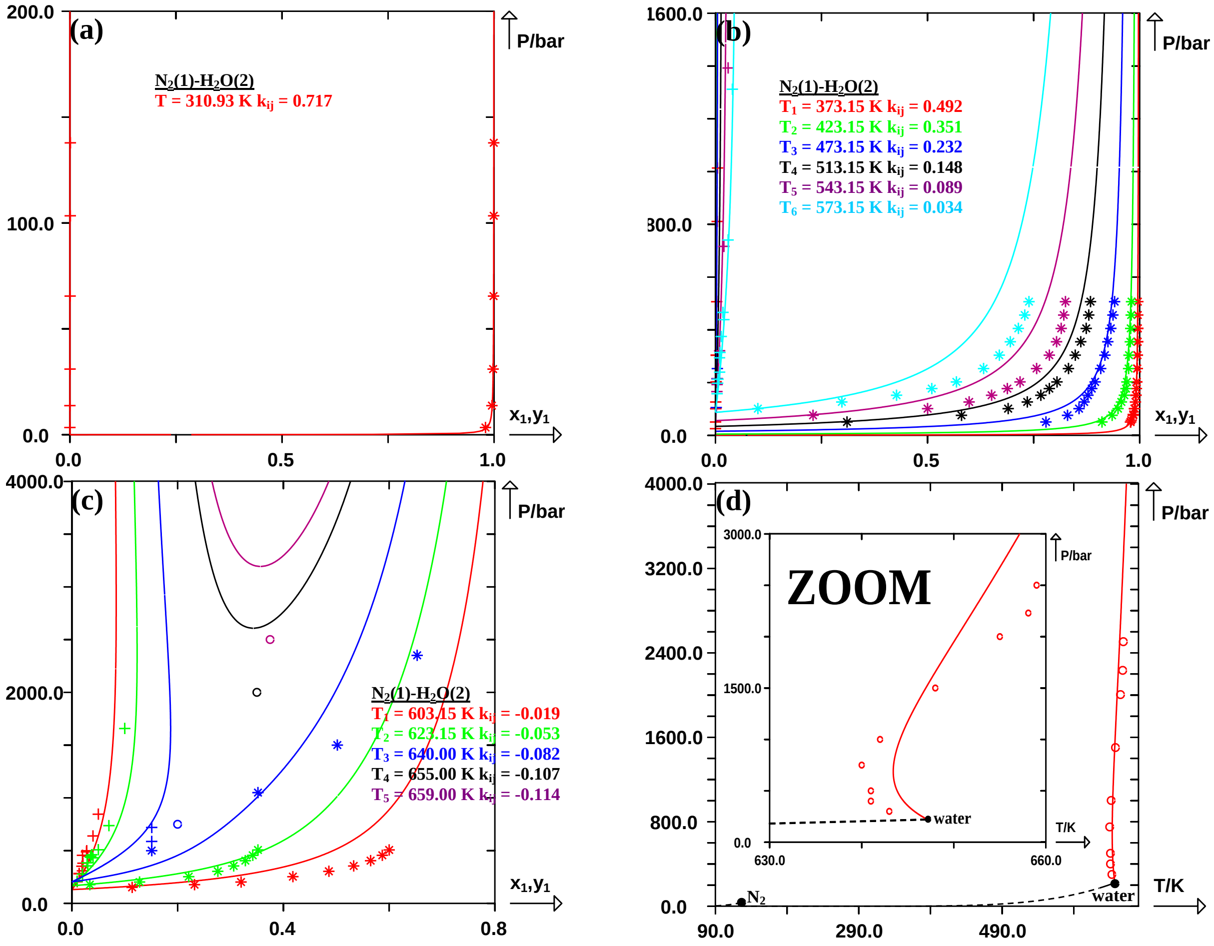

Figure II‒17. Prediction of isothermal curves and prediction of the critical locus for the binary system: (N_2(1) + H_2O(2)) using the PPR78 model. (+) experimental bubble points, (✳) experimental dew points, (○) experimental critical points, (●) critical points of the pure compounds. Solid line: predicted curves with the PPR78 model. Dashed line: vaporization curve of the pure compounds. **(a)** System (N_2(1) + H_2O(2)) at T = 310.93 K (k_{ij} = 0.717). **(b)** System (N_2(1) + H_2O(2)) at six different temperatures: T_1 = 373.15 K (k_{ij} = 0.492), T_2 = 423.15 K (k_{ij} = 0.351), T_3 = 473.15 K (k_{ij} = 0.232), T_4 = 513.15 K (k_{ij} = 0.148), T_5 = 543.15 K (k_{ij} = 0.089), T_6 = 573.15 K (k_{ij} = 0.034). **(c)** System (N_2(1) + H_2O(2)) at five different temperatures: T_1 = 603.15 K (k_{ij} = -0.019), T_2 = 623.15 K (k_{ij} = -0.053), T_3 = 640.00 K (k_{ij} = -0.082), T_4 = 655.00 K (k_{ij} = -0.107), T_5 = 659.00 K (k_{ij} = -0.114). **(d)** Critical locus of the system (N_2(1) + H_2O(2)).

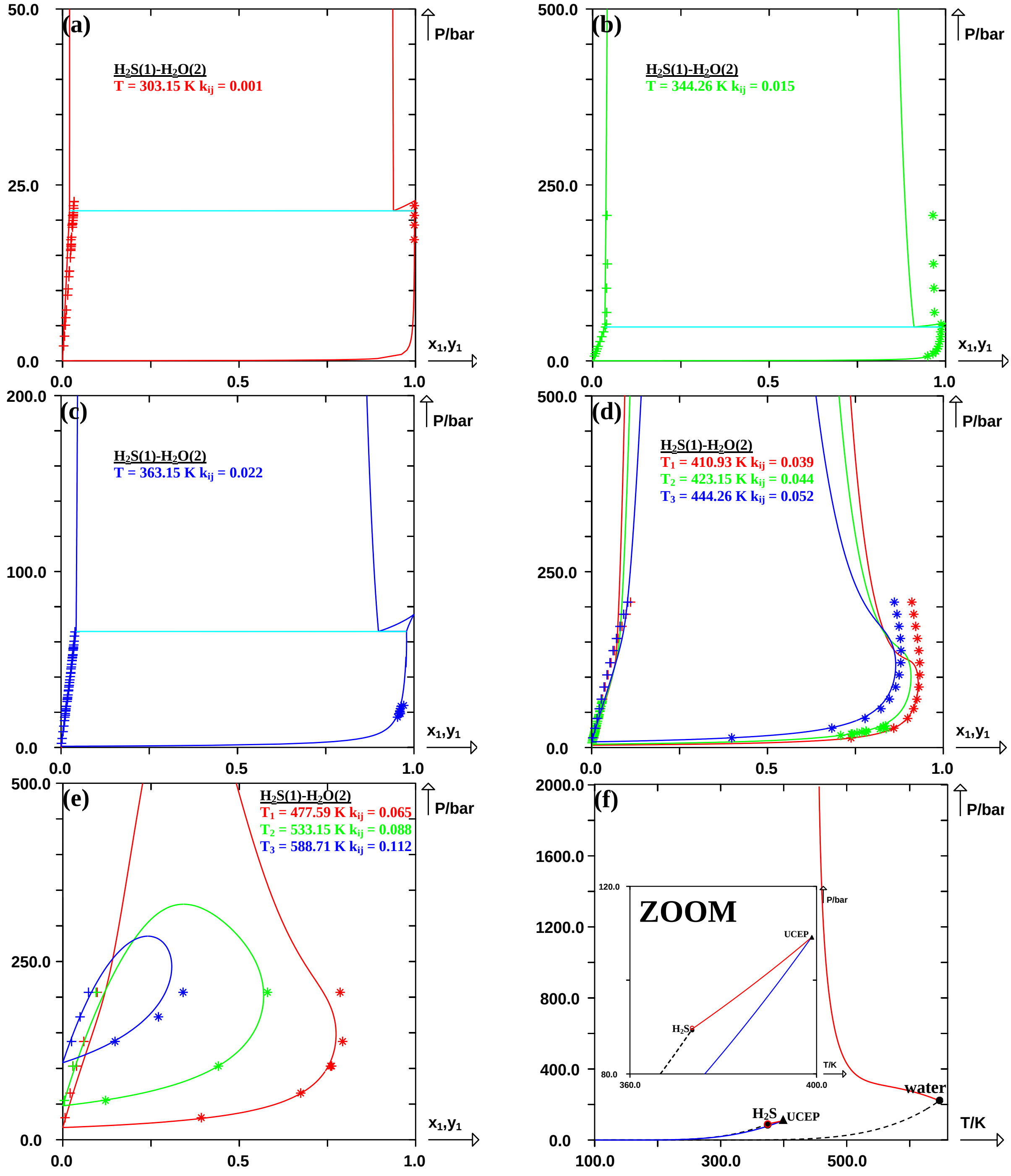

Figure II−18. Prediction of isothermal curves and prediction of the critical locus for the binary system: (H_2S(1) + H_2O(2)) using the PPR78 model. (+) experimental bubble points, (✳) experimental dew points, (○) experimental critical points, (●) critical points of the pure compounds, (▲) upper critical endpoint, UCEP. Solid line: predicted curves with the PPR78 model. Dashed line: vaporization curve of the pure compounds. **(a)** System (H_2S(1) + H_2O(2)) at T = 303.15 K (k_{ij} = 0.001). **(b)** System (H_2S(1) + H_2O(2)) at T = 344.26 K (k_{ij} = 0.015). **(c)** System (H_2S(1) + H_2O(2)) at T = 363.15 K (k_{ij} = 0.022). **(d)** System (H_2S(1) + H_2O(2)) at three different temperatures: T_1 = 410.93 K (k_{ij} = 0.039), T_2 = 423.15 K (k_{ij} = 0.044), T_3 = 444.26 K (k_{ij} = 0.052). **(e)** System (H_2S(1) + H_2O(2)) at three different temperatures: T_1 = 477.59 K (k_{ij} = 0.065), T_2 = 533.15 K (k_{ij} = 0.088), T_3 = 588.71 K (k_{ij} = 0.112). **(f)** Critical locus of the system (H_2S(1) + H_2O(2)).

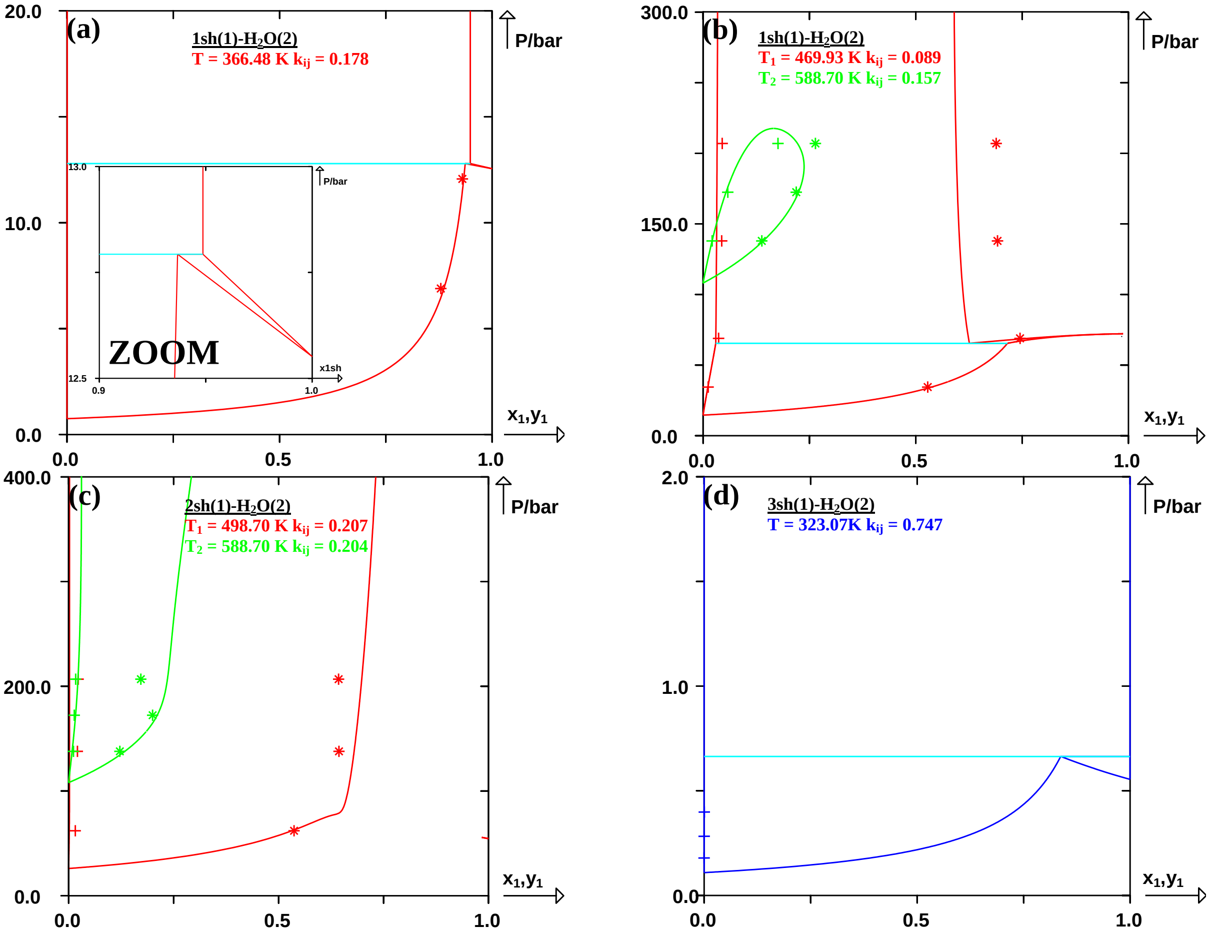

Figure II‒19. Prediction of isothermal curves for the three binary systems: (methyl mercaptan(1) + water(2)), (ethyl mercaptan(1) + water(2)) and (n-propyl mercaptan(1) + water(2)) using the PPR78 model. (+) experimental bubble points, (✳) experimental dew points. Solid line: predicted curves with the PPR78 model. Dashed line: vaporization curve of the pure compounds. **(a)** System (methyl mercaptan(1) + water(2)) at T = 366.48 K (k_{ij} = 0.178). **(b)** System (methyl mercaptan(1) + water(2)) at two different temperatures: T_1 = 469.93 K (k_{ij} = 0.089), T_2 = 588.70 K (k_{ij} = 0.157). **(c)** System (ethyl mercaptan(1) + water(2)) at two different temperatures: T_1 = 498.70 K (k_{ij} = 0.207), T_2 = 588.70 K (k_{ij} = 0.204). **(d)** System (n-propyl mercaptan(1) + water(2)) at T = 323.07 K (k_{ij} = 0.747).

II.5 Conclusion

In this study, the PPR78 model has been extended to systems containing water that are highly non-ideal and most of them exhibit Type III phase behavior. It is really difficult to correctly predict the phase behaviors of such systems by using a cubic EoS, even with temperature-dependent BIP ($k_{ij}(T)$), for the following reasons:

- Temperature-dependent BIP ($k_{ij}(T)$) could not correlate simultaneously the critical behaviors and the subcritical phase equilibria with quite high accuracy.
- For some of the mixtures in our study, it is impossible to perfectly reproduce both the water-rich liquid phase and the hydrocarbon-rich liquid phase at one temperature by using a single k_{ij} value.
- In the vicinity of the low-pressure critical line, there is no k_{ij} value that could well predict at the same time, the LLE at high-pressure region and the VLE at low-pressure region.
- The quality of the prediction of critical locus decreases with the chain length of alkane.

From a general overview on the results obtained in this study, we can conclude that although quantitative predictions may not be of high quality for some of the studied systems, the predictions using PPR78 model are qualitatively accurate for so many systems over wide ranges of temperature and pressure. From now on, it is possible to estimate the BIP ($k_{ij}(T)$) for any mixture containing water, mercaptans, H_2S, N_2, CO_2, naphthenes, aromatics and alkanes at any temperature.

References

(1) Van Konynenburg, P. H.; Scott, R. L. Critical lines and phase equilibria in binary van der Waals mixtures. *Philos. Trans. R. Soc. London, Ser. A* **1980**, *298*, 495-540.
(2) Mohammadi, A. M. Estimation of water content in sour gases. *67th European Association of Geoscientists and Engineers, EAGE Conference and Exhibition, incorporating SPE EUROPE2005 - Extended Abstracts* **2005**, 2603-2612.
(3) Montel, F. Phase equilibria needs for petroleum exploration and production industry. *Fluid Phase Equilib.* **1993**, *84* (C), 343-367.
(4) Yakoumis, I. V.; Nikitin, E.; Kontogeorgis, G. M. Validation of a recent generalized expression of Tc/Pc vs. the van der Waals surface area according to recent measurements. *Fluid Phase Equilib.* **1998**, *153* (1), 23-27.
(5) Dutkiewicz, A.; Ridley, J.; Buick, R. Oil-bearing CO2-CH4-H2O fluid inclusions: oil survival since the Palaeoproterozoic after high temperature entrapment. *Chemical Geology* **2003**, *194* (1-3), 51-79.
(6) Houghton, J. Global warming. *Reports on Progress in Physics* **2005**, *68* (6), 1343-1403.
(7) Tsonopoulos, C.; Heidman, J. L. High-pressure vapor-liquid equilibria with cubic equations of state. *Fluid Phase Equilib.* **1986**, *29* (C), 391-414.
(8) Economou, I. G.; Donohue, M. D. Equations of state for hydrogen bonding systems. *Fluid Phase Equilib.* **1996**, *116* (1-2), 518-529.
(9) Mathias, P. M.; Copeman, T. W. Extension of the Peng-Robinson equation of state to complex mixtures: evaluation of the various forms of the local composition concept. *Fluid Phase Equilib.* **1983**, *13*, 91-108.
(10) Michel, S.; Hooper, H. H.; Prausnitz, J. M. Mutual solubilities of water and hydrocarbons from an equation of state. Need for an unconventional mixing rule. *Fluid Phase Equilib.* **1989**, *45* (2-3), 173-189.
(11) Wong, D. S. H.; Orbey, H.; Sandler, S. I. Equation of state mixing rule for nonideal mixtures using available activity coefficient model parameters and that allows extrapolation over large ranges of temperature and pressure. *Ind. Eng. Chem. Res.* **1992**, *31* (8), 2033-2039.
(12) Michelsen, M. L. A modified Huron-Vidal mixing rule for cubic equations of state. *Fluid Phase Equilib.* **1990**, *60* (1-2), 213-219.
(13) Dahl, S.; Michelsen, M. L. High-pressure vapor-liquid equilibrium with a UNIFAC-based equation of state. *AIChE J.* **1990**, *36* (12), 1829-1836.
(14) Kolár, P.; Kojima, K. Prediction of critical points in multicomponent systems using the PSRK group contribution equation of state. *Fluid Phase Equilib.* **1996**, *118* (2), 175-200.
(15) Alvarado, G. E.; Castier, M.; Sandler, S. I. Predictions of critical behavior using the Wong-Sandler mixing rule. *Journal of Supercritical Fluids, The* **1998**, *13* (1-3), 49-54.
(16) Polishuk, I.; Wisniak, J.; Segura, H. Simultaneous prediction of the critical and sub-critical phase behavior in mixtures using equation of state I. Carbon dioxide-alkanols. *Chem. Eng. Sci.* **2001**, *56* (23), 6485-6510.
(17) Castier, M.; Sandler, S. I. Critical points with the Wong-Sandler mixing rule--II. Calculations with a modified Peng-Robinson equation of state. *Chem. Eng. Sci.* **1997**, *52* (20), 3579-3588.
(18) Wang, M.-C.; Wong, D. S.-H. Calculation of critical lines of hydrocarbon/water systems by extrapolating mixing rules fitted to subcritical equilibrium data. *Fluid Phase Equilib.* **2005**, *227* (2), 183-196.
(19) Galindo, A.; Whitehead, P. J.; Jackson, G., Predicting the High-Pressure Phase Equilibria of Water + n-Alkanes Using a Simplified SAFT Theory with Transferable Intermolecular Interaction Parameters. In *The Journal of Physical Chemistry*, American Chemical Society: 1996; Vol. 100, pp 6781-6792.
(20) Economou, I. G.; Tsonopoulos, C. Associating models and mixing rules in equations of state for water/hydrocarbon mixtures. *Chem. Eng. Sci.* **1997**, *52* (4), 511-525.
(21) Voutsas, E. C.; Boulougouris, G. C.; Economou, I. G.; Tassios, D. P. Water/Hydrocarbon Phase Equilibria Using the Thermodynamic Perturbation Theory. *Ind. Eng. Chem. Res.* **2000**, *39* (3), 797-804.
(22) Aparicio-Martínez, S.; Hall, K. R. Phase equilibria in water containing binary systems from molecular based equations of state. *Fluid Phase Equilib.* **2007**, *254* (1-2), 112-125.
(23) Jaubert, J.-N.; Mutelet, F. VLE predictions with the Peng-Robinson equation of state and temperature dependent kij calculated through a group contribution method. *Fluid Phase Equilib.* **2004**, *224* (2), 285-304.
(24) Jaubert, J.-N.; Vitu, S.; Mutelet, F.; Corriou, J.-P. Extension of the PPR78 model (predictive 1978, Peng-Robinson EOS with temperature dependent kij calculated through a group contribution method) to systems containing aromatic compounds. *Fluid Phase Equilib.* **2005**, *237* (1-2), 193-211.
(25) Privat, R.; Jaubert, J. N.; Mutelet, F. Addition of the nitrogen group to the PPR78 model (predictive 1978, Peng Robinson EOS with temperature-dependent kij calculated through a group contribution method. *Ind. Eng. Chem. Res.* **2008**, *47* (6), 2033-2048.

(26) Privat, R.; Jaubert, J. N.; Mutelet, F. Addition of the sulfhydryl group (-SH) to the PPR78 model (predictive 1978, Peng-Robinson EOS with temperature dependent kij calculated through a group contribution method). *Journal of Chemical Thermodynamics* **2008**, *40* (9), 1331-1341.
(27) Privat, R.; Mutelet, F.; Jaubert, J. N. Addition of the hydrogen sulfide group to the PPR 78, Model (Predictive 1978, Peng-Robinson equation of state with temperature dependent kij- calculated through a group contribution method). *Ind. Eng. Chem. Res.* **2008**, *47* (24), 10041-10052.
(28) Vitu, S.; Jaubert, J.-N.; Mutelet, F. Extension of the PPR78 model (Predictive 1978, Peng-Robinson EOS with temperature dependent kij calculated through a group contribution method) to systems containing naphtenic compounds. *Fluid Phase Equilib.* **2006**, *243* (1-2), 9-28.
(29) Vitu, S.; Privat, R.; Jaubert, J. N.; Mutelet, F. Predicting the phase equilibria of CO2 + hydrocarbon systems with the PPR78 model (PR EOS and kij calculated through a group contribution method). *Journal of Supercritical Fluids* **2008**, *45* (1), 1-26.
(30) Poling, B. E.; Prausnitz, J. M.; O'Connell, J. P. *The Properties of Gases and Liquids, 5th Ed.* **2000**, 11-18.
(31) Azarnoosh, A.; McKetta, J. J. The Solubility of Propane in Water. *Pet. Refiner* **1958**, *37* (11), 275-278.
(32) Blanco, S. T.; Velasco, I.; Rauzy, E.; Otin, S. Water dew points of binary nitrogen + water and propane + water mixtures. Measurement and correlation. *Fluid Phase Equilib.* **1999**, *161* (1), 107-117.
(33) Chapoy, A.; Mokraoui, S.; Valtz, A.; Richon, D.; Mohammadi, A. H.; Tohidi, B. Solubility measurement and modeling for the system propane-water from 277.62 to 368.16K. *Fluid Phase Equilib.* **2004**, *226*, 213-220.
(34) De Loos, T. W.; Wijen, A. J. M.; Diepen, G. A. M. Phase equilibriums and critical phenomena in fluid (propane + water) at high pressures and temperatures. *J. Chem. Thermodyn.* **1980**, *12* (2), 193-204.
(35) Klausutis, N. Phase equilibrium in the propane - propylene - water system in the three - phase region. *Ph.D. thesis, Austin, Texas* **1968**, 1-113.
(36) Kobayashi, R.; Katz, D. L. Vapor-liquid equilibria for binary hydrocarbon-water systems. *J. Ind. Eng. Chem. (Washington, D. C.)* **1953**, *45*, 440-446.
(37) Sanchez, M.; Coll, R. Propane-water system at high pressures and temperatures. I. Two-phase region. *An. Quim.* **1978**, *74* (11), 1329-1335.
(38) Umano, S.; Nakano, Y. Solubility of propane and butane in salt solution. *Kogyo Kagaku Zasshi* **1958**, *61*, 536-542.
(39) Wehe, A. H.; McKetta, J. J. Method for Determining Total Hydrocarbons Dissolved in Water. *Anal. Chem.* **1961**, *33* (2), 291-293.
(40) Brooks, W. B.; Gibbs, G. B.; McKetta, J. J. Mutual Solubilities of Light Hydrocarbon - Water Systems. *Pet. Refiner* **1951**, *30*, 118-120.
(41) Carroll, J. J.; Jou, F.-Y.; Mather, A. E. Fluid phase equilibria in the system n-butane+water. *Fluid Phase Equilib.* **1997**, *140* (1-2), 157-169.
(42) Le Breton, J. G.; McKetta, J. J. Low Pressure Solubility of n-Butane in Water. *Hydrocarbon Process. Pet. Refiner* **1964**, *43* (6), 136-138.
(43) Reamer, H. H.; Olds, R. H.; Sage, B. H.; Lacey, W. N. Phase equilibria in hydrocarbon systems. XLIII. Compositions of the coexisting phases of n-butane-water system in the 3-phase region. *J. Ind. Eng. Chem. (Washington, D. C.)* **1944**, *36*, 381-383.
(44) Reamer, H. H.; Sage, B. H.; Lacey, W. N. Phase equilibria in hydrocarbon systems. n-Butane-water system in the two-phase region. *J. Ind. Eng. Chem. (Washington, D. C.)* **1952**, *44*, 609-615.
(45) Tian, Y.; Michelberger, T.; Franck, E. U. High-pressure phase equilibria and critical curves of (water + n-butane) and (water + n-hexane) at temperatures to 700 K and pressures to 300 MPa. *J. Chem. Thermodyn.* **1991**, *23* (1), 105-112.
(46) Tian, Y.; Zhao, X.; Chen, L.; Zhu, H.; Fu, H. High pressure phase equilibria and critical phenomena of water + iso-butane and water + n-butane systems to 695 K and 306 MPa. *J. Supercrit. Fluids* **2004**, *30* (2), 145-153.
(47) De Loos, T. W.; Van, D. J. H.; Lichtenthaler, R. N. Phase equilibriums and critical phenomena in fluid (n-alkane + water) systems at high pressures and temperatures. *Fluid Phase Equilib.* **1983**, *10* (2-3), 279-287.
(48) Jou, F.-Y.; Mather, A. E. Vapor-Liquid-Liquid Locus of the System Pentane + Water. *J. Chem. Eng. Data* **2000**, *45* (5), 728-729.
(49) Barrufet, M. A.; Liu, K.; Rahman, S.; Wu, C. Simultaneous Vapor-Liquid-Liquid Equilibria and Phase Molar Densities of a Quaternary System of Propane + Pentane + Octane + Water. *J. Chem. Eng. Data* **1996**, *41* (4), 918-922.
(50) Namiot, A. Y.; Skripka, V. G.; Lotter, Y. G. Phase Equilibria in Hydrocarbon - Water Systems at High Temperatures. *Deposited Doc. VINITI* **1976**, (1213-76), 1-13.
(51) Rasulov, S. M.; Rasulov, A. R. Experimental investigation of the thermal properties of a binary n-hexane-water mixture at high temperatures and pressures. *High Temp.* **2000**, *38* (3), 389-393.

(52) Rebert, C. J.; Hayworth, K. E. Gas and liquid solubility relations in hydrocarbon-water systems. *AIChE J.* **1967**, *13* (1), 118-121.

(53) Rezanova, E. N.; Toikka, A. M.; Markuzin, N. P. Equilibrium of two and three liquid phases with vapor in the n-heptane-nitromethane-water system. I. Experimental data. *Vestn. Leningr. Univ., Ser. 4: Fiz., Khim.* **1991**, (3), 53-56.

(54) Skripka, V. G.; Gubkina, G. V.; Boksha, O. A. Phase Equilibria Between n-Alkanes and Water at Elevated Temperatures and Pressures. *Deposited Doc. VINITI* **1973**, (7271-73), 1-6.

(55) Brady, C. J.; Cunningham, J. R.; Wilson, G. M. Water - Hydrocarbon Liquid-Liquid-Vapor Equilibrium Measurements to 530 degrees F. *GPA Research Report* **1982**, (RR-62), 1-66.

(56) Sultanov, R. G.; Skripka, V. G. Solubility of Water in n-Alkanes at Elevated Temperatures and Pressures. *Deposited Doc. VINITI* **1972**, (4386-72), 1-13.

(57) Tu, M.; Fei, D.; Liu, Y.; Wang, J. Phase Equilibrium for Partially Miscible System of Octane - Water. *Gaoxiao Huaxue Gongcheng Xuebao* **1998**, *12* (4), 325-330.

(58) Haruki, M.; Iwai, Y.; Nagao, S.; Yahiro, Y.; Arai, Y. Measurement and Correlation of Phase Equilibria for Water + Hydrocarbon Systems near the Critical Temperature and Pressure of Water. *Ind. Eng. Chem. Res.* **2000**, *39* (12), 4516-4520.

(59) Wang, Q.; Chao, K. C. Vapor-liquid and liquid-liquid equilibria and critical states of water + n-decane mixtures. *Fluid Phase Equilib.* **1990**, *59* (2), 207-215.

(60) Wang, Q.; Chen, G.; Han, S. Critical locus of water-n-decane mixtures. *Shiyou Huagong* **1995**, *24* (1), 35-38.

(61) Stevenson, R. L.; LaBracio, D. S.; Beaton, T. A.; Thies, M. C. Fluid phase equilibria and critical phenomena for the dodecane-water and squalane-water systems at elevated temperatures and pressures. *Fluid Phase Equilib.* **1994**, *93*, 317-336.

(62) Breman, B. B.; Beenackers, A. A. C. M.; Rietjens, E. W. J.; Stege, R. J. H. Gas-Liquid Solubilities of Carbon Monoxide, Carbon Dioxide,Hydrogen, Water, 1-Alcohols ($1 \leq n \leq 6$), and n-Paraffins ($2 \leq n \leq 6$) in Hexadecane, Octacosane, 1-Hexadecanol, Phenanthrene, and Tetraethylene Glycol at Pressures up to 5.5 MPa and Temperatures from 293 to 553 K. *J. Chem. Eng. Data* **1994**, *39* (4), 647-666.

(63) Sultanov, R. G.; Skripka, V. G.; Namiot, A. Y. Phase Equilibria in the System Water - n-Hexadecane at elevated Temperatures. *Deposited Doc. VINITI* **1971**, (3139-71), 1-11.

(64) Black, C.; Joris, G. G.; Taylor, H. S. The solubility of water in hydrocarbons. *J. Chem. Phys.* **1948**, *16*, 537-543.

(65) McAuliffe, C. Solubility in water of paraffin, cycloparaffin, olefin, acetylene, cycloolefin, and aromatic hydrocarbons. *J. Phys. Chem.* **1966**, *70* (4), 1267-1275.

(66) Wetlaufer, D. B.; Malik, S. K.; Stoller, L.; Coffin, R. L. Nonpolar group participation in the denaturation of proteins by urea and guanidinium salts. Model compound studies. *J. Am. Chem. Soc.* **1964**, *86* (3), 508-514.

(67) Connolly, J. F. Solubility of hydrocarbons in water near the critical solution temperatures. *J. Chem. Eng. Data* **1966**, *11* (1), 13-16.

(68) Pereda, S.; Awan, J. A.; Mohammadi, A. H.; Valtz, A.; Coquelet, C.; Brignole, E. A.; Richon, D. Solubility of hydrocarbons in water: Experimental measurements and modeling using a group contribution with association equation of state (GCA-EoS). *Fluid Phase Equilib.* **2009**, *275* (1), 52-59.

(69) Addicks, J.; Owren, G. A.; Fredheim, A. O.; Tangvik, K. Solubility of Carbon Dioxide and Methane in Aqueous Methyldiethanolamine Solutions. *J. Chem. Eng. Data* **2002**, *47* (4), 855-860.

(70) Carroll, J. J.; Jou, F.-Y.; Mather, A. E.; Otto, F. D. The solubility of methane in aqueous solutions of monoethanolamine, diethanolamine and triethanolamine. *Can. J. Chem. Eng.* **1998**, *76*, 945-951.

(71) Chapoy, A.; Coquelet, C.; Richon, D. Solubility measurement and modeling of water in the gas phase of the methane/water binary system at temperatures from 283.08 to 318.12 K and pressures up to 34.5 MPa. *Fluid Phase Equilib.* **2003**, *214* (1), 101-117.

(72) Chapoy, A.; Mohammadi, A. H.; Richon, D.; Tohidi, B. Gas solubility measurement and modeling for methane-water and methane-ethane-n-butane-water systems at low temperature conditions. *Fluid Phase Equilib.* **2004**, *220* (1), 113-121.

(73) Chapoy, A.; Mohammadi, A. H.; Tohidi, B.; Richon, D. Estimation of Water Content for Methane + Water and Methane + Ethane + n-Butane + Water Systems Using a New Sampling Device. *J. Chem. Eng. Data* **2005**, *50* (4), 1157-1161.

(74) Crovetto, R.; Fernandez-Prini, R.; Japas, M. L. Solubilities of inert gases and methane in water and in heavy water in the temperature range of 300 to 600 K. *J. Chem. Phys.* **1982**, *76* (2), 1077-1086.

(75) Culberson, O. L.; Horn, A. B.; McKetta, J. J., Jr. Phase equilibria in hydrocarbon - water systems. The Solubility of Ethane in Water at Pressures to 1200 Pounds Per Square Inch. *Trans. Am. Inst. Min. Metall. Pet. Eng.* **1950**, *189*, 1-6.

(76) Culberson, O. L.; McKetta, J. J., Jr. Phase Equilibria in Hydrocarbon - Water Systems. IV. Vapor-Liquid Equilibrium Constants in the Methane - Water and Ethane - Water System. *Trans. Am. Inst. Min. Metall. Pet. Eng.* **1951**, *192*, 297-300.
(77) Culberson, O. L.; McKetta, J. J., Jr. Phase equilibria in hydrocarbon - water systems. III- The Solubility of Methane in Water at Pressures to 10,000 PSIA. *Trans. Am. Inst. Min. Metall. Pet. Eng.* **1951**, *192*, 223-226.
(78) Davis, J. E.; McKetta, J. J. Solubility of Methane in Water. *Pet. Refiner* **1960**, *39*, 205-206.
(79) Dhima, A. *Ph.D. thesis, Univ. Claude Bernard - Lyon 1* **1998**, 1-169.
(80) Duffy, J. R.; Smith, N. O.; Nagy, B. Solubility of Natural Gases in Aqueous Salt Solutions. I. Liquidus Surfaces in the System CH4 - H2O - NaCl2 - CaCl2 at Room Temperatures and at Pressures Below 1000 PSIA. *Geochim. Cosmochim. Acta* **1961**, *24*, 23-31.
(81) Fenghour, A.; Wakeham, W. A.; Watson, J. T. R. Densities of (water+methane) in the temperature range 430 K to 699 K and at pressures up to 30 MPa. *J. Chem. Thermodyn.* **1996**, *28* (4), 447-458.
(82) Gillespie, P. C.; Wilson, G. M. Vapor-Liquid and Liquid-Liquid Equilibria: Water - Methane, Water - Carbon Dioxide, Water - Hydrogen Sulfide, Water - n-Pentane, Water - Methane - n-Pentane. *GPA Research Report* **1982**, 1-73.
(83) Kiepe, J.; Horstmann, S.; Fischer, K.; Gmehling, J. Experimental Determination and Prediction of Gas Solubility Data for Methane + Water Solutions Containing Different Monovalent Electrolytes. *Ind. Eng. Chem. Res.* **2003**, *42* (21), 5392-5398.
(84) Kim, Y. S.; Ryu, S. K.; Yang, S. O.; Lee, C. S. Liquid Water-Hydrate Equilibrium Measurements and Unified Predictions of Hydrate-Containing Phase Equilibria for Methane, Ethane, Propane, and Their Mixtures. *Ind. Eng. Chem. Res.* **2003**, *42* (11), 2409-2414.
(85) Lekvam, K.; Bishnoi, P. R. Dissolution of methane in water at low temperatures and intermediate pressures. *Fluid Phase Equilib.* **1997**, *131* (1-2), 297-309.
(86) Malegaonkar, M. B.; Dholabhai, P. D.; Bishoi, P. R. Kinetics of carbon dioxide and methane hydrate formation. *Can. J. Chem. Eng.* **1997**, *75* (6), 1090-1099.
(87) Michels, A.; Gerver, J.; Bijl, A. Effect of pressure on the solubility of gases. *Physica (Amsterdam)* **1936**, *3*, 797-808.
(88) Mohammadi, A. H.; Chapoy, A.; Richon, D.; Tohidi, B. Experimental Measurement and Thermodynamic Modeling of Water Content in Methane and Ethane Systems. *Ind. Eng. Chem. Res.* **2004**, *43* (22), 7148-7162.
(89) Olds, R. H.; Sage, B. H.; Lacey, W. N. Phase equilibria in hydrocarbon systems. Composition of the dew-point gas of the methane-water system. *J. Ind. Eng. Chem. (Washington, D. C.)* **1942**, *34*, 1223-1227.
(90) Reichl, A. Measurement and Correlation of the Gas Solubility of Halogenated Hydrocarbons. *Dissertation. Berlin* **1996**.
(91) Rigby, M.; Prausnitz, J. M. Solubility of water in compressed nitrogen, argon, and methane. *J. Phys. Chem.* **1968**, *72* (1), 330-334.
(92) Sanchez, M.; De, M. F. Liquid-vapor equilibrium in the methanol-water system measured at high pressures and temperatures between 150 and 300°C. *An. Quim.* **1978**, *74* (11), 1325-1328.
(93) Servio, P.; Englezos, P. Measurement of Dissolved Methane in Water in Equilibrium with Its Hydrate. *J. Chem. Eng. Data* **2002**, *47* (1), 87-90.
(94) Shmonov, V. M.; Sadus, R. J.; Franck, E. U. High-pressure phase equilibria and supercritical pVT data of the binary water + methane mixture to 723 K and 200 MPa. *J. Phys. Chem.* **1993**, *97* (35), 9054-9059.
(95) Sultanov, R. G.; Skripka, V. G.; Namiot, A. Y. Moisture content of methane at high temperatures and pressures. *Gazov. Prom.* **1971**, *16* (4), 6-8.
(96) Sultanov, R. G.; Skripka, V. G.; Namiot, A. Y. Solubility of methane in water at high temperatures and pressures. *Gazov. Prom.* **1972**, *17* (5), 6-7.
(97) Ugrozov, V. V. Equilibrium Compositions of Vapor-Gas Mixtures over Solutions. *Russ. J. Phys. Chem.* **1996**, *70* (7), 1240-1241.
(98) Wang, L.-K.; Chen, G.-J.; Han, G.-H.; Guo, X.-Q.; Guo, T.-M. Experimental study on the solubility of natural gas components in water with or without hydrate inhibitor. *Fluid Phase Equilib.* **2003**, *207* (1-2), 143-154.
(99) Wang, Y.; Han, B.; Yan, H.; Liu, R. Solubility of CH4 in the mixed solvent t-butyl alcohol and water. *Thermochim. Acta* **1995**, *253*, 327-334.
(100) Yang, S. O.; Cho, S. H.; Lee, H.; Lee, C. S. Measurement and prediction of phase equilibria for water + methane in hydrate forming conditions. *Fluid Phase Equilib.* **2001**, *185* (1-2), 53-63.
(101) Yarym-Agaev, N. L.; Sinyavskaya, R. P.; Koliushko, I. I.; Levinton, L. Y. Phase Equilibria in the Water - Methane and Methanol - Methane Binary Systems under High Pressures. *J. Appl. Chem. USSR* **1985**, *58* (1), 154-157.
(102) Yokoyama, C.; Wakana, S.; Kaminishi, G.; Takahashi, S. Vapor-liquid equilibria in the methane-diethylene glycol-water system at 298.15 and 323.15 K. *J. Chem. Eng. Data* **1988**, *33* (3), 274-276.

(103) Zheng, D.; Gao, J.; Sun, D.; Guo, T. Gas solubilities in water/formation water at high temperature and high pressure -- an apparatus and its reliability. *Gaoxiao Huaxue Gongcheng Xuebao* **1996**, *10* (1), 59-63.
(104) Anthony, R. G.; McKetta, J. J. Phase equilibrium in the ethylene-water system. *J. Chem. Eng. Data* **1967**, *12* (1), 17-20.
(105) Chapoy, A.; Coquelet, C.; Richon, D. Measurement of the Water Solubility in the Gas Phase of the Ethane + Water Binary System near Hydrate Forming Conditions. *J. Chem. Eng. Data* **2003**, *48* (4), 957-966.
(106) Coan, C. R.; King, A. D. Solubility of Water in Compressed Carbon Dioxide, Nitrous Oxide, and Ethane. Evidence for Hydration of Carbon Dioxide and Nitrous Oxide in the Gas Phase. *J. Am. Chem. Soc.* **1971**, *93* (8), 1857-1862.
(107) Culberson, O. L.; McKetta, J. J. Phase Equilibria in Hydrocarbon - Water Systems. II - The Solubility of Ethane in Water at Pressures to 10,000 psi. *Trans. Am. Inst. Min. Metall. Pet. Eng.* **1950**, *189*, 319-322.
(108) Danneil, A.; Toedheide, K.; Franck, E. U. Vaporization equilibriums and critical curves in the systems ethane/water and n-butane/water at high pressures. *Chem.-Ing.-Tech.* **1967**, *39* (13), 816-822.
(109) Dhima, A.; de, H. J.-C.; Moracchini, G. Solubility of light hydrocarbons and their mixtures in pure water under high pressure. *Fluid Phase Equilib.* **1998**, *145* (1), 129-150.
(110) Mohammadi, A. H.; Chapoy, A.; Tohidi, B.; Richon, D. Measurements and Thermodynamic Modeling of Vapor-Liquid Equilibria in Ethane-Water Systems from 274.26 to 343.08 K. *Ind. Eng. Chem. Res.* **2004**, *43* (17), 5418-5424.
(111) Reamer, H. H.; Olds, R. H.; Sage, B. H.; Lacey, W. N. Phase equilibria in hydrocarbon series. Composition of dew-point gas in ethane-water system. *J. Ind. Eng. Chem. (Washington, D. C.)* **1943**, *35*, 790-793.
(112) Sparks, K. A.; Sloan, E. D. Water Content of NGL in the Presence of Hydrates. *GPA Research Report* **1983**, (RR-71), 1-26.
(113) Alwani, Z.; Schneider, G. Influence of the Pressure on the Separation of liquid Systems. Phase Equilibria and Critical Phenomena in the System Benzene - Water between 250 and 368 C and up to 3700 bar. *Ber. Bunsen-Ges. Phys. Chem.* **1967**, *71* (6), 633-638.
(114) Anderson, F. E.; Prausnitz, J. M. Mutual solubilities and vapor pressures for binary and ternary aqueous systems containing benzene, toluene, m-xylene, thiophene and pyridine in the region 100-200°C. *Fluid Phase Equilib.* **1986**, *32* (1), 63-76.
(115) Bader, M. S. H.; Gasem, K. A. M. Determination of Infinite Dilution Activity Coefficients for Organic - Aqueous Systems Using a Dilute Vapor-Liquid Equilibrium Method. *Chem. Eng. Commun.* **1996**, *140*, 41-72.
(116) Chmara, Y. I. Possible interpretation of azeotropism as properties of vapor-liquid systems with chemical reactions. *Zh. Fiz. Khim.* **1982**, *56* (5), 1065-1078.
(117) Fischer, K. Experimental determination of the boiling curve in the system benzene - water in the homogeneous benzene-rich range at 90.48 C by a synthetic static experimental method. *Unpublished Data* **1994**.
(118) Niini, A. Determination of the Pressure Isotherm for Water, Methanol and Ethanol Mixtures and an Estimation of the van der Waals Forces in Liquids. I. Non-Polar Solvents. *Ann. Acad. Sci. Fennicae Ser. A* **1940**, *55*, 1-52.
(119) Rebert, C. J.; Kay, W. B. The phase behavior and solubility relations of the benzenewater system. *AIChE J.* **1959**, *5* (3), 285-289.
(120) Tsonopoulos, C.; Wilson, G. M. High-temperature mutual solubilities of hydrocarbons and water. Part I: Benzene, cyclohexane and n-hexane. *AIChE J.* **1983**, *29* (6), 990-999.
(121) Valtz, A.; Guilbot, P.; Richon, D. Amine BTEX Solubility. *GPA Research Report* **2002**, (RR-180), 1-103.
(122) Valtz, A.; Hegarty, M.; Richon, D. Experimental determination of the solubility of aromatic compounds in aqueous solutions of various amines. *Fluid Phase Equilib.* **2003**, *210* (2), 257-276.
(123) Rabezkii, M. G.; Bazaev, A. R.; Abdulagatov, I. M.; Magee, J. W.; Bazaev, E. A. PVTx Measurements for Water + Toluene Mixtures in the Near-Critical and Supercritical Regions. *J. Chem. Eng. Data* **2001**, *46* (6), 1610-1618.
(124) Wobst, M.; Moerke, K. Determination of the vapor-liquid equilibria in binary systems formed by maleic anhydride, maleic acid, o-xylene, and water. *FIZ Report* **1990**, 5311.
(125) Heidman, J. L.; Tsonopoulos, C.; Brady, C. J.; Wilson, G. M. High-temperature mutual solubilities of hydrocarbons and water. Part II: ethylbenzene, ethylcyclohexane, and n-octane. *AIChE J.* **1985**, *31* (3), 376-384.
(126) Christensen, S. P.; Paulaitis, M. E. Phase equilibria for tetralin-water and 1-methylnaphthalene-water mixtures at elevated temperatures and pressures. *Fluid Phase Equilib.* **1992**, *71* (1-2), 63-83.
(127) Inga, R. F.; McKetta, J. J. Solubility of Cyclopropane in Water. *Pet. Refiner* **1961**, *40* (3), 191-193.
(128) Broellos, K.; Peter, K.; Schneider, G. M. Fluid mixed systems under high pressure. Phase equilibriums and critical points in the binary systems cyclohexane-water, n-heptane-water, biphenyl-water, and benzene-water-d2 at 420.deg. and 3000 bars. *Ber. Bunsenges. Phys. Chem.* **1970**, *74* (7), 682-686.

(129) Anderson, G. K. Solubility of Carbon Dioxide in Water under Incipient Clathrate Formation Conditions. *J. Chem. Eng. Data* **2002**, *47* (2), 219-222.
(130) Bamberger, A.; Sieder, G.; Maurer, G. High-pressure (vapor-liquid) equilibrium in binary mixtures of (carbon dioxide + water or acetic acid) at temperatures from 313 to 353 K. *J. Supercrit. Fluids* **2000**, *17* (2), 97-110.
(131) Bando, S.; Takemura, F.; Nishio, M.; Hihara, E.; Akai, M. Solubility of CO2 in Aqueous Solutions of NaCl at (30 to 60) °C and (10 to 20) MPa. *J. Chem. Eng. Data* **2003**, *48* (3), 576-579.
(132) Briones, J. A.; Mullins, J. C.; Thies, M. C.; Kim, B. U. Ternary phase equilibria for acetic acid-water mixtures with supercritical carbon dioxide. *Fluid Phase Equilib.* **1987**, *36*, 235-246.
(133) Cai, Z.; Wu, Z. Measurement and correlation of vapor-liquid equilibrium with CO2 systems at high pressure. *Huaxue Gongcheng (Xi'an, People's Repub. China)* **1996**, *24* (4), 71-73.
(134) Crovetto, R.; Wood, R. H. Solubility of carbon dioxide in water and density of aqueous CO2 near the solvent critical temperature. *Fluid Phase Equilib.* **1992**, *74*, 271-288.
(135) Dalmolin, I.; Skovroinski, E.; Biasi, A.; Corazza, M. L.; Dariva, C.; Oliveira, J. V. Solubility of carbon dioxide in binary and ternary mixtures with ethanol and water. *Fluid Phase Equilib.* **2006**, *245* (2), 193-200.
(136) Dhima, A.; de, H. J.-C.; Jose, J. Solubility of Hydrocarbons and CO2 Mixtures in Water under High Pressure. *Ind. Eng. Chem. Res.* **1999**, *38* (8), 3144-3161.
(137) Dohrn, R.; Buenz, A. P.; Devlieghere, F.; Thelen, D. Experimental measurements of phase equilibria for ternary and quaternary systems of glucose, water, carbon dioxide and ethanol with a novel apparatus. *Fluid Phase Equilib.* **1993**, *83*, 149-158.
(138) D'Souza, R.; Patrick, J. R.; Teja, A. S. High pressure phase equilibria in the carbon dioxide-n-hexadecane and carbon dioxide-water systems. *Can. J. Chem. Eng.* **1988**, *66* (2), 319-323.
(139) Fischer, K.; Petri, M.; Chen, J.; Noll, O.; Gmehling, J. *Unpublished Data* **1995**.
(140) Gu, F. Solubility of carbon dioxide in aqueous sodium chloride solution under high pressure. *Gaoxiao Huaxue Gongcheng Xuebao* **1998**, *12* (2), 118-123.
(141) Iwai, Y.; Uno, M.; Nagano, H.; Arai, Y. Measurement of solubilities of palmitic acid in supercritical carbon dioxide and entrainer effect of water by FTIR spectroscopy. *J. Supercrit. Fluids* **2004**, *28* (2-3), 193-200.
(142) Kiepe, J.; Horstmann, S.; Fischer, K.; Gmehling, J. Experimental Determination and Prediction of Gas Solubility Data for CO2 + H2O Mixtures Containing NaCl or KCl at Temperatures between 313 and 393 K and Pressures up to 10 MPa. *Ind. Eng. Chem. Res.* **2002**, *41* (17), 4393-4398.
(143) King, M. B.; Mubarak, A.; Kim, J. D.; Bott, T. R. The mutual solubilities of water with supercritical and liquid carbon dioxide. *J. Supercrit. Fluids* **1992**, *5* (4), 296-302.
(144) Malinin, S. D. The system H2O-CO2 at high temperatures and pressures. *Geokhimiya* **1959**, *3*, 235-45.
(145) Mueller, G. Experimental Study of the Vapor-Liquid Equilibrium in the System Ammonia - Carbon Dioxide - Water from 100 to 200 C at Pressure up to 90 bar. *Ph.D. thesis, Univ. Kaiserslautern* **1983**, 1-174.
(146) Nakayama, T.; Sagara, H.; Arai, K.; Saito, S. High pressure liquid-liquid equilibria for the system of water, ethanol and 1,1-difluoroethane at 323.2 K. *Fluid Phase Equilib.* **1987**, *38* (1-2), 109-127.
(147) Prutton, C. F.; Savage, R. L. The solubility of carbon dioxide in calcium chloridewater solutions at 75, 100, 120° and high pressures. *J. Am. Chem. Soc.* **1945**, *67*, 1550-1554.
(148) Sako, T.; Sugeta, T.; Nakazawa, N.; Okubo, T.; Sato, M.; Taguchi, T.; Hiaki, T. Phase equilibrium study of extraction and concentration of furfural produced in reactor using supercritical carbon dioxide. *J. Chem. Eng. Jpn.* **1991**, *24* (4), 449-55.
(149) Sayegh, S. G.; Najman, J. CO2 - SO2 - Brine Phase Behavior Studies. *Report. Petroleum Recovery Institute, Calgary, Alberta* **1984**, (1984-2).
(150) Sidorov, I. P.; Kazarnovskii, Y. S.; Goldman, A. M. The Solubility of Water in compressed Gases. *Tr. Gos. Nauchno Issled. Proektn. Inst. Azotn. Promst. Prod. Org. Sin.* **1953**, *1*, 48-67.
(151) Silkenbaeumer, D.; Rumpf, B.; Lichtenthaler, R. N. Solubility of Carbon Dioxide in Aqueous Solutions of 2-Amino-2-methyl-1-propanol and N-Methyldiethanolamine and Their Mixtures in the Temperature Range from 313 to 353 K and Pressures up to 2.7 MPa. *Ind. Eng. Chem. Res.* **1998**, *37* (8), 3133-3141.
(152) Takenouchi, S.; Kennedy, G. C. The binary system H2O-CO2 at high temperatures and pressures. *Am. J. Sci.* **1964**, *262*, 1055-1074.
(153) Takenouchi, S.; Kennedy, G. C. Solubility of carbon dioxide in NaCl solutions at high temperatures and pressures. *Am. J. Sci.* **1965**, *263* (5), 445-454.
(154) Teng, H.; Yamasaki, A.; Chun, M. K.; Lee, H. Solubility of liquid CO2 in water at temperatures from 278 K to 293 K and pressures from 6.44 MPa to 29.49 MPa and densities of the corresponding aqueous solutions. *J. Chem. Thermodyn.* **1997**, *29* (11), 1301-1310.
(155) Toedheide, K.; Franck, E. U. Two-phase range and the critical curve in the system carbon dioxide-water up to 3500 bar. *Z. Phys. Chem. (Muenchen, Ger.)* **1963**, *37* (5/6), 387-401.

(156) Valtz, A.; Chapoy, A.; Coquelet, C.; Paricaud, P.; Richon, D. Vapour-liquid equilibria in the carbon dioxide-water system, measurement and modelling from 278.2 to 318.2K. *Fluid Phase Equilib.* **2004**, *226*, 333-344.
(157) Vilcu, R.; Gainar, I. Solubility of gases in liquids under pressure. I. The system carbon dioxide - water. *Rev. Roum. Chim.* **1967**, *12*, 181-189.
(158) Wiebe, R.; Gaddy, V. L. The solubility of carbon dioxide in water at various temperatures from 12° to 40° and at pressures to 500 atmospheres. Critical phenomena. *J. Am. Chem. Soc.* **1940**, *62*, 815-817.
(159) Wiebe, R.; Gaddy, V. L. Vapor-phase composition of carbon dioxide-water mixtures at various temperatures and at pressures to 700 atmospheres. *J. Am. Chem. Soc.* **1941**, *63*, 475-477.
(160) Zaalishvili, S. D. Solubility of carbon dioxide from its mixtures with hydrogen and nitrogen in water under pressure. *Zh. Fiz. Khim.* **1940**, *14*, 413-417.
(161) Zawisza, A.; Malesinska, B. Solubility of carbon dioxide in liquid water and of water in gaseous carbon dioxide in the range 0.2-5 MPa and at temperatures up to 473 K. *J. Chem. Eng. Data* **1981**, *26* (4), 388-391.
(162) Zel'venskii, Y. D. The solubility of carbon dioxide in water under pressure. *Zh. Khim. Prom-sti.* **1937**, *14*, 1250-1257.
(163) Zhang, G.; Wu, Y.; Ma, P.; Wu, G.; Li, D. The Measurement and Correlation of Carbon Monoxide and Other Gases Solubility in Phenol. *Proceedings. Nanjing, China* **2004**, 1-7.
(164) Zheng, D.-Q.; Guo, T.-M.; Knapp, H. Experimental and modeling studies on the solubility of CO2, CHClF2, CHF3, C2H2F4 and C2H4F2 in water and aqueous NaCl solutions under low pressures. *Fluid Phase Equilib.* **1997**, *129* (1-2), 197-209.
(165) Alvarez, J.; Fernandez-Prini, R. A semiempirical procedure to describe the thermodynamics of dissolution of nonpolar gases in water. *Fluid Phase Equilib.* **1991**, *66* (3), 309-326.
(166) Blanco, S. T.; Velasco, I.; Otin, S. Dew points of binary nitrogen-water mixtures. *Phys. Chem. Liq.* **2002**, *40* (2), 167-172.
(167) Chapoy, A.; Mohammadi, A. H.; Tohidi, B.; Richon, D. Gas Solubility Measurement and Modeling for the Nitrogen + Water System from 274.18 K to 363.02 K. *J. Chem. Eng. Data* **2004**, *49* (4), 1110-1115.
(168) Gillespie, P. C.; Wilson, G. M. Vapor-Liquid Equilibrium Data on Water-Substitute Gas Components: N2 - H2O, H2 - H2O, CO - H2O, H2 - CO - H2O, and H2S - H2O. *GPA Research Report* **1980**, (RR-41), 1-34.
(169) Goodman, J. B.; Krase, N. W. Solubility of nitrogen in water at high pressures and temperatures. *Ind. Eng. Chem. Ind. Ed.* **1931**, *23* (4), 401-404.
(170) Japas, M. L.; Franck, E. U. High pressure phase equilibria and PVT-data of the water-nitrogen system to 673 K and 250 MPa. *Ber. Bunsen-Ges. Phys. Chem.* **1985**, *89* (7), 793-800.
(171) Maslennikova, V. Y. Solubility of Nitrogen in Water. *Tr. Gos. Nauchno Issled. Proektn. Inst. Azotn. Promst. Prod. Org. Sin.* **1971**, *12*, 82-87.
(172) Maslennikova, V. Y.; Vdovina, N. A.; Tsiklis, D. S. Solubility of Water in Compressed Nitrogen. *Russ. J. Phys. Chem.* **1971**, *45* (9), 1354-1354.
(173) Mohammadi, A. H.; Chapoy, A.; Tohidi, B.; Richon, D. Water Content Measurement and Modeling in the Nitrogen + Water System. *J. Chem. Eng. Data* **2005**, *50* (2), 541-545.
(174) O'Sullivan, T. D.; Smith, N. O.; Nagy, B. Solubility of natural gases in aqueous salt solutions. III. Nitrogen in aqueous NaCl at high pressures. *Geochim. Cosmochim. Acta* **1966**, *30*, 617-619.
(175) Prokhorova, V. M.; Tsiklis, D. S. Vapor-vapor equilibrium in the system nitrogen - water. *Zh. Fiz. Khim.* **1970**, *44* (8), 2069-2070.
(176) Smith, N. O.; Kelemen, S.; Nagy, B. Solubility of natural gases in aqueous salt solutions - II. Nitrogen in aqueous NaCl, CaCl2, Na2SO4 and MgSO4 at room temperatures and at pressures below 1000 psia. *Geochim. Cosmochim. Acta* **1962**, *26*, 921-926.
(177) Wiebe, R.; Gaddy, V. L.; Heins, C. Solubility of Nitrogen in Water at 25 degrees C from 25 to 1000 Atmospheres. *Ind. Eng. Chem. Ind. Ed.* **1932**, *24*, 927-927.
(178) Wiebe, R.; Gaddy, V. L.; Heins, C. The Solubility of Nitrogen in Water at 50, 75 and 100 degrees C from 25 to 1000 Atmospheres. *J. Am. Chem. Soc.* **1933**, *55*, 947-953.
(179) Burgess, M. P.; Germann, R. P. Physical properties of hydrogen sulfide-water mixtures. *AIChE J.* **1969**, *15* (2), 272-275.
(180) Carroll, J. J.; Mather, A. E. Phase equilibrium in the system water-hydrogen sulfide: experimental determination of the LLV locus. *Can. J. Chem. Eng.* **1989**, *67* (3), 468-470.
(181) Chapoy, A.; Mohammadi, A. H.; Tohidi, B.; Valtz, A.; Richon, D. Experimental measurement and phase behavior modeling of hydrogen sulfide-water binary system. *Ind. Eng. Chem. Res.* **2005**, *44* (19), 7567-7574.
(182) Kozintseva, T. N. Solubility of H2S in Water and Salt-solutions a high Temperatures. *Sb. Geokhim. Issl. Pov. Davl. Temp. Moskva 1965* **1965**, 121-134.
(183) Lee, J. I.; Mather, A. E. Solubility of hydrogen sulfide in water. *Ber. Bunsen-Ges. Phys. Chem.* **1977**, *81* (10), 1020-1023.

(184) Selleck, F. T.; Carmichael, L. T.; Sage, B. H. Phase behavior in the hydrogen sulfide-water system. *J. Ind. Eng. Chem. (Washington, D. C.)* **1952**, *44*, 2219-2226.
(185) Gillespie, P. C.; Wilson, G. M. Sulfur Compounds and Water V-L-E and Mutual Solubility MeSH - H2O; EtSH - H2O; CS2 - H2O and COS - H2O. *GPA Research Report* **1984**, (RR-78), 1-40.
(186) Kilner, J.; McBain, S. E.; Roffey, M. G. (Vapor + liquid) equilibria of (methanethiol or ethanethiol or propan-1-thiol or butan-1-thiol + n-hexane or n-decane or toluene or water) for mole fractions x = 0 to 0.2 of thiol at temperatures between 323 and 373 K. *J. Chem. Thermodyn.* **1990**, *22* (2), 203-210.
(187) Brunner, E. Fluid mixtures at high pressures IX. Phase separation and critical phenomena in 23 (n-alkane + water) mixtures. *The Journal of Chemical Thermodynamics* **1990**, *22* (4), 335-353.
(188) Alwani, Z.; Schneider, G. Phase equilibriums, critical phenomena, and pressure-volume-temperature data on binary water-aromatic hydrocarbon mixtures up to 420.deg. and 2200 bars. *Ber. Bunsenges. Phys. Chem.* **1969**, *73* (3), 294-301.
(189) Jockers, R.; Paas, R.; Schneider, G. M. Fluid mixtures at high pressures. Liquid-liquid phase equilibriums and critical phenomena in the systems 1,2,3,4-tetrahydronaphthalene + water, decahydronaphthalene(cis) + water, decahydronaphthalene(trans) + water, and methane + trifluoromethane up to 2600 bar. *Ber. Bunsenges. Phys. Chem.* **1977**, *81* (10), 1093-1096.

Chapitre III. Extension du modèle PPR78 aux systèmes contenant des alcènes

Les alcènes sont des molécules qui possèdent une ou plusieurs doubles liaisons. Les alcènes légers, en particulier l’éthylène et le propène sont obtenus par craquage du pétrole brut. Au travers de diverses réactions (polymérisation, hydroformylation, alkylation, oligomérisation…) ils entrent dans la fabrication de nombreuses molécules. La production des alcènes plus lourds, comme par exemple le 1-hexène, provient principalement de la séparation par distillation du vaste mélange d’alcènes issu de l’oligomérisation de l’éthylène. En bref, au cours des années passées, l’utilisation des alcènes comme des réactifs, des intermédiaires de synthèse, ou des produits finis s’est énormément développée dans les industries chimique, pétrochimique et polymérique. Par conséquent, la connaissance précise des équilibres entre phases des systèmes contenant des alcènes est essentielle pour le dimensionnement et l’optimisation des procédés. Nous nous intéresserons dans ce chapitre à la présentation des équilibres entre phases de ces systèmes binaires.

III.1 Introduction

The development of novel processes and products requires efficient thermodynamic models capable of predicting the equilibrium properties without the use of experimental data. Over the past years, the use of alkenes and cycloalkenes as reactants, intermediates, or end products has significantly increased in the chemical, petrochemical and polymer industries. Consequently, the accurate knowledge of the phase equilibria of systems containing alkenes is vital for the optimal design of processes and products. In spite of this, systematic studies of alkenes containing mixtures are really limited. In order to meet these requirements, Jaubert and coworkers[1] developed a group contribution method allowing the estimation of the temperature-dependent binary interaction parameters ($k_{ij}(T)$) for the widely used Peng-Robinson equation of state. This model relies on the Peng-Robinson EoS as published by Peng and Robinson in 1978 and the addition of a group contribution method to estimate the k_{ij} makes it predictive. It was thus simply called PPR78 (predictive 1978, Peng-Robinson EoS).

In our previous papers[1-7] and Chapter II, sixteen groups are defined: CH_3, CH_2, CH, C, CH_4 (methane), C_2H_6 (ethane), CH_{aro}, C_{aro}, $C_{fused\ aromatic\ rings}$, $CH_{2,cyclic}$, $CH_{cyclic} = C_{cyclic}$, CO_2, N_2, H_2S, mercaptans and water. It was decided to add the alkenes and cycloalkenes to the PPR78 model, in order to predict the phase behavior of petroleum fluids containing these unsaturated hydrocarbons. To do so, four groups are defined: C_2H_4(ethylene), $CH_{2,alkenic} = CH_{alkenic}$, $C_{alkenic}$ and $CH_{cycloalkenic} = C_{cycloalkenic}$. The interactions between these four new groups and the sixteen ones previously defined are determined. It is thus possible to estimate, at any temperature, the k_{ij} between two components in any mixture containing paraffins, aromatics, naphthenes, CO_2, N_2, H_2S, mercaptans, water and alkenes.

III.2 Database and reduction procedure

Table III−1. List of the 76 pure components used in this study

Component	Short name	Component	Short name
methane	1	1-butene	1a4
ethane	2	cis-2-butene	c2a4
propane	3	trans-2-butene	t2a4
n-butane	4	1-pentene	1a5
n-pentane	5	1-hexene	1a6
n-hexane	6	1-heptene	1a7
n-heptane	7	1-octene	1a8
n-octane	8	cis-3-octene	c3a8
n-nonane	9	trans-3-octene	t3a8
n-decane	10	cis-4-octene	c4a8
n-dodecane	12	trans-4-octene	t4a8
n-tetradecane	14	1-decene	1a10
n-hexadecane	16	1-undecene	1a11
n-eicosane	20	1-hexadecene	1a16
2-methylpropane(isobutane)	2m3	1-octadecene	1a18
2-methylbutane	2m4	1,2-propadiene	aa3
2,2,4-trimethylpentane(isooctane)	224m5	1,3-butadiene	13a4
benzene	B	2-methylpropene	2ma3
methylbenzene(toluene)	mB	2-methyl-1-butene	2m1a4
1,3-dimethylbenzene(m-xylene)	13mB	2-methyl-2-butene	2m2a4
1,2-dimethylbenzene(o-xylene)	12mB	3-methyl-1-butene	3m1a4
1,4-dimethylbenzene(p-xylene)	14mB	2-ethyl-1-butene	2e1a4
ethylbenzene	eB	2-methyl-1-pentene	2m1a5
1,2,4-trimethylbenzene	124mB	4-methyl-1-pentene	4m1a5
1-metylethylbenzene(cumene)	iprB	2-methyl-1,3-butadiene	2m13a4
propylbenzene	prB	cyclopentene	aC5
naphthalene	BB	cyclohexene	aC6
1-methylnaphthalene	1mBB	1-methylcyclohexene	1maC6
phenanthrene	Phe	vinylbenzene(styrene)	Ba2
cyclopentane	C5	alpha-methylstyrene	Bma2
cyclohexane	C6	1,5-cyclooctadiene	15aC8
1,2,3,4-tetrahydronaphthalene(tetralin)	tet	dicyclopentadiene	gama
trans-decalin	tCC6	p-cemene	pcy
carbon dioxide	CO_2	alpha-pinene	ap
nitrogen	N_2	beta-pinene	bp
water	H_2O	myrcene	myr
ethylene	a2	limonene(R+S)	lamda
propene	a3	limonene(R)	xi

Table (III−1) presents the list of the 76 pure components involved in this study. The pure fluid physical properties (T_c, P_c and ω) used in this study originate from two sources. We have used Poling et al.[8] for alkanes, cyclo alkanes, aromatic compounds, CO_2, N_2, H_2S, H_2O and alkenes. For the missing components (some mercaptans and alkenes), the DIPPR database was chosen instead. Table (III−2) details the sources of the binary experimental data used in our evaluations[9-283] along with the temperature, pressure and composition range for each binary system. Most of the data available in the open literature (9263 bubble points + 6413 dew points + 143 mixture critical points) have been collected. Our database includes VLE data on 196 binary systems. The 140 parameters (70 A_{kl} and 70 B_{kl}) determined in this study [see Table (I−2)], are those which minimize the objective function defined in equation (I−105).

Table III−2. Binary systems database

Binary system (1^{st} compound-2^{nd} compound)	Temperature range (K)	Pressure range (bar)	x_1 range (1^{st} compound liquid mole fraction)	y_1 range (1^{st} compound gas mole fraction)	Number of bubble points (T,P,x)	Number of dew points (T,P,y)	Number of binary critical points (T_{cm}, P_{cm}, x_c)	References
a2-3	199.83-283.15	1.40-40.53	0.0440-0.9950	0.2608-0.9990	101	91	0	9-13
a2-4	322.04-388.71	13.79-67.02	0.0010-0.8250	0.0065-0.8720	31	31	4	14
a2-5	333.15-443.15	53.90-80.76	0.2900-0.8650	0.2900-0.8650	0	0	6	15
a2-6	293.15-491.28	2.79-95.65	0.0250-0.8550	0.2002-0.9880	137	41	12	15-20
a2-7	212.30-535.40	0.81-108.42	0.0038-0.9699	0.0622-0.9998	364	202	14	15, 17, 21-25
a2-8	318.15-338.15	15.00-95.00	0.1924-0.8897	0.9605-0.9949	20	20	0	26
a2-9	293.15-333.15	2.78-30.89	0.0350-0.5620	-	12	0	0	17
a2-10	283.65-353.15	20.27-58.01	0.2100-0.9560	0.9984-0.9999	16	8	0	27-28
a2-12	263.95-348.15	1.01-91.19	0.0131-0.9500	-	62	0	0	23, 29
a2-16	283.65-448.15	10.35-76.12	0.5493-0.9280	0.9440-1.0000	10	24	0	28, 30
a2-20	295.00-573.15	4.90-244.40	0.0659-0.9520	0.9350-1.0000	118	49	5	31-35
a2-2m3	292.95-393.15	10.10-65.76	0.0050-0.9490	0.0080-0.9500	36	35	5	36-38
a2-224m5	346.65-346.65	6.20-90.00	0.3000-0.6030	0.8890-0.9770	12	14	0	39-40
1-a2	103.94-248.15	0.10-60.80	0.0297-0.9851	0.1873-0.9996	193	218	0	12, 41-45
a2-2	140.00-293.15	0.06-52.01	0.0335-0.9861	0.0500-0.9928	462	279	2	12, 44, 46-53
a2-B	210.00-552.75	0.84-118.55	0.0030-0.9244	0.1000-0.9920	163	60	9	17, 19, 22, 39-40, 54-63
a2-mB	228.05-563.15	0.98-128.68	0.0220-0.9693	0.2530-0.9985	84	16	5	17, 28, 39, 64-67
a2-14mB	283.15-303.15	3.95-9.83	0.0500-0.1770	-	10	0	0	68
a2-12mB	243.15-333.15	2.77-31.09	0.0240-0.4820	-	29	0	0	17, 68
a2-13mB	223.15-293.15	1.82-12.77	0.0580-0.5100	-	16	0	0	68
a2-eB	273.15-423.15	2.45-14.71	0.0130-0.2010	-	20	0	0	58, 68
a2-BB	285.15-540.15	7.50-303.98	0.2447-0.8300	0.7114-1.0000	33	240	7	69-76
a2-1mBB	348.15-448.15	15.29-38.67	-	0.9925-0.9997	0	7	0	30
a2-Phe	298.15-343.15	69.90-311.30	-	0.9894-1.0000	0	49	0	71, 77-78
a2-C6	180.00-423.15	0.66-113.28	0.0040-0.8600	0.6990-0.9910	50	24	0	19, 22, 62
a2-tCC6	195.00-235.00	3.55-7.53	0.2012-0.9689	-	9	0	0	62
a2-CO_2	223.15-298.15	7.32-69.17	0.0200-0.9880	0.0300-0.9640	301	301	4	79-87
N_2-a2	120.00-260.00	2.68-110.38	0.0132-0.9658	0.1138-0.9994	87	132	0	12, 88-90
a2-H_2O	298.15-573.15	1.17-945.00	0.0000-0.0470	0.1600-0.9990	216	178	0	91-98
a3-3	228.65-360.93	0.95-41.61	0.0370-0.9940	0.0450-0.9950	621	534	0	49, 99-109
a3-6	238.15-333.15	0.13-7.41	0.0282-0.7010	-	25	0	0	17, 110
a3-7	238.15-333.15	0.13-7.39	0.0171-0.6830	-	40	0	0	17, 22, 110
a3-8	238.15-343.15	0.13-17.23	0.0282-0.9050	-	46	0	0	110-113
a3-9	293.15-333.15	2.43-7.46	0.0990-0.6980	-	9	0	0	17
a3-1a4	277.59-410.93	2.07-46.99	0.0170-0.9830	0.0480-0.9940	67	48	3	114
a3-13a4	273.20-333.20	1.60-24.43	0.0430-0.9720	0.1600-0.9930	25	25	0	115
1a4-4	310.93-344.26	3.62-9.73	0.1000-0.9313	0.1140-0.9351	58	58	0	116-117
1a4-7	353.15-443.15	2.05-40.65	0.0210-0.9350	-	49	0	0	24
1a4-1a6	373.60-373.60	4.05-14.30	0.0930-0.7690	0.3220-0.9190	5	5	0	118
1a5-5	273.15-468.50	0.26-35.30	0.1420-0.8600	0.2102-0.7511	50	9	3	119-120

Table III−2. (continued-1)

Binary system (1^{st} compound-2^{nd} compound)	Temperature range (K)	Pressure range (bar)	x_1 range (1^{st} compound liquid mole fraction)	y_1 range (1^{st} compound gas mole fraction)	Number of bubble points (T,P,x)	Number of dew points (T,P,y)	Number of binary critical points (T_{cm}, P_{cm}, x_c)	References
1a6-6	302.92-333.15	0.30-0.89	0.0050-0.9750	0.0070-0.9790	84	62	0	121-124
1a6-7	313.15-365.72	0.14-0.94	0.0494-0.9860	0.1490-0.9960	49	43	0	125-127
1a6-8	328.15-328.15	0.12-0.73	0.0500-0.9500	0.3060-0.9950	11	11	0	122
1a7-7	328.15-371.00	0.24-1.01	0.0830-0.9390	0.1240-0.9100	51	14	0	128-130
1a7-8	328.15-328.15	0.11-0.27	0.1000-0.9400	0.2940-0.9720	11	11	0	130
1a8-8	352.97-398.43	0.27-1.01	0.1050-0.9000	0.1170-0.9210	40	20	0	131-132
6-1a10	348.52-438.51	1.01-1.01	0.0152-0.8250	0.1317-0.9899	19	19	0	133
8-1a10	400.03-442.37	1.01-1.01	0.0182-0.9618	0.0471-0.9891	34	34	0	133
6-1a16	472.10-572.50	7.84-40.07	0.2160-0.9787	0.8000-0.9995	21	21	2	134
12-1a16	368.95-544.25	0.01-1.01	0.0690-0.8320	0.2940-0.9900	45	45	0	135
14-1a16	396.75-502.15	0.01-0.27	0.0580-0.9470	0.1140-0.9800	65	65	0	136-137
12-1a18	374.95-576.95	0.01-1.01	0.0100-0.8200	0.2050-0.9920	75	75	0	138
13a4-5	273.15-293.15	0.31-2.35	0.0474-0.9636	-	14	0	0	139
13a4-6	233.15-413.15	0.03-33.44	0.0380-0.9620	0.1560-0.9997	60	60	0	140-141
13a4-7	233.15-413.15	0.03-33.44	0.0400-0.9760	0.2800-0.9997	61	61	0	140-141
13a4-8	233.15-413.15	0.03-33.44	0.0220-0.9720	0.2840-0.9999	65	65	0	140-141
13a4-c2a4	278.15-338.15	1.10-7.83	0.0882-0.7498	-	16	0	0	142
13a4-t2a4	278.15-318.15	1.20-4.96	0.0529-0.9515	-	15	0	0	142
13a4-1a5	273.15-293.15	0.39-2.29	0.0702-0.9283	-	12	0	0	143
13a4-4	278.15-338.71	1.30-8.36	0.0944-0.9000	0.1172-0.9061	58	9	0	116, 142
t3a8-8	388.35-398.48	0.80-1.01	0.1540-0.8860	0.1660-0.8930	15	10	0	131
c3a8-8	388.01-398.54	0.80-1.01	0.1260-0.8990	0.1370-0.9060	15	10	0	131
t4a8-8	387.52-398.54	0.80-1.01	0.1030-0.8990	0.1130-0.9070	15	10	0	131
c4a8-8	374.47-398.55	0.53-1.01	0.0990-0.8940	0.1090-0.9010	20	10	0	131
4-c2a4	278.15-358.15	1.14-11.21	0.2642-0.8937	-	20	0	0	142
t2a4-c2a4	298.15-338.15	2.19-6.99	0.2755-0.8870	-	12	0	0	142
2m3-1a4	277.00-416.00	1.61-38.50	0.2464-0.8420	0.4000-0.8420	12	0	4	144-145
2m3-13a4	278.00-338.00	1.66-9.65	0.2525-0.7522	-	12	0	0	145
1a4-4m1a5	323.15-423.15	1.32-32.51	0.0848-0.9703	-	90	0	0	146-147
1a6-224m5	313.15-365.23	0.14-0.94	0.0470-0.9550	-	39	0	0	148-149
a3-224m5	289.20-330.20	1.01-1.01	0.0601-0.2031	-	7	0	0	150
1-a3	100.00-273.15	0.04-42.28	0.0260-0.9940	0.1666-0.9999	109	55	0	12, 49, 151-153
1-1a6	134.80-134.80	0.72-4.68	0.0725-0.8710	-	12	0	0	154
1-1a8	295.00-295.00	69.90-173.30	0.2883-0.5701	-	4	0	0	155
2-a3	197.85-344.26	0.32-49.78	0.0140-0.9770	0.0450-0.9968	168	194	2	12, 49, 156-159
2-1a11	298.15-318.15	3.03-52.77	0.0972-0.9853	-	30	0	0	160
a3-B	293.15-555.95	0.63-67.40	0.0310-0.9509	0.0792-0.9981	78	42	13	17, 161-165
1a4-B	298.15-298.15	0.41-1.02	0.0660-0.2450	-	4	0	0	166
13a4-B	298.15-413.15	0.25-33.44	0.0376-0.9740	0.2600-0.9995	41	41	0	140, 167
1a6-B	283.15-348.80	0.07-0.94	0.0320-0.9616	0.0910-0.9620	90	38	0	168-172

Table III−2. (continued-2)

Binary system (1^{st} compound-2^{nd} compound)	Temperature range (K)	Pressure range (bar)	x_1 range (1^{st} compound liquid mole fraction)	y_1 range (1^{st} compound gas mole fraction)	Number of bubble points (T,P,x)	Number of dew points (T,P,y)	Number of binary critical points (T_{cm}, P_{cm}, x_c)	References
B-1a7	328.15-328.15	0.29-0.43	0.0500-0.9500	0.1000-0.9540	11	11	0	122
B-1a8	283.15-323.15	0.02-0.33	0.1650-0.8870	-	24	0	0	170
4m1a5-B	283.15-323.15	0.09-0.86	0.1050-0.9140	-	24	0	0	170
a3-mB	238.15-333.15	0.13-7.34	0.0200-0.5980	-	44	0	0	17, 110, 173
13a4-mB	233.15-413.15	0.03-33.44	0.0280-0.9820	0.2500-0.9999	64	64	0	140-141
1a6-mB	283.15-381.30	0.04-1.01	0.0222-0.9715	0.0881-0.9920	63	21	0	148, 170, 174
1a7-mB	328.15-328.15	0.16-0.27	0.0500-0.9500	0.1180-0.9600	11	11	0	122
13a4-Ba2	243.15-363.15	0.10-4.55	0.0023-0.8110	0.3780-0.9995	27	17	0	175-176
mB-Ba2	312.35-413.25	0.07-1.01	0.0654-0.9000	0.1806-0.9677	19	19	0	177-178
1a6-12mB	337.27-414.60	1.01-1.01	0.0094-0.9792	0.0830-0.9983	21	21	0	174
a3-13mB	293.15-353.15	2.03-5.07	0.0300-0.4470	-	16	0	0	163
1a6-13mB	337.36-408.23	1.01-1.01	0.0195-0.9779	0.1171-0.9977	20	20	0	174
14mB-Ba2	323.15-323.15	0.03-0.04	0.0233-0.9465	0.0309-0.9603	25	25	0	179
1a6-eB	337.53-403.55	1.01-1.01	0.0290-0.9703	0.1666-0.9966	20	20	0	174
1a8-eB	394.95-408.45	1.01-1.01	0.0410-0.9470	0.0720-0.9610	16	16	0	180
eB-Ba2	324.38-370.15	0.05-0.27	0.0390-0.9780	0.0550-0.9840	65	65	0	181-182
a3-124mB	293.15-353.15	2.03-5.07	0.0520-0.4000	-	16	0	0	163
a3-iprB	293.15-614.55	2.03-80.40	0.0520-0.8950	0.2160-0.8950	16	0	7	163-164
BB-1a16	441.95-497.05	0.27-0.27	0.0630-0.9620	0.2470-0.9900	8	8	0	137
BB-1a18	364.85-572.25	0.01-1.01	0.0330-0.9200	0.3060-0.9940	56	56	0	183
a3-C6	298.15-318.15	0.32-1.27	0.0132-0.0714	-	12	0	0	22
1a4-C6	298.15-298.15	0.41-1.02	0.0830-0.2870	-	4	0	0	166
13a4-C6	303.15-413.15	0.25-33.44	0.0200-0.9820	0.1480-0.9980	36	36	0	140
1a6-C6	313.15-313.15	0.26-0.44	0.0323-0.9584	-	29	0	0	168, 184
C6-1a8	313.15-313.15	0.10-0.24	0.2236-0.9834	-	12	0	0	185
a3-tet	273.15-293.15	1.13-9.97	0.1114-0.9822	-	31	0	0	107
CO_2-a3	229.65-355.15	1.31-71.80	0.0140-0.9490	0.1190-0.9620	157	154	6	82-83, 86, 159, 186-187
CO_2-1a4	273.15-318.15	3.14-75.07	0.0246-0.9400	0.2188-0.9850	53	48	2	86, 188
CO_2-13a4	303.00-333.00	6.00-79.30	0.0320-0.9080	0.2450-0.9660	73	76	0	189
CO_2-1a5	303.15-328.60	13.50-84.30	0.1462-0.9300	0.8390-0.9826	37	37	0	190
CO_2-1a6	303.15-393.15	9.95-120.90	0.0820-0.9769	0.8140-0.9929	154	94	5	191-194
CO_2-1a7	303.15-343.15	10.10-73.15	0.0740-0.8030	0.9560-0.9950	24	24	0	193
CO_2-1a8	333.15-333.15	12.17-102.39	0.1019-0.9607	0.9607-0.9607	10	0	1	195
CO_2-Ba2	308.00-393.20	14.39-162.40	0.0820-0.9908	0.8608-0.9989	111	108	7	196-201
CO_2-1a16	314.20-531.30	9.85-51.40	0.0463-0.5050	0.9383-0.9806	15	5	0	202
N_2-a3	194.65-295.65	1.19-214.45	0.0090-0.4882	0.2320-0.9920	39	69	0	12, 89, 203
N_2-13a4	273.15-293.15	4.05-11.15	0.0025-0.0125	-	12	0	0	204
a3-H_2O	294.26-623.15	1.50-2200.00	0.0000-0.9989	0.1830-0.9963	205	108	0	95, 205-209
1a4-H_2O	279.15-417.15	1.83-68.26	0.0001-0.0010	0.5278-0.9994	32	42	0	210-214
13a4-H_2O	280.15-377.59	1.32-19.01	0.0001-0.0011	0.9980-0.9986	33	6	0	210, 215

Table III−2. (continued-3)

Binary system (1st compound-2nd compound)	Temperature range (K)	Pressure range (bar)	x_1 range (1st compound liquid mole fraction)	y_1 range (1st compound gas mole fraction)	Number of bubble points (T,P,x)	Number of dew points (T,P,y)	Number of binary critical points (T_{cm}, P_{cm}, x_c)	References
1a6-H_2O	366.48-496.26	3.18-53.78	0.0000-0.9898	0.5647-0.7481	8	4	0	216
H_2O-1a8	366.48-549.82	1.24-92.60	0.0087-0.9999	0.5870-0.7060	8	5	0	216
a2-a3	233.15-357.95	1.67-55.69	0.0200-0.9840	0.0640-0.9890	152	178	7	9, 12, 82, 159, 217-218
a2-1a4	273.14-393.15	2.05-66.40	0.0230-0.9610	0.1331-0.9980	141	84	0	147, 217, 219-221
a2-1a6	293.20-373.60	7.70-87.80	0.0810-0.9440	0.7730-0.9858	18	18	0	220
a2-4m1a5	293.15-423.15	3.43-85.10	0.0143-0.8670	0.6300-0.9870	47	23	0	118, 147
a2-1a8	303.00-342.40	10.00-89.70	0.1170-0.9090	0.9651-0.9962	10	10	0	220
3-aa3	253.15-353.15	1.83-31.49	0.0009-0.9459	-	38	0	0	222
2m1a4-5	283.15-298.15	0.40-0.81	0.1507-0.8001	-	24	0	0	119
2m13a4-5	298.15-313.10	0.71-1.25	0.0950-0.9500	-	37	0	0	119, 223
5-2m2a4	278.15-298.15	0.27-0.68	0.1501-0.8002	-	25	0	0	119
2m1a4-6	307.66-341.05	1.01-1.01	0.0120-0.8450	0.0358-0.9520	12	12	0	224
2m13a4-6	273.15-340.34	0.09-1.01	0.0207-0.9817	0.0575-0.9925	76	14	0	119, 225-226
2m2a4-6	313.94-340.58	1.01-1.01	0.0260-0.8817	0.0555-0.9522	13	13	0	227
2ma3-8	298.15-343.15	1.01-8.53	0.1840-0.9375	-	23	0	0	111
13a4-2m13a4	273.15-293.15	0.39-2.30	0.1264-0.9469	-	13	0	0	228
1a5-2m13a4	293.15-298.15	0.65-0.85	0.0680-0.9560	-	17	0	0	119
2ma3-2m13a4	318.55-367.55	5.07-10.30	0.0340-0.9778	0.0880-0.9900	26	26	0	229-230
2m13a4-2m2a4	298.15-311.70	0.64-1.14	0.0050-0.9950	0.0060-0.9957	96	75	0	119, 231-241
2m1a4-2m13a4	293.15-293.15	0.62-0.67	0.1080-0.8849	-	7	0	0	119
2m1a4-2m2a4	278.15-311.58	0.28-1.01	0.0109-0.9005	0.0131-0.7350	46	11	0	119, 237
aa3-8	217.17-253.15	0.01-1.01	0.0060-0.9340	-	29	0	0	242
3-2ma3	321.48-412.04	13.79-41.37	0.0860-0.8530	0.1250-0.9030	29	29	1	243
2ma3-4	277.59-344.26	1.32-9.69	0.2500-0.7500	-	30	0	0	244
7-bP	358.15-368.15	0.10-0.91	0.0140-0.9790	0.1550-0.9970	25	25	0	245
1a8-bP	368.15-388.15	0.13-0.84	0.0300-0.9830	0.1510-0.9970	23	23	0	245
2m3-2ma3	277.59-346.43	1.65-10.96	0.1000-0.9000	0.1059-0.9052	39	9	0	244, 246
2m4-2m13a4	301.60-313.15	0.90-1.52	0.0369-0.9472	-	23	0	0	238, 247
2m4-2m2a4	302.53-308.80	1.01-1.01	0.1840-0.7760	-	5	0	0	238
3m1a4-2m13a4	294.55-305.35	1.01-1.01	0.0597-0.9140	0.1130-0.9510	12	9	0	234, 238
2m13a4-B	278.15-298.15	0.08-0.68	0.0860-0.8930	-	45	0	0	119
2m1a5-B	283.15-323.15	0.07-0.66	0.0450-0.9340	-	24	0	0	170
12mB-Bma2	419.05-437.15	1.01-1.01	0.0500-0.9000	-	10	0	0	248
2m1a4-mB	305.90-380.26	1.01-1.01	0.0105-0.9300	0.0919-0.9955	13	13	0	224
2m13a4-mB	308.41-375.65	1.01-1.01	0.0344-0.9510	0.2075-0.9895	11	11	0	224
2m2a4-mB	311.61-377.72	1.01-1.01	0.0249-0.9994	0.1681-0.9999	18	18	0	224
mB-Bma2	293.15-313.15	0.01-0.08	0.1202-0.8901	-	40	0	0	249
Ba2-Bma2	420.25-437.55	1.01-1.01	0.0400-0.9000	-	11	0	0	248
2m13a4-C6	278.15-298.15	0.11-0.69	0.1460-0.8810	-	59	0	0	119
C6-bP	343.15-358.15	0.05-1.10	0.0020-0.9580	0.0560-0.9980	23	23	0	245

Table III−2. (continued-4)

Binary system (1st compound-2nd compound)	Temperature range (K)	Pressure range (bar)	x_1 range (1st compound liquid mole fraction)	y_1 range (1st compound gas mole fraction)	Number of bubble points (T,P,x)	Number of dew points (T,P,y)	Number of binary critical points (T_{cm}, P_{cm}, x_c)	References
CO_2-2m1a5	303.15-343.15	10.20-74.30	0.0830-0.8480	0.8820-0.9930	24	24	0	[193]
CO_2-Bma2	308.00-393.10	29.80-180.90	0.1894-0.9257	0.9430-0.9988	67	60	0	[197, 250]
CO_2-2e1a4	313.15-373.15	24.30-115.50	0.2250-0.9770	0.8220-0.9770	30	0	3	[191]
CO_2-myr	323.15-323.15	70.40-94.60	0.5142-0.8560	0.9680-0.9972	6	6	0	[251]
N_2-2ma3	273.15-293.15	4.05-11.15	0.0023-0.0126	-	12	0	0	[204]
a2-bP	288.15-308.15	43.73-74.99	0.7228-0.9933	0.9512-0.9986	49	17	0	[252]
5-aC6	278.15-298.15	0.09-0.60	0.1440-0.8420	-	40	0	0	[119]
6-aC6	278.15-298.15	0.05-0.19	0.0860-0.8680	-	40	0	0	[119]
7-1maC6	372.05-381.65	1.01-1.01	0.0890-0.9320	0.1500-0.9440	17	17	0	[253]
13aC5-6	283.15-337.37	0.12-1.01	0.0600-0.9650	0.2050-0.4152	13	2	0	[119, 254]
C5-aC6	324.15-353.50	1.01-1.01	0.0467-0.9171	0.1216-0.9679	16	16	0	[255]
C6-aC6	353.84-355.94	1.01-1.01	0.0240-0.9420	0.0270-0.9440	19	19	0	[124]
13aC5-gama	293.45-333.75	0.12-1.57	0.1680-0.8640	-	18	0	0	[256]
aC6-aP	343.15-358.15	0.11-1.06	0.0250-0.9820	0.2810-0.9960	31	31	0	[245]
5-gama	313.10-323.10	0.10-1.44	0.0500-0.9000	-	46	0	0	[223]
C6-aP	338.15-353.15	0.10-0.79	0.0520-0.8140	0.3770-0.9990	18	18	0	[245]
7-aP	358.15-368.15	0.14-0.91	0.0440-0.9880	0.2690-0.9960	30	30	0	[245]
B-aC6	348.15-354.65	0.81-1.02	0.0680-0.9430	0.0820-0.9380	42	42	0	[257-259]
13aC5-B	278.15-351.76	0.07-1.01	0.0272-0.8100	0.0607-0.4556	30	6	0	[119, 254]
B-gama	356.65-372.25	1.01-1.01	0.5466-0.9361	0.9358-0.9946	8	8	0	[260]
aC6-13mB	329.05-405.75	0.40-0.99	0.0280-0.9350	0.1840-0.9900	30	30	0	[261]
aC5-eB	271.25-396.65	0.13-1.01	0.0370-0.9480	0.3260-0.9980	18	18	0	[262]
aC5-iprB	278.65-398.65	0.13-1.01	0.0480-0.8960	0.5430-0.9980	17	17	0	[262]
mB-15aC8	313.85-336.15	0.08-0.08	0.1000-0.9000	0.4000-0.9750	9	9	0	[263]
aP-pcy	429.95-448.05	1.01-1.01	0.0427-0.9041	0.0948-0.9492	17	17	0	[264]
CO_2-aC6	315.45-347.25	19.53-112.06	0.1604-0.9554	0.9410-0.9889	45	45	0	[265]
CO_2-lamda	293.32-348.12	8.30-129.35	0.0732-0.9966	0.9562-0.9998	100	135	4	[266-274]
CO_2-aP	295.85-335.25	32.50-109.30	0.3007-0.9896	0.9718-0.9988	64	148	0	[266, 275-276]
CO_2-xi	315.00-323.20	3.00-100.50	0.0281-0.9540	0.9670-0.9998	53	37	0	[277-279]
a2-aP	288.15-308.15	44.71-73.69	0.7471-0.9950	0.9572-0.9980	52	17	0	[252]
a2-xi	288.15-308.15	40.67-77.97	0.5864-0.9935	0.9742-0.9961	32	6	0	[280]
2m13a4-13aC5	307.50-312.80	1.01-1.01	0.0500-0.9500	0.0650-0.9560	27	20	0	[235, 239, 281]
2m2a4-13aC5	310.87-313.00	1.01-1.01	0.0500-0.9500	0.0615-0.9440	18	18	0	[235, 239]
2m13a4-gama	313.10-323.10	0.09-1.52	0.0490-0.9000	-	25	0	0	[223]
aP-lamda	429.50-450.00	1.01-1.01	0.0207-0.9843	0.0334-0.9905	47	47	0	[264, 282]
bP-lamda	439.35-449.45	1.01-1.01	0.0752-0.9712	0.1033-0.9759	16	16	0	[283]
Total number of points:					**9263**	**6413**	**143**	

III.3 Difficulties in predicting the phase behavior of alkenes containing mixtures

III.3.1 Uncertainty on the pure component vapor pressure

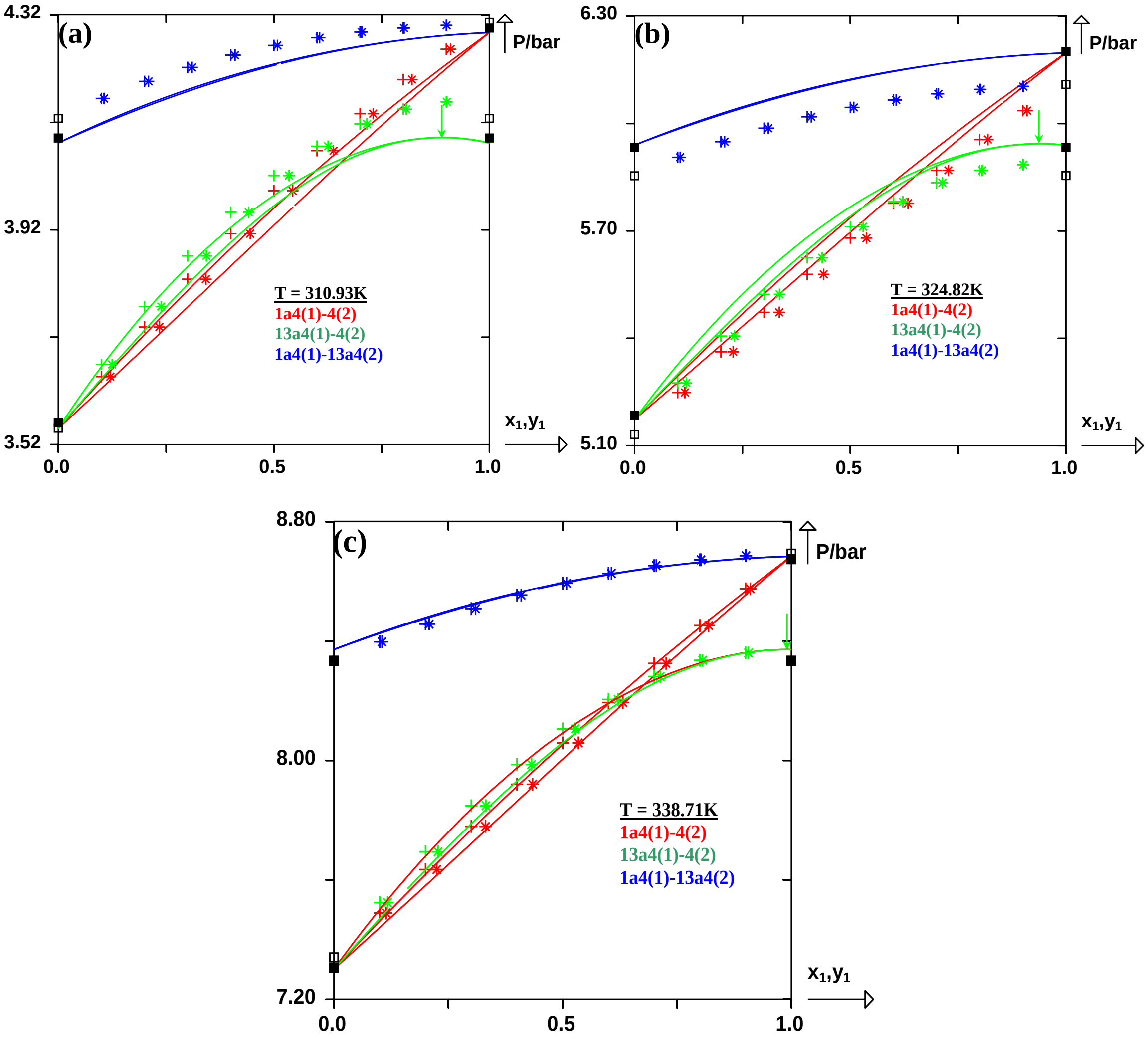

Figure III−1. Prediction of isothermal curves for the three binary systems: (1-butene(1) + n-butane(2)), (1,3-butadiene(1) + n-butane(2)) and (1-butene(1) + 1,3-butadiene(2)) using the PPR78 model. (+) experimental bubble points, (✳) experimental dew points, (☐) experimental saturated vapor pressure of pure component, (■) saturated vapor pressure of pure component according to Prosim. Solid line: predicted curves with the PPR78 model. **(a)** (1-butene(1) + n-butane(2)) at T = 310.93 K (k_{ij} = 0.0043), (1,3-butadiene(1) + n-butane(2)) at T = 310.93 K (k_{ij} = 0.0156), (1-butene(1) + 1,3-butadiene(2)) at T = 310.93 K (k_{ij} = 0.0035).**(b)** (1-butene(1) + n-butane(2)) at T = 324.82 K (k_{ij} = 0.0040), (1,3-butadiene(1) + n-butane(2)) at T = 324.82 K (k_{ij} = 0.0144), (1-butene(1) + 1,3-butadiene(2)) at T = 324.82 K (k_{ij} = 0.0032). **(c)** (1-butene(1) + n-butane(2)) at T = 338.71 K (k_{ij} = 0.0037), (1,3-butadiene(1) + n-butane(2)) at T = 338.71 K (k_{ij} = 0.0133), (1-butene(1) + 1,3-butadiene(2)) at T = 338.71 K (k_{ij} = 0.0029).

Pure components which are similar in size, shape and chemical nature tend to form nearly ideal or even azeotropic solutions. These types of solutions occur frequently in industrial applications and are well-known for the difficulty of their separations. Consequently, the accurate design of distillation units for these solutions requires models to accurately predict the experimental VLE data. It is important to notice that even though our model is capable to represent this kind of phase behavior, the uncertainty on the saturated vapor pressure of pure component has increased the objective function and made our parameters-fitting more difficult. In order to illustrate this problem, we take the measurements of Laurance et al.[116] that concern the three binary systems composed of C4 hydrocarbons as n-butane, 1-butene and 1,3-butadiene.

The P-xy diagrams for the three binary mixtures ((1-butene(1) + n-butane(2)), (1,3-butadiene(1) + n-butane(2)) and (1-butene(1) + 1,3-butadiene(2))) at T = 310.93 K are shown in figure (III−1a). The calculated saturated vapor pressures of n-butane, 1-butene and 1,3-butadiene underestimate the experimental value (black hollow square) of 0.0009 bar (i.e. 0.03%), 0.0189 bar (i.e. 0.44%) and 0.0457 bar (i.e. 1.11%), respectively. As a result, the phase envelopes calculated by our model are shifted to lower pressures. In addition, the predicted P-xy diagrams for these three mixtures at T = 324.82 K are shifted to higher pressures [see figure (III−1b)], which is a direct consequence of the feature that the pure component saturated vapor pressures are overestimated. When the temperature reaches T = 338.71 K [see figure (III−1c)], our model yields the phase envelopes in good agreement with experimental data except for the left side of (1-butene(1) + 1,3-butadiene(2)), for which a small difference between the calculated saturated vapor pressure and the experimental one can still be observed. For comparison, we have plotted in figure (III−1) (solid black squares) the pure component saturated pressures at three different temperatures, obtained from correlations available in the software Prosim, which indicates that the PR EoS predicts more or less well the saturated pressures. In this case, only the experimental points at T = 338.71 K were used for our data-fitting, although there are still some deviations on the saturated pressure. It is indeed clear that the inaccuracy on the pure component vapor pressure observed for these binary systems is not linked to the k_{ij} value.

III.3.2 Difficulties of temperature-dependent BIP ($k_{ij}(T)$) optimization

For some of the studied alkenes containing mixtures, it is really difficult to restitute both the critical pressure and the critical composition. By looking at the binary system (ethylene(1) + n-butane(2)) at T = 338.71 K [see figure (III−2a)], k_{ij} = 0.0000 makes the PR EoS able to well reproduce the critical pressure, while the value needed for the critical composition is: k_{ij} = 0.3000. It is therefore difficult to restitute both the critical pressure and the critical composition with the same k_{ij} value. Another difficulty is the simultaneous correlation of the bubble and dew curves for binary systems containing 1,3-butadiene. Taking (1,3-butadiene(1) + n-hexane(2)) at T = 233.15 K for example, two P-xy diagrams calculated with two different k_{ij} values are plotted in figure (III−2b), which indicate that it is not possible to well predict both the bubble and dew curves at one temperature, by using a single k_{ij} value. Moreover, most of the binary mixtures containing 1,3-butadiene, show high mole fraction of the light component in the vapor phase [see figure (III−2b)], close to one, which will make the objective function defined by equation (I−105) more important.

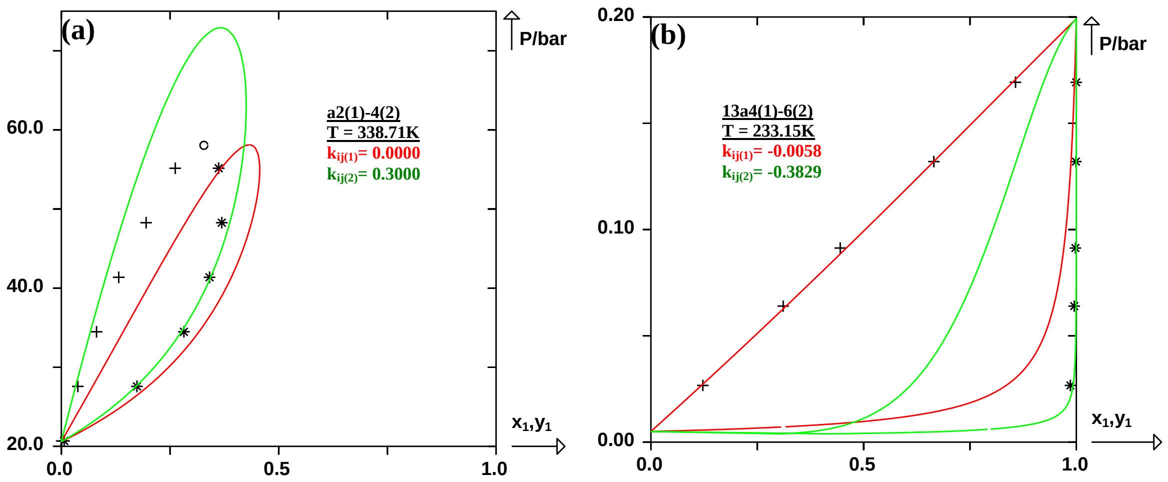

Figure III−2. Prediction of isothermal curves for the two binary systems: (ethylene(1) + n-butene(2)) and (1,3-butadiene(1) + n-hexane(2)). (+) experimental bubble points, (✳) experimental dew points, (○) experimental critical points. **(a)** System (ethylene(1) + n-butene(2)) at T = 338.71 K with two different k_{ij} values: $k_{ij(1)}$ = 0.0000 and $k_{ij(2)}$ = 0.3000. **(b)** System (1,3-butadiene(1) + n-hexane(2)) at T = 233.15 K with two different k_{ij} values: $k_{ij(1)}$ = -0.0058 and $k_{ij(2)}$ = -0.3829.

III.4 Results and discussion

For all the data points included in our database, the objective function defined by equation (I−105) is: F_{obj}=8.80 %.

The average overall deviation on the liquid phase composition is:

$$\overline{\Delta x_1} = \frac{\sum_{i=1}^{n_{bubble}} \left(\left| x_{1,exp} - x_{1,cal} \right| \right)_i}{n_{bubble}} = 0.023 \text{. Moreover } \frac{F_{obj,bubble}}{n_{bubble}} = 7.95 \ \%$$

The average overall deviation on the gas phase composition is:

$$\overline{\Delta y_1} = \frac{\sum_{i=1}^{n_{dew}} \left(\left| y_{1,exp} - y_{1,cal} \right| \right)_i}{n_{dew}} = 0.016 \text{. Moreover } \frac{F_{obj,dew}}{n_{dew}} = 10.08 \ \%$$

The average overall deviation on the critical composition is:

$$\overline{\Delta x_{c1}} = \frac{\sum_{i=1}^{n_{crit}} \left(\left| x_{c1,exp} - x_{c1,cal} \right| \right)_i}{n_{crit}} = 0.029 \text{. Moreover } \frac{F_{obj,crit.\ comp}}{n_{crit}} = 10.29 \ \%$$

The average overall deviation on the binary critical pressure is:

$$\overline{\Delta P_c} \% = \frac{F_{obj,crit.\ pressure}}{n_{crit}} = \frac{100 \sum_{i=1}^{n_{crit}} \left(\frac{\left| P_{cm,exp} - P_{cm,cal} \right|}{P_{cm,exp}} \right)_i}{n_{crit}} = 3.49\%$$

The value of the objective function indicates that the PPR78 model can give a good representation of the systems studied in this work, although the results are not as good as those obtained for the hydrocarbons and CO_2. This slightly higher objective function value can be explained by the following reasons:

(1) Some experimental data reported in the literatures are generally inconsistent and there are obvious scatters among them.

(2) Several binary systems containing water, cannot be correlated accurately with a cubic equation of state even with temperature-dependent $k_{ij}(T)$.

(3) The deviation between the calculated pure component saturated vapor pressures and the experimental ones increases naturally the objective function.

(4) Nearly ideal or even azeotropic behavior is largely investigated in this study, which results in significant objective function.

(5) A number of dew point compositions are not far away from one, which inevitably increases the objective function. As we can see, the absolute deviation on the gas phase composition is smaller than that on the liquid phase, however, the percent deviation on the gas phase composition is two percent bigger.

In order to illustrate the accuracy and the limitations of our model, it was decided to define several families of binary systems which could give a good representation of the whole data base.

III.4.1 Results for mixtures of [alkene (or cycloalkene) + n-alkane (or branched alkane)]

In this family, 75 binary systems (4335 bubble points + 2676 dew points + 60 mixture critical points) have been collected. It is therefore impossible to show graphically all the results for this family. In order to well illustrate the accuracy of our model, it was decided to present the results in several figures [figure (III−3) to figure (III−9)] according to the differences of phase phenomena.

Figure (III−3) shows the isothermal and isobaric phase diagrams in the sub-critical region for ten binary systems. For the mixtures of (methane(1) + ethylene(2)), (ethylene(1) + propane(2)) and (1,3-butadiene(1) + n-octane(2)) [see figures (III−3a,3b,3c)], the liquid branch is nearly a straight line which means that the liquid phase is close to an ideal solution, and the interval between the vapor and liquid branch is significant. The BIP(k_{ij}(T)) is close to zero and decreases slightly with temperature. The results for six other binary systems are shown in figures (III−3d,3e,3f). In general, quite good agreements between VLE predictions and experimental data points are obtained except that the dew curve of (1,3-butadiene(1) + n-octane(2)) is not very accurate. Indeed, as discussed in section III.3.2, it is difficult to well predict both the bubble and dew curve simultaneously for the systems containing 1,3-butadiene.

Figure (III−4) shows the isothermal and isobaric phase diagrams in both the sub-critical and super-critical regions for six binary systems. It is important to notice that the whole phase envelope and the critical points for (ethylene(1) + n-butane(2)) are not very satisfactory [see figure (III−4b)], owing to the fact that the critical pressure and the critical composition can not be simultaneously predicted, as discussed in section III.3.2. After our data-fitting over the whole database, the critical pressures of (ethylene(1) + n-butane(2)) are better reproduced than the critical compositions. Nevertheless, accurate results are obtained for all these binary systems over wide ranges of temperature and pressure, with BIP(k_{ij}(T)) increasing with temperature except for (n-hexane(1) + 1-hexadecene(2)) [see figure (III−4f)].

Figure (III−5) shows the isothermal phase diagrams at low pressures for six different binary systems. The predicted phase envelops are in good agreement with experimental data. Regarding two binary systems containing cycloalkene: (n-pentane(1) + cyclohexene(2)), (n-hexane(1) + cyclohexene(2)), accurate results are obtained by PPR78, with negative BIP(k_{ij}(T)) values decreasing and then increasing with temperature for both of them.

Figures (III−6,7) show the isothermal and isobaric phase diagrams for twelve binary systems that contain two components of very similar volatility. The nearly ideal and azeotropic phase phenomena, shown in figure (III−6) and figure (III−7) respectively, are not easy to be well reproduced and they will inevitably increase the objective function. Even though small deviations between the calculated pure component vapor pressure and the experimental one still exist for some of these binary systems, all these P-xy and T-xy diagrams indicate that the PPR78 model is capable to well predict this kind of phase behavior. BIP(k_{ij}(T)) is always near zero and it is interesting to notice that BIP(k_{ij}(T)) for each of these ten systems decreases slightly with temperature.

Figure (III−8) shows the isothermal phase diagrams for four asymmetric binary systems. As we can see, the phase envelops for (ethylene(1) + n-dodecane(2)) and (ethylene(1) + n-hexadecane(2)) are slightly overestimated, however, the critical loci, the bubble and dew curves for (ethylene(1) + n-eicosane(2)) are in good agreement with experimental data. From a general view of these binary systems, we can conclude that PPR78 remains an accurate model, regardless of the length of n-alkanes and alkenes.

Among these 75 binary systems of [alkene (or cycloalkene) + n-alkane (or branched alkane)], only 13 ones present experimental critical points, and the predictions of the critical loci are shown in figure (III−9). All these systems except for (ethylene(1) + n-eicosane(2)), exhibit a continuous vapor-liquid critical curve between the critical points of the two pure components, which corresponds to Type I or Type II behavior in the classification of Van Konynenburg and Scott[284]. Generally, these types of critical loci are accurately predicted by our model. We have to indicate that obvious scatters can be observed for several systems. In particular, the experimental critical points of (ethylene(1) + n-octane(2)) on the right side of the mixture critical pressure maximum, appears in the critical locus of (ethylene(1) + n-heptane(2)) [see figure (III−9b)]. That is why these experimental points in that region are slightly overestimated by our model. Meanwhile, Type IV phase behavior is exhibited by (ethylene(1) + n-eicosane(2)) [see figure (III−9c)], the mixture critical line extending between the critical point of n-eicosane and the LCEP (lower critical end point) is well predicted, and that extending between the critical point of ethylene and the UCEP (upper critical end point) is out of the experimental support.

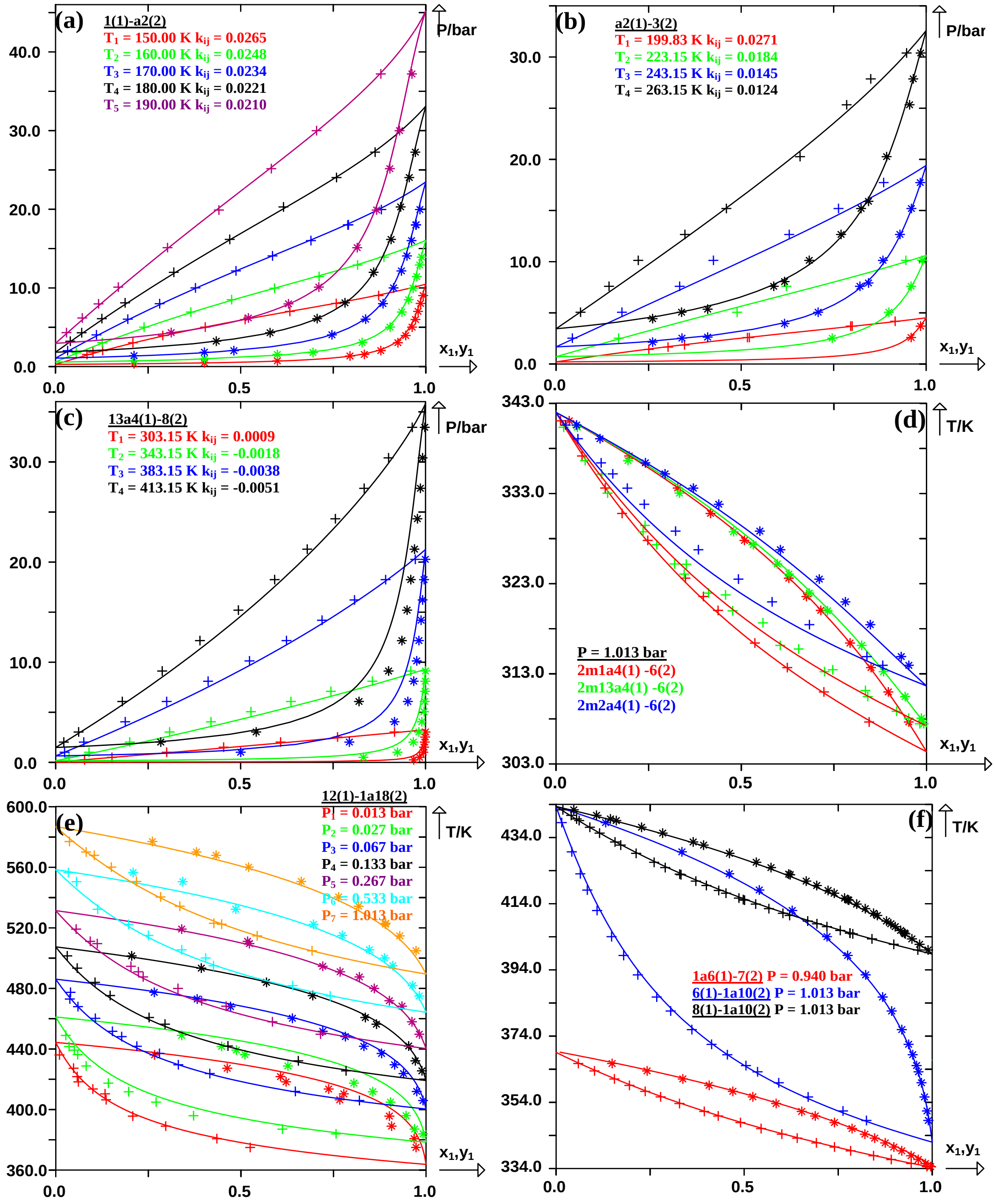

Figure III−3. Prediction of isothermal and isobaric curves in the sub-critical region for ten binary systems using the PPR78 model. (+) experimental bubble points, (✳) experimental dew points. Solid line: predicted curves with the PPR78 model. **(a)** System (methane(1) + ethylene(2)) at five different temperatures: T_1 = 150.00 K (k_{ij} = 0.0265), T_2 = 160.00 K (k_{ij} = 0.0248), T_3 = 170.00 K (k_{ij} = 0.0234), T4 = 180.00 K (k_{ij} = 0.0221), T_5 = 190.00 K (k_{ij} = 0.0210). **(b)** System (ethylene(1) + propane(2)) at four different temperatures: T_1 = 199.83 K (k_{ij} = 0.0271), T_2 = 223.15 K (k_{ij} = 0.0184), T_3 = 243.15 K (k_{ij} = 0.0145), T_4 = 263.15 K (k_{ij} = 0.0124). **(c)** System (1,3-butadiene(1) + n-octane(2)) at four different temperatures: T_1 = 303.15 K (k_{ij} = 0.0009), T_2 = 343.15 K (k_{ij} = -0.0018), T_3 = 383.15 K (k_{ij} = -0.0038), T4 = 413.15 K (k_{ij} = -0.0051). **(d)** System (2-methyl-1-butene(1) + n-hexane(2)) at P = 1.013 bar, system (2-methyl-1,3-butadiene(1) + n-hexane(2)) at P = 1.013 bar, system (2-methyl-2-butene(1) + n-hexane(2)) at P = 1.013 bar. **(e)** System (n-dodecane(1) + 1-octadecene(2)) at seven different pressures: P_1 = 0.013 bar, P_2 = 0.027 bar, P_3 = 0.067 bar, P_4 = 0.133 bar, P_5 = 0.267 bar, P_6 = 0.533 bar, P_7 = 1.013 bar. **(f)** System (1-hexene(1) + n-heptane(2)) at P = 0.940 bar, system (n-hexane(1) + 1-decene(2)) at P = 1.013 bar, system (n-octane(1) + 1-decene(2)) at P_4 = 1.013 bar.

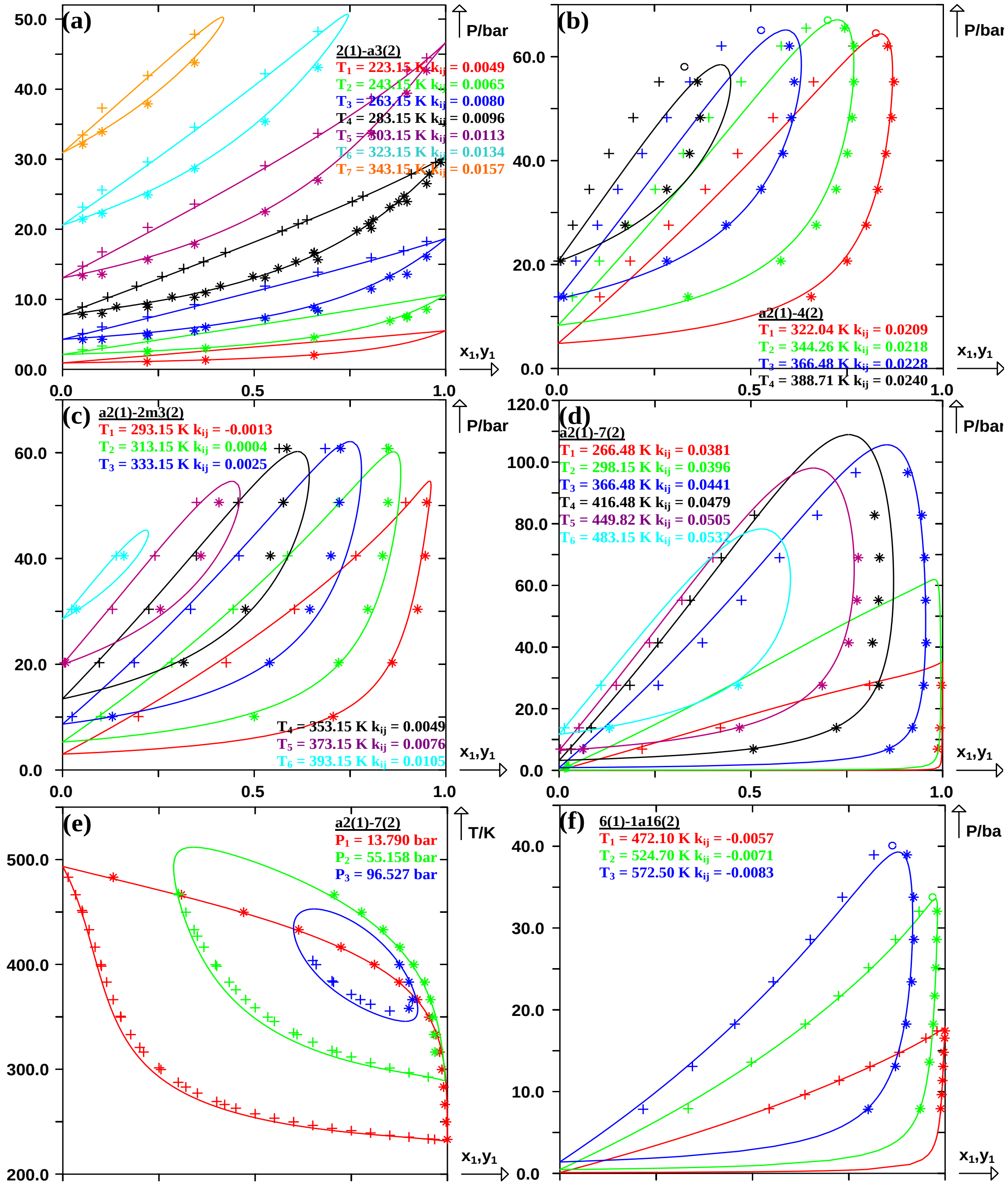

Figure III−4. Prediction of isothermal and isobaric curves in the sub-critical and super-critical regions for five binary systems using the PPR78 model. (+) experimental bubble points, (✳) experimental dew points, (○) experimental critical points. Solid line: predicted curves with the PPR78 model. **(a)** System (ethane(1) + propene(2)) at seven different temperatures: T_1 = 223.15 K (k_{ij} = 0.0049), T_2 = 243.15 K (k_{ij} = 0.0065), T_3 = 263.15 K (k_{ij} = 0.0080), T4 = 283.15 K (k_{ij} = 0.0096), T_5 = 303.15 K (k_{ij} = 0.0113), T_6 = 323.15 K (k_{ij} = 0.0134), T_7 = 343.15 K (k_{ij} = 0.0157). **(b)** System (ethylene(1) + n-butane(2)) at four different temperatures: T_1 = 322.04 K (k_{ij} = 0.0209), T_2 = 344.26 K (k_{ij} = 0.0218), T_3 = 366.48 K (k_{ij} = 0.0228), T4 = 388.71 K (k_{ij} = 0.0240). **(c)** System (ethylene(1) + isobutane(2)) at six different temperatures: T_1 = 293.15 K (k_{ij} = -0.0013), T_2 = 313.15 K (k_{ij} = 0.0004), T_3 = 333.15 K (k_{ij} = 0.0025), T_4 = 353.15 K (k_{ij} = 0.0049), T_5 = 373.15 K (k_{ij} = 0.0076), T_6 = 393.15 K (k_{ij} = 0.0105). **(d)** System (ethylene(1) + n-heptane(2)) at six different temperatures: T_1 = 266.48 K (k_{ij} = 0.0381), T_2 = 298.15 K (k_{ij} = 0.0396), T_3 = 366.48 K (k_{ij} = 0.0441), T_4 = 416.48 K (k_{ij} = 0.0479), T_5 = 449.82 K (k_{ij} = 0.0505), T_6 = 483.15 K (k_{ij} = 0.0532). **(e)** System (ethylene(1) + n-heptane(2)) at three different pressures: P_1 = 13.790 bar, P_2 = 55.158 bar, P_3 = 96.527 bar. **(f)** System (n-hexane(1) + 1-hexadecene(2)) at three different temperatures: T_1 = 472.10 K (k_{ij} = -0.0057), T_2 = 524.70 K (k_{ij} = -0.0071), T_3 = 572.50 K (k_{ij} = -0.0083).

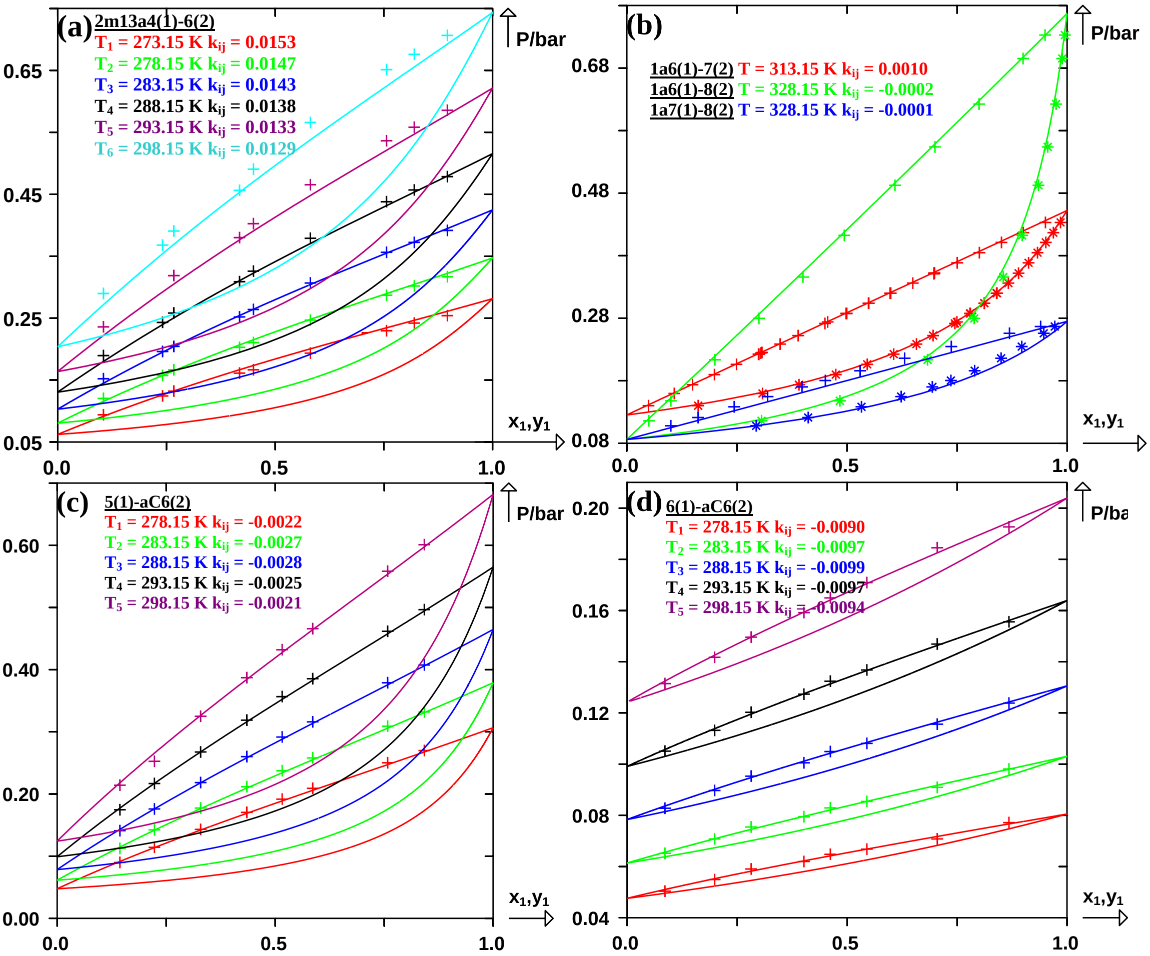

Figure III‒5. Prediction of isothermal curves at low pressures for six binary systems using the PPR78 model. (+) experimental bubble points, (✳) experimental dew points. Solid line: predicted curves with the PPR78 model. **(a)** System (2-methyl-1,3-butadiene(1) + n-hexane(2)) at six different temperatures: T_1 = 273.15 K (k_{ij} = 0.0153), T_2 = 278.15 K (k_{ij} = 0.0147), T_3 = 283.15 K (k_{ij} = 0.0143), T_4 = 288.15 K (k_{ij} = 0.0138), T_5 = 293.15 K (k_{ij} = 0.0133), T_6 = 298.15 K (k_{ij} = 0.0129). **(b)** System (1-hexene(1) + n-heptane(2)) at T = 313.15 K (k_{ij} = 0.0010), system (1-hexene(1) + n-octane(2)) at T = 328.15 K (k_{ij} = -0.0002), system (1-heptene(1) + n-octane(2)) at T = 328.15 K (k_{ij} = -0.0001). **(c)** System (n-pentane(1) + cyclohexene(2)) at five different temperatures: T_1 = 278.15 K (k_{ij} = -0.0022), T_2 = 283.15 K (k_{ij} = -0.0027), T_3 = 288.15 K (k_{ij} = -0.0028), T_4 = 293.15 K (k_{ij} = -0.0025), T_5 = 298.15 K (k_{ij} = -0.0021). **(d)** System (n-hexane(1) + cyclohexene(2)) at five different temperatures: T_1 = 278.15 K (k_{ij} = -0.0090), T_2 = 283.15 K (k_{ij} = -0.0097), T_3 = 288.15 K (k_{ij} = -0.0099), T_4 = 293.15 K (k_{ij} = -0.0097), T_5 = 298.15 K (k_{ij} = -0.0094).

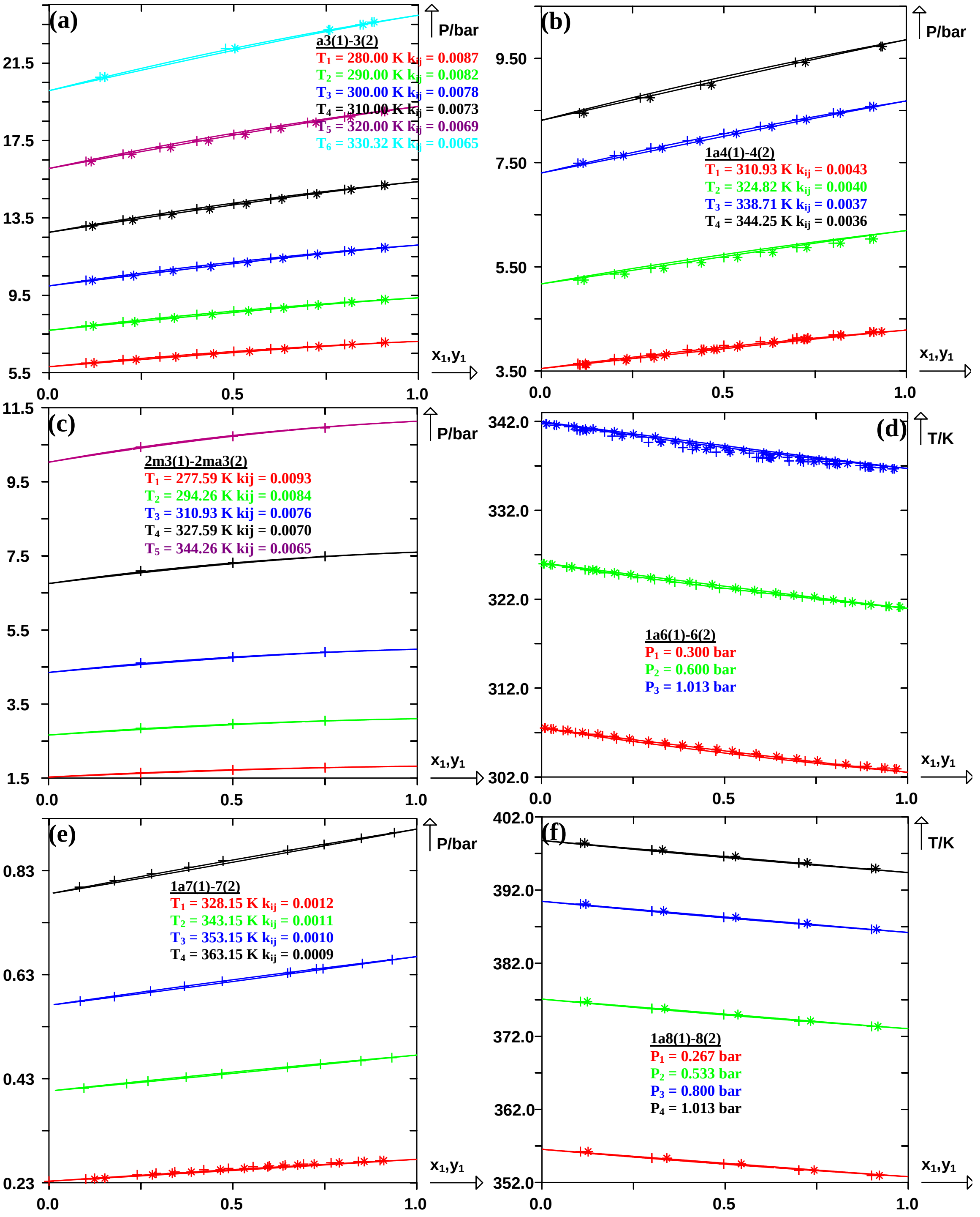

Figure III−6. Prediction of isothermal curves for six binary systems that contain two components of very similar volatility, using the PPR78 model. (+) experimental bubble points, (✳) experimental dew points. Solid line: predicted curves with the PPR78 model. **(a)** System (propene(1) + propane(2)) at six different temperatures: T_1 = 280.00 K (k_{ij} = 0.0087), T_2 = 290.00 K (k_{ij} = 0.0082), T_3 = 300.00 K (k_{ij} = 0.0078), T_4 = 310.00 K (k_{ij} = 0.0073), T_5 = 320.00 K (k_{ij} = 0.0069), T_6 = 330.32 K (k_{ij} = 0.0065). **(b)** System (1-butene(1) + n-butane(2)) at four different temperatures: T_1 = 310.93 K (k_{ij} = 0.0043), T_2 = 324.82 K (k_{ij} = 0.0040), T_3 = 338.71 K (k_{ij} = 0.0037), T_4 = 344.25 K (k_{ij} = 0.0036). **(c)** System (isobutane(1) + 2-methylpropene (2)) at five different temperatures: T_1 = 277.59 K (k_{ij} = 0.0093), T_2 = 294.26 K (k_{ij} = 0.0084), T_3 = 310.93 K (k_{ij} = 0.0076), T_4 = 327.59 K (k_{ij} = 0.0070), T_5 = 344.26 K (k_{ij} = 0.0065). **(d)** System (1-hexene(1) + n-hexane(2)) at three different pressures: P_1 = 0.300 bar, P_2 = 0.600 bar, P_3 = 1.013 bar. **(e)** System (1-heptene(1) + n-heptane(2)) at four different temperatures: T_1 = 328.15 K (k_{ij} = 0.0012), T_2 = 343.15 K (k_{ij} = 0.0011), T_3 = 353.15 K (k_{ij} = 0.0010), T_4 = 363.15 K (k_{ij} = 0.0009). **(f)** System (1-octene(1) + n-octane(2)) at four different pressures: P_1 = 0.267 bar, P_2 = 0.533 bar, P_3 = 0.800 bar, P_4 = 1.013 bar.

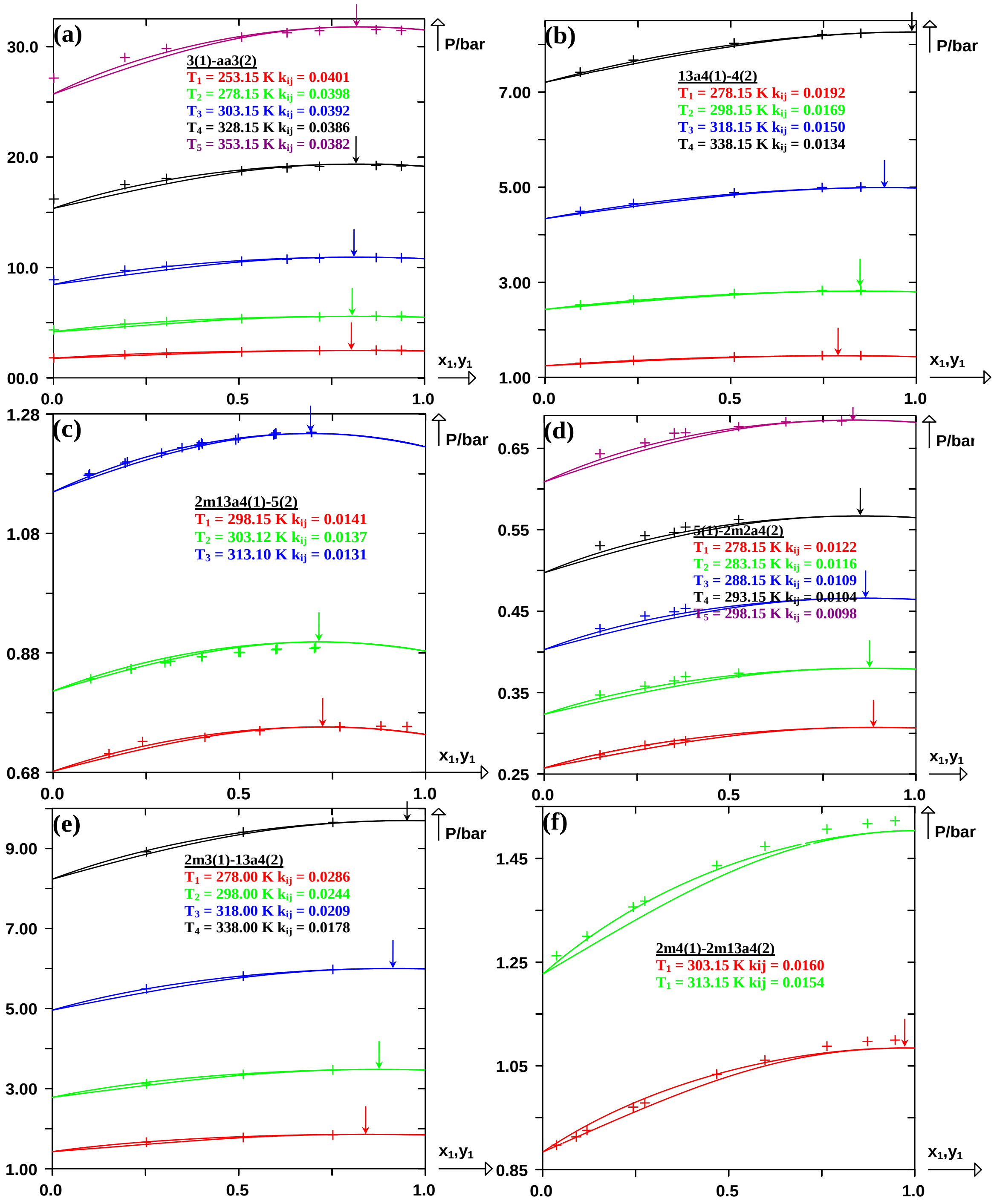

Figure III−7. Prediction of isothermal curves for six binary systems that contain two components of very similar volatility, using the PPR78 model. (+) experimental bubble points, (✳) experimental dew points. Solid line: predicted curves with the PPR78 model. **(a)** System (propane(1) + 1,2-propadiene(2)) at five different temperatures: T_1 = 253.15 K (k_{ij} = 0.0401), T_2 = 278.15 K (k_{ij} = 0.0398), T_3 = 303.15 K (k_{ij} = 0.0392), T_4 = 328.15 K (k_{ij} = 0.0386), T_5 = 353.15 K (k_{ij} = 0.0382). **(b)** System (1,3-butadiene(1) + n-butane(2)) at four different temperatures: T_1 = 278.15 K (k_{ij} = 0.0192), T_2 = 298.15 K (k_{ij} = 0.0169), T_3 = 318.15 K (k_{ij} = 0.0150), T_4 = 338.15 K (k_{ij} = 0.0134). **(c)** System (2-methyl-1,3-butadiene(1) + n-pentane(2)) at three different temperatures: T_1 = 298.15 K (k_{ij} = 0.0141), T_2 = 303.12 K (k_{ij} = 0.0137), T_3 = 313.10 K (k_{ij} = 0.0131). **(d)** System (n-pentane(1) + 2-methyl-2-butene(2)) at five different temperatures: T_1 = 278.15 K (k_{ij} = 0.0122), T_2 = 283.15 K (k_{ij} = 0.0116), T_3 = 288.15 K (k_{ij} = 0.0109), T_4 = 293.15 K (k_{ij} = 0.0104), T_5 = 298.15 K (k_{ij} = 0.0098). **(e)** System (isobutane(1) + 1,3-butadiene(2)) at four different temperatures: T_1 = 278.00 K (k_{ij} = 0.0286), T_2 = 298.00 K (k_{ij} = 0.0244), T_3 = 318.00 K (k_{ij} = 0.0209), T_4 = 338.00 K (k_{ij} = 0.0178). **(f)** System (2-methylbutane(1) + 2-methyl-1,3-butadiene(2)) at two different temperatures: T_1 = 303.15 K (k_{ij} = 0.0160), T_2 = 313.15 K (k_{ij} = 0.0154).

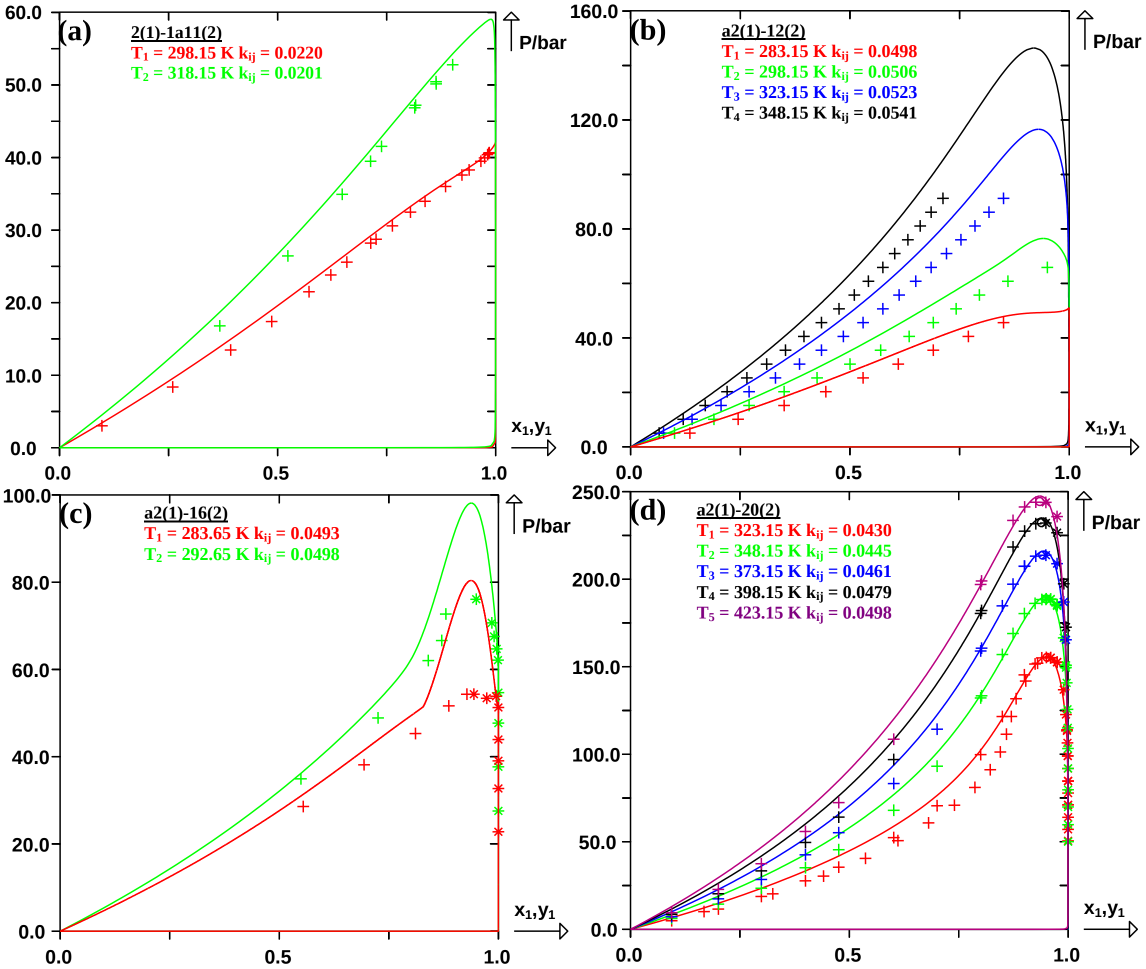

Figure III−8. Prediction of isothermal curves for four asymmetric binary systems using the PPR78 model. (+) experimental bubble points, (✳) experimental dew points, (○) experimental critical points. Solid line: predicted curves with the PPR78 model. **(a)** System (ethane(1) + 1-undecene(2)) at two different temperatures: T_1 = 298.15 K (k_{ij} = 0.0220), T_2 = 318.15 K (k_{ij} = 0.0201). **(b)** System (ethylene(1) + n-dodecane(2)) at four different temperatures: T_1 = 283.15 K (k_{ij} = 0.0498), T_2 = 298.15 K (k_{ij} = 0.0506), T_3 = 323.15 K (k_{ij} = 0.0523), T_4 = 348.15 K (k_{ij} = 0.0541). **(c)** System (ethylene(1) + n-hexadecane(2)) at two different temperatures: T_1 = 283.65 K (k_{ij} = 0.0493), T_2 = 292.65 K (k_{ij} = 0.0498). **(d)** System (ethylene(1) + n-eicosane(2)) at five different temperatures: T_1 = 323.15 K (k_{ij} = 0.0430), T_2 = 348.15 K (k_{ij} = 0.0445), T_3 = 373.15 K (k_{ij} = 0.0461), T_4 = 398.15 K (k_{ij} = 0.0479), T_5 = 423.15 K (k_{ij} = 0.0498).

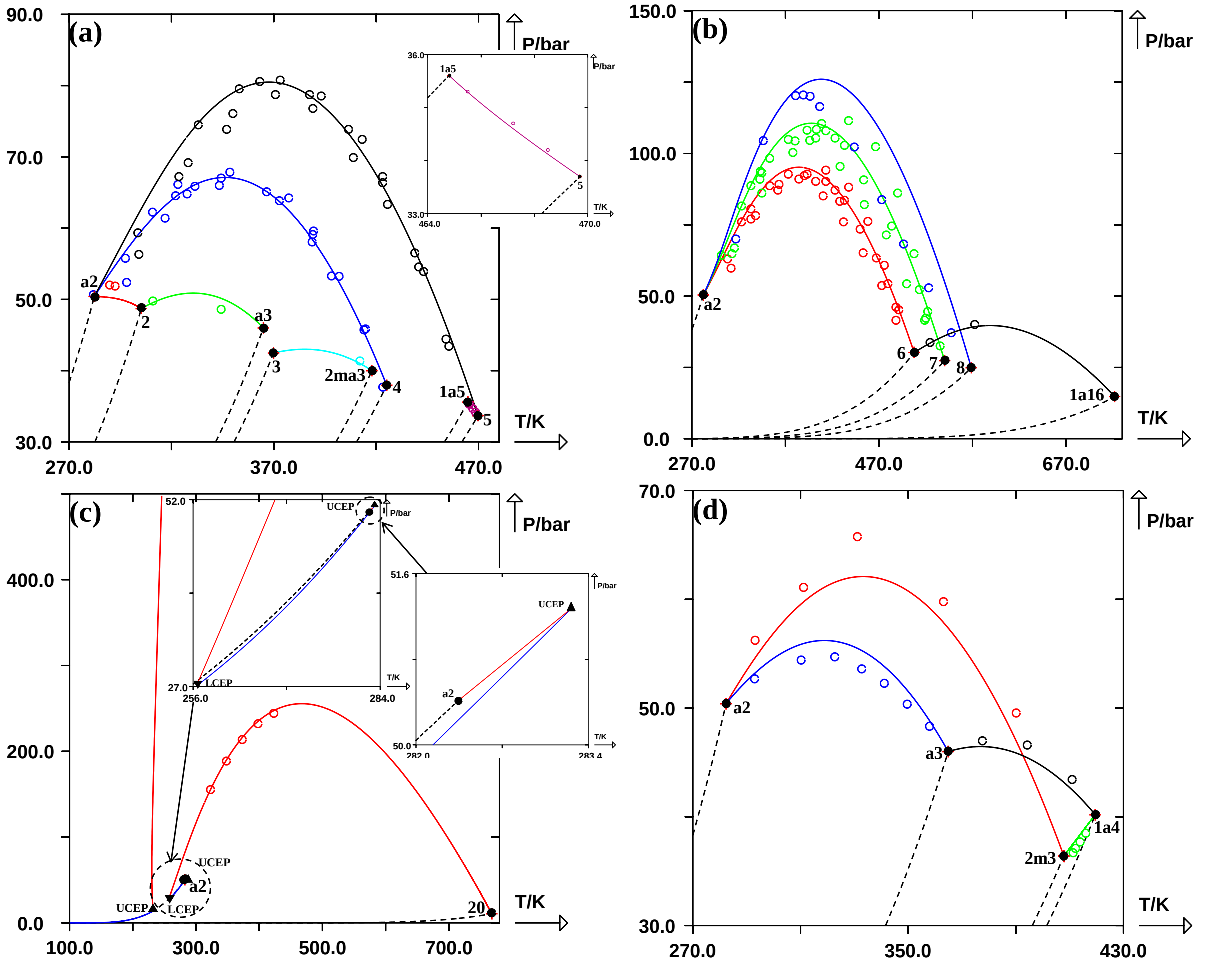

Figure III–9. (a-d) Predictions of the critical locus for fifteen binary systems using the PPR78 model. (○) experimental critical points, (●) critical points of the pure compounds, (▲) Upper critical end point (UCEP), (▼) Lower critical end point (LCEP). Solid line: predicted curves with the PPR78 model. Dashed line: vaporization curve of the pure compounds.

III.4.2 Results for mixtures of [alkene (or cycloalkene) + alkene (or cycloalkene)]

Figure (III−10) shows the isothermal and isobaric phase diagrams for five binary systems that contain two components of very similar volatility. From a general view over the results obtained, the nearly ideal phase behavior and the azeotropes are predicted with satisfactory accuracy, regardless of the uncertainty of pure component saturated pressure and some scatter among experimental data points. At the same time, P-xy and T-xy phase diagrams in the sub-critical area for nine different binary systems are shown in figure (III−11), and perfect results are obtained by our model.

Figure (III−12) shows the isothermal phase diagrams in both the sub-critical and super-critical regions for six binary systems. All the experimental VLE data for (ethylene(1) + propene(2)), (ethylene(1) + 1-butene(2)), (ethylene(1) + 4-methyl-1-pentene(2)) and (propene(1) + 1-butene(2)) from low to high temperatures are predicted with excellent accuracy. When the formula of the alkene mixed with ethylene becomes more complex (e.g. alpha-pinene, beta-pinene), the mixture becomes highly asymmetric. And as a result, the predictions are less satisfactory [see figure (III−12e,12f)].

The predictions of the critical loci for two binary systems in this family: (ethylene(1) + propene(2)), (propene(1) + 1-butene(2)) are plotted in figure (III−9d). Generally, accurate results are obtained for various binary systems belonging to this family.

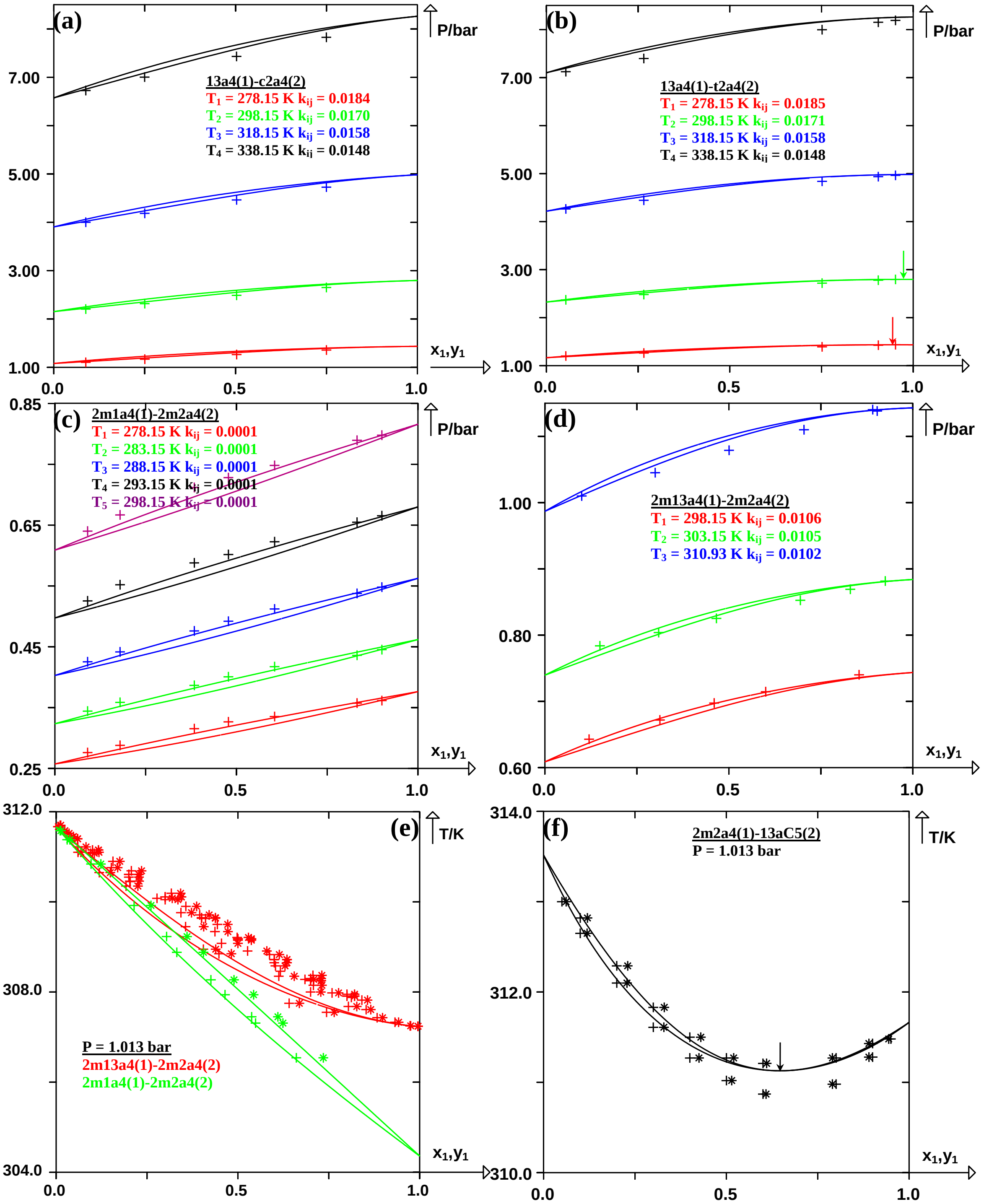

Figure III−10. Prediction of isothermal and isobaric curves for six binary systems that contain two components of very similar volatility, using the PPR78 model. (+) experimental bubble points, (✳) experimental dew points. Solid line: predicted curves with the PPR78 model. **(a)** System (1,3-butadiene(1) + cis-2-butene(2)) at four different temperatures: T_1 = 278.15 K (k_{ij} = 0.0184), T_2 = 298.15 K (k_{ij} = 0.0170), T_3 = 318.15 K (k_{ij} = 0.0158), T_4 = 338.15 K (k_{ij} = 0.0148). **(b)** System (1,3-butadiene(1) + trans-2-butene(2)) at four different temperatures: T_1 = 278.15 K (k_{ij} = 0.0185), T_2 = 298.15 K (k_{ij} = 0.0171), T_3 = 318.15 K (k_{ij} = 0.0158), T_4 = 338.15 K (k_{ij} = 0.0148). **(c)** System (2-methyl-1-butene(1) + 2-methyl-2-butene(2)) at five different temperatures: T_1 = 278.15 K (k_{ij} = 0.0001), T_2 = 283.15 K (k_{ij} = 0.0001), T_3 = 288.15 K (k_{ij} = 0.0001), T_4 = 293.15 K (k_{ij} = 0.0001), T_5 = 298.15 K (k_{ij} = 0.0001). **(d)** System (2-methyl-1,3-butadiene(1) + 2-methyl-2-butene(2)) at three different temperatures: T_1 = 298.15 K (k_{ij} = 0.0106), T_2 = 303.15 K (k_{ij} = 0.0105), T_3 = 310.93 K (k_{ij} = 0.0102). **(e)** System (2-methyl-1,3-butadiene(1) + 2-methyl-2-butene(2)) at P = 1.013 bar, system (2-methyl-1-butene(1) + 2-methyl-2-butene(2)) at P = 1.013 bar. **(f)** System (2-methyl-2-butene(1) + 1,3-cyclopentadiene(2)) at P = 1.013 bar.

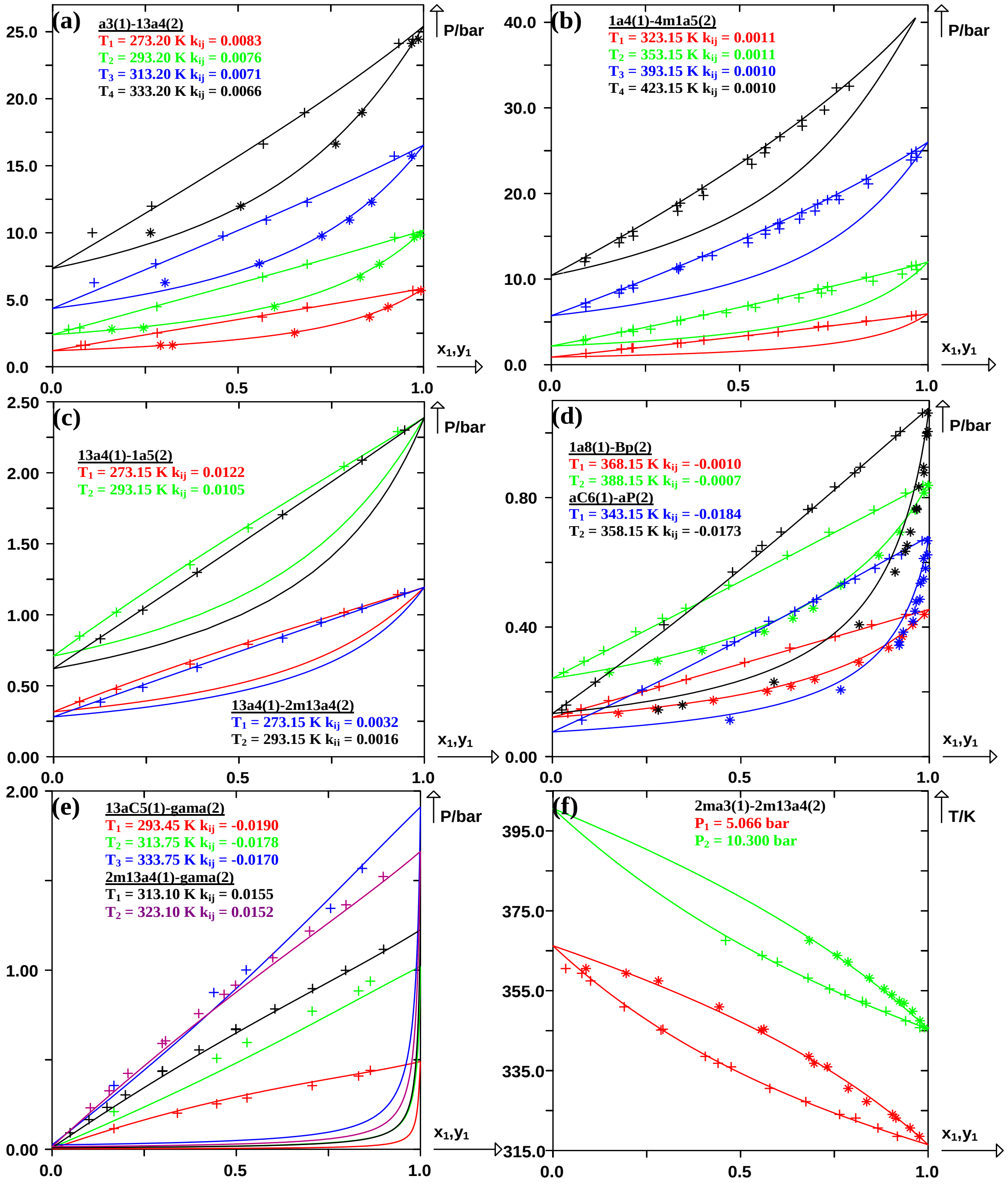

Figure III‒11. Prediction of isothermal and isobaric curves in the sub-critical region for nine binary systems using the PPR78 model. (+) experimental bubble points, (✳) experimental dew points. Solid line: predicted curves with the PPR78 model. **(a)** System (propene(1) + 1,3-butadiene(2)) at four different temperatures: T_1 = 273.20 K (k_{ij} = 0.0083), T_2 = 293.20 K (k_{ij} = 0.0076), T_3 = 313.20 K (k_{ij} = 0.0071), T_4 = 333.20 K (k_{ij} = 0.0066). **(b)** System (1-butene(1) + 4-methyl-1-pentene(2)) at four different temperatures: T_1 = 323.15 K (k_{ij} = 0.0011), T_2 = 353.15 K (k_{ij} = 0.0011), T_3 = 393.15 K (k_{ij} = 0.0010), T_4 = 423.15 K (k_{ij} = 0.0010). **(c)** System (1,3-butadiene(1) + 1-pentene(2)) at two different temperatures: T_1 = 273.15 K (k_{ij} = 0.0122), T_2 = 293.15 K (k_{ij} = 0.0105), and system (1,3-butadiene(1) + 2-methyl-1,3-butadiene(2)) at two different temperatures: T_1 = 273.15 K (k_{ij} = 0.0032), T_2 = 293.15 K (k_{ij} = 0.0016). **(d)** System (1-octene(1) + beta-pinene(2)) at two different temperatures: T_1 = 368.15 K (k_{ij} = -0.0010), T_2 = 388.15 K (k_{ij} = -0.0007), and system (cyclohexene(1) + alpha-pinene(2)) at two different temperatures: T_1 = 343.15 K (k_{ij} = -0.0184), T_2 = 358.15 K (k_{ij} = -0.0173). **(e)** System (1,3-cyclopentadiene(1) + dicyclopentadiene(2)) at three different temperatures: T_1 = 293.45 K (k_{ij} = -0.0190), T_2 = 313.75 K (k_{ij} = -0.0178), T_3 = 333.75 K (k_{ij} = -0.0170), and system (2-methyl-1,3-butadiene(1) + dicyclopentadiene(2)) at two different temperatures: T_1 = 313.10 K (k_{ij} = 0.0155), T_2 = 323.10 K (k_{ij} = 0.0152). **(f)** System (2-methylpropene(1) + 2-methyl-1,3-butadiene(2)) at two different pressures: P_1 = 5.066 bar, P_2 = 10.300 bar.

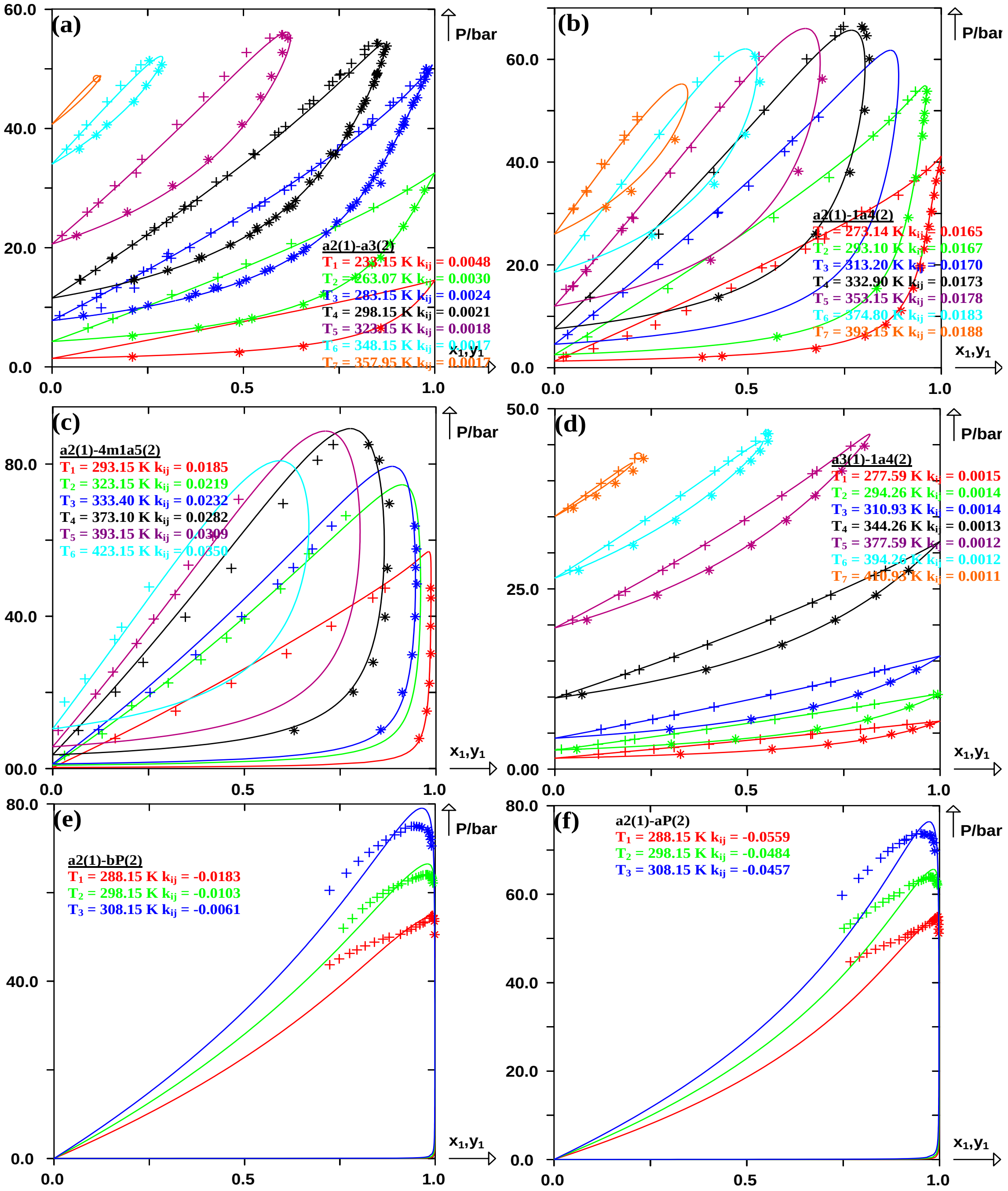

Figure III‒12. Prediction of isothermal curves in the sub-critical and super-critical regions for six binary systems using the PPR78 model. (+) experimental bubble points, (✳) experimental dew points, (○) experimental critical points. Solid line: predicted curves with the PPR78 model. **(a)** System (ethylene(1) + propene(2)) at seven different temperatures: T_1 = 233.15 K (k_{ij} = 0.0048), T_2 = 263.07 K (k_{ij} = 0.0030), T_3 = 283.15 K (k_{ij} = 0.0024), T_4 = 298.15 K (k_{ij} = 0.0021), T_5 = 323.15 K (k_{ij} = 0.0018), T_6 = 348.15 K (k_{ij} = 0.0017), T_7 = 357.95 K (k_{ij} = 0.0017). **(b)** System (ethylene(1) + 1-butene(2)) at seven different temperatures: T_1 = 273.14 K (k_{ij} = 0.0165), T_2 = 293.10 K (k_{ij} = 0.0167), T_3 = 313.20 K (k_{ij} = 0.0170), T_4 = 332.90 K (k_{ij} = 0.0173), T_5 = 353.15 K (k_{ij} = 0.0178), T_6 = 374.80 K (k_{ij} = 0.0183), T_7 = 393.15 K (k_{ij} = 0.0188). **(c)** System (ethylene(1) + 4-methyl-1-pentene(2)) at six different temperatures: T_1 = 293.15 K (k_{ij} = 0.0185), T_2 = 323.15 K (k_{ij} = 0.0219), T_3 = 333.40 K (k_{ij} = 0.0232), T_4 = 373.10 K (k_{ij} = 0.0282), T_5 = 393.15 K (k_{ij} = 0.0309), T_6 = 423.15 K (k_{ij} = 0.0350). **(d)** System (propene(1) + 1-butene(2)) at seven different temperatures: T_1 = 277.59 K (k_{ij} = 0.0015), T_2 = 294.26 K (k_{ij} = 0.0014), T_3 = 310.93 K (k_{ij} = 0.0014), T_4 = 344.26 K (k_{ij} = 0.0013), T_5 = 377.59 K (k_{ij} = 0.0012), T_6 = 394.26 K (k_{ij} = 0.0012), T_7 = 410.93 K (k_{ij} = 0.0011). **(e)** System (ethylene(1) + beta-pinene(2)) at three different temperatures: T_1 = 288.15 K (k_{ij} = -0.0183), T_2 = 298.15 K (k_{ij} = -0.0103), T_3 = 308.15 K (k_{ij} = -0.0061). **(f)** System (ethylene(1) + alpha-pinene(2)) at three different temperatures: T_1 = 288.15 K (k_{ij} = -0.0559), T_2 = 298.15 K (k_{ij} = -0.0484), T_3 = 308.15 K (k_{ij} = -0.0457).

III.4.3 Results for mixtures of [alkene (or cycloalkene) + aromatic compound] and [alkene (or cycloalkene) + naphthenic compound]

Figure (III−13) shows the isothermal phase diagrams at low pressures for six binary systems. The only drawback is that the small positive deviation from ideality of the system (toluene(1) + alpha-methylstyrene(2)) has not been well predicted [see figure (III−13d)]. However, very good results have been obtained for the other five binary systems, including the system (cyclohexane(1) + beta-pinene(2)) that contains a compound more complex.

Figure (III−14) shows the isothermal and isobaric phase diagrams in the sub-critical region for eight systems. From the P-xy diagrams [figures (III−14a,14b,14c)] we can see that the liquid and vapor branches of (1,3-butadiene(1) + benzene(2)) and (1,3-butadiene(1) + cyclohexane(2)) can not be simultaneously restituted, as discussed in section III.3.2, while that of (1,3-butadiene(1) + toluene(2)) are in close agreement with experimental data. The T-xy diagrams [figures (III−14d,14e,14f)] indicate that PPR78 can accurately predict the phase envelops for the other five binary systems, including those containing a cycloalkene or a long-chain alkene.

Figure (III−15) shows the isothermal phase diagrams in both the sub-critical and super-critical regions for four binary systems. As shown in figures (III−15a,15b,15c), very good results are obtained for (ethylene(1) + benzene(2)), (ethylene(1) + toluene(2)) and (ethylene(1) + cyclohexane(2)). Unfortunately, (ethylene (1) + naphthalene (2)) presents the worst results in this study: F_{obj} = 18.35% over 33 bubble points, 240 dew points and 7 critical points. As shown in figure (III−15d), most of the experimental data are dew points and most of the vapor compositions are not far from one, which inevitably increases the objective function. Furthermore, we have tried to find the best k_{ij} to correlate the experimental data at each of these temperatures: T = 332.10 K, 341.85 K and 352.00 K, nevertheless, there is no k_{ij} value that is able to exactly reproduce the phase envelope (liquid branch, vapor branch, critical composition and critical pressure). By looking at the prediction of isothermal curves at five different temperatures, reasonable results are obtained except for the P-xy diagram at T = 308.15 K. Moreover, it is surprising that BIP(k_{ij}(T)) varies much more significantly with temperature (k_{ij} decreases from 0.1098 to 0.0011 as the temperature varies from 285.15 K to 352.15 K), compared to other systems investigated.

Figure (III−16) shows the isothermal and isobaric phase diagrams for three binary systems that contain two components of very similar volatility, and the predictions of critical loci for five different binary systems. Two azeotropic curves for the system (benzene(1) + cyclohexene(2)), the nearly ideal phase behavior of (ethylbenzene(1) + styrene(2)) and two T-xy curves of (cyclohexane(1) + cyclohexene(2)) and (benzene(1) + cyclohexene(2)) are respectively shown in figures (III−16a,16b,16c). Once again, the PPR78 model is capable to well predict this kind of phase behavior. Regarding the predictions of critical loci [see figure (III−16d)], the experimental critical points for (ethylene(1) + benzene(2)), (ethylene(1) + toluene(2)), (propene(1) + benzene(2)) and (propene(1) + isopropylbenzene(2)) are predicted with satisfactory accuracy. However, considering (ethylene(1) + naphthalene(2)), the critical curve shows a pressure minimum and a pressure maximum, and the slope of the critical curve at low temperature is very steep (a small change of temperature induces a large change of pressure). Such Type III systems are really difficult to be well predicted by our model, which was demonstrated in our previous parpers[3-4]. That is why the predicted P-xy diagram for (ethylene(1) + naphthalene(2)) was so poor [see figure (III−15d)].

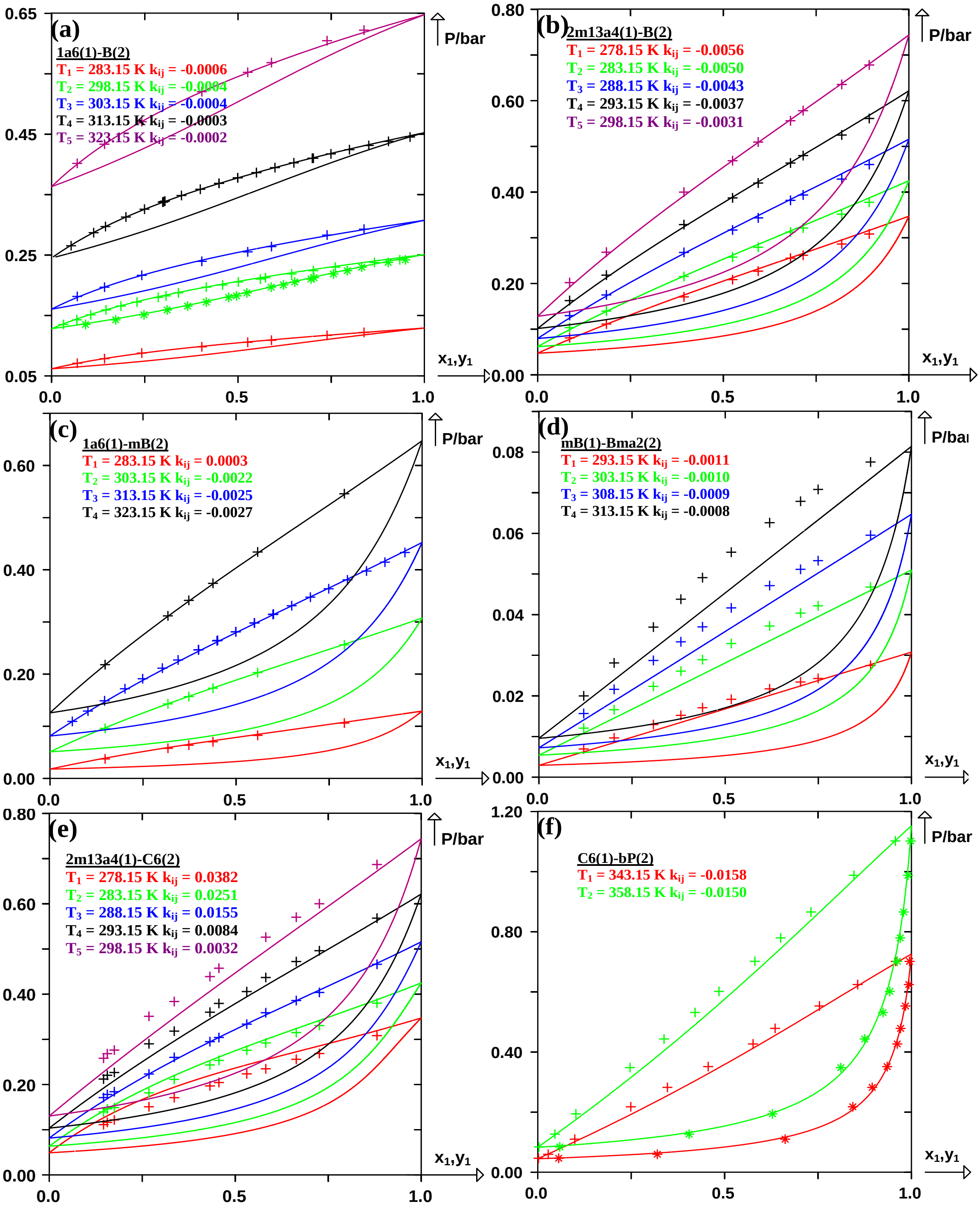

Figure III‒13. Prediction of isothermal curves at low pressures for six binary systems using the PPR78 model. (+) experimental bubble points, (✳) experimental dew points. Solid line: predicted curves with the PPR78 model. **(a)** System (1-hexene(1) + benzene(2)) at five different temperatures: T_1 = 283.15 K (k_{ij} = -0.0006), T_2 = 298.15 K (k_{ij} = -0.0004), T_3 = 303.15 K (k_{ij} = -0.0004), T_4 = 313.15 K (k_{ij} = -0.0003), T_5 = 323.15 K (k_{ij} = -0.0002). **(b)** System (2-methyl-1,3-butadiene(1) + benzene(2)) at five different temperatures: T_1 = 278.15 K (k_{ij} = -0.0056), T_2 = 283.15 K (k_{ij} = -0.0050), T_3 = 288.15 K (k_{ij} = -0.0043), T_4 = 293.15 K (k_{ij} = -0.0037), T_5 = 298.15 K (k_{ij} = -0.0031). **(c)** System (1-hexene(1) + methylbenzene(2)) at four different temperatures: T_1 = 283.15 K (k_{ij} = 0.0003), T_2 = 303.15 K (k_{ij} = -0.0022), T_3 = 313.15 K (k_{ij} = -0.0025), T_4 = 323.15 K (k_{ij} = -0.0027). **(d)** System (methylbenzene(1) + alpha-methylstyrene(2)) at four different temperatures: T_1 = 293.15 K (k_{ij} = -0.0011), T_2 = 303.15 K (k_{ij} = -0.0010), T_3 = 308.15 K (k_{ij} = -0.0009), T_4 = 313.15 K (k_{ij} = 0.0008). **(e)** System (2-methyl-1,3-butadiene(1) + cyclohexane(2)) at five different temperatures: T_1 = 278.15 K (k_{ij} = 0.0382), T_2 = 283.15 K (k_{ij} = 0.0251), T_3 = 288.15 K (k_{ij} = 0.0155), T_4 = 293.15 K (k_{ij} = 0.0084), T_5 = 298.15 K (k_{ij} = 0.0032). **(f)** System (cyclohexane(1) + beta-pinene(2)) at two different temperatures: T_1 = 343.15 K (k_{ij} = -0.0158), T_2 = 358.15 K (k_{ij} = -0.0150).

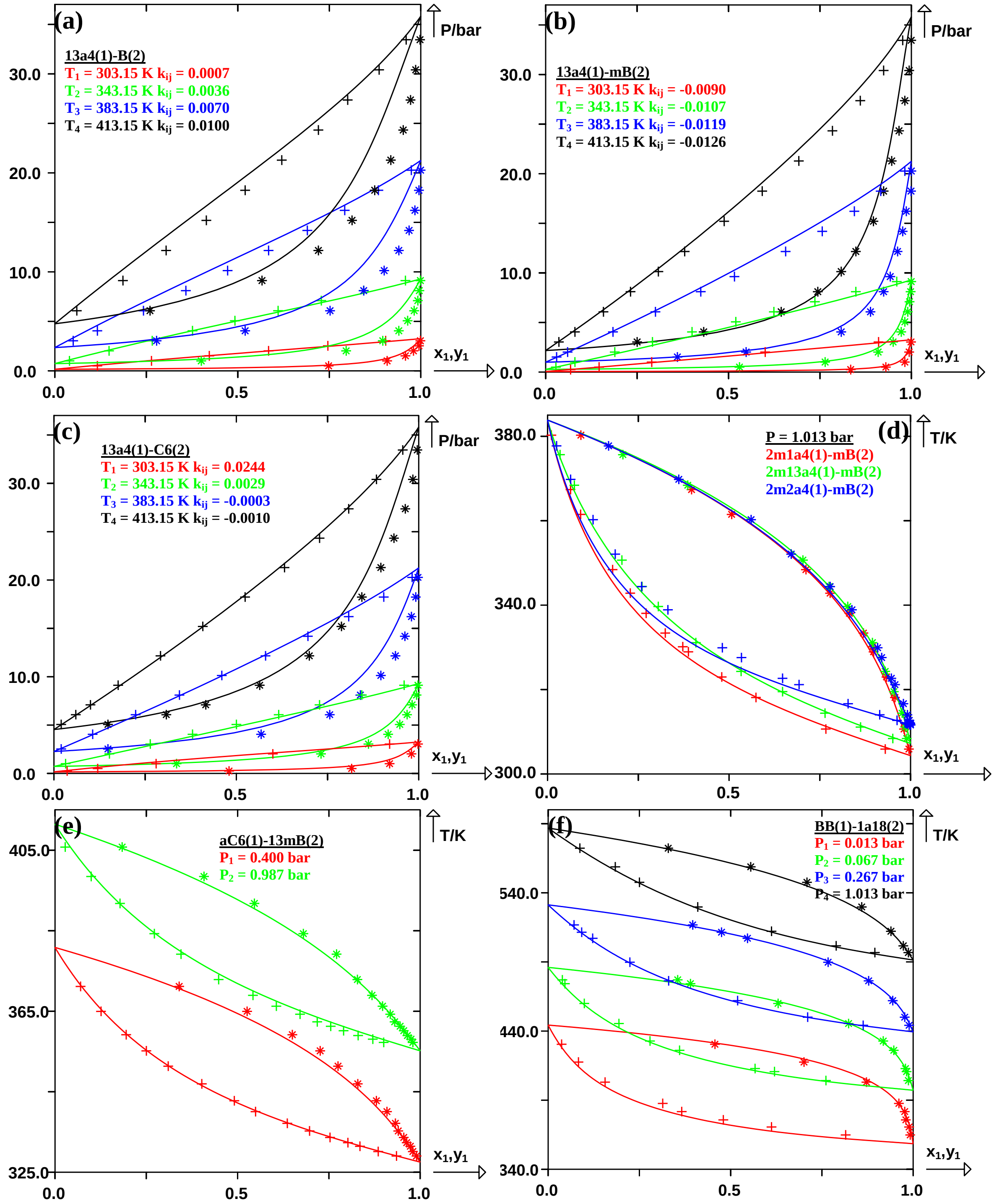

Figure III−14. Prediction of isothermal and isobaric curves in the sub-critical region for eight binary systems using the PPR78 model. (+) experimental bubble points, (✳) experimental dew points. Solid line: predicted curves with the PPR78 model. **(a)** System (1,3-butadiene(1) + benzene(2)) at four different temperatures: T_1 = 303.15 K (k_{ij} = 0.0007), T_2 = 343.15 K (k_{ij} = 0.0036), T_3 = 383.15 K (k_{ij} = 0.0070), T_4 = 413.15 K (k_{ij} = 0.0100). **(b)** System (1,3-butadiene(1) + methylbenzene(2)) at four different temperatures: T_1 = 303.15 K (k_{ij} = -0.0090), T_2 = 343.15 K (k_{ij} = -0.0107), T_3 = 383.15 K (k_{ij} = -0.0119), T_4 = 413.15 K (k_{ij} = -0.0126). **(c)** System (1,3-butadiene(1) + cyclohexane(2)) at four different temperatures: T_1 = 303.15 K (k_{ij} = 0.0244), T_2 = 343.15 K (k_{ij} = 0.0029), T_3 = 383.15 K (k_{ij} = -0.0003), T_4 = 413.15 K (k_{ij} = -0.0010). **(d)** System (2-methyl-1-butene(1) + methylbenzene(2)) at P = 1.013 bar, system (2-methyl-1,3-butadiene(1) + methylbenzene(2)) at P = 1.013 bar, system (2-methyl-2-butene(1) + methylbenzene(2)) at P = 1.013 bar. **(e)** System (cyclohexene(1) + 1,3-dimethylbenzene(2)) at two different pressures: P_1 = 0.400 bar, P_2 = 0.987 bar. **(f)** System (naphthalene(1) + 1-octadecene(2)) at four different pressures: P_1 = 0.013 bar, P_2 = 0.067 bar, P_3 = 0.267 bar, P_4 = 1.013 bar.

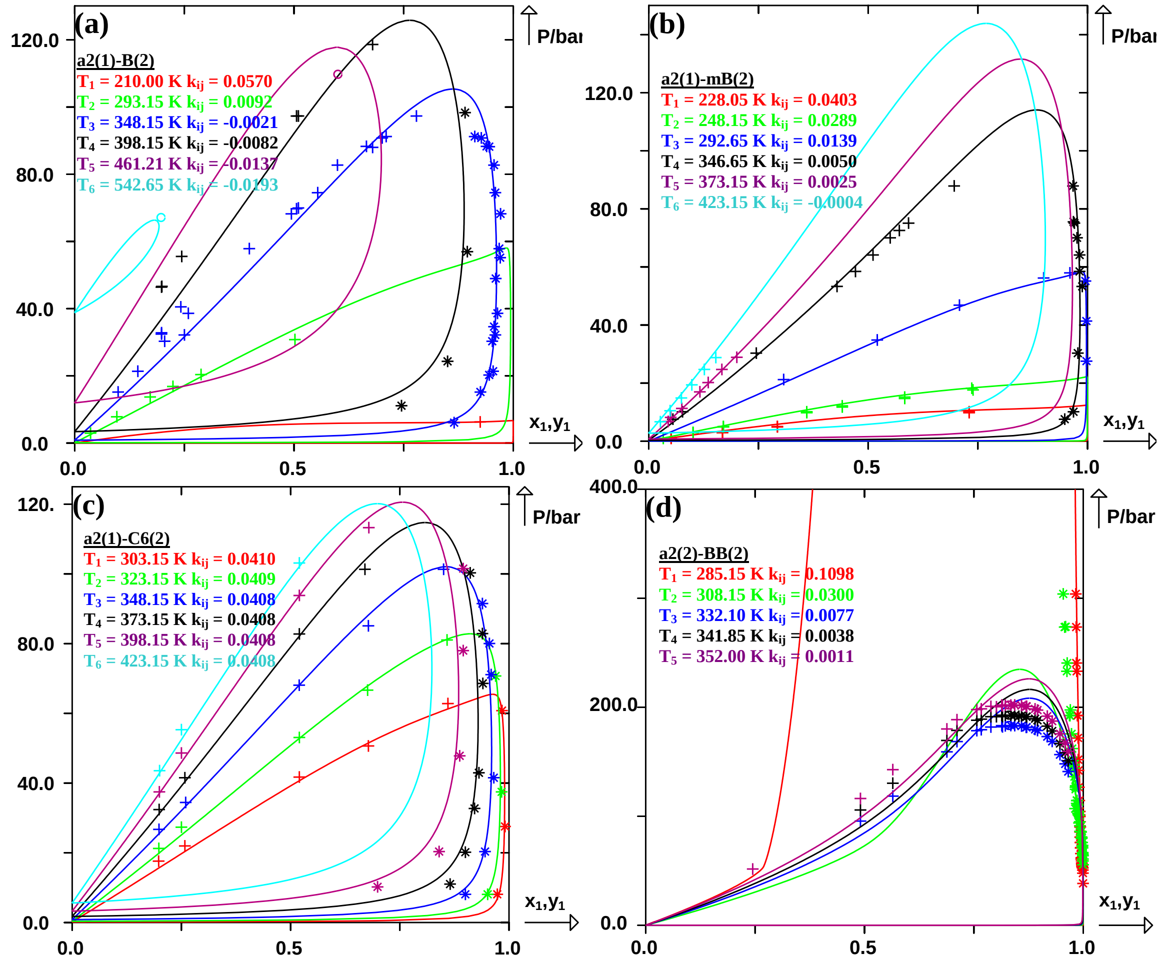

Figure III‒15. Prediction of isothermal curves in the sub-critical and super-critical regions for four binary systems using the PPR78 model. (+) experimental bubble points, (✳) experimental dew points, (○) experimental critical points. Solid line: predicted curves with the PPR78 model. **(a)** System (ethylene(1) + benzene(2)) at six different temperatures: T_1 = 210.00 K (k_{ij} = 0.0570), T_2 = 293.15 K (k_{ij} = 0.0092), T_3 = 348.15 K (k_{ij} = -0.0021), T_4 = 398.15 K (k_{ij} = -0.0082), T_5 = 461.21 K (k_{ij} = -0.0137), T_6 = 542.65 K (k_{ij} = -0.0193). **(b)** System (ethylene(1) + toluene(2)) at six different temperatures: T_1 = 228.05 K (k_{ij} = 0.0403), T_2 = 248.15 K (k_{ij} = 0.0289), T_3 = 292.65 K (k_{ij} = 0.0139), T_4 = 346.65 K (k_{ij} = 0.0050), T_5 = 373.15 K (k_{ij} = 0.0025), T_6 = 423.15 K (k_{ij} = -0.0004). **(c)** System (ethylene(1) + cyclohexane(2)) at six different temperatures: T_1 = 303.15 K (k_{ij} = 0.0410), T_2 = 323.15 K (k_{ij} = 0.0409), T_3 = 348.15 K (k_{ij} = 0.0408), T_4 = 373.15 K (k_{ij} = 0.0408), T_5 = 398.15 K (k_{ij} = 0.0408), T_6 = 423.15 K (k_{ij} = 0.0408). **(d)** System (ethylene(1) + naphthalene(2)) at five different temperatures: T_1 = 285.15 K (k_{ij} = 0.1098), T_2 = 308.15 K (k_{ij} = 0.0300), T_3 = 332.10 K (k_{ij} = 0.0077), T_4 = 341.85 K (k_{ij} = 0.0038), T_5 = 352.00 K (k_{ij} = 0.0011).

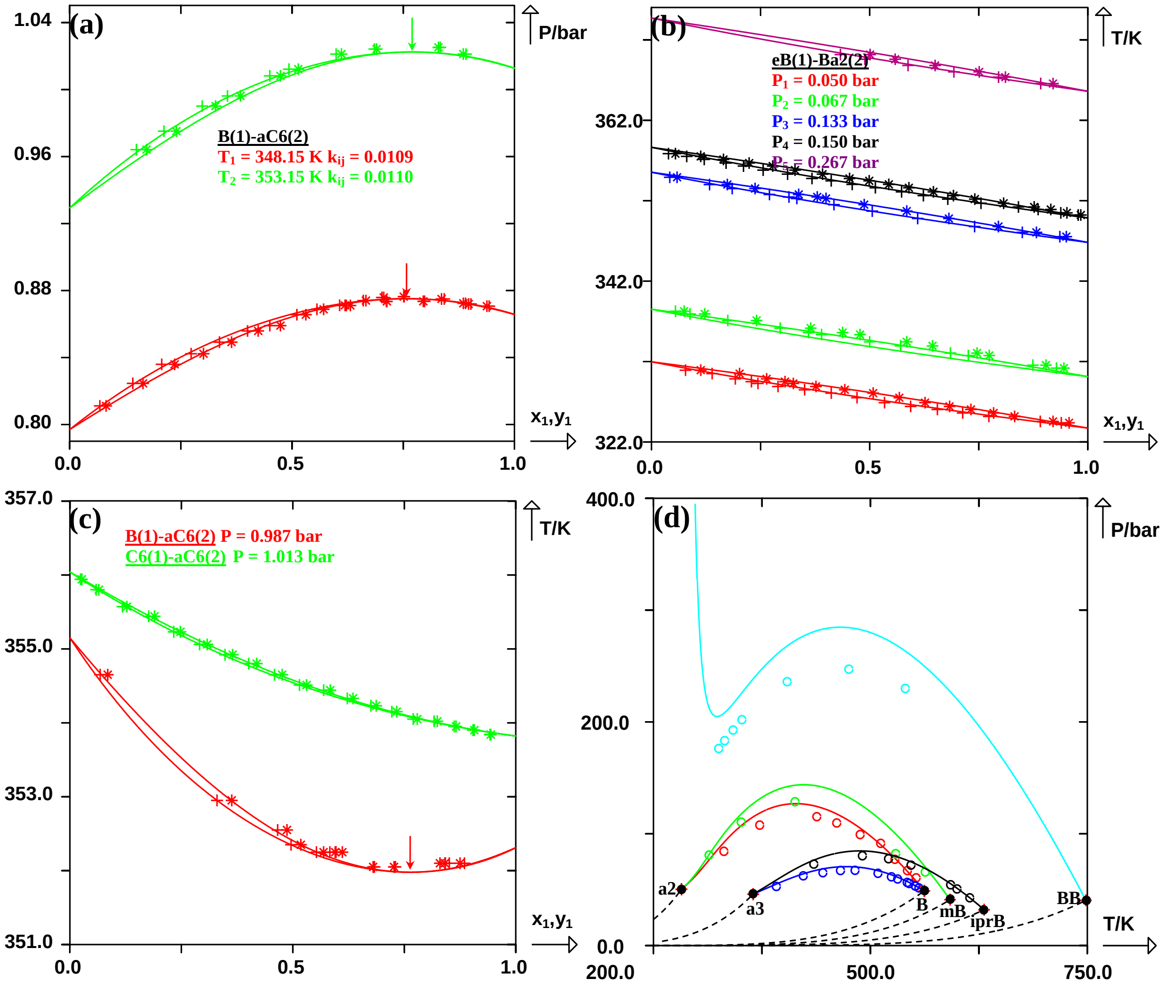

Figure III−16. Prediction of isothermal and isobaric curves for three binary systems that contain two components of very similar volatility, and predictions of critical locus for five binary systems using the PPR78 model. (+) experimental bubble points, (✳) experimental dew points, (○) experimental critical points, (●) critical points of the pure compounds. Solid line: predicted curves with the PPR78 model, dashed line: vaporization curve of the pure compounds. **(a)** System (benzene(1) + cyclohexene(2)) at two different temperatures: T_1 = 348.15 K (k_{ij} = 0.0109), T_2 = 353.15 K (k_{ij} = 0.0110). **(b)** System (ethylbenzene(1) + styrene(2)) at five different pressures: P_1 = 0.050 bar, P_2 = 0.067 bar, P_3 = 0.133 bar, P_4 = 0.150 bar, P_5 = 0.267 bar. **(c)** System (benzene(1) + cyclohexene(2)) at P = 0.987 bar, systeme(cyclohexane(1) + cyclohexene(2)) at P = 1.013 bar. **(d)** Prediction of the critical locus for five binary systems.

III.4.4 Results for mixtures of [alkene (or cycloalkene) + CO_2(or N_2)]

VLE measurements for the binary systems of [alkene (or cycloalkene) + CO_2] were extensively carried out by lots of investigators. Only four binary mixtures containing an alkene and N_2 have been found, without any experimental critical point. Furthermore, no experimental VLE data points of (alkene + H_2S) is available in the open literature.

The (ethylene(1) + CO_2(2)) system exhibits homogeneous positive azeotrope [see figure (III−17)], and the phase behavior is very similar to that of (CO_2(1) + ethane(2)) studied in our previous paper[4] except that there is no temperature minimum in the critical locus of (ethylene(1) + CO_2(2)) [see figure (III−17e)]. The BIP($k_{ij}(T)$) varies from 0.0535 to 0.0572 as the temperature changes from 223.15 K to 293.15 K, and accurate results are obtained at any temperature. Working with long chain or branched alkenes, or even with dienes, our model can still give good representations of the experimental data in both the sub-critical and super-critical areas [see figures (III−18,19)]. The accuracy of our model remains constant, regardless of the alkene chain length (e.g. 1-hexadecene), as shown in figure (III−20a). Moreover, the predicted phase envelops of (CO_2(1) + alpha-methylstyrene(2)) and (CO_2(1) + cyclohexene(2)) are both in good agreement with experimental data [see figures (III−20b,20c)]. As the cycloalkene becomes more complex (alpha-pinene, (R+S)-limonene), the liquid branches are slightly underestimated by our model. It is important to indicate that for (CO_2(1) + (R+S)-limonene(2)) [see figure (III−20e)], when the experimental temperature varies from $T = 323.00$ K to $T = 323.20$ K, the difference in bubble pressure can be as high as 15 bar, which indicates that these experimental data have a great deal of scatter among them. Figure (III−20f) shows the prediction quality of critical loci for five different binary mixtures in this family. They all exhibit Type II phase behavior in the classification of van Konynenburg and Scott [284].

Regarding the mixtures of (alkene + N_2), experimental data points are only available for four binary systems. The bubble points of (N_2(1) + 1,3-butadiene(2)) and (N_2(1) + 2-methylpropene(2)) [see table (III−2)] describe only the small solubility of N_2 in alkenes at low temperatures, which have not been plotted here. Figures (III−21a,21b) present several isothermal diagrams predicted by our model for two binary systems: (N_2(1) + ethylene(2)) and (N_2(1) + propene(2)). The objective function is: $F_{obj} = 5.38$ %, which demonstrates that the PPR78 is able to predict accurately the phase behavior of these mixtures from low to high temperatures, in spite of the overestimation of critical pressure at intermediate temperatures.

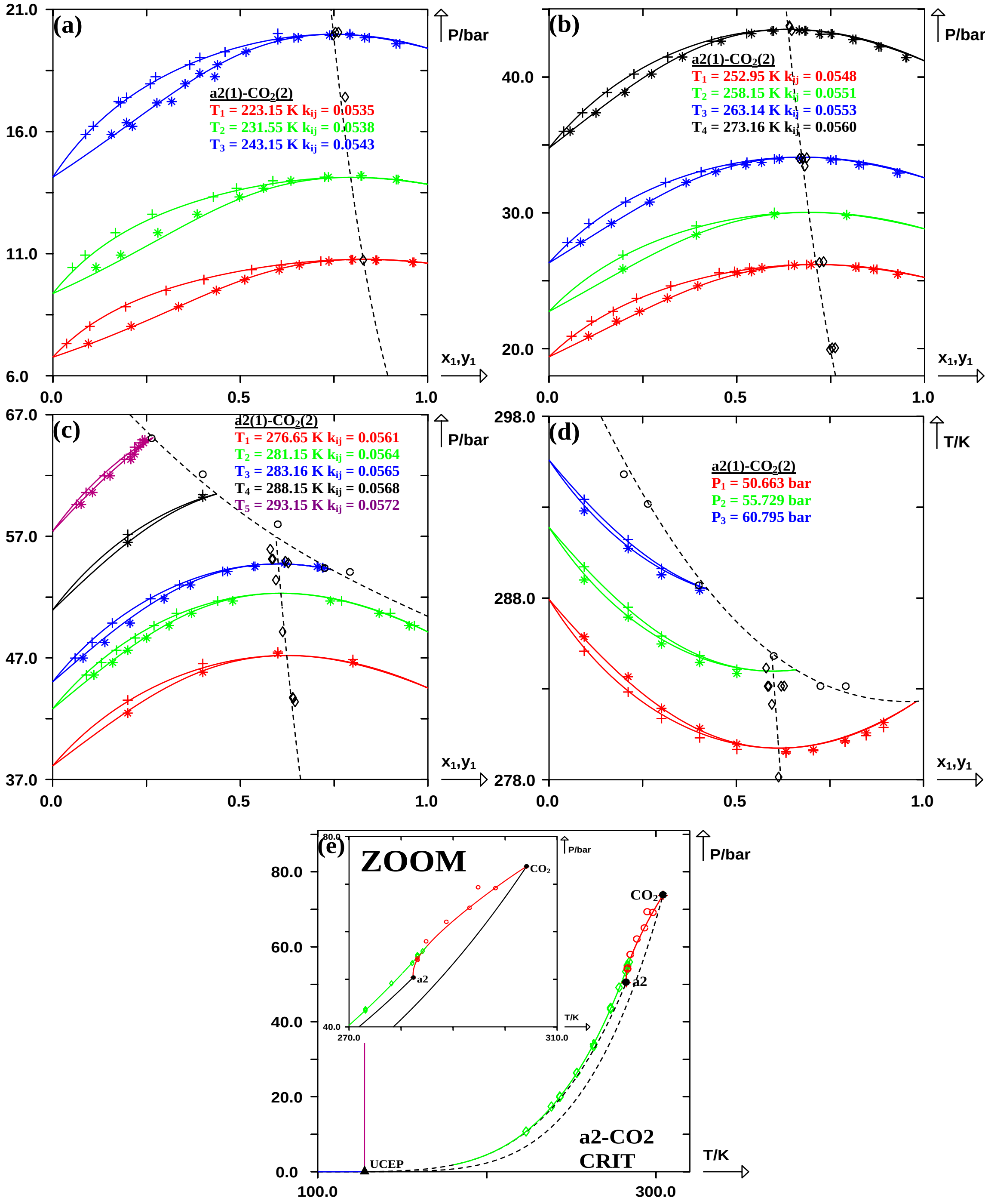

Figure III−17. Prediction of isothermal and isobaric curves and prediction of the critical locus for the binary systems: (ethylene(1) + carbon dioxide(2)) using the PPR78 model. (+) experimental bubble points, (✳) experimental dew points, (○) experimental critical points, (◇) experimental azeotropic points (●) critical points of the pure compounds, (▲) Upper critical end point (UCEP). Solid line: predicted curves with the PPR78 model. Dashed line: predicted critical curves and azeotropic curves (Pxy and Txy diagrams) and vaporization curve of the pure compounds (PT diagram). **(a)** System (ethylene(1) + carbon dioxide(2)) at three different temperatures: T_1 = 223.15 K (k_{ij} = 0.0535), T_2 = 231.55 K (k_{ij} = 0.0538), T_3 = 243.15 K (k_{ij} = 0.0543). **(b)** System (ethylene(1) + carbon dioxide(2)) at four different temperatures: T_1 = 252.95 K (k_{ij} = 0.0548), T_2 = 258.15 K (k_{ij} = 0.0551), T_3 = 263.14 K (k_{ij} = 0.0553), T_4 = 273.16 K (k_{ij} = 0.0560). **(c)** System (ethylene(1) + carbon dioxide(2)) at five different temperatures: T_1 = 276.65 K (k_{ij} = 0.0561), T_2 = 281.15 K (k_{ij} = 0.0564), T_3 = 283.16 K (k_{ij} = 0.0565), T_4 = 288.15 K (k_{ij} = 0.0568), T_5 = 293.15 K (k_{ij} = 0.0572). **(d)** System (ethylene(1) + carbon dioxide(2)) at three different pressures: P_1 = 50.663 bar, P_2 = 55.729 bar, P_3 = 60.795 bar. **(e)** Prediction of the critical locus for the binary system (ethylene(1) + carbon dioxide(2)).

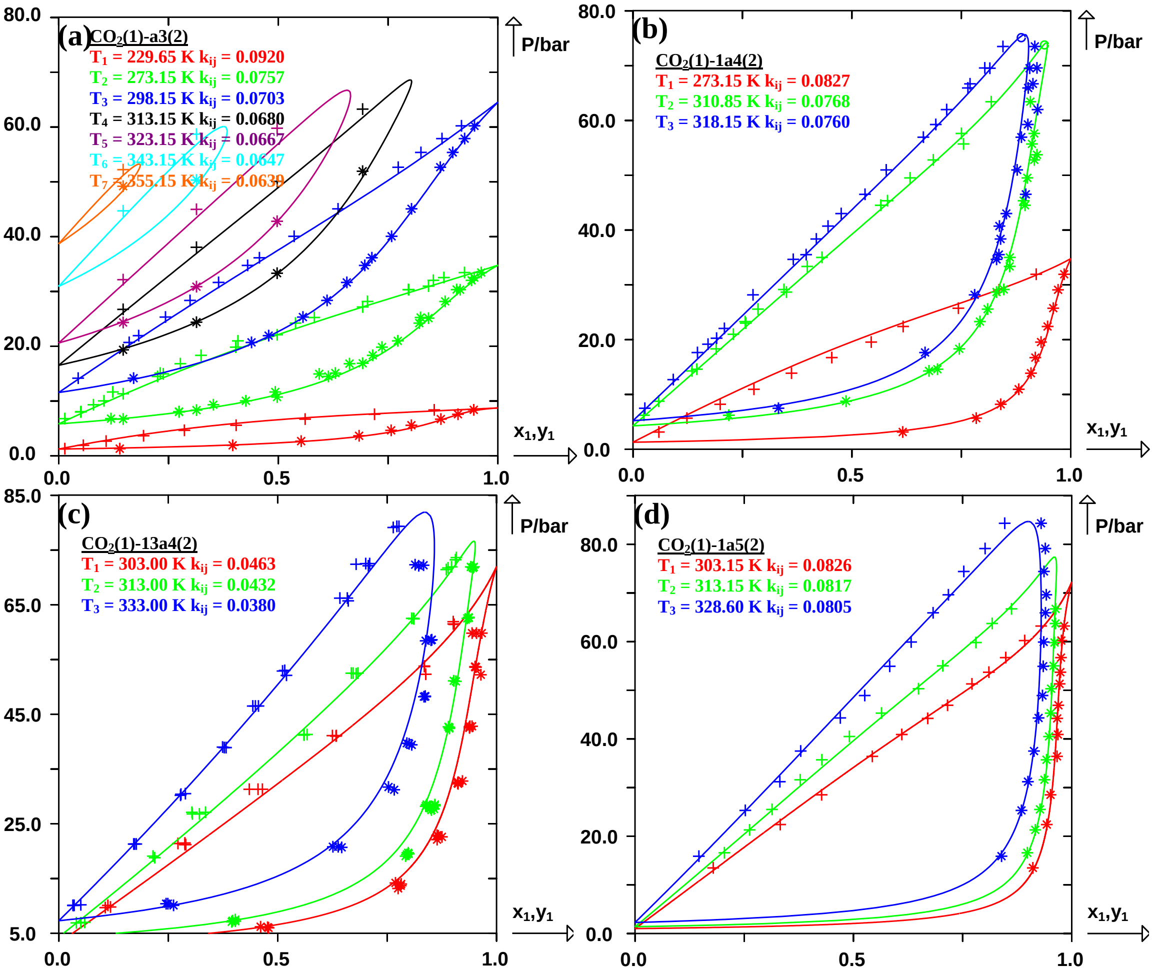

Figure III−18. Prediction of isothermal curves for four binary systems using the PPR78 model. (+) experimental bubble points, (✳) experimental dew points. Solid line: predicted curves with the PPR78 model. **(a)** System (carbon dioxide(1) + propene(2)) at seven different temperatures: T_1 = 229.65 K (k_{ij} = 0.0920), T_2 = 273.15 K (k_{ij} = 0.0757), T_3 = 298.15 K (k_{ij} = 0.0703), T_4 = 313.15 K (k_{ij} = 0.0680), T_5 = 323.15 K (k_{ij} = 0.0667), T_6 = 343.15 K (k_{ij} = 0.0647), T_7 = 355.15 K (k_{ij} = 0.0639). **(b)** System (carbon dioxide(1) + 1-butene(2)) at three different temperatures: T_1 = 273.15 K (k_{ij} = 0.0827), T_2 = 310.85 K (k_{ij} = 0.0768), T_3 = 318.15 K (k_{ij} = 0.0760). **(c)** System (carbon dioxide(1) + 1,3-butadiene(2)) at three different temperatures: T_1 = 303.00 K (k_{ij} = 0.0463), T_2 = 313.00 K (k_{ij} = 0.0432), T_3 = 333.00 K (k_{ij} = 0.0380). **(d)** System (carbon dioxide(1) + 1-pentene(2)) at three different temperatures: T_1 = 303.15 K (k_{ij} = 0.0826), T_2 = 313.15 K (k_{ij} = 0.0817), T_3 = 328.60 K (k_{ij} = 0.0805).

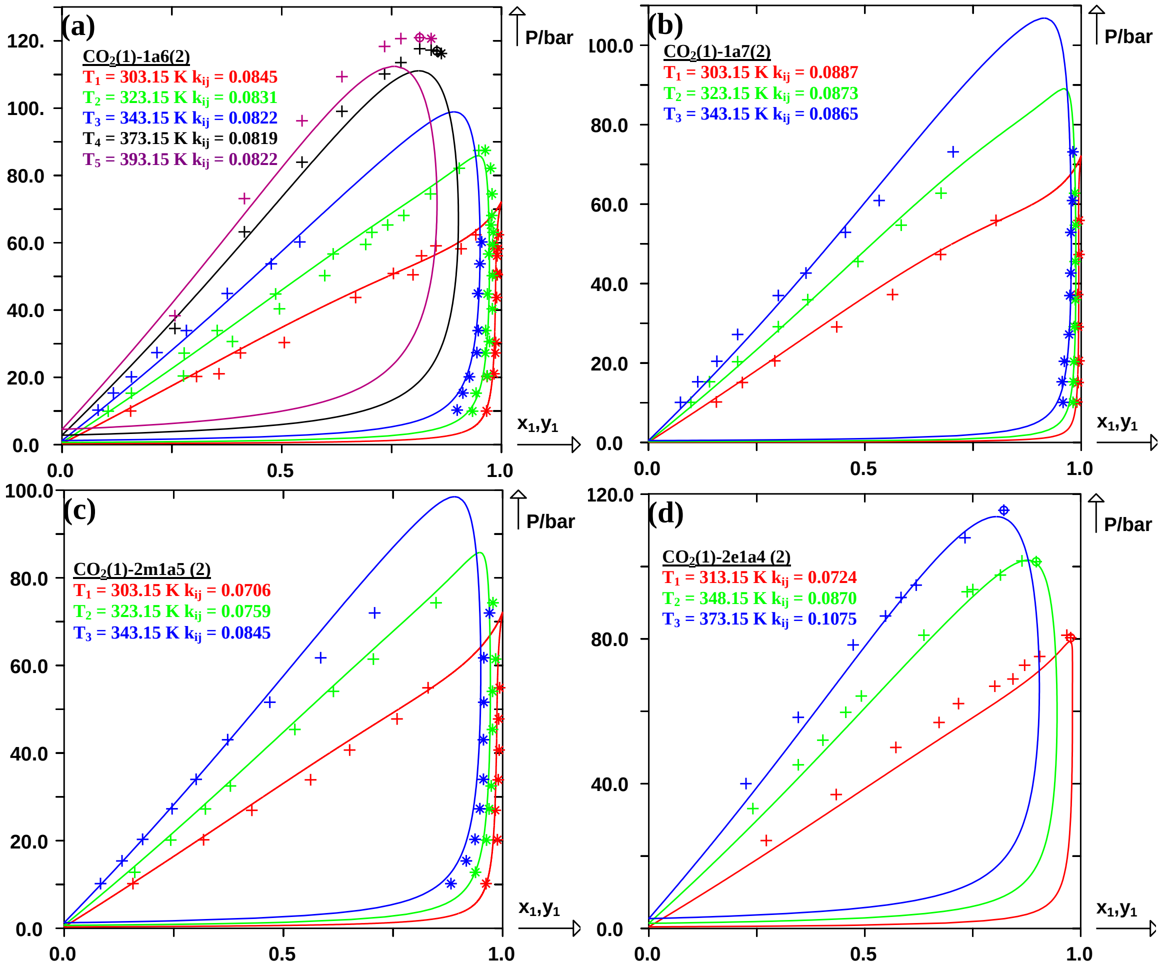

Figure III−19. Prediction of isothermal curves for four binary systems using the PPR78 model. (+) experimental bubble points, (✳) experimental dew points, (○) experimental critical points. Solid line: predicted curves with the PPR78 model. **(a)** System (carbon dioxide(1) + 1-hexene(2)) at five different temperatures: T_1 = 303.15 K (k_{ij} = 0.0845), T_2 = 323.15 K (k_{ij} = 0.0831), T_3 = 343.15 K (k_{ij} = 0.0822), T_4 = 373.15 K (k_{ij} = 0.0819), T_5 = 393.15 K (k_{ij} = 0.0822). **(b)** System (carbon dioxide(1) + 1-heptene(2)) at three different temperatures: T_1 = 303.15 K (k_{ij} = 0.0887), T_2 = 323.15 K (k_{ij} = 0.0873), T_3 = 343.15 K (k_{ij} = 0.0865). **(c)** System (carbon dioxide(1) + 2-methyl-1-pentene(2)) at three different temperatures: T_1 = 303.15 K (k_{ij} = 0.0706), T_2 = 323.15 K (k_{ij} = 0.0759), T_3 = 343.15 K (k_{ij} = 0.0845). **(d)** System (carbon dioxide(1) + 2-ethyl-1-butene(2)) at three different temperatures: T_1 = 313.15 K (k_{ij} = 0.0724), T_2 = 348.15 K (k_{ij} = 0.0870), T_3 = 373.15 K (k_{ij} = 0.1075).

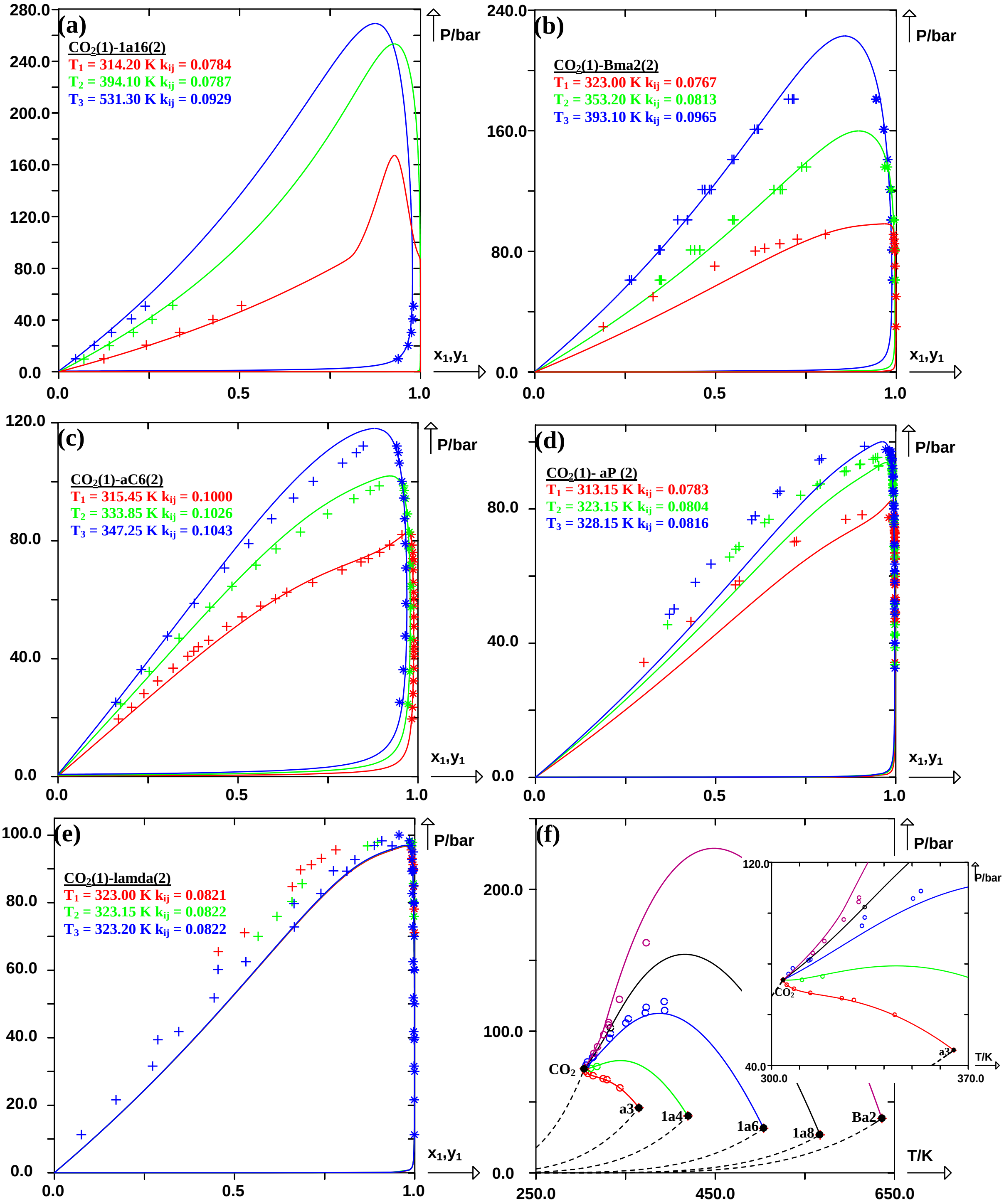

Figure III−20. Prediction of isothermal curves for five binary systems, and prediction of the critical locus for five binary systems using the PPR78 model. (+) experimental bubble points, (✳) experimental dew points, (○) experimental critical points, (●) critical points of the pure compounds. Solid line: predicted curves with the PPR78 model. Dashed line: vaporization curve of the pure compounds. **(a)** System (carbon dioxide(1) + 1-hexadecene(2)) at three different temperatures: T_1 = 314.20 K (k_{ij} = 0.0784), T_2 = 394.10 K (k_{ij} = 0.0787), T_3 = 531.30 K (k_{ij} = 0.0929). **(b)** System (carbon dioxide(1) + alpha-methylstyrene(2)) at three different temperatures: T_1 = 323.00 K (k_{ij} = 0.0767), T_2 = 353.20 K (k_{ij} = 0.0813), T_3 = 393.10 K (k_{ij} = 0.0965). **(c)** System (carbon dioxide(1) + cyclohexene(2)) at three different temperatures: T_1 = 315.45 K (k_{ij} = 0.1000), T_2 = 333.85 K (k_{ij} = 0.1026), T_3 = 347.25 K (k_{ij} = 0.1043). **(d)** System (carbon dioxide(1) + alpha-pinene(2)) at three different temperatures: T_1 = 313.15 K (k_{ij} = 0.0783), T_2 = 323.15 K (k_{ij} = 0.0804), T_3 = 328.15 K (k_{ij} = 0.0816). **(e)** System (carbon dioxide(1) + (R+S)-limonene(2)) at three different temperatures: T_1 = 323.00 K (k_{ij} = 0.0821), T_2 = 323.15 K (k_{ij} = 0.0822), T_3 = 323.20 K (k_{ij} = 0.0822). **(f)** Prediction of the critical locus for five binary systems.

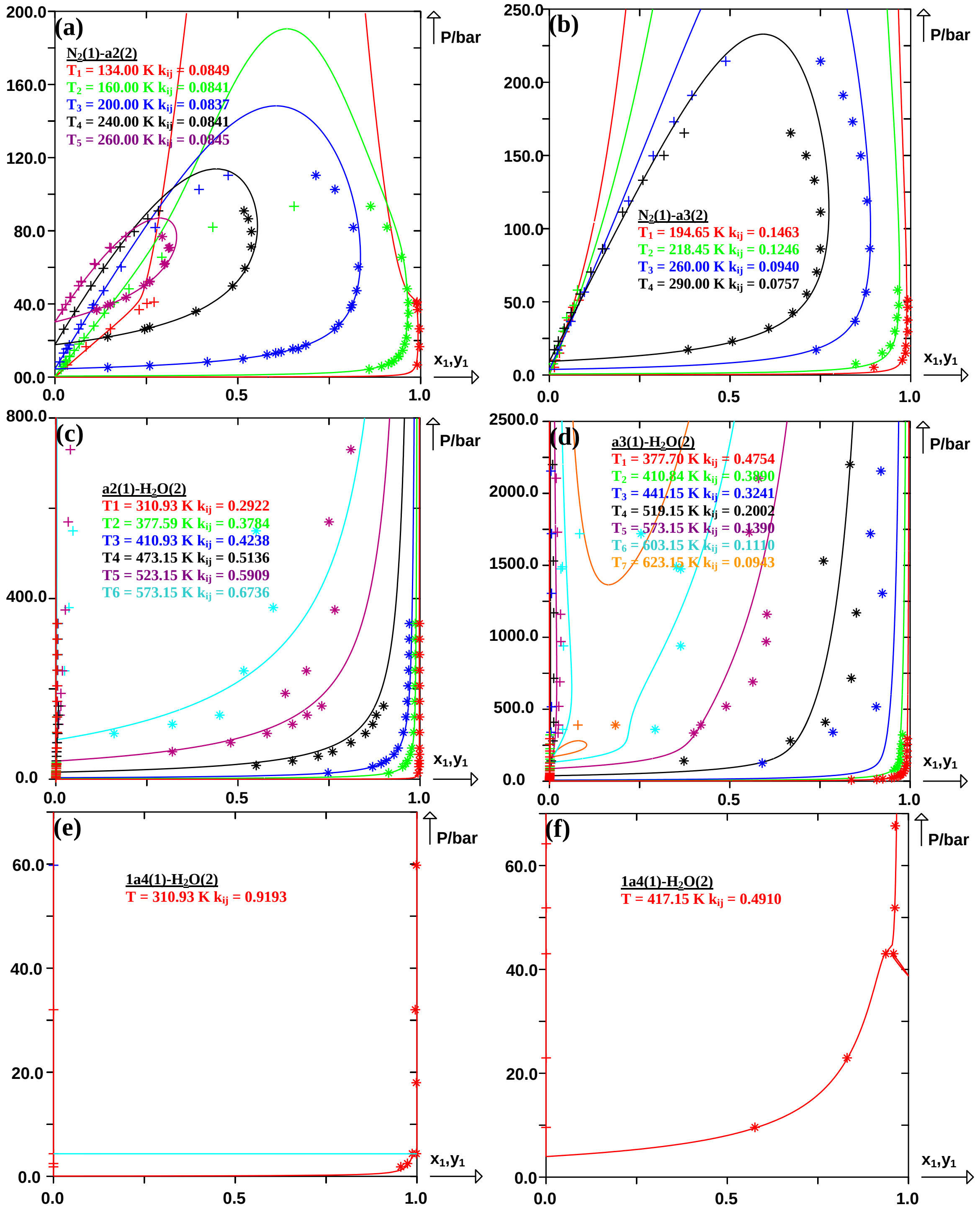

Figure III−21. Prediction of isothermal curves for six binary systems using the PPR78 model. (+) experimental bubble points, (✳) experimental dew points. Solid line: predicted curves with the PPR78 model. **(a)** System (nitrogen(1) + ethylene(2)) at five different temperatures: T_1 = 134.00 K (k_{ij} = 0.0849), T_2 = 160.00 K (k_{ij} = 0.0841), T_3 = 200.00 K (k_{ij} = 0.0837), T_4 = 240.00 K (k_{ij} = 0.0841), T_5 = 260.00 K (k_{ij} = 0.0845). **(b)** System (nitrogen(1) + propene(2)) at four different temperatures: T_1 = 194.65 K (k_{ij} = 0.1463), T_2 = 218.45 K (k_{ij} = 0.1246), T_3 = 260.00 K (k_{ij} = 0.0940), T_4 = 290.00 K (k_{ij} = 0.0757). **(c)** System (ethylene(1) + water(2)) at six different temperatures: T_1 = 310.93 K (k_{ij} = 0.2922), T_2 = 377.59 K (k_{ij} = 0.3784), T_3 = 410.93 K (k_{ij} = 0.4238), T_4 = 473.15 K (k_{ij} = 0.5136), T_5 = 523.15 K (k_{ij} = 0.5909), T_6 = 573.15 K (k_{ij} = 0.6736). **(d)** System (propene(1) + water(2)) at seven different temperatures: T_1 = 377.70 K (k_{ij} = 0.4754), T_2 = 410.84 K (k_{ij} = 0.3890), T_3 = 441.15 K (k_{ij} = 0.3241), T_4 = 519.15 K (k_{ij} = 0.2002), T_5 = 573.15 K (k_{ij} = 0.1390), T_6 = 603.15 K (k_{ij} = 0.1110), T_7 = 623.15 K (k_{ij} = 0.0943). **(e)** System (1-butene(1) + water(2)) at T = 310.93 K (k_{ij} = 0.9193). **(f)** System (1-butene(1) + water(2)) at T = 417.15 K (k_{ij} = 0.4910).

III.4.5 Results for mixtures of (alkenes + water)

According to our data base, 502 bubble points, 343 dew points and no critical point have been collected over 6 binary systems which consist of an alkene and water. Figure (III−21c) shows six isothermal phase diagrams for (ethylene(1) + H_2O(2)). At low temperature T = 310.93 K, immiscibility dominates the phase area. As the temperature increases, the mutual solubility increases and the solubility of water in ethylene-rich liquid is more significant. It is really difficult for our model to quantitatively describe these LLE in a wide temperature range. Similar phase phenomena can also be observed for the mixture of (propene(1) + H_2O(2)) at seven different temperatures [see figure (III−21d)]. Once again, solubility of water in propene-rich liquid at low temperatures seems to be well predicted while the mutual solubility at moderate temperatures becomes less accurate, especially the isothermal curves at T = 441.15K. At T = 603.15 K, the experimental isotherm seems to form a closed phase envelop, while the predicted curves still present an open phase envelop to higher pressures. At T = 623.15 K, the predicted phase diagram presents two coexistent regions: VLE and LLE, but the VLE are underestimated, compared to the experimental data. Considering (1-butene(1) + water(2)), experimental points at two different temperatures are perfectly predicted, including VLE and LLE [figures (III−21e,21f)]. The performance of our model for this system at higher temperatures has not been verified.

III.5 Conclusion

In this paper, the alkenic and cycloalkenic groups were added to the PPR78 model, and accurate results are obtained over wide temperature ranges, owing to the fact that most of the 196 binary systems investigated here exhibit Type I or Type II phase behavior in the classification of van Konynenburg and Scott. It is important to notice that for the mixtures that present nearly ideal phase behavior, small deviation between the calculated pure component saturated pressure and the experimental one will induce a large change of the phase envelop, especially for the azeotropic phase phenomena.

For all the binary mixtures studied, the BIP(k_{ij}(T)) is always near zero and it has a necessary dependence on temperature, except that BIP(k_{ij}(T)) varies a lot from low to high temperatures for the water containing systems. In conclusion, this paper makes it possible to estimate the k_{ij} for any mixtures that contain cycloalkenes, alkenes, water, N_2, CO_2, naphthenes, aromatics and alkanes at any temperature.

References

(1) Jaubert, J.-N.; Mutelet, F. VLE predictions with the Peng-Robinson equation of state and temperature dependent kij calculated through a group contribution method. *Fluid Phase Equilib.* **2004**, *224* (2), 285-304.
(2) Jaubert, J.-N.; Vitu, S.; Mutelet, F.; Corriou, J.-P. Extension of the PPR78 model (predictive 1978, Peng-Robinson EOS with temperature dependent kij calculated through a group contribution method) to systems containing aromatic compounds. *Fluid Phase Equilib.* **2005**, *237* (1-2), 193-211.
(3) Vitu, S.; Jaubert, J.-N.; Mutelet, F. Extension of the PPR78 model (Predictive 1978, Peng-Robinson EOS with temperature dependent kij calculated through a group contribution method) to systems containing naphtenic compounds. *Fluid Phase Equilib.* **2006**, *243* (1-2), 9-28.
(4) Vitu, S.; Privat, R.; Jaubert, J. N.; Mutelet, F. Predicting the phase equilibria of CO2 + hydrocarbon systems with the PPR78 model (PR EOS and kij calculated through a group contribution method). *Journal of Supercritical Fluids* **2008**, *45* (1), 1-26.
(5) Privat, R.; Jaubert, J. N.; Mutelet, F. Addition of the nitrogen group to the PPR78 model (predictive 1978, Peng Robinson EOS with temperature-dependent kij calculated through a group contribution method. *Ind. Eng. Chem. Res.* **2008**, *47* (6), 2033-2048.
(6) Privat, R.; Mutelet, F.; Jaubert, J. N. Addition of the hydrogen sulfide group to the PPR 78, Model (Predictive 1978, Peng-Robinson equation of state with temperature dependent kij- calculated through a group contribution method). *Ind. Eng. Chem. Res.* **2008**, *47* (24), 10041-10052.
(7) Privat, R.; Jaubert, J. N.; Mutelet, F. Addition of the sulfhydryl group (-SH) to the PPR78 model (predictive 1978, Peng-Robinson EOS with temperature dependent kij calculated through a group contribution method). *Journal of Chemical Thermodynamics* **2008**, *40* (9), 1331-1341.
(8) Poling, B. E.; Prausnitz, J. M.; O'Connell, J. P. *The Properties of Gases and Liquids, 5th Ed.* **2000**, 11-18.
(9) Vapor-liquid Equilibrium of the System Ethylene - Propylene. *Confidential Company Research Report* **1982**, (LC6611).
(10) Elshayal, I. M.; Lu, B. C. Y. Measurement of total pressures for ethylene-propane mixtures. *Can. J. Chem. Eng.* **1975**, *53* (1), 83-7.
(11) Machat, V.; Boublik, T. Vapor-liquid equilibrium at elevated pressures from the BACK equation of state. II. Binary systems. *Fluid Phase Equilib.* **1985**, *21* (1-2), 11-24.
(12) Rozhnov, M. S.; Kozya, V. G.; Zhdanov, V. I. Phase ratios in two-component systems of C1-3 hydrocarbons and nitrogen. *Khim. Prom-st. (Moscow)* **1988**, (11), 674-5.
(13) Smith, P. *Ph.D. thesis, University of Wisconsin* **1974**.
(14) Williams, B. Pressure-Volume-Temperature Relationships and Phase Equilibria in the System Ethylene - Normal Butane. *Ph.D. thesis, University of Michigan* **1947**.
(15) Raetzsch, M. T.; Soell, W. Critical liquid-vapor phenomena of binary systems containing ethylene. *Z. Phys. Chem. (Leipzig)* **1975**, *256* (5), 815-28.
(16) Vapor-liquid Equilibrium of the System Ethylene - Hexane. *Confidential Company Research Report* **1979**, (LC5327).
(17) Konobeev, B. I.; Lyapin, V. V. Solubility of ethylene and propylene in organic solvents. *Khim. Prom-st. (Moscow)* **1967**, *43* (2), 114-16.
(18) Nagy, I.; Krenz, R. A.; Heidemann, R. A.; de, L. T. W. Vapor-Liquid Equilibrium Data for the Ethylene + Hexane System. *J. Chem. Eng. Data* **2005**, *50* (4), 1492-1495.
(19) Zhuze, T. P.; Zhurba, A. S. Solubilities of ethylene in hexane, cyclohexane, and benzene under pressure. *Bulletin of the Academy of Sciences of the USSR Division of Chemical Science* **1960**, *9* (2), 335-337.
(20) Zhuze, T. P.; Zhurba, A. S.; Esakov, E. A. Solubilities of hexane, cyclohexane, and benzene in compressed ethylene. *Bulletin of the Academy of Sciences of the USSR Division of Chemical Science* **1960**, *9* (2), 331-334.
(21) Kay, W. B. Liquid-vapor equilibrium relations in binary systems. Ethylene-heptane system. *J. Ind. Eng. Chem. (Washington, D. C.)* **1948**, *40*, 1459-64.
(22) Pacheco, C. R. N.; Ferreira Filho, J. P.; Uller, A. M. C. Gas Solubility - Experimental Studies in Nonpolar Systems. *World Congress III of Chemical Engineering, Tokyo* **1986**, 104-107.
(23) Sahgal, A.; La, H. M.; Hayduk, W. Solubility of ethylene in several polar and non-polar solvents. *Can. J. Chem. Eng.* **1978**, *56* (3), 354-7.
(24) Thoedtmann, I.; Preuss, H.; Pape, D. Determination of the vapor-liquid equilibria in binary systems formed by n-heptane, but-1-ene, and ethene. *FIZ Report* **1989**, 12011.
(25) Zernov, V. S.; Kogan, V. B.; Egudina, O. G.; Kobyakov, V. M.; Babayants, T. V.; Kalichava, L. I. Phase Equilibria and Volume Ratios in the Systems Heptane - Ethylene. *J. Appl. Chem. USSR* **1990**, *63* (7), 1469-1472.
(26) Weng, W. L.; Lee, M. J. Vapor-liquid equilibrium of the octane/carbon dioxide, octane/ethane, and octane/ethylene systems. *J. Chem. Eng. Data* **1992**, *37* (2), 213-15.

(27) Nederbragt, G. W. Gas-liquid equilibria in hydrocarbon systems. *Appl. Sci. Res., Sect. A* **1948**, *A1*, 237-48.
(28) Todd, D. B.; Elgin, J. C. Phase equilibria in systems with ethylene above its critical temperature. *AIChE J.* **1955**, *1*, 20-7.
(29) Ribeiro, J. V.; Susu, A. A.; Kohn, J. P. Heterogeneous-phase equilibrium in ethylene-n-dodecane system. *J. Chem. Eng. Data* **1972**, *17* (3), 279-80.
(30) Kaul, B. K. Solubilities and Dew-Point Temperature in Hydrocarbon and Coal Processing. *Ph.D. thesis, University of California, Berkeley* **1977**, 1-128.
(31) Chou, J. S.; Chao, K. C. Solubility of ethylene in n-eicosane, n-octacosane, and n-hexatriacontane. *J. Chem. Eng. Data* **1989**, *34* (1), 68-70.
(32) De Loos, T. W.; Poot, W.; Lichtenthaler, R. N. Fluid phase equilibria in binary ethylene + n-alkane systems. *Ber. Bunsen-Ges. Phys. Chem.* **1984**, *88* (9), 855-9.
(33) Gregorowicz, J. Solubility of eicosane in supercritical ethane and ethylene. *J. Supercrit. Fluids* **2003**, *26* (2), 95-113.
(34) Gregorowicz, J. Phase behaviour in the vicinity of the three-phase solid-liquid-vapour line in asymmetric nonpolar systems at high pressures. *Fluid Phase Equilib.* **2006**, *240* (1), 29-39.
(35) Kohn, J. P.; Andrle, E. S.; Luks, K. D.; Colmenares, J. D. Phase equilibriums of ethylene and certain normal paraffins. *J. Chem. Eng. Data* **1980**, *25* (4), 348-50.
(36) The binary vapor-liquid equilibria of hydrogen, ethane, ethylene, propylene and 1-butene with n-butane and isobutane. *Confidential Company Research Report* **1979**, (LC5322).
(37) Naumova, A. A.; Tyvina, T. N. Critical liquid-gas phenomena in the isobutane-ethylene system. *Zh. Prikl. Khim. (Leningrad)* **1981**, *54* (6), 1416-17.
(38) Naumova, A. A.; Tyvina, T. N. Liquid-Gas Equilibrium in the Isobutane - Ethylene System. *J. Appl. Chem. USSR* **1981**, *54* (12), 2440-2441.
(39) Fallaha, F. H. Phase Equilibria at high Pressures with Application to Vapor Phase Extraction. *Ph.D. thesis, University of Birmingham* **1974**.
(40) King, M. B.; Alderson, D. A.; Fallah, F. H.; Kassim, D. M.; Kassim, K. M.; Sheldon, J. R.; Mahmud, R. S. Some vapor/liquid and vapor/solid equilibrium measurements of relevance for supercritical extraction operations, and their correlation. *Chem. Eng. Supercrit. Fluid Cond.* **1983**, 31-80.
(41) Calado, J. C. G.; Soares, V. A. M. Thermodynamics of liquid mixtures of methane and ethene. *J. Chem. Soc., Faraday Trans. 1* **1977**, *73* (8), 1271-80.
(42) Hsi, C.; Lu, B. C. Y. Vapor-liquid equilibriums in the methane-ethylene-ethane system. *Can. J. Chem. Eng.* **1971**, *49* (1), 140-3.
(43) Miller, R. C.; Kidnay, A. J.; Hiza, M. J. Liquid + vapor equilibriums in methane + ethene and in methane + ethane from 150.00 to 190.00 K. *J. Chem. Thermodyn.* **1977**, *9* (2), 167-78.
(44) Moran, D. W. Low temperature equilibria in binary systems, including the solid phases. *Ph.D. thesis, University of London* **1959**, 1-192.
(45) Sagara, H.; Arai, Y.; Saito, S. Vapor-liquid equilibriums of binary and ternary systems containing hydrogen and light hydrocarbons. *J. Chem. Eng. Jap.* **1972**, *5* (4), 339-48.
(46) Barclay, D. A.; Flebbe, J. L.; Manley, D. B. Relative volatilities of the ethane-ethylene system from total pressure measurements. *J. Chem. Eng. Data* **1982**, *27* (2), 135-42.
(47) Calado, J. C. G.; Gomes, d. A. E. J. S.; Clancy, P.; Gubbins, K. E. Thermodynamic study of liquid mixtures of ethane and ethene. *J. Chem. Soc., Faraday Trans. 1* **1983**, *79* (11), 2657-67.
(48) Clark, A. M.; Din, F. Equilibria between solid, liquid, and gaseous phases at low temperatures. The system carbon dioxide plus ethane plus ethylene. *Discuss. Faraday Soc.* **1953**, *15*, 202-7.
(49) Eubank, P. T.; Barrufet, M. A.; Duarte-Garza, H.; Yurttas, L. Pressure-volume-temperature (PVT) experiments for precise VLE data for mixtures of similar volatility. *Fluid Phase Equilib.* **1989**, *52*, 219-27.
(50) Fredenslund, A.; Mollerup, J.; Hall, K. R. Vapor-liquid equilibrium data for the systems ethylene + ethane and carbon dioxide + ethylene + ethane. *J. Chem. Eng. Data* **1976**, *21* (3), 301-4.
(51) Hanson, G. H.; Hogan, R. J.; Ruehlen, F. N.; Cines, M. R. Ethane-ethylene system; vapor-liquid equilibria at 0°, -40°, and -100°F. *Chem. Eng. Prog., Symp. Ser.* **1953**, *49* (6), 37-44.
(52) Kharakhorin, F. F. Phase Relations in Systems of Liquefied Gases. Equilibrium of co-existent liquid and vapor phases in the system ethane - ethylene. *Foreign Petr. Techn.* **1941**, *9* (11), 411-422.
(53) McCurdy, J. L.; Katz, D. L. Phase equilibria in the system ethane-ethylene-acetylene. *J. Ind. Eng. Chem. (Washington, D. C.)* **1944**, *36*, 674-80.
(54) Coan, C. R.; King, A. D., Jr. Second cross virial coefficients of benzene-gas mixtures from high-pressure solubility measurements. Comparison with gas-chromatographic values. *J. Chromatogr.* **1969**, *44* (3-4), 429-36.
(55) Ellis, S. R. M.; Valteris, R. L.; Harris, G. J. High pressure equilibrium still for vapor-phase extraction studies. *Chem. Eng. Progr., Symp. Ser.* **1968**, *64* (88), 16-21.
(56) Hiraoka, H. Solubilities of ethylene in benzene at high pressures. *Rev. Phys.-Chem. Japan* **1958**, *28*, 64-6.

(57) Holder, G. A.; Macauley, D. Solubility of ethylene in benzene at pressures to 9 MPa and temperatures from 353 to 433 K. *J. Chem. Eng. Data* **1992**, *37* (1), 100-4.
(58) Kozorezov, Y. I.; Rusakov, A. P.; Pikalo, N. M. Solubility of ethylene in benzene, ethylbenzene, and diethylbenzene. *Khim. Prom. (Moscow)* **1969**, *45* (5), 343-5.
(59) Liu, T.; Fu, J.-Y.; Wang, K.; Gao, Y.; Yuan, W.-K. Gas-Liquid Critical Properties of Ethylene + Benzene. *J. Chem. Eng. Data* **2001**, *46* (4), 809-812.
(60) Lyubetskii, S. G. Liquid-Vapor Equilibrium in the System Ethylene - Benzene. *J. Appl. Chem. USSR* **1962**, *35* (1), 125-129.
(61) Lyubetskii, S. G. Liquid-vapor equilibrium in the system ethylene-benzene. *Zh. Prikl. Khim. (S.-Peterburg, Russ. Fed.)* **1962**, *35*, 141-7.
(62) Tiffin, D. L.; Kohn, J. P.; Luks, K. D. Three-phase solid-liquid-vapor equilibriums of the systems ethylene-cyclohexane, ethylene-trans-decalin, ethylene-benzene, and ethylene-2-methylnaphthalene. *J. Chem. Eng. Data* **1979**, *24* (2), 96-8.
(63) Zhurba, A. S.; Zhuze, T. P. Investigation of the p-V-T-n-relations and of the phase equilibrium in the system ethylene - benzene. *Izv. Vyssh. Uchebn. Zaved. Neft Gaz* **1960**, *1*, 93-106.
(64) Lee, L.-s.; Ou, H.-j.; Hsu, H.-l. The experiments and correlations of the solubility of ethylene in toluene solvent. *Fluid Phase Equilib.* **2005**, *231* (2), 221-230.
(65) Shenderei, E. R.; Zel'venskii, Y. D.; Ivanoskii, F. P. The solubility of ethylene in acetone, methyl ethyl ketone, and toluene at low temperatures. *Zh. Fiz. Khim.* **1962**, *36*, 801-7.
(66) Shenderei, E. R.; Zel'venskii, Y. D.; Ivanovskii, F. P. Solubility of ethylene in acetone, ethyl methyl ketone, and toluene at low temperatures. *Russ. J. Phys. Chem.* **1962**, *36* (4), 415-419.
(67) Tyvina, T. N.; Naumova, A. A.; Polyakov, S. A. Critical Effects and Phase and Volume Behavior of Solutions of Ethylene in Toluene. *J. Appl. Chem. USSR* **1979**, *52*, 910-913.
(68) Nakamura, E.; Koguchi, K.; Amemiya, T. Solubilities of ethylene in C8 aromatic hydrocarbons. *Kogyo Kagaku Zasshi* **1966**, *69* (10), 1940-4.
(69) Diepen, G. A. M.; Scheffer, F. E. C. The solubility of naphthalene in supercritical ethylene. *J. Am. Chem. Soc.* **1948**, *70*, 4085-9.
(70) Diepen, G. A. M.; Scheffer, F. E. C. The solubility of naphthalene in supercritical ethylene. II. *J. Phys. Chem.* **1953**, *57*, 575-7.
(71) Johnston, K. P.; Eckert, C. A. An analytical Carnahan-Starling-van der Waals model for solubility of hydrocarbon solids in supercritical fluids. *AIChE J.* **1981**, *27* (5), 773-9.
(72) Seiichi, S.; Kazunari, O.; Takashi, K. Solubilities of naphthalene and indole in supercritical fluids. *J. Supercrit. Fluids* **1988**, *1* (1), 1-6.
(73) Tsekhanskaya, Y. V.; Iomtev, M. B.; Mushkina, E. V. Solubility of naphthalene in ethylene and carbon dioxide under pressure. *Russ. J. Phys. Chem.* **1964**, *38* (9), 1173-1176.
(74) van Welie, G. S. A.; Diepen, G. A. M. The P-T-x Space Model of the System Ethylene - Naphthalene. (I). *Recl. Trav. Chim. Pays Bas* **1961**, *80*, 659-665.
(75) van Welie, G. S. A.; Diepen, G. A. M. The P-T-x Space Model of the System Ethylene - Naphthalene. (III). *Recl. Trav. Chim. Pays Bas* **1961**, *80*, 673-680.
(76) van Welie, G. S. A.; Diepen, G. A. M. The P-T-x Space Model of the System Ethylene - Naphthalene. (II). *Recl. Trav. Chim. Pays Bas* **1961**, *80*, 666-672.
(77) Johnston, K. P.; Ziger, D. H.; Eckert, C. A. Solubilities of hydrocarbon solids in supercritical fluids. The augmented van der Waals treatment. *Ind. Eng. Chem. Fundam.* **1982**, *21* (3), 191-7.
(78) Kurnik, R. T.; Holla, S. J.; Reid, R. C. Solubility of solids in supercritical carbon dioxide and ethylene. *J. Chem. Eng. Data* **1981**, *26* (1), 47-51.
(79) Bae, H. K.; Nagahama, K.; Hirata, M. Isothermal vapor-liquid equilibriums for the ethylene-carbon dioxide system at high pressure. *J. Chem. Eng. Data* **1982**, *27* (1), 25-7.
(80) Cook, D.; Longuet-Higgins, H. C. Application of the theory of conformal solutions to the system carbon dioxide-ethylene. *Proc. R. Soc. London, Ser. A* **1951**, *209*, 28-38.
(81) Hakuta, T.; Nagahama, K.; Suda, S. Binary vapor-liquid equilibriums of carbon dioxide-C2 hydrocarbons. *Kagaku Kogaku* **1969**, *33* (9), 904-7.
(82) Haselden, G. G.; Holland, F. A.; King, M. B.; Strickland-Constable, R. F. Two-phase equilibrium in binary and ternary systems. X. Phase equilibriums and compressibility of the systems carbon dioxide-propylene, carbon dioxide-ethylene, and ethylene-propylene, and an account of the thermodynamic functions of the system carbon dioxide-propylene. *Proc. R. Soc. London, Ser. A* **1957**, *240*, 1-28.
(83) Haselden, G. G.; Newitt, D. M.; Shah, S. M. Two-phase equilibrium in binary and ternary systems. V. Carbon dioxide-ethylene. VI. Carbon dioxide-propylene. *Proc. R. Soc. London, Ser. A* **1951**, *209*, 1-14.

(84) Khazanova, N. E.; Sominskaya, E. E.; Zakharova, A. V.; Rozovskii, M. B.; Nechitailo, N. L. Systems with azeotropism at high pressures. X. Phase and volume relations in the ethylene-carbon dioxide system. *Zh. Fiz. Khim.* **1979**, *53* (6), 1594-7.
(85) Mollerup, J. Vapor-liquid equilibrium in ethylene-carbon dioxide and ethane-carbon dioxide. *J. Chem. Soc., Faraday Trans. 1* **1975**, *71* (12), 2351-60.
(86) Nagahama, K.; Konishi, H.; Hoshino, D.; Hirata, M. Binary vapor-liquid equilibriums of carbon dioxide-light hydrocarbons at low temperature. *J. Chem. Eng. Jpn.* **1974**, *7* (5), 323-8.
(87) Rowlinson, J. S.; Sutton, J. R.; Weston, F. Liquid - Vapor Equilibrium in a Ternary System. *Proceedings, International Conference Thermodynamics and Transport Properties Fluids, 1957* **1957**, 3-7.
(88) Gasem, K. A. M.; Hiza, M. J.; Kidnay, A. J. Phase behavior in the nitrogen + ethylene system from 120 to 200 K. *Fluid Phase Equilib.* **1981**, *6* (3-4), 181-9.
(89) Grauso, L.; Fredenslund, A.; Mollerup, J. Vapor-liquid equilibrium data for the systems ethane + molecular nitrogen, ethene + molecular nitrogen, propane + molecular nitrogen, and propene + molecular nitrogen. *Fluid Phase Equilib.* **1977**, *1* (1), 13-26.
(90) Zeck, S.; Knapp, H. Vapor-liquid and vapor-liquid-liquid phase equilibria of binary and ternary systems of nitrogen, ethene and methanol: experiment and data evaluation. *Fluid Phase Equilib.* **1986**, *26* (1), 37-58.
(91) Anthony, R. G.; McKetta, J. J. Phase equilibrium in the ethylene-water system. *J. Chem. Eng. Data* **1967**, *12* (1), 17-20.
(92) Bradbury, E. J.; McNulty, D.; Savage, R. L.; McSweeney, E. E. Solubility of ethylene in water. Effect of temperature and pressure. *J. Ind. Eng. Chem. (Washington, D. C.)* **1952**, *44*, 211-12.
(93) Davis, J. E.; McKetta, J. J., Jr. Solubility of ethylene in H2O. *J. Chem. Eng. Data* **1960**, *5* (3), 374-5.
(94) Diepen, G. A. M.; Scheffer, F. E. C. The solubility of water in supercritical ethene. *Recl. Trav. Chim. Pays-Bas Belg.* **1950**, *69*, 604-9.
(95) Sanchez, M.; Lentz, H. Phase equilibrium of water-propene and water-ethene systems at high temperatures and pressures. *High Temp. - High Pressures* **1973**, *5* (6), 689-99.
(96) Sidorov, I. P.; Kazarnovskii, Y. S.; Goldman, A. M. The Solubility of Water in compressed Gases. *Tr. Gos. Nauchno Issled. Proektn. Inst. Azotn. Promst. Prod. Org. Sin.* **1953**, *1*, 48-67.
(97) Tsiklis, D. S.; Kulikova, A. I.; Shenderei, L. I. Phase-equilibriums in the system ethanol-ethylene-water. *Khim. Prom-st. (St. Petersburg, Russ. Fed.)* **1960**, 401-6.
(98) Tsiklis, D. S.; Mushkina, E. V.; Shenderei, L. I. Phase Equilibria in the System Ethylene - Water at high Pressures and Temperatures. *Inzh. Fiz. Zh.* **1958**, *1* (8), 3-7.
(99) Hakuta, T.; Nagahama, K.; Hirata, M. Binary vapor-liquid equilibrium for C3 hydrocarbons. *Bull. Jap. Petrol. Inst.* **1969**, *11*, 10-15.
(100) Hanson, G. H.; Hogan, R. J.; Nelson, W. T.; Cines, M. R. Propane-propylene system-vapor-liquid equilibrium relationships. *J. Ind. Eng. Chem. (Washington, D. C.)* **1952**, *44*, 604-9.
(101) Harmens, A. Propylene-propane phase equilibrium from 230 to 350 K. *J. Chem. Eng. Data* **1985**, *30* (2), 230-3.
(102) Hirata, M.; Hakuta, T. Vapor-Liquid Equilibrium Data for Propylene - Propane. *Mem. Fac. Technol. Tokyo Metropol. Univ.* **1968**, *18*, 1595-1606.
(103) Hirata, M.; Hakuta, T.; Onoda, T. Vapor-liquid equilibria of the propylene - propane system at low temperature. *Int. Chem. Eng.* **1968**, *8* (1), 175-179.
(104) Ho, Q. N.; Yoo, K. S.; Lee, B. G.; Lim, J. S. Measurement of vapor-liquid equilibria for the binary mixture of propylene (R-1270) + propane (R-290). *Fluid Phase Equilib.* **2006**, *245* (1), 63-70.
(105) Laurance, D. R.; Swift, G. W. Relative volatility of propane-propene system from 100-160.deg.F. *J. Chem. Eng. Data* **1972**, *17* (3), 333-7.
(106) Manley, D. B.; Swift, G. W. Relative volatility of propane-propene system by integration of general coexistence equation. *J. Chem. Eng. Data* **1971**, *16* (3), 301-7.
(107) Noda, K.; Sakai, M.; Ishida, K. Isothermal vapor-liquid equilibriums for the propane-propylene-tetralin system. *J. Chem. Eng. Data* **1982**, *27* (1), 32-4.
(108) Onken, U.; Arlt, W. Recommended Test Mixtures for Distillation Columns. *Monograph. The Institution of Chemical Engineers, Rugby, Warwickshire* **1990**, 1-61.
(109) Reamer, H. H.; Sage, B. H. Volumetric and phase behavior of propene-propane system. *J. Ind. Eng. Chem. (Washington, D. C.)* **1951**, *43*, 1628-34.
(110) Shenderei, E. R.; Zel'venskii, Y. D.; Ivanovskii, F. P. Solubility of Propylene inorganic Solvents at low Temperatures. *Tr. Gos. Nauchno Issled. Proektn. Inst. Azotn. Promst. Prod. Org. Sin.* **1963**, *15*, 161-175.
(111) Asatani, H.; Hayduk, W. A Constant Flow Apparatus for the Determination of Gas Solubilities at High Pressures. *World Congress III of Chemical Engineering, Tokyo* **1986**.
(112) Hayduk, W.; Asatani, H.; Miyano, Y. Solubilities of propene, butane, isobutane, and isobutene gases in n-octane, chlorobenzene, and n-butanol solvents. *Can. J. Chem. Eng.* **1988**, *66* (3), 466-73.

(113) Hayduk, W.; Asatani, H.; Miyano, Y. A high pressure solubility apparatus for gases of high solubility. *Can. J. Chem. Eng.* **1991**, *69* (5), 1197-203.
(114) Goff, G. H.; Farrington, P. S.; Sage, B. H. Volumetric and phase behavior of propene-1-butene system. *J. Ind. Eng. Chem. (Washington, D. C.)* **1950**, *42*, 735-43.
(115) Oscarson, J. L.; Lundell, S. O.; Cunningham, J. R. Phase equilibria for ten binary systems. *AIChE Symp. Ser.* **1987**, *83* (256), 1-17.
(116) Laurance, D. R.; Swift, G. W. Vapor-liquid equilibriums in three binary and ternary systems composed of butane, 1-butene, and 1,3-butadiene. *J. Chem. Eng. Data* **1974**, *19* (1), 61-7.
(117) Sage, B. H.; Lacey, W. N. System 1-butene-butane. Composition of coexisting phases. *J. Ind. Eng. Chem. (Washington, D. C.)* **1948**, *40*, 1299-1301.
(118) Laugier, S.; Richon, D. High-Pressure Vapor-Liquid Equilibria for Ethylene + 4-Methyl-1-pentene and 1-Butene + 1-Hexene. *J. Chem. Eng. Data* **1996**, *41* (2), 282-4.
(119) Gumpert, H. J.; Koehler, H.; Schiller, W.; Bittrich, H. J. Vapor pressure measurements of binary systems of olefins and diolfeins. *Wiss. Z. Tech. Hochsch. Chem. Carl Schorlemmer Leuna-Merseburg* **1973**, *15* (3), 179-87.
(120) Wolfe, D.; Kay, W. B.; Teja, A. S. Phase equilibriums in the n-pentane + pent-1-ene system. 2. Dew and bubble points. *J. Chem. Eng. Data* **1983**, *28* (3), 322-4.
(121) Hanson, D. O.; Van, W. M. Alteration of the relative volatility of hexane-1-hexene by oxygenated and chlorinated solvents. *J. Chem. Eng. Data* **1967**, *12* (3), 319-25.
(122) Kirss, H.; Kudryavtseva, L. S.; Eisen, O. Liquid-vapor equilibrium in 1-hexene-hexane-octane, benzene-1-heptane-heptane, 1-heptene-heptane-toluene ternary systems and in corresponding binary systems at 55.deg. *Eesti NSV Tead. Akad. Toim., Keem., Geol.* **1975**, *24* (1), 15-22.
(123) Lozano, L. M.; Montero, E. A.; C, M. M.; Villamanan, M. A. Isothermal vapor-liquid equilibria of binary mixtures containing methyl tert-butyl ether (MTBE) and/or substituted hydrocarbons. *Fluid Phase Equilib.* **1997**, *133* (1-2), 155-162.
(124) Marrufo, B.; Aucejo, A.; Sanchotello, M.; Loras, S. Isobaric vapor-liquid equilibrium for binary mixtures of 1-hexene+ n-hexane and cyclohexane+cyclohexene at 30, 60 and 101.3kPa. *Fluid Phase Equilib.* **2009**, *279* (1), 11-16.
(125) Chamorro, C. R.; Segovia, J. J.; Martin, M. C.; Villamanan, M. A. Thermodynamics of Octane-Enhancing Additives in Gasolines: Vapor-Liquid Equilibrium of Binary and Ternary Mixtures Containing Di-isopropyl Ether or Heptane and 1-Hexene + Cyclohexane at 313.15 K. *J. Chem. Eng. Data* **2001**, *46* (6), 1574-1579.
(126) Segovia, J. J.; Martin, M. C.; Chamorro, C. R.; Montero, E. A.; Villamanan, M. A. Excess thermodynamic functions for ternary systems containing fuel oxygenates and substitution hydrocarbons 2. Total-pressure data and GE for methyl tert-butyl ether/n-heptane/1-hexene at 313.15 K. *Fluid Phase Equilib.* **1998**, *152* (2), 265-276.
(127) Segura, H.; Wisniak, J.; Galindo, G.; Reich, R. Phase equilibria in the systems 1-hexene + heptane and 1-hexene + ethyl 1,1-dimethylethyl ether + heptane at 94.00 kPa. *Phys. Chem. Liq.* **2002**, *40* (1), 67-81.
(128) Bittrich, H. J.; Zimmermann, G.; Schaar, E. Studies of selective separation of substances. VI. Ortho ester as a selective solvent for hydrocarbon separations. *Z. Phys. Chem. (Leipzig)* **1979**, *260* (5), 1005-8.
(129) Kudryavtseva, L. S.; Toome, M.; Otsa, E. Liquid-vapor equilibrium in the 1-heptene-heptane-1-heptyne system. *Eesti NSV Tead. Akad. Toim., Keem.* **1981**, *30* (2), 147-9.
(130) Kudryavtseva, L. S.; Viit, H.; Eisen, O. Vapor-liquid equilibrium in 1-heptene-heptane, 1-heptene-octane, heptane-octane, benzene-thiophene, benzene-heptane, and thiophene-heptane binary systems at 55.deg. *Eesti NSV Tead. Akad. Toim., Keem., Geol.* **1971**, *20* (4), 292-6.
(131) Kuus, M.; Toome, M.; Kudryavtseva, L. S.; Eisen, O. Thermodynamic properties of the mixtures of n-octane with isomers of n-octene. 2. Vapor-liquid equilibriums. *Eesti NSV Tead. Akad. Toim., Keem.* **1980**, *29* (1), 32-7.
(132) Mikhelson, V.; Kirss, H.; Kudryavtseva, L. S.; Eizen, O. G. Vapor-Liquid Equilibrium T-x Measurements by a New Semi-Micro Method. *Fluid Phase Equilib.* **1977**, *1*, 201-209.
(133) Jalili, A. H.; Sina, M. Isobaric Vapor-Liquid Equilibria of Hexane + 1-Decene and Octane + 1-Decene Mixtures. *J. Chem. Eng. Data* **2008**, *53* (2), 398-402.
(134) Joyce, P. C.; Leggett, B. E.; Thies, M. C. Vapor-liquid equilibrium for model Fischer-Tropsch waxes (hexadecane, 1-hexadecene, and 1-hexadecanol) in supercritical hexane. *Fluid Phase Equilib.* **1999**, *158-160*, 723-731.
(135) Keistler, J. R.; Van, W. M. Vapor-liquid equilibria at subatmospheric pressures-system dodecane-hexadecene. *J. Ind. Eng. Chem. (Washington, D. C.)* **1952**, *44* (3), 622-4.
(136) Rasmussen, R. R.; Van, W. M. Vapor-liquid equilibria at subatmospheric pressures-tetradecane-hexadecene system. *J. Ind. Eng. Chem. (Washington, D. C.)* **1950**, *42* (10), 2121-4.

(137) Ward, S. H.; Van, W. M. Vapor-liquid equilibria at 200 mm. of mercury. Binary systems naphthalene-tetradecane, naphthalene-1-hexadecane, tetradecane-1-hexadecene, ternary systems naphthalene-tetradecane-1-hexadecene. *J. Ind. Eng. Chem. (Washington, D. C.)* **1954**, *46* (2), 338-50.
(138) Jordan, B. T., Jr.; Van, W. M. Vapor-liquid equilibrium at subatmospheric pressures; dodecane-octadecene system. *J. Ind. Eng. Chem. (Washington, D. C.)* **1951**, *43* (12), 2908-12.
(139) Doering, K. E.; Preuss, H. Vapor pressures of mixtures 1,3-butadiene - n-pentane. *FIZ Report* **1967**, 3061.
(140) Rozhnov, M. S. Phase and volume parameters in the butadiene-hydrocarbon systems. *Khim. Prom-st. (Moscow)* **1967**, *43* (4), 288-90.
(141) Rozhnov, M. S.; Efremova, G. D. Liquid-gas equilibrium in butadiene-hydrocarbon systems at low temperatures. *Khim. Prom. Ukr.* **1970**, *6*, 33-5.
(142) Flebbe, J. L.; Barclay, D. A.; Manley, D. B. Vapor pressures of some C4 hydrocarbons and their mixtures. *J. Chem. Eng. Data* **1982**, *27* (4), 405-12.
(143) Doering, K. E.; Preuss, H. Vapor pressures of mixtures 1,3-butadiene - 1-pentene. *FIZ Report* **1967**, 4141.
(144) Li, J.; Qin, Z.; Wang, G.; Dong, M.; Wang, J. Critical temperatures and pressures of several binary and ternary mixtures concerning the alkylation of 2-methylpropane with 1-butene in the presence of methane or carbon dioxide. *J. Chem. Eng. Data* **2007**, *52* (5), 1736-1740.
(145) Steele, K.; Poling, B. E.; Manley, D. B. Vapor pressures for the system 1-butene, isobutane, and 1,3-butadiene. *J. Chem. Eng. Data* **1976**, *21* (4), 399-403.
(146) Thoedtmann, I.; Preuss, H.; Pape, D. Determination of the vapor-liquid equilibria in systems formed by ethene, but-1-ene and 4-methylpent-1-ene. *FIZ Report* **1989**, 9151.
(147) Wohlfarth, C.; Finck, U.; Schultz, R.; Heuer, T. Investigation of phase equilibria in mixtures composed of ethene, 1-butene, 4-methyl-1-pentene, and a polyethylene wax. *Angew. Makromol. Chem.* **1992**, *198*, 91-110.
(148) Chamorro, C. R.; Martin, M. C.; Villamanan, M. A.; Segovia, J. J. Characterization and modelling of a gasoline containing 1,1-dimethylethyl methyl ether (MTBE), diisopropyl ether (DIPE) or 1,1-dimethylpropyl methyl ether (TAME) as fuel oxygenate based on new isothermal binary vapour-liquid data. *Fluid Phase Equilib.* **2004**, *220* (1), 105-112.
(149) Segura, H.; Wisniak, J.; Galindo, G.; Reich, R. Phase Equilibria in the Systems 1-Hexene + 2,2,4-Trimethylpentane and 1-Hexene + Ethyl 1,1-Dimethylethyl Ether + 2,2,4-Trimethylpentane at 94.00 kPa. *J. Chem. Eng. Data* **2001**, *46* (3), 511-515.
(150) Popescu, R.; Stanescu, L.; Sandulescu, D. Propylene solubility in liquid hydrocarbons at atmospheric pressure. I. *Rev. Roum. Chim.* **1992**, *37* (10), 1117-24.
(151) Blagoi, Y. P.; Orobinskii, N. A. Liquid-Vapor Phase Equilibrium in the Systems Propene - Methane and Propene - Carbon Tetrafluoride. *Russ. J. Phys. Chem.* **1966**, *40* (12), 1625-1629.
(152) Orobinskii, N. A.; Blagoi, Y. P.; Semyannikova, E. L.; V'yunnik, L. N. Phase Equilibrium Liquid-Vapor. Systems Methane - Propylene and Carbon Tetrafluoride - Propylene at high Temperatures. *Fiz. Khim. Rastvorov* **1972**, 233-238.
(153) Steckel, F. Vapor-liquid equilibria under pressure of some binary hydrogen sulfide-containing systems. *Sven. Kem. Tidskr.* **1945**, *57*, 209-16.
(154) Sandri, V. Molecular interactions and phase separation. *Corsi Semin. Chim.* **1967**, *5*, 63-71.
(155) Peramanu, S.; Pruden, B. B. Solubility study for the purification of hydrogen from high pressure hydrocracker off-gas by an absorption-stripping process. *Can. J. Chem. Eng.* **1997**, *75* (3), 535-543.
(156) Hirata, M.; Suda, S.; Hakuta, T.; Nagahama, K. Light hydrocarbon vapor-liquid equilibria. *Mem. Fac. Technol., Tokyo Metrop. Univ.* **1969**, *19*, 103-22.
(157) Lu, H.; Newitt, D. M.; Ruhemann, M. Two-phase equilibrium in binary and ternary systems. IV. The system ethane-propylene. *Proc. R. Soc. London, Ser. A* **1941**, *178*, 506-525.
(158) McKay, R. A.; Reamer, H. H.; Sage, B. H.; Lacey, W. N. Volumetric and phase behavior in the ethane-propene system. *J. Ind. Eng. Chem. (Washington, D. C.)* **1951**, *43* (9), 2112-2117.
(159) Ohgaki, K.; Nakai, S.; Nitta, S.; Katayama, T. Isothermal vapor-liquid equilibriums for the binary systems propylene-carbon dioxide, propylene-ethylene and propylene-ethane at high pressure. *Fluid Phase Equilib.* **1982**, *8* (2), 113-122.
(160) Estrera, S. S.; Arbuckle, M. M.; Luks, K. D. Solubility and partial miscibility of ethane in certain hydrocarbon liquids. *Fluid Phase Equilib.* **1987**, *35* (1-3), 291-307.
(161) Guo, J.; Liu, T.; Dai, Y.-C.; Yuan, W.-K. Vapor-Liquid Equilibria of Benzene and Propylene under Elevated Temperature and Pressure. *J. Chem. Eng. Data* **2001**, *46* (3), 668-670.
(162) Guzechak, O. Y.; Sarancha, V. N.; Romanyuk, I. M.; Yavorskaya, O. M.; Churik, G. P. Solubility of propylene in organic solvents. *J. Appl. Chem. USSR* **1984**, *57* (8), 1662-1665.
(163) Kozorezov, Y. I.; Novozhilova, T. S. Solubility of propylene in aromatic hydrocarbons. *Sov. Chem. Ind. Engl. Transl.* **1971**, *47* (6), 399-401.

(164) Wang, G.; Qin, Z.; Liu, J.; Tian, Z.; Hou, X.; Wang, J. Critical Properties of the Reacting Mixture in the Alkylation of Benzene with Propene. *Ind. Eng. Chem. Res.* **2003**, *42* (25), 6531-6535.
(165) Yamamoto, H.; Ohgaki, K.; Katayama, T. Isothermal vapor-liquid equilibrium data of the benzene-propylene system at 25°C. *Fluid Phase Equilib.* **1989**, *46* (1), 53-58.
(166) Miyano, Y.; Nakanishi, K. Solubilities of 1-butene in (methanol + benzene) and (methanol + cyclohexane) at T=298.15 K and p=40 kPa to 102 kPa. *J. Chem. Thermodyn.* **2003**, *35* (3), 519-528.
(167) Wong, K. F.; Eckert, C. A. Vapor-liquid equilibriums of 1,3-butadiene systems. *J. Chem. Eng. Data* **1969**, *14* (4), 432-436.
(168) Chamorro, C. R.; Segovia, J. J.; Martin, M. C.; Villamanan, M. A. Thermodynamics of Octane-Enhancing Additives in Gasolines: Vapor-Liquid Equilibrium of Ternary Mixtures Containing Di-isopropyl Ether or Cyclohexane and 1-Hexene + Benzene at 313.15 K. *J. Chem. Eng. Data* **2002**, *47* (2), 316-321.
(169) Dojcansky, J.; Heinrich, J.; Surovy, J. Gas-liquid equilibriums in the system 1-hexene-benzene at 25°. *Chem. Zvesti* **1967**, *21* (9-10), 713-717.
(170) Prausnitz, J. M.; Vera, J. H. Vapor-liquid equilibriums in binary aromatic-olefin systems. *J. Chem. Eng. Data* **1971**, *16* (2), 149-154.
(171) Segovia, J. J.; Martin, M. C.; Chamorro, C. R.; Villamanan, M. A. Thermodynamics of Octane-Enhancing Additives in Gasolines: Vapor-Liquid Equilibrium of the Ternary Mixtures Methyl tert-Butyl Ether + Heptane + Benzene and Methyl tert-Butyl Ether + Benzene + 1-Hexene at 313.15 K. *J. Chem. Eng. Data* **1998**, *43* (Copyright (C) 2010 American Chemical Society (ACS). All Rights Reserved.), 1014-1020.
(172) Segura, H.; Wisniak, J.; Galindo, G.; Reich, R. Phase Equilibria in the Systems 1-Hexene + Benzene and 1-Hexene + Ethyl 1,1-Dimethylethyl Ether + Benzene at 94.00 kPa. *J. Chem. Eng. Data* **2001**, *46* (3), 506-510.
(173) Dariva, C.; Lovisi, H.; Mariac, L. C. S.; Coutinho, F. M. B.; Oliveira, J. V.; Pinto, J. C. Propylene solubility in toluene and isododecane. *Can. J. Chem. Eng.* **2003**, *81* (1), 147-152.
(174) Diaz, C.; Dominguez, A.; Tojo, J. Phase Equilibria of the Binary Systems 1-Hexene with o-Xylene, m-Xylene, p-Xylene, Toluene, and Ethylbenzene at 101.3 kPa. *J. Chem. Eng. Data* **2002**, *47* (4), 867-871.
(175) Lu, B. C. Y.; Ni, L.-W.; Taylor, M. Reevaluation of Vapor-Liquid Equilibria for Butadiene + Styrene. *J. Chem. Eng. Data* **1996**, *41* (2), 287-291.
(176) Wilhelm, R. H.; Collier, D. W. Vapor-liquid equilibriums of the system butadiene-styrene. *J. Ind. Eng. Chem. (Washington, D. C.)* **1948**, *40*, 2350-2353.
(177) Laevskaya, N. S.; Bagrov, I. V.; Dobroserdov, L. L. Vapor-Liquid Equilibrium in Systems which are Created During the Production of Styrene-Copolymers. *Deposited Doc. VINITI* **1977**, (421-77), 1-7.
(178) Martirosyan, R. S.; Beregovykh, V. V.; Pluzhnikova, Z. A.; Kolyuchkina, G. A.; L'vov, S. V.; Serafimov, L. A. Physico-chemical Properties of Binary Systems Formed by Products of the Dehydrogenation of Ethylbenzene. *Tr. Mosk. Inst. Tonkoi Khim. Tekhnol.* **1974**, *4* (1), 122-125.
(179) Determination of the Vapor Pressures and the real Separation Factors for the Systems Ethylbenzene - p-Xylene and p-Xylene - Styrene by Measurements. *Confidential Company Research Report* **1977**, (LC3521).
(180) Weber, J. H. Vapor-liquid equilibriums at atmospheric pressure - systems 2,2,5-trimethylhexane-ethylbenzene and 1-octene-ethylbenzene. *J. Ind. Eng. Chem. (Washington, D. C.)* **1956**, *48*, 134-136.
(181) Aucejo, A.; Loras, S.; Martinez-Soria, V.; Becht, N.; Del, R. G. Isobaric Vapor-Liquid Equilibria for the Binary Mixtures of Styrene with Ethylbenzene, o-Xylene, m-Xylene, and p-Xylene. *J. Chem. Eng. Data* **2006**, *51* (3), 1051-1055.
(182) Chaiyavech, P.; Van, W. M. Styrene-ethylbenzene vapor-liquid equilibrium at reduced pressures. *J. Chem. Eng. Data* **1959**, *4*, 53-6.
(183) Martin, W. L.; Van, W. M. Vapor-liquid equilibria of the naphthalene-1-octadecene system at subatmospheric pressures. *J. Ind. Eng. Chem. (Washington, D. C.)* **1954**, *46*, 1477-1481.
(184) Segovia, J. J.; Martin, M. C.; Chamorro, C. R.; Villamanan, M. A. Vapor-Liquid Equilibrium of Ternary Mixtures Containing Methyl tert-Butyl Ether and/or Substitution Hydrocarbons. Methyl tert-Butyl Ether + Heptane + Cyclohexane and Methyl tert-Butyl Ether + Cyclohexane + 1-Hexene at 313.15 K. *J. Chem. Eng. Data* **1998**, *43* (6), 1021-1026.
(185) Young, K. L.; Mentzer, R. A.; Greenkorn, R. A.; Chao, K. C. Vapor-liquid equilibrium in mixtures of cyclohexane + benzene, + 1-octene, + m-xylene, and + n-heptane. *J. Chem. Thermodyn.* **1977**, *9* (10), 979-85.
(186) Ke, J.; Han, B.; George, M. W.; Yan, H.; Poliakoff, M. How Does the Critical Point Change during a Chemical Reaction in Supercritical Fluids? A Study of the Hydroformylation of Propene in Supercritical CO2. *J. Am. Chem. Soc.* **2001**, *123* (16), 3661-3670.
(187) Yorizane, M.; Yoshimura, S.; Masuoka, H. Vapor-Liquid Equilibria of Carbon Dioxide - Propylene System. *Kagaku Kogaku* **1966**, *30*, 1093-1096.
(188) Behrens, P. K.; Sandler, S. I. Vapor-liquid equilibriums for the carbon dioxide-1-butene system at 37.7 and 45.0°C. *J. Chem. Eng. Data* **1983**, *28* (1), 52-56.

(189) Wagner, K. D.; Zappe, J.; Reeps, A.; Dahmen, N.; Dinjus, E. Vapor-liquid equilibria for the binary system of carbon dioxide and 1,3-butadiene at 303, 313 and 333 K. *Fluid Phase Equilib.* **1998**, *153* (1), 135-142.
(190) Wu, G.; Zhang, N.; Zheng, X.; Kubota, H.; Makita, T. High pressure vapor-liquid equilibria of four binary systems containing carbon dioxide. *J. Chem. Eng. Jpn.* **1988**, *21* (1), 25-29.
(191) Byun, H.-S.; Choi, T.-H. Vapor-liquid equilibria measurement of carbon dioxide + 1-hexene and carbon dioxide + 2-ethyl-1-butene systems at high pressure. *Korean Journal of Chemical Engineering* **2004**, *21* (5), 1032-1037.
(192) Jennings, D. W.; Teja, A. S. Vapor-liquid equilibria in the carbon dioxide-1-hexene and carbon dioxide-1-hexyne systems. *J. Chem. Eng. Data* **1989**, *34* (3), 305-309.
(193) Vera, J. H.; Orbey, H. Binary vapor-liquid equilibria of carbon dioxide with 2-methyl-1-pentene, 1-hexene, 1-heptene, and m-xylene at 303.15, 323.15, and 343.15 K. *J. Chem. Eng. Data* **1984**, *29* (3), 269-272.
(194) Wagner, Z.; Wichterle, I. High-pressure vapor-liquid equilibrium in systems containing carbon dioxide, 1-hexene, and n-hexane. *Fluid Phase Equilib.* **1987**, *33* (1-2), 109-123.
(195) Ren, W.; Rutz, B.; Scurto, A. M. High-pressure phase equilibrium for the hydroformylation of 1-octene to nonanal in compressed CO2. *J. Supercrit. Fluids* **2009**, *51* (2), 142-147.
(196) Akgun, M.; Emel, D.; Baran, N.; Akgun, N. A.; Deniz, S.; Dincer, S. Styrene-carbon dioxide phase equilibria at high pressures. *J. Supercrit. Fluids* **2004**, *31* (1), 27-32.
(197) Bamberger, A.; Schmelzer, J. u.; Walther, D.; Maurer, G. High-pressure vapor-liquid equilibria in binary mixtures of carbon dioxide and benzene compounds: experimental data for mixtures with ethylbenzene, isopropylbenzene, 1,2,4-trimethylbenzene, 1,3,5-trimethylbenzene, ethenylbenzene and isopropenylbenzene, and their correlation with the generalized Bender and Skjold-Jorgensen's group contribution equation of state. *Fluid Phase Equilib.* **1994**, *97* (1-2), 167-189.
(198) Suppes, G. J.; McHugh, M. A. Phase behavior of the carbon dioxide-styrene system. *J. Chem. Eng. Data* **1989**, *34* (3), 310-312.
(199) Tan, C. S.; Yarn, S. J.; Hsu, J. H. Vapor-liquid equilibria for the systems carbon dioxide-ethylbenzene and carbon dioxide-styrene. *J. Chem. Eng. Data* **1991**, *36* (1), 23-25.
(200) Wang, B.; He, J.; Sun, D.; Zhang, R.; Han, B. Solubility of chlorobutane, ethyl methacrylate and trifluoroethyl acrylate in supercritical carbon dioxide. *Fluid Phase Equilib.* **2006**, *239* (1), 63-68.
(201) Zhang, J.; Gao, L.; Zhang, X.; Zong, B.; Jiang, T.; Han, B. Phase Behaviors, Density, and Isothermal Compressibility of Styrene + CO2, Ethylbenzene + CO2, and Ethylbezene + Styrene + CO2 Systems. *J. Chem. Eng. Data* **2005**, *50* (6), 1818-1822.
(202) Kim, H.; Lin, H. M.; Chao, K. C. Vapor-liquid equilibrium in binary mixtures of carbon dioxide + phenyloctane and carbon dioxide + 1-hexadecene. *AIChE Symp. Ser.* **1985**, *81*, 86-89.
(203) Yorizane, M.; Sadamoto, S.; Yoshimura, S.; Masuoka, H.; Shiki, N.; Kimura, T.; Toyama, A. Low temperature vapor-liquid equilibriums. Nitrogen-propylene and carbon monoxide-methane systems. *Kagaku Kogaku* **1968**, *32* (3), 257-264.
(204) Steinbach, H. G.; Steinbrecher, M. Solubility of nitrogen C4-liquefied gases. *Chem. Tech. (Leipzig)* **1966**, *18* (10), 633-633.
(205) Azarpoor, A.; McKetta, J. J. Solubility of propylene in water. *J. Chem. Eng. Data* **1959**, *4*, 211-212.
(206) Chen, X.; Xu, X. Phase Equilibria of Propylene - Methanol - Water System. *Huagong Xuebao (Chinese Edition)* **1998**, *49* (5), 632-638.
(207) Klausutis, N. Phase equilibrium in the propane - propylene - water system in the three - phase region. *Ph.D. thesis, Austin, Texas* **1968**, 1-113.
(208) Li, C. C.; McKetta, J. J. Vapor-liquid equilibrium in the propylene-water system. *J. Chem. Eng. Data* **1963**, *8*, 271-275.
(209) Liu, G.; Ren, Y.; Mi, Z. Measurement and Correlation of Solubility for Propylene in 2-Propanol - Water Solutions. *Chemweb Preprint Server* **2002**, 1-5.
(210) Black, C.; Joris, G. G.; Taylor, H. S. The solubility of water in hydrocarbons. *J. Chem. Phys.* **1948**, *16*, 537-543.
(211) Brooks, W. B.; Haughn, J. E.; McKetta, J. J. The 1-butene-water system in the vapor and three-phase regions. *Pet. Refin.* **1955**, *34* (8), 129-130.
(212) Brooks, W. B.; McKetta, J. J. The solubility of water in 1-butene. *Pet. Refin.* **1955**, *34* (4), 138.
(213) Brooks, W. B.; McKetta, J. J. The solubility of 1-butene in water. *Pet. Refin.* **1955**, *34* (2), 143-144.
(214) Josten, H. The separation of liquid mixtures with the aid of pressure-liquefied gases. *Ph.D. thesis, RWTH Aachen* **1986**, 1-244.
(215) Reed, C. D.; McKetta, J. J. Solubility of 1,3-butadiene in water. *J. Chem. Eng. Data* **1959**, *4* (4), 294-295.
(216) Brady, C. J.; Cunningham, J. R.; Wilson, G. M. Water - Hydrocarbon Liquid-Liquid-Vapor Equilibrium Measurements to 530 degrees F. *GPA Research Report* **1982**, (RR-62), 1-66.

(217) Bae, H. K.; Nagahama, K.; Hirata, M. Measurement and correlation of high pressure vapor-liquid equilibriums for the systems ethylene-1-butene and ethylene-propylene. *J. Chem. Eng. Jpn.* **1981**, *14* (1), 1-6.
(218) Kubota, H.; Inatome, H.; Tanaka, Y.; Makita, T. Vapor-liquid equilibriums of the ethylene-propylene system under high pressure. *J. Chem. Eng. Jpn.* **1983**, *16* (2), 99-103.
(219) Vapor-liquid equilibrium of the System Ethylene - 1-Butene. *Confidential Company Research Report* **1981**, (LC4483).
(220) Laugier, S.; Richon, D.; Renon, H. Ethylene + Olefin Binary Systems: Vapor-Liquid Equilibrium Experimental Data and Modeling. *J. Chem. Eng. Data* **1994**, *39* (2), 388-391.
(221) Preuss, H.; Moerke, K. Determination of the VLE in the system ethene - but-1-ene. *FIZ Report* **1984**, 9261.
(222) Burcham, A. F.; Trampe, M. D.; Poling, B. E.; Manley, D. B. Phase equilibria for the propane-propadiene system from total pressure measurements. *ACS Symp. Ser.* **1986**, *300*, 86-107.
(223) Howat, C. S.; Swift, G. W. Vapor-liquid phase equilbiria for the isoprene - n-pentane binary system from 300 to 330 K. *Fluid Phase Equilib.* **1985**, *21* (1-2), 113-134.
(224) Kozhenkov, A. V.; Malenko, Y. I.; Nikolaev, S. N.; Sobolev, D. M. Vapor-Liquid Equilibrium in the System Methylethylene (2-Methylbutylene-1) - Hexane - Toluene. *Promst. Sint. Kauch. Shin. Rezinotekh. Izdel.* **1988**, *7*, 2-3.
(225) Kozhenkov, A. V.; Malenko, Y. I.; Nikolaev, S. N.; Sobolev, D. M. Vapor-Liquid Equilibrium in the System Isoprene - Hexane - Toluene. *Promst. Sint. Kauch. Shin. Rezinotekh. Izdel.* **1987**, *1*, 3-4.
(226) Roscher, T. Vapor-liquid equilibria of the systems n-pentane - toluene and isoprene - n-hexane. *FIZ Report* **1970**, 12281.
(227) Kozhenkov, A. V.; Nikolaev, S. N.; Sobolev, D. M.; Malenko, Y. I. Vapor-Liquid Equilibrium in the system Trimethylethylene - Hexane - Toluene. *Promst. Sint. Kauch. Shin. Rezinotekh. Izdel.* **1987**, *11* (4), 4-5.
(228) Doering, K. E.; Preuss, H. Vapor pressures of mixtures 1-butyne - vinylacetylene and isoprene - 1,3-butadiene. *FIZ Report* **1967**, 2041.
(229) Mervart, Z. Phase equilibriums in the system isobutene-isoprene at 5 atmospheres. *Collection of Czechoslovak Chemical Communications* **1959**, *24* (12), 4034-4036.
(230) Wu, Z.; Chen, Z.; Shou, Z.; Zhu, S. Isobaric Vapor-Liquid Equilibrium of Isobutene - Isopropene - Chloromethane. *Huagong Xuebao (Chinese Edition)* **1987**, *38* (4), 406-415.
(231) Doering, K. E.; Preuss, H. Vapor pressures of mixtures isoprene - 2-methyl-2-butene. *FIZ Report* **1968**, 7091.
(232) Dolejsek, Z.; Grubner, O.; Hala, E.; Hanus, V.; Kossler, I. The purification and analyses of isoprene. II. *Chem. Prum.* **1961**, *11*, 361-363.
(233) Ezekwe, J. N.; Howat, C. S., III; Swift, G. W. Vapor-liquid equilibriums for the binary system 2-methylbutene-2 and 2-methyl-1,3-butadiene at 310.93, 316.48, and 322.04 K. *Fluid Phase Equilib.* **1981**, *7* (1), 75-85.
(234) Frolov, A. F.; Korotkova, V. N. Vapor-Liquid Equilibrium in the System of Isoprene with Hydrocarbons of C5 Fractions. *Khim. Promst. Moscow* **1961**, (6), 376-378.
(235) Korotkova, V. N.; Pavlov, S. Y.; Karpacheva, L. L.; Kofman, L. S.; Serafimov, L. A. Vapor-Liquid Equilibrium in the Systems Isoprene - 2-Methyl-2-butene - Cyclopentadiene and Isoprene - 2-Methyl-2-butene - Pentin-1. *Promst. Sint. Kauch.* **1971**, (7), 1-4.
(236) Kozhenkov, A. V.; Nikolaev, S. N.; Reshetova, L. I.; Malenko, Y. I. Vapor-Liquid Equilibrium in System Containing C5-hydrocarbons. *Proizvod. Ispolz. Elastom.* **1991**, (6), 8-12.
(237) Lianzhou Research Inst. of Chem. Machinery., Z. U. *Huaxue Gongcheng* **1973**, *3*, 110-120.
(238) Ogorodnikov, S. K.; Kogan, V. B.; Nemtsov, M. S. Properties of Binary Systems Formed from C5 Hydrocarbons. *J. Appl. Chem. USSR* **1960**, *33* (7), 1581-1587.
(239) Shestakova, L. A.; Kofman, L. S.; Matveeva, T. N.; Savel'eva, T. N. Liquid-vapor phase equilibrium in binary and ternary mixtures of isoprene, 2-methyl-2-butene, and cyclopentadiene. *Prom. Sin. Kauch. Nauch.-Tekh. Sb.* **1970**, *11*, 10-13.
(240) Tianjin University, L. R. I. o. C. I. Vapor-Liquid Equilibria for Isoprene + 2-Methyl-2-butene and 2-Methyl-2-butene + N-Methyl-2-pyrrolidone at 760 mmHg. *Huaxue Gongcheng* **1978**, *5*, 74-92.
(241) Vostrikova, V. N.; Moiseeva, T. P.; Grinfeld, A. A.; Markhovskaya, Z. V. Vapor-Liquid Equilibrium of Binary and Ternary Systems Made up by Isoprene, Trimethylethylene and Methylenecyclobutane. *Promst. Sint. Kauch. Shin. Rezinotekh. Izdel.* **1986**, *12*, 2-4.
(242) Shenderei, E. R. Solubility of Acetylene, Methylacetylene, Propadiene and Diacetylene in n-Octane. *Khim. Promst. Moscow* **1965**, *41* (8), 580-585.
(243) Scheeline, H. W.; Gilliland, E. R. Vapor-liquid equilibrium in the system propane-isobutylene. *J. Ind. Eng. Chem. (Washington, D. C.)* **1939**, *31*, 1050-1057.

(244) Martinez-Ortiz, J. A.; Manley, D. B. Vapor pressures for the system isobutane-isobutylene-n-butane. *J. Chem. Eng. Data* **1978**, *23* (2), 165-167.
(245) Reich, R.; Sanhueza, V. Vapor-liquid equilibria for α-pinene and β-pinene and for these pinenes with heptane, cyclohexane, 1-octene and cyclohexene. *Fluid Phase Equilib.* **1992**, *77* (1), 313-325.
(246) Hirata, M.; Suda, S.; Hakuta, T.; Nagahama, K. Vapor-liquid equilibriums of binary C4-hydrocarbon systems. *Sekiyu Gakkai Shi* **1969**, *12* (10), 773-777.
(247) Doering, K. E.; Preuss, H. Vapor pressures of mixtures isopentane - isoprene. *FIZ Report* **1968**, 1221.
(248) Prikhodko, S. I.; Komarova, L. F.; Gorelova, O. M.; Gorlova, N. N.; Bondaletov, V. G. Study of phase equilibrium of vapor-liquid in binary and ternary systems formed by components of pyrolysis of short-way distillation of gasolines. *Zh. Prikl. Khim. (Leningrad)* **2005**, *78* (3), 403-407.
(249) Bui, V. T.; Hamdouni, A.; Leonard, J. Interactive behavior of the α-methylstyrene-toluene mixture. *Can. J. Chem. Eng.* **1992**, *70* (1), 153-158.
(250) Phiong, H.-S.; Lucien, F. P. Volumetric expansion and vapour-liquid equilibria of α-methylstyrene and cumene with carbon dioxide at elevated pressure. *J. Supercrit. Fluids* **2003**, *25* (2), 99-107.
(251) Bogel-Lukasik, E.; Szudarska, A.; Bogel-Lukasik, R.; Nunes, d. P. M. Vapour-liquid equilibrium for β-myrcene and carbon dioxide and/or hydrogen and the volume expansion of β-myrcene or limonene in CO2 at 323.15K. *Fluid Phase Equilib.* **2009**, *282* (1), 25-30.
(252) Costa, M. A. M.; Matos, H. A. S.; Nunes, d. P. M.; Gomes, d. A. E. J. S. Binary and Ternary Phase Behavior of α-Pinene, β-Pinene, and Supercritical Ethene. *J. Chem. Eng. Data* **1996**, *41* (5), 1104-1110.
(253) Ruiz, B. F.; Fernandez, T. M. J. Vapor-liquid equilibrium for the binary system 1-methylcyclohexene + heptane at 101.3 kPa. *ELDATA: Int. Electron. J. Phys.-Chem. Data* **1999**, *5* (3), 143-148.
(254) Vostrikova, V. N.; Ambrozaitis, E. V.; Savostina, L. A.; Reshetov, S. A. Liquid-Vapor Equilibrium in Cyclopentadiene - Benzene, Cyclopentadiene - Hexane, Isoprene - Dicyclopentadiene and Piperylene - Dicyclopentadiene Binary Systems. *J. Appl. Chem. USSR* **1982**, *55* (6), 1178-1179.
(255) Jan, D. S.; Xie, Y. C.; Tsai, F. N. Isobaric vapor-liquid equilibria for cyclopentane + cyclohexene + 1,2-dichloroethane and the three constituent binary systems. *J. Chem. Eng. Data* **1993**, *38* (3), 383-385.
(256) Stoeck, S. Determination of the vapor-liquid equilibrium in the system cyclopentadiene - dicyclopentadiene. *FIZ Report* **1975**, 12011.
(257) Dojcansky, J.; Heinrich, J.; Surovy, J. Liquid-vapor equilibrium isotherm in the benzene-cyclohexene system at 25,50, and 75.deg. *Chem. Zvesti* **1968**, *22* (7), 514-520.
(258) Harrison, J. M.; Berg, L. Vapor-liquid equilibria of binary hydrocarbon systems. *J. Ind. Eng. Chem. (Washington, D. C.)* **1946**, *38*, 117-120.
(259) Sander, A.; Wagner, H. G. *Private Communication* **1987**.
(260) Vostrikova, V. N.; Komarova, T. V.; Aerov, M. E.; Sidorkova, A. V.; Savostina, L. A. Liquid Vapor Equilibrium of Binary Systems Containing Dicyclopentadiene. *J. Appl. Chem. USSR* **1975**, *48* (4), 960-961.
(261) Comelli, F.; Francesconi, R. Isobaric vapor-liquid equilibrium in binary mixtures of m- and p-xylenes with cyclohexene and cyclohexanone. *Can. J. Chem. Eng.* **1985**, *63* (2), 344-347.
(262) Afanas'ev, V. V.; Demidov, A. E.; Grishunin, A. V. Vapor-liquid equilibrium in binary systems formed by epoxidation products of cyclopentene with hydroperoxides of ethylbenzene and isopropylbenzene. *Deposited Doc. Oniitekhim* **1984**, (904 khp-D 84), 1-16.
(263) Karaseva, N. V.; Karavaeva, A. P.; Antonova, T. N.; Chabutkina, E. M.; Koshel, G. N. Liquid-vapor equilibria of the binary systems toluene - 1,5-cyclooctadiene and 1,5-cyclooctadiene - 5,6-epoxy-cis-cyclooctene. *Izv. Vyssh. Uchebn. Zaved. Khim. Khim. Tekhnol.* **1997**, *40* (3), 18-20.
(264) Bernardo-Gil, M. G.; Ribeiro, M. A. Vapor-liquid equilibria of binary systems based on pine resin. *Fluid Phase Equilib.* **1989**, *53*, 15-22.
(265) Bendale, P. G.; Enick, R. M. Use of carbon dioxide to shift benzene/acetonitrile and benzene/cyclohexane azeotropes. *Fluid Phase Equilib.* **1994**, *94*, 227-253.
(266) Akgun, M.; Akgun, N. A.; Dincer, S. Phase behavior of essential oil components in supercritical carbon dioxide. *J. Supercrit. Fluids* **1999**, *15* (2), 117-125.
(267) Berna, A.; Chafer, A.; Monton, J. B. Solubilities of Essential Oil Components of Orange in Supercritical Carbon Dioxide. *J. Chem. Eng. Data* **2000**, *45* (5), 724-727.
(268) Chang, C.-M. J.; Chen, C.-C. High-pressure densities and P-T-x-y diagrams for carbon dioxide + linalool and carbon dioxide + limonene. *Fluid Phase Equilib.* **1999**, *163* (1), 119-126.
(269) Di, G. G.; Brandani, V.; Del, R. G.; Mucciante, V. Solubility of essential oil components in compressed supercritical carbon dioxide. *Fluid Phase Equilib.* **1989**, *52*, 405-411.
(270) Gamse, T.; Marr, R. High-pressure phase equilibria of the binary systems carvone-carbon dioxide and limonene-carbon dioxide at 30°C, 40°C, and 50°C. *Fluid Phase Equilib.* **2000**, *171* (1-2), 165-174.
(271) Iwai, Y.; Morotomi, T.; Sakamoto, K.; Koga, Y.; Arai, Y. High-Pressure Vapor-Liquid Equilibria for Carbon Dioxide + Limonene. *J. Chem. Eng. Data* **1996**, *41* (5), 951-952.

(272) Marteau, P.; Obriot, J.; Tufeu, R. Experimental determination of vapor-liquid equilibria of CO2 + Limonene and CO2 + Citral mixtures. *J. Supercrit. Fluids* **1995**, *8* (1), 20-24.
(273) Raeissi, S.; Peters, C. J. Experimental determination of high-pressure phase equilibria of the ternary system carbon dioxide+limonene+linalool. *J. Supercrit. Fluids* **2005**, *35* (1), 10-17.
(274) Vieira de Melo, S. A. B.; Pallado, P.; Guarise, G. B.; Bertucco, A. High-pressure vapor-liquid equilibrium data for binary and ternary systems formed by supercritical CO2, limonene and linalool. *Braz. J. Chem. Eng.* **1999**, *16* (1), 7-17.
(275) Pavlicek, J.; Richter, M. High pressure vapor-liquid equilibrium in the carbon dioxide-α-pinene system. *Fluid Phase Equilib.* **1993**, *90* (1), 125-133.
(276) Richter, M.; Sovova, H. The solubility of two monoterpenes in supercritical carbon dioxide. *Fluid Phase Equilib.* **1993**, *85*, 285-300.
(277) Benvenuti, F.; Gironi, F. High-Pressure Equilibrium Data in Systems Containing Supercritical Carbon Dioxide, Limonene, and Citral. *J. Chem. Eng. Data* **2001**, *46* (4), 795-799.
(278) Leeke, G. A.; Santos, R.; King, M. B. Vapor-Liquid Equilibria for the Carbon Dioxide + Carvacrol System at Elevated Pressures. *J. Chem. Eng. Data* **2001**, *46* (3), 541-545.
(279) Matos, H. A.; Gomes, d. A. E.; Simoes, P. C.; Carrondo, M. T.; Nunes, d. P. M. Phase equilibria of natural flavors and supercritical solvents. *Fluid Phase Equilib.* **1989**, *52*, 357-364.
(280) Gomes de Azevedo, E.; Matos, H. A.; Nunes, d. P. M. Phase equilibria of ethene + limonene and ethene + cineole from 285 K to 308 K and pressures to 8 MPa. *Fluid Phase Equilib.* **1993**, *83*, 193-202.
(281) Lesteva, T. M.; Ogorodnikov, S. K.; Morozova, A. I. Kinetics of Cyclopentadiene Dimerization and Liquid-Vapor Equilibrium in the System Isoprene - Cyclopentadiene. *J. Appl. Chem. USSR* **1967**, *40* (4), 853-856.
(282) Farelo, F.; Santos, F.; Serrano, L. Isobaric vapor liquid equilibrium in binary mixtures of α-pinene, limonene and 1,8-cineole. *Can. J. Chem. Eng.* **1991**, *69* (3), 794-799.
(283) Bernardo-Gil, M. G.; Ribeiro, A. Vapor-liquid equilibria of binary mixtures of β-pinene with limonene and p-cymene at atmospheric pressure. *Fluid Phase Equilib.* **1993**, *85*, 153-160.
(284) Van Konynenburg, P. H.; Scott, R. L. Critical lines and phase equilibria in binary van der Waals mixtures. *Philos. Trans. R. Soc. London, Ser. A* **1980**, *298*, 495-540.

Chapitre IV. Extension du modèle PPR78 aux systèmes contenant de l’hydrogène

Depuis de nombreuses années, l’hydrogène est utilisé pour de multiples applications industrielles. La principale utilisation de l’hydrogène est l’élimination du soufre, naturellement contenu dans le pétrole, pour produire des carburants propres : la désulfuration. L’hydrogène est aussi le carburant de fusées ou de lanceurs spatiaux comme ARIANE 5. Il est aussi utilisé :

- dans la chimie pour fabriquer des fibres textiles comme le nylon, des mousse polyuréthanes ou des matières plastiques ;
- dans l’industrie du verre, pour fabriquer du verre plat ;
- dans l’électronique, comme gaz vecteur ;
- dans la métallurgie pour le traitement thermique de l’acier.

De plus, la pollution et l’effet de serre sont de plus en plus des sujets couramment discutés, c’est pourquoi la transition de l’énergie ‘fossile’ à l’énergie utilisant H_2 (e.g. dans la pile à combustible), sera nécessaire. Dans ce chapitre le groupe H_2 sera inclus au modèle PPR78 et nous présenterons les résultats concernant la prédiction du comportement des mélanges binaires asymétriques.

IV.1 Introduction

Hydrogen has wide applications in the petroleum and chemical industries, including hydrodealkylation, hydrodesulfurization and hydrocracking. Apart from these, the great attraction of hydrogen is that, once isolated, it is a clean burning fuel that produces neither carbon dioxide (a greenhouse gas) nor toxic emissions and can be used for electricity production, transportation, and other energy needs. It can be treated as the long-run solution by reason of the environment problems associated with fossil fuels.

In many industrial processes, the VLE behavior of hydrogen containing mixtures in wide temperature and pressure ranges is required to design and optimize the processes. It is therefore necessary to develop models able to accurately predict the VLE in both the sub-critical and critical regions, without the use of experimental data.

It is well known that cubic equations of state (cubic EoSs) are largely used for the calculations in the refinery industry because they are simple, robust and predictive in certain extent. However, at high densities, the properties of H_2 containing mixtures are likely to be influenced by the quantization of translational motion as demonstrated by Sadus[1]. Therefore, the description of the VLE of these mixtures with cubic EoS will be a challenge, owing to the asymmetric nature of these mixtures and the quantum behavior of hydrogen.

In order to meet these requirements, many authors have used a cubic EoS with either a modified alpha function (El-Twaty and Prausnitz.[2], Wang and Zhong[3], and Twu et al.[4]), or different methods for computing hydrogen-hydrocarbon binary interaction parameters k_{ij} (Moysan et al.[5-6], Gray et al.[7] and Valderrama et al.[8]). Other authors (Huang et al.[9], Ioannidis and Knox.[10] and Gao et al.[11]) used a cubic EoS, together with complex mixing rules. Recently, the SAFT equation of state has been successfully applied to predict hydrogen-hydrocarbon phase equilibrium by Ghosh et al.[12], Florusse et al.[13] and Thi et al.[14].

However, additional pure and binary parameters required in the cubic EoS can be used only for the selected experimental data and they are usually unsuitable for extrapolation. The SAFT equation of state is actually restricted to linear alkanes and alkenes. Among all the authors that investigated the H_2-containing mixtures, only Sadus[1] and Polishuk and Vera[15] have calculated the critical loci in the P-T projection. However, their pressure domain was limited (up to 600 bar for Sadus[1] and 850 bar for Polishuk and Vera[15]) and they did not analyze all the mixtures available in the open literature.

In this work, the hydrogen group is added to the PPR78 model (predictive 1978, Peng-Robonson EoS) so as to predict the VLE and critical loci of hydrogen containing mixtures. Such a model combines the widely used Peng-Robinson EoS with a group contribution method aimed at estimating the temperature dependent binary interaction parameters ($k_{ij}(T)$). In our previous papers[16-22] and Chapter II, III, twenty groups were defined: CH_3, CH_2, CH, C, CH_4 (methane), C_2H_6 (ethane), CH_{aro}, C_{aro}, $C_{fused\ aromatic\ rings}$, $CH_{2,cyclic}$, $CH_{cyclic} = C_{cyclic}$, CO_2, N_2, H_2S, -SH, H_2O, $CH_2{=}CH_2$ (ethylene), $CH_{2alkenic} = CH_{alkenic}$, $C_{alkenic}$ and $CH_{cycloalkenic} = C_{cycloalkenic}$. In this paper, the interactions between this new group (H_2) and the twenty ones previously defined are determined. It is thus possible to estimate, at any temperature, the k_{ij} between two components in any mixture containing paraffins, aromatics, naphthenes, CO_2, N_2, H_2S, mercaptan, water, olefins and H_2.

IV.2 Database and reduction procedure

Table IV−1. List of the 47 pure components used in this study

Component	Short name	Component	Short name
hydrogen	H_2	1,3,5-trimethylbenzene	135mB
methane	1	isopropylbenzene	iprB
ethane	2	naphthalene	BB
propane	3	1-methylnaphthalene	1mBB
n-butane	4	2-methylnaphthalene	2mBB
n-pentane	5	diphenylmethane	Dph
n-hexane	6	phenanthrene	phe
n-heptane	7	cyclohexane	C6
n-octane	8	methylcyclohexane	mC6
n-nonane	9	1,2,3,4-tetrahydronaphthalene(tetralin)	tet
n-decane	10	trans-decalin	tCC6
n-dodecane	12	1,1’-bicyclohexyl	bcy
n-tetradecane	14	carbon dioxide	CO_2
n-hexadecane	16	Nitrogen	N_2
n-eicosane	20	hydrogen sulfide	H_2S
2-methylpropane(isobutane)	2m3	Water	H_2O
2,3-dimethylbutane	23m4	Ethylene	a2
2,2,4-trimethylpentane(isooctane)	224m5	Propene	a3
Benzene	B	1-hexadecene	1a6
methylbenzene(toluene)	mB	1-heptene	1a7
1,3-dimethylbenzene(m-xylene)	13mB	1-octene	1a8
1,4-dimethylbenzene(p-xylene)	14mB	alpha-methylstyrene	Bma2
ethylbenzene	eB	cyclohexene	aC6
1,2,4-trimethylbenzene	124mB		

Table (IV−1) presents the list of the 47 pure components involved in this study. The pure fluid physical properties (T_c, P_c and ω) used in this study originate from two sources. We have used Poling et al.[23] for alkanes, cyclo alkanes, aromatic compounds, CO_2, N_2, H_2S, H_2O, alkenes and H_2. As some mercaptans and alkenes were missing in this book, the DIPPR database was used instead. Table (IV−2) details the sources of the binary experimental data used in our evaluations[24-142] along with the temperature, pressure and composition range for each binary system. Most of the data available in the open literature (5446 bubble points + 3784 dew points + 114 mixture critical points) have been collected. Our database includes VLE data on 46 binary systems. The 40 parameters (20 A_{kl} and 20 B_{kl}) determined in this study [see Table (I−2)], are those which minimize the objective function defined in equation (I−105).

Table IV−2. Binary systems database

Binary system (1^{st} compound-2^{nd} compound)	Temperature range (K)	Pressure range (bar)	x_1 range (1^{st} compound liquid mole fraction)	y_1 range (1^{st} compound gas mole fraction)	Number of bubble points (T,P,x)	Number of dew points (T,P,y)	Number of binary critical points (T_{cm}, P_{cm}, x_c)	References
H_2-3	93.15-366.40	6.89-551.58	0.0013-0.6690	0.1100-0.9990	445	319	14	24-28
H_2-4	144.26-394.25	20.68-534.34	0.0080-0.3410	0.2130-0.9985	124	100	0	29-32
H_2-5	273.15-463.15	6.93-275.90	0.0044-0.2590	0.3730-0.9965	110	29	0	33-34
H_2-6	277.59-506.48	12.40-689.48	0.0105-0.7000	0.1000-0.9980	159	98	8	35-38
H_2-7	238.15-498.85	1.01-784.54	0.0005-0.8100	0.2500-0.9650	66	48	2	39-44
H_2-8	248.15-543.15	1.01-173.30	0.0005-0.2500	0.0305-0.9068	145	115	0	35, 39-42, 45-47
H_2-9	298.15-324.65	1.01-1.01	0.0007-0.0008	-	3	0	0	40
H_2-10	283.17-583.45	1.01-303.98	0.0007-0.5013	0.6025-0.9998	267	32	0	33, 35, 40, 48-53
H_2-12	344.30-422.00	14.20-347.15	0.0144-0.2990	0.9868-0.9993	36	12	0	54-55
H_2-14	328.15-473.15	40.53-303.98	0.0330-0.3260	-	12	0	0	53
H_2-16	298.13-664.05	11.51-300.00	0.0180-0.5192	0.6054-0.9994	190	32	0	48, 56-58
H_2-20	323.20-573.25	9.94-129.10	0.0113-0.1289	0.9617-0.9996	37	10	0	49, 59
H_2-2m3	310.93-394.26	34.48-206.85	0.0225-0.2470	0.2480-0.9571	22	22	0	54
H_2-23m4	308.15-483.15	27.17-164.50	0.0268-0.1273	-	92	0	0	33
H_2-224m5	26.50-523.15	1.01-1078.70	0.0006-0.8160	0.2470-0.9984	94	88	2	39-40, 42-43, 50, 54, 60
H_2-1	66.89-183.12	2.20-1414.00	0.0018-0.6800	0.0338-0.9998	606	643	15	30, 61-71
H_2-2	83.00-283.15	2.67-5625.00	0.0022-0.7980	0.0847-1.0000	400	425	11	28, 68, 72-75
H_2-B	283.15-533.15	1.01-2941.99	0.0002-0.5940	0.0110-0.9984	227	191	0	39, 42, 45, 76-84
H_2-mB	208.15-575.15	1.01-327.00	0.0002-0.5140	0.2100-0.9976	125	60	0	35, 39, 42, 50, 60, 80, 85-86
H_2-13mB	295.00-593.15	8.51-254.41	0.0053-0.3241	0.1741-0.9898	143	52	0	33, 42, 87-88
H_2-14mB	308.15-573.15	26.66-148.75	0.0281-0.1550	-	117	0	0	33
H_2-eB	295.00-298.15	44.13-294.20	0.0161-0.0839	-	7	0	0	42, 80
H_2-135mB	298.15-298.15	49.03-294.20	0.0151-0.0895	-	3	0	0	80
H_2-124mB	295.00-295.00	69.90-173.30	0.0248-0.0571	-	4	0	0	42
H_2-iprB	323.00-488.15	6.89-303.98	0.0034-0.2870	-	27	0	0	53, 89-90
H_2-Dph	462.75-701.65	20.27-253.31	0.0123-0.3056	0.4497-0.9989	27	27	0	85
H_2-BB	373.20-423.20	42.90-193.90	0.0157-0.0567	-	14	0	0	82
H_2-1mBB	328.15-730.05	20.27-303.98	0.0100-0.3362	0.3084-0.9980	110	36	0	33, 53, 91-92
H_2-2mBB	353.15-433.15	19.20-131.30	0.0061-0.0529	-	23	0	0	93
H_2-phe	383.20-699.82	13.79-252.30	0.0038-0.0840	0.8275-1.0000	71	6	0	56, 82, 94-95
H_2-C6	293.15-523.15	1.01-690.37	0.0004-0.3667	0.5490-0.9973	279	69	0	33, 42, 76, 80, 84, 89, 96-99
H_2-tet	423.15-662.59	17.37-273.30	0.0100-0.2824	0.3765-0.9985	89	77	0	83, 100-104
H_2-mC6	295.00-498.65	24.52-961.05	0.0170-0.7900	0.4640-0.9780	36	27	1	42-43, 80
H_2-tCC6	338.15-473.15	40.53-303.98	0.0140-0.1950	-	12	0	0	53
H_2-bcy	462.15-701.65	20.27-253.31	0.0054-0.4239	0.0602-0.9977	28	28	0	105
H_2-CO_2	219.90-298.15	9.30-1918.00	0.0013-0.6400	0.0425-0.9335	302	300	11	30, 106-113
H_2-N_2	25.10-122.04	1.32-580.00	0.0119-0.6200	0.0821-1.0000	307	398	11	30, 67, 70, 112, 114-126
H_2-H_2S	243.15-273.15	10.13-50.66	0.0020-0.0200	0.3220-0.9100	11	11	0	127
H_2-H_2O	273.15-636.10	3.45-1013.25	0.0000-0.0164	0.1000-0.9994	146	82	0	57, 128-135
H_2-a2	112.00-281.70	2.00-5998.30	0.0043-0.7800	0.0207-0.9997	304	309	23	28, 68, 136-139
H_2-a3	173.15-364.70	17.23-551.21	0.0044-0.4625	0.0288-0.9970	46	42	16	28, 136, 140
H_2-1a6	313.20-453.20	40.53-303.98	0.0400-0.4140	0.6415-0.9977	60	48	0	53, 141
H_2-1a7	333.15-473.15	40.53-303.98	0.0280-0.3530	-	12	0	0	53
H_2-1a8	295.00-463.15	40.53-303.98	0.0240-0.3410	0.8740-0.9997	65	48	0	42, 53, 141
H_2-Bma2	287.95-373.15	1.01-130.00	0.0000-0.0407	-	33	0	0	89-90, 142
H_2-aC6	303.15-373.15	6.89-68.95	0.0024-0.0397	-	10	0	0	89
Total number of points:					**5446**	**3784**	**114**	

IV.3 Difficulties in predicting the phase behavior of hydrogen containing mixtures

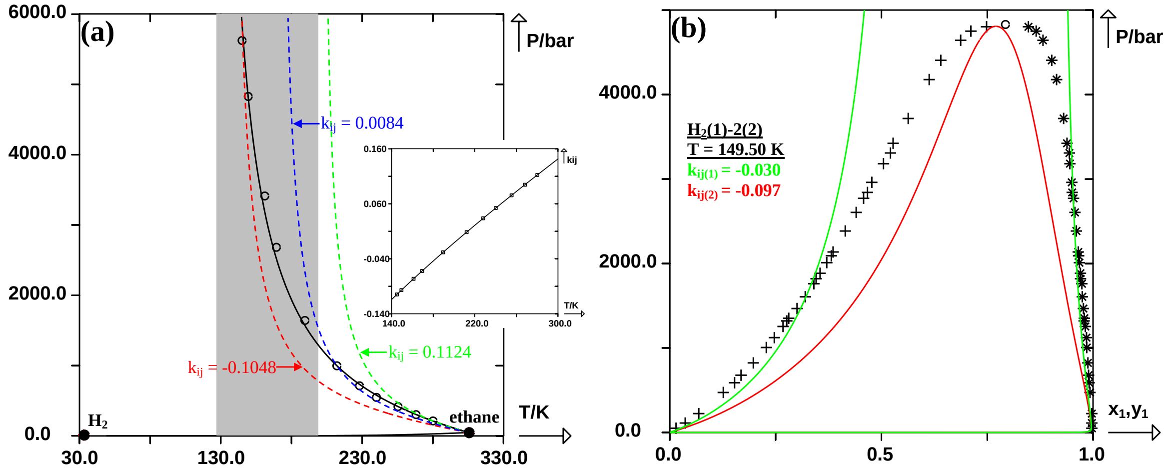

Figure IV−1. Prediction of the critical loci and prediction of isothermal curves for the binary system: (H_2(1) + ethane(2)). (+) experimental bubble points, (✳) experimental dew points, (○) experimental critical points, (●) critical points of the pure compounds. (□) k_{ij} value corresponding to the temperature of experimental critical point **(a)** (solid line) prediction of the critical locus using the Peng-Robonson EoS with classical mixing rules and a temperature-dependent k_{ij}; (dashed lines) prediction of the critical loci using the Peng-Robonson EoS with classical mixing rules and three constant k_{ij} values. **(b)** Prediction of isothermal curves at T = 149.50 K, using the Peng-Robonson EoS with classical mixing rules and two constant k_{ij} values: $k_{ij(1)} = -0.030$ and $k_{ij(2)} = -0.097$.

Most of the hydrogen containing systems exhibit Type III phase behavior in the classification scheme of Van Konynenburg and Scott[143]. By considering our previous studies, we can conclude that, even with a temperature-dependent $k_{ij}(T)$, the Peng-Robinsen equation of state (EoS) is not able to predict accurately two kinds of Type III critical loci: (1) The critical curve shows a pressure minimum and a pressure maximum, and the slope of the critical curve at low temperature (near the upper critical end point) is often very steep (a small change of temperature induces a large change of pressure). The example of (ethylene(1) + naphthalene(2)) can be found in section III.4.3, Chapter III. (2) The critical line which starts at the critical point of the less volatile substance goes through a temperature minimum and goes steeply to high pressure. The example of (methane(1) + water(2)) can be found in section II.3.1, Chapter II.

As shown in figure (IV−1a), the experimental critical data of (hydrogen(1) + ethane(2)) mixture starts from the critical point of ethane, then rises slowly until P = 1000 bar, and finally goes steeply to extremely high pressure (P > 1000 bar). It seems to have a temperature minimum at high pressures but we do not have any experimental support, even if the highest critical pressure is as high as 5625 bar. In figure (IV−1a), were plotted three calculated critical loci (dashed lines) by using the Peng-Robinson EoS with classical mixing rules and three constant k_{ij} value ($k_{ij} = 0.1124$, $k_{ij} = 0.0084$, and $k_{ij} = -0.1048$). From this figure, it is obvious that a single k_{ij} value can not manage this Type III phase phenomena.

In the same time, we have fitted the 11 critical points by using temperature-dependent BIP($k_{ij}(T)$) and good results have been obtained [solid line in figure (IV−1a)]. The corresponding k_{ij}-T curve is plotted in an enlarged scale in figure (IV−1a). These results indicate that by using the Peng-Robinson EoS with classical mixing rules, the k_{ij} value has a huge influence on the calculated critical locus and it has a significant dependence on temperature. However, as discussed in chapter II section II.3.1, the parameters ($A_{6\text{-}21}$, $B_{6\text{-}21}$) fitted on these critical points here could not describe very well the entire phase space in a wide range of temperature and pressure. Furthermore, by varying the two parameters ($A_{6\text{-}21}$, $B_{6\text{-}21}$), it was found that the more accurate the critical locus is, the worse the objective function defined by equation (I−105) would be. In these conditions, a compromise between the restitution of VLE (or LLE) and that of critical loci appears to be necessary.

In spite of that, VLE in the temperature range [the gray part in figure (IV−1a)] where a small change of temperature induces a large change of pressure is not an easy task. Firstly, it is necessary to notice that even if we do not consider the experimental critical points in this temperature range, the objective function over VLE is significant. To illuminate this point, we have plotted in figure (IV−1b) the isothermal diagram at T = 149.50 K by using the best k_{ij} value ($k_{ij} = -0.03$) for this isotherm. The objective function over the 34 bubble points and 34 dew points is: $F_{obj} = 18.71$ %. Secondly, the objective function over VLE will be much more significant if we consider only the mixture critical points in this temperature range. In figure (IV−1b) we have plotted the isothermal diagram at T = 149.50 K ($k_{ij} = -0.097$) by using the parameters ($A_{6\text{-}21}$, $B_{6\text{-}21}$) fitted on critical points. As can be seen, huge deviations appear on both the bubble curve and the dew curve, and the objective function is: $F_{obj} = 43.59$ %. For these reasons, we can conclude that the compromise between the representation of critical points and that of the whole phase envelope in this temperature range become very weak. As a result, the critical pressures in this region will be always overestimated.

IV.4 Results and discussion

For all the data points included in our database, the objective function defined by equation (I−105) is: $F_{obj} = 8.79\,\%$.

The average overall deviation on the liquid phase composition is:

$$\overline{\Delta x_1} = \frac{\sum_{i=1}^{n_{bubble}} \left(\left| x_{1,exp} - x_{1,cal} \right| \right)_i}{n_{bubble}} = 0.015 \text{. Moreover } \frac{F_{obj,bubble}}{n_{bubble}} = 8.44\ \%$$

The average overall deviation on the gas phase composition is:

$$\overline{\Delta y_1} = \frac{\sum_{i=1}^{n_{dew}} \left(\left| y_{1,exp} - y_{1,cal} \right| \right)_i}{n_{dew}} = 0.014 \text{. Moreover } \frac{F_{obj,dew}}{n_{dew}} = 9.32\ \%$$

The average overall deviation on the critical composition is:

$$\overline{\Delta x_{c1}} = \frac{\sum_{i=1}^{n_{crit}} \left(\left| x_{c1,exp} - x_{c1,cal} \right| \right)_i}{n_{crit}} = 0.020 \text{. Moreover } \frac{F_{obj,crit.\ comp}}{n_{crit}} = 5.84\ \%$$

The average overall deviation on the binary critical pressure is:

$$\overline{\Delta P_c}\,\% = \frac{F_{obj,crit.\ pressure}}{n_{crit}} = \frac{100 \sum_{i=1}^{n_{crit}} \left(\frac{\left| P_{cm,exp} - P_{cm,cal} \right|}{P_{cm,exp}} \right)_i}{n_{crit}} = 11.02\%$$

The value of the objective function indicates that the PPR78 remains capable to predict the phase behavior for binary systems involving hydrogen with good accuracy. Moreover, this objective function value can be explained by the following reasons:

(1) Some experimental data reported in the literature are generally inconsistent and there are obvious scatters among them.

(2) Large immiscibility at low temperature inevitably increases the objective function.

(3) All the binary systems in this study present Type III phase behavior, which is difficult to predict with a cubic equation of state even with temperature dependent $k_{ij}(T)$.

(4) We have made a compromise between the restitution of VLE (or LLE) and that of critical loci.

(5) Some binary systems: (hydrogen(1) + ethane(2)) and (hydrogen(1) + ethylene(2)) are really difficult to correlate even if we do not consider the experimental critical points, as discussed in section IV.3.

In order to illustrate the accuracy and the limitations of our model, it was decided to define several families of binary systems which could give a good representation of the whole data base.

IV.4.1 Results for mixtures of [hydrogen + n-alkanes (or branched alkanes)]

In this family, various binary mixtures have been investigated experimentally and there is a vast amount of VLE, LLE and critical points in our data base although we have not found any critical point for mixtures containing an n-alkane heavier than n-heptane. All the 18 binary mixtures belonging to this family exhibit Type III phase behavior in the classification scheme of van Konynenburg and Scott[143].

We have plotted in figures (IV−2,3,4a,4b), the predicted isothermal diagrams for 12 binary mixtures containing H_2 and an alkane. At low temperatures, the relatively low solubility of H_2 in the alkane-rich phase and the high purity of H_2 in the other phase can be observed. As the temperature increases, most of the isotherms form a closed phase envelop at moderate and high temperatures. Considering the mixtures which consist of H_2 and a long chain n-alkane, only the mutual solubility at low and moderate pressures can be observed and the prediction of isothermal diagrams at higher pressures has not been verified because of the lack of experimental data. These graphic results together with the objective function over all the experimental points in this family: $F_{obj} = 9.05$ %, indicate that our model is able to correlate these experimental data over wide ranges of temperature and pressure.

It is important to notice that the predicted phase envelope of (H_2(1) + n-hexane(2)) at T = 477.59 K [figure (IV−3a)] and that of (H_2(1) + isooctane(2)) at T = 523.15 K [figure (IV−4b)] are not in good agreement with experimental data, because of the compromise between the restitution of VLE (or LLV) and that of critical loci that was made in our study. Moreover, as discussed in section IV.3, the phase behavior of (H_2(1) + ethane(2)) between T = 129.80 K and T = 169.40 K is very difficult to be well predicted [see figure (IV−2c)]. The experimental points of this mixture in figure (IV−2c) indicate that the two isotherms at T = 149.50 K and T = 169.40 K form a closed phase envelop, the critical pressure of which are at P = 4830 and 2685 bar, respectively. However, in spite of the compromise, the critical pressures are still largely overestimated by our model.

As shown in figure (IV−4c), satisfactory results are obtained for all the experimental critical points in this family. In order to compare our prediction with that of Polishuk et al.[15], we have plotted the critical locus in an enlarged scale [see figure (IV−4d)] and the predictions obtained here are a little better, especially for (H_2(1) + ethane(2)).

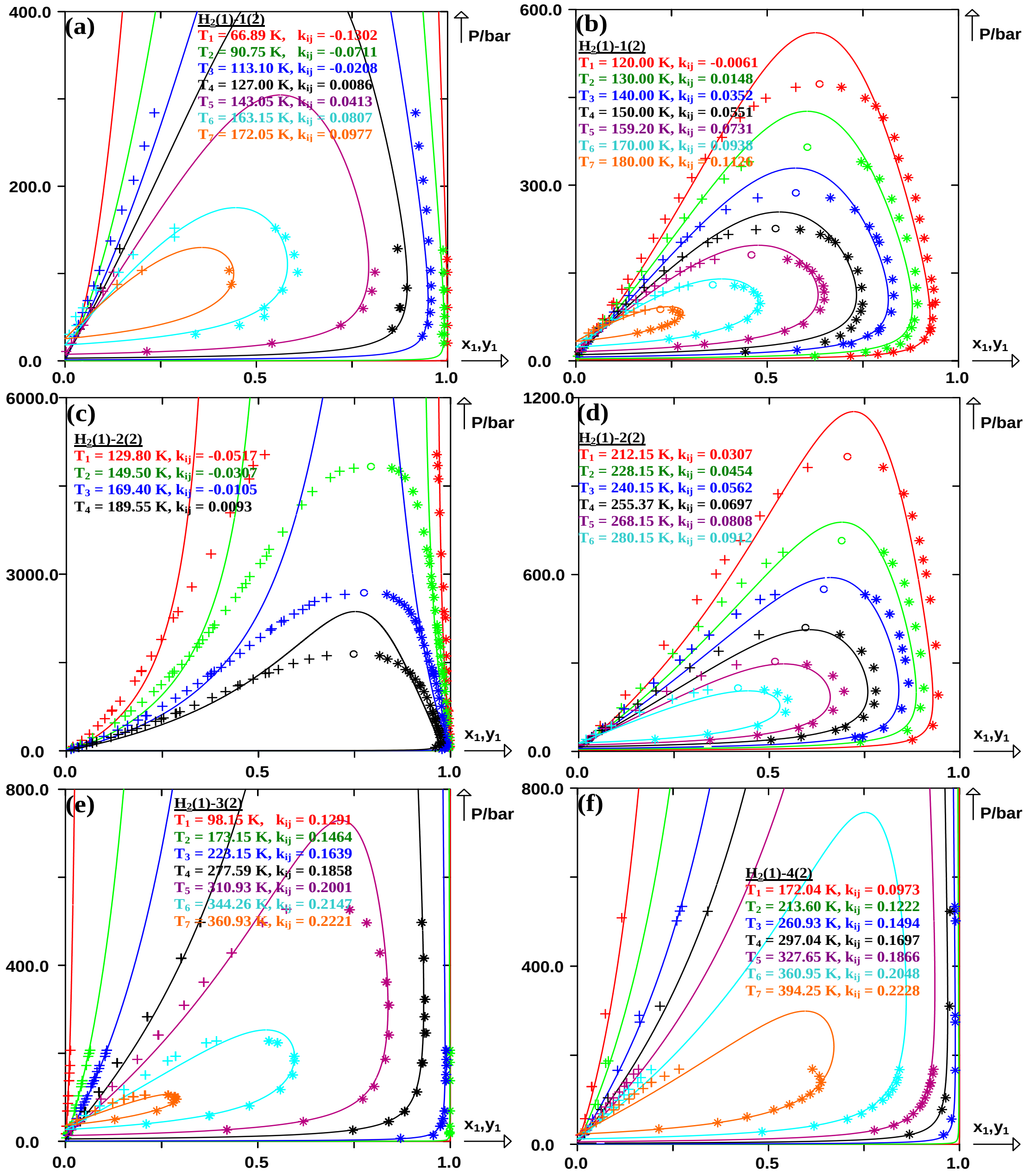

Figure IV‒2. Prediction of isothermal curves for four binary systems: (hydrogen(1) + methane(2)), (hydrogen(1) + ethane(2)), (hydrogen(1) + propane(2)) and (hydrogen(1) + n-butane(2)) using the PPR78 model. (+) experimental bubble points, (✳) experimental dew points, (○) experimental critical points. Solid line: predicted curves with the PPR78 model. **(a)** System (hydrogen(1) + methane(2)) at seven different temperatures: T_1 = 66.89 K (k_{ij} = -0.1302), T_2 = 90.75 K (k_{ij} = -0.0711), T3 = 113.10 K (k_{ij} = -0.0208), T4 = 127.00 K (k_{ij} = 0.0086), T_5 = 143.05 K (k_{ij} = 0.0413), T_6 = 163.15 K (k_{ij} = 0.0807), T_7 = 172.05 K (k_{ij} = 0.0977). **(b)** System (hydrogen(1) + methane(2)) at seven different temperatures: T_1 = 120.00 K (k_{ij} = -0.0061), T_2 = 130.00 K (k_{ij} = 0.0148), T3 = 140.00 K (k_{ij} = 0.0352), T4 = 150.00 K (k_{ij} = 0.0551), T_5 = 159.20 K (k_{ij} = 0.0731), T_6 = 170.00 K (k_{ij} = 0.0938), T_7 = 180.00 K (k_{ij} = 0.1126). **(c)** System (hydrogen(1) + ethane(2)) at four different temperatures: T_1 = 129.80 K (k_{ij} = -0.0517), T_2 = 149.50 K (k_{ij} = -0.0307), T3 = 169.40 K (k_{ij} = -0.0105), T4 = 189.55 K (k_{ij} = 0.0093). **(d)** System (hydrogen(1) + ethane(2)) at six different temperatures: T_1 = 212.15 K (k_{ij} = 0.0307), T_2 = 228.15 K (k_{ij} = 0.0454), T3 = 240.15 K (k_{ij} = 0.0562), T4 = 255.37 K (k_{ij} = 0.0697), T_5 = 268.15 K (k_{ij} = 0.0808), T_6 = 280.15 K (k_{ij} = 0.0912). **(e)** System (hydrogen(1) + propane(2)) at seven different temperatures: T_1 = 98.15 K (k_{ij} = 0.1291), T_2 = 173.15 K (k_{ij} = 0.1464), T_3 = 223.15 K (k_{ij} = 0.1639), T_4 = 277.59 K (k_{ij} = 0.1858), T_5 = 310.93 K (k_{ij} = 0.2001), T_6 = 344.26 K (k_{ij} = 0.2147), T_7 = 360.93 K (k_{ij} = 0.2221). **(f)** System (hydrogen(1) + n-butane(2)) at seven different temperatures: T_1 = 172.04 K (k_{ij} = 0.0973), T_2 = 213.60 K (k_{ij} = 0.1222), T_3 = 260.93 K (k_{ij} = 0.1494), T_4 = 297.04 K (k_{ij} = 0.1697), T_5 = 327.65 K (k_{ij} = 0.1866), T_6 = 360.95 K (k_{ij} = 0.2048), T_7 = 394.25 K (k_{ij} = 0.2228).

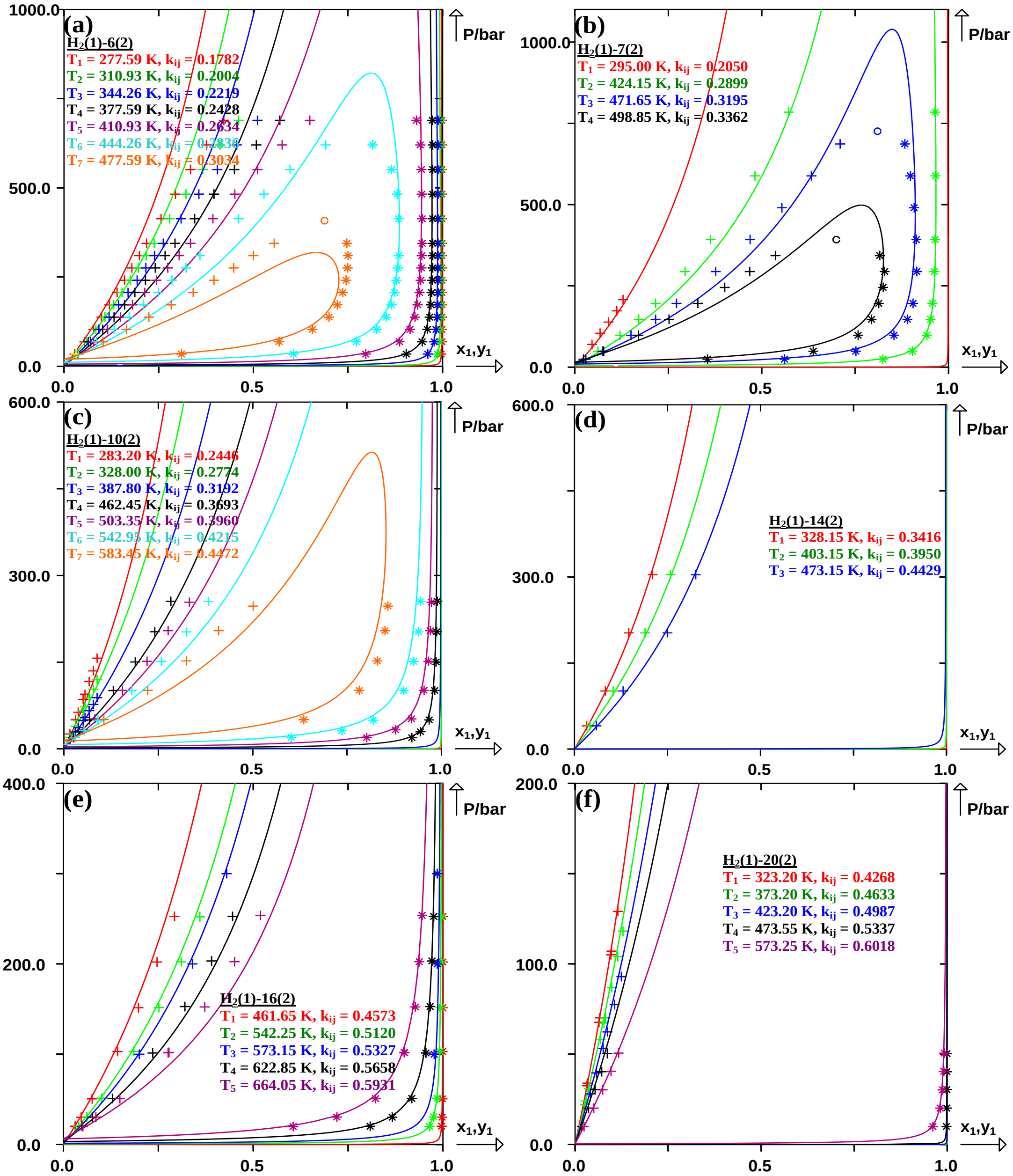

Figure IV−3. Prediction of isothermal curves for six binary systems: (hydrogen(1) + n-hexane(2)), (hydrogen(1) + n-heptane(2)), (hydrogen(1) + n-decane(2)) , (hydrogen(1) + n-tetradecane(2)) , (hydrogen(1) + n-hexadecane(2)) and (hydrogen(1) + n-eicosane(2)) using the PPR78 model. (+) experimental bubble points, (✳) experimental dew points, (○) experimental critical points. Solid line: predicted curves with the PPR78 model. **(a)** System (hydrogen(1) + n-hexane(2)) at seven different temperatures: T_1 = 277.59 K (k_{ij} = 0.1782), T_2 = 310.93 K (k_{ij} = 0.2004), T_3 = 344.26 K (k_{ij} = 0.2219), T_4 = 377.59 K (k_{ij} = 0.2428), T_5 = 410.93 K (k_{ij} = 0.2634), T_6 = 444.26 K (k_{ij} = 0.2836), T_7 = 477.59 K (k_{ij} = 0.3034). **(b)** System (hydrogen(1) + n-heptane(2)) at four different temperatures: T_1 = 295.00 K (k_{ij} = 0.2050), T_2 = 424.15 K (k_{ij} = 0.2899), T_3 = 471.65 K (k_{ij} = 0.3195), T_4 = 498.85 K (k_{ij} = 0.3362). **(c)** System (hydrogen(1) + n-decane(2)) at seven different temperatures: T_1 = 283.20 K (k_{ij} = 0.2446), T_2 = 328.00 K (k_{ij} = 0.2774), T_3 = 387.80 K (k_{ij} = 0.3192), T_4 = 462.45 K (k_{ij} = 0.3693), T_5 = 503.35 K (k_{ij} = 0.3960), T_6 = 542.95 K (k_{ij} = 0.4215), T_7 = 583.45 K (k_{ij} = 0.4472). **(d)** System (hydrogen(1) + n-tetradecane(2)) at three different temperatures: T_1 = 328.15 K (k_{ij} = 0.3416), T_2 = 403.15 K (k_{ij} = 0.3950), T_3 = 473.15 K (k_{ij} = 0.4429). **(e)** System (hydrogen(1) + n-hexadecane(2)) at five different temperatures: T_1 = 461.65 K (k_{ij} = 0.4573), T_2 = 542.25 K (k_{ij} = 0.5120), T_3 = 573.15 K (k_{ij} = 0.5327), T_4 = 622.85 K (k_{ij} = 0.5658), T_5 = 664.05 K (k_{ij} = 0.5931). **(f)** System (hydrogen(1) + n-eicosane(2)) at five different temperatures: T_1 = 323.20 K (k_{ij} = 0.4268), T_2 = 373.20 K (k_{ij} = 0.4633), T_3 = 423.20 K (k_{ij} = 0.4987), T_4 = 473.55 K (k_{ij} = 0.5337), T_5 = 573.25 K (k_{ij} = 0.6018).

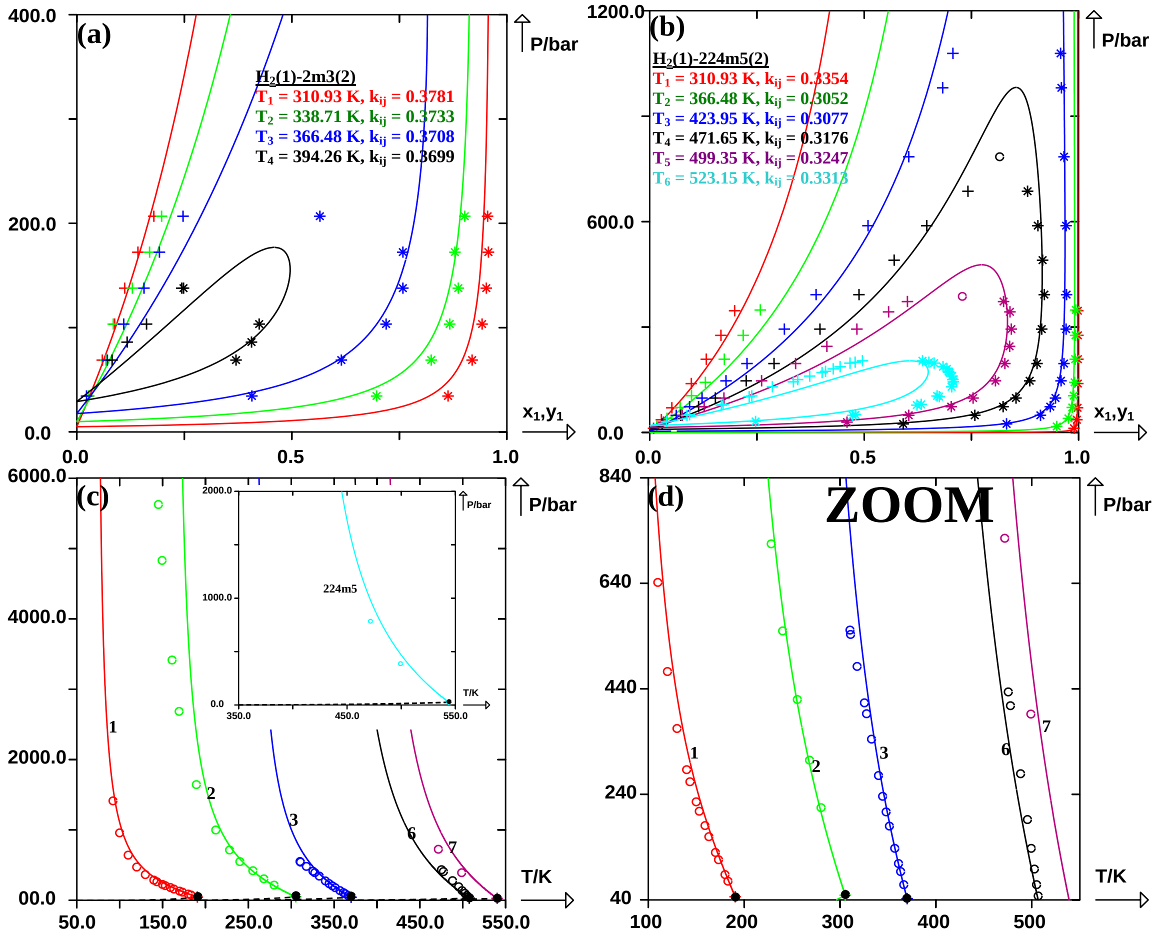

Figure IV−4. Prediction of isothermal curves for two binary systems: (hydrogen(1) + isobutane(2)) and (hydrogen(1) + isooctane(2)), and prediction of the critical locus for six binary systems containing hydrogen and an alkane using the PPR78 model. (+) experimental bubble points, (✳) experimental dew points, (○) experimental critical points, (●) critical points of the pure compounds. Solid line: predicted curves with the PPR78 model. Dashed line: vaporization curve of the pure compounds. **(a)** System (hydrogen(1) + isobutane(2)) at four different temperatures: T_1 = 310.93 K (k_{ij} = 0.3781), T_2 = 338.71 K (k_{ij} = 0.3733), T_3 = 366.48 K (k_{ij} = 0.3708), T_4 = 394.26 K (k_{ij} = 0.3699). **(b)** System (hydrogen(1) + isooctane(2)) at six different temperatures: T_1 = 310.93 K (k_{ij} = 0.3354), T_2 = 366.48 K (k_{ij} = 0.3052), T_3 = 423.95 K (k_{ij} = 0.3077), T_4 = 471.65 K (k_{ij} = 0.3176), T_5 = 499.35 K (k_{ij} = 0.3247), T_6 = 523.15 K (k_{ij} = 0.3313). **(c,d)** Prediction of the critical locus for the six binary systems containing hydrogen and an alkane using the PPR78 model.

IV.4.2 Results for mixtures of (hydrogen + aromatic compound)

According to our data base, we have collected 1270 experimental data points over 13 binary mixtures, unfortunately, no critical point has been found. As a result, the prediction quality of critical locus has not been verified. Due to the fact that our data-fitting procedure was carried out by using VLE (or LLE) data, it is not surprising that the objective function obtained in this family is quite good: F_{obj} = 4.85 %. As shown in figure (IV−5), the predicted isothermal diagrams are in close agreement with experimental data. On the other hand, we need to notice that the predicted curves of (H_2(1) + methylbenzene(2)) at T = 568.15 K [see figure (IV−5b)] are not very accurate because no compromise between the prediction of VLE (or LLV) and that of critical loci was made in this family. By looking at six different binary mixtures in figure (IV−5), BIP (k_{ij}(T) is very significant and it is an increasing function of temperature for each system.

IV.4.3 Results for mixtures of (hydrogen + naphthenic compound)

Considering 5 binary mixture belonging to this family, only one critical point of (H_2(1) + methylcyclohexane(2)) was found, among 647 experimental points available in the open literature. The compromise between this critical point and the bubble and dew curves representation was adopted. As a result, the bubble curve of (H_2(1) + 1,1'-bicylcohexyl(2)) at T = 701.65 K is not very accurate [see figure (IV−6d)]. In spite of that, the objective function obtained here is still quite good: F_{obj} = 4.88 %. The corresponding prediction of isothermal curves for four different binary mixtures is plotted in figure (IV−6).

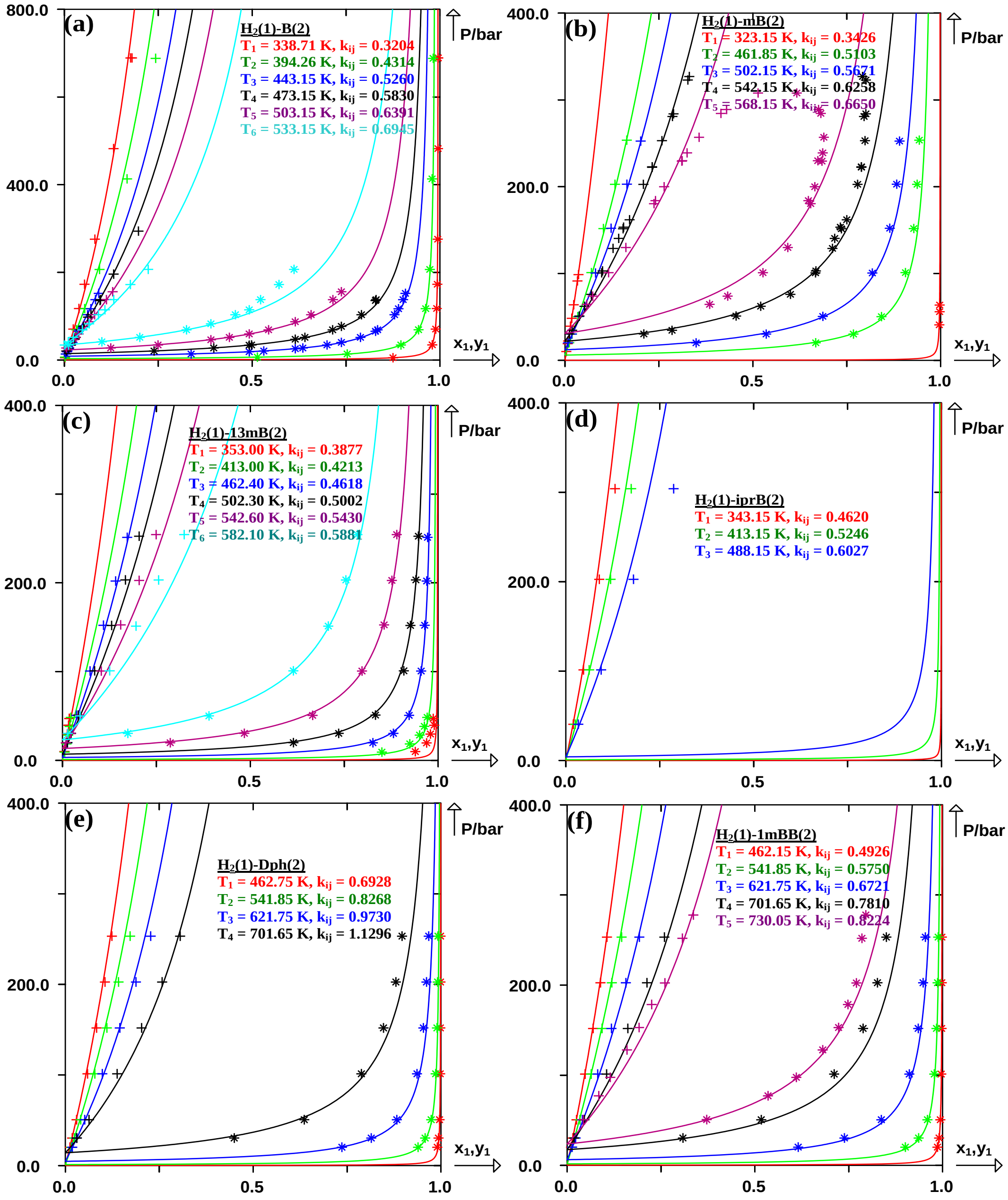

Figure IV−5. Prediction of isothermal curves for six binary systems: (hydrogen(1) + benzene(2)), (hydrogen(1) + toluene(2)), (hydrogen(1) + 1,3-dimethylbenzene(2)), (hydrogen(1) + isopropylbenzene(2)), (hydrogen(1) + diphenylmethane(2)) and (hydrogen(1) + 1-methylnaphthalene(2)) using the PPR78 model. (+) experimental bubble points, (✳) experimental dew points. Solid line: predicted curves with the PPR78 model. **(a)** System (hydrogen(1) + benzene(2)) at six different temperatures: T_1 = 338.71 K (k_{ij} = 0.3204), T_2 = 394.26 K (k_{ij} = 0.4314), T_3 = 443.15 K (k_{ij} = 0.5260), T_4= 473.15 K (k_{ij} = 0.5830), T_5 = 503.15 K (k_{ij} = 0.6391), T_6 = 533.15 K (k_{ij} = 0.6945). **(b)** System (hydrogen hydrogen(1) + toluene(2)) at five different temperatures: T_1 = 323.15 K (k_{ij} = 0.3426), T_2 = 461.85 K (k_{ij} = 0.5103), T_3 = 502.15 K (k_{ij} = 0.5671), T_4 = 542.15 K (k_{ij} = 0.6258), T_5 = 568.15 K (k_{ij} = 0.6650). **(c)** System (hydrogen(1) + 1,3-dimethylbenzene(2)) at six different temperatures: T_1 = 353.00 K (k_{ij} = 0.3877), T_2 = 413.00 K (k_{ij} = 0.4213), T_3 = 462.40 K (k_{ij} = 0.4618), T_4 = 502.30 K (k_{ij} = 0.5002), T_5 = 542.60 K (k_{ij} = 0.5430), T_6 = 582.10 K (k_{ij} = 0.5881). **(d)** System (hydrogen(1) + isopropylbenzene(2)) at three different temperatures: T_1 = 343.15 K (k_{ij} = 0.4620), T_2 = 413.15 K (k_{ij} = 0.5246), T_3 = 488.15 K (k_{ij} = 0.6027). **(e)** System (hydrogen(1) + diphenylmethane(2)) at four different temperatures: T_1 = 462.75 K (k_{ij} = 0.6928), T_2 = 541.85 K (k_{ij} = 0.8268), T_3 = 621.75 K (k_{ij} = 0.9730), T_4 = 701.65 K (k_{ij} = 1.1296). **(f)** System (hydrogen(1) + 1-methylnaphthalene(2)) at five different temperatures: T_1 = 462.15 K (k_{ij} = 0.4926), T_2 = 541.85 K (k_{ij} = 0.5750), T_3 = 621.75 K (k_{ij} = 0.6721), T_4 = 701.65 K (k_{ij} = 0.7810), T_5 = 730.05 K (k_{ij} = 0.8224).

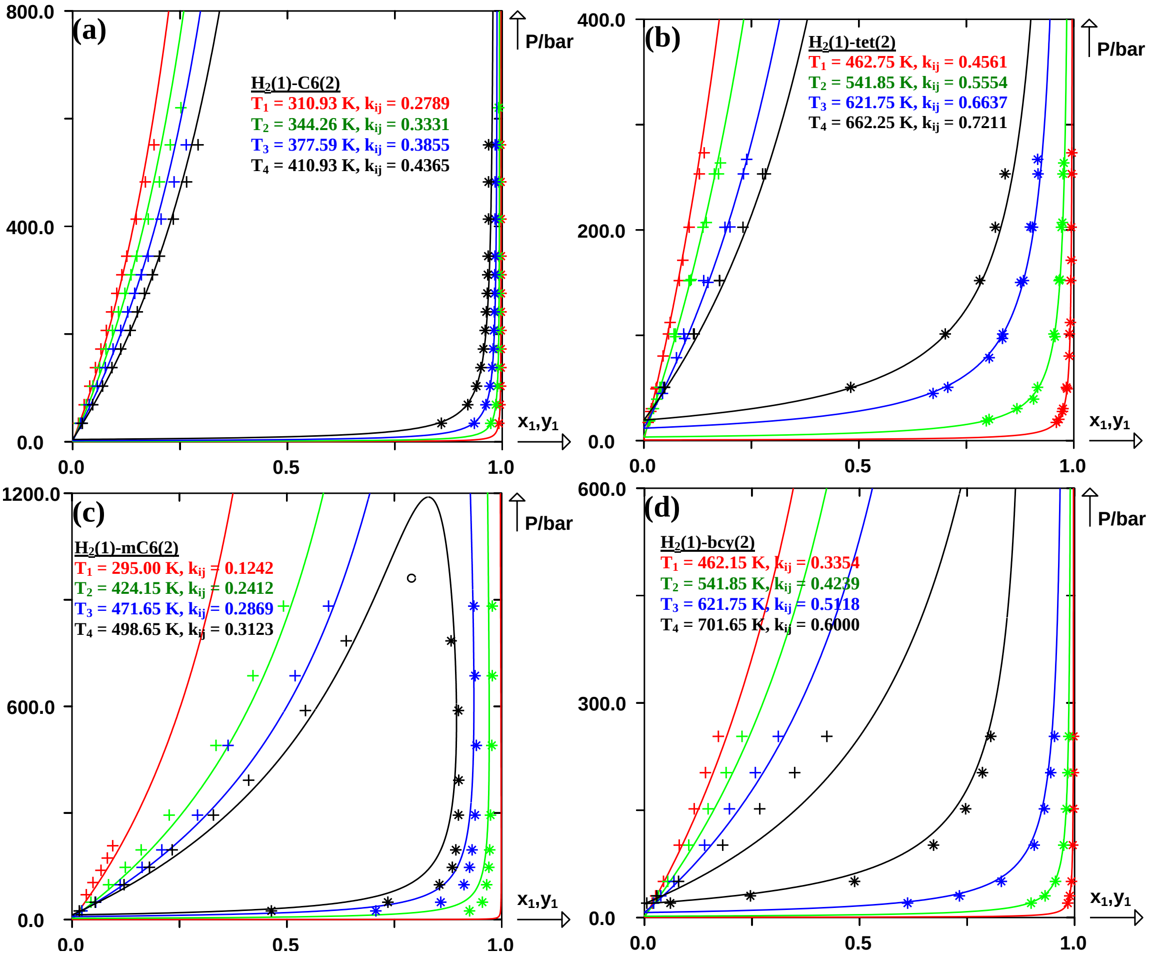

Figure IV−6. Prediction of isothermal curves for four binary systems: (hydrogen(1) + cyclohexane(2)), (hydrogen(1) + tetralin(2)), (hydrogen(1) + methylcyclohexane(2)) and (hydrogen(1) + 1,1'-bicyclohexyl(2)) using the PPR78 model. (+) experimental bubble points, (✳) experimental dew points, (○) experimental critical points. Solid line: predicted curves with the PPR78 model. **(a)** System (hydrogen(1) + cyclohexane(2)) at four different temperatures: T_1 = 310.93 K (k_{ij} = 0.2789), T_2 = 344.26 K (k_{ij} = 0.3331), T_3 = 377.59 K (k_{ij} = 0.3855), T_4 = 410.93 K (k_{ij} = 0.4365). **(b)** System (hydrogen(1) + tetralin(2)) at four different temperatures: T_1 = 462.75 K (k_{ij} = 0.4561), T_2 = 541.85 K (k_{ij} = 0.5554), T_3 = 621.75 K (k_{ij} = 0.6637), T_4 = 662.25 K (k_{ij} = 0.7211). **(c)** System (hydrogen(1) + methylcyclohexane(2)) at four different temperatures: T_1 = 295.00 K (k_{ij} = 0.1242), T_2 = 424.15 K (k_{ij} = 0.2412), T_3 = 471.65 K (k_{ij} = 0.2869), T_4 = 498.65 K (k_{ij} = 0.3123). **(d)** System (hydrogen(1) + 1,1'-bicyclohexyl(2)) at four different temperatures: T_1 = 462.15 K (k_{ij} = 0.3354), T_2 = 541.85 K (k_{ij} = 0.4239), T_3 = 621.75 K (k_{ij} = 0.5118), T_4= 701.65 K (k_{ij} = 0.6000).

IV.4.4 Results for mixtures of [hydrogen + CO_2 (or N_2 or H_2S or H_2O)]

Mixtures of (H_2(1) + CO_2(2)) and (H_2(1) + N_2(2)) present many reliable experimental data. As shown in figure (IV−9a), Type III phase behavior can be observed for both of them. In the vicinity of the critical point of the less volatile component (CO_2 or N_2), the critical loci are perfectly predicted, as well as the corresponding P-xy diagrams [see figures (IV−7a,7b,7c,7d)]. As the temperature decreases, our model has a tendency to overestimate the critical pressure, which can be seen in some isotherms in figure (IV−7b) and figure (IV−7d). In general, LLE and VLE of these two binary systems over wide ranges of temperature and pressure are fairly predicted.

Considering (H_2(1) + H_2S(2)), only 22 bubble points were collected. As a result, the determination of the interaction parameters between group 14 (H_2S) and group 21 (H_2) becomes uncertain, although values of $A_{21\text{-}14}$ and $B_{21\text{-}14}$ have been proposed [see table (I−2)]. The P-xy diagrams of this mixture can be found in figure (IV−7e).

In figure (IV−7f), we have plotted the phase diagrams of (H_2(1) + H_2O(2)) at five different temperatures. All these experimental data points are predicted with reasonable accuracy. The prediction of P-xy curves at higher temperatures and that of critical locus have not been checked here because of the lack of experimental data. It is obvious that the solubility of H_2 in the water-rich liquid phase has little temperature dependence and this low solubility of H_2 inevitably increases our objective function. In spite of that, the objective function obtained for (H_2(1) + H_2O(2)) is: $F_{obj} = 8.61$ %, which indicates that PPR78 can give a good representation of these available experimental data in the sub-critical region.

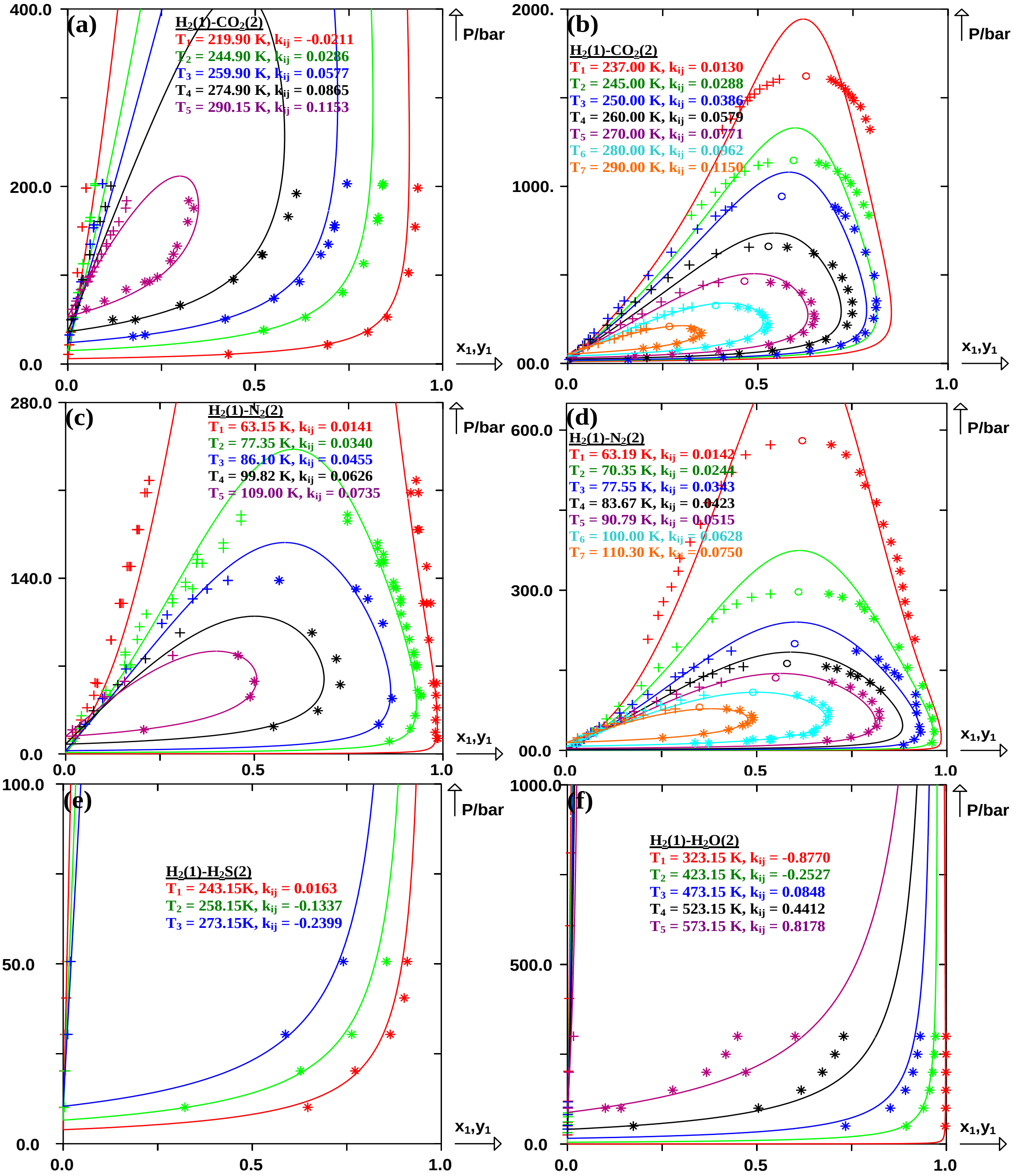

Figure IV−7. Prediction of isothermal curves for four binary systems: (hydrogen(1) + carbon dioxide(2)), (hydrogen(1) + nitrogen(2)), (hydrogen(1) + hydrogen sulfide(2)) and (hydrogen(1) + water(2)) using the PPR78 model. (+) experimental bubble points, (✳) experimental dew points, (○) experimental critical points. Solid line: predicted curves with the PPR78 model. **(a)** System (hydrogen(1) + carbon dioxide(2)) at five different temperatures: T_1 = 219.90 K (k_{ij} = -0.0211), T_2 = 244.90 K (k_{ij} = 0.0286), T_3 = 259.90 K (k_{ij} = 0.0577), T_4 = 274.90 K (k_{ij} = 0.0865), T_5 = 290.15 K (k_{ij} = 0.1153). **(b)** System (hydrogen(1) + carbon dioxide(2)) at seven different temperatures: T_1 = 237.00 K (k_{ij} = 0.0130), T_2 = 245.00 K (k_{ij} = 0.0288), T_3 = 250.00 K (k_{ij} = 0.0386), T_4 = 260.00 K (k_{ij} = 0.0579), T_5 = 270.00 K (k_{ij} = 0.0771), T_6 = 280.00 K (k_{ij} = 0.0962), T_7 = 290.00 K (k_{ij} = 0.1150). **(c)** System (hydrogen(1) + nitrogen(2)) at five different temperatures: T_1 = 63.15 K (k_{ij} = 0.0141), T_2 = 77.35 K (k_{ij} = 0.0340), T_3 = 86.10 K (k_{ij} = 0.0455), T_4 = 99.82 K (k_{ij} = 0.0626), T_5 = 109.00 K (k_{ij} = 0.0735). **(d)** System (hydrogen(1) + nitrogen(2)) at seven different temperatures: T_1 = 63.19 K (k_{ij} = 0.0142), T_2 = 70.35 K (k_{ij} = 0.0244), T_3 = 77.55 K (k_{ij} = 0.0343), T_4 = 83.67 K (k_{ij} = 0.0423), T_5 = 90.79 K (k_{ij} = 0.0515), T_6 = 100.00 K (k_{ij} = 0.0628), T_7 = 110.30 K (k_{ij} = 0.0750). **(e)** System (hydrogen(1) + hydrogen sulfide(2)) at three different temperatures: T_1 = 243.15 K (k_{ij} = 0.0163), T_2 = 258.15 K (k_{ij} = -0.1337), T_3 = 273.15 K (k_{ij} = -0.2399). **(f)** System (hydrogen(1) + water(2)) at five different temperatures: T_1 = 323.15 K (k_{ij} = -0.8770), T_2 = 423.15 K (k_{ij} = -0.2527), T_3 = 473.15 K (k_{ij} = 0.0848), T_4 = 523.15 K (k_{ij} = 0.4412), T_5 = 573.15 K (k_{ij} = 0.8178).

IV.4.5 Results for mixtures of [hydrogen + alkene (or cycloalkene)]

According to our data base, VLE data are only known for six binary systems in this family. The data-fitting procedure was well accomplished for the binary mixture (H_2(1) + ethylene(2)) because enough experimental points have been collected, including 20 critical points. We have plotted in figure (IV−8a,8b) fourteen isothermal curves for this mixture. As mentioned in section IV.3, even though we have made a compromise between the representation of the critical points and that of the whole phase envelop, the critical pressures are still overestimated at T = 166.15 K and T = 175.15 K [see figure (IV−8b)]. Meanwhile, LLE at low temperatures and VLE in the vicinity of the critical points of ethylene are well described by our model. The prediction of critical locus of this mixture is plotted in figure (IV−9b).

Regarding the binary mixtures which consist of H_2 and a linear alkene, critical points are only available for (H_2(1) + propene(2)) and all the experimental VLE (or LLE) points were measured at low and moderate pressures. As shown in figure (IV−8c), the P-xy diagrams of (H_2(1) + propene(2)) at five different temperatures are well reproduced, as well as the 16 critical points in the vicinity of the critical point of propene [figure (IV−9b)]. In figure (IV−8d), we have plotted four predicted isotherms of (H_2(1) + 1-hexene(2)), together with the experimental points published by Vasil’eva et al.[141]. These authors have demonstrated that the solubility of 1-hexene in the H_2-rich liquid phase at P = 300 bar has little temperature dependence, which is very difficult to predict by our model.

The determination of the interaction parameters between group 19 (branched alkene) and group 21 (H_2) seems to be impossible because only 26 experimental points (H_2(1) + alpha-methylstyrene(2)) were collected in our data base. Similarly, only 10 experimental points of (H_2(1) + cyclohexene(2)) are available to fit the interaction parameters between group 20 (cycloalkene) and group 21 (H_2). It is therefore an easy task for our model to properly represent these measurements with a good accuracy, however, extrapolation of our model to these two groups will thus be uncertain [see figure (IV−8e,8f)].

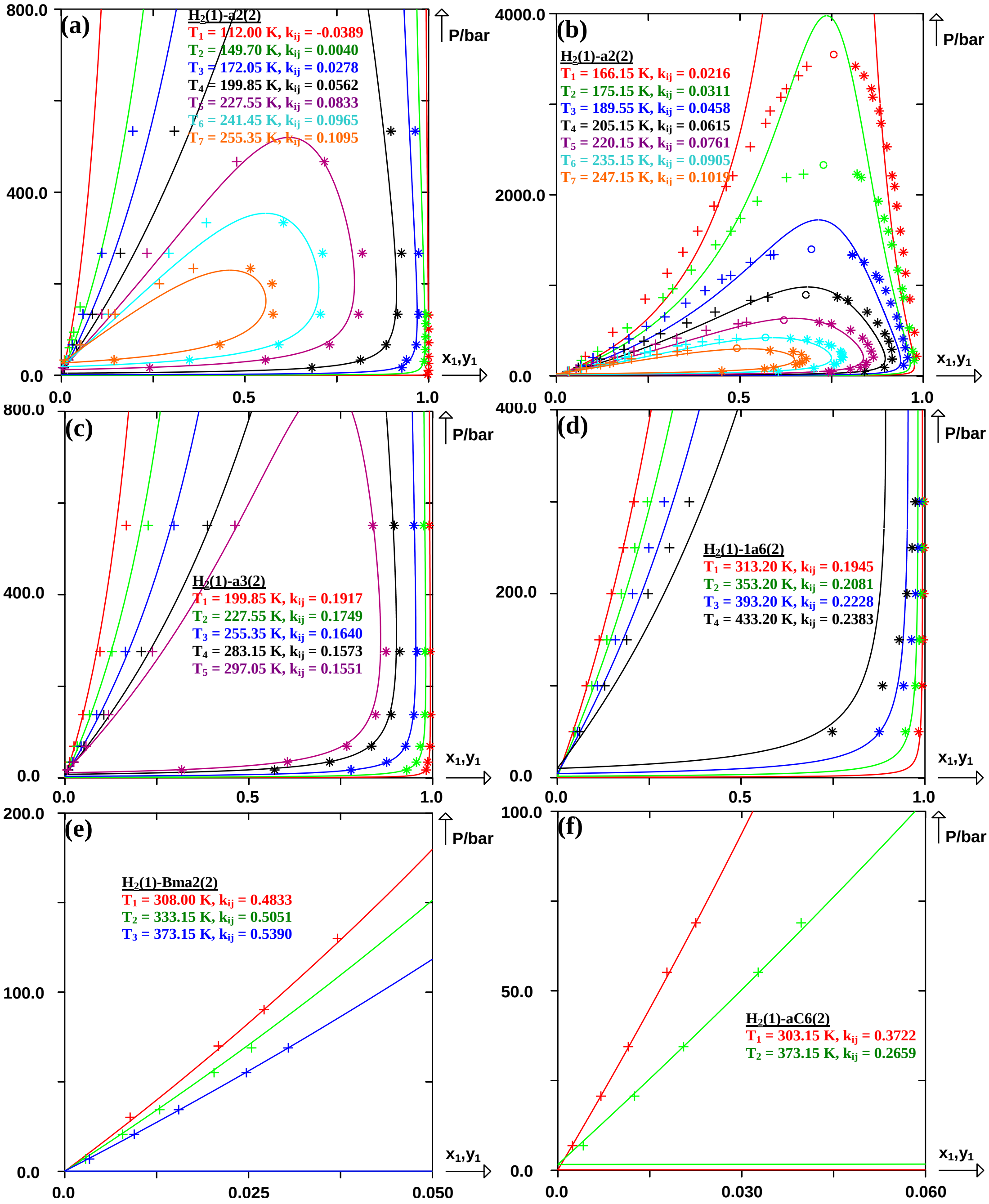

Figure IV−8. Prediction of isothermal curves for five binary systems: (hydrogen(1) + ethylene(2)), (hydrogen(1) + propene(2)), (hydrogen(1) + 1-hexene(2)), (hydrogen(1) + alpha-methylstyrene(2)) and (hydrogen(1) + cyclohexene(2)) using the PPR78 model. (+) experimental bubble points, (✳) experimental dew points, (○) experimental critical points. Solid line: predicted curves with the PPR78 model. **(a)** System (hydrogen(1) + ethylene(2)) at seven different temperatures: T_1 = 112.00 K (k_{ij} = -0.0389), T_2 = 149.70 K (k_{ij} = 0.0040), T_3 = 172.05 K (k_{ij} = 0.0278), T_4 = 199.85 K (k_{ij} = 0.0562), T_5 = 227.55 K (k_{ij} = 0.0833), T_6 = 241.45 K (k_{ij} = 0.0965), T_7 = 255.35 K (k_{ij} = 0.1095). **(b)** System (hydrogen(1) + ethylene(2)) at seven different temperatures: T_1 = 166.15 K (k_{ij} = 0.0216), T_2 = 175.15 K (k_{ij} = 0.0311), T_3 = 189.55 K (k_{ij} = 0.0458), T_4 = 205.15 K (k_{ij} = 0.0615), T_5 = 220.15 K (k_{ij} = 0.0761), T_6 = 235.15 K (k_{ij} = 0.0905), T_7 = 247.15 K (k_{ij} = 0.1019). **(c)** System (hydrogen(1) + propene(2)) at five different temperatures: T_1 = 199.85 K (k_{ij} = 0.1917), T_2 = 227.55 K (k_{ij} = 0.1749), T_3 = 255.35 K (k_{ij} = 0.1640), T_4 = 283.15 K (k_{ij} = 0.1573), T_5 = 297.05 K (k_{ij} = 0.1551). **(d)** System (hydrogen(1) + 1-hexene(2)) at four different temperatures: T_1 = 313.20 K (k_{ij} = 0.1945), T_2 = 353.20 K (k_{ij} = 0.2081), T_3 = 393.20 K (k_{ij} = 0.2228), T_4 = 433.20 K (k_{ij} = 0.2383). **(e)** System (hydrogen(1) + alpha-methylstyrene(2)) at three different temperatures: T_1 = 308.00 K (k_{ij} = 0.4833), T_2 = 333.15 K (k_{ij} = 0.5051), T_3 = 373.15 K (k_{ij} = 0.5390). **(f)** System (hydrogen(1) + cyclohexene(2)) at two different temperatures: T_1 = 303.15 K (k_{ij} = 0.3722), T_2 = 373.15 K (k_{ij} = 0.2659).

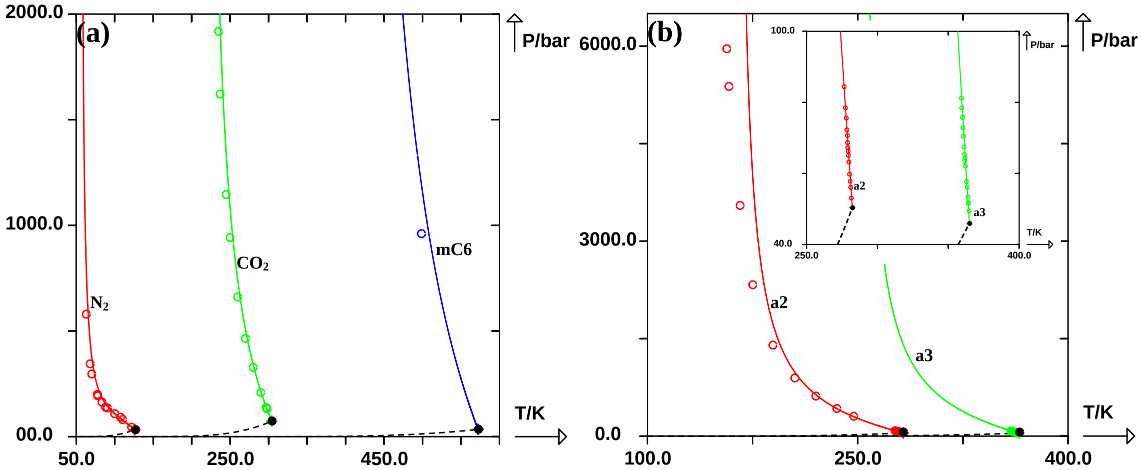

Figure IV−9. Prediction of the critical locus for five binary systems using the PPR78 model. (○) experimental critical points, (●) critical points of the pure compounds. Solid line: predicted curves with the PPR78 model. Dashed line: vaporization curve of the pure compounds. **(a)** Prediction of the critical locus for three binary systems: (hydrogen(1) + nitrogen(2)), (hydrogen(1) + carbon dioxide(2)) and (hydrogen(1) + methylcyclohexane(2)). **(b)** Prediction of the critical locus for two binary systems: (hydrogen(1) + ethylene(2)) and (hydrogen(1) + propene(2)).

IV.5 Conclusion

The PPR78 model was extended to systems containing hydrogen with an objective function of 8.79 % over 46 binary systems. In this work, all the systems exhibit Type III phase behavior and it is necessary to make a compromise between the restitution of VLE (or LLE) and that of critical loci. Concerning the binary systems consisting of H_2 and a mercaptan, no experimental data is available in the open literature and the parameters $A_{21\text{-}15}$ and $B_{21\text{-}15}$ have not been determined. Moreover, although the values of $A_{21\text{-}14}$, $B_{21\text{-}14}$, $A_{21\text{-}19}$, $B_{21\text{-}19}$, $A_{21\text{-}20}$ and $B_{21\text{-}20}$ have been proposed, their use is uncertain.

Generally, this paper allows us to conclude that, in spite of the asymmetric nature of mixtures containing H_2, the quantum behavior of H_2 and the Type III phase behavior for all the binary mixtures investigated, the representations and predictions of LLE and VLE over a wide range of temperature and pressure obtained here, using such a simple PR EoS, together with classical mixing rules and temperature-dependant BIP ($k_{ij}(T)$), can be considered as satisfactory. Finally, it is possible to estimate the k_{ij} for any system containing hydrogen, alkenes, water, mercaptan, H_2S, N_2, CO_2, naphthenes, aromatics and alkanes whatever the temperature.

References

(1) Sadus, R. J. Influence of quantum effects on the high-pressure phase behavior of binary mixtures containing hydrogen. *J. Phys. Chem.* **1992**, *96* (9), 3855-3860.
(2) El-Twaty, A. I.; Prausnitz, J. M. Correlation of K-factors for mixtures of hydrogen and heavy hydrocarbons. *Chem. Eng. Sci.* **1980**, *35* (8), 1765-1768.
(3) Wang, W.; Zhong, C. Mixing rules for hydrogen-containing systems. *Fluid Phase Equilib.* **1989**, *47* (1), 103-114.
(4) Twu, C.; Coon, J. E.; Harvey, A. H.; Cunningham, J. R. An Approach for the Application of a Cubic Equation of State to Hydrogen-Hydrocarbon Systems. *Ind. Eng. Chem. Res.* **1996**, *35* (3), 905.
(5) Moysan, J. M.; Huron, M. J.; Paradowski, H.; Vidal, J. Prediction of the solubility of hydrogen in hydrocarbon solvents through cubic equations of state. *Chem. Eng. Sci.* **1983**, *38* (7), 1085.
(6) Moysan, J. M.; Paradowski, H.; Vidal, J. Prediction of phase behavior of gas-containing systems with cubic equations of state. *Chem. Eng. Sci.* **1986**, *41* (8), 2069-2074.
(7) Gray, R. D., Jr.; Heidman, J. L.; Springer, R. D.; Tsonopoulos, C. VLE predictions for multicomponent hydrogen systems with cubic equations of state. *Gas Process. Assoc., Proc. 64th Annu. Conv.* **1985**, 289-298.
(8) Valderrama, J. O.; Cisternas, L. A.; Vergara, M. E.; Bosse, M. A. Binary interaction parameters in cubic equations of state for hydrogen-hydrocarbon mixtures. *Chem. Eng. Sci.* **1990**, *45* (1), 49-54.
(9) Huang, H.; Sandler, S. I.; Orbey, H. Vapor-liquid equilibria of some hydrogen + hydrocarbon systems with the Wong-Sandler mixing rule. *Fluid Phase Equilib.* **1994**, *96* (1-2), 143.
(10) Ioannidis, S.; Knox, D. E. Vapor-liquid equilibria predictions of hydrogen-hydrocarbon mixtures with the Huron-Vidal mixing rule. *Fluid Phase Equilib.* **1999**, *165* (1), 23.
(11) Gao, W.; Robinson, R. L.; Gasem, K. A. M. Alternate equation of state combining rules and interaction parameter generalizations for asymmetric mixtures. *Fluid Phase Equilib.* **2003**, *213* (1-2), 19-37.
(12) Ghosh, A.; Chapman, W. G.; French, R. N. Gas solubility in hydrocarbons-a SAFT-based approach. *Fluid Phase Equilib.* **2003**, *209* (2), 229-243.
(13) Florusse, L. J.; Peters, C. J.; Pamies, J. C.; Vega, L. F.; Meijer, H. Solubility of hydrogen in heavy n-alkanes: Experiments and SAFT modeling. *AlChE J.* **2003**, *49* (12), 3260-3269.
(14) Thi, C.; Tamouza, S.; Passarello, J.-P.; Tobaly, P.; de Hemptinne, J.-C. Modeling Phase Equilibrium of H2 + n-Alkane and CO2 + n-Alkane Binary Mixtures Using a Group Contribution Statistical Association Fluid Theory Equation of State (GC-SAFT-EOS) with a kij Group Contribution Method. *Ind. Eng. Chem. Res.* **2006**, *45* (20), 6803-6810.
(15) Polishuk, I.; Vera, J. H. A novel EOS that combines van der Waals and Dieterici potentials. *AlChE J.* **2005**, *51* (7), 2077-2088.
(16) Jaubert, J.-N.; Mutelet, F. VLE predictions with the Peng-Robinson equation of state and temperature dependent kij calculated through a group contribution method. *Fluid Phase Equilib.* **2004**, *224* (2), 285-304.
(17) Jaubert, J.-N.; Vitu, S.; Mutelet, F.; Corriou, J.-P. Extension of the PPR78 model (predictive 1978, Peng-Robinson EOS with temperature dependent kij calculated through a group contribution method) to systems containing aromatic compounds. *Fluid Phase Equilib.* **2005**, *237* (1-2), 193-211.
(18) Vitu, S.; Jaubert, J.-N.; Mutelet, F. Extension of the PPR78 model (Predictive 1978, Peng-Robinson EOS with temperature dependent kij calculated through a group contribution method) to systems containing naphtenic compounds. *Fluid Phase Equilib.* **2006**, *243* (1-2), 9-28.
(19) Vitu, S.; Privat, R.; Jaubert, J. N.; Mutelet, F. Predicting the phase equilibria of CO2 + hydrocarbon systems with the PPR78 model (PR EOS and kij calculated through a group contribution method). *Journal of Supercritical Fluids* **2008**, *45* (1), 1-26.
(20) Privat, R.; Jaubert, J. N.; Mutelet, F. Addition of the nitrogen group to the PPR78 model (predictive 1978, Peng Robinson EOS with temperature-dependent kij calculated through a group contribution method. *Ind. Eng. Chem. Res.* **2008**, *47* (6), 2033-2048.
(21) Privat, R.; Mutelet, F.; Jaubert, J. N. Addition of the hydrogen sulfide group to the PPR 78, Model (Predictive 1978, Peng-Robinson equation of state with temperature dependent kij- calculated through a group contribution method). *Ind. Eng. Chem. Res.* **2008**, *47* (24), 10041-10052.
(22) Privat, R.; Jaubert, J. N.; Mutelet, F. Addition of the sulfhydryl group (-SH) to the PPR78 model (predictive 1978, Peng-Robinson EOS with temperature dependent kij calculated through a group contribution method). *Journal of Chemical Thermodynamics* **2008**, *40* (9), 1331-1341.
(23) Poling, B. E.; Prausnitz, J. M.; O'Connell, J. P. *The Properties of Gases and Liquids, 5th Ed.* **2000**, 11-18.
(24) Bol'shakov, P. E.; Linshits, L. R. Phase equilibria in liquid-gas systems at high pressures. *Tr. Gos. Nauchno Issled. Proektn. Inst. Azotn. Promst. Prod. Org. Sin.* **1954**, *3*, 18-27.

(25) Burriss, W. L.; Hsu, N. T.; Reamer, H. H.; Sage, B. H. Phase behavior of the hydrogen-propane system. *J. Ind. Eng. Chem. (Washington, D. C.)* **1953**, *45*, 210-213.
(26) Trust, D. B. The Hetergeneous Phase Behavior of the Hydrogen - Propane, Carbon Monoxide - Propane and Hydrogen - Carbon Monoxide - Propane Systems. *Ph.D. thesis, Kansas Univ.* **1968**.
(27) Trust, D. B.; Kurata, F. Vapor-liquid phase behavior of the hydrogen-propane and hydrogen-carbon monoxide-propane systems. *AIChE J.* **1971**, *17* (1), 86-91.
(28) Williams, R. B.; Katz, D. L. Vapor-liquid equilibria in binary systems. Hydrogen with ethylene, ethane, propylene, and propane. *J. Ind. Eng. Chem. (Washington, D. C.)* **1954**, *46*, 2512-2520.
(29) Aroyan, H. J.; Katz, D. L. Low-temperature vapor-liquid equilibria in hydrogen-butane system. *J. Ind. Eng. Chem. (Washington, D. C.)* **1951**, *43* (1), 185-189.
(30) Augood, D. R. The Separation of HD and H_2 by Absorptive Fractionation. *Trans. Inst. Chem. Eng.* **1957**, *35*, 394-408.
(31) Klink, A. E.; Cheh, H. Y.; Amick, E. H., Jr. Vapor-liquid equilibrium of the hydrogen-butane system at elevated pressures. *AIChE J.* **1975**, *21* (6), 1142-1148.
(32) Nelson, E. E.; Bonnell, W. S. Solubility of hydrogen in butane. *J. Ind. Eng. Chem. (Washington, D. C.)* **1943**, *35* (2), 204-206.
(33) Connolly, J. F.; Kandalic, G. A. Gas solubilities, vapor-liquid equilibria, and partial molal volumes in some hydrogen-hydrocarbon systems. *J. Chem. Eng. Data* **1986**, *31* (4), 396-406.
(34) Freitag, N. P.; Robinson, D. B. Equilibrium phase properties of the hydrogen-methane-carbon dioxide, hydrogen-carbon dioxide-n-pentane and hydrogen-n-pentane systems. *Fluid Phase Equilib.* **1986**, *31* (2), 183-201.
(35) Brunner, E. Solubility of hydrogen in 10 organic solvents at 298.15, 323.15, and 373.15 K. *J. Chem. Eng. Data* **1985**, *30* (3), 269-273.
(36) Fu, M.-S.; Tan, C.-S. Solubility of hydrogen in a mixture of n-hexane and dicyclopentadiene from 313 to 363 K and from 2.0 to 5.5 MPa. *Fluid Phase Equilib.* **1994**, *93*, 233-247.
(37) Gao, W.; Robinson, R. L., Jr.; Gasem, K. A. M. Solubilities of Hydrogen in Hexane and of Carbon Monoxide in Cyclohexane at Temperatures from 344.3 to 410.9 K and Pressures to 15 MPa. *J. Chem. Eng. Data* **2001**, *46* (3), 609-612.
(38) Nichols, W. B.; Reamer, H. H.; Sage, B. H. Volumetric and phase behavior in the hydrogen-hexane system. *AIChE J.* **1957**, *3* (2), 262-267.
(39) Cook, M. W.; Hanson, D. N.; Alder, B. J. Solubility of hydrogen and deuterium in nonpolar solvents. *The Journal of Chemical Physics* **1957**, *26* (4), 748-751.
(40) Ene, R.; Bica, I.; Sandulescu, D. Determination of hydrogen solubility in liquid hydrocarbons at atmospheric pressure. *Rev. Roum. Chim.* **1982**, *27*, 609-613.
(41) Lachowicz, S. K.; Newitt, D. M.; Weale, K. E. Solubility of hydrogen and deuterium in heptane and octane at high pressures. *Trans. Faraday Soc.* **1955**, *51*, 1198-1205.
(42) Peramanu, S.; Pruden, B. B. Solubility study for the purification of hydrogen from high pressure hydrocracker off-gas by an absorption-stripping process. *Can. J. Chem. Eng.* **1997**, *75* (3), 535-543.
(43) Peter, S.; Reinhartz, K. Phase equilibrium in the systems H2-n-heptane, H2-methylcyclohexane, and H2-2,2,4-trimethylpentane at elevated pressures and temperatures. *Z. Phys. Chem. (Muenchen, Ger.)* **1960**, *24*, 103-118.
(44) Zernov, V. S.; Kogan, V. B.; Egudina, O. G.; Kobyakov, V. M.; Babayants, T. V.; Kalichava, L. I. Phase Equilibria and Volume Ratios in the Systems Heptane - Ethylene. *J. Appl. Chem. USSR* **1990**, *63* (7), 1469-1472.
(45) Connolly, J. F. Vapor-liquid equilibrium ratios for four binary systems. *Proc. Am. Petrol. Inst. Sect. III* **1965**, *45*, 62-67.
(46) Connolly, J. F.; Kandalic, G. A. Thermodynamic properties of solutions of hydrogen in n-octane. *J. Chem. Thermodyn.* **1989**, *21* (8), 851-858.
(47) Kim, K. J.; Way, T. R.; Feldman, K. T., Jr.; Razani, A. Solubility of Hydrogen in Octane, 1-Octanol, and Squalane. *J. Chem. Eng. Data* **1997**, *42* (1), 214-215.
(48) Florusse, L. J.; Peters, C. J.; Pamies, J. C.; Vega, L. F.; Meijer, H. Solubility of hydrogen in heavy n-alkanes: Experiments and SAFT modeling. *AIChE J.* **2003**, *49* (12), 3260-3269.
(49) Park, J.; Robinson, R. L., Jr.; Gasem, K. A. M. Solubilities of Hydrogen in Heavy Normal Paraffins at Temperatures from 323.2 to 423.2 K and Pressures to 17.4 MPa. *J. Chem. Eng. Data* **1995**, *40* (1), 241-244.
(50) Prausnitz, J. M.; Benson, P. R. Solubility of liquids in compressed hydrogen, nitrogen, and carbon dioxide. *AIChE J.* **1959**, *5*, 161-164.
(51) Schofield, B. A.; Ring, Z. E.; Missen, R. W. Solubility of hydrogen in a white oil. *Can. J. Chem. Eng.* **1992**, *70* (4), 822-824.
(52) Sebastian, H. M.; Simnick, J. J.; Lin, H.-M.; Chao, K.-C. Gas-liquid equilibrium in the hydrogen + n-decane system at elevated temperatures and pressures. *J. Chem. Eng. Data* **1980**, *25* (1), 68-70.

(53) Sokolov, V. I.; Polyakov, A. A. Solubility of hydrogen in n-decane, n-tetradecane, 1-hexene, 1-pentene, 4-octene, isopropylbenzene, 1-methylnaphthalene, and decalin. *J. Appl. Chem. USSR* **1977**, *50* (6), 1347-1349.
(54) Dean, M. R.; Tooke, J. W. Vapor-liquid equilibria in three hydrogen-paraffin systems. *J. Ind. Eng. Chem. (Washington, D. C.)* **1946**, *38*, 389-393.
(55) Gao, W.; Robinson, R. L., Jr.; Gasem, K. A. M. High-Pressure Solubilities of Hydrogen, Nitrogen, and Carbon Monoxide in Dodecane from 344 to 410 K at Pressures to 13.2 MPa. *J. Chem. Eng. Data* **1999**, *44* (1), 130-132.
(56) Breman, B. B.; Beenackers, A. A. C. M.; Rietjens, E. W. J.; Stege, R. J. H. Gas-Liquid Solubilities of Carbon Monoxide, Carbon Dioxide,Hydrogen, Water, 1-Alcohols (1 ≤ n ≤ 6), and n-Paraffins (2 ≤ n ≤ 6) in Hexadecane, Octacosane, 1-Hexadecanol, Phenanthrene, and Tetraethylene Glycol at Pressures up to 5.5 MPa and Temperatures from 293 to 553 K. *J. Chem. Eng. Data* **1994**, *39* (4), 647-666.
(57) Dohrn, R.; Brunner, G. Phase equilibria in ternary and quaternary systems of hydrogen, water and hydrocarbons at elevated temperatures and pressures. *Fluid Phase Equilib.* **1986**, *29*, 535-544.
(58) Lin, H.-M.; Sebastian, H. M.; Chao, K.-C. Gas-liquid equilibrium in hydrogen + n-hexadecane and methane + n-hexadecane at elevated temperatures and pressures. *J. Chem. Eng. Data* **1980**, *25* (3), 252-254.
(59) Huang, S. H.; Lin, H. M.; Tsai, F. N.; Chao, K. C. Solubility of synthesis gases in heavy n-paraffins and Fischer-Tropsch wax. *Ind. Eng. Chem. Res.* **1988**, *27* (1), 162-169.
(60) Laugier, S.; Richon, D.; Renon, H. Vapor-liquid equilibriums of hydrogen-2,2,4-trimethylpentane and hydrogen-toluene systems at high pressures and temperatures. *J. Chem. Eng. Data* **1980**, *25* (3), 274-276.
(61) Benham, A. L.; Katz, D. L. Vapor-liquid equilibriums for hydrogen-light hydrocarbon systems at low temperatures. *AIChE J.* **1957**, *3*, 33-36.
(62) Fastovskii, V. G.; Gonikberg, M. G. Solubility of gases in liquids at low temperatures and high pressures. III. Solubility of hydrogen in liquid methane. *Acta Physicochim. URSS* **1940**, *12*, 485-488.
(63) Fastovskii, V. G.; Gonikberg, M. G. Solubility of Gases in Liquids at low Temperatures and high Pressures. III. Solubility of Hydrogen in liquid Methane. *Zh. Fiz. Khim.* **1940**, *14* (3), 427-428.
(64) Hong, J. H.; Kobayashi, R. Vapor Liquid Equilibrium Study of the H2 - CH4 System at Low Temperatures and Elevated Pressures. *GPA Research Report* **1980**, (RR-46), 1-25.
(65) Hong, J. H.; Kobayashi, R. Vapor-liquid equilibrium study of the hydrogen-methane system at low temperatures and elevated pressures. *J. Chem. Eng. Data* **1981**, *26* (2), 127-131.
(66) Kirk, B. S.; Ziegler, W. T. A phase-equilibrium apparatus for gas-liquid systems and the gas phase of gas-solid systems: application to methane-hydrogen from 66.88° to 116.53°K. and up to 125 atmospheres. *Adv. Cryog. Eng.* **1965**, *10*, 160-170.
(67) Kremer, H.; Knapp, H. Vapor-liquid equilibriums in ternary mixtures of hydrogen, nitrogen, carbon monoxide, and methane. *Fluid Phase Equilib.* **1983**, *11* (3), 289-310.
(68) Sagara, H.; Arai, Y.; Saito, S. Vapor-liquid equilibriums of binary and ternary systems containing hydrogen and light hydrocarbons. *J. Chem. Eng. Jap.* **1972**, *5* (4), 339-348.
(69) Tsang, C. Y.; Clancy, P.; Calado, J. C. G.; Streett, W. B. Phase equilibriums in the hydrogen/methane system at temperatures from 92.3 to 180.0 K and pressures to 140 MPa. *Chem. Eng. Commun.* **1980**, *6* (6), 365-383.
(70) Yorizane, M.; Yoshimura, S.; Masuoka, H. Low Temperature Vapor-Liquid Equilibria of Hydrogen - Containing Binaries. *Proc. Int. Cryog. Eng. Conf.* **1968**, *1*, 57-62.
(71) Yorizane, M.; Yoshimura, S.; Masuoka, H.; Funada, I.; Fu, C. T.; Lu, B. C. Y. Phase Behavior of three Hydrogen-Containing Ternary Systems. *Adv. Cryog. Eng.* **1979**, *24*, 654-661.
(72) Cohen, A. E.; Hipkin, H. G.; Koppany, C. R. Experimental vapor-liquid equilibrium data for hydrogen-ethane and hydrogen-methane-ethane. *Chem. Eng. Progr., Symp. Ser.* **1967**, *63* (81), 10-17.
(73) Heintz, A.; Streett, W. B. Phase equilibriums in the hydrogen/ethane system at temperatures from 92.5 to 280.1 K and pressures to 560 MPa. *J. Chem. Eng. Data* **1982**, *27* (4), 465-469.
(74) Hiza, M. J.; Heck, C. K.; Kidnay, A. J. Liquid-Vapor and Solid-Vapor Equilibrium in the System Hydrogen - Ethane. *Adv. Cryog. Eng.* **1967**, *13*, 343-356.
(75) Levitskaya, E.; Pryannikov, K. Equilibrium between liquid and vapor in the binary system of hydrogen and ethane. *Zh. Tekh. Fiz.* **1939**, *9*, 1849-1853.
(76) Brainard, A. J.; Williams, G. B. Vapor-liquid equilibrium for the system hydrogen-benzene-cyclohexane-n-hexane. *AIChE J.* **1967**, *13* (1), 60-69.
(77) Chao, K. C.; Lin, H. M.; Liu, K. D.; Lawson, C. C.; Sebastian, H. M.; Simnick, J. J.; Yao, J. Phase Equilibrium in Coal Liquefaction Processes. *Research Project 367-1, Electric Power Research Institute AF-466* **1976**, (EPRI AF-466).
(78) Coan, C. R.; King, A. D., Jr. Second cross virial coefficients of benzene-gas mixtures from high-pressure solubility measurements. Comparison with gas-chromatographic values. *J. Chromatogr.* **1969**, *44* (3-4), 429-436.

(79) Connolly, J. F. Thermodynamic properties of hydrogen in benzene solutions. *J. Chem. Phys.* **1962**, *36* (11), 2897-2904.
(80) Ipat'ev, V. V., Jr.; Levin, M. I. Equilibrium between liquid and gas at high pressures and temperatures. I. Solubility of hydrogen in individual hydrocarbons of the aromatic and the naphthenic series. *Zh. Fiz. Khim.* **1935**, *6* (5), 632-639.
(81) Ipat'ev, V. V.; Teodorovich, V. P.; Brestkin, A. P.; Artemovich, V. S. The region of ultrahigh pressures. I. The equilibrium between the liquid and the vapor phases in the system hydrogen-benzene at pressures up to 3000 atmospheres. *Zh. Fiz. Khim.* **1948**, *22* (7), 833-845.
(82) Park, J.; Robinson, R. L., Jr.; Gasem, K. A. M. Solubilities of Hydrogen in Aromatic Hydrocarbons from 323 to 433 K and Pressures to 21.7 MPa. *J. Chem. Eng. Data* **1996**, *41* (1), 70-73.
(83) Simnick, J. J.; Lawson, C. C.; Lin, H. M.; Chao, K. C. Vapor-liquid equilibrium of hydrogen/tetralin system at elevated temperatures and pressures. *AIChE J.* **1977**, *23* (4), 469-476.
(84) Thompson, R. E.; Edmister, W. C. Vapor-liquid equilibriums in hydrogen-benzene and hydrogen-cyclohexane mixtures. *AIChE J.* **1965**, *11* (3), 457-461.
(85) Simnick, J. J.; Liu, K. D.; Lin, H.-M.; Chao, K.-C. Gas-liquid equilibrium in mixtures of hydrogen and diphenylmethane. *Ind. Eng. Chem. Process Des. Dev.* **1978**, *17* (2), 204-208.
(86) Yin, J.-Z.; Tan, C.-S. Solubility of hydrogen in toluene for the ternary system H2 + CO2 + toluene from 305 to 343 K and 1.2 to 10.5MPa. *Fluid Phase Equilib.* **2006**, *242* (2), 111-117.
(87) Simnick, J. J.; Sebastian, H. M.; Lin, H. M.; Chao, K. C. Gas-liquid equilibrium in mixtures of hydrogen + m-xylene and + m-cresol. *J. Chem. Thermodyn.* **1979**, *11* (6), 531-537.
(88) Zhao, L.; Zhao, Y.; Lu, Z.; Zhang, B. Solubility of H2 and CO in mixed xylene. *Huaxue Fanying Gongcheng Yu Gongyi* **2000**, *16* (4), 396-400.
(89) Herskowitz, M.; Wisniak, J.; Skladman, L. Hydrogen solubility in organic liquids. *J. Chem. Eng. Data* **1983**, *28* (2), 164-166.
(90) Phiong, H.-S.; Lucien, F. P. Solubility of Hydrogen in α-Methylstyrene and Cumene at Elevated Pressure. *J. Chem. Eng. Data* **2002**, *47* (3), 474-477.
(91) Lin, H. M.; Sebastian, H. M.; Chao, K. C. Gas-liquid equilibriums of hydrogen + 1 methylnaphthalene at 457°C. *Fluid Phase Equilib.* **1980**, *4* (3-4), 321-323.
(92) Yao, J.; Sebastian, H. M.; Lin, N. M.; Chao, K. C. Gas-Liquid Equilibria in Mixtures of Hydrogen and 1-Methylnaphthalene. *Fluid Phase Equilib.* **1977**, *1*, 293-304.
(93) Partzsch, S. Examination of vapor-liquid equilibria in mixtures of hydrocarbons with phenols and hydrogen. *Ph.D. thesis, Univ. Leipzig* **1992**.
(94) Malone, P. V.; Kobayashi, R. Light gas solubility in phenanthrene: the hydrogen-phenanthrene and methane-phenanthrene systems. *Fluid Phase Equilib.* **1990**, *55* (1-2), 193-205.
(95) Zudkevitch, D.; Weinstein, N. J.; Daubert, T. E. Applicability of Phase Equilibrium Data Correlations to High Temperature - High Pressure Aromatic Systems and Liquid Fuels from Coal. *Proc.conf. Nat. Phys. Lab. Symp.* **1978**, *87*, 1-26.
(96) Berty, T. E.; Reamer, H. H.; Sage, B. H. Phase behavior in the hydrogen-cyclohexane system. *J. Chem. Eng. Data* **1966**, *11* (1), 25-30.
(97) Dymond, J. H. Solubility of a series of gases in cyclohexane and dimethylsulfoxide. *J. Phys. Chem.* **1967**, *71* (6), 1829-1831.
(98) Krichevskii, I. R.; Sorina, G. A. Phase and volume relations in liquid-gas systems at high pressures. VI. The cyclohexane-hydrogen system. *Zh. Fiz. Khim.* **1958**, *32* (9), 2080-2086.
(99) Ronze, D.; Fongarland, P.; Pitault, I.; Forissier, M. Hydrogen solubility in straight run gas oil. *Chem. Eng. Sci.* **2002**, *57* (4), 547-553.
(100) Harrison, R. H.; Scheppele, S. E.; Sturm, G. P., Jr.; Grizzle, P. L. Solubility of hydrogen in well-defined coal liquids. *J. Chem. Eng. Data* **1985**, *30* (2), 183-189.
(101) Lin, H. M.; Lin, Y. R. Flow apparatus for phase equilibrium measurement at elevated temperatures. *AIChE J.* **1990**, *36* (10), 1597-1600.
(102) Nasir, P.; Martin, R. J.; Kobayashi, R. A novel apparatus for the measurement of the phase and volumetric behavior at high temperatures and pressures and its application to study VLE in the hydrogen-tetralin system. *Fluid Phase Equilib.* **1981**, *5* (3-4), 279-288.
(103) Sung, S. Phase Equilibrium of the Hydrogen - Coal Liquid System. *Ph.D. thesis, Pittsburgh* **1981**.
(104) Wiegand, K. W.; Strobel, B.; Hofmann, H. Phase equilibria measurements between hydrocarbon liquids and hydrogen under high temperatures and high pressures. *Erdoel Kohle, Erdgas, Petrochem.* **1987**, *40* (5), 216-221.
(105) Sebastian, H. M.; Yao, J.; Lin, H.-M.; Chao, K.-C. Gas-liquid equilibrium of the hydrogen/bicyclohexyl system at elevated temperatures and pressures. *J. Chem. Eng. Data* **1978**, *23* (2), 167-170.

(106) Barrick, P. L.; Heck, C. K.; Spano, J. O. Liquid-vapor equilibriums of the hydrogen-carbon dioxide system. *Tech. Rep. AFML-TR - Air Force Mater. Lab. (U. S.)* **1966**, *No. 66-390*, 69 pp.
(107) Bezanehtak, K.; Combes, G. B.; Dehghani, F.; Foster, N. R.; Tomasko, D. L. Vapor-Liquid Equilibrium for Binary Systems of Carbon Dioxide + Methanol, Hydrogen + Methanol, and Hydrogen + Carbon Dioxide at High Pressures. *J. Chem. Eng. Data* **2002**, *47* (2), 161-168.
(108) Kaminishi, G.; Toriumi, T. Gas-liquid equilibrium under high pressures. VI. Vapor-liquid phase equilibrium in the CO2-H2, CO2-N2, and CO2-O2 systems. *Kogyo Kagaku Zasshi* **1966**, *69* (2), 175-178.
(109) Ke, J.; Han, B.; George, M. W.; Yan, H.; Poliakoff, M. How Does the Critical Point Change during a Chemical Reaction in Supercritical Fluids? A Study of the Hydroformylation of Propene in Supercritical CO2. *J. Am. Chem. Soc.* **2001**, *123* (16), 3661-3670.
(110) Spano, J. O.; Heck, C. K.; Barrick, P. L. Liquid-vapor equilibria of the hydrogen-carbon dioxide system. *J. Chem. Eng. Data* **1968**, *13* (2), 168-171.
(111) Tsang, C. Y.; Streett, W. B. Phase equilibriums in the hydrogen/carbon dioxide system at temperatures from 220 to 290 K and pressures to 172 MPa. *Chem. Eng. Sci.* **1981**, *36* (6), 993-1000.
(112) Yorizane, M. Determination of vapor-liquid equilibrium data at high pressure and low temperature. *Asahi Garasu Kogyo Gijutsu Shoreikai Kenkyu Hokoku* **1971**, *18*, 61-76.
(113) Yorizane, M.; Yoshimura, S.; Masuoka, H. Vapor liquid equilibrium at high pressures. N2-CO2, H2-CO2 systems. *Kagaku Kogaku* **1970**, *34* (9), 953-957.
(114) Akers, W. W.; Eubanks, L. S. Vapor-Liquid Equilibria in the System Hydrogen - Nitrogen - Carbon Monoxide. *Adv. Cryog. Eng.* **1957**, *3*, 275-293.
(115) Dokoupil, Z.; van, S. G.; Swenker, M. D. P. The equilibrium between the solid phase and the gas phase of the systems hydrogen-nitrogen, hydrogen-carbon monoxide, and hydrogen-nitrogen-carbon monoxide. *Appl. Sci. Res., Sect. A* **1955**, *A5*, 182-241.
(116) Eubanks, L. S. Vapor-Liquid Equilibria in the System Hydrogen - Nitrogen - Carbon Monoxide. *Ph.D. thesis, Houston, Texas* **1957**.
(117) Gonikberg, M. G.; Fastovskii, V. G.; Gurvich, I. G. Solubility of gases in liquids at low temperatures and high pressures. I. Solubility of hydrogen in liquid nitrogen at temperatures from 79.0 to 109.0°K. and at pressures up to 190 atmospheres. *Acta Physicochim. URSS* **1939**, *11*, 865-882.
(118) Gonikberg, M. G.; Fastovstkii, V. G.; Gurvich, I. G. The Solubility of Gases in Liquids at low Temperatures and high Pressures. I. *Zh. Fiz. Khim.* **1939**, *13* (11), 1669-1679.
(119) Knapp, H.; Schmoelling, K.; Neumann, A. Measurement of the molal heat capacity of hydrogen-nitrogen mixtures. *Cryogenics* **1976**, *16* (4), 231-237.
(120) Maimoni, A. Liquid-vapor equilibriums in the hydrogen-nitrogen and deuterium-nitrogen systems. *AIChE J.* **1961**, *7*, 371-375.
(121) Omar, M. H.; Dokoupil, Z. Some supplementary measurements on the vapor-liquid equilibrium of the system hydrogen-nitrogen at temperatures higher than the triple point of nitrogen. *Physica (The Hague)* **1962**, *28*, 33-43.
(122) Shtekkel, F. A.; Tsin, N. M. Determination of the composition diagram for the liquid-gas system methane-nitrogen-hydrogen. *Zh. Khim. Prom-sti.* **1939**, *16* (No. 8), 24-28.
(123) Streett, W. B.; Calado, J. C. G. Liquid-vapor equilibrium for hydrogen + nitrogen at temperatures from 63 to 110 K and pressures to 57 MPa. *J. Chem. Thermodyn.* **1978**, *10* (11), 1089-1100.
(124) Verschoyle, T. T. H. The ternary system: carbon monoxide-nitrogen-hydrogen and the component binary systems between temperatures of -185° and -215° and between pressures of 0 and 225 atm. *Trans. Roy. Soc. (London)* **1931**, *A230*, 189-220.
(125) Xiao, J.; Liu, K. H2 - N2 - Ar ... *Huaxue Gongcheng* **1990**, *18*, 8-12.
(126) Yorizane, M.; Yoshimura, S.; Masuoka, H.; Naka, T. Measurement and prediction of the vapor-liquid equilibrium relation at low temperature and high pressure for the hydrogen-nitrogen system. *Kagaku Kogaku* **1971**, *35* (6), 691-693.
(127) Yorizane, M.; Sadamoto, S.; Masuoka, H.; Eto, Y. Solubility of gases in methanol at high pressures. *Kogyo Kagaku Zasshi* **1969**, *72* (10), 2174-2177.
(128) Alvarez, J.; Crovetto, R.; Fernandez-Prini, R. The dissolution of nitrogen and of hydrogen in water from room temperature to 640 K. *Ber. Bunsen-Ges. Phys. Chem.* **1988**, *92* (8), 935-940.
(129) Gillespie, P. C.; Wilson, G. M. Vapor-Liquid Equilibrium Data on Water-Substitute Gas Components: N2-H_2O, H_2-H_2O, CO-H_2O, H_2-CO-H_2O, and H_2S-H_2O. *GPA Research Report* **1980**, (RR-41), 1-34.
(130) Ipat'ev, V. V.; Teodorovich, V. P. Solubility of hydrogen in water under pressure at elevated temperatures. *Zh. Obshch. Khim.* **1934**, *4*, 395-399.
(131) Kling, G.; Maurer, G. The solubility of hydrogen in water and in 2-aminoethanol at temperatures between 323 K and 423 K and pressures up to 16 MPa. *J. Chem. Thermodyn.* **1991**, *23* (6), 531-541.

(132) Maslennikova, V. Y.; Goryunova, N. P.; Subbotina, L. A.; Tsiklis, D. S. The Solubility of Water in Compressed Hydrogen. *Russ. J. Phys. Chem.* **1976**, *50* (2), 240-243.
(133) Ugrozov, V. V. Equilibrium Compositions of Vapor-Gas Mixtures over Solutions. *Russ. J. Phys. Chem.* **1996**, *70* (7), 1240-1241.
(134) Wiebe, R.; Gaddy, V. L. The solubility of hydrogen in water at 0°, 50°, 75° and 100° from 25 to 1000 atmospheres. *J. Am. Chem. Soc.* **1934**, *56*, 76-79.
(135) Zoss, L. M. A Study of the Hydrogen and Water and Oxygen and Water Systems at Various Temperatures and Pressures. *Ph.D. thesis, Purdue Univ., West Lafayette* **1952**, 1-76.
(136) Chen, Z.-h.; Yao, Z.; Zhu, F.-j.; Cao, K.; Li, Y.; Huang, Z.-m. Gas-Liquid Critical Properties of Ethylene + Hydrogen and Propylene + Hydrogen Binary Mixtures. *J. Chem. Eng. Data* **2010**, *55* (5), 2004-2007.
(137) Heintz, A.; Streett, W. B. Phase equilibriums in the hydrogen/ethylene system at temperatures from 114.1 to 247.1 K and pressures to 600 MPa. *Ber. Bunsen-Ges. Phys. Chem.* **1983**, *87* (4), 298-303.
(138) Hiza, M. J.; Heck, C. K.; Kidnay, A. J. Liquid-vapor and solid-vapor equilibrium in the system hydrogen-ethylene. *Chem. Eng. Progr., Symp. Ser.* **1968**, *64* (88), 57-65.
(139) Likhter, A. I.; Tikhonovich, N. P. Equilibrium between vapor and liquid in the system ethylene-methane-hydrogen. I. The binary system ethylene-hydrogen. *Zh. Tekh. Fiz.* **1939**, *9*, 1916-1922.
(140) Sagara, H.; Mihara, S.; Arai, Y.; Saito, S. Vapor-liquid equilibriums and Henry's constants for ternary systems containing hydrogen and light hydrocarbons. *J. Chem. Eng. Jpn.* **1975**, *8* (2), 98-104.
(141) Vasil'eva, I. I.; Naumova, A. A.; Polyakov, A. A.; Tyvina, T. N.; Fokina, V. V. Phase and volume-dependent relationships in hydrogen - 1-hexene, hydrogen - 1-octene, and hydrogen - C15-C18 olefin systems. *J. Appl. Chem. USSR* **1986**, *59* (6), 1180-1183.
(142) Herskowitz, M.; Morita, S.; Smith, J. M. Solubility of hydrogen in α-methylstyrene. *J. Chem. Eng. Data* **1978**, *23* (3), 227-228.
(143) Van Konynenburg, P. H.; Scott, R. L. Critical lines and phase equilibria in binary van der Waals mixtures. *Philos. Trans. R. Soc. London, Ser. A* **1980**, *298*, 495-540.

Chapitre V. Définition d’un nouveau modèle baptisé *E*-PPR78 par ajustement simultané des paramètres de groupes sur des données d’équilibres entre phases et des données d’excès

Afin de concevoir, optimiser les procédés chimiques, il est essentiel d’avoir des informations sur les propriétés thermodynamiques des systèmes concernés. Les équilibres entre phases, mais également les grandeurs d’excès (enthalpie d’excès, capacité calorifique d’excès) sont particulièrement utiles dans les calculs de génie chimique. Pour cette raison, il est très important d’avoir un modèle capable de prédire avec précision l’ensemble de ces données.

Depuis 2004, le modèle PPR78 a été développé en prenant uniquement en compte des données d’équilibres entre phases (équilibres liquide-vapeur, liquide-liquide et liquide-liquide-vapeur). Les résultats obtenus indiquent clairement que ce modèle est un modèle prédictif précis concernant la prévision des équilibres entre phases. Nous nous somme cependant redus compte que sans être mauvaise, la restitution des h^E et des c_P^E n’était pas toujours satisfaisante. Dans ce chapitre nous nous proposons de réajuster les 420 paramètres du modèle PPR78 sur des données expérimentales incluant, entre des données d’équilibres entre phases, de multiples données de grandeurs d’excès. Nous espérons ainsi ne pas trop dégrader la restitution des équilibres entre phases et simultanément grandement améliorer la prédiction des grandeurs d’excès. Ce nouveau modèle a été baptisé *E*-PPR78 (enhanced PPR78).

V.1 Introduction

Today, the synthesis design and optimization steps of chemical processes require efficient thermodynamic models to give a simultaneous representation of phase equilibria and excess thermodynamic properties without having to perform costly and fastidious experiments. To do so, Demiriel and Gecegormez[1] examined the performance of activity coefficient models like NRTL and UNIQUAC and it was necessary to introduce temperature-dependent parameters for both models to correlate simultaneously the vapor-liquid equilibria (VLE) and excess enthalpy (h^E) data. Chen et al.[2] used the virial-like Martin-Hou equation of state (EoS) to correlate h^E data of both liquid mixtures and gaseous mixtures. They also predicted the isothermal binary VLE data using the parameters determined by correlating h^E data. In recent decades, the capability and the flexibility of cubic EoSs have been much improved, particularly by introducing Gibbs energy (g^E) mixings rules. These EoS/g^E models can be used to solve phase equilibrium problems even for some very complicated systems. Ohta[3] applied the PRSV EoS with the modified Huron-Vidal first order (MHV1) and Wong-Sandler (WS) mixing rules to correlate h^E for some kinds of binary systems at low and high pressures. The simultaneous representation of VLE and h^E data over wide ranges of temperature and pressure was performed only for four binary mixtures.

Despite the relative success of the above-mentioned approaches, none of them could simultaneously predict the phase equilibria and excess properties for various binary mixtures, covering a wide range of temperature and pressure. Since soon one decade, Jaubert and coworkers[4-10] developed the PPR78 model (predictive 1978, Peng-Robonson EoS). This predictive model relies on the combination of the Peng-Robinson equation in its 1978 version with classical Van der Waals mixing rules (linear on b and quadratic on a). In addition a group contribution method is used to accurately quantify the interactions between each pair of molecules. Nowadays, the PPR78 model can manage complex mixtures containing alkanes, aromatics, naphthenes, alkenes, carbon dioxide, nitrogen, hydrogen sulfide, mercaptans, hydrogen and water. Successes and failures of PPR78 in the representation of phase equilibrium properties (bubble and dew points, critical points, azeotropes, liquid-liquid phase equilibria and so on) were largely studied, published and discussed by all PPR78 contributors.

Note that besides the phase equilibria, the excess thermodynamic properties, such as h^E and excess heat capacity (c_P^E) are also important in chemical engineering designs and optimizations because they are used to calculate the energy and exergy balances of any process for the development of heat pumps and other applications in heat exchange, heat transport and heat storage. Hence, the capacity of the PPR78 model to predict h^E and c_P^E data has been evaluated. A surprising feature of this model is that the predictions of h^E and c_P^E using the parameters determined by correlating phase equilibrium data, are in many cases accurate over a wide temperature and pressure range, although quantitative predictions are not very satisfactory for some of the studied systems.

The aim of the present work is to simultaneously correlate h^E, c_P^E and VLE data. The new model *E*-PPR78 (enhanced PPR78) thus obtained is capable to describe h^E, c_P^E and phase equilibrium properties (bubble and dew points, critical points, azeotropes, liquid-liquid phase equilibria) in mixtures formed by alkanes, aromatics, naphthenes, alkenes, carbon dioxide, nitrogen, hydrogen sulfide, mercaptans, hydrogen and water.

V.2 Why this work was conducted?

Before this work, the performance of the original PPR78 model to predict h^E and c_P^E data has been evaluated, showing reasonable results. Due to the fact that only VLE data were employed in optimizing those original parameters, it could not always ensure an exact representation of h^E and c_P^E. In this work, a simultaneous correlation of h^E, c_P^E and VLE data is carried out to develop the *E*-PPR78 model, which can be explained by the reasons as follows:

♣ In 1996, Orbey and Sandler[11] investigated the simultaneous correlation of VLE and h^E with cubic EoS and various types of mixing rules, such as two-parameter version of the Van der Waals one-fluid mixing rule, several g^E mixings rules, as well as the direct use of activity coefficient models. Their study indicated that although these models could give good correlations of VLE and h^E separately, attempting to predict the values of one property with parameters obtained from the other did not give satisfactory results with any model.

♣ Due to the fact that the predictions of h^E and c_P^E are much less accurate than that of VLE by using the original PPR78 model, a simultaneous correlation of h^E, c_P^E and VLE data by making a compromise among them is really possible. We can expect that the accuracy of VLE will not decrease significantly and that of h^E and c_P^E will be highly improved.

♣ The PPR78 model has been extended to systems containing hydrogen and twenty-one groups have been defined until now. The 420 parameters (210 A_{kl} and 210 B_{kl}) determined are shown in table (I−2), among which 54 parameters (27 A_{kl} and 27 B_{kl}) are not available because of the absence of experimental data. We have to notice that several parameters in table (I−2) were proposed in spite of the limited quantity of experimental data, as discussed in our previous articles[4-10] and chapters II, III and IV. Fortunately, a great deal of experimental h^E and c_P^E data have been collected in our database, which can be used as an excellent complement to these groups where experimental VLE data are not sufficient. Consequently, it is necessary to re-determine the parameters of our model by using VLE, h^E and c_p^E data.

♣ As shown in our previous studies, the temperature-dependent binary interaction parameters $k_{ij}(T)$ of PPR78 plays an important role in the VLE prediction. Thanks to the parameters A_{kl} and B_{kl} determined by using experimental VLE data, a group contribution method allowing the estimation of BIP($k_{ij}(T)$) was well established. By looking at the equations from (I−106) to (I−122) in sections I.4.4 and I.4.5 in chapter I, the influence of the first derivative of $k_{ij}(T)$ with temperature (dk_{ij}/dT) on h^E becomes obvious, as well as that of dk_{ij}/dT and the second derivative d^2k_{ij}/dT^2 on $c_P{}^E$. In order to give an illustration, we have plotted in figure (V−1a) three calculated h^E-x curves of (benzene(1) + isooctane(2)) at T = 298.15 K and under P = 1.00 atm, with the Peng-Robinson EoS and Van der Waals mixing rules, together with experimental points. The BIP(k_{ij}) chosen here is: $k_{ij} = 0.0029$, according to the PPR78 model. h^E-x curves in figure (V−1a) are calculated with three different dk_{ij}/dT values: $dk_{ij}/dT = -1.7\times10^{-4}$ (in red), $dk_{ij}/dT = -5.7\times10^{-5}$ (in green) and $dk_{ij}/dT = 0.00$ (in blue), among which $dk_{ij}/dT = -1.7\times10^{-4}$ (in red) is the value obtained from the PPR78 model, and $dk_{ij}/dT = -5.7\times10^{-5}$ (in green) is the best value to well describe these experimental h^E points. The influence of dk_{ij}/dT on h^E is very significant, despite of its small magnitude. Similar illustration [see figure (V−1b)] and explanation apply to the influence of d^2k_{ij}/dT^2 on $c_P{}^E$. We must indicate that $k_{ij} = 0.0029$ and $dk_{ij}/dT = -1.7\times10^{-4}$ taken here are those obtained from the PPR78 model and only the influence of d^2k_{ij}/dT^2 on $c_P{}^E$ have been checked. It is obvious that the $c_P{}^E$ values change a lot as d^2k_{ij}/dT^2 varies from -1.0×10^{-7} to 2.0×10^{-6} and the best value fitted on experimental $c_P{}^E$ points is: $d^2k_{ij}/dT^2 = -1.0\times10^{-7}$ (in green). Although the original PPR78 model can give a good estimation of BIP($k_{ij}(T)$), the estimation of temperature-dependent dk_{ij}/dT and d^2k_{ij}/dT^2 remains uncertain. For this reason, it is important to re-fit the parameters A_{kl} and B_{kl} by using VLE, h^E and $c_p{}^E$ data, so as to establish a group contribution aimed at estimating the temperature-dependent BIP($k_{ij}(T)$), dk_{ij}/dT and d^2k_{ij}/dT^2.

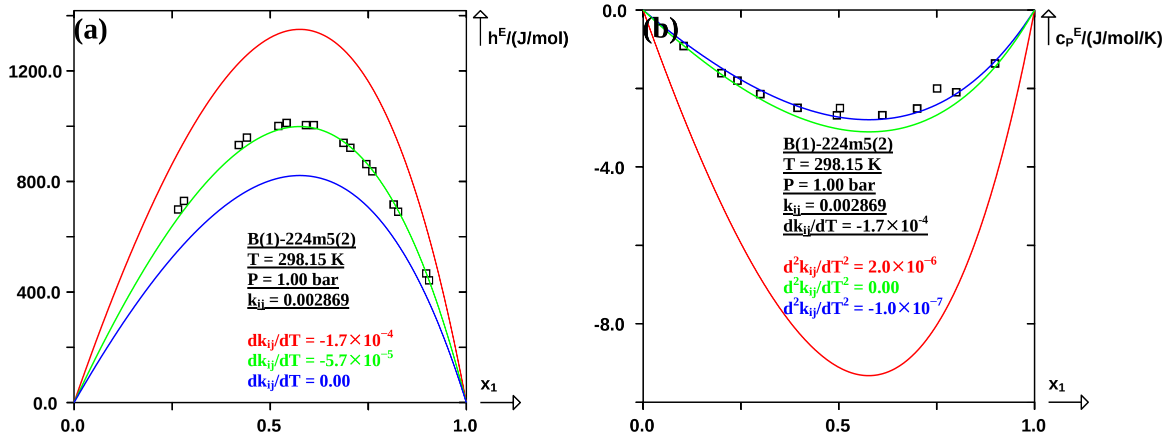

Figure V−1. Prediction of h^E-x and $c_P{}^E$-x curves for the binary system: (benzene(1) + isooctane(2)) at T = 298.15 K and under one atmosphere (P = 1.00 atm). (☐) experimental h^E and $c_P{}^E$ points. Solid line: calculated curves. **(a)** Calculated h^E curves with Peng-Robinson EoS and Van der Waals mixing rules, using $k_{ij} = 0.0029$ (PPR78) and three different dk_{ij}/dT values: $dk_{ij}/dT = -1.7\times10^{-4}$ (PPR78), $dk_{ij}/dT = -5.7\times10^{-5}$ (best fit) and $dk_{ij}/dT = 0.00$. **(b)** Calculated h^E curves with Peng-Robinson EoS and Van der Waals mixing rules, using $k_{ij} = 0.0029$, $dk_{ij}/dT = -1.7\times10^{-4}$ (PPR78), and three different d^2k_{ij}/dT^2 values: $d^2k_{ij}/dT^2 = 2.0\times10^{-6}$ (PPR78), $d^2k_{ij}/dT^2 = 0.00$ and $d^2k_{ij}/dT^2 = -1.0\times10^{-7}$ (best fit).

V.3 Database and reduction procedure

Table V−1. List of the 148 pure component used in this study

Component	Short name	Component	Short name	Component	Short name
methane	1	1,2,3-trimethylbenzene	123mB	cis-2-butene	c2a4
ethane	2	1,2,4-trimethylbenzene	124mB	2-methyl-1-butene	2m1a4
propane	3	1,3,5-trimethylbenzene	135mB	2-methyl-2-butene	2m2a4
n-butane	4	1-metylethylbenzene(cumene)	iprB	3-methyl-1-butene	3m1a4
n-pentane	5	propylbenzene	prB	2-ethyl-1-butene	2e1a4
n-hexane	6	butylbenzene	buB	1,3-butadiene	13a4
n-heptane	7	tertiobutylbenzene	tbuB	1-pentene	1a5
n-octane	8	p-cymene	pcy	4-methyl-1-pentene	4m1a5
n-nonane	9	naphthalene	BB	1-hexene	1a6
n-decane	10	1-methylnaphthalene	1mBB	trans-2-hexene	t2a6
n-undecane	11	2-methylnaphthalene	2mBB	cis-2-hexene	c2a6
n-dodecane	12	1,1’-biphenyl	Bph	trans-3-hexene	t3a6
n-tridecane	13	diphenylmethane	Dph	trans-trans-2,4-hexadiene	tt24a6
n-tetradecane	14	phenanthrene	phe	1,5-hexadiene	15a6
n-pentadecane	15	cyclopropane	C3	1-heptene	1a7
n-hexadecane	16	cyclopentane	C5	trans-2-heptene	t2a7
n-heptadecane	17	methylcyclopentane	mC5	cis-2-heptene	c2a7
n-octadecane	18	trans-1,3-dimethylcyclopentane	t13mC5	trans-3-heptene	t3a7
n-nonadecane	19	cis-1,2-dimethylcyclopentane	c12mC5	1-octene	1a8
n-eicosane	20	1,1-dimethylcyclopentane	11mC5	trans-3-octene	t3a8
2-methylpropane(isobutane)	2m3	ethylcyclopentane	eC5	cis-3-octene	c3a8
2,2-dimethylpropane	22m3	cyclohexane	C6	trans-4-octene	t4a8
2,2,3-trimethylbutane	223m4	methylcyclohexane	mC6	cis-4-octene	c4a8
2-methylbutane	2m4	ethylcyclohexane	eC6	myrcene	myr
2,2-dimethylbutane	22m4	propylcyclohexane	prC6	1-nonene	1a9
2,3-dimethylbutane	23m4	isopropylcyclohexane	iprC6	1-decene	1a10
2-methylpentane	2m5	cycloheptane	C7	1-undecene	1a11
3-methylpentane	3m5	cyclooctane	C8	1-dodecene	1a12
2,2-dimethylpentane	22m5	1,2,3,4-	tet	1-hexadecene	1a16
2,3-dimethylpentane	23m5	trans-decalin	tCC6	1-octadecene	1a18
2,4-dimethylpentane	24m5	cis-decalin	cCC6	styrene	Ba2
2,2,4-trimethylpentane(isooctane)	224m5	1,1’-bicyclohexyl	bcy	alpha-methylstyrene	Bma2
2-methylhexane	2m6	carbon dioxide	CO_2	2-methylpropene	2ma3
3-methylhexane	3m6	nitrogen	N_2	2-methyl-1,3-butadiene	2m13a4
2,2-dimethylhexane	22m6	hydrogen sulfide	H_2S	2-methyl-1-pentene	2m1a5
2,5-dimethylhexane	25m6	methyl mercaptan	1sh	beta-pinene	bp
3,3-dimethylhexane	33m6	ethyl mercaptan	2sh	cyclopentene	aC5
3,4-dimethylhexane	34m6	propyl mercaptan	3sh	1,3-cyclopentadiene	13aC5
2,2,5-trimethylhexane	225m6	butyl mercaptan	4sh	3-methylcyclopentene	3maC5
2-methylheptane	2m7	isopropyl mercaptan	iprsh	cyclohexene	aC6
4-methylheptane	4m7	isobutyl mercaptan	ibush	1,3-cyclohexadiene	13aC6
2,2-dimethylheptane	22m7	tert-butyl mercaptan	tbush	1,4-cyclohexadiene	14aC6
2-methyloctane	2m8	sec-butyl mercaptan	sbush	1-methyl-cyclohexene	1maC6
2,2,4,4,6,8,8-heptamethylnonane	Hm9	hydrogen	H_2	1,5-cyclooctadiene	15aC8
benzene	B	water	H_2O	dicyclopentadiene	gama
methylbenzene(toluene)	mB	ethylene	a2	limonene(R+S)	lamda
1,2-dimethylbenzene(o-xylene)	12mB	propene	a3	limonene(R)	xi
1,3-dimethylbenzene(m-xylene)	13mB	1,2-propadiene	aa3	alpha-pinene	ap
1,4-dimethylbenzene(p-xylene)	14mB	1-butene	1a4		
ethylbenzene	eB	trans-2-butene	t2a4		

Table (V−1) presents the list of the 148 pure components involved in this study. The pure fluid physical properties (T_c, P_c and ω) used in this study originate from two sources. We have used Poling et al.[12] for alkanes, aromatics, naphthenes, alkenes, CO_2, N_2, H_2S, H_2 and H_2O. As some mercaptans and alkenes were missing in this book, the DIPPR database was chosen instead. The sources of the experimental phase equilibrium data can be found in our previous articles[4-10] and chapters II, III and IV. Table (V−5) and table (V−6) in appendix detail the sources of the experimental excess molar enthalpy (h^E) and excess molar heat capacity ($c_P{}^E$) data used in our evaluations along with the temperature, pressure, h^E (or $c_P{}^E$) and composition range for each binary system. The experimental h^E data points have been collected for the mixtures formed by alkanes, aromatics, naphthenes, alkenes, carbon dioxide, nitrogen, hydrogen sulfide, mercaptans, hydrogen and water, while the experimental $c_P{}^E$ data points have been found only for the mixtures containing alkanes, aromatics and naphthenes. Indeed, most of the h^E and $c_P{}^E$ data available in the open literature have been collected. Furthermore, for some binary mixtures, obvious discrepancy can be observed on experimental h^E and $c_P{}^E$ data points [figure (V−2)].

In summary, our database includes 98757 VLE data points (55874 bubble points + 41412 dew points + 1471 critical points) over 800 binary systems, 28934 h^E data points (18254 points in the liquid single-phase region, 5224 points in the gaseous single-phase region and 5456 points referring to the two-phase region) over 483 binary systems, and 2251 $c_P{}^E$ data points in the liquid single-phase region over 107 binary systems. The 420 parameters (210 A_{kl} and 210 B_{kl}) determined [see table (V−2)], are those which minimize the following objective function:

$$F_{obj,global} = \frac{F_{obj,b}\cdot n_b + F_{obj,d}\cdot n_d + F_{obj,c.\ comp}\cdot n_c + F_{obj,c.\ pres}\cdot n_c + F_{obj,hE}\cdot n_{hE} + F_{obj,cPE}\cdot n_{cPE}}{n_b + n_d + n_c + n_c + n_{hE} + n_{cPE}}$$

$$\begin{cases} F_{obj,b} = \dfrac{100}{n_b}\displaystyle\sum_{i=1}^{n_b} 0.5\left(\dfrac{\Delta x}{x_{1,exp}} + \dfrac{\Delta x}{x_{2,exp}}\right)_i \text{ with } \Delta x = \left|x_{1,exp} - x_{1,cal}\right| = \left|x_{2,exp} - x_{2,cal}\right| \\ F_{obj,d} = \dfrac{100}{n_d}\displaystyle\sum_{i=1}^{n_d} 0.5\left(\dfrac{\Delta y}{y_{1,exp}} + \dfrac{\Delta y}{y_{2,exp}}\right)_i \text{ with } \Delta y = \left|y_{1,exp} - y_{1,cal}\right| = \left|y_{2,exp} - y_{2,cal}\right| \\ F_{obj,c.\ comp} = \dfrac{100}{n_c}\displaystyle\sum_{i=1}^{n_c} 0.5\left(\dfrac{\Delta x_c}{x_{c1,exp}} + \dfrac{\Delta x_c}{x_{c2,exp}}\right)_i \text{ with } \Delta x_c = \left|x_{c1,exp} - x_{c1,cal}\right| = \left|x_{c2,exp} - x_{c2,cal}\right| \\ F_{obj,c.\ pres} = \dfrac{100}{n_c}\displaystyle\sum_{i=1}^{n_c}\left(\dfrac{\Delta P_{cm}}{P_{cm,exp}}\right)_i \text{ with } \Delta P_{cm} = \left|P_{cm,exp} - P_{cm,cal}\right| \\ F_{obj,hE} = \dfrac{100}{n_{hE}}\displaystyle\sum_{i=1}^{n_{hE}}\left(\dfrac{\Delta h^E}{h^E_{exp}}\right)_i \text{ with } \Delta h^E = \left|h^E_{exp} - h^E_{cal}\right| \\ F_{obj,cPE} = \dfrac{100}{n_{cPE}}\displaystyle\sum_{i=1}^{n_{cPE}}\left(\dfrac{\Delta c^E_P}{c^E_{P,exp}}\right)_i \text{ with } \Delta c^E_P = \left|c^E_{P,exp} - c^E_{P,cal}\right| \end{cases} \quad (V-1)$$

n_b, n_d, n_{crit}, n_{hE} and n_{cPE} are the number of bubble points, dew points, mixture critical points, h^E points and c_P^E points respectively. In a similar way, $F_{obj,b}$, $F_{obj,d}$, $F_{obj,c.comp}$, $F_{obj,c.pres}$, $F_{obj,hE}$ and $F_{obj,cPE}$ are the objective function of predicted bubble curves, dew curves, mixture critical point composition, mixture critical point pressure, h^E curves and c_P^E curves, respectively. x_1 is the mole fraction in the liquid phase of the most volatile component and x_2 the mole fraction of the heaviest component (it is obvious that $x_2 = 1 - x_1$). Similarly, y_1 is the mole fraction in the gas phase of the most volatile component and y_2 the mole fraction of the heaviest component (it is obvious that $y_2 = 1 - y_1$). x_{c1} is the critical mole fraction of the most volatile component and x_{c2} the critical mole fraction of the heaviest component. P_{cm} is the binary critical pressure.

The objective function of h^E and c_P^E ($F_{obj,hE/cPE}$) can be written as:

$$F_{obj,hE/cPE} = \frac{F_{obj,hE} \cdot n_{hE} + F_{obj,cPE} \cdot n_{cPE}}{n_{hE} + n_{cPE}} \tag{V−2}$$

In contrast to $F_{obj,hE}$, $F_{obj,cPE}$, the objective function of VLE ($F_{obj,VLE}$) can be expressed as:

$$F_{obj,VLE} = \frac{F_{obj,b} \cdot n_b + F_{obj,d} \cdot n_d + F_{obj,c.\ comp} \cdot n_c + F_{obj,c.\ pres} \cdot n_c}{n_b + n_d + n_c + n_c} \tag{V−3}$$

Particularly, the objective function of critical points is:

$$F_{obj,crit} = \frac{1}{2}\left(F_{obj,c.\ comp} + F_{obj,c.\ pres}\right) \tag{V−4}$$

In order to properly evaluate the uncertainty on the predicted h^E: Δh^E, which is the difference between the calculated value and the experimental one, we have defined the average value of temperature changes ($\overline{\Delta T}$) by:

$$\overline{\Delta T} = \frac{1}{n_{hE}} \sum_{i=1}^{n_{hE}} (\Delta T)_i \text{ with } \Delta T = \frac{\Delta h^E}{c_P} \tag{V−5}$$

where c_P is the molar heat capacity of the binary mixture, ΔT is the temperature change for one experimental h^E point.

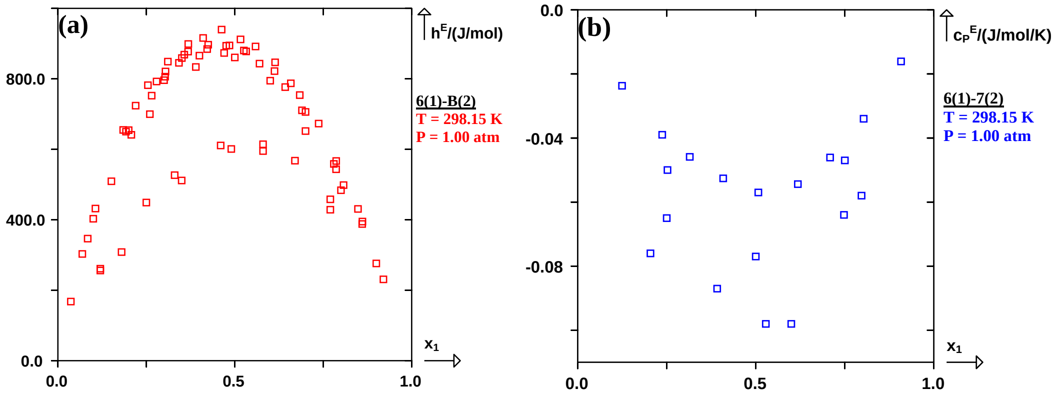

Figure V−2. (a) Experimental h^E points (☐) for the binary system (n-hexane(1) + benzene(2)) at T = 298.15 K and under one atmosphere (P = 1.00 atm). **(b)** Experimental c_P^E points (☐) for the binary system (n-hexane(1) + n-heptane(2)) at T = 298.15 K and under one atmosphere (P = 1.00 atm).

Table V−2. Group interaction parameters: ($A_{kl} = A_{lk}$)/MPa and ($B_{kl} = B_{lk}$)/MPa. N.A. = Not Available

	CH_3 (G 1)	CH_2 (G 2)	CH (G 3)	C (G 4)	CH_4 (G 5)	C_2H_6 (G 6)	CH_{aro} (G 7)	C_{aro} (G 8)	$C_{poly\ aro}$ (G 9)	$CH_{2,cycl}$ (G 10)	CH_{cycl}/C_{cycl} (G 11)	CO_2 (G 12)	N_2 (G 13)	H_2S (G 14)	SH (G 15)	H_2O (G 16)	C_2H_4 (G 17)	$CH_{2,alc}$ /CH_{alc} (G18)	C_{alc} (G 19)	$CH_{cyclalc}$ /$C_{cyclalc}$ (G 20)	H_2 (G 21)
CH_3 (G 1)	0	-	-	-	-	-	-	-	-	-	-	-	-	-	-	-	-	-	-	-	-
CH_2 (G 2)	$A_{12}=65.54$ $B_{12}=105.7$	0	-	-	-	-	-	-	-	-	-	-	-	-	-	-	-	-	-	-	-
CH (G 3)	$A_{13}=214.9$ $B_{13}=294.9$	$A_{23}=39.05$ $B_{23}=41.59$	0	-	-	-	-	-	-	-	-	-	-	-	-	-	-	-	-	-	-
C (G 4)	$A_{14}=431.6$ $B_{14}=575.0$	$A_{24}=134.5$ $B_{24}=183.9$	$A_{34}=-86.13$ $B_{34}=85.10$	0	-	-	-	-	-	-	-	-	-	-	-	-	-	-	-	-	-
CH_4 (G 5)	$A_{15}=28.48$ $B_{15}=20.25$	$A_{25}=37.75$ $B_{25}=74.81$	$A_{35}=131.4$ $B_{35}=157.5$	$A_{45}=309.5$ $B_{45}=35.69$	0	-	-	-	-	-	-	-	-	-	-	-	-	-	-	-	-
C_2H_6 (G 6)	$A_{16}=3.775$ $B_{16}=8.922$	$A_{26}=29.85$ $B_{26}=65.88$	$A_{36}=156.1$ $B_{36}=96.77$	$A_{46}=388.1$ $B_{46}=-224.8$	$A_{56}=9.951$ $B_{56}=13.73$	0	-	-	-	-	-	-	-	-	-	-	-	-	-	-	-
CH_{aro} (G 7)	$A_{17}=98.83$ $B_{17}=136.2$	$A_{27}=25.05$ $B_{27}=64.51$	$A_{37}=56.62$ $B_{37}=129.7$	$A_{47}=170.5$ $B_{47}=284.1$	$A_{57}=67.26$ $B_{57}=167.5$	$A_{67}=41.18$ $B_{67}=50.79$	0	-	-	-	-	-	-	-	-	-	-	-	-	-	-
C_{aro} (G 8)	$A_{18}=103.60$ $B_{18}=103.60$	$A_{28}=5.147$ $B_{28}=-7.549$	$A_{38}=48.73$ $B_{38}=-89.22$	$A_{48}=128.3$ $B_{48}=189.1$	$A_{58}=106.7$ $B_{58}=190.8$	$A_{68}=67.94$ $B_{68}=210.7$	$A_{78}=-16.47$ $B_{78}=16.47$	0	-	-	-	-	-	-	-	-	-	-	-	-	-
$C_{poly\ aro}$ (G 9)	$A_{19}=624.9$ $B_{19}=774.10$	$A_{29}=-17.84$ $B_{29}=-4.118$	NA	NA	$A_{59}=249.1$ $B_{59}=408.3$	NA	$A_{79}=52.50$ $B_{79}=251.2$	$A_{89}=-328.0$ $B_{89}=-569.3$	0	-	-	-	-	-	-	-	-	-	-	-	-
$CH_{2,cycl}$ (G 10)	$A_{1-10}=43.58$ $B_{1-10}=60.05$	$A_{2-10}=8.579$ $B_{2-10}=27.79$	$A_{3-10}=73.09$ $B_{3-10}=71.37$	$A_{4-10}=208.6$ $B_{4-10}=294.4$	$A_{5-10}=33.97$ $B_{5-10}=5.490$	$A_{6-10}=12.70$ $B_{6-10}=73.43$	$A_{7-10}=28.82$ $B_{7-10}=65.54$	$A_{8-10}=37.40$ $B_{8-10}=53.53$	$A_{9-10}=140.7$ $B_{9-10}=277.6$	0	-	-	-	-	-	-	-	-	-	-	-
CH_{cycl}/C_{cycl} (G 11)	$A_{1-11}=293.4$ $B_{1-11}=170.9$	$A_{2-11}=63.48$ $B_{2-11}=-74.46$	$A_{3-11}=-120.8$ $B_{3-11}=18.53$	$A_{4-11}=25.05$ $B_{4-11}=81.33$	$A_{5-11}=188.0$ $B_{5-11}=473.9$	$A_{6-11}=118.0$ $B_{6-11}=-212.8$	$A_{7-11}=129.0$ $B_{7-11}=36.72$	$A_{8-11}=-99.17$ $B_{8-11}=-193.5$	$A_{9-11}=-99.17$ $B_{9-11}=-193.5$	$A_{10-11}=139.0$ $B_{10-11}=35.69$	0	-	-	-	-	-	-	-	-	-	-
CO_2 (G 12)	$A_{1-12}=144.8$ $B_{1-12}=401.5$	$A_{2-12}=141.4$ $B_{2-12}=237.1$	$A_{3-12}=191.8$ $B_{3-12}=380.9$	$A_{4-12}=377.5$ $B_{4-12}=162.7$	$A_{5-12}=134.9$ $B_{5-12}=219.3$	$A_{6-12}=136.2$ $B_{6-12}=235.7$	$A_{7-12}=98.48$ $B_{7-12}=253.6$	$A_{8-12}=154.4$ $B_{8-12}=374.4$	$A_{9-12}=331.1$ $B_{9-12}=276.6$	$A_{10-12}=144.1$ $B_{10-12}=354.1$	$A_{11-12}=216.2$ $B_{11-12}=-132.8$	0	-	-	-	-	-	-	-	-	-
N_2 (G 13)	$A_{1-13}=38.09$ $B_{1-13}=88.19$	$A_{2-13}=83.73$ $B_{2-13}=188.7$	$A_{3-13}=383.6$ $B_{3-13}=375.4$	$A_{4-13}=341.8$ $B_{4-13}=635.2$	$A_{5-13}=30.88$ $B_{5-13}=37.06$	$A_{6-13}=61.59$ $B_{6-13}=84.92$	$A_{7-13}=185.3$ $B_{7-13}=490.7$	$A_{8-13}=343.8$ $B_{8-13}=1712$	$A_{9-13}=702.4$ $B_{9-13}=1889$	$A_{10-13}=179.5$ $B_{10-13}=546.6$	$A_{11-13}=331.5$ $B_{11-13}=389.8$	$A_{12-13}=95.05$ $B_{12-13}=255.6$	0	-	-	-	-	-	-	-	-
H_2S (G 14)	$A_{1-14}=159.6$ $B_{1-14}=227.8$	$A_{2-14}=136.6$ $B_{2-14}=124.6$	$A_{3-14}=192.5$ $B_{3-14}=562.8$	$A_{4-14}=330.8$ $B_{4-14}=-297.2$	$A_{5-14}=181.9$ $B_{5-14}=304.0$	$A_{6-14}=157.2$ $B_{6-14}=217.1$	$A_{7-14}=21.28$ $B_{7-14}=6.177$	$A_{8-14}=9.608$ $B_{8-14}=-36.72$	$A_{9-14}=9.608$ $B_{9-14}=-36.72$	$A_{10-14}=117.4$ $B_{10-14}=166.4$	$A_{11-14}=71.37$ $B_{11-14}=-127.7$	$A_{12-14}=134.9$ $B_{12-14}=201.4$	$A_{13-14}=319.5$ $B_{13-14}=550.1$	0	-	-	-	-	-	-	-
SH (G 15)	$A_{1-15}=789.6$ $B_{1-15}=1829$	$A_{2-15}=439.9$ $B_{2-15}=504.8$	$A_{3-15}=374.0$ $B_{3-15}=520.9$	$A_{4-15}=685.9$ $B_{4-15}=1547$	$A_{5-15}=701.7$ $B_{5-15}=1318$	NA	$A_{7-15}=277.6$ $B_{7-15}=449.5$	$A_{8-15}=1002$ $B_{8-15}=-736.4$	$A_{9-15}=1002$ $B_{9-15}=-736.4$	$A_{10-15}=493.1$ $B_{10-15}=832.1$	$A_{11-15}=463.2$ $B_{11-15}=-337.7$	NA	NA	$A_{14-15}=-157.8$ $B_{14-15}=153.7$	0	-	-	-	-	-	-
H_2O (G 16)	$A_{1-16}=3557$ $B_{1-16}=11195$	$A_{2-16}=4324$ $B_{2-16}=12126$	$A_{3-16}=971.4$ $B_{3-16}=567.6$	NA	$A_{5-16}=2265$ $B_{5-16}=4722$	$A_{6-16}=2333$ $B_{6-16}=5147$	$A_{7-16}=2268$ $B_{7-16}=6218$	$A_{8-16}=543.5$ $B_{8-16}=411.8$	$A_{9-16}=1340$ $B_{9-16}=-65.88$	$A_{10-16}=4211$ $B_{10-16}=13031$	$A_{11-16}=244.0$ $B_{11-16}=-60.39$	$A_{12-16}=559.3$ $B_{12-16}=277.9$	$A_{13-16}=2574$ $B_{13-16}=5490$	$A_{14-16}=603.9$ $B_{14-16}=599.1$	$A_{15-16}=30.88$ $B_{15-16}=-113.6$	0	-	-	-	-	-
C_2H_4 (G 17)	$A_{1-17}=7.892$ $B_{1-17}=35.00$	$A_{2-17}=59.71$ $B_{2-17}=82.35$	$A_{3-17}=147.9$ $B_{3-17}=-55.59$	$A_{4-17}=366.8$ $B_{4-17}=-219.3$	$A_{5-17}=19.22$ $B_{5-17}=33.29$	$A_{6-17}=7.549$ $B_{6-17}=20.93$	$A_{7-17}=25.74$ $B_{7-17}=78.92$	$A_{8-17}=97.80$ $B_{8-17}=67.94$	$A_{9-17}=209.7$ $B_{9-17}=3819$	$A_{10-17}=35.34$ $B_{10-17}=52.50$	$A_{11-17}=297.2$ $B_{11-17}=-647.2$	$A_{12-17}=73.09$ $B_{12-17}=106.7$	$A_{13-17}=45.30$ $B_{13-17}=92.65$	NA	NA	$A_{16-17}=1650$ $B_{16-17}=1661$	0	-	-	-	-
$CH_{2,alc}/CH_{alc}$ (G 18)	$A_{1-18}=48.73$ $B_{1-18}=44.27$	$A_{2-18}=9.608$ $B_{2-18}=50.79$	$A_{3-18}=84.76$ $B_{3-18}=193.2$	$A_{4-18}=181.2$ $B_{4-18}=419.0$	$A_{5-18}=48.73$ $B_{5-18}=68.29$	$A_{6-18}=26.77$ $B_{6-18}=-5.147$	$A_{7-18}=9.951$ $B_{7-18}=19.90$	$A_{8-18}=-48.38$ $B_{8-18}=27.79$	$A_{9-18}=669.8$ $B_{9-18}=589.5$	$A_{10-18}=-15.44$ $B_{10-18}=24.36$	$A_{11-18}=260.1$ $B_{11-18}=134.9$	$A_{12-18}=60.74$ $B_{12-18}=183.9$	$A_{13-18}=59.71$ $B_{13-18}=227.2$	NA	NA	$A_{16-18}=2243$ $B_{16-18}=5199$	$A_{17-18}=14.76$ $B_{17-18}=11.32$	0	-	-	-
C_{alc} (G 19)	$A_{1-19}=102.6$ $B_{1-19}=260.1$	$A_{2-19}=64.85$ $B_{2-19}=51.82$	$A_{3-19}=91.62$ $B_{3-19}=54.90$	NA	NA	NA	$A_{7-19}=-16.47$ $B_{7-19}=61.42$	$A_{8-19}=343.1$ $B_{8-19}=880.2$	NA	$A_{10-19}=159.6$ $B_{10-19}=140.7$	NA	$A_{12-19}=74.81$ $B_{12-19}=-266.6$	$A_{13-19}=541.5$ $B_{13-19}=94.71$	NA	NA	NA	$A_{17-19}=-518.2$ $B_{17-19}=6815$	$A_{18-19}=24.71$ $B_{18-19}=121.8$	0	-	-
$CH_{cyclalc}/C_{cyclalc}$ (G 20)	$A_{1-20}=47.01$ $B_{1-20}=169.5$	$A_{2-20}=34.31$ $B_{2-20}=51.13$	NA	NA	NA	NA	$A_{7-20}=3.775$ $B_{7-20}=1.716$	$A_{8-20}=242.9$ $B_{8-20}=-7.206$	NA	$A_{10-20}=31.91$ $B_{10-20}=69.32$	$A_{11-20}=151.3$ $B_{11-20}=2.745$	$A_{12-20}=87.85$ $B_{12-20}=66.91$	NA	NA	NA	NA	$A_{17-20}=-98.83$ $B_{17-20}=1809$	$A_{18-20}=14.07$ $B_{18-20}=-12.35$	$A_{19-20}=23.68$ $B_{19-20}=87.50$	0	-
H_2 (G 21)	$A_{1-21}=174.0$ $B_{1-21}=239.5$	$A_{2-21}=155.4$ $B_{2-21}=240.9$	$A_{3-21}=326.0$ $B_{3-21}=287.9$	$A_{4-21}=548.3$ $B_{4-21}=2343$	$A_{5-21}=156.1$ $B_{5-21}=92.99$	$A_{6-21}=137.6$ $B_{6-21}=150.0$	$A_{7-21}=288.9$ $B_{7-21}=189.1$	$A_{8-21}=400.1$ $B_{8-21}=1201$	$A_{9-21}=602.9$ $B_{9-21}=1463$	$A_{10-21}=236.1$ $B_{10-21}=192.5$	$A_{11-21}=-51.82$ $B_{11-21}=34.31$	$A_{12-21}=265.9$ $B_{12-21}=268.3$	$A_{13-21}=65.20$ $B_{13-21}=70.10$	$A_{14-21}=145.8$ $B_{14-21}=823.5$	NA	$A_{16-21}=830.8$ $B_{16-21}=-137.9$	$A_{17-21}=151.3$ $B_{17-21}=165.1$	$A_{18-21}=175.7$ $B_{18-21}=373.0$	$A_{19-21}=621.4$ $B_{19-21}=873.6$	$A_{20-21}=460.8$ $B_{20-21}=2167$	0

V.4 Results and discussion

Table V−3. Several objective functions obtained by the original PPR78 model and the recent *E*-PPR78 model

Objective functions	PPR78	*E*-PPR78
$F_{obj,VLE}$ (%)	7.62	7.79
$F_{obj,hE/cPE}$ (%)	851.24	52.00
$F_{obj,global}$ (%)	216.40	18.73

Table V−4. Several objective functions by family obtained by the original PPR78 model and the recent *E*-PPR78 model

Families	$F_{obj,b}$ (%)		$F_{obj,d}$ (%)		$F_{obj,c.comp}$ (%)		$F_{obj,c.pres}$ (%)		$F_{obj,VLE}$ (%)		$F_{obj,hE}$ (%)		$F_{obj,cPE}$ (%)	
	PPR78	*E*-PPR78	PPR78	*E*-PPR78	PPR78	*E*-PPR78	PPR78	*E*-PPR78	PPR78	*E*-PPR78	PPR78	*E*-PPR78	PPR78	*E*-PPR78
Alkanes	3.76	3.99	5.51	5.49	5.99	6.19	4.18	4.03	4.52	4.64	628.73	48.77	327.75	25.73
Aromatics	5.82	6.09	6.10	6.28	6.53	5.00	4.97	4.26	5.93	6.13	88.20	34.90	3001.31	129.61
Naphthenes	3.92	4.11	4.52	4.63	2.88	4.52	1.56	1.65	4.01	4.23	1489.68	71.65	7037.97	58.44
CO_2	7.47	7.96	8.42	8.39	6.96	6.20	3.30	3.22	7.79	8.03	64.96	45.56	0.00	0.00
N_2	10.03	10.19	7.30	7.35	9.01	8.93	6.68	5.75	8.61	8.70	16.34	14.73	0.00	0.00
H_2S	10.21	10.06	7.54	7.61	9.67	9.37	3.02	3.39	9.04	8.99	56.42	55.27	0.00	0.00
Mercaptans	13.73	12.81	7.91	8.47	0.00	0.00	0.00	0.00	12.06	11.56	362.89	27.58	0.00	0.00
H_2O	18.33	18.42	15.67	15.73	22.29	21.95	19.97	20.10	17.09	17.16	54.84	54.85	0.00	0.00
Alkenes	7.95	8.33	10.08	10.33	10.29	10.84	3.49	3.39	8.80	9.12	235.09	39.95	0.00	0.00
H_2	8.44	8.61	9.32	9.36	5.84	5.70	11.02	10.27	8.79	8.89	21.10	21.10	0.00	0.00
Total	7.42	7.66	8.01	8.08	7.12	7.26	4.87	4.68	7.62	7.79	568.82	49.62	4481.40	82.59

For the reasons discussed in section V.2, we have simultaneously correlated excess molar enthalpy (h^E), excess molar heat capacity (c_P^E) and vapor-liquid equilibrium (VLE) data in this study. Table (V−3) presents the objective function of VLE ($F_{obj,VLE}$), hE/cPE ($F_{obj,hE/cPE}$) and the global one ($F_{obj,global}$), obtained by the original PPR78 model and recent *E*-PPR78 model. In table (V−4), the objective function of predicted bubble curves ($F_{obj,b}$), dew curves ($F_{obj,d}$), mixture critical point composition ($F_{obj,c.comp}$), mixture critical point pressure ($F_{obj,c.pres}$), VLE ($F_{obj,VLE}$), h^E curves ($F_{obj,hE}$) and c_P^E curves ($F_{obj,cPE}$) are shown family by family, according to our previous articles and chapters II, III and IV. In addition, the objective function over all the different families is shown at the bottom of table (V−4). Moreover, we have presented several histograms in figure (V−3), so as to have an explicit observation concerning $F_{obj,ELV}$, $F_{obj,crit}$, $F_{obj,hE}$, $\overline{\Delta T}$ (average value of temperature changes), $F_{obj,cPE}$ and $\overline{\Delta c_P^E}$ (average deviation on c_P^E).

Because of the simultaneous correlation of VLE, h^E and c_P^E, the objective function over all the VLE data (10 different families) in this study ($F_{obj,VLE}$ = 7.79 %) becomes a littler higher than that obtained by the original PPR78 model ($F_{obj,VLE}$ = 7.62 %). However, the small variation is absolutely acceptable and the objective function of the two families of binary mixtures containing H_2S and mercaptans seems to be better [see table (V−4) or figure (V−3a)]. Furthermore, the objective function of critical points ($F_{obj,crit}$) over nine different families is retained as shown in figure (V−3b) (dashed line), for which the original PPR78 model exhibits a better $F_{obj,c.comp}$ while the recent *E*-PPR78 gives a better $F_{obj,c.press}$ [see table (V−4)].

On the other hand, thanks to the simultaneous correlation of VLE, h^E and c_P^E, both the objective function of h^E ($F_{obj,hE}$) and that of c_P^E ($F_{obj,cPE}$) have been remarkably improved, as well as the average value of temperature changes ($\overline{\Delta T}$), as shown in table (V−4) and figures (V−3c,3d,3e). It is necessary to notice that h^E data points in the liquid single-phase region and c_P^E data points (available only in the liquid single-phase region) are much better correlated. Meanwhile, the improvements in h^E in the gaseous single-phase region and that referring to the two-phase region are not so significant.

Although the simultaneous correlation of h^E, c_P^E and VLE data has been carried out in this study, the objective functions of h^E and c_P^E is still much higher than that of VLE, which can be explained by the reasons as follows:

(1) Some experimental h^E and c_P^E data reported in the literatures are generally inconsistent and there are obvious scatters among them.

(2) A number of h^E and c_P^E values are very close to zero and the small magnitudes inevitably increase the objective function.

(3) The binary system in the gaseous single-phase region at low temperature and under one atmosphere shows small endothermic mixing which is not easy to be well predicted by our model.

What is more, the simultaneous correlation of h^E and VLE data for the binary systems containing H_2O is always a difficult task, and the average temperature changes of this family is: $\overline{\Delta T}$ = 4.51 K.

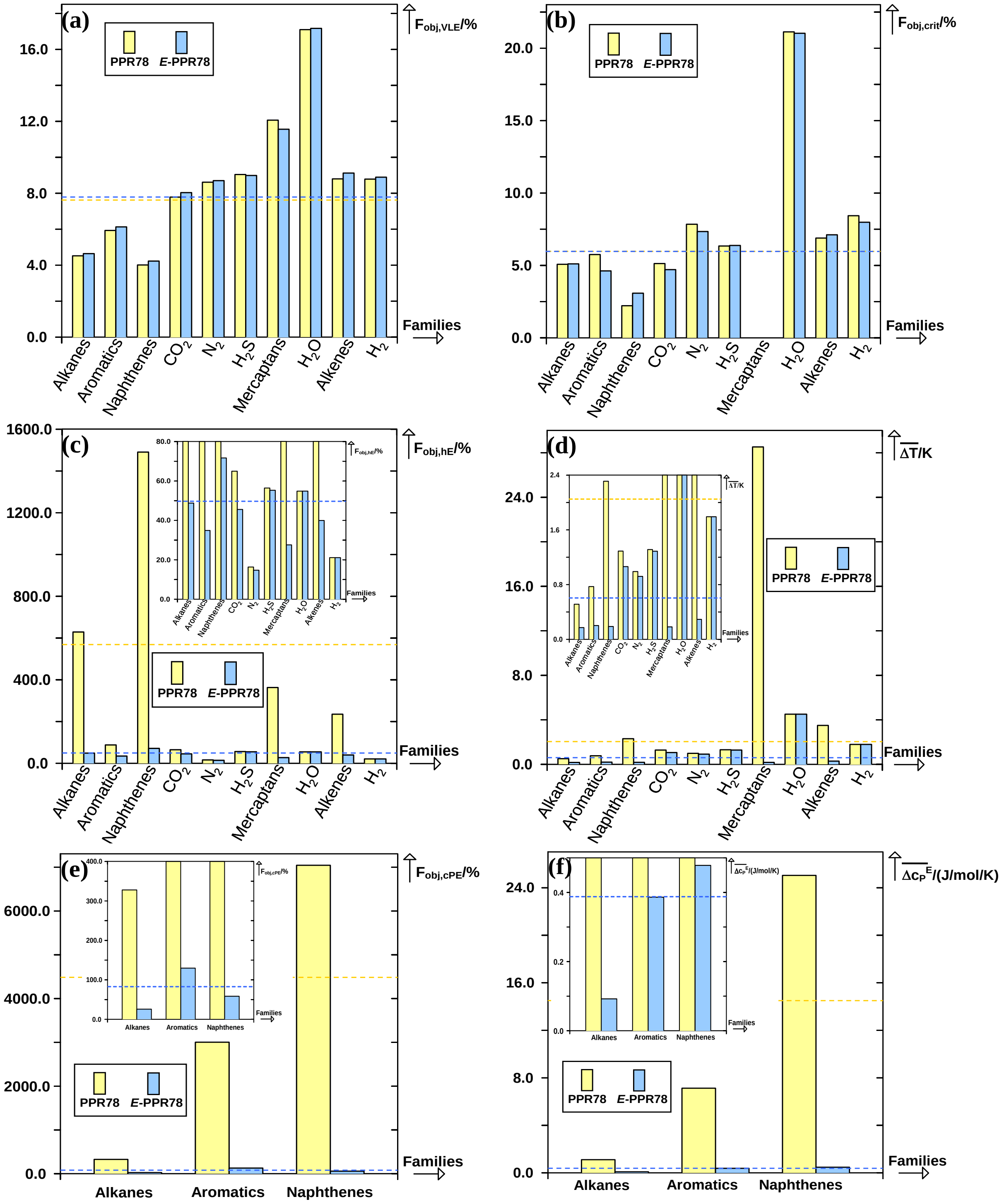

Figure V−3. Histograms of several objective functions (F_{obj}), average overall deviation on c_P^E ($\overline{\Delta c_P^E}$) and average value of temperature changes ($\overline{\Delta T}$), obtained by the original PPR78 model (in yelow) and the recent *E*-PPR78 model (in blue), according to different families: alkanes, aromatics, naphthenes, CO_2, N_2, H_2S, mercaptans, H_2O, alkenes and H_2. Dashed line: objective function over all the families. **(a)** Objective function of VLE ($F_{obj,VLE}$). **(b)** Objective function of critical points ($F_{obj,crit}$). **(c)** Objective function of h^E ($F_{obj,hE}$). **(d)** Average value of temperature changes ($\overline{\Delta T}$). **(e)** Objective function of c_P^E ($F_{obj,cPE}$). **(f)** Average deviation on c_P^E ($\overline{\Delta c_P^E}$).

Considering that 1075 different binary mixtures have been investigated in this study, it is impossible to illustrate system by system, why the recent *E*-PPR78 model could give a better simultaneous representation of VLE, h^E and c_P^E. Taking the binary mixture: (benzene(1) + isooctane(2)) for example, we have plotted in figure (V−4), the predictions of VLE, h^E and c_P^E, by using the original PPR78 model (dashed line) and the recent *E*-PPR78 model (solid line). By using this recent model, the accuracy of predicted P-xy curves at six different temperatures is retained, moreover, the predicted h^E-x and c_P^E-x curves in the liquid singe-phase region are in better agreement with experimental data [see figures (V−4a,4b,4c)]. Thanks to these recently obtained parameters A_{kl} and B_{kl}, reasonable values of BIP(k_{ij}(T)) can be observed in the temperature range: 200K < T < 600K [see figure (V−4d)], giving a good representation of VLE. At the same time, the effect of temperature on BIP(k_{ij}(T)) has been remarkably mitigated and as a result, the magnitude of dk_{ij}/dT becomes less significant and dk_{ij}/dT itself appears to be less temperature-dependent, especially at low and moderate temperatures. The same explanation can be applied to d^2k_{ij}/dT^2. After our examination over all the mixtures, we have found that by using these recently determined parameters (A_{kl}, B_{kl}), both dk_{ij}/dT and d^2k_{ij}/dT^2 for most of the binary mixtures at low and moderate temperatures, become less temperature-dependent showing a magnitude less significant, as (benzene(1) + isooctane(2)). However, both dk_{ij}/dT and d^2k_{ij}/dT^2 at low and moderate temperatures can also be more temperature-dependent showing a magnitude more significant. Such a behavior is observed for the mixtures containing benzene (or cyclohexane) and an n-alkane. Briefly, the recent *E*-PPR78 model can give a better estimation of temperature-dependent k_{ij}, dk_{ij}/dT and d^2k_{ij}/dT^2, and that is why a better prediction of h^E and c_P^E are obtained, by retaining the good prediction of VLE.

Since our database includes 98757 VLE data points (55874 bubble points + 41412 dew points + 1471 critical points) over 800 binary systems and the prediction of VLE using the recent model is very similar to that obtained by the original one, only the graphic results of h^E and c_P^E are presented in order to illustrate the accuracy and limitations of the recent *E*-PPR78 model. The following illustration is divided into four parts: h^E in the liquid single-phase region, h^E in the gaseous single-phase region, h^E referring to the two-phase region and c_P^E in the liquid single-phase region.

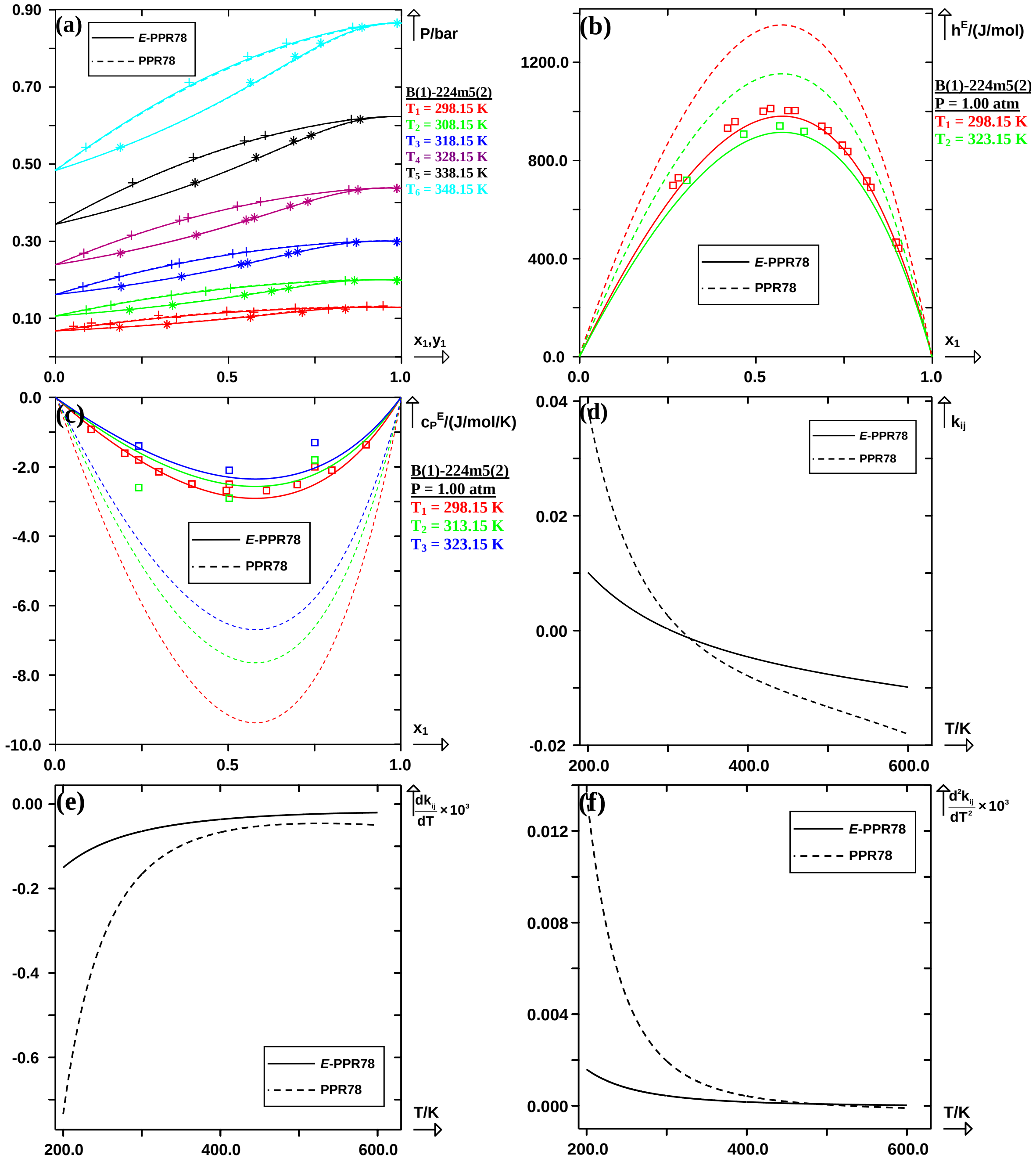

Figure V−4. Prediction of P-xy, h^E-x, c_P^E-x k_{ij}-T, dk_{ij}/dT-T and d^2k_{ij}/dT^2-T curves for the binary system: (benzene(1) + isooctane(2)). (+) experimental bubble points, (✳) experimental dew points, (☐) experimental h^E and c_P^E points. Solid line: predicted curves with the recent *E*-PPR78 model. Dashed line: predicted curves with the original PPR78 model. **(a)** Predicted P-xy curves at six different temperatures: T_1 = 298.15 K, T_2 = 308.15 K, T_3 = 318.15 K, T_4 = 328.15 K, T_5 = 338.15 K, T_6 = 348.15 K. **(b)** Predicted h^E-x curves at two different temperatures: T_1 = 298.15 K, T_2 = 323.15 K. **(c)** Predicted c_P^E-x curves at three different temperatures: T_1 = 298.15 K, T_2 = 313.15 K T_3 = 323.15 K. **(d)** k_{ij}-T curves calculated with the recent model and the original one. **(e)** dk_{ij}/dT-T curves calculated with the recent model and the original one. **(f)** d^2k_{ij}/dT^2-T curves calculated with the recent model and the original one.

V.4.1 Results of excess molar enthalpy (h^E) in the liquid single-phase region

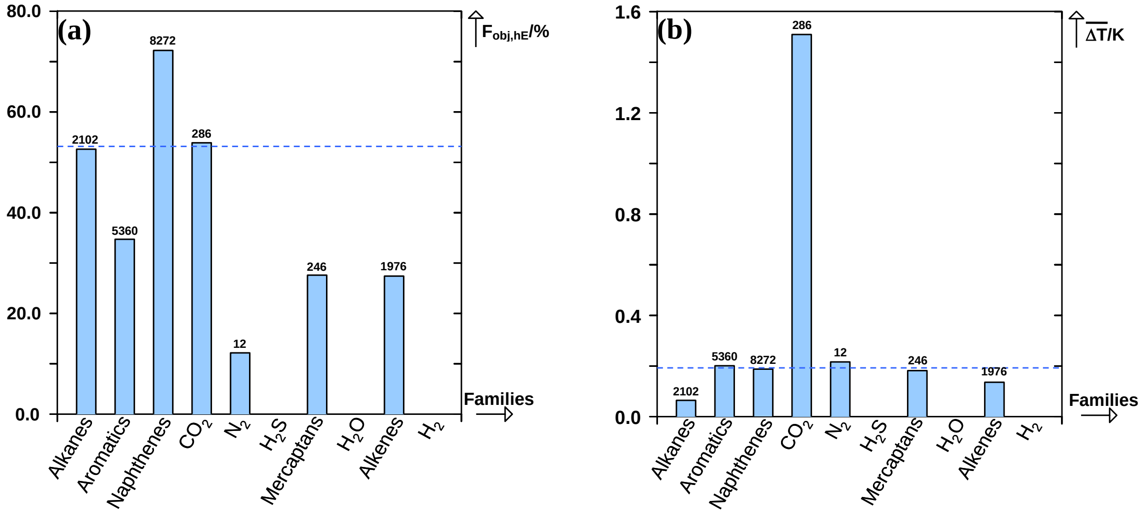

Figure V−5. (a) Histogram of the objective functions of h^E in the liquid single-phase region for ten families of binary systems, with the number of experimental points on top. **(b)** Histogram of the average value of temperature changes generated by the uncertainty on the predicted h^E in the liquid single-phase region for ten families of binary systems, with the number of experimental points on top.

The excess molar enthalpy (h^E) in the liquid single-phase region has been extensively measured and we have collected 18254 experimental points over 435 binary mixtures. For all the data points in the liquid single-phase region, the objective function is: $F_{obj,hE} = 53.14$ % [see blue dashed line in figure (V−5a)]. This objective function was caused by some nearly zero experimental h^E points and the relatively low h^E values in the liquid single-phase region. In addition, the objective function for each family is presented in figure (V−5a), except for the mixtures containing H_2S, H_2O and H_2 where experimental data is not available. Similarly, the average value of the temperature changes ($\overline{\Delta T}$) generated by the uncertainty on the predicted h^E (difference between the calculated value and the experimental one) can be seen in figure (V−5b). By looking at the mixtures containing CO_2, its objective function is very close to the average one, however, its $\overline{\Delta T}$ appears to be 1.51 K, being about 7.5 times higher than that obtained for all the binary mixtures. That's why we have introduced $\overline{\Delta T}$ to evaluate the performance of our model. In order to have a further understanding of the prediction of h^E in the liquid phase, it is decided to present the h^E-x curves family by family so as to illustrate the accuracy and limitations of our model.

V.4.1.1 Binary mixtures containing alkanes (n-alkanes and branched-alkanes)

Figure (V−6) shows the predictions of h^E curves for the binary systems containing n-alkanes, together with the experimental points. The excess enthalpies (h^E) at the temperatures and pressures investigated are homogeneous (liquid state) over the entire composition range. The predicted h^E-x curves of (methane(1) + ethane(2)) at two different temperatures under P = 1.00 atm are almost symmetrical which are in good agreement with the experimental points, including the effect of temperature on h^E [see figure (V−6a)]. Regarding (ethane(1) + propane(2)), the experimental h^E values at T = 273.15 K and under five different pressures are negative and the minimums appear at about $x_1 = 0.6$. Accurate results are obtained by our model in a wide range of pressure except for the underestimation of the h^E at P = 50.00 bar [see figure (V−6b)]. Figures (V−6c,6d) present the accurate predictions of our model for two binary systems: (n-hexane(1) + n-octane(2)) and (n-hexane(1) + n-dodecane(2)). We can see that once again both the temperature and pressure have an obvious influence over the h^E value, which are well predicted by our model. On the other hand, the accuracy could not be kept for the mixture of (n-hexane(1) + n-dodecane(2)) [see figure (V−6e)], which is also confirmed by the results obtained for the mixtures containing n-heptane [see figure (V−6f)]. Although the *E*-PPR78 model could not give a perfect representation of h^E for the binary mixtures consisting of a normal n-alkane and a long-chain n-alkane, the average value of temperature changes are very small ($\overline{\Delta T}$ = 0.15 K) for the five experimental points of (n-heptane(1) + n-hexadecane(2)) at T = 298.15 K and P = 1.00 atm, plotted in figure (V−6f), which is the worst case among the binary mixtures containing n-alkanes.

Figure (V−7) shows the prediction of h^E curves for the binary systems containing branched-alkanes. It is important to notice that the recent *E*-PPR78 model is much more accurate than the original one in predicting the h^E behavior for the mixtures containing branched-alkanes. This is due to the fact that 10 parameters (5 A_{kl} and 5 B_{kl}) were re-determined for the mixtures consisting of two branched-alkanes and consequently, the most of the experimental h^E points are better reproduced and at the same time the high performance of our model for the VLE data is retained. Figures (V−7a,7b,7c,7d) show the results obtained for 16 different binary systems containing branched-alkanes at T = 298.15 K and P = 1.00 atm, from which we can see that our model is generally capable to have a satisfactory representation of the h^E behavior for these mixtures. Once again, the h^E-x curves for the systems containing a long-chain n-alkane are underestimated [see figure (V−7b)], except that the results of (2,3-dimethylbutane(1) + n-hexadecane(2)) appear to be correct. As shown in figures (V−7e,7f), the effect of temperature on h^E value can be observed for the two binary systems investigated, which is well predicted by the *E*-PPR78 model.

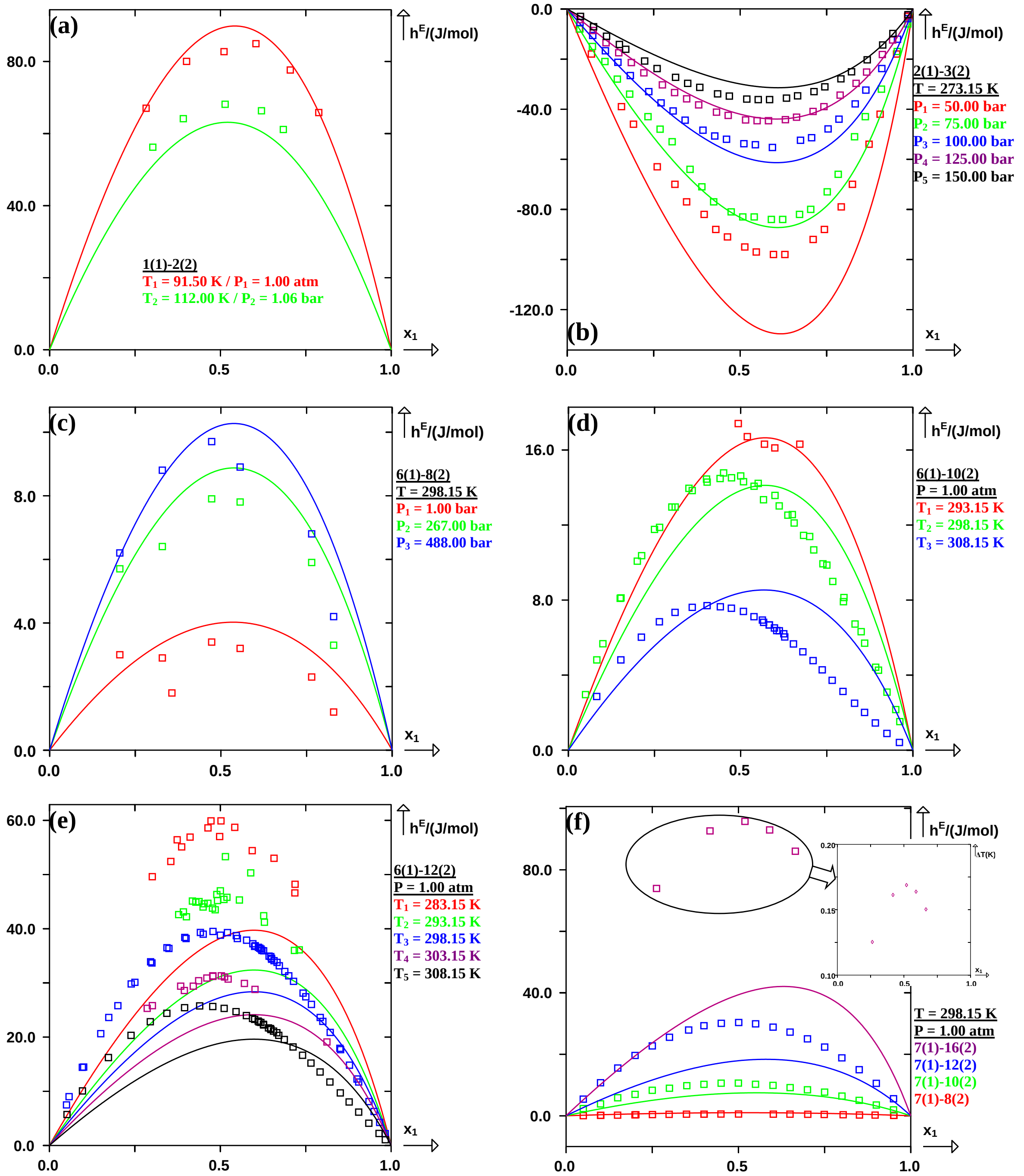

Figure V−6. Prediction of h^E curves in the liquid single-phase region for the binary systems containing n-alkanes using the *E*-PPR78 model. (☐) experimental h^E points, (◊) temperature changes (ΔT). Solid line: predicted curves with the *E*-PPR78 model. **(a)** System (methane(1) + ethane(2)) at : T_1 = 91.50 K and P_1 = 1.00 atm, T_2 = 112.00 K and P_2 = 1.06 bar. **(b)** System (ethane(1) + propane(2)) at T = 273.15 K and under five different pressures: P_1 = 50.00 bar, P_2 = 75.00 bar, P_3 = 100.00 bar, P_4 = 125.00 bar, P_5 = 150.00 bar. **(c)** System (n-hexane(1) + n-octane(2)) at T = 298.15 K and under three different pressures: P_1 = 1.00 bar, P_2 = 267.00 bar, P_3 = 488.00 bar. **(d)** System (n-hexane(1) + n-decane(2)) under one atmosphere (P = 1.00 atm) and at three different temperatures: T_1 = 293.15 K, T_2 = 298.15 K, T_3 = 308.15 K. **(e)** System (n-hexane(1) + n-dodecane(2)) under one atmosphere (P = 1.00 atm) and at five different temperatures: T_1 = 283.15 K, T_2 = 293.15 K, T_3 = 298.15 K, T_4 = 303.15 K, T_5 = 308.15 K. **(f)** Four different systems at T = 298.15 K and under one atmosphere (P = 1.00 atm): (n-heptane(1) + n-octane(2)), (n-heptane(1) + n-decane(2)), (n-heptane(1) + n-dodecane(2)), (n-heptane(1) + n-hexadecane(2)) and the temperature changes (ΔT) generated by the uncertainty on h^E for five experimental points of (n-heptane(1) + n-hexadecane(2)).

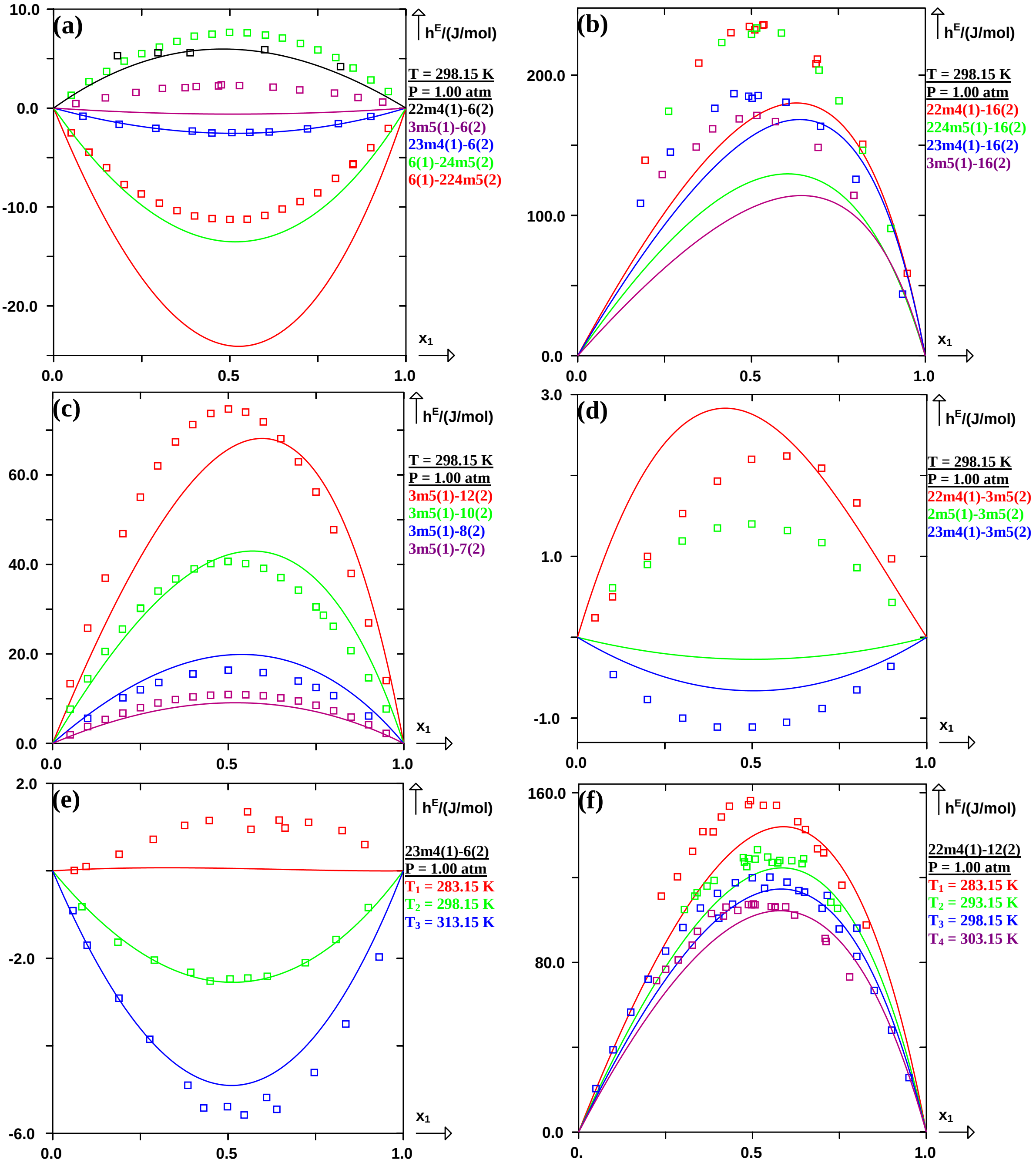

Figure V−7. Prediction of h^E curves in the liquid single-phase region for the binary systems containing branched-alkanes using the *E*-PPR78 model. (□) experimental h^E points. Solid line: predicted curves with the *E*-PPR78 model. **(a)** Five different systems at T = 298.15 K and under one atmosphere (P = 1.00 atm): (n-hexane(1) + 2,2,4-trimethylpentane(2)), (n-hexane(1) + 2,4-dimethylpentane(2)), (2,3-dimethylbutane(1) + n-hexane(2)), (3-methylpentane(1) + n-hexane(2)), (2,2-dimethylbutane(1) + n-hexane(2)). **(b)** Four different systems at T = 298.15 K and under one atmosphere (P = 1.00 atm): (2,2-dimethylbutane(1) + n-hexadecane(2)), (2,2,4-trimethylpentane(1) + n-hexadecane(2)), (2,3-dimethylbutane(1) + n-hexadecane(2)), (3-methylpentane(1) + n-hexadecane(2)). **(c)** Four different systems at T = 298.15 K and under one atmosphere (P = 1.00 atm): (3-methylpentane(1) + n-dodecane(2)), (3-methylpentane(1) + n-decane(2)), (3-methylpentane(1) + n-octane(2)), (3-methylpentane(1) + n-heptane(2)). **(d)** Three different systems at T = 298.15 K and under one atmosphere (P = 1.00 atm): (2,2-dimethylbutane(1) + 3-methylpentane(2)), (2-methylpentane(1) + 3-methylpentane(2)), (2,3-dimethylbutane(1) + 3-methylpentane(2)). **(e)** System (2,3-dimethylbutane(1) + n-hexane(2)) under one atmosphere (P = 1.00 atm) and at three different temperatures: T_1 = 283.15 K, T_2 = 298.15 K, T_3 = 313.15 K. **(f)** System (2,2-dimethylbutane(1) + n-dodecane(2)) under one atmosphere (P = 1.00 atm) and at four different temperatures: T_1 = 283.15 K, T_2 = 293.15 K, T_3 = 298.15 K, T_4 = 303.15 K.

V.4.1.2 Binary mixtures containing aromatics

Figure (V−8) presents the predictions of h^E curves in the liquid single-phase for the binary systems which consist of an aromatic and an alkane. For the five binary mixtures containing benzene at T = 323.15 K and P = 1.00 atm [see figure (V−8a)], the predicted h^E are in perfect agreement with the experimental points regardless of the chain length of n-alkane. It is interesting to notice that the h^E maximum of (n-hexane(1) + benzene(2)) is located at x_1 = 0.45, while the h^E-x curve is skewed gradually to the right side as the chain length of the n-alkane increases and finally the h^E maximum of (benzene(1) + n-eicosane(2)) appears at x_1 = 0.71. We can therefore get some information that the difference in volatility between two components in the binary mixture changes not only the h^E value but also the shape of the h^E-x curve. Similarly, perfect results are obtained for five binary mixtures containing ethylbenzene at T = 298.15 K and P = 1.00 atm [see figure (V−8b)]. As the aromatic becomes more complex (1-methylnaphthalene), our model can always give a good representation of the experimental h^E points for the five different binary mixtures at T = 298.15 K and P = 1.00 atm [see figure (V−8c)]. Considering the mixtures consisting of an aromatic and a branched-alkane, we have plotted in figure (V−8d) four h^E-x curves for the mixtures containing benzene and an isomers of n-hexane at T = 298.15 K and P = 1.00 atm. In this case, the difference in volatility between the two components in these four mixtures is not so obvious and as a consequence, the h^E values and the shapes of h^E-x curve are very similar over the entire composition range, which is accurately predicted by our model. Figure (V−8e) shows the results obtained for the mixtures consisting of toluene and an n-alkane, from which we can see that the experimental points of (n-hexane(1) + toluene(2)) are well predicted, unfortunately, the others are overestimated little by little as the chain length of the n-alkane increases. In this case, if we take the systems: (ethylbenzene(1) + n-hexadecane(2)) at T = 298.15 K and P = 1.00 atm [see figure (V−8b)], and (toluene(1) + n-hexadecane(2)) at T = 298.15 K and P = 1.00 atm [see figure (V−8e)] for comparison, it is really difficult for our model to well reproduce simultaneously two sets of experimental h^E points being nearly identical for two different binary systems under the same condition. Worse still, the comparisons between the predicted h^E curves and the experimental points for five binary mixtures containing 1,2,4-trimethylbenzene [see figure (V−8f)], indicate that the effect of the chain length of n-alkane on the predicted h^E values is much more significant than that on the experimental ones. Although the maximum difference between the predicted h^E and the experimental one for (1,2,4-trimethylbenzene(1) + n-hexadecane(2)) arrives at 267 J/mol, the average value of temperature changes ($\overline{\Delta T}$ = 0.64 K) for this mixture remains inappreciable.

Figure (V−9) presents the predictions of h^E curves for the binary systems which consist of two aromatics. As plotted in figure (V−9a), the experimental h^E data are predicted with accuracy for four different mixtures containing benzene, as well as the other three mixtures plotted in figure (V−9b). Considering four mixtures containing toluene [see figure (V−9c)], slightly positive (or negative) experimental h^E values can be observed, which are unfortunately overestimated by our model, with acceptable uncertainty. For the binary mixtures containing two xylenes (or pseudocumene), it is necessary to indicate that we could do nothing to improve the results shown in figure (V−9d), owing to the fact that the parameters A_{kl} and B_{kl} have no effect on this kind of binary mixture. From the h^E curves of two mixtures at P = 1.00 atm and at four different temperatures [see figures (V−9e,9f)], we can see that the results of (benzene(1) + 1,4-dimethylbenzene(2)) predicted by our model are satisfactory while for (toluene(1) + 1,4-dimethylbenzene(2)), only the h^E-x curve at T = 338.15 K seems to be accurate and the effect of temperature on h^E is underestimated.

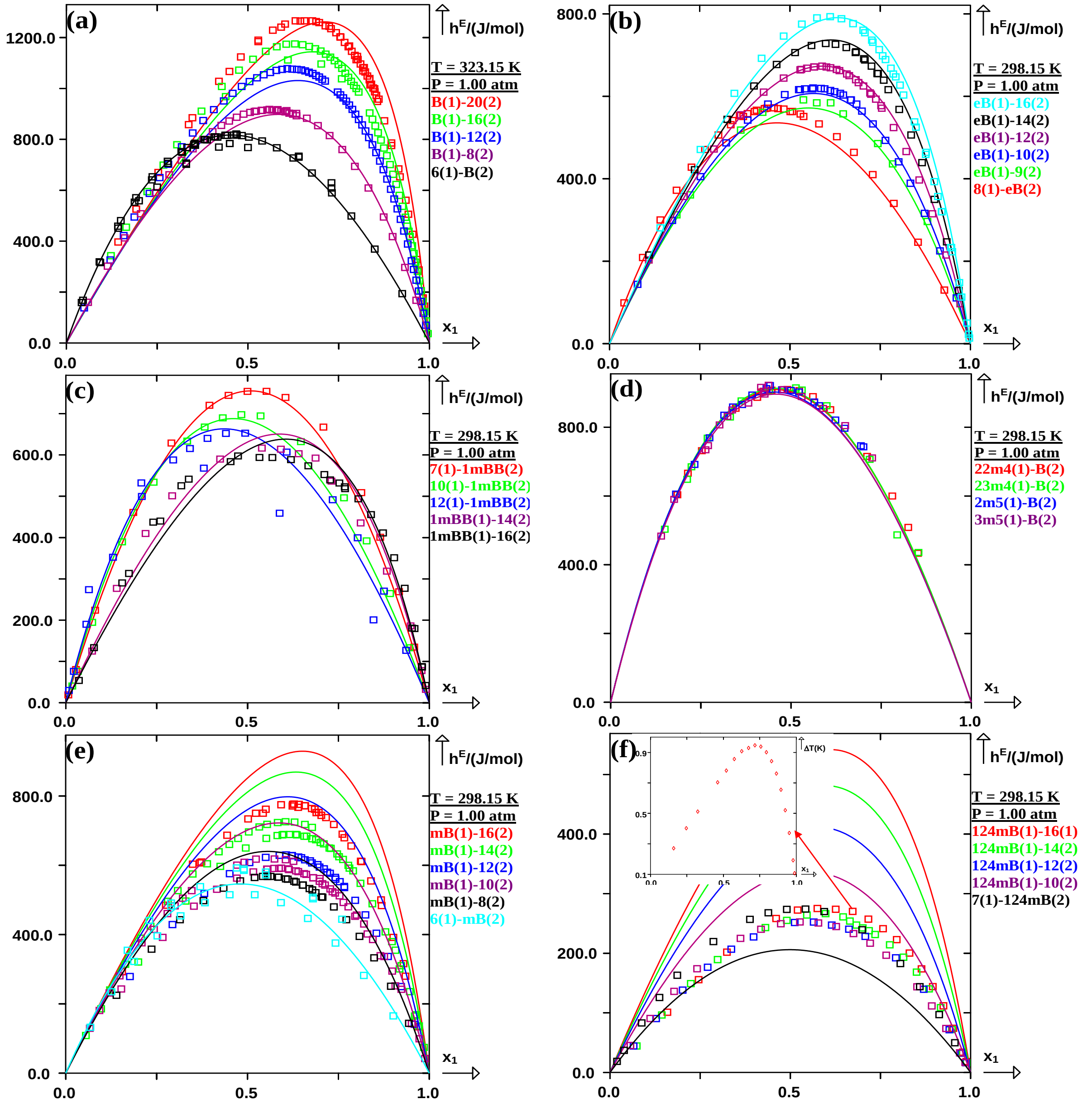

Figure V−8. Prediction of h^E curves in the liquid single-phase region for the binary systems consist of an aromatic and an alkane using the *E*-PPR78 model. (□) experimental h^E points, (◇) temperature changes (ΔT). Solid line: predicted curves with the *E*-PPR78 model. **(a)** Five different systems at T = 323.15 K and under one atmosphere (P = 1.00 atm): (benzene(1) + n-eicosane(2)), (benzene(1) + n-hexadecane(2)), (benzene(1) + n-dodecane(2)), (benzene(1) + n-octane(2)), (n-hexane(1) + benzene(2)). **(b)** Six different systems at T = 298.15 K and under one atmosphere (P = 1.00 atm): (n-octane(1) + ethylbenzene(2)), (ethylbenzene(1) + n-nonane(2)), (ethylbenzene(1) + n-decane(2)), (ethylbenzene(1) + n-dodecane(2)), (ethylbenzene(1) + n-tetradecane(2)), (ethylbenzene(1) + n-hexadecane(2)). **(c)** Five different systems at T = 298.15 K and under one atmosphere (P = 1.00 atm): (n-heptane(1) + 1-methylnaphthalene(2)), (n-decane(1) + 1-methylnaphthalene(2)), (n-dodecane(1) + 1-methylnaphthalene(2)), (1-methylnaphthalene(1) + n-tetradecane(2)), (1-methylnaphthalene(1) + n-hexadecane(2)). **(d)** Four different systems at T = 298.15 K and under one atmosphere (P = 1.00 atm): (2,2-dimethylbutane(1) + benzene(2)), (2,3-dimethylbutane(1) + benzene(2)), (2-methylpentane(1) + benzene(2)), (3-methylpentane(1) + benzene(2)). **(e)** Six different systems at T = 298.15 K and under one atmosphere (P = 1.00 atm): (toluene(1) + n-hexadecane(2)), (toluene(1) + n-tetradecane(2)), (toluene(1) + n-dodecane(2)), (toluene(1) + n-decane(2)), (toluene(1) + n-octane(2)), (n-hexane(1) + toluene(2)). **(f)** Five different systems at T = 298.15 K and under one atmosphere (P = 1.00 atm): (1,2,4-trimethylbenzene(1) + n-hexadecane(2)), (1,2,4-trimethylbenzene(1) + n-tetradecane(2)), (1,2,4-trimethylbenzene(1) + n-dodecane(2)), (1,2,4-trimethylbenzene(1) + n-decane(2)), (n-heptane(1) + 1,2,4-trimethylbenzene(2)) and the temperature changes (ΔT) generated by the uncertainty on h^E for eighteen experimental points of (1,2,4-trimethylbenzene(1) + n-hexadecane(2)).

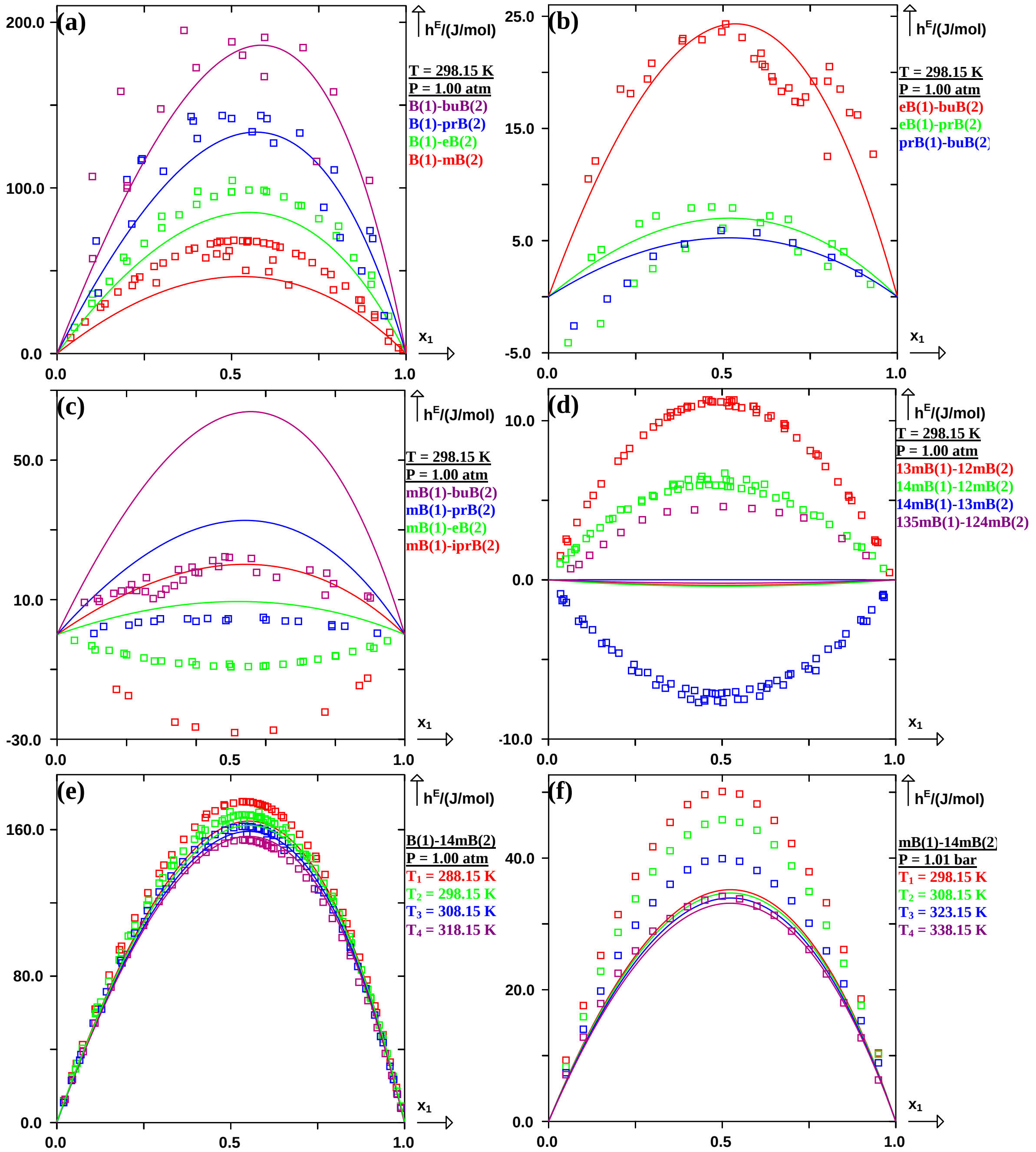

Figure V−9. Prediction of h^E curves in the liquid single-phase region for the binary systems consist of two aromatics using the *E*-PPR78 model. (☐) experimental h^E points. Solid line: predicted curves with the *E*-PPR78 model. **(a)** Four different systems at T = 298.15 K and under one atmosphere (P = 1.00 atm): (benzene(1) + toluene(2)), (benzene(1) + ethylbenzene(2)), (benzene(1) + n-propylbenzene(2)), (benzene(1) + n-butylbenzene(2)). **(b)** Three different systems at T = 298.15 K and under one atmosphere (P = 1.00 atm): (ethylbenzene(1) + n-butylbenzene(2)), (ethylbenzene(1) + n-propylbenzene(2)), (n-propylbenzene(1) + n-butylbenzene(2)). **(c)** Four different systems at T = 298.15 K and under one atmosphere (P = 1.00 atm): (toluene(1) + isopropylbenzene(2)), (toluene(1) + ethylbenzene(2)), (toluene(1) + n-propylbenzene(2)), (toluene(1) + n-butylbenzene(2)). **(d)** Four different systems at T = 298.15 K and under one atmosphere (P = 1.00 atm): (1,3-dimethylbenzene(1) + 1,2-dimethylbenzene(2)), (1,4-dimethylbenzene(1) + 1,2-dimethylbenzene(2)), (1,4-dimethylbenzene(1) + 1,3-dimethylbenzene(2)), (1,3,5-trimethylbenzene(1) + 1,2,4-trimethylbenzene(2)). **(e)** System (benzene(1) + 1,4-dimethylbenzene(2)) under one atmosphere (P = 1.00 atm) and at four different temperatures: T_1 = 288.15 K, T_2 = 298.15 K, T_3 = 308.15 K, T_4 = 318.15 K. **(f)** System (toluene(1) + 1,4-dimethylbenzene(2)) under P = 1.01 bar and at four different temperatures: T_1 = 298.15 K, T_2 = 308.15 K, T_3 = 323.15 K, T_4 = 338.15 K.

V.4.1.3 Binary mixtures containing naphthenes

As shown in figure (V−5), this family presents the highest objective function among seven families investigated, meanwhile, its $\overline{\Delta T}$ is even lower than the average one. This is because some of the h^E values are relatively low and the small magnitude of h^E inevitably increases the objective function. Due to the fact that 8272 experimental points have been collected, it is decided to present the prediction of h^E-x_1 curves in three different figures.

Figure (V−10) shows the predictions of h^E curves for the binary systems which consist of a naphthene and an alkane. The predicted h^E for five different binary mixtures containing cyclohexane and an n-alkane at T = 313.15 K and P = 1.00 atm [see figure (V−10a)] are in close agreement with experimental data. We have to notice that the h^E behavior observed here is very similar to that of the mixtures containing benzene and an n-alkane [see figure (V−8a)], while the magnitude of h^E value here is less important and the predicted h^E-x curve for the mixture containing a long chain n-alkane is less accurate. As shown in figure (V−10b), accurate results are obtained for the mixtures containing 1,1'-bicyclohexyl except that the experimental points of (1,1'-bicyclohexyl(1) + n-hexadecane(2)) are a little underestimated. Figure (V−10c) is the plots of four h^E curves for mixtures containing methylcyclohexane and an n-alkane at T = 298.15 K and P = 1.00 atm, from which we can see that the effect of the chain length of the n-alkane is not well predicted by our model, as a result, only the h^E curves of (methylcyclohexane(1) + n-octane(2)) and (n-heptane(2) + methylcyclohexane (2)) appear to be accurate and the experimental points are overestimated and underestimated for (n-hexane(2) + methylcyclohexane (2)) and (methylcyclohexane (2) + n-decane(2)), respectively. In figures (V−10d,10e), we have plotted the prediction of h^E curves for ten different mixtures. Even though the results of some mixtures are not in good agreement with experimental data, the uncertainties are still acceptable. Furthermore, The h^E curves of (cyclopentane(1) + 2,3-dimethylbutane(2)) under one atmosphere and at three different temperatures [see figure (V−10f)] indicate that the effect of temperature is significant on the small magnitude of h^E, which is well predicted by our model.

Figure (V−11) shows the prediction of h^E curves in the liquid single-phase for the binary systems which consist of a naphthene and an aromatic. Most of the predicted h^E curves are in perfect agreement with experimental data. By looking at the binary systems containing two naphthenes [see figure (V−12)], the results obtained are not very satisfactory, especially for the mixture containing 1,1’-bicyclohexyl or cis-decalin, plotted in figure (V−12e) and figure (V−12f). As discussed previously, the parameters A_{kl} and B_{kl} have no effect on the binary mixtures shown in figures (V−12a,12b). The results of (cyclopentane(1) + cyclooctane(2)) are surprisingly good including the effect of temperature on h^E, while the experimental data of (cyclohexane(1) + cyclooctane(2)) are underestimated and the effect of temperature predicted by our model seems to be wrong. It is important to notice that a small magnitude of h^E value increases the objective function. Moreover, the mixture like (cyclohexane(1) + cis-decalin(2)) shows an endothermic and an exothermic mixing in the cis-decalin-rich and cyclohexane-rich region, respectively [see figure (V−12f)]. For this mixture showing a flexuous h^E behavior, the experimental points close to zero will generate a huge objective function. The same explanation can be applied to the mixtures: (cyclohexane(1) + cyclooctane(2)) and (cyclohexane(1) + methylcyclohexane(2)) shown in figures (V−12b,12c).

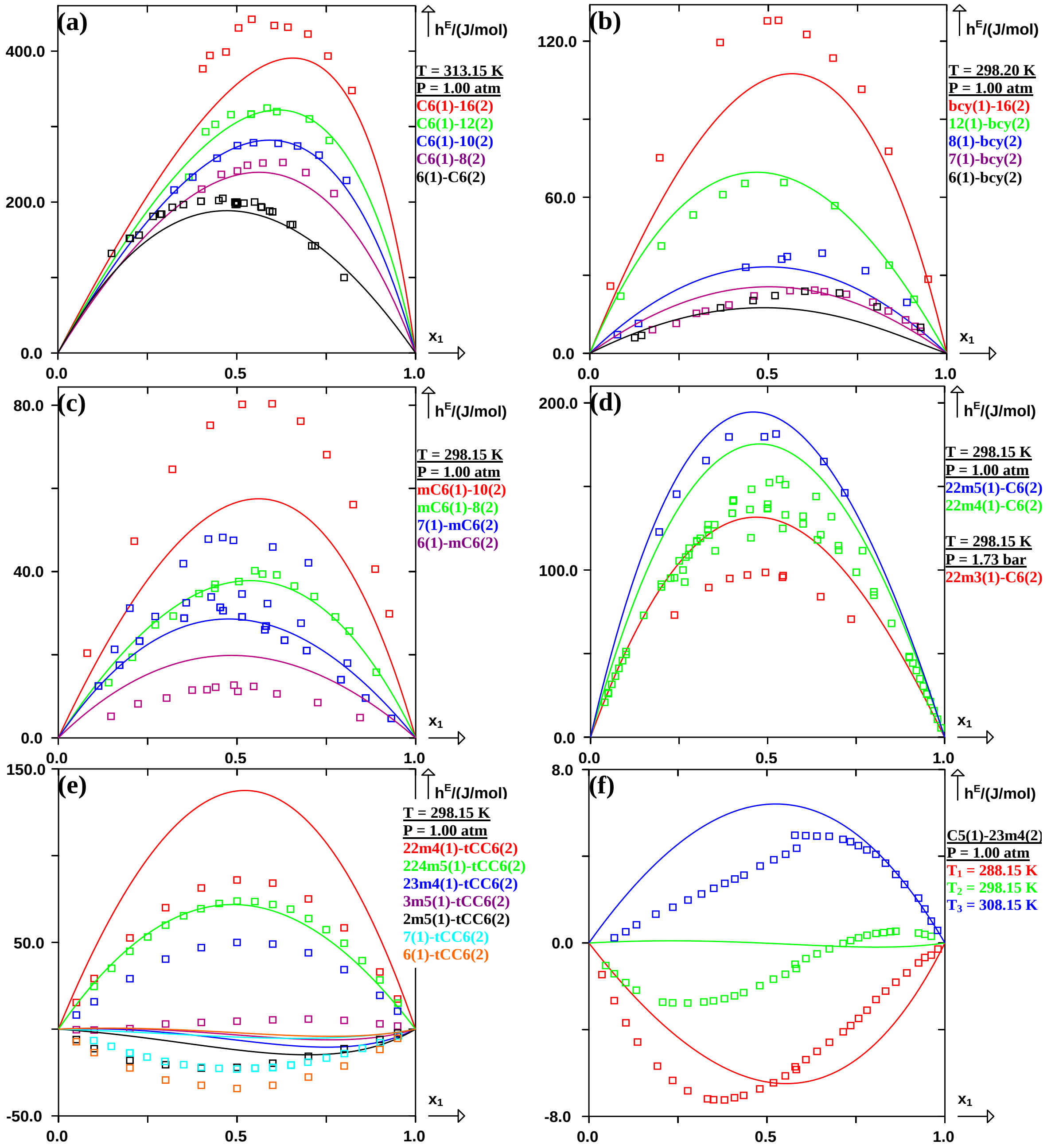

Figure V−10. Prediction of h^E curves in the liquid single-phase region for the binary systems consist of a naphthene and an alkane using the *E*-PPR78 model. (☐) experimental h^E points. Solid line: predicted curves with the *E*-PPR78 model. **(a)** Five different systems at T = 313.15 K and under one atmosphere (P = 1.00 atm): (cyclohexane(1) + n-hexadecane(2)), (cyclohexane(1) + n-dodecane(2)), (cyclohexane(1) + n-decane(2)), (cyclohexane(1) + n-octane(2)), (n-hexane(1) + cyclohexane(2)). **(b)** Four different systems at T = 298.20 K and under one atmosphere (P = 1.00 atm): (1,1'-bicyclohexyl(1) + n-hexadecane(2)), (n-dodecane(1) + 1,1'-bicyclohexyl(2)), (n-octane(1) + 1,1'-bicyclohexyl(2)), (n-heptane(1) + 1,1'-bicyclohexyl(2)), (n-hexane(1) + 1,1'-bicyclohexyl(2)). **(c)** Four different systems at T = 298.15 K and under one atmosphere (P = 1.00 atm): (methylcyclohexane(1) + n-decane(2)), (methylcyclohexane(1) + n-octane(2)), (n-heptane(1) + methylcyclohexane(2)), (n-hexane(1) + methylcyclohexane(2)). **(d)** One system at T = 298.15 K and under P = 1.73 bar: (2,2-dimethylpropane(1) + cyclohexane(2)), and two different systems at T = 298.15 K and under one atmosphere (P = 1.00 atm): (2,2-dimethylbutane(1) + cyclohexane(2)), (2,2-dimethylpentane(1) + cyclohexane(2)). **(e)** Seven different systems at T = 298.15 K and under one atmosphere (P = 1.00 atm): (2,2-dimethylbutane(1) + trans-decalin(2)), (2,2,4-trimethylpentane(1) + trans-decanlin(2)), (2,3-dimethylbutane(1) + trans-decalin(2)), (3-methylpentane(1) + trans-decalin(2)), (2-methylpentane(1) + trans-decalin(2)), (n-heptane(1) + trans-decalin(2)), (n-hexane(1) + trans-decalin(2)). **(f)** System (cyclopentane(1) + 2,3-dimethylbutane(2)) under one atmosphere (P = 1.00 atm) and at three different temperatures: T_1 = 288.15 K, T_2 = 298.15 K, T_3 = 308.15 K.

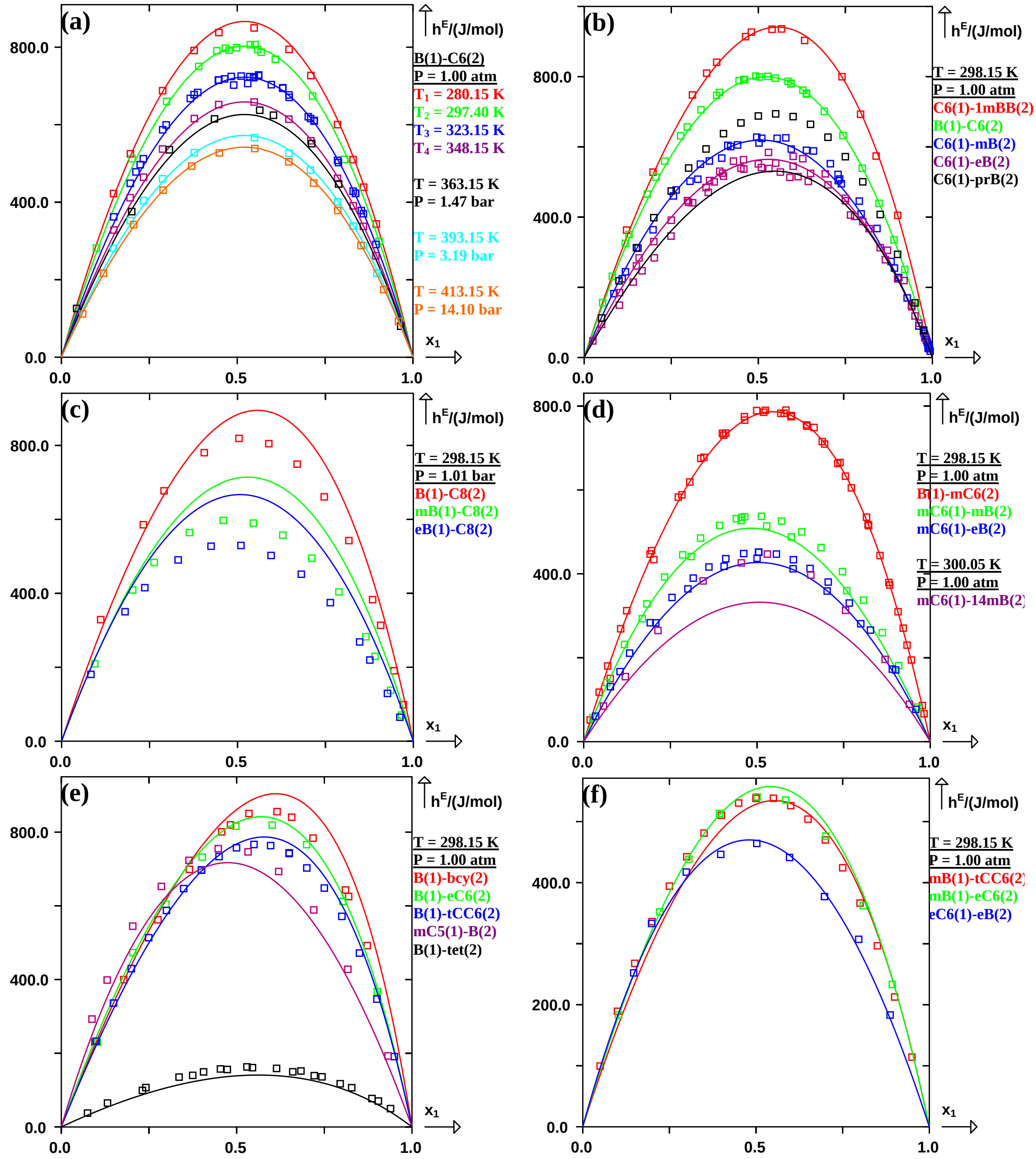

Figure V−11. Prediction of h^E curves in the liquid single-phase region for the binary systems consist of a naphthene and an aromatic using the *E*-PPR78 model. (☐) experimental h^E points. Solid line: predicted curves with the *E*-PPR78 model. **(a)** System (benzene(1) + cyclohexane(2)) under one atmosphere (P = 1.00 atm) and at four different temperatures: T_1 = 280.15 K, T_2 = 297.40 K, T_3 = 323.15 K, T_4 = 348.15 K, under P = 1.47 bar and at T = 363.15 K, under P = 3.19 bar and at T = 393.15 K, under P = 14.10 bar and at T = 413.15 K. **(b)** Five different systems at T = 298.15 K and under one atmosphere (P = 1.00 atm): (cyclohexane(1) + 1-methylnaphthalene(2)), (benzene(1) + cyclohexane(2)), (cyclohexane(1) + toluene(2)), (cyclohexane(1) + ethylbenzene(2)), (cyclohexane(1) + n-propylbenzene(2)). **(c)** Three different systems at T = 298.15 K and under P = 1.01 bar: (benzene(1) + cyclooctane(2)), (toluene(1) + cyclooctane(2)), (ethylbenzene(1) + cyclooctane(2)). **(d)** Three different systems at T = 298.15 K and under one atmosphere (P = 1.00 atm): (benzene(1) + methylcyclohexane(2)), (methylcyclohexane(1) + toluene(2)), (methylcyclohexane(1) + ethylbenzene(2)), one system at T = 300.05 K and under one atmosphere (P = 1.00 atm): (methylcyclohexane(1) + 1,4-dimethylbenzene(2)). **(e)** Five different systems at T = 298.15 K and under one atmosphere (P = 1.00 atm): (benzene(1) + 1,1’-bicyclohexyl(2)), (benzene(1) + ethylcyclohexane(2)), (benzene(1) + trans-decalin(2)), (methylcyclopentane(1) + benzene(2)), (benzene(1) + tetralin(2)). **(f)** Three different systems at T = 298.15 K and under one atmosphere (P = 1.00 atm): (toluene(1) + trans-decalin(2)), (toluene(1) + ethylcyclohexane(2)), (ethylcyclohexane(1) + ethylbenzene(2)).

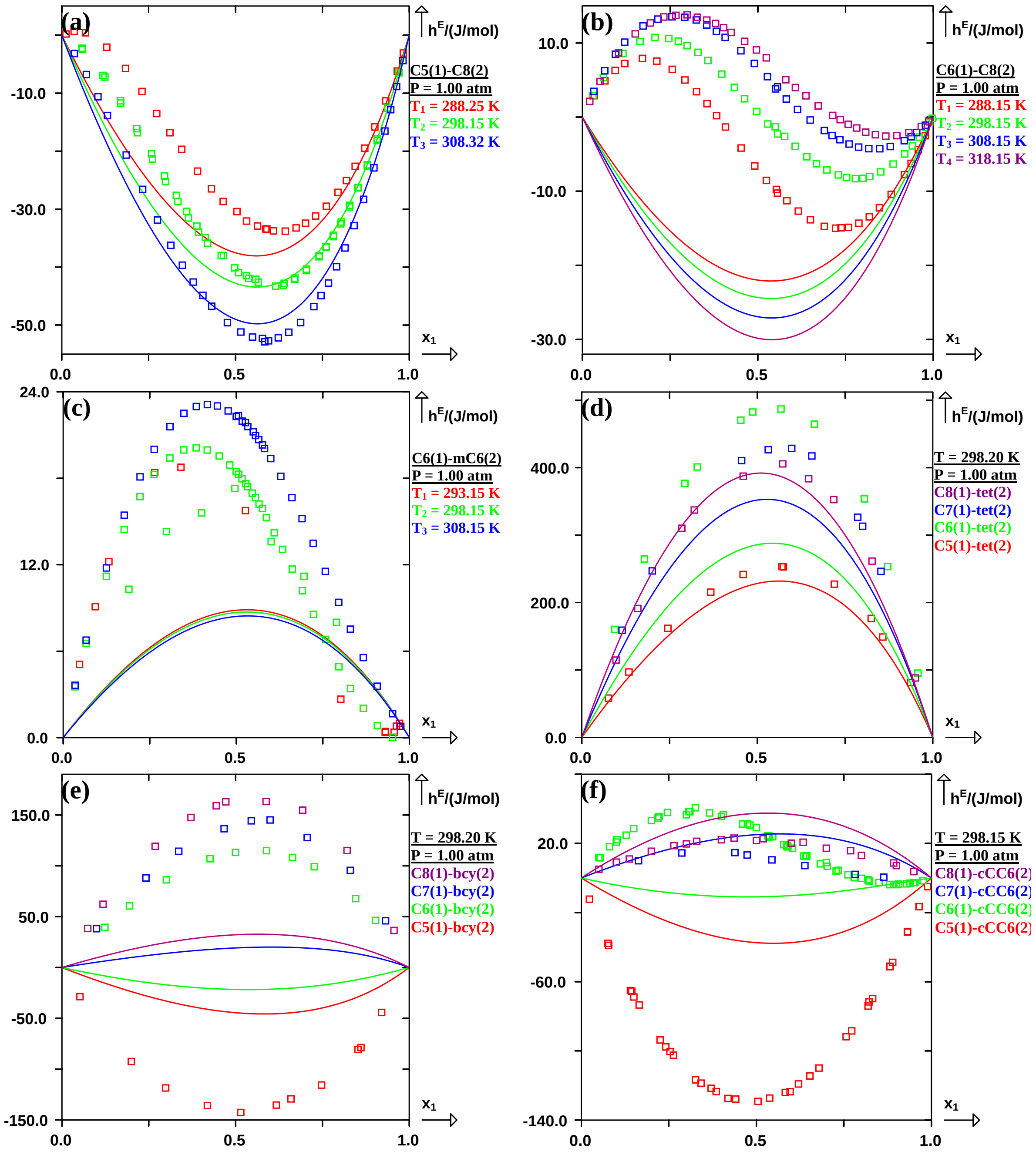

Figure V−12. Prediction of h^E curves in the liquid single-phase region for the binary systems consist of two naphthenes using the *E*-PPR78 model. (☐) experimental h^E points. Solid line: predicted curves with the *E*-PPR78 model. **(a)** System (cyclopentane(1) + cyclooctane(2)) under one atmosphere (P = 1.00 atm) and at three different temperatures: T_1 = 288.25 K, T_2 = 298.15 K, T_3 = 308.32 K. **(b)** System (cyclohexane(1) + cyclooctane(2)) under one atmosphere (P = 1.00 atm) and at four different temperatures: T_1 = 288.15 K, T_2 = 298.15 K, T_3 = 308.15 K, T_4 = 318.15 K. **(c)** System (cyclohexane(1) + methylcyclohexane(2)) under one atmosphere (P = 1.00 atm) and at three different temperatures: T_1 = 293.15 K, T_2 = 298.15 K, T_3 = 308.15 K. **(d)** Four different systems at T = 298.20 K and under one atmosphere (P = 1.00 atm): (cyclopentane(1) + tetralin(2)), (cyclohexane(1) + tetralin(2)), (cycloheptane(1) + tetralin(2)), (cyclooctane(1) + tetralin(2)). **(e)** Four different systems at T = 298.20 K and under one atmosphere (P = 1.00 atm): (cyclopentane(1) + 1,1’-bicyclohexyl(2)), (cyclohexane(1) + 1,1’-bicyclohxyl(2)), (cycloheptane(1) + 1,1’-bicyclohexyl(2)), (cyclooctane(1) + 1,1’-bicyclohexyl(2)). **(f)** Four different systems at T = 298.15 K and under one atmosphere (P = 1.00 atm): (cyclopentane(1) + cis-decalin(2)), (cyclohexane(1) + cis-decalin(2)), (cycloheptane(1) + cis-decalin(2)), (cyclooctane(1) + cis-decalin(2)).

V.4.1.4 Binary mixtures containing CO_2 (or mercaptans, or ethylene)

Figure (V−13) presents the predictions of h^E curves in the liquid single-phase for the binary systems containing CO_2 (or mercaptans, or ethylene). Considering the mixtures containing CO_2 for which the average value of the temperature changes ($\overline{\Delta T}$) is the highest among the families investigated [see figure (V−5b)], we have plotted in figures (V−13a,13b,13c) the h^E-x curves of such mixtures. As shown in figure (V−13a), the predicted h^E curves of (CO_2(1) + ethane(2)) at T = 272.10 K and under two different pressures are in close agreement with experimental data. Meanwhile, the results of (CO_2(1) + toluene(2)) at T = 298.15 K which is 6 K below than the critical temperature of CO2 (T_C = 304.20 K) and under two different pressures, become less accurate, especially for the h^E curve at P = 106.00 bar [see figure (V−13b)]. As for the mixture (CO_2(1) + n-decane(2)) at T = 303.15 K which is just 1 K below the critical temperature of CO_2 and under two different pressures, both the two h^E curves are underestimated by our model, and the average value of the temperature changes for 48 experimental points shown in figure (V−13c) is: $\overline{\Delta T}$ = 2.40 K. In the open literature, 246 experimental points are available for the mixtures containing mercaptans and perfect results are obtained for four binary mixtures containing n-butyl mercaptans at T = 298.15 K and under P = 5.00 bar, as shown in figure (V−13d). Figures (V−13e,13f) give the h^E-x plots for the two binary mixtures containing ethylene. Reasonable results are obtained for the mixture (methane(1) + ethylene(2)). By looking at (ethylene(1) + propane(2)) at T = 273.15 K and under four different pressures, the effect of pressure on h^E value is correctly predicted and the h^E-x curve at P = 100.00 bar is perfectly reproduced. In general, the experimental points of the mixtures containing ethylene are predicted with acceptable accuracy.

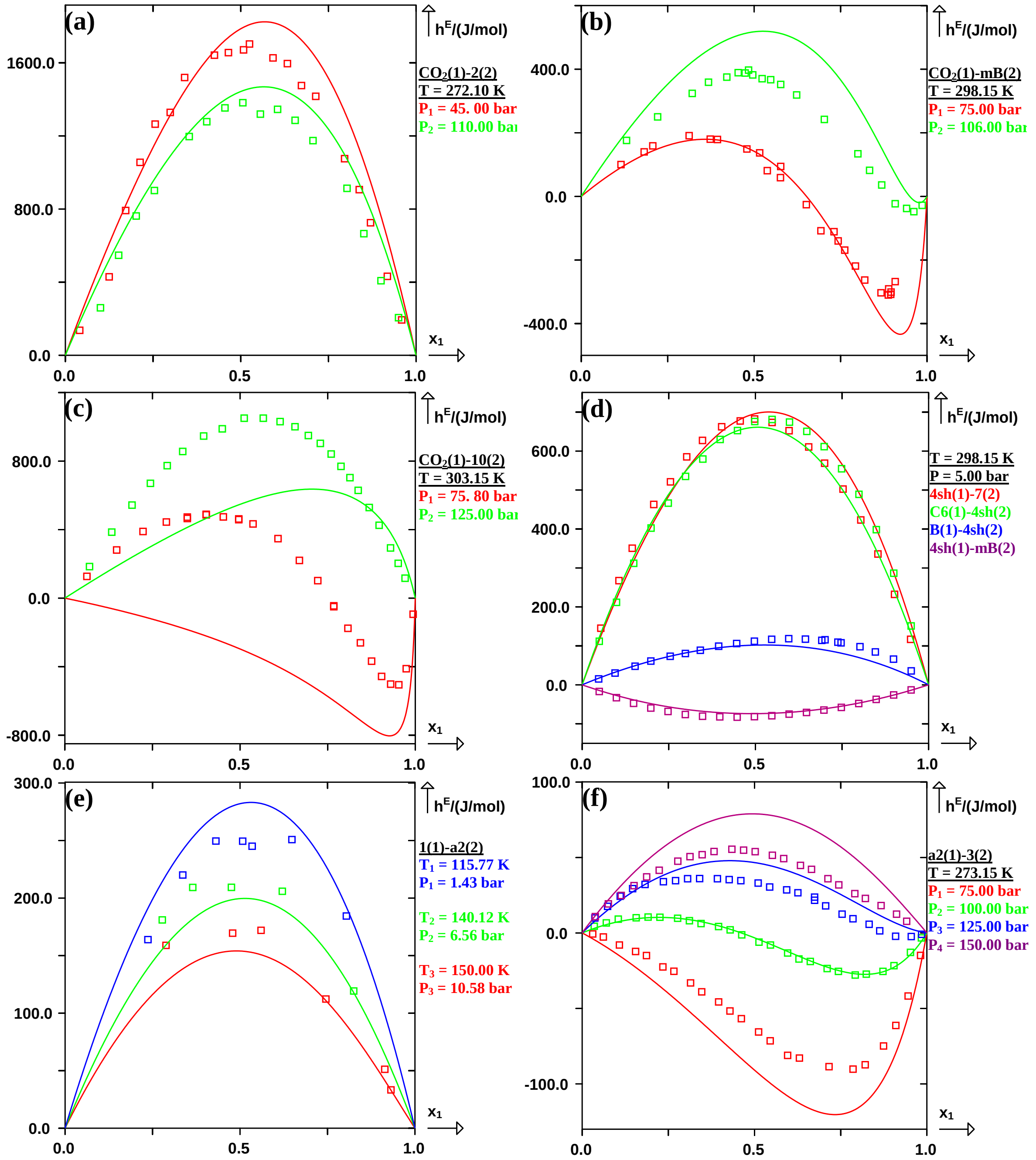

Figure V−13. Prediction of h^E curves in the liquid single-phase region for the binary systems containing CO_2 (or mercaptans, or ethylene) using the *E*-PPR78 model. (☐) experimental h^E points. Solid line: predicted curves with the *E*-PPR78 model. **(a)** System (CO_2(1) + ethane(2)) at T = 272.10 K and under two different pressures: P_1 = 45.00 bar, P_2 = 110.00 bar. **(b)** System (CO_2(1) + toluene(2)) at T = 298.15 K and under two different pressures: P_1 = 75.00 bar, P_2 = 106.00 bar. **(c)** System (CO_2(1) + n-decane(2)) at T = 303.15 K and under two different pressures: P_1 = 75.80 bar, P_2 = 125.00 bar. **(d)** Four different systems at T = 298.15 K and under P = 5.00 bar: (n-butyl mercaptan(1) + n-heptane(2)), (cyclohexane(1) + n-butyl mercaptan(2)), (benzene(1) + n-butyl mercaptan(2)), (n-butyl mercaptan(1) + toluene(2)). **(e)** System (methane(1) + ethylene(2)) at T_1 = 150.00 K and P_1 = 10.58 bar, T_2 = 140.12 K and P_2 = 6.56 bar, T_3 = 115.77 K and P_3 = 1.43 bar. **(f)** System (ethylene(1) + propane(2)) at T = 273.15 K and under four different pressures: P_1 = 75.00 bar, P_2 = 100.00 bar, P_3 = 125.00 bar, P_4 = 150.00 bar.

V.4.1.5 Binary mixtures containing alkenes

Figure (V−14) shows the predictions of h^E curves for the binary systems containing linear alkenes (one double bond or two double bonds). Considering the mixtures which consist of a 1-alkene and its corresponding n-alkane, we have plotted five h^E-x curves for these mixtures at T = 298.15 K and P = 1.00 atm [see figure (V−14a)]. Obvious scatters can be observed for the mixture (1-heptene(1) + n-heptane(2)) and it is interesting to notice that the h^E value is a decreasing function of the carbon number of 1-alkene (or n-alkane). Although the experimental data are underestimated by our model, the uncertainty seems to be reasonable. As plotted in figure (V−14b), perfect results are obtained for the mixtures containing 1-hexene and a branched-alkane, as well as the mixtures containing a 1-alkene and a naphthenic compound [see figure (V−14c)]. The prediction of h^E curves for four binary mixtures containing two linear alkenes are plotted in figure (V−14d), from which we can see that it is really difficult to well predict the h^E behavior for these mixtures where the volatility of two components is very close. In figures (V−14e,14f), we have plotted the h^E-x curves for the mixtures consisting of an alkene and benzene (or cyclohexane). Reasonable results are obtained by our model and the mixtures containing benzene are a little better predicted than those containing cyclohexane.

Figure (V−15) shows the h^E curves for the binary systems containing branched alkenes (or cycloalkenes) in the liquid single-phase region. Only 241 points are available for the mixture containing branched alkenes. It is therefore an easy task for our model to properly represent these experimental points with a good accuracy [see figures (V−15a,15b)]. In figure (V−15c), we have plotted the h^E-x curves for five different binary mixtures which consist of cyclohexene and n-alkane at T = 298.15 K and under one atmosphere. Perfect results are obtained for the mixtures containing a normal n-alkane (n-octane, n-decane and n-dodecane), while the prediction appears to be less accurate as the chain length of n-alkane increases. The prediction of h^E curves for the other 10 mixtures [see figures (V−15d,15e,15f)] indicates that our model is capable to give a good representation of h^E for the mixtures containing cycloalkenes.

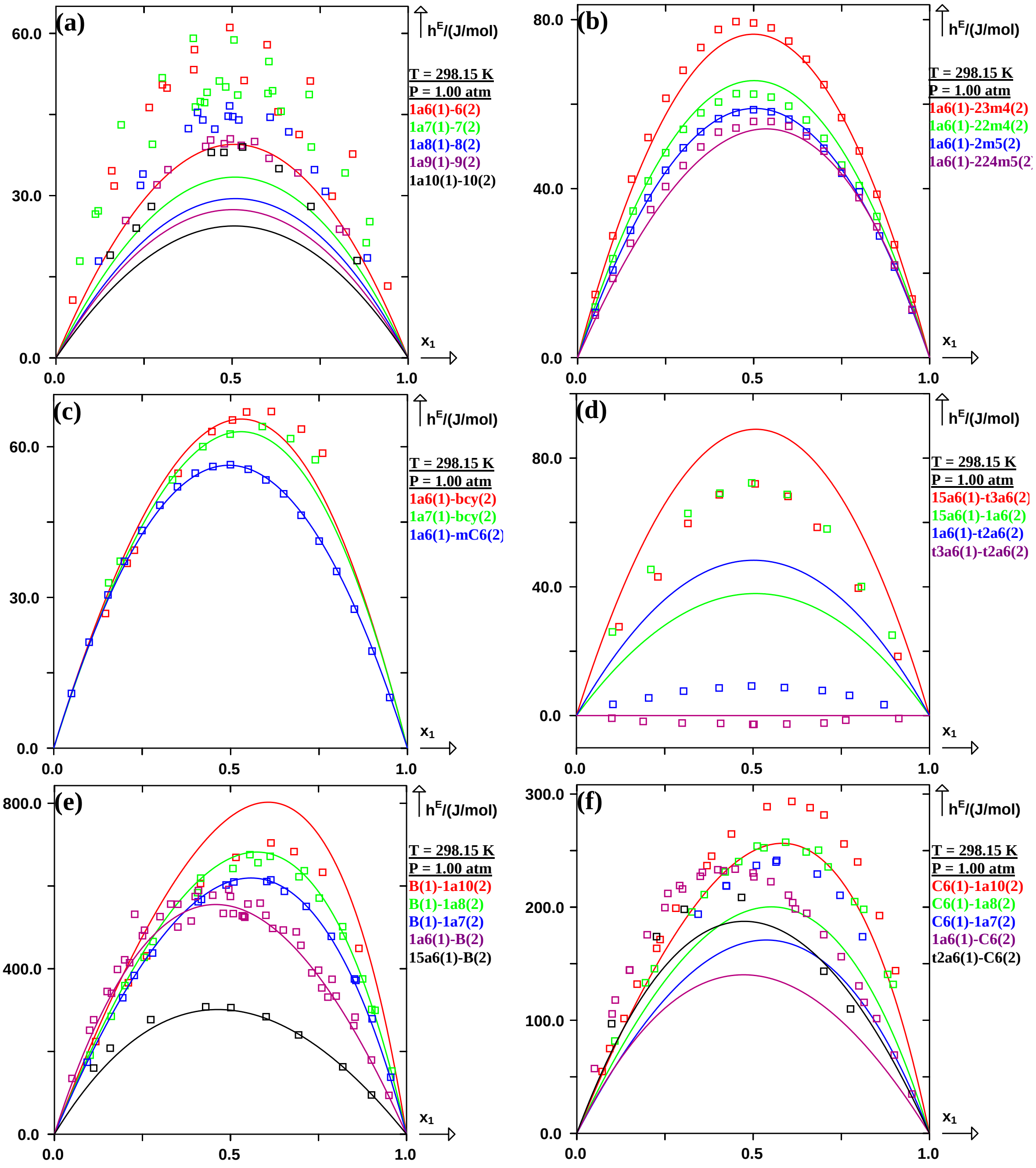

Figure V−14. Prediction of h^E curves in the liquid single-phase region for the binary systems containing linear alkenes using the *E*-PPR78 model. (☐) experimental h^E points. Solid line: predicted curves with the *E*-PPR78 model. **(a)** Five different systems at T = 298.15 K and under one atmosphere (P = 1.00 atm): (1-hexene(1) + n-hexane(2)), (1-heptene(1) + n-heptane(2)), (1-octene(1) + n-octane(2)), (1-nonene(1) + n-nonane(2)), (1-decene(1) + n-decane(2)). **(b)** Four different systems at T = 298.15 K and under one atmosphere (P = 1.00 atm): (1-hexene(1) + 2,3-dimethylbutane(2)), (1-hexene(1) + 2,2-dimethylbutane(2)), (1-hexene(1) + 2-methylpentane(2)), (1-hexene(1) + 2,2,4-trimethylpentane(2)). **(c)** Three different systems at T = 298.15 K and under one atmosphere (P = 1.00 atm): (1-hexene(1) + 1,1'-bicyclohexyl(2)), (1-heptene(1) + 1,1'-bicyclohexyl(2)), (1-hexene(1) + methylcyclohexane(2)). **(d)** Four different systems at T = 298.15 K and under one atmosphere (P = 1.00 atm): (1,5-hexadiene(1) + trans-3-hexene(2)), (1,5-hexadiene(1) + 1-hexene(2)), (1-hexene(1) + trans-2-hexene(2)), (trans-3-hexene(1) + trans-2-hexene(2)). **(e)** Five different systems at T = 298.15 K and under one atmosphere (P = 1.00 atm): (benzene(1) + 1-decene(2)), (benzene(1) + 1-octene(2)), (benzene(1) + 1-heptene(2)), (1-hexene(1) + benzene(2)), (1,5-hexadiene(1) + benzene(2)). **(f)** Five different systems at T = 298.15 K and under one atmosphere (P = 1.00 atm): (cyclohexane(1) + 1-decene(2)), (cyclohexane(1) + 1-octene(2)), (cyclohexane(1) + 1-heptene(2)), (1-hexene(1) + cyclohexane(2)), (trans-2-hexene(1) + cyclohexane(2)).

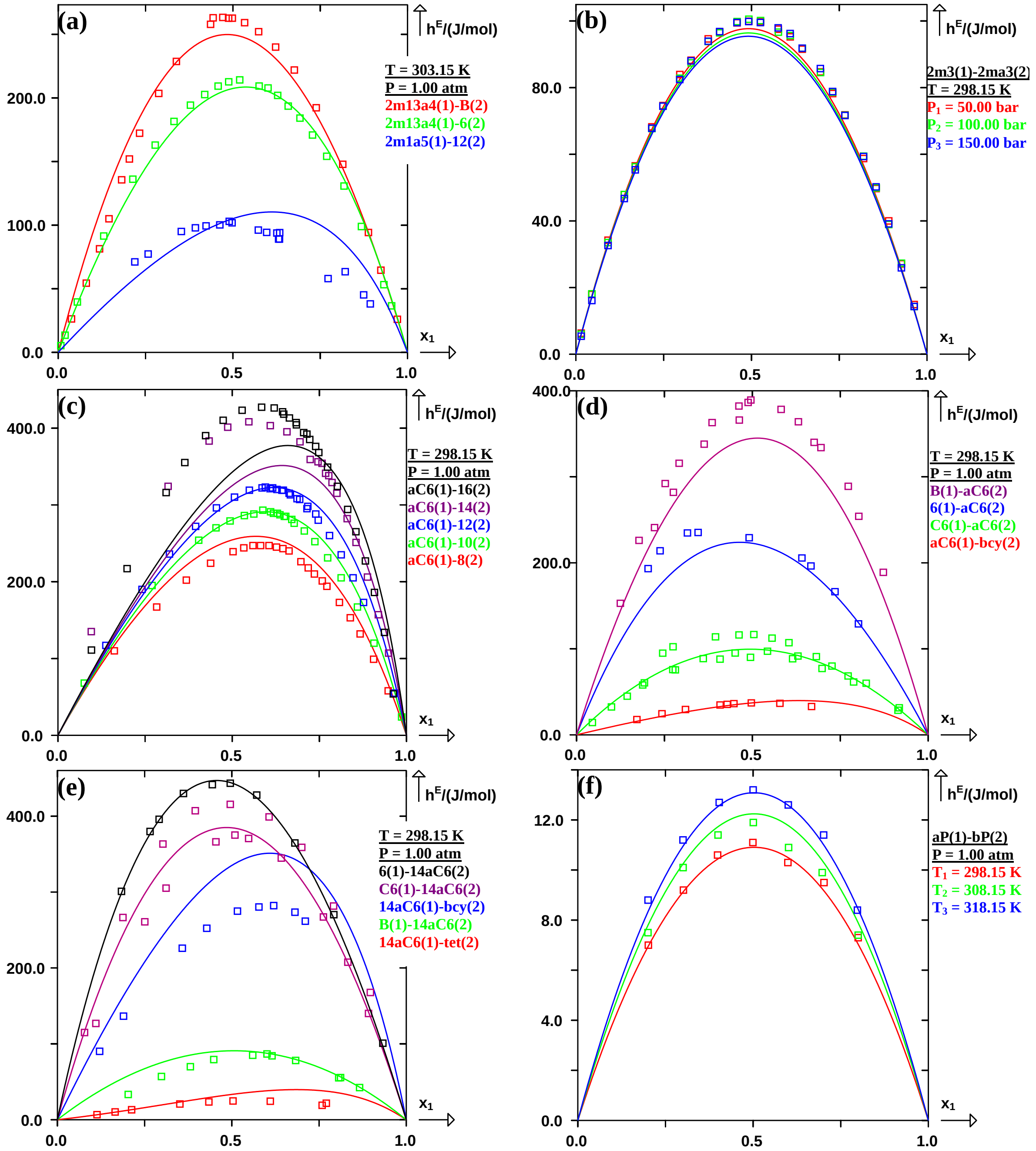

Figure V−15. Prediction of h^E curves in the liquid single-phase region for the binary systems containing branched alkenes (or cycloalkenes) using the *E*-PPR78 model. (☐) experimental h^E points. Solid line: predicted curves with the *E*-PPR78 model. **(a)** Three different systems at T = 303.15 K and under one atmosphere (P = 1.00 atm): (2-methyl-1,3-butadiene(1) + benzene(2)), (2-methyl-1,3-butadiene(1) + n-hexane(2)), (2-methyl-1-pentene(1) + n-dodecane(2)). **(b)** System (2-methylpropane(1) + 2-methylpropene(2)) at T = 298.15 K and under three different pressures: P_1 = 50.00 bar, P_2 = 100.00 bar, P_3 = 150.00 bar. **(c)** Five different systems at T = 298.15 K and under one atmosphere (P = 1.00 atm): (cyclohexene(1) + n-octane(2)), (cyclohexene(1) + n-decane(2)), (cyclohexene(1) + n-dodecane(2)), (cyclohexene(1) + n-tetradecane(2)), (cyclohexene(1) + n-hexadecane(2)). **(d)** Four different systems at T = 298.15 K and under one atmosphere (P = 1.00 atm): (cyclohexene(1) + 1,1'-bicyclohexyl(2)), (cyclohexane(1) + cyclohexene(2)), (n-hexane(1) + cyclohexene(2)), (benzene(1) + cyclohexene(2)). **(e)** Five different systems at T = 298.15 K and under one atmosphere (P = 1.00 atm): (1,4-cyclohexadiene(1) + tetralin(2)), (benzene(1) + 1,4-cyclohexadiene(2)), (1,4-cyclohexadiene(1) + 1,1'-bicyclohexyl(2)), (cyclohexane(1) + 1,4-cyclohexadiene(2)), (n-hexane(1) + 1,4-cyclohexadiene(2)). **(f)** System (alpha-pinene(1) + beta-pinene(2)) under one atmosphere (P = 1.00 atm) and at three different temperaures: T_1 = 298.15 K, T_2 = 308.15 K, T_3 = 318.15 K.

V.4.2 Results of excess molar enthalpy (h^E) in the gaseous single-phase region

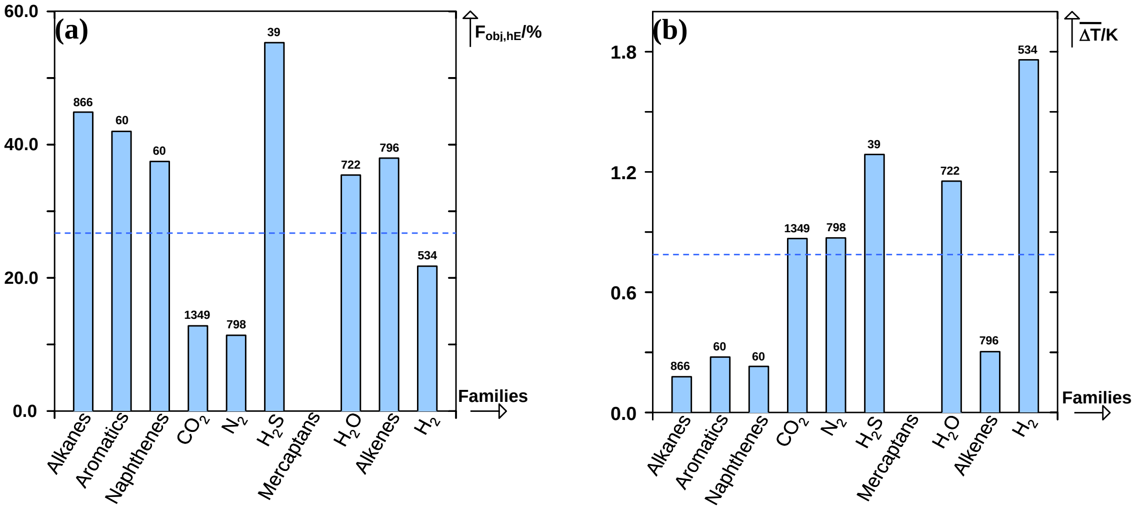

Figure V−16. (a) Histogram of the objective functions of h^E in the gaseous single-phase region for ten families of binary systems, with the number of experimental points on top. **(b)** Histogram of the average value of temperature changes generated by the uncertainty on the predicted h^E in the gaseous single-phase region for ten families of binary systems, with the number of experimental points on top.

In the open literature, only 55 binary mixtures present experimental h^E in the gaseous single-phase region, nevertheless, 5224 experimental points have been collected. For all the experimental points in the gaseous single-phase region, the objective function is: $F_{obj,hE}$ = 26.70% [blue dashed line in figure (V−16a)]. The objective function here is much lower than the one obtained in the previous case (h^E in the liquid single-phase region), however, the average value of temperature changes ($\overline{\Delta T}$ = 0.79 K) obtained here is 4 times higher. It can be argued that the mixture in the liquid state (always in sub-critical region) exhibits small or moderate endothermic (or exothermic) mixing, whereas, the mixture in the gaseous state could be in both the sub-critical and super-critical regions. We have observed that the mixture exhibits huge or moderate endothermic effects if the mixing takes place in the vicinity of the critical point of the pure component and otherwise, the mixture exhibits small or moderate endothermic mixing. Because quite a good deal of experimental points in the gaseous state are measured at temperatures close to the critical temperature of the pure component, and at different pressures, the huge experimental h^E value will make our objective function (relative deviations) less important and at the same time, the absolute deviation (difference between the calculated value and the experimental one) being more significant will inevitably increase the average value of temperature changes ($\overline{\Delta T}$). This explanation can be applied to the family of binary mixtures containing CO_2 (or N_2, or H_2) shown in figure (V−16b), displaying $F_{obj,hE}$ lower than the average one with $\overline{\Delta T}$ greater than the average one.

In order to clearly illustrate the results obtained by our model, we have defined two different temperature ranges: $T < T_{C2}$ where the temperatures (T) are lower than the critical temperature of the less volatile component (T_{C2}) and $T > T_{C2}$ where the temperatures (T) are higher than the critical temperature of the less volatile component (T_{C2}).

V.4.2.1 h^E in the gaseous state over the temperature range: $T < T_{C2}$

Figures (V−17,18,19) present the predictions of h^E curves in the gaseous state where the temperatures (T) investigated are below the critical temperature of the less volatile component (T_{C2}).

As shown in figure (V−17), it is really difficult to predict accurately the h^E behavior while $T < T_{C2}$ and under low pressures, for the binary mixtures which exhibit small endothermic mixings. Most of the 215 experimental h^E points are underestimated ($F_{obj,hE}$ = 40.20 %), however, the temperature changes are very small ($\overline{\Delta T}$ = 0.16 K). On the other hand, regarding the h^E-x curves of two binary mixtures containing CO_2 [see figures (V−18a,18b)] at T = 293.15 K which is a little below the critical temperature of CO_2 (T_C = 304.12 K), the h^E increase from low values to moderate values as the pressure increases for both mixtures. Moreover, the prediction of h^E curves seems to be more accurate ($F_{obj,hE}$ = 18.05 % for these 85 points). Meanwhile, the average value of temperature changes become more significant ($\overline{\Delta T}$ = 0.73 K) due to the relatively higher uncertainty on the predicted h^E at higher pressures. In addition, the prediction of h^E curves at the pressures near the critical pressure of CO_2 (P_C = 73.74 bar) has not been examined because of the absence of experimental data.

In figure (V−18c), we have plotted the h^E-y curves for six different binary mixtures consisting of methane and an n-alkanes, under one atmosphere, where most of the experimental points are underestimated by our model. Acceptable results are obtained for the mixture (methane(1) + ethane(2)) at T = 303.20 K which is slightly below the critical temperature of ethane (T_C = 305.32 K) and the mixture (methane(1) + n-butane(2)) at T = 394.30 K near the critical temperature of n-butane (T_C = 425.15 K). Figure (V−18d) presents the h^E behavior for six binary mixtures containing n-octane at T = 403.20 K being far away from the critical temperature of n-octane (T_C = 568.70 K), from which we observe that most of the experimental points are underestimated by our model and better results can be obtained if the mixtures are less asymmetric (n-heptane(1) + n-octane(2)). Considering the mixture (methane(1) + H_2S(2)) at T = 305.15 K and under three different pressures, shown in figure

(V−18e), the h^E curve at P = 5.07 bar are predicted with acceptable uncertainty, however, it becomes much worse at P = 15.20 bar. The effect of pressure on h^E predicted here is far away from accuracy and that is why the objective function and the average value of temperature changes are very high for the family of the mixture containing H_2S (methane(1) + H_2S(2) only) [see figure (V−16)].

As shown in figure (V−19a), the predictions of h^E-y curves of the mixtures containing H_2O at T = 373.20 K and under one atmosphere, are more or less accurate except for the very asymmetric system: (methane(1) + H_2O(2)). This is confirmed by the results of the other two mixtures: (H_2O(1) + cyclohexane(2)) (less asymmetric) and (N_2(1) + H_2O(2)) (more asymmetric) under P = 1.01 bar and at different temperatures [see figures (V−19b,19c)]. Obviously, these asymmetric systems result in significant objective function. Considering the h^E-y curves of (H_2O(1) + n-heptane(2)) [see figures (V−19d,19e)] at three different pressure-temperature points in the super-critical region of n-heptane, huge endothermic mixings can be observed. The objective function for these 15 experimental points in figure (V−19e) is only 10.65%, however, the average value of temperature changes arrives at 3.46 K. At the same time, we have to notice that the large objective function and high average value of temperature changes for the family of binary mixtures containing H_2 [see figure (V−16)] are caused by the mixture (H_2(1) + H_2O(2)).

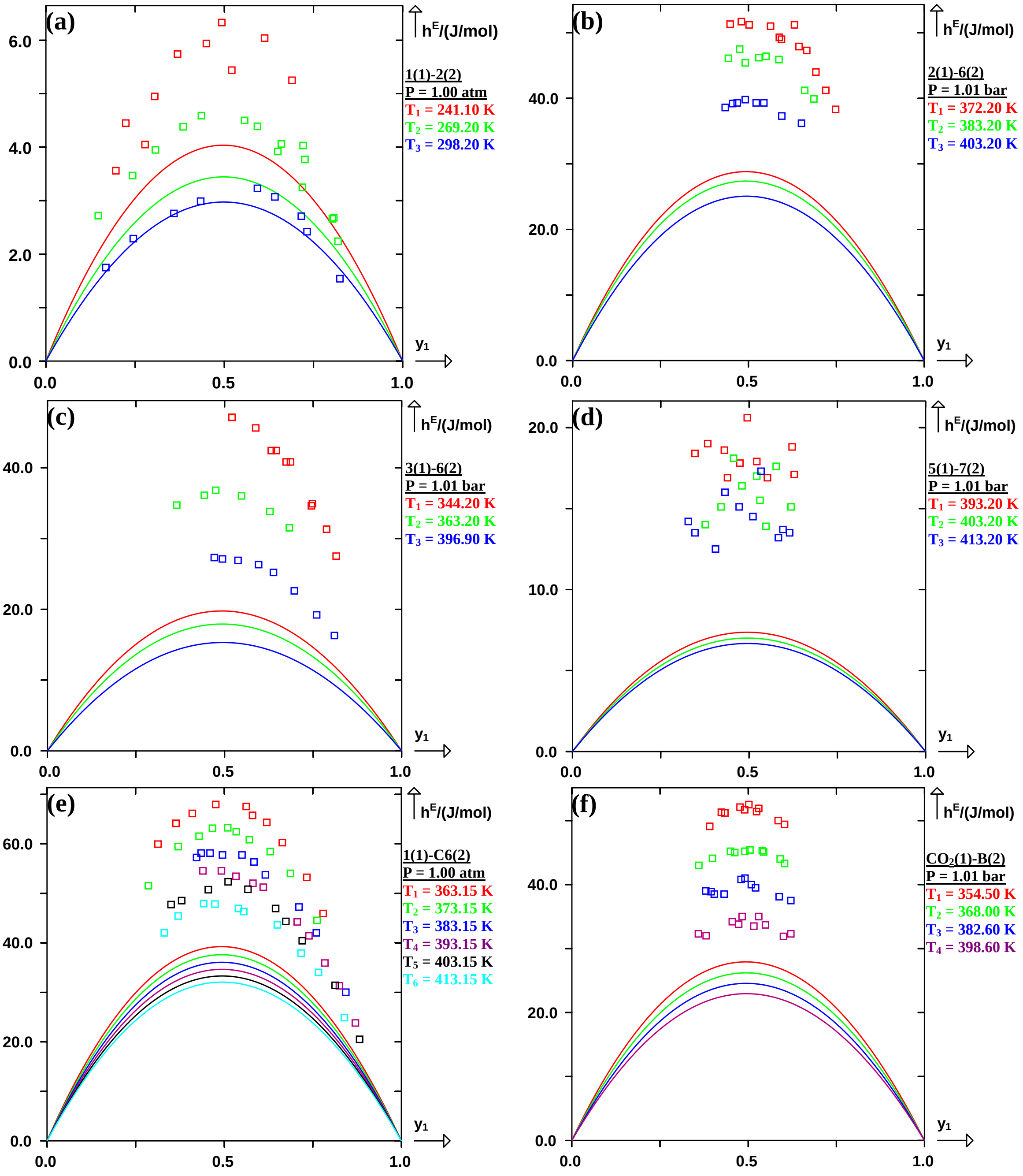

Figure V−17. Prediction of h^E curves in the gaseous single-phase region for the binary systems using the *E*-PPR78 model. (☐) experimental h^E points. Solid line: predicted curves with the *E*-PPR78 model. **(a)** System (methane(1) + ethane(2)) under one atmosphere (P = 1.00 atm) and at three different temperatures: T_1 = 241.10 K, T_2 = 269.20 K, T_3 = 298.20 K. **(b)** System (ethane(1) + hexane(2)) under P = 1.01 bar and at three different temperatures: T_1 = 372.20 K, T_2 = 383.20 K, T_3 = 403.20 K. **(c)** System (propane(1) + n-hexane(2)) under P = 1.01 bar and at three different temperatures: T_1 = 344.20 K, T_2 = 363.20 K, T_3 = 396.90 K. **(d)** System (n-pentane(1) + n-heptane(2)) under P = 1.01 bar and at three different temperatures: T_1 = 393.20 K, T_2 = 403.20 K, T_3 = 413.20 K. **(e)** System (methane(1) + cyclohexane(2)) under one atmosphere (P = 1.00 atm) and at six different temperatures: T_1 = 363.15 K, T_2 = 373.15 K, T_3 = 383.15 K, T_4 = 393.15 K, T_5 = 403.15 K, T_6 = 413.15 K. **(f)** System (CO_2(1) + benzene(2)) under P = 1.01 bar and at four different temperatures: T_1 = 354.50 K, T_2 = 368.00 K, T_3 = 382.60 K, T_4 = 398.60 K.

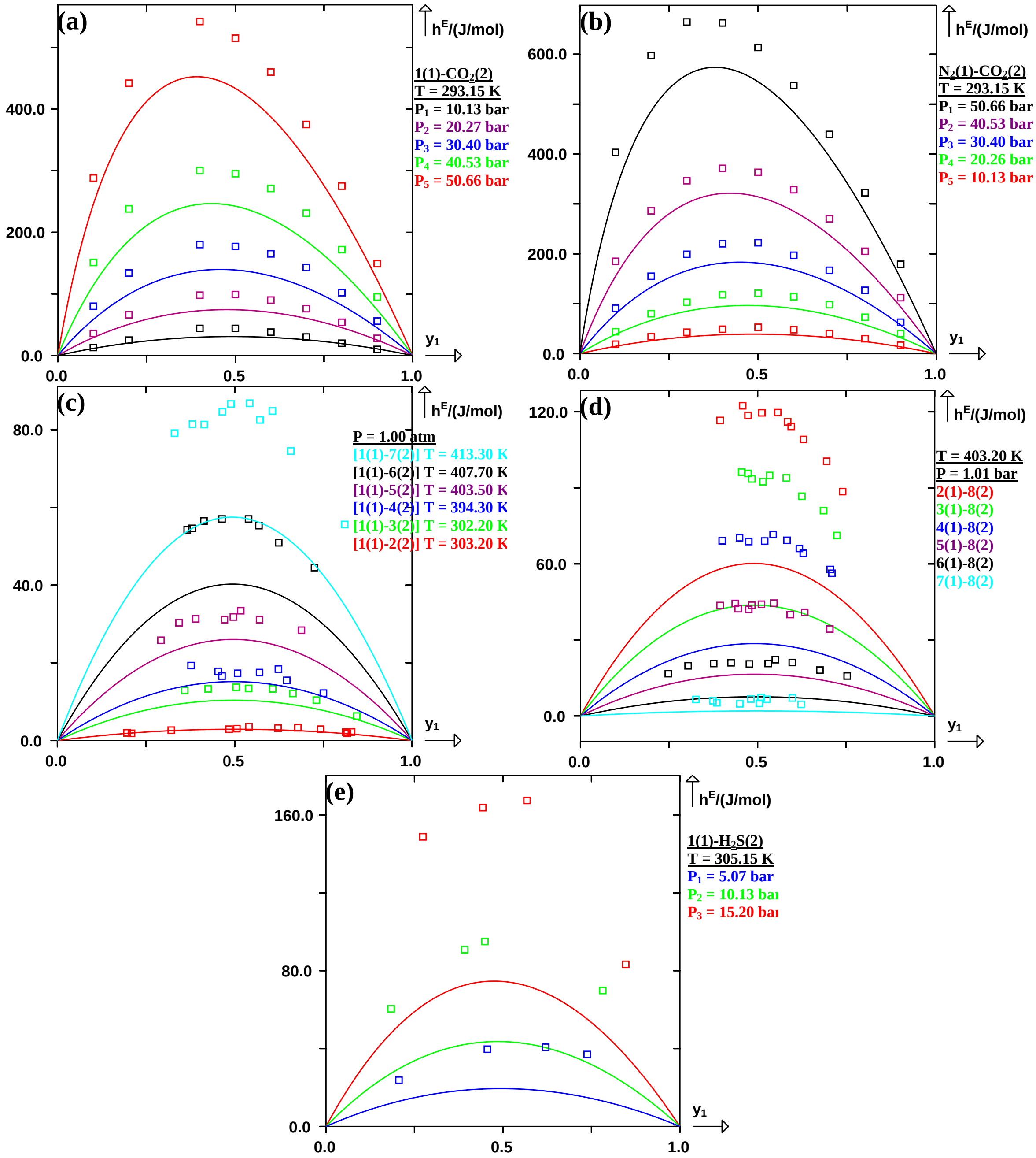

Figure V−18. Prediction of h^E curves in the gaseous single-phase region for the binary systems using the *E*-PPR78 model. (☐) experimental h^E points. Solid line: predicted curves with the *E*-PPR78 model. **(a)** System (methane(1) + CO_2(2)) at T = 293.15 K and under five different pressures: P_1 = 50.66 bar, P_2 = 40.53 bar, P_3 = 30.40 bar, P_4 = 20.27 bar, P_5 = 10.13 bar. **(b)** System (N_2(1) + CO_2(2)) at T = 293.15 K and under five different pressures: P_1 = 10.13 bar, P_2 = 20.26 bar, P_3 = 30.40 bar, P_4 = 40.53 bar, P_5 = 50.66 bar. **(c)** Six different systems under one atmosphere (P = 1.00 atm): (methane(1) + ethane(2)) at T = 303.20 K, (methane(1) + propane(2)) at T = 302.20 K, (methane(1) + n-butane(2)) at T = 394.30 K, (methane(1) + n-pentane(2)) at T = 403.50 K, (methane(1) + n-hexane(2)) at T = 407.70 K, (methane(1) + n-heptane(2)) at T = 413.30 K. **(d)** Six different systems at T = 403.20 K and under P = 1.01 bar: (ethane(1) + n-octane(2)), (propane(1) + n-octane(2)), (n-butane(1) + n-octane(2)), (n-pentane(1) + n-octane(2)), (n-hexane(1) + n-octane(2)), (n-heptane(1) + n-octane(2)). **(e)** System (methane(1) + H_2S(2)) at T = 305.15 K and under three different pressures: P_1 = 15.20 bar, P_2 = 10.13 bar, P_3 = 5.07 bar.

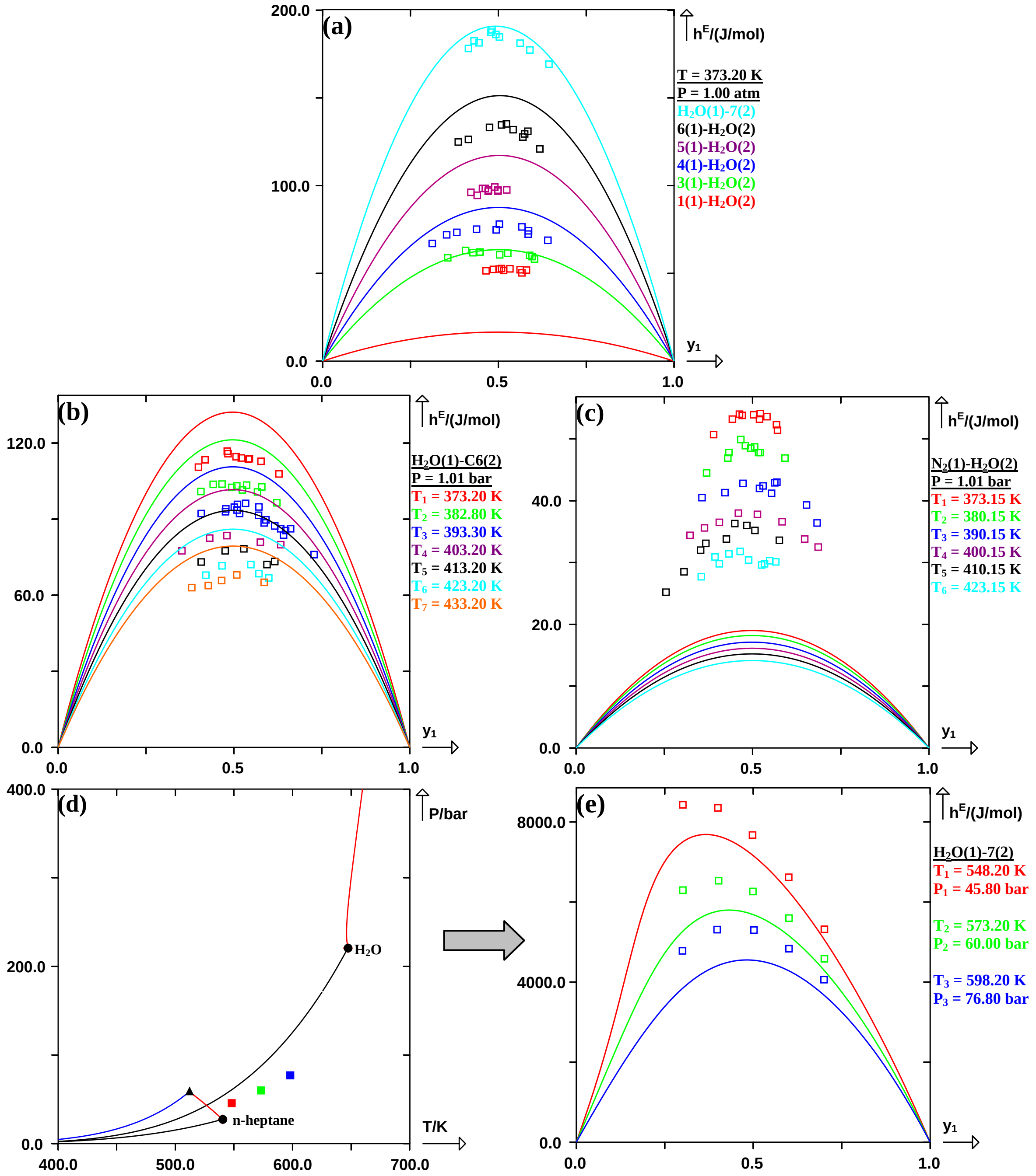

Figure V−19. Projection of pressure-temperature and prediction of h^E curves in the gaseous single-phase region for the binary systems containing H_2O using the *E*-PPR78 model. (□) experimental h^E points, (■) pressure-temperature points, (●) critical points of the pure compounds, (▲) upper critical endpoint, UCEP. Solid line: predicted curves with the *E*-PPR78 model. **(a)** Six different systems at T = 373.20 K and under one atmosphere (P = 1.00 atm): (methane(1) + $H_2O(2)$), (propane(1) + $H_2O(2)$), (n-butane(1) + $H_2O(2)$), (n-pentane(1) + $H_2O(2)$), (n-hexane(1) + $H_2O(2)$), ($H_2O(1)$ + n-heptane(2)). **(b)** System ($H_2O(1)$ + cyclohexane(2)) under P = 1.01 bar and at seven different temperatures: T_1 = 373.20 K, T_2 = 382.80 K, T_3 = 393.30 K, T_4 = 403.20 K, T_5 = 413.20 K, T_6 = 423.20 K, T_7 = 433.20 K. **(c)** System (N_2 (1) + $H_2O(2)$) under P = 1.01 bar and at six different temperatures: T_1 = 373.15 K, T_2 = 380.15 K, T_3 = 390.15 K, T_4 = 400.15 K, T_5 = 410.15 K, T_6 = 423.15 K. **(d)** Pressure-temperature projection for system ($H_2O(1)$ + n-heptane(2)) with the pressure-temperature points where the h^E curves are predicted. **(e)** System ($H_2O(1)$ + n-heptane(2)) at: T_1 = 548.20 K and P_1 = 45.80 bar, T_2 = 573.20 K and P_2 = 60.00 bar, T_3 = 598.20 K and P_3 = 76.80 bar.

V.4.2.2 h^E in the gaseous state over the temperature range: $T > T_{c2}$

Figures (V−20,21,22) present the predictions of h^E curves in the gaseous state where the temperatures (T) investigated are higher than the critical temperature of the less volatile component (T_{C2}). We have plotted the P-T projections for each binary mixture studied, together with the P-T points, indicating at which temperature and pressure the h^E behavior is examined.

As shown in figure (V−20), the h^E-y curves are well predicted for two binary mixtures (methane(1) + ethylene(2)) and (N_2(1) + ethylene(2)) over the temperature range: $T > T_{C2}$ and the pressure range: $P < P_{C2}$ (critical pressure of the less volatile component). It is obvious that both the temperature and pressure have a significant effect on h^E in this region. The maximum value of h^E is a decreasing function of the temperature and an increasing function of the pressure.

In order to well understand the h^E behavior over the pressure range: $P > P_{C2}$, we have plotted in figure (V−21) the h^E-y curves for two mixtures: (methane(1) + CO_2(2)) and (N_2(1) + methane(2)). At temperatures much higher than the critical temperature of the less volatile component (T_{C2}), the maximum h^E values are still a monotonic function of pressure but over a pressure range wider than in the previous case [see figures (V−21c,21e)]. Once again, accurate results are obtained by our model. At the temperature slightly above the critical temperature of the less volatile component (T_{C2}), the effect of pressure on the maximum of h^E is no longer monotonic. Taking the mixture (methane(1) + CO_2(2)) at T = 305.15 K for example [see figure (V−21b)], as the pressure increases from 20.27 to 101.33 bar, the h^E maximum increases, reaches the maximum at P = 81.06 bar and then it drops a little. Similar phenomena can be found for the mixture (N_2(1) + methane(2)) at T = 201.00 K [see figure (V−21d)]. It is difficult for our model to perfectly predict the highest (or near highest) h^E-y curve.

It is well known that, close to the critical point, small changes in pressure or temperature result in large changes in density. And as a result, it is not surprising that the effect of pressure on h^E at temperatures slightly above T_{C2} is complex. In order to illustrate this complexity, h^E-y curves of the other two binary mixtures: (H_2(1) + methane(2)) and (CO_2(1) + ethane(2)) are plotted in figure (V−22). As shown in figure (V−22b), the maximum of the h^E-y curves for (H_2(1) + methane(2)) is a monotonic increasing function of the pressure and the predicted curves at seven different pressures are in good agreement with experimental data. As for the mixture (CO_2(1) + ethane(2)) [see figure (V−22d)], the effect of pressure on h^E at T = 308.40 K is completely different, owing to the fact that the critical temperatures of two components in the mixture are very similar. At P = 40.00 bar and P = 110.00 bar, the h^E-x curves are almost symmetric, while the curve at P = 55.00 bar and P = 83.00 bar is skewed a lot, presenting a peak value on the left and right side respectively. Acceptable results are obtained except for the underestimation of two peak values. In addition, we have plotted the h^E-y curves for the mixture (ethylene(1) + propane(2)) at T = 373.15 K and under four different pressures in figure (V−22f), where the h^E value is an decreasing function of pressure. It is interesting to notice that the experimental points under each pressure show an endothermic mixing and an exothermic mixing in the ethylene-rich and propane-rich region respectively and the effect of pressure on both the endothermic and exothermic phenomena can also be observed. In this case, even though the predicted h^E curves are in close agreement with experimental data, huge objective function will be generated by the small magnitude or even the nearly zero value of experimental h^E point.

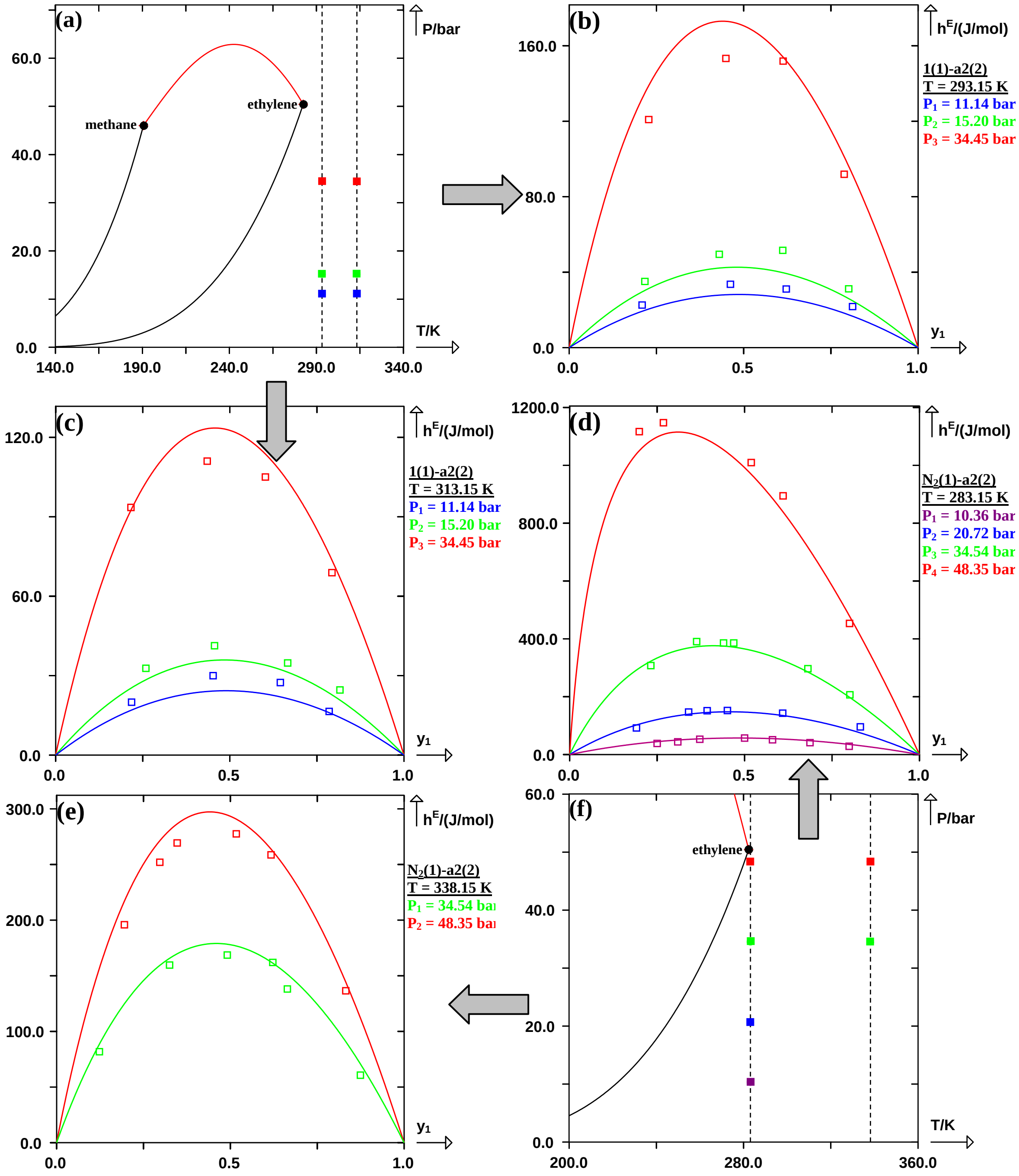

Figure V−20. Projection of pressure-temperature and prediction of h^E curves in the gaseous high-temperature region for two binary systems: (methane(1) + ethylene(2)) and (N_2(1) + ethylene(2)), using the *E*-PPR78 model. (□) experimental h^E points, (■) pressure-temperature points, (●) critical points of the pure compounds. Solid line: predicted curves with the *E*-PPR78 model. Dashed line: constant temperature. **(a)** Pressure-temperature projection for system (methane(1) + ethylene(2)) with the pressure-temperature points where the h^E curves are predicted. **(b)** h^E curves for system (methane(1) + ethylene(2)) at T = 293.15 K and under three different pressures: P_1 = 34.45 bar, P_2 = 15.20 bar, P_3 = 11.14 bar. **(c)** h^E curves for system (methane(1) + ethylene(2)) at T = 313.15 K and under three different pressures: P_1 = 34.45 bar, P_2 = 15.20 bar, P_3 = 11.14 bar. **(d)** h^E curves for system (N_2(1) + ethylene(2)) at T = 283.15 K and under four different pressures: P_1 = 48.35 bar, P_2 = 34.54 bar, P_3 = 20.72 bar, P_4 = 10.36 bar. **(e)** h^E curves for system (N_2(1) + ethylene(2)) at T = 338.15 K and under two different pressures: P_1 = 48.35 bar, P_2 = 34.54 bar. **(f)** Pressure-temperature projection for system (N_2(1) + ethylene(2)) with the pressure-temperature points where the h^E curves are predicted.

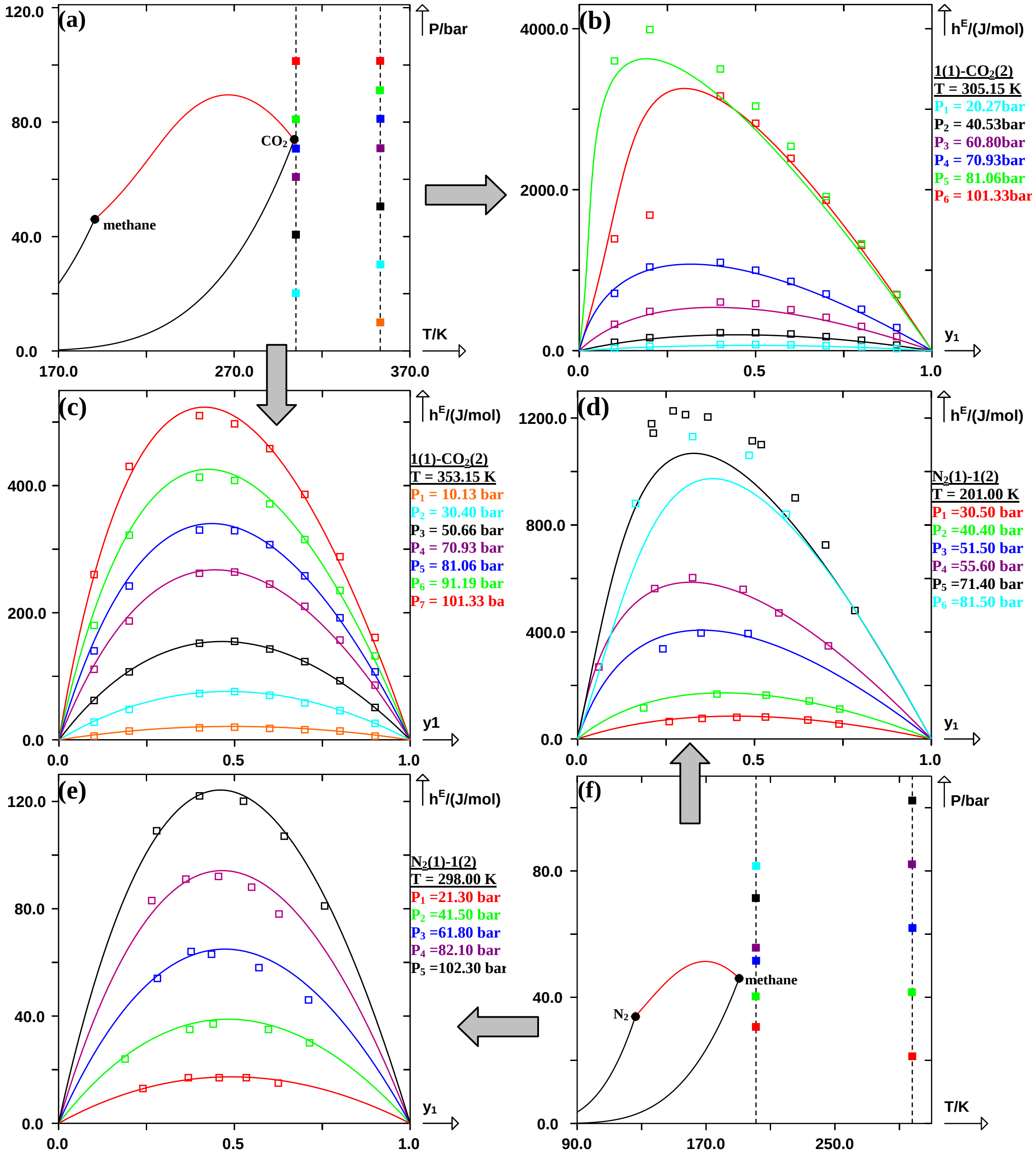

Figure V−21. Projection of pressure-temperature and prediction of h^E curves in the gaseous high-temperature region for two binary systems: (methane(1) + CO_2(2)) and (N_2(1) + methane(2)), using the *E*-PPR78 model. (☐) experimental h^E points, (■) pressure-temperature points, (●) critical points of the pure compounds. Solid line: predicted curves with the *E*-PPR78 model. Dashed line: constant temperature. **(a)** Pressure-temperature projection for system (methane(1) + CO_2(2)) with the temperature-pressure points where the h^E curves are predicted. **(b)** h^E curves for system (methane(1) + CO_2(2)) at T = 305.15 K and under six different pressures: P_1 = 101.33 bar, P_2 = 81.06 bar, P_3 = 70.93 bar, P_4 = 60.80 bar, P_5 = 40.53 bar, P_6 = 20.27 bar. **(c)** h^E curves for system (methane(1) + CO_2(2)) at T = 353.15 K and under seven different pressures: P_1 = 101.33 bar, P_2 = 91.19 bar, P_3 = 81.06 bar, P_4 = 70.93 bar, P_5 = 50.66 bar, P_6 = 30.40 bar, P_7 = 10.13 bar. **(d)** h^E curves for system (N_2(1) + methane(2)) at T = 201.00 K and under six different pressures: P_1 = 30.50 bar, P_2 = 40.40 bar, P_3 = 51.50 bar, P_4 = 55.60 bar, P_5 = 71.40 bar, P_6 = 81.50 bar. **(e)** h^E curves for system (N_2(1) + methane(2)) at T = 298.00 K and under five different pressures: P_1 = 21.30 bar, P_2 = 41.50 bar, P_3 = 61.80 bar, P_4 = 82.10 bar, P_5 = 102.30 bar. **(f)** Pressure-temperature projection for system (N_2(1) + methane(2)) with the temperature-pressure points where the h^E curves are predicted.

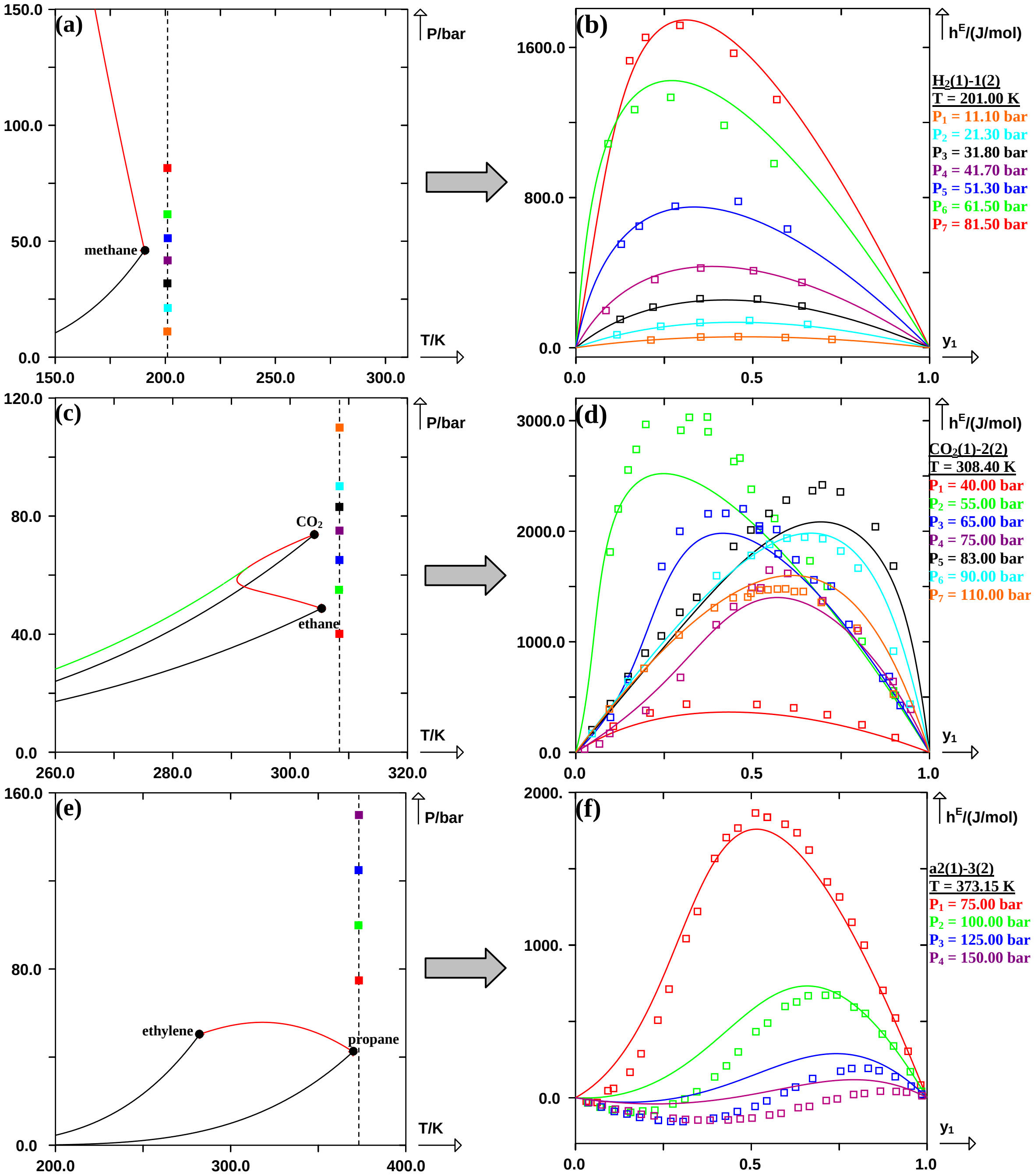

Figure V−22. Projection of pressure-temperature and prediction of h^E curves in the gaseous high-temperature region for two binary systems: (CO_2(1) + ethane(2)) and (H_2(1) + methane(2)), using the *E*-PPR78 model. (☐) experimental h^E points, (■) pressure-temperature points, (●) critical points of the pure compounds. Solid line: predicted curves with the *E*-PPR78 model. Dashed line: constant temperature. **(a)** Pressure-temperature projection for system (H_2(1) + methane(2)) with the pressure-temperature points where the h^E curves are predicted. **(b)** h^E curves for system (H_2(1) + methane(2)) at T = 201.00 K and under seven different pressures: P_1 = 81.50 bar, P_2 = 61.50 bar, P_3 = 51.30 bar, P_4 = 41.70 bar, P_5 = 31.80 bar, P_6 = 21.30 bar, P_7 = 11.10 bar. **(c)** Pressure-temperature projection for system (CO_2(1) + ethane(2)) with the pressure-temperature points where the h^E curves are predicted. **(d)** h^E curves for system (CO_2(1) + ethane(2)) at T = 308.40 K and under seven different pressures: P_1 = 40.00 bar, P_2 = 55.00 bar, P_3 = 65.00 bar, P_4 = 75.00 bar, P_5 = 83.00 bar, P_6 = 90.00 bar, P_7 = 110.00 bar. **(e)** Pressure-temperature projection for system (ethylene(1) + propane(2)) with the pressure-temperature points where the h^E curves are predicted. **(f)** h^E curves for system (ethylene(1) + propane(2)) at T = 373.15 K and under four different pressures: P_1 = 75.00 bar, P_2 = 100.00 bar, P_3 = 125.00 bar, P_4 = 150.00 bar.

V.4.3 Results of excess molar enthalpy (h^E) referring to the two-phase region

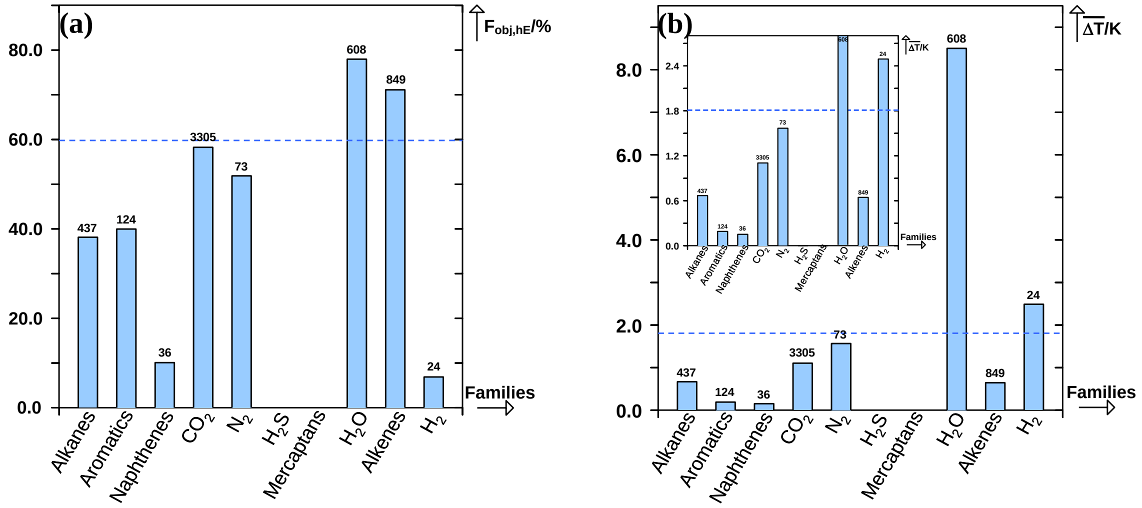

Figure V−23. (a) Histogram of the objective functions of h^E referring to the two-phase region for ten families of binary systems, with the number of experimental points on top. **(b)** Histogram of the average value of temperature changes generated by the uncertainty on the predicted h^E referring to the two-phase region for ten families of binary systems, with the number of experimental points on top.

According to our data base, 5456 experimental h^E points referring to the two-phase (vapor-liquid or liquid-liquid) region over 23 binary mixtures have been collected, among which 3305 points have been measured for 9 mixtures containing CO_2. For all the experimental points referring to the two-phase region, the objective function is: $F_{obj,hE} = 59.77\%$ [blue dashed line in figure (V−23)]. The objective function here is close to that obtained in the previous case (h^E in the liquid single-phase region), however, the average value of temperature changes ($\overline{\Delta T} = 1.81$ K) obtained here is much higher. This is because the binary mixtures exhibit huge h^E values at the temperatures and pressures where the two-phase region is crossed, or even at the pressure-temperature points being a little above the critical point of the mixture. As a result, the uncertainty (difference between the calculated value and the experimental one) will be more significant and inevitably increase the average value of temperature changes ($\overline{\Delta T}$). On the other hand, nearly zero experimental points especially for the mixtures showing flexuous h^E behavior and the relatively low h^E values for the mixtures in the liquid-like super-critical region, will make the objective function more significant.

In this study, besides the prediction of h^E curves at the temperatures and pressures where the two-phase (VL or LL) region is crossed over the composition range, we will also present the results of the mixture in the single-phase region over the entire composition range, in order to illustrate the accuracy and limitations of our model and well understand the h^E

behavior during the phase transition from single-phase to two-phase (or two-phase to single-phase).

Figure (V−24) shows the h^E curves referring to the two-phase region for three different binary mixtures, together with the isothermal diagram on the left side where the horizontal dashed lines across the diagram correspond to the different pressures examined. Taking (CO_2(1) + toluene(2)) at T = 413.15 K and P = 76.00 bar for example [see figures (V−24a,24b)], the pure component toluene is in liquid state because the temperature is lower than its critical temperature (T_C = 591.75 K) and the pressure is higher than its critical pressure (P_C = 41.08 bar), while CO_2 is a supercritical fluid (gas-like) because the temperature is much greater than its T_C (304.12 K) and the pressure is a little higher than its P_C (73.74 bar). As shown in the isothermal diagram in figure (V−24a), the mixture is liquid over the composition range: $0.00 < x_1 < 0.32$ and consequently, the h^E value decreases up to $x_1 = 0.32$ (exothermic mixing) due to the condensation effect of CO_2 [see figure (V−24b)]. On the other hand, the mixture is in the gaseous state over the narrow composition range: $0.93 < y_1 < 1.00$, and as a consequence, the maximum h^E value is located at $y_1 = 0.93$ (endothermic mixing) owing to the vaporization effect of toluene. The section between $x_1 = 0.32$ and $y_1 = 0.93$ in the h^E diagram corresponds to a change in the amount of liquid and gaseous phases across the two-phase region. The other h^E curves under four different pressures can be explained in a similar way and moreover, very accurate results are obtained for this mixture. In figure (V−24d), we have plotted the h^E curves of (ethane(1) + propane(2)) at T = 323.15 K and under three different pressures. At P = 50.00 bar where the pressure is slightly under the critical pressure of the mixture, huge exothermic mixing and moderate endothermic mixing takes place respectively in the liquid and gaseous states. As the pressure increases, moderate negative h^E values can be observed at P = 100.00 bar which is above the critical pressure of the mixture. In this case, we can see that, the liquid-like fluid mixture is formed by liquid propane and liquid-like fluid ethane. At P = 150.00 bar which is much higher than P_C of the mixture, the h^E values are still negative with less important magnitude. In general, the experimental points at three different pressures are predicted with acceptable accuracy. In addition, we have plotted in figure (V−24f) the h^E curves of (n-hexane(1) + toluene(2)) at T = 573.15 K and under three different pressures. By looking at the h^E curve of the same mixture at T = 298.15 K and P = 1.00 atm (h^E-x curve in the liquid single-phase region) plotted in figure (V−8e) in section V.4.1, we can observe that the h^E behavior at the pressures above P_C

of the mixture is surprisingly similar to that in the liquid single-phase region at a much lower temperature and pressure. Considering the results obtained here, except for the h^E curve at P = 75.00 bar, the experimental points are well represented by our model.

Figure (V−25) shows the h^E curves referring to the two-phase region for three binary mixtures at a temperature slightly below the critical temperature of the less volatile component, together with the isothermal diagram where a small phase envelop can be observed. Regarding the mixture (H_2(1) + methane(2)) at T = 183.00 K, the maximum h^E value is observed at P = 41.40 K which is a little above the saturated pressure of methane. On the other hand, the h^E values at P = 77.10 bar (near P_C of the mixture) is less significant because less methane is vaporized at this pressure. Generally, the h^E-x curves of (H_2(1) + methane(2)) in both the two-phase and single-phase region [see figure (V−25b)] are in good agreement with experimental data, as well as that of (N_2(1) + methane(2)) shown in figure (V−25d). At the same time, seven h^E curves of (CO_2(1) + ethane(2)) at T = 291.60 K and under different pressures are plotted in figure (V−25f). The h^E curves at P = 40.00, 48.80 and 54.00 bar are similar to the ones of (H_2(1) + methane(2)) and (N_2(1) + methane(2)) across the two-phase region, except for the exothermic mixing in the ethane-rich region. As the pressure increases, another phase envelop is crossed at P = 56.00 bar and the mixture exhibits huge endothermic mixing in the CO_2-rich region due to the fact that a great deal of CO_2 is vaporized during the mixing procedure. Once again, accurate results are obtained.

Figure (V−26) shows the h^E curves referring to the two-phase region for three binary mixtures, together with the isobaric diagram where the horizontal dashed lines across the diagram correspond to the different temperatures examined. At this step, we can notice that a good representation of h^E referring to the two-phase region depends not only on the accuracy of volumic property but accurate prediction of phase equilibria as well. As we know, the *E*-PPR78 model is able to predict perfectly the phase equilibria for the binary mixtures containing alkanes, aromatics, naphthenes, CO_2, N_2 and H_2, thanks to which, the predicted h^E-xy curves of these mixtures are in good agreement with experimental points [see figures (V−24,25,26b,26d)]. Meanwhile, the h^E values of (H_2O(1) + benzene(2)) in figure (V−26f) are overestimated by our model, and the uncertainty of h^E can also be explained by reasons that the prediction of the solubility of water in benzene (the branch of benzene-rich liquid) is not accurate.

As previously discussed in section V.4.2, the h^E behavior over the temperature range: $T > T_{C2}$ (in the gaseous single-phase region) is complex, because small changes in pressure or temperature result in large changes in density near the critical point. It is also interesting to present the h^E behavior over the pressure range: $P > P_{CM}$ where the pressures investigated are above the critical pressure of the mixture. In figure (V−27), we have plotted the predicted h^E curves of two binary mixtures: (CO_2(1) + n-pentane(2)) and (ethylene(1) + propane(2)) over the pressure range: $P > P_{CM}$. The points in the P-T projections indicate at which temperature and pressure the h^E behavior is examined. The h^E curves of (CO_2(1) + n-pentane(2)) under P = 103.70 bar and at seven different temperatures are shown in figure (V−27b). The huge negative h^E values can be explained as resulting principally from the condensation effect of gas-like CO_2, while the huge positive h^E values are a result of the vaporization effect of liquid (or liquid-like) n-pentane. As the pressure increases at P = 124.50 bar, the huge endothermic and exothermic mixings can still be observed, with less important magnitude on the extreme h^E values [see figure (V−27c)]. The same explanation applies to the mixture (ethylene(1) + propane(2)) at P = 60.00 bar shown in figures (V−27d,27e). Particularly, the h^E curves of (ethylene(1) + propane(2)) at P = 150.00 bar [see figures (V−27e,27f)] which is much higher than the critical pressure of the mixture. Both the supercritical ethylene and the mixture become more liquid-like and, hence, the condensation and vaporization effects become less important. Although the h^E curves at T = 348.15, 363.15 and 373.15 K are not very accurate (objective function: 161.37%), the average value of temperature changes ($\overline{\Delta T} = 0.68$ K) is still acceptable.

In general, by looking at the h^E behavior of the binary mixtures referring to the two-phase (VL or LL) region, huge (or moderate) endothermic mixing is exhibited when one liquid (or liquid-like fluid) pure component and one gaseous (or gas-like fluid) pure component form a gaseous (or gas-like) mixture, or even when two liquid (or liquid-like fluid) pure components form a gaseous (or gas-like) mixture ; contrarily, huge (or moderate) exothermic mixing is exhibited when one liquid (or liquid-like fluid) pure component and one gaseous (or gas-like fluid) pure component form a liquid (or liquid-like) mixture, or even when two gaseous (or gas-like fluid) pure components form a liquid (or liquid-like) mixture. These phenomena seem to be a consequence of change of state (vaporization or condensation) of the pure components during the mixing. In summary, our model is capable to predict the h^E behavior for the binary mixtures referring to the two-phase region.

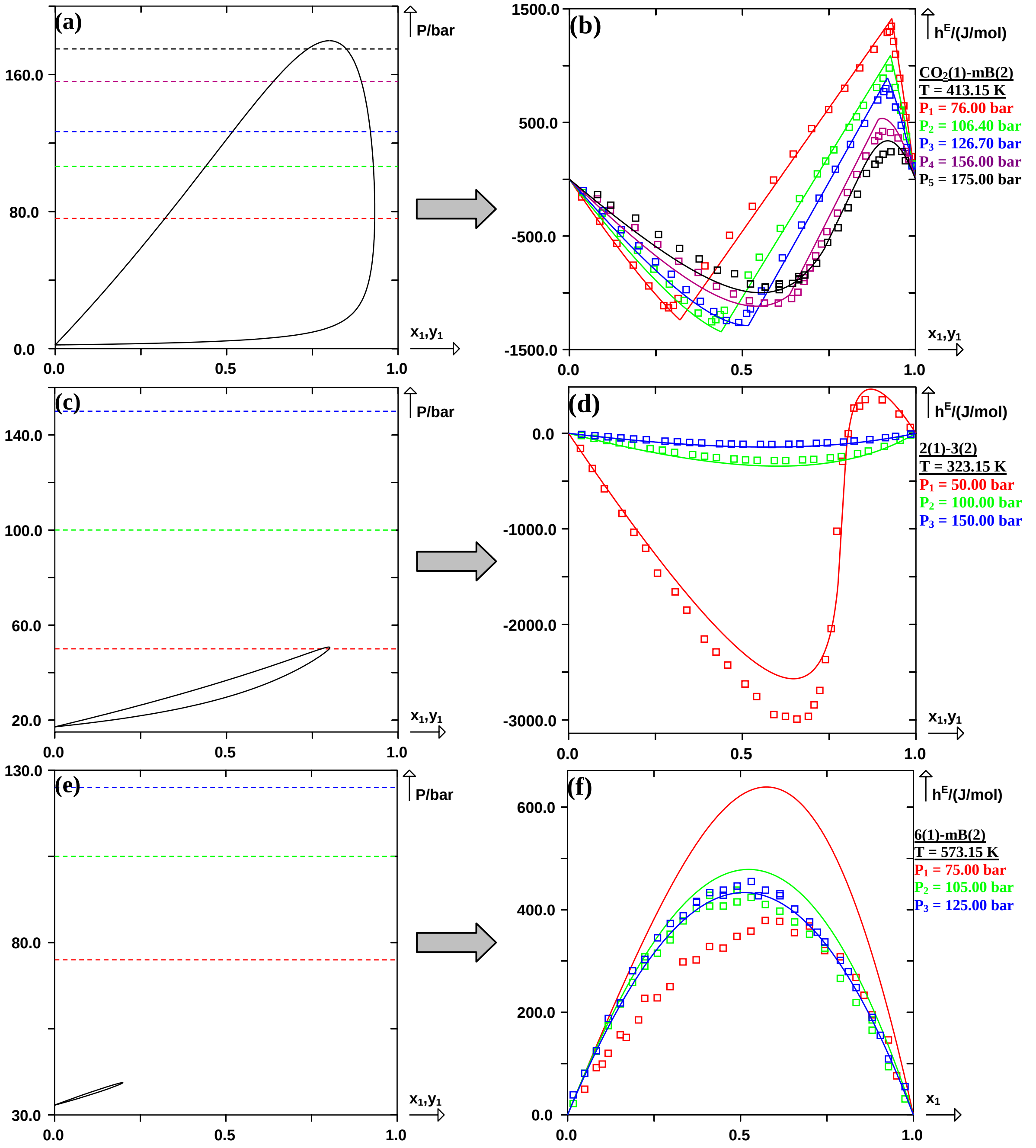

Figure V−24. Isothermal diagram and prediction of h^E curves referring to the two-phase region for three different binary systems: (CO_2(1) + toluene(2)), (ethane(1) + propane(2)) and (n-hexane(1) + toluene(2)), using the *E*-PPR78 model. (☐) experimental h^E points. Solid line: predicted curves with the *E*-PPR78 model. Dashed line: constant pressure. **(a)** Isothermal curves for system (CO_2(1) + toluene(2)) at T = 413.15 K. **(b)** h^E curves for system (CO_2(1) + toluene(2)) at T = 413.15 K and under five different pressures: P_1 = 76.00 bar, P_2 = 106.40 bar, P_3 = 126.70 bar, P_4 = 156.00 bar, P_5 = 175.00 bar. **(c)** Isothermal curves for system (ethane(1) + propane(2)) at T = 323.15 bar. **(d)** h^E curves for system (ethane(1) + propane(2)) at T = 323.15 K and under three different pressures: P_1 = 50.00 bar, P_2 = 100.00 bar, P_3 = 150.00 bar. **(e)** Isothermal curves for system (n-hexane(1) + toluene(2)) at T = 573.15 K. **(f)** h^E curves for system (n-hexane(1) + toluene(2)) at T = 573.15 K and under three different pressures: P_1 = 75.00 K, P_2 = 105.00 K, P_3 = 125.00 K.

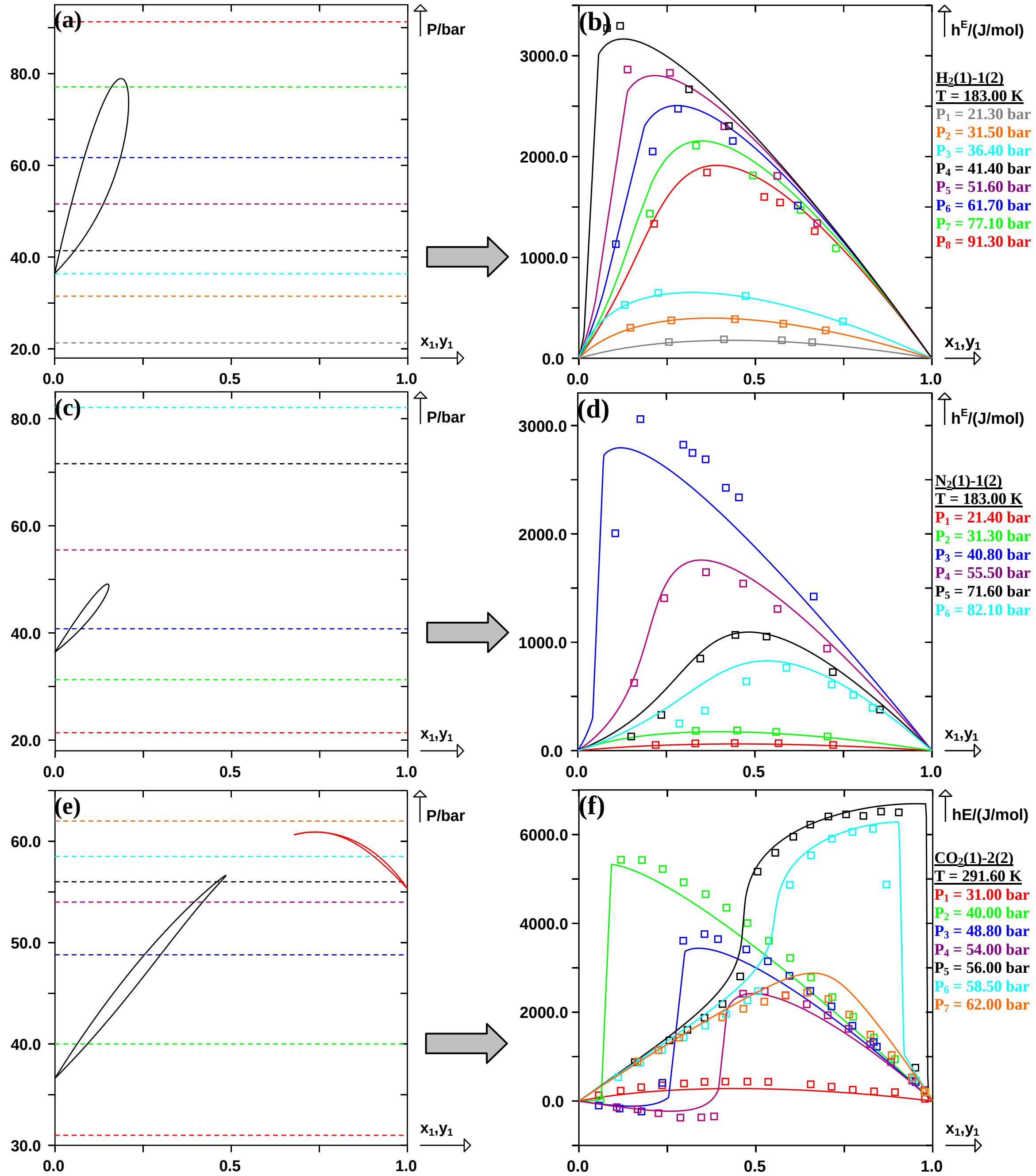

Figure V‒25. Isothermal diagram and prediction of h^E curves referring to the two-phase region for three different binary systems: (H_2(1) + methane(2)), (N_2(1) + methane(2)) and (CO_2(1) + ethane(2)), using the *E*-PPR78 model. (☐) experimental h^E points. Solid line: predicted curves with the *E*-PPR78 model. Dashed line: constant pressure. **(a)** Isothermal curves for system (H_2(1) + methane(2)) at T = 183.00 K. **(b)** h^E curves for system (H_2(1) + methane(2)) at T = 183.00 K and under eight different pressures: P_1 = 91.30 bar, P_2 = 77.10 bar, P_3 = 61.70 bar, P_4 = 51.60 bar, P_5 = 41.40 bar, P_6 = 36.40 bar, P_7 = 31.50 bar, P_8 = 21.30 bar. **(c)** Isothermal curves for system (N_2(1) + methane(2)) at T = 183.00 K. **(d)** h^E curves for system (N_2(1) + methane(2)) at T = 183.00 K and under six different pressures: P_1 = 21.40 bar, P_2 = 31.30 bar, P_3 = 40.80 bar, P_4 = 55.50 bar, P_5 = 71.60 bar, P_6 = 82.10 bar. **(e)** Isothermal curves for system (CO_2(1) + ethane(2)) at T = 291.60 K. **(f)** h^E curves for system (CO_2(1) + ethane(2)) at T = 291.60 K and under seven different pressures: P_1 = 31.00 bar, P_2 = 40.00 bar, P_3 = 48.80 bar, P_4 = 54.00 bar, P_5 = 56.00 bar, P_6 = 58.50 bar, P_7 = 62.00 bar.

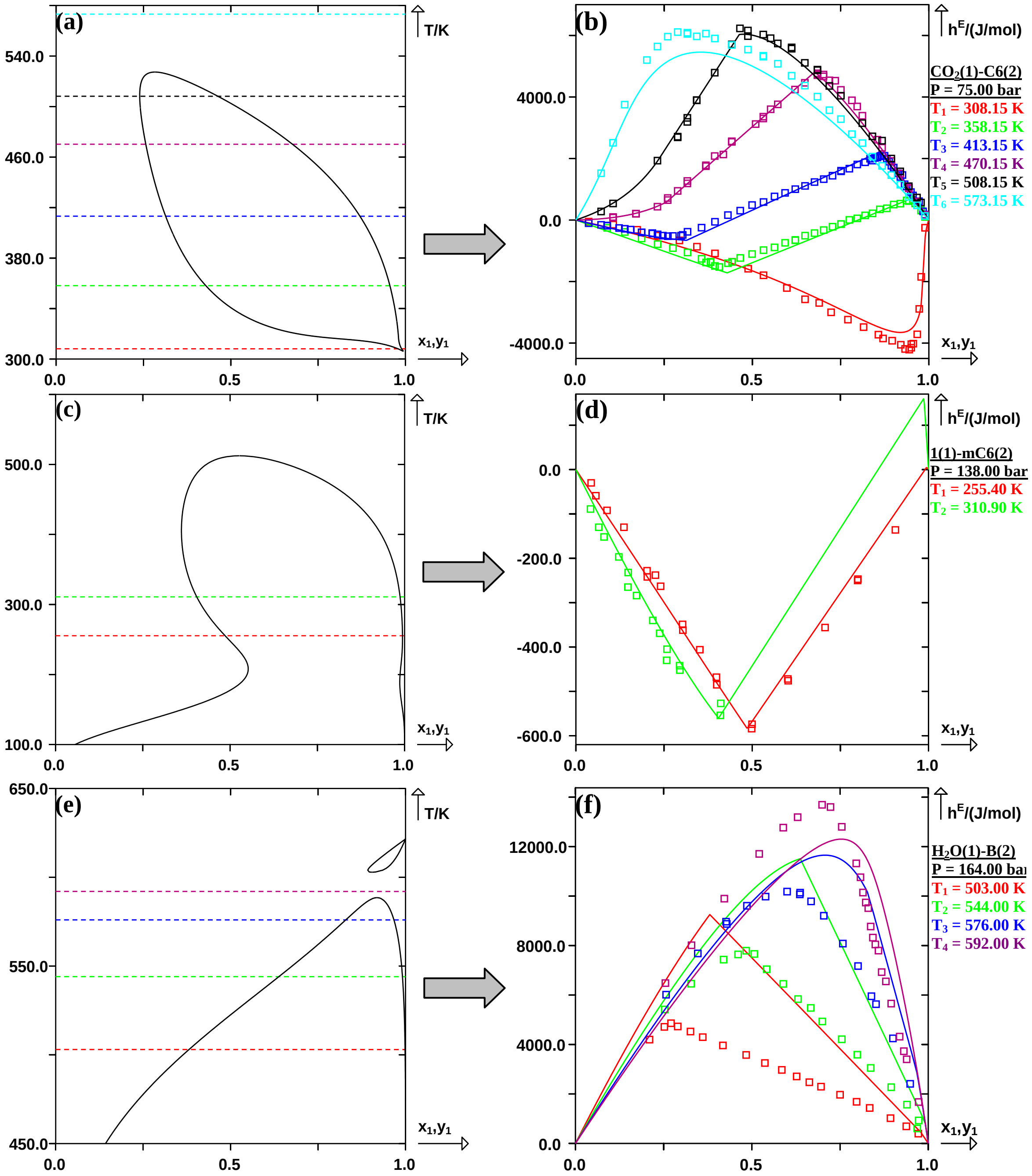

Figure V‒26. Isobaric diagram and prediction of h^E curves referring to the two-phase region for three different binary systems: (CO_2(1) + cyclohexane(2)), (methane(1) + methylcyclohexane(2)) and (H_2O(1) + benzene(2)), using the *E*-PPR78 model. (☐) experimental h^E points. Solid line: predicted curves with the *E*-PPR78 model. Dashed line: constant temperature. **(a)** Isobaric curves for system (CO_2(1) + cyclohexane(2)) under P = 75.00 bar. **(b)** h^E curves for system (CO_2(1) + cyclohexane(2)) under P = 75.00 bar and at six different temperatures: T_1 = 308.15 K, T_2 = 358.15 K, T_3 = 413.15 K, T_4 = 470.15 K, T_5 = 508.15 K, T_6 = 573.15 K. **(c)** Isobaric curves for system (methane(1) + methylcyclohexane(2)) under P = 138.00 bar. **(d)** h^E curves for system (methane(1) + methylcyclohexane(2)) under P = 138.00 bar and at two different temperatures: T_1 = 255.40 K, T_2 = 310.90 K. **(e)** Isobaric curves for system (H_2O(1) + benzene(2)) under P = 164.00 bar. **(f)** h^E curves for system (H_2O(1) + benzene(2)) under P = 164.00 bar and at four different temperatures: T_1 = 503.00 K, T_2 = 544.00 K, T_3 = 576.00 K, T_4 = 592.00 K.

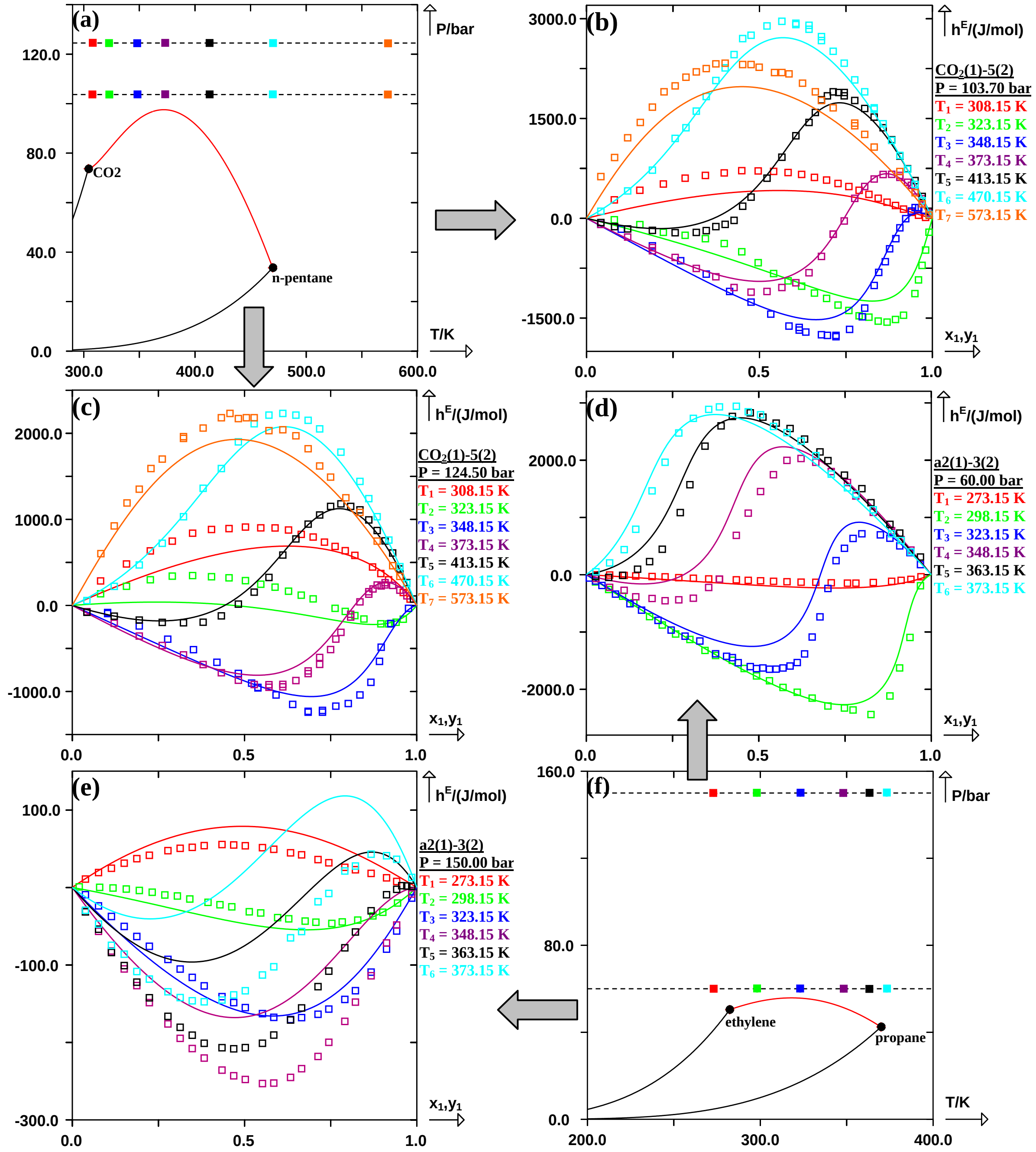

Figure V−27. Projection of pressure-temperature and prediction of h^E curves referring to the two-phase region for two binary systems: (CO_2(1) + n-pentane(2)) and (ethylene(1) + propane(2)), using the *E*-PPR78 model. (☐) experimental h^E points, (■) pressure-temperature points, (●) critical points of the pure compounds. Solid line: predicted curves with the *E*-PPR78 model. Dashed line: constant pressure. **(a)** Pressure-temperature projection for system (CO_2(1) + n-pentane(2)) with the pressure-temperature points where the h^E curves are predicted. **(b)** h^E curves for system (CO_2(1) + n-pentane(2)) under P = 103.70 bar and at seven different temperatures: T_1 = 308.15 K, T_2 = 323.15 K, T_3 = 348.15 K, T_4 = 373.15 K, T_5 = 413.15 K, T_6 = 470.15 K, T_7 = 573.15 K. **(c)** h^E curves for system (CO_2(1) + n-pentane(2)) under P = 124.50 bar and at seven different temperatures: T_1 = 308.15 K, T_2 = 323.15 K, T_3 = 348.15 K, T_4 = 373.15 K, T_5 = 413.15 K, T_6 = 470.15 K, T_7 = 573.15 K. **(d)** Pressure-temperature projection for system (ethylene(1) + propane(2)) with the pressure-temperature points where the h^E curves are predicted. **(e)** h^E curves for system (ethylene(1) + propane(2)) under P = 60.00 bar and at six different temperatures: T_1 = 273.15 K, T_2 = 298.15 K, T_3 = 323.15 K, T_4 = 348.15 K, T_5 = 363.15 K, T_6 = 373.15 K. **(f)** (ethylene(1) + propane(2)) under P = 150.00 bar and at six different temperatures: T_1 = 273.15 K, T_2 = 298.15 K, T_3 = 323.15 K, T_4 = 348.15 K, T_5 = 363.15 K, T_6 = 373.15 K.

V.4.4 Results of excess molar heat capacity at constant pressure (c_P^E)

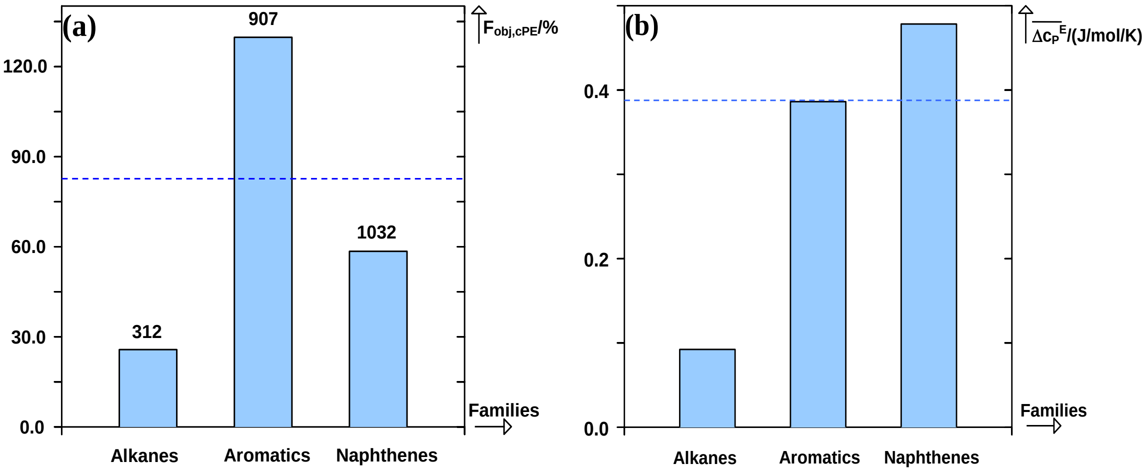

Figure V−28. (a) Histogram of the objective functions of c_P^E in the liquid single-phase region for three families of binary systems, with the number of experimental points on top. **(b)** Histogram of the average deviation on c_P^E ($\overline{\Delta c_P^E}$).

In this study, we have collected 2251 experimental c_P^E points, over 107 binary mixtures. Contrarily to what was observed for h^E, only c_P^E data in the liquid single-phase region are available. For all the data points, the objective function is: $F_{obj,cPE}$ = 82.59% [blue dashed line in figure (V−28a)]. It is necessary to notice that the c_P^E-x curves could not be perfectly predicted by our model because of the small magnitude of c_P^E value. In addition, some c_P^E values are very close to zero which inevitably increases the objective function of c_P^E during the adjustment, making our data-fitting more difficult.

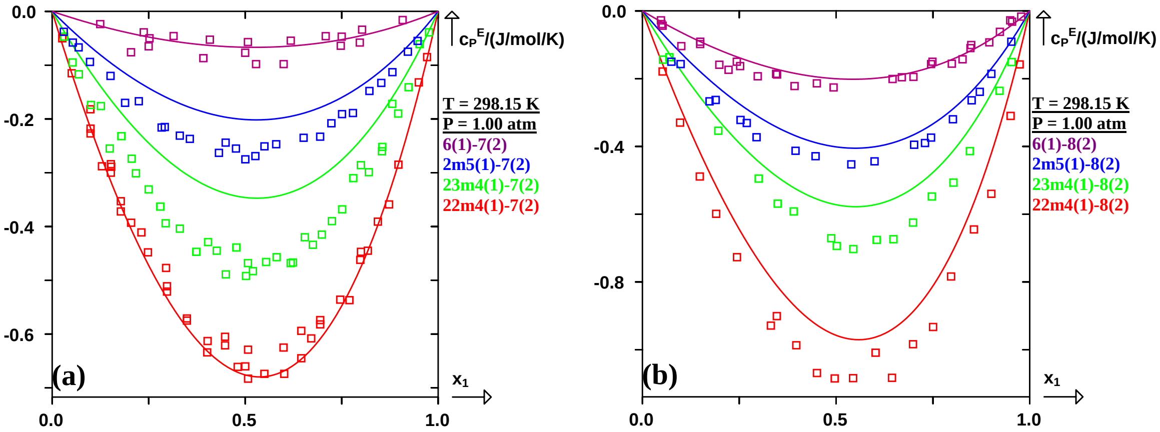

Figure V−29. Prediction of c_P^E curves in the liquid single-phase region for the binary systems containing alkanes using the *E*-PPR78 model. (☐) experimental c_P^E points. Solid line: predicted curves with the *E*-PPR78 model. **(a)** Four different systems at T = 298.15 K and under one atmosphere (P = 1.00 atm): (2,2-dimethylbutane(1) + n-heptane(2)), (2,3-dimethylbutane(1) + n-heptane(2)), (2-methylpentane(1) + n-heptane(2)), (n-hexane(1) + n-heptane(2)). **(b)** Four different systems at T = 298.15 K and under one atmosphere (P = 1.00 atm): (2,2-dimethylbutane(1) + n-octane(2)), (2,3-dimethylbutane(1) + n-octane(2)), (2-methylpentane(1) + n-octane(2)), (n-hexane(1) + n-octane(2)).

Figure (V−29) shows the c_P^E-x curves for 8 different mixtures containing two alkanes at T = 298.15 K and under one atmosphere. The objective function of this family of binary mixtures is: $F_{obj,cPE}$ = 25.73 % and the absolute uncertainty on the predicted c_P^E (difference between the calculated value and the experimental one) is only: 0.09 J/(mol·K). By looking at the mixtures which consist of an isomer of n-hexane and n-heptane (or n-octane), all the c_P^E values are slightly negative and the c_P^E-x curves are almost symmetric. Generally, the prediction for the mixtures containing alkanes is in close agreement with experimental data, and the effect of isomer structure on c_P^E value is well described by our model.

Figure (V−30) presents the results for the mixtures containing aromatics. The objective function of this family is: $F_{obj,cPE}$ = 129.61 %, because poor results are obtained for the mixtures containing 1,2,4-trimethylbenzene and the mixtures consisting of two xylenes. Regarding the c_P^E-x curves of the mixtures containing 1,2,4-trimethylbenzene and an n-alkane plotted in figure (V−30e), all the experimental points are underestimated by our model, and unfortunately, the objective function is 1763.44 %. Moreover, as previously discussed, the parameters A_{kl} and B_{kl} have no effect on the mixtures containing two xylenes [see figure (V−30f)] and the objective function obtained for these binary mixtures is approximately 100 %. Despite of that, accurate results are obtained for most of the binary mixtures in this family. As shown in figures (V−30a,30b), it is interesting to notice that the c_P^E-x curves of the mixtures consisting of n-alkane and benzene (or ethylbenzene) are less symmetric and that the change in c_P^E value with the chain length of the n-alkane is also well predicted by our model. Figure (V−30c) gives the plots of well predicted c_P^E-x curves for four binary mixtures which consist of an aromatic compound and 2,3-dimethylbutane. It is obvious that the magnitude of c_P^E value is a decreasing function of the chain length of the alkyl chain in the substituted benzene ring according to the prediction of the *E*-PPR78 model. Unfortunately, this effect is ambiguous for the experimental investigation. Considering four mixtures containing two aromatics [see figure (V−30d)], all the predicted c_P^E-x curves are above the experimental data, however, the maximum uncertainty presented by the mixture (benzene(1) + n-butylbenzene(2)) at $x_1 \approx 0.56$, is only: $\Delta c_P^E \approx 0.5$ J/(mol·K).

Figure (V−31) shows the c_P^E-x curves for 22 different mixtures containing naphthenes at T = 298.15 K and under one atmosphere. The results of this family are reasonable although they are less accurate than those obtained for the mixtures containing alkanes [see figure (V−28)]. It is really difficult for our model to well predict the c_P^E-x curves for the mixture (cyclohexane(1) + n-tetradecane(2)) [see figure (V−31a)], the mixtures containing a branched-alkane and trans-decalin [see figure (V−31b)] and the mixtures containing two naphthenes [see figure (V−31f)]. In addition, the c_P^E-x curves for 6 different mixtures under one atmosphere and at different temperatures are plotted in figure (V−32). We can see that the temperature has a positive effect on the c_P^E value for these mixtures which is well predicted by the *E*-PPR78 model.

In general, all these graphic results together with the average overall deviation on c_P^E (0.39 J/(mol·K)) [blue dashed line in figure (V−28b)] indicate that the *E*-PPR78 model is capable to give a satisfactory representation of c_P^E for most of the binary mixtures investigated.

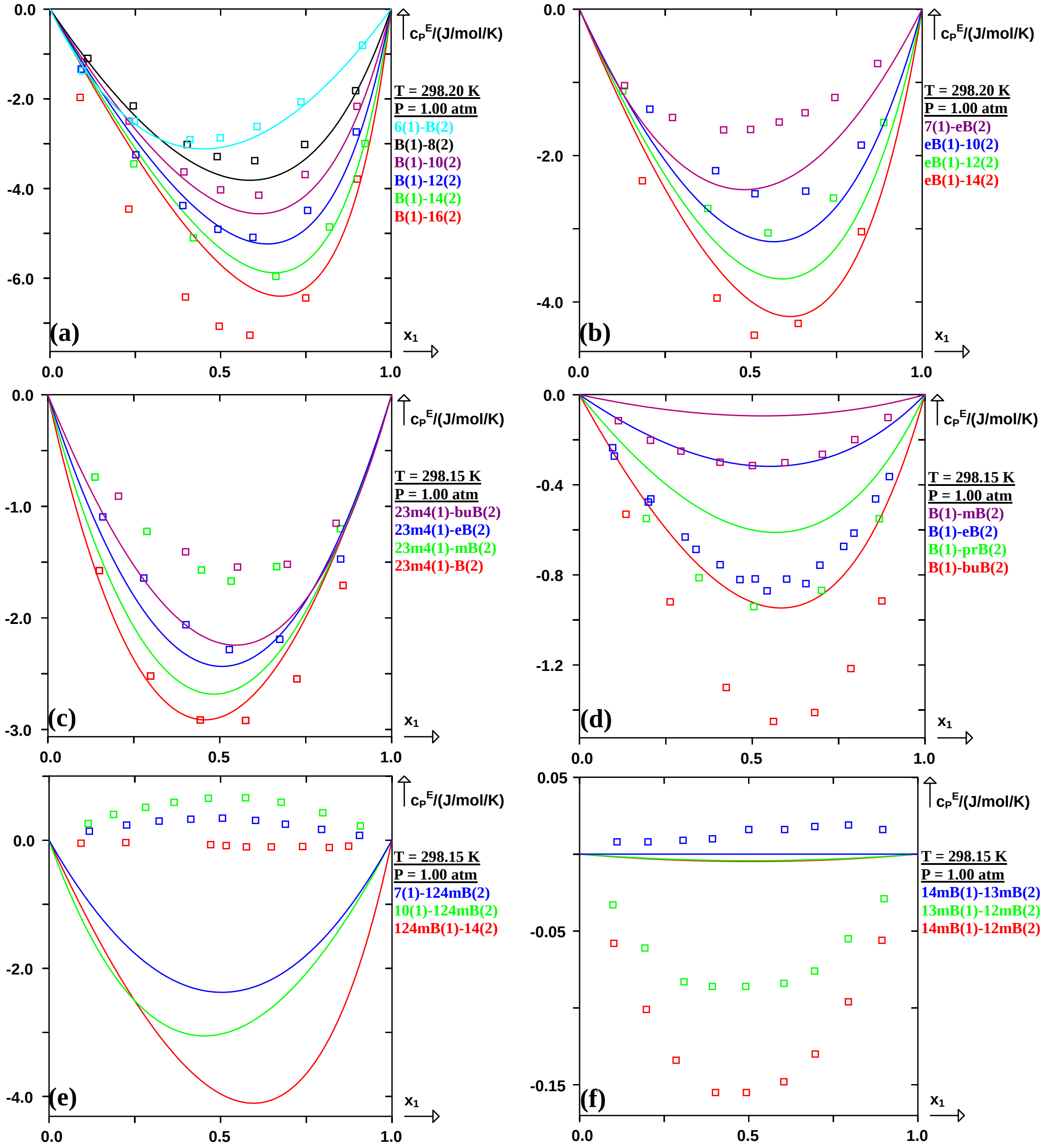

Figure V‒30. Prediction of c_P^E curves in the liquid single-phase region for the binary systems containing aromatics using the *E*-PPR78 model. (□) experimental c_P^E points. Solid line: predicted curves with the *E*-PPR78 model. **(a)** Six different systems at T = 298.20 K and under one atmosphere (P = 1.00 atm): (benzene(1) + n-hexadecane(2)), (benzene(1) + n-tetradecane(2)), (benzene(1) + n-dodecane(2)), (benzene(1) + n-decane(2)), (benzene(1) + n-octane(2)), (n-hexane(1) + benzene(2)). **(b)** Four different systems at T = 298.20 K and under one atmosphere (P = 1.00 atm): (ethylbenzene(1) + n-tetradecane(2)), (ethylbenzene(1) + n-dodecane(2)), (ethylbenzene(1) + n-decane(2)), (n-heptane(1) + ethylbenzene(2)). **(c)** Four different systems at T = 298.15 K and under one atmosphere (P = 1.00 atm): (2,3-dimethylbutane(1) + benzene(2)), (2,3-dimethylbutane(1) + toluene(2)), (2,3-dimethylbutane(1) + ethylbenzene(2)), (2,3-dimethylbutane(1) + n-butylbenzene(2)). **(d)** Four different systems at T = 298.15 K and under one atmosphere (P = 1.00 atm): (benzene(1) + n-butylbenzene(2)), (benzene(1) + n-propylbenzene(2)), (benzene(1) + ethylbenzene(2)), (benzene(1) + toluene(2)). **(e)** Three different systems at T = 298.15 K and under one atmosphere (P = 1.00 atm): (1,2,4-trimethylbenzene(1) + n-tetradecane(2)), (n-decane(1) + 1,2,4-trimethylbenzene(2)), (n-heptane(1) + 1,2,4-trimethylbenzene(2)). **(f)** Three different systems at T = 298.15 K and under one atmosphere (P = 1.00 atm): (1,4-dimethylbenzene(1) + 1,2-dimethylbenzene(2)), (1,3-dimethylbenzene (1) + 1,2-dimethylbenzene(2)), (1,4-trimethylbenzene (1) + 1,3-trimethylbenzene(2)).

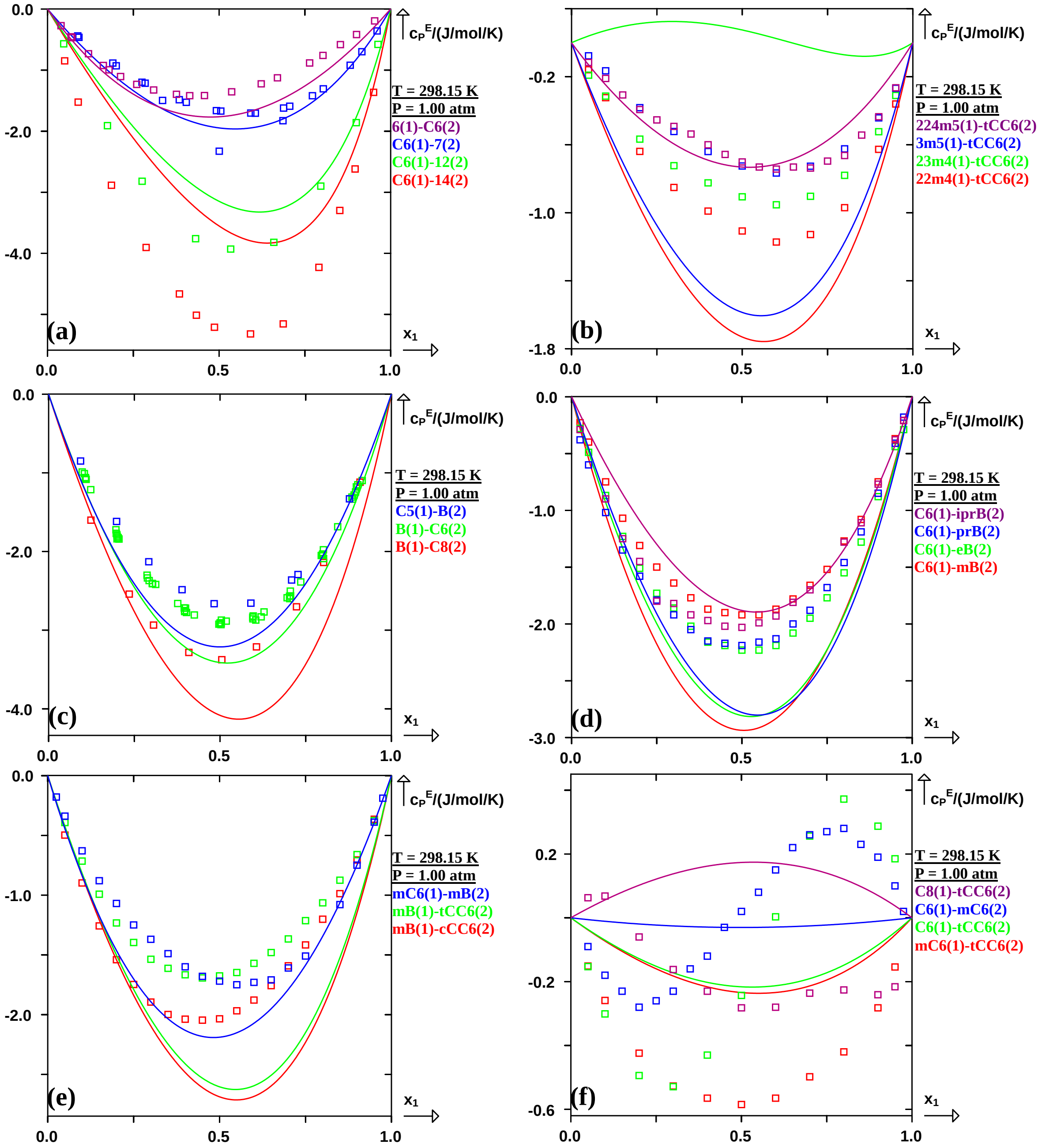

Figure V−31. Prediction of c_P^E curves in the liquid single-phase region for the binary systems containing aromatics using the *E*-PPR78 model. (☐) experimental c_P^E points. Solid line: predicted curves with the *E*-PPR78 model. **(a)** Four different systems at T = 298.15 K and under one atmosphere (P = 1.00 atm): (cyclohexane(1) + n-tetradecane(2)), (cyclohexane(1) + n-dodecane(2)), (cyclohexane(1) + n-heptane(2)), (n-hexane(1) + cyclohexane(2)). **(b)** Four different systems at T = 298.15 K and under one atmosphere (P = 1.00 atm): (2,2-dimethylbutane(1) + trans-decalin(2)), (2,3-dimethylbutane(1) + trans-decalin(2)), (3-methylpentane(1) + trans-decalin(2)), (2,2,4-trimethylpentane(1) + trans-decalin(2)). **(c)** Three different systems at T = 298.15 K and under one atmosphere (P = 1.00 atm): (benzene(1) + cyclooctane(2)), (benzene(1) + cyclohexane(2)), (cyclopentane(1) + benzene(2)). **(d)** Four different systems at T = 298.15 K and under one atmosphere (P = 1.00 atm): (cyclohexane(1) + toluene(2)), (cyclohexane(1) + ethylbenzene(2)), (cyclohexane(1) + n-propylbenzene(2)), (cyclohexane(1) + isopropylbenzene(2)). **(e)** Three different systems at T = 298.15 K and under one atmosphere (P = 1.00 atm): (toluene(1) + cis-decalin(2)), (toluene(1) + trans-decalin(2)), (methylcyclohexane(1) + toluene(2)). **(f)** Four different systems at T = 298.15 K and under one atmosphere (P = 1.00 atm): (methylcyclohexane(1) + trans-decalin(2)), (cyclohexane(1) + trans-decalin(2)), (cyclohexane(1) + methylcyclohexane(2)), (cyclooctane(1) + trans-decalin(2)).

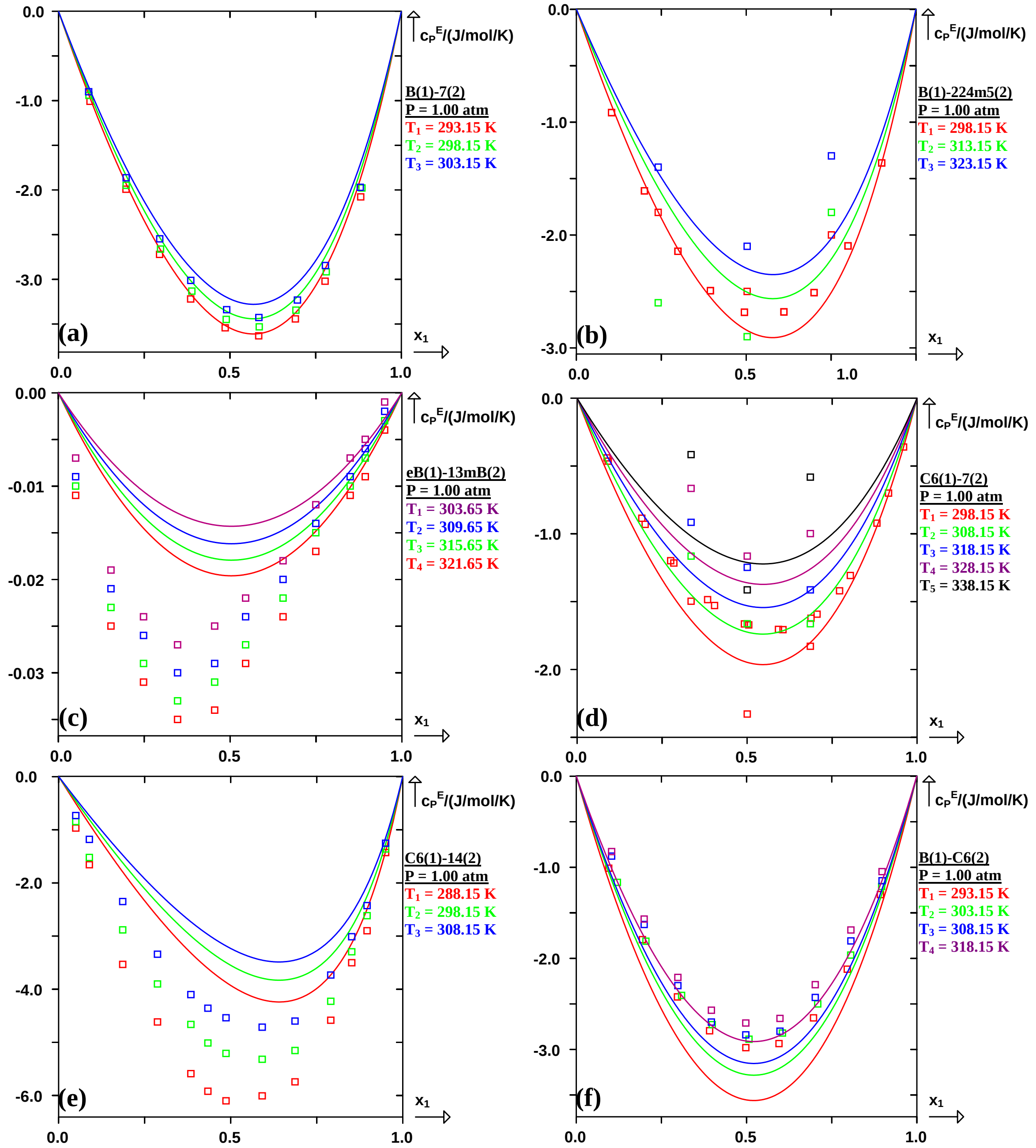

Figure V−32. Prediction of c_P^E curves in the liquid single-phase region for the binary systems using the *E*-PPR78 model. (☐) experimental c_P^E points. Solid line: predicted curves with the *E*-PPR78 model. **(a)** System (benzene(1) + n-heptane(2)) under one atmosphere (P = 1.00 atm) and at three different temperatures: T_1 = 293.15 K, T_2 = 298.15 K, T_3 = 303.15 K. **(b)** System (benzene(1) + 2,2,4-trimethylpentane(2)) under one atmosphere (P = 1.00 atm) and at three different temperatures: T_1 = 298.15 K, T_2 = 313.15 K, T_3 = 323.15 K. **(c)** System (ethylbenzene(1) + 1,3-dimethylbenzene(2)) under one atmosphere (P = 1.00 atm) and at four different temperatures: T_1 = 321.65 K, T_2 = 315.65 K, T_3 = 309.65 K, T_4 = 303.65 K. **(d)** System (cyclohexane(1) + n-heptane(2)) under one atmosphere (P = 1.00 atm) and at five different temperatures: T_1 = 298.15 K, T_2 = 308.15 K, T_3 = 318.15 K, T_4 = 328.15 K. **(e)** System (cyclohexane(1) + n-tetradecane(2)) under one atmosphere (P = 1.00 atm) and at three different temperatures: T_1 = 288.15 K, T_2 = 298.15 K, T_3 = 308.15 K. **(f)** System (benzene(1) + cyclohexane(2)) under one atmosphere (P = 1.00 atm) and at four different temperatures: T_1 = 293.15 K, T_2 = 303.15 K, T_3 = 308.15 K, T_4 = 318.15 K.

V.5 Conclusion

Before this study, the PPR78 model was capable to describe the phase equilibria for complex mixtures containing alkanes, aromatics, naphthenes, alkenes, carbon dioxide, nitrogen, hydrogen sulfide, mercaptans, hydrogen and water. Moreover, by fitting the group parameters on vapor-liquid equilibrium (VLE) data only, the predictions of excess molar enthalpy (h^E) and excess molar heat capacity (c_P^E), although reasonable, could be highly improved (the quality of predicted h^E (or c_P^E) curves for some of the studied binary systems were far away from being satisfactory). In this study, the parameters of the PPR78 model have been readjusted by using VLE, h^E and c_P^E data, in order to have a simultaneous correlation and prediction of VLE, h^E and c_P^E. Several conclusions can be made from this work.

(1) By using this recent *E*-PPR78 model, the prediction quality of VLE is retained, as well as that of mixture critical points. The accuracy of the predicted h^E (or c_P^E) curves has been remarkably improved.

(2) Both h^E and c_P^E in the liquid single-phase region are well described by our model. The results of h^E in the gaseous single-phase region at low temperature and under one atmosphere are less accurate but still acceptable which can be explained by the small average value of temperature changes ($\overline{\Delta T}$).

(3) The predicted h^E referring to the two-phase region and that in the temperature range: $T > T_{C2}$ (critical temperature of the less volatile component) are in close agreement with experimental data, although the average value of temperature changes ($\overline{\Delta T}$) is relatively higher owing to the huge magnitude of h^E values.

(4) Considering all the binary systems studied, simultaneous correlation of h^E and VLE for the mixtures containing H_2O is always the most difficult.

In general, the results obtained in this work indicate that it is possible for our model to represent simultaneously the VLE, h^E and c_P^E over a wide temperature and pressure range. From now on, the recent *E*-PPR78 model was capable to describe both the phase equilibria and excess thermodynamic properties such as h^E and c_P^E, for complex mixtures containing alkanes, aromatics, naphthenes, alkenes, carbon dioxide, nitrogen, hydrogen sulfide, mercaptans, hydrogen and water.

Appendix

Table V−5. Binary systems database (h^E)

Binary system (1st compound-2nd compound)	Temperature rage (K)	Pressure range (bar)	Excess enthalpy range (J/mol)	x_1 range (1st compound liquid mole fraction)	y_1 range (1st compound gas mole fraction)	z_1 range (1st compound mole fraction)	Number of points (T,P,h^E,x)	Number of points (T,P,h^E,y)	Number of points (T,P,h^E,z)	References
3-6	344.20-396.90	1.01000-1.01000	16.3000-47.1000	-	0.3650-0.8150	-	0	24	0	[13]
3-7	383.20-413.20	1.01000-1.01000	23.8000-63.7000	-	0.3660-0.8970	-	0	31	0	[13]
3-8	403.20-413.30	1.01000-1.01000	70.7000-96.2000	-	0.3630-0.7240	-	0	29	0	[13]
4-6	363.20-393.20	1.01000-1.01000	9.6000-20.3000	-	0.3310-0.7810	-	0	37	0	[13]
4-8	403.20-413.20	1.01000-1.01000	44.4000-71.6000	-	0.4000-0.7550	-	0	28	0	[13]
5-6	293.15-403.20	1.01000-1.01325	2.7000-9.0000	0.5000-0.5000	0.3970-0.6000	-	1	27	0	[13-14]
5-7	293.15-413.20	1.01000-1.01325	10.0000-20.6000	0.5000-0.5000	0.3280-0.6280	-	1	29	0	[13-14]
5-8	403.20-413.20	1.01000-1.01000	34.3000-44.5000	-	0.3940-0.7040	-	0	20	0	[13]
5-10	293.15-293.15	1.01325-1.01325	20.1000-25.5000	0.4876-0.6906	-	-	3	0	0	[15]
5-16	293.15-293.15	1.01325-1.01325	149.1000-151.2000	0.4732-0.5589	-	-	3	0	0	[15]
6-7	293.15-298.15	1.01325-1.01325	-28.4700-23.4000	0.0500-0.9500	-	-	31	0	0	[16-18]
6-8	298.15-413.20	1.00000-488.00000	0.4200-22.2000	0.1004-0.9003	0.2480-0.7530	-	32	20	0	[13, 19-21]
6-9	298.15-298.15	1.01000-1.01000	1.9000-9.9000	0.1061-0.8931	-	-	19	0	0	[22]
6-10	293.15-308.15	1.00000-485.00000	0.4100-37.4000	0.0498-0.9620	-	-	120	0	0	[15, 20, 23-25]
6-11	298.15-308.15	1.01325-1.01325	0.5900-25.9800	0.0474-0.9818	-	-	68	0	0	[26]
6-12	283.15-308.15	1.01000-1.01325	1.0600-59.9000	0.0499-0.9829	-	-	168	0	0	[22, 27-32]
6-14	298.15-298.15	1.01000-1.01000	6.7000-67.9000	0.0486-0.8986	-	-	21	0	0	[33]
6-16	293.15-349.15	1.00000-1.01325	-31.6000-129.8900	0.0380-0.9860	-	-	198	0	0	[32, 34-41]
7-8	298.15-413.20	1.01000-1.01325	0.0560-7.2000	0.0501-0.9510	0.3260-0.7440	-	22	20	0	[13, 42]
7-10	298.15-298.15	1.01325-1.01325	1.9300-10.6400	0.0500-0.9500	-	-	19	0	0	[43]
7-12	298.15-298.15	1.01325-1.01325	5.4300-30.3300	0.0501-0.9500	-	-	19	0	0	[44]
7-16	293.15-323.15	1.01325-1.01325	33.4000-111.6000	0.2625-0.6651	-	-	19	0	0	[15, 32, 45]
8-10	298.15-298.15	1.01325-1.01325	1.0390-4.9610	0.0500-0.9500	-	-	19	0	0	[46]
8-12	298.15-298.15	1.01325-1.01325	3.4900-20.5100	0.0502-0.9499	-	-	30	0	0	[44, 47]
8-16	293.15-323.15	1.01325-1.01325	33.0000-87.2000	0.4654-0.6417	-	-	7	0	0	[15, 32]
10-12	298.15-298.15	1.01325-1.01325	0.9400-5.1700	0.0501-0.9499	-	-	19	0	0	[44]
10-16	293.15-293.15	1.01325-1.01325	45.0000-49.2000	0.5000-0.6279	-	-	5	0	0	[15, 32]
22m3-8	323.15-323.15	1.01325-1.01325	-92.5280-0.0000	0.2990-0.8550	-	-	17	0	0	[48]
22m4-6	298.15-298.15	1.01000-1.01000	4.2000-5.9000	0.1811-0.8142	-	-	5	0	0	[49]
22m4-7	298.15-298.15	1.01325-1.01325	3.9700-23.3700	0.0500-0.9500	-	-	20	0	0	[16]
22m4-8	298.15-298.15	1.01000-1.01325	11.3600-35.2000	0.1002-0.9000	-	-	13	0	0	[19, 50]
22m4-10	298.15-298.15	1.01325-1.01325	12.7800-73.5500	0.0506-0.9498	-	-	20	0	0	[23]
22m4-12	283.15-303.15	1.01000-1.01325	20.5300-156.3000	0.0501-0.9501	-	-	83	0	0	[27-28, 51]
22m4-16	293.15-298.15	1.01325-1.01325	58.7000-254.9000	0.1941-0.9482	-	-	20	0	0	[27, 37]
23m4-6	283.15-313.15	1.01325-1.01325	-5.5800-1.3500	0.0580-0.9309	-	-	37	0	0	[52]

Table V−5. (continued-1)

Binary system (1st compound-2nd compound)	Temperature rage (K)	Pressure range (bar)	Excess enthalpy range (J/mol)	x_1 range (1st compound liquid mole fraction)	y_1 range (1st compound gas mole fraction)	z_1 range (1st compound mole fraction)	Number of points (T,P,h^E,x)	Number of points (T,P,h^E,y)	Number of points (T,P,h^E,z)	References
23m4-7	298.15-298.15	1.01325-1.01325	1.6700-9.9300	0.0500-0.9500	-	-	20	0	0	[16]
23m4-8	298.15-298.15	1.01325-1.01325	5.9700-17.1800	0.1001-0.9000	-	-	9	0	0	[19]
23m4-10	298.15-298.15	1.01325-1.01325	6.4400-46.8800	0.0390-0.9500	-	-	20	0	0	[23]
23m4-12	283.15-303.15	1.01325-1.01325	14.9400-122.1000	0.0501-0.9501	-	-	67	0	0	[27-28]
23m4-16	293.15-298.15	1.01325-1.01325	43.9000-209.2000	0.1808-0.9347	-	-	17	0	0	[27, 37]
2m5-6	283.15-313.15	1.01325-1.01325	0.6400-5.6200	0.0501-0.9377	-	-	37	0	0	[52]
2m5-7	298.15-298.15	1.01325-1.01325	2.4800-13.0500	0.0500-0.9500	-	-	20	0	0	[16]
2m5-8	283.15-313.15	1.01325-1.01325	6.9900-27.2000	0.1001-0.9000	-	-	38	0	0	[19, 53]
2m5-10	298.15-298.15	1.01325-1.01325	7.0300-44.4100	0.0433-0.9460	-	-	19	0	0	[23]
2m5-12	283.15-303.15	1.01325-1.01325	14.3400-104.0000	0.0503-0.9501	-	-	73	0	0	[27-28]
2m5-16	293.15-298.15	1.01325-1.01325	102.9000-194.8000	0.1664-0.8079	-	-	22	0	0	[27, 37]
3m5-6	283.15-313.15	1.01325-1.01325	0.0700-4.7500	0.0337-0.9473	-	-	44	0	0	[52]
3m5-7	298.15-298.15	1.01325-1.01325	1.9400-10.9500	0.0500-0.9500	-	-	20	0	0	[16]
3m5-8	283.15-313.15	1.01325-1.01325	5.6200-25.0000	0.1001-0.9001	-	-	41	0	0	[19, 53-54]
3m5-10	298.15-298.15	1.01325-1.01325	7.6600-40.6700	0.0500-0.9499	-	-	23	0	0	[23, 54]
3m5-12	283.15-303.15	1.01325-1.01325	13.3500-104.8000	0.0501-0.9499	-	-	76	0	0	[27-28]
3m5-16	293.15-298.15	1.01325-1.01325	114.3000-189.1000	0.2434-0.7947	-	-	19	0	0	[27, 37]
6-24m5	298.15-298.15	1.01325-1.01325	1.3000-7.6600	0.0501-0.9498	-	-	19	0	0	[55]
24m5-7	298.15-298.15	1.01325-1.01325	8.1400-22.9900	0.1001-0.9005	-	-	9	0	0	[55]
24m5-8	298.15-298.15	1.01325-1.01325	12.8900-34.6100	0.1041-0.8999	-	-	12	0	0	[55]
24m5-12	298.15-298.15	1.01325-1.01325	17.8300-113.3000	0.0501-0.9500	-	-	13	0	0	[55]
6-224m5	298.15-298.15	1.01000-1.01325	-11.6000-0.0000	0.0500-0.9498	-	-	25	0	0	[56-57]
7-224m5	298.15-313.15	1.01325-1.01325	1.0000-21.0000	0.0500-0.9780	-	-	54	0	0	[57-58]
224m5-8	298.15-323.15	1.01325-1.01325	5.0400-26.1600	0.0500-0.9500	-	-	34	0	0	[45, 57]
224m5-10	298.15-298.15	1.01325-1.01325	12.3600-69.5700	0.0501-0.9500	-	-	19	0	0	[57]
224m5-12	298.15-298.15	1.01325-1.01325	20.5100-117.9400	0.0500-0.9500	-	-	19	0	0	[59]
224m5-16	298.15-323.15	1.01325-1.01325	90.7000-233.5000	0.2615-0.9009	-	-	13	0	0	[32, 45]
22m4-23m4	298.15-298.15	1.01325-1.01325	0.4100-1.3500	0.0999-0.8999	-	-	9	0	0	[60]
22m4-2m5	298.15-298.15	1.01325-1.01325	-2.6000-0.0000	0.1001-0.9001	-	-	10	0	0	[60]
22m4-3m5	298.15-298.15	1.01325-1.01325	0.2400-2.2400	0.0501-0.8990	-	-	10	0	0	[60]
22m4-224m5	298.15-298.15	1.01000-1.01000	-10.2000-0.0000	0.2176-0.7456	-	-	4	0	0	[61]
23m4-2m5	298.15-298.15	1.01325-1.01325	-6.9600-0.0000	0.1002-0.9005	-	-	9	0	0	[60]
23m4-3m5	298.15-298.15	1.01325-1.01325	-1.1100-0.0000	0.1023-0.8972	-	-	9	0	0	[60]
2m5-3m5	298.15-298.15	1.01325-1.01325	0.4300-1.4000	0.1000-0.9003	-	-	9	0	0	[60]
1-3	91.50-302.20	1.01325-1.01325	5.1000-155.3000	0.3019-0.8274	0.1380-0.8920	-	11	83	0	[62-63]
1-4	277.00-394.30	1.01325-1.01325	7.5000-51.2000	-	0.2090-0.8980	-	0	96	0	[62]
1-5	318.50-403.50	1.01325-1.01325	25.8000-67.9000	-	0.2550-0.7080	-	0	75	0	[62]
1-6	343.20-407.70	1.01325-1.01325	43.6000-99.3000	-	0.2940-0.8220	-	0	61	0	[62]
1-7	255.40-413.30	1.01325-138.00000	-729.0000-105.1000	-	0.3300-0.8420	0.0196-0.6019	0	37	33	[62, 64]
1-8	410.20-418.30	1.01325-1.01325	84.0000-140.7000	-	0.3800-0.7960	-	0	19	0	[62]

Table V−5. (continued-2)

Binary system (1st compound-2nd compound)	Temperature rage (K)	Pressure range (bar)	Excess enthalpy range (J/mol)	x_1 range (1st compound liquid mole fraction)	y_1 range (1st compound gas mole fraction)	z_1 range (1st compound mole fraction)	Number of points (T,P,h^E,x)	Number of points (T,P,h^E,y)	Number of points (T,P,h^E,z)	References
2-3	200.00-373.15	1.01325-150.00000	-2991.000-3547.000	0.0344-0.9855	0.0344-0.9850	0.0171-0.9855	199	75	404	[65-66]
2-4	304.50-363.20	1.01000-1.01000	8.9000-19.0000	-	0.3770-0.6690	-	0	26	0	[13]
2-6	372.20-403.20	1.01000-1.01000	36.2000-51.7000	-	0.4340-0.7480	-	0	28	0	[13]
2-8	403.20-413.20	1.01000-1.01000	69.4000-122.4000	-	0.3940-0.7920	-	0	20	0	[13]
1-2	91.50-303.20	1.01325-1.01325	1.1500-84.9000	0.2825-0.7879	0.1470-0.8660	-	11	81	0	[62-63]
5-B	298.15-298.15	1.01325-1.01325	175.0000-886.3450	0.0434-0.8994	-	-	37	0	0	[67-68]
6-B	290.65-323.15	0.80000-1.01325	19.7620-940.0000	0.0043-0.9918	-	-	251	0	0	[18, 69-79]
B-7	288.15-323.15	1.01000-1.01325	30.1000-1008.4300	0.0102-0.9756	-	-	320	0	0	[45, 80-92]
B-8	291.15-323.15	1.01000-1.01325	158.3100-1037.0000	0.0560-0.9636	-	-	85	0	0	[67, 72, 91, 93-94]
B-10	298.15-323.15	1.01325-1.01325	112.5000-1072.3000	0.0384-0.9828	-	-	155	0	0	[68, 72, 83, 87]
B-11	298.15-298.15	1.01325-1.01325	257.0000-1108.0000	0.1502-0.9588	-	-	24	0	0	[67]
B-12	298.15-323.15	1.01325-1.01325	70.0000-1164.0000	0.0490-0.9902	-	-	83	0	0	[67, 72]
B-13	298.15-298.15	1.01325-1.01325	270.8860-1198.6800	0.1284-0.9649	-	-	9	0	0	[68]
B-14	293.15-323.15	1.01325-1.01325	46.2000-1263.0000	0.0353-0.9952	-	-	277	0	0	[67, 72, 83, 95]
B-15	298.15-298.15	1.01325-1.01325	172.0000-1293.0000	0.1613-0.9808	-	-	25	0	0	[67]
B-16	293.15-323.15	1.01325-1.01325	34.4000-1347.6000	0.0371-0.9965	-	-	228	0	0	[45, 67, 72, 95]
B-17	298.15-298.15	1.01325-1.01325	176.0000-1390.0000	0.1662-0.9827	-	-	27	0	0	[67]
B-18	323.15-323.15	1.01325-1.01325	127.0000-1213.0000	0.1265-0.9868	-	-	46	0	0	[72]
B-20	323.15-323.15	1.01325-1.01325	145.0000-1266.0000	0.1428-0.9860	-	-	61	0	0	[72]
22m4-B	298.15-298.15	1.01325-1.01325	433.2000-909.1000	0.1852-0.8522	-	-	15	0	0	[79]
23m4-B	298.15-298.15	1.01325-1.01325	435.4000-913.8000	0.1500-0.8536	-	-	13	0	0	[79]
2m5-B	298.15-298.15	1.01325-1.01325	605.2000-920.5000	0.1810-0.7010	-	-	18	0	0	[79]
3m5-B	298.15-298.15	1.01325-1.01325	483.0000-921.3000	0.1400-0.7252	-	-	17	0	0	[79]
B-224m5	298.15-323.15	1.01325-1.01325	427.0500-1018.2300	0.1566-0.9047	-	-	26	0	0	[45, 96]
1-B	363.15-413.15	1.01325-1.01325	19.0000-62.6000	-	0.2880-0.8710	-	0	60	0	[97]
6-mB	293.15-573.15	1.01325-125.00000	22.0000-592.5000	0.0164-0.9758	-	0.0164-0.9757	425	0	92	[18, 69, 98-99]
7-mB	255.40-323.15	0.79000-138.00000	36.4000-594.0000	0.0128-0.9687	-	-	198	0	0	[18, 45, 83, 91, 100-105]
mB-8	298.15-298.15	1.01325-1.01325	144.0000-568.0000	0.1396-0.9438	-	-	29	0	0	[106]
mB-10	298.15-308.15	1.01325-1.01325	42.4000-618.4000	0.0349-0.9883	-	-	119	0	0	[83, 106]
mB-12	298.15-298.15	1.01325-1.01325	141.0000-630.0000	0.1767-0.9593	-	-	31	0	0	[106]
mB-14	298.15-298.15	1.01325-1.01325	74.3000-725.9000	0.0554-0.9855	-	-	58	0	0	[83, 106]
mB-16	298.15-323.15	1.01325-1.01325	134.0000-777.0000	0.1552-0.9713	-	-	41	0	0	[45, 106]
6-12mB	298.15-323.15	1.01325-1.01325	236.0000-446.5000	0.1600-0.8200	-	-	35	0	0	[69, 107]
7-12mB	298.15-298.15	1.01325-1.01325	287.5000-420.0000	0.2400-0.7700	-	-	6	0	0	[108]
12mB-9	298.15-318.15	1.01325-1.01325	185.0000-440.0000	0.1590-0.8950	-	-	31	0	0	[109-110]
6-13mB	298.15-323.15	1.01325-1.01325	200.0000-381.0000	0.1600-0.8300	-	-	30	0	0	[69, 111]
7-13mB	298.15-323.15	1.01325-1.01325	229.4000-401.4000	0.1599-0.7918	-	-	23	0	0	[45, 108]
13mB-9	298.15-298.15	1.01325-1.01325	198.0000-377.5000	0.1859-0.8807	-	-	11	0	0	[110]
6-14mB	298.15-323.15	1.01325-1.01325	163.3000-349.0000	0.1600-0.8300	-	-	23	0	0	[69]
7-14mB	298.15-298.15	1.01325-1.01325	50.1000-347.0000	0.0690-0.9653	-	-	35	0	0	[83, 108]

Table V−5. (continued-3)

Binary system (1st compound-2nd compound)	Temperature rage (K)	Pressure range (bar)	Excess enthalpy range (J/mol)	x_1 range (1st compound liquid mole fraction)	y_1 range (1st compound gas mole fraction)	z_1 range (1st compound mole fraction)	Number of points (T,P,h^E,x)	Number of points (T,P,h^E,y)	Number of points (T,P,h^E,z)	References
14mB-9	298.15-298.15	1.01325-1.01325	134.8000-319.9000	0.1854-0.9025	-	-	10	0	0	110
14mB-10	298.15-308.15	1.01325-1.01325	32.0000-330.1000	0.0306-0.9779	-	-	88	0	0	83
14mB-14	298.15-298.15	1.01325-1.01325	55.1000-369.1000	0.0716-0.9783	-	-	27	0	0	83
14mB-16	298.15-298.15	1.01325-1.01325	180.6000-412.7000	0.2010-0.9180	-	-	10	0	0	108
7-eB	288.15-308.15	1.01325-1.01325	34.3000-568.9000	0.0143-0.9792	-	-	81	0	0	104, 112-114
8-eB	298.15-298.15	1.01325-1.01325	99.0000-708.9000	0.0408-0.9277	-	-	39	0	0	115-116
eB-9	293.60-298.15	1.01325-1.01325	296.3000-744.0000	0.1864-0.8810	-	-	12	0	0	110, 117
eB-10	298.15-298.15	1.01325-1.01325	111.0000-620.0000	0.0780-0.9613	-	-	29	0	0	118
eB-12	298.15-298.15	1.01325-1.01325	97.0000-673.0000	0.1090-0.9718	-	-	32	0	0	115
eB-14	298.15-298.15	1.01325-1.01325	129.0000-728.0000	0.1095-0.9680	-	-	25	0	0	118
eB-16	298.15-330.00	1.01325-1.01325	13.7000-793.0000	0.1407-0.9971	-	-	48	0	0	115, 119
eB-18	303.15-330.00	1.01325-1.01325	117.0000-531.0000	0.8435-0.9706	-	-	12	0	0	119
eB-19	311.45-330.00	1.01325-1.01325	115.0000-510.0000	0.8521-0.9732	-	-	12	0	0	119
eB-20	313.02-330.00	1.01325-1.01325	90.6000-545.0000	0.8491-0.9799	-	-	13	0	0	119
7-124mB	298.15-298.15	1.01325-1.01325	18.7000-274.1000	0.0195-0.9564	-	-	16	0	0	120
124B -10	298.15-298.15	1.01325-1.01325	16.9000-252.4000	0.0567-0.9852	-	-	18	0	0	120
124mB-12	298.15-298.15	1.01325-1.01325	16.5000-252.3000	0.0655-0.9873	-	-	16	0	0	120
124mB-14	298.15-298.15	1.01325-1.01325	16.3000-266.4000	0.0743-0.9889	-	-	22	0	0	120
124mB-16	298.15-298.15	1.01325-1.01325	18.4000-275.0000	0.1592-0.9885	-	-	18	0	0	120
7-135mB	298.15-298.15	1.01325-1.01325	238.0000-308.6000	0.2640-0.7370	-	-	6	0	0	108
135mB-16	298.15-298.15	1.01325-1.01325	157.6000-389.6000	0.1410-0.8960	-	-	7	0	0	108
7-prB	298.15-298.15	1.01325-1.01325	410.0000-445.0000	0.3580-0.6150	-	-	4	0	0	113
8-prB	298.15-308.15	1.01325-1.01325	259.0000-430.5000	0.1650-0.8015	-	-	36	0	0	114
7-iprB	298.15-298.15	1.01325-1.01325	348.2000-507.0000	0.2750-0.7920	-	-	7	0	0	108
7-1mBB	298.15-298.15	1.01325-1.01325	19.2000-753.9000	0.0070-0.9584	-	-	15	0	0	120
10-1mBB	298.15-298.15	1.01325-1.01325	40.6000-697.5000	0.0178-0.9452	-	-	15	0	0	120
12-1mBB	298.15-298.15	1.01325-1.01325	30.0000-652.6000	0.0088-0.9361	-	-	20	0	0	120-121
1mBB-14	298.15-298.15	1.01325-1.01325	32.5000-616.5000	0.0724-0.9904	-	-	15	0	0	120
1mBB-16	298.15-298.15	1.01325-1.01325	42.1000-597.5000	0.0361-0.9898	-	-	29	0	0	120
phe-20	391.75-391.75	1.01325-1.01325	354.2630-1343.1500	0.0999-0.9007	-	-	10	0	0	122
224m5-mB	293.15-363.15	1.01325-16.50000	39.4500-662.6000	0.0162-0.9615	-	-	80	0	0	96, 123-124
1-mB	255.40-310.90	138.0000-138.0000	-97.0000-19.0000	-	-	0.0128-0.9036	0	0	32	64
B-mB	279.45-337.65	1.01325-1.01325	2.6000-79.1310	0.0358-0.9913	-	-	154	0	0	18, 70, 91, 125-133
B-12mB	293.15-323.15	1.01325-1.01325	23.2000-214.9000	0.0332-0.9753	-	-	57	0	0	134-137
B-13mB	289.45-323.15	1.01325-1.01325	30.3000-238.6480	0.0447-0.9701	-	-	60	0	0	130, 134-137
B-14mB	287.85-328.45	1.01325-1.01325	7.8700-177.6000	0.0197-0.9897	-	-	302	0	0	126, 129, 133, 135-140
B-eB	293.15-298.15	1.01325-1.01325	15.8200-104.5000	0.0500-0.9500	-	-	31	0	0	141-143
B-124mB	298.15-298.15	1.01325-1.01325	96.5670-379.4050	0.0953-0.9422	-	-	13	0	0	129
B-135mB	298.15-303.15	1.01325-1.01325	119.1180-441.9140	0.0965-0.9428	-	-	22	0	0	129, 144
B-prB	298.15-318.15	1.01325-1.01325	12.7000-143.7000	0.0820-0.9627	-	-	44	0	0	145-146

Table V−5. (continued-4)

Binary system (1st compound-2nd compound)	Temperature rage (K)	Pressure range (bar)	Excess enthalpy range (J/mol)	x_1 range (1st compound liquid mole fraction)	y_1 range (1st compound gas mole fraction)	z_1 range (1st compound mole fraction)	Number of points (T,P,h^E,x)	Number of points (T,P,h^E,y)	Number of points (T,P,h^E,z)	References
B-iprB	298.15-318.15	1.01325-1.01325	37.4000-107.1000	0.1972-0.9088	-	-	39	0	0	144, 147
B-buB	298.15-318.15	1.01325-1.01325	57.3000-195.1000	0.1014-0.8952	-	-	30	0	0	145-146
B-1mBB	298.15-298.15	1.01325-1.01325	88.0000-173.0000	0.1587-0.8493	-	-	13	0	0	148
B-2mBB	309.15-318.15	1.01325-1.01325	54.0000-143.0000	0.1590-0.8833	-	-	14	0	0	148
B-Bph	344.75-344.75	1.01325-1.01325	57.7780-144.8630	0.1354-0.8747	-	-	12	0	0	149
B-Dph	308.15-308.15	1.01325-1.01325	1.3820-9.5880	0.1682-0.9094	-	-	12	0	0	150
mB-12mB	298.15-298.15	1.01325-1.01325	9.4000-47.0000	0.0687-0.9476	-	-	36	0	0	131
mB-13mB	298.15-298.15	1.01325-1.01325	7.3000-43.0000	0.0603-0.9574	-	-	17	0	0	131
mB-14mB	290.65-338.15	1.01000-1.01325	4.1000-50.1000	0.0500-0.9500	-	-	123	0	0	70, 126, 129, 131, 151
mB-eB	298.15-303.15	1.01325-1.01325	-12.7300-0.0000	0.0500-0.9500	-	-	43	0	0	142-143, 152-153
mB-124mB	298.15-298.15	1.01325-1.01325	38.6180-121.5030	0.1468-0.9063	-	-	10	0	0	129
mB-135mB	298.15-298.15	1.01325-1.01325	31.3800-153.4270	0.1105-0.9509	-	-	13	0	0	129
mB-prB	298.15-318.15	1.01325-1.01325	0.3000-4.9000	0.1061-0.9210	-	-	39	0	0	145, 154
mB-iprB	298.15-318.15	1.01325-1.01325	-28.1000-0.0000	0.1708-0.8930	-	-	30	0	0	147, 153
mB-buB	298.15-318.15	1.01325-1.01325	7.9000-22.3000	0.0789-0.9006	-	-	50	0	0	145, 154
13mB-12mB	288.65-298.15	1.01325-1.01325	0.4610-11.3000	0.0347-0.9822	-	-	59	0	0	130, 155-156
14mB-12mB	288.65-298.15	1.01325-1.01325	0.7120-10.5510	0.0338-0.9649	-	-	55	0	0	130, 155-156
eB-12mB	298.15-343.15	1.01325-1.01325	2.5540-39.4400	0.0324-0.9650	-	-	78	0	0	142, 155
12mB-iprB	298.15-298.15	1.01325-1.01325	18.9600-92.5900	0.0997-0.9241	-	-	18	0	0	157
14mB-13mB	288.65-298.15	1.01325-1.01325	-10.8860-0.0000	0.0351-0.9666	-	-	63	0	0	130, 155-156
eB-13mB	298.15-343.15	1.01325-1.01325	3.2240-35.1500	0.0353-0.9652	-	-	80	0	0	142, 155
13mB-iprB	298.15-298.15	1.01325-1.01325	18.3300-97.7900	0.0904-0.9179	-	-	18	0	0	157
eB-14mB	298.15-298.15	1.01325-1.01325	-9.9500-0.0000	0.0365-0.9663	-	-	50	0	0	142, 155
14mB-124mB	298.15-298.15	1.01325-1.01325	14.9370-38.8280	0.1291-0.8929	-	-	11	0	0	129
14mB-135mB	298.15-298.15	1.01325-1.01325	8.1590-28.6600	0.0968-0.9224	-	-	13	0	0	129
14mB-iprB	298.15-298.15	1.01325-1.01325	-20.3100-0.0000	0.0888-0.9610	-	-	19	0	0	157
eB-prB	298.15-318.15	1.01325-1.01325	-4.1000-8.0000	0.0562-0.9230	-	-	43	0	0	145, 158
eB-iprB	298.15-318.15	1.01325-1.01325	-3.7000-0.0000	0.1875-0.8489	-	-	24	0	0	147
eB-buB	298.15-318.15	1.01325-1.01325	9.1000-24.3000	0.1139-0.9306	-	-	49	0	0	145, 158
135mB-124mB	298.15-298.15	1.01325-1.01325	0.7030-4.6020	0.0643-0.9144	-	-	14	0	0	129
prB-buB	298.15-298.15	1.01325-1.01325	-2.6000-5.9000	0.0727-0.8893	-	-	10	0	0	145
2mBB-1mBB	318.15-318.15	1.01325-1.01325	7.3000-44.4000	0.0550-0.9500	-	-	8	0	0	86
5-C5	288.20-298.20	1.01325-1.01325	16.0000-58.4000	0.0663-0.9316	-	-	25	0	0	159
C5-6	288.20-298.20	1.01325-1.01325	13.0000-60.8000	0.0635-0.9336	-	-	28	0	0	159
C5-7	288.20-298.20	1.01325-1.01325	11.2000-71.1000	0.0688-0.9642	-	-	38	0	0	159-160
C5-8	288.20-298.20	1.01325-1.01325	27.3000-87.2000	0.0939-0.9276	-	-	26	0	0	159
C5-10	298.15-298.15	1.01325-1.01325	10.6000-108.9000	0.2011-0.9728	-	-	11	0	0	160
C5-12	288.20-298.20	1.01325-1.01325	33.4000-166.9000	0.0833-0.9474	-	-	26	0	0	159
C5-16	293.20-308.20	1.01325-1.01325	43.6000-268.1000	0.1051-0.9524	-	-	37	0	0	159, 161
5-C6	298.15-298.15	1.01325-1.01325	7.9400-61.7100	0.0077-0.0623	-	-	8	0	0	162

Table V−5. (continued-5)

Binary system (1st compound-2nd compound)	Temperature rage (K)	Pressure range (bar)	Excess enthalpy range (J/mol)	x_1 range (1st compound liquid mole fraction)	y_1 range (1st compound gas mole fraction)	z_1 range (1st compound mole fraction)	Number of points (T,P,h^E,x)	Number of points (T,P,h^E,y)	Number of points (T,P,h^E,z)	References
6-C6	288.15-413.21	0.79000-300.00000	1.7000-241.6000	0.0018-0.9909	-	-	1535	0	0	18, 48, 69-70, 73, 76, 78, 99, 102, 162-208
C6-7	293.15-323.15	1.00000-285.00000	4.9200-293.0000	0.2030-0.9969	-	-	68	0	0	20, 45, 81, 162, 182, 209
C6-8	298.15-313.15	1.00000-290.00000	3.6200-288.2000	0.0895-0.9979	-	-	120	0	0	20, 162, 165, 182, 205, 210-212
C6-9	298.15-313.15	1.01325-1.01325	176.1500-296.2000	0.2948-0.8578	-	-	32	0	0	182, 213
C6-10	298.15-313.15	1.00000-290.00000	2.5100-365.9000	0.0500-0.9988	-	-	115	0	0	20, 162, 165, 182, 214-215
C6-11	298.15-313.15	1.01325-1.01325	86.0000-354.9000	0.1642-0.9535	-	-	53	0	0	165, 182
C6-12	293.15-313.15	1.00000-291.00000	2.1000-415.0000	0.1213-0.9992	-	-	100	0	0	20, 162, 182, 205, 213, 216
C6-13	298.15-298.15	1.01325-1.01325	102.0000-401.0000	0.1236-0.9540	-	-	27	0	0	165
C6-14	293.15-308.15	1.00000-1.01325	2.2100-483.2000	0.0292-0.9993	-	-	176	0	0	95, 162, 165, 214
C6-15	298.15-298.15	1.01325-1.01325	104.0000-478.0000	0.1275-0.9612	-	-	27	0	0	165
C6-16	293.15-323.15	1.01325-1.01325	1.7300-562.2000	0.0091-0.9995	-	-	218	0	0	45, 95, 161-162, 165, 182, 217
C6-17	298.15-298.15	1.01325-1.01325	119.0000-565.0000	0.1593-0.9641	-	-	28	0	0	165
6-C7	288.20-298.20	1.01325-1.01325	62.4000-226.2000	0.0598-0.8765	-	-	22	0	0	218
7-C7	288.20-298.20	1.01000-1.01325	20.1000-261.9000	0.0641-0.9706	-	-	52	0	0	218-220
C7-8	288.20-298.20	1.01325-1.01325	72.9000-293.7000	0.0915-0.9367	-	-	23	0	0	218
C7-9	298.15-298.15	1.01325-1.01325	44.8000-274.6000	0.0605-0.9467	-	-	10	0	0	219
C7-12	288.20-298.20	1.01325-1.01325	109.7000-398.7000	0.1095-0.9332	-	-	21	0	0	218
C7-14	298.15-298.15	1.01325-1.01325	79.2000-365.8000	0.0857-0.9628	-	-	10	0	0	219
C7-16	298.20-308.20	1.01325-1.01325	139.3000-480.6000	0.1366-0.8741	-	-	21	0	0	218
6-C8	288.15-298.15	1.01325-1.01325	48.0000-219.8000	0.0827-0.9232	-	-	22	0	0	221
7-C8	288.15-298.15	1.01000-1.01325	19.3000-253.5000	0.0706-0.9734	-	-	49	0	0	219-221
8-C8	288.15-298.15	1.01325-1.01325	65.1000-279.0000	0.0845-0.9078	-	-	25	0	0	221
9-C8	298.15-298.15	1.01325-1.01325	40.0000-254.1000	0.0587-0.9451	-	-	10	0	0	219
C8-12	288.15-298.15	1.01325-1.01325	112.0000-392.8000	0.1166-0.9299	-	-	26	0	0	221
C8-14	298.15-298.15	1.01325-1.01325	77.1000-329.5000	0.0779-0.9589	-	-	10	0	0	219
C8-16	298.15-308.15	1.01325-1.01325	102.3000-456.4000	0.1022-0.9360	-	-	25	0	0	221
6-tet	288.20-298.20	1.01325-1.01325	139.1000-476.6000	0.0970-0.9339	-	-	19	0	0	222
7-tet	288.20-323.15	1.01000-1.01325	60.3000-530.0000	0.1034-0.9736	-	-	59	0	0	45, 220, 222-223
tet-12	288.20-298.20	1.01325-1.01325	138.4000-598.9000	0.1599-0.9515	-	-	21	0	0	222
tet-16	298.15-323.15	1.01325-1.01325	156.4000-712.9000	0.0775-0.9497	-	-	30	0	0	45, 222
C5-23m4	288.15-308.15	1.01325-1.01325	-7.2400-4.9700	0.0367-0.9805	-	-	94	0	0	224
22m3-C6	298.15-298.15	1.01325-1.01325	70.6000-98.5700	0.2370-0.7360	-	-	9	0	0	225
22m4-C6	298.15-298.15	1.01325-1.01325	5.6000-154.2000	0.0400-0.9900	-	-	69	0	0	202, 226-228
23m4-C6	288.15-308.15	1.01325-1.01325	4.4700-167.0000	0.0070-0.9900	-	-	148	0	0	202, 227, 229
2m5-C6	298.15-298.15	1.01325-1.01325	6.5000-205.6000	0.0068-0.9900	-	-	53	0	0	162, 202, 227
3m5-C6	298.15-298.15	1.01325-1.01325	5.8000-185.6000	0.0200-0.9900	-	-	50	0	0	202, 227
22m5-C6	298.15-313.15	1.01325-1.01325	108.1000-181.4000	0.1880-0.7430	-	-	16	0	0	182
24m5-C6	301.15-301.15	1.01325-1.01325	102.1600-172.0800	0.1758-0.7115	-	-	5	0	0	96
C6-224m5	293.15-323.15	1.00000-290.00000	18.7000-190.5000	0.0571-0.9737	-	-	131	0	0	20, 45, 124, 182, 211, 230

Table V−5. (continued-6)

Binary system (1st compound-2nd compound)	Temperature rage (K)	Pressure range (bar)	Excess enthalpy range (J/mol)	x_1 range (1st compound liquid mole fraction)	y_1 range (1st compound gas mole fraction)	z_1 range (1st compound mole fraction)	Number of points (T,P,h^E,x)	Number of points (T,P,h^E,y)	Number of points (T,P,h^E,z)	References
C6-34m6	308.15-308.15	1.01325-1.01325	156.4000-224.3000	0.3478-0.8218	-	-	8	0	0	211
C6-4m7	308.15-308.15	1.01325-1.01325	164.3000-219.5000	0.3953-0.8221	-	-	9	0	0	211
23m4-C7	288.15-313.15	1.01325-1.01325	15.7700-168.3100	0.0249-0.9713	-	-	96	0	0	231
23m4-C8	288.15-313.15	1.01325-1.01325	15.3400-185.3500	0.0275-0.9741	-	-	96	0	0	232
1-C6	363.15-413.15	1.01325-1.01325	20.5000-67.9000	-	0.2860-0.8820	-	0	60	0	97
C5-B	298.15-308.15	1.01325-1.01325	145.7000-647.0000	0.1030-0.9423	-	-	36	0	0	160, 233-234
B-C6	280.15-413.21	0.80000-17.54000	3.3000-867.4800	0.0012-0.9987	-	-	1397	0	0	41, 45, 70, 73, 76, 78, 81, 88, 94, 103, 129, 162, 167-168, 177, 180, 191, 195-196, 203-204, 207-209, 234-276
B-C7	298.15-298.15	1.01000-1.01325	98.3000-820.9000	0.1016-0.9689	-	-	32	0	0	234, 277-278
B-C8	298.15-298.15	1.01000-1.01325	98.8000-818.4000	0.1113-0.9719	-	-	36	0	0	234, 277-278
B-tet	298.15-323.15	1.01325-1.01325	37.7000-163.0000	0.0750-0.9387	-	-	25	0	0	45, 279
C5-mB	298.15-298.15	1.01325-1.01325	146.0000-365.4000	0.1293-0.8932	-	-	8	0	0	234
C6-mB	290.65-413.21	1.01325-17.54000	18.5200-627.5160	0.0530-0.9937	-	-	132	0	0	18, 69-70, 128-129, 132, 162, 178, 234, 252, 280
C6-12mB	298.15-300.05	1.01325-1.01325	157.0000-631.7000	0.1003-0.8992	-	-	30	0	0	93, 112, 281
C6-13mB	298.15-323.15	1.01325-1.01325	93.7080-575.6000	0.1800-0.9664	-	-	32	0	0	45, 281-282
C6-14mB	288.15-313.15	1.01325-1.01325	20.1290-587.6900	0.0161-0.9930	-	-	174	0	0	70, 93, 129, 138, 281, 283-285
C6-eB	298.15-298.15	1.01325-1.01325	47.4000-584.2000	0.0250-0.9779	-	-	57	0	0	112, 282, 286
C6-124mB	298.15-298.15	1.01325-1.01325	146.8580-640.4870	0.0796-0.9303	-	-	13	0	0	129
C6-135mB	298.15-298.15	1.01325-1.01325	142.0890-623.4160	0.0806-0.9312	-	-	13	0	0	129
C6-prB	298.15-298.15	1.01325-1.01325	78.2000-694.1000	0.0500-0.9750	-	-	20	0	0	286
C6-iprB	298.15-298.15	1.01325-1.01325	37.1000-542.4000	0.0250-0.9750	-	-	19	0	0	286
mB-C7	298.15-298.15	1.01000-1.01325	73.7000-622.3000	0.0864-0.9631	-	-	23	0	0	234, 278
C7-eB	298.15-298.15	1.01000-1.01000	73.7000-548.8000	0.0423-0.9241	-	-	13	0	0	278
mB-C8	298.15-298.15	1.01000-1.01325	70.6000-619.7000	0.0949-0.9666	-	-	26	0	0	234, 278
eB-C8	298.15-298.15	1.01000-1.01000	65.1000-529.1000	0.0834-0.9617	-	-	13	0	0	278
C6-1mBB	298.15-298.15	1.01325-1.01325	363.0000-936.0000	0.1218-0.9003	-	-	14	0	0	148
C6-2mBB	309.15-318.15	1.01325-1.01325	395.0000-927.0000	0.1578-0.9154	-	-	13	0	0	148
C5-C6	288.15-308.15	1.01325-1.01325	0.8600-35.4700	0.0106-0.9918	-	-	98	0	0	173, 233, 287
C5-C7	288.15-308.15	1.01325-1.01325	-16.0400-12.8800	0.0335-0.9790	-	-	100	0	0	173, 288
C5-C8	283.15-313.15	1.01325-1.01325	-56.6000-0.6300	0.0123-0.9831	-	-	162	0	0	173, 289-290
C6-C7	288.15-318.15	1.01325-1.01325	-0.1100-9.1000	0.0299-0.9761	-	-	104	0	0	173, 291
C6-C8	283.15-318.15	1.01325-1.01325	-19.4000-19.3000	0.0212-0.9973	-	-	174	0	0	173, 288
C7-C8	283.15-353.15	1.01325-1.01325	-11.8000-4.7000	0.0296-0.9762	-	-	137	0	0	173, 291
C5-tet	288.20-298.20	1.01325-1.01325	58.3000-258.6000	0.0762-0.9370	-	-	19	0	0	222
C6-tet	288.20-323.15	1.01325-1.01325	95.3000-503.0000	0.0944-0.9579	-	-	31	0	0	45, 222
C7-tet	288.20-298.20	1.01325-1.01325	158.9000-451.9000	0.1148-0.8712	-	-	17	0	0	222
C8-tet	288.20-298.20	1.01325-1.01325	88.2000-436.7000	0.0976-0.9508	-	-	18	0	0	222
6-mC5	298.15-298.15	1.01325-1.01325	52.3000-107.1000	0.2700-0.8400	-	-	7	0	0	164

Table V−5. (continued-7)

Binary system (1st compound-2nd compound)	Temperature rage (K)	Pressure range (bar)	Excess enthalpy range (J/mol)	x_1 range (1st compound liquid mole fraction)	y_1 range (1st compound gas mole fraction)	z_1 range (1st compound mole fraction)	Number of points (T,P,h^E,x)	Number of points (T,P,h^E,y)	Number of points (T,P,h^E,z)	References
mC5-7	298.15-298.15	1.01325-1.01325	18.4000-96.0000	0.1369-0.9576	-	-	11	0	0	160
mC5-10	298.15-298.15	1.01325-1.01325	22.8000-148.9000	0.1741-0.9677	-	-	11	0	0	160
mC5-16	298.20-308.20	1.01325-1.01325	104.0000-300.0000	0.1139-0.9224	-	-	13	0	0	161
6-mC6	273.15-298.15	1.01325-1.01325	4.9000-18.6000	0.0919-0.9116	-	-	18	0	0	124, 292
7-mC6	255.40-323.15	1.01325-138.00000	4.7000-89.0000	0.0958-0.9378	-	-	77	0	0	45, 101, 164, 292-294
mC6-8	298.15-298.15	1.01325-1.01325	13.3000-40.2000	0.1408-0.8898	-	-	16	0	0	292
mC6-10	298.15-298.15	1.01325-1.01325	20.3900-80.3300	0.0810-0.9262	-	-	11	0	0	294
mC6-16	273.15-308.20	1.01325-1.01325	65.0000-259.1000	0.1213-0.9366	-	-	21	0	0	124, 161
8-eC6	298.15-298.15	1.01325-1.01325	23.5000-41.1000	0.2500-0.8100	-	-	6	0	0	164
6-tCC6	298.15-298.15	1.01325-1.01325	-34.2000-0.0000	0.0500-0.9500	-	-	11	0	0	295
7-tCC6	298.15-298.15	1.01000-1.01325	-33.9000-0.0000	0.0990-0.9521	-	-	36	0	0	220, 247
6-cCC6	298.15-298.15	1.01325-1.01325	19.1000-111.0000	0.0500-0.9500	-	-	11	0	0	295
7-cCC6	298.15-298.15	1.01000-1.01325	21.4000-139.2000	0.0500-0.9500	-	-	32	0	0	220, 296
6-bcy	288.20-298.20	1.01325-1.01325	6.0000-33.0000	0.1261-0.9265	-	-	17	0	0	297
7-bcy	298.15-298.15	1.01000-1.01000	8.5000-24.3000	0.1756-0.9274	-	-	15	0	0	220
8-bcy	288.20-298.20	1.01325-1.01325	7.2000-46.2000	0.0774-0.9164	-	-	16	0	0	297
12-bcy	288.20-300.05	1.01325-1.01325	20.8000-84.1000	0.0864-0.9085	-	-	20	0	0	297-298
bcy-16	298.20-308.20	1.01325-1.01325	24.0000-128.0000	0.0579-0.9478	-	-	18	0	0	297
22m3-mC6	273.15-273.15	1.01325-1.01325	27.3000-34.0000	0.3410-0.7370	-	-	4	0	0	124
224m5-mC6	273.15-298.15	1.01325-1.01325	11.0100-54.3900	0.0467-0.9500	-	-	28	0	0	124, 299
22m4-tCC6	298.15-298.15	1.01325-1.01325	15.4000-86.0000	0.0500-0.9500	-	-	11	0	0	295
23m4-tCC6	298.15-298.15	1.01325-1.01325	8.2000-50.0000	0.0500-0.9500	-	-	11	0	0	295
2m5-tCC6	298.15-298.15	1.01325-1.01325	-22.4000-0.0000	0.0500-0.9500	-	-	11	0	0	295
3m5-tCC6	298.15-298.15	1.01325-1.01325	-0.5000-5.8000	0.0500-0.9500	-	-	11	0	0	295
224m5-tCC6	298.15-298.15	1.01325-1.01325	15.0300-73.8800	0.0996-0.9507	-	-	18	0	0	247
22m4-cCC6	298.15-298.15	1.01325-1.01325	29.5000-158.4000	0.0500-0.9500	-	-	11	0	0	295
23m4-cCC6	298.15-298.15	1.01325-1.01325	25.9000-142.1000	0.0500-0.9500	-	-	11	0	0	295
2m5-cCC6	298.15-298.15	1.01325-1.01325	20.9000-112.9000	0.0500-0.9500	-	-	11	0	0	295
3m5-cCC6	298.15-298.15	1.01325-1.01325	23.8000-124.3000	0.0500-0.9500	-	-	11	0	0	295
2m7-cCC6	298.15-298.15	1.01325-1.01325	33.3000-178.7000	0.0500-0.9500	-	-	20	0	0	296
1-mC6	255.40-310.90	138.0000-138.0000	-584.0000-0.0000	-	-	0.0415-0.9060	0	0	36	64
mC5-B	298.15-298.15	1.01325-1.01325	192.8000-755.0000	0.0877-0.9319	-	-	11	0	0	160
B-mC6	298.15-308.15	1.01325-1.01325	51.9000-790.0000	0.0188-0.9855	-	-	66	0	0	294, 300-301
B-eC6	283.15-298.15	1.01325-1.01325	230.0000-876.0000	0.1030-0.9011	-	-	12	0	0	302
B-tCC6	298.15-298.15	1.01325-1.01325	190.8900-766.4600	0.0997-0.9500	-	-	20	0	0	247
B-cCC6	298.15-298.15	1.01325-1.01325	126.7000-776.3000	0.0500-0.9500	-	-	24	0	0	45, 296
B-bcy	298.15-298.15	1.01325-1.01325	229.9000-855.5000	0.0958-0.8723	-	-	13	0	0	279
mC6-mB	255.40-310.90	0.79000-138.00000	57.2000-557.0000	0.0262-0.9622	-	-	87	0	0	101-102, 124, 276, 301
mC6-14mB	300.05-300.05	1.01325-1.01325	85.0000-447.0000	0.0570-0.9400	-	-	10	0	0	138
mC6-eB	283.15-298.15	1.01325-1.01325	60.7000-458.0000	0.0344-0.9583	-	-	31	0	0	301-302

Table V−5. (continued-8)

Binary system (1st compound-2nd compound)	Temperature rage (K)	Pressure range (bar)	Excess enthalpy range (J/mol)	x_1 range (1st compound liquid mole fraction)	y_1 range (1st compound gas mole fraction)	z_1 range (1st compound mole fraction)	Number of points (T,P,h^E,x)	Number of points (T,P,h^E,y)	Number of points (T,P,h^E,z)	References
mB-eC6	283.15-298.15	1.01325-1.01325	183.0000-584.0000	0.1033-0.8932	-	-	12	0	0	[302]
eC6-eB	283.15-298.15	1.01325-1.01325	183.0000-502.0000	0.1469-0.8868	-	-	12	0	0	[302]
mB-tCC6	298.15-298.15	1.01325-1.01325	166.1600-486.8300	0.0994-0.9011	-	-	17	0	0	[247]
mB-cCC6	298.15-298.15	1.01325-1.01325	99.5000-539.1000	0.0500-0.9500	-	-	20	0	0	[296]
C5-mC5	298.15-298.15	1.01325-1.01325	-12.3700-0.0000	0.0678-0.9554	-	-	10	0	0	[294]
C5-mC6	298.15-298.15	1.01325-1.01325	-112.3000-0.0000	0.0762-0.9605	-	-	10	0	0	[294]
C5-tCC6	298.15-298.15	1.01325-1.01325	-270.5600-0.0000	0.0307-0.9736	-	-	36	0	0	[303]
C5-cCC6	298.15-298.15	1.01325-1.01325	-129.1400-0.0000	0.0232-0.9894	-	-	37	0	0	[303]
C5-bcy	288.20-298.20	1.01325-1.01325	-142.6000-0.0000	0.0519-0.9205	-	-	19	0	0	[297]
mC5-C6	298.15-298.15	1.01325-1.01325	9.1000-46.8000	0.0526-0.8876	-	-	11	0	0	[160]
C6-mC6	293.15-308.15	1.01325-1.01325	0.0300-23.1200	0.0342-0.9751	-	-	87	0	0	[124, 143, 304]
C6-eC6	298.15-298.15	1.01325-1.01325	27.9000-72.0000	0.1030-0.8896	-	-	9	0	0	[143]
C6-tCC6	298.15-298.15	1.01325-1.01325	-7.4300-25.2200	0.0500-0.9753	-	-	55	0	0	[305-307]
C6-cCC6	298.15-298.15	1.01325-1.01325	-3.8500-40.6000	0.0500-0.9765	-	-	55	0	0	[305-307]
C6-bcy	288.20-298.20	1.01325-1.01325	39.5000-126.0000	0.1237-0.9285	-	-	19	0	0	[297]
C7-tCC6	298.15-298.15	1.01325-1.01325	-7.9000-0.0000	0.1450-0.9238	-	-	8	0	0	[306]
C7-cCC6	298.15-298.15	1.01325-1.01325	0.5000-14.7000	0.1632-0.8638	-	-	8	0	0	[306]
C7-bcy	288.20-298.20	1.01325-1.01325	38.2000-158.4000	0.0997-0.9318	-	-	17	0	0	[297]
C8-tCC6	298.15-298.15	1.01325-1.01325	-1.5000-8.4800	0.0500-0.9500	-	-	20	0	0	[306-307]
C8-cCC6	298.15-298.15	1.01325-1.01325	3.7300-23.1000	0.0500-0.9500	-	-	19	0	0	[306-307]
C8-bcy	288.20-298.20	1.01325-1.01325	36.4000-178.2000	0.0742-0.9564	-	-	18	0	0	[297]
tet-tCC6	298.15-298.15	1.01325-1.01325	124.0000-245.0000	0.2046-0.8634	-	-	9	0	0	[308]
mC5-mC6	298.15-298.15	1.01325-1.01325	-52.0400-0.0000	0.0595-0.9491	-	-	10	0	0	[294]
mC6-eC6	298.15-298.15	1.01325-1.01325	1.1000-4.2000	0.1183-0.8783	-	-	10	0	0	[143]
mC6-tCC6	298.15-298.15	1.01325-1.01325	1.2200-7.2000	0.0500-0.9500	-	-	11	0	0	[307]
mC6-cCC6	298.15-298.15	1.01325-1.01325	8.9900-49.2600	0.0500-0.9500	-	-	11	0	0	[307]
CO2-5	308.15-573.15	75.80000-124.50000	-4022.000-4460.000	-	0.0387-0.9905	0.0387-0.9907	0	175	414	[309-310]
CO2-6	308.15-573.15	62.90000-125.00000	-4090.000-5050.000	-	0.0244-0.9918	0.0200-0.9918	0	176	547	[311-313]
CO2-9	373.15-373.15	75.00000-125.00000	-1980.000-252.000	-	-	0.0584-0.9934	0	0	49	[314]
CO2-10	283.15-573.15	75.80000-125.00000	-4750.000-3370.000	0.0631-0.9939	-	0.0362-0.9945	102	0	301	[315-316]
CO2-12	318.15-318.15	40.00000-140.00000	-2974.800-688.600	-	-	0.0500-0.9980	0	0	170	[317]
CO2-22m3	310.00-313.15	62.90000-104.40000	-4300.000-493.000	-	-	0.0600-0.9800	0	0	118	[318]
1-CO2	283.15-353.15	5.07000-111.45700	6.000-3990.000	-	0.0950-0.9000	-	0	636	0	[319-320]
CO2-2	217.00-323.15	1.01325-110.00000	-373.000-6514.000	0.0410-0.9790	0.0250-0.9780	0.0460-0.9790	118	185	105	[321-324]
CO2-B	354.50-398.60	1.01000-1.01000	31.9000-52.5000	-	0.3590-0.6210	-	0	40	0	[325]
CO2-mB	298.15-573.15	69.80000-175.00000	-5660.000-7060.000	0.1150-0.9870	-	0.0347-0.9946	66	0	885	[326-330]
CO2-C6	308.15-573.15	1.01000-143.90000	-4212.000-6510.000	-	0.0393-0.9902	0.0364-0.9902	0	137	716	[325, 331-333]
N2-1	91.50-298.00	1.01325-102.30000	13.0000-3059.0000	0.1170-0.7140	0.0600-0.7840	0.1060-0.8530	12	75	28	[334-336]
N2-2	92.10-92.30	6.31000-7.90000	17.4000-178.0000	-	-	0.0500-0.9980	0	0	41	[337-338]
N2-B	333.20-433.20	0.47000-1.02000	41.0000-71.7000	-	0.5000-0.5000	-	0	15	0	[339]

Table V−5. (continued-9)

Binary system (1st compound-2nd compound)	Temperature rage (K)	Pressure range (bar)	Excess enthalpy range (J/mol)	x_1 range (1st compound liquid mole fraction)	y_1 range (1st compound gas mole fraction)	z_1 range (1st compound mole fraction)	Number of points (T,P,h^E,x)	Number of points (T,P,h^E,y)	Number of points (T,P,h^E,z)	References
N2-C6	333.20-433.20	0.44000-1.02000	40.3000-75.1000	-	0.5000-0.5000	0.5000-0.5000	0	15	4	339-340
N2-CO2	283.15-353.15	10.13000-121.59000	9.0000-4400.0000	-	0.1000-0.9000	-	0	693	0	341-342
1-H2S	293.15-313.15	5.07000-15.20000	23.8000-190.8000	-	0.1840-0.8470	-	0	39	0	343
3SH-7	298.15-298.15	1.01325-1.01325	217.2000-724.1000	0.0900-0.8690	-	-	12	0	0	344
4sh-7	283.15-333.15	5.00000-5.00000	72.0000-698.3000	0.0406-0.9630	-	-	60	0	0	345
B-4sh	283.15-333.15	5.00000-5.00000	9.9000-146.7000	0.0479-0.9498	-	-	58	0	0	345
4sh-mB	283.15-333.15	5.00000-5.00000	-91.2000-0.0000	0.0198-0.9495	-	-	59	0	0	345
C6-4sh	283.15-333.15	5.00000-5.00000	103.0000-682.5000	0.0497-0.9497	-	-	57	0	0	345
3-H2O	363.20-393.20	1.01000-1.01000	43.3000-71.8000	-	0.3030-0.6920	-	0	40	0	346
4-H2O	363.20-393.20	1.01000-1.01000	51.6000-88.4000	-	0.3120-0.7020	-	0	40	0	346
5-H2O	363.20-698.20	1.01325-45.00000	57.9000-1877.0000	-	0.2020-0.7480	-	0	65	0	347-348
6-H2O	363.20-648.20	1.01325-114.80000	82.0000-4467.0000	-	0.2980-0.7030	-	0	55	0	348-349
H2O-7	363.20-598.20	1.01000-76.80000	96.8000-8428.0000	-	0.3000-0.7010	-	0	86	0	348-350
H2O-8	363.20-648.20	1.01325-70.00000	153.3000-7700.0000	-	0.2060-0.7650	-	0	75	0	348, 351
1-H2O	373.20-648.20	1.01000-105.10000	26.7000-1699.0000	-	0.2890-0.7040	-	0	90	0	352-353
H2O-B	363.20-592.00	1.01000-164.00000	47.6000-13680.0000	-	0.3810-0.6380	0.2100-0.9870	0	60	124	354-356
H2O-C6	363.20-433.20	1.01000-1.01000	63.0000-126.7000	-	0.3520-0.7280	-	0	68	0	354-355
CO2-H2O	308.15-648.20	1.01000-202.00000	-231.000-18379.000	-	0.2980-0.7020	0.0020-0.9690	0	55	484	357-361
N2-H2O	373.15-698.20	1.01000-125.80000	25.2000-1315.0000	-	0.2550-0.7980	-	0	77	0	350, 362
H2S-H2O	383.15-483.15	1.01325-1.01325	12.0000-35.5000	-	0.5000-0.5000	-	0	11	0	363
a2-3	273.15-373.15	50.00000-150.00000	-2440.000-3026.000	0.0211-0.9850	0.0281-0.9855	0.0088-0.9861	146	125	567	364
1-a2	115.77-313.15	1.01325-34.45000	16.5000-250.7000	0.2368-0.9313	0.2030-0.8160	-	18	36	0	365-366
a2-2	273.15-363.15	50.00000-150.00000	-436.200-2355.400	0.0205-0.9834	0.0143-0.9824	0.0152-0.9667	121	471	206	367
a2-CO2	260.95-306.62	35.00000-110.00000	98.0000-2340.0000	0.0410-0.8510	0.0500-0.9010	0.0420-0.9640	51	47	76	368
N2-a2	283.15-338.15	10.36000-48.35000	28.7200-1147.0000	-	0.1230-0.9090	-	0	75	0	369
a3-3	323.15-323.15	50.00000-100.00000	17.1120-97.9830	0.0533-0.9531	-	-	35	0	0	248
1a6-6	298.15-298.15	1.01325-1.01325	10.7000-61.1000	0.0475-0.9419	-	-	17	0	0	188, 370
1a6-12	293.15-293.15	1.01325-1.01325	96.5000-136.9000	0.2737-0.6299	-	-	17	0	0	27
t2a6-6	298.15-298.15	1.01325-1.01325	22.6000-55.8000	0.1251-0.8495	-	-	9	0	0	370
t2a6-7	298.15-298.15	1.01325-1.01325	24.1000-56.6000	0.1294-0.8771	-	-	5	0	0	371
c2a6-6	298.15-298.15	1.01325-1.01325	21.4000-74.9000	0.0759-0.9037	-	-	9	0	0	370
c2a6-7	298.15-298.15	1.01325-1.01325	32.5000-72.7000	0.1304-0.8781	-	-	5	0	0	371
t3a6-6	298.15-298.15	1.01325-1.01325	21.4000-63.1000	0.1270-0.9058	-	-	9	0	0	370
t3a6-7	298.15-298.15	1.01325-1.01325	28.7000-65.7000	0.1292-0.8769	-	-	7	0	0	371
15a6-6	298.15-298.15	1.01325-1.01325	82.6000-246.6000	0.0968-0.8953	-	-	9	0	0	372
6-1a7	298.15-298.15	1.01325-1.01325	30.1000-47.1000	0.1982-0.8115	-	-	8	0	0	373
1a7-7	298.15-303.15	1.01000-1.01325	0.6090-59.1000	0.0021-0.8908	-	-	26	0	0	370, 374-375
1a7-12	298.15-298.15	1.01325-1.01325	37.0000-97.0000	0.1790-0.9000	-	-	9	0	0	376
t2a7-7	298.15-298.15	1.01325-1.01325	13.8000-45.5000	0.1309-0.8985	-	-	9	0	0	370
c2a7-7	298.15-298.15	1.01325-1.01325	11.6000-63.0000	0.0692-0.8868	-	-	9	0	0	370

Table V−5. (continued-10)

Binary system (1st compound-2nd compound)	Temperature rage (K)	Pressure range (bar)	Excess enthalpy range (J/mol)	x_1 range (1st compound liquid mole fraction)	y_1 range (1st compound gas mole fraction)	z_1 range (1st compound mole fraction)	Number of points (T,P,h^E,x)	Number of points (T,P,h^E,y)	Number of points (T,P,h^E,z)	References
t3a7-7	298.15-298.15	1.01325-1.01325	21.0000-67.8000	0.0865-0.9076	-	-	9	0	0	370
6-1a8	298.15-298.15	1.01325-1.01325	13.4000-29.4000	0.1813-0.8690	-	-	10	0	0	377
7-1a8	298.15-323.15	1.01325-1.01325	22.1000-39.8000	0.1727-0.8463	-	-	12	0	0	45
1a8-8	298.15-318.15	1.01325-1.01325	17.2000-46.6000	0.1130-0.8850	-	-	40	0	0	378
1a8-16	298.15-323.15	1.01325-1.01325	60.1000-163.8000	0.2656-0.9036	-	-	12	0	0	45
t3a8-8	298.15-318.15	1.01325-1.01325	20.1000-55.1000	0.1250-0.8880	-	-	33	0	0	378
c3a8-8	298.15-318.15	1.01325-1.01325	48.1000-57.6000	0.4640-0.5560	-	-	7	0	0	378
t4a8-8	298.15-318.15	1.01325-1.01325	21.7000-64.0000	0.1220-0.8730	-	-	36	0	0	378
c4a8-8	298.15-318.15	1.01325-1.01325	57.3000-66.3000	0.4490-0.6180	-	-	6	0	0	378
1a9-9	298.15-298.15	1.01325-1.01325	23.3000-40.5000	0.1980-0.8240	-	-	13	0	0	379
7-1a10	298.15-298.15	1.01325-1.01325	9.9000-26.7000	0.0971-0.8856	-	-	9	0	0	371
1a10-10	298.15-298.15	1.01325-1.01325	18.0000-45.4000	0.1540-0.8550	-	-	10	0	0	376, 380
8-1a12	298.15-298.15	1.01325-1.01325	77.0000-77.0000	0.6300-0.6300	-	-	1	0	0	380
9-1a12	298.15-298.15	1.01325-1.01325	73.0000-73.0000	0.6000-0.6000	-	-	1	0	0	380
1a12-12	298.15-298.15	1.01325-1.01325	88.0000-88.0000	0.4000-0.4000	-	-	1	0	0	380
1a12-16	298.15-298.15	1.01325-1.01325	133.5000-133.5000	0.4700-0.4700	-	-	1	0	0	380
2m4-1a5	363.13-363.13	15.00000-15.00000	19.7500-57.7900	0.1051-0.9049	-	-	9	0	0	381
1a6-22m4	298.15-298.15	1.01325-1.01325	11.3900-62.4600	0.0500-0.9500	-	-	19	0	0	382
1a6-23m4	298.15-298.15	1.01325-1.01325	13.8800-79.5200	0.0500-0.9499	-	-	19	0	0	382
1a6-2m5	298.15-298.15	1.01325-1.01325	10.7200-58.6700	0.0501-0.9500	-	-	19	0	0	382
1a6-3m5	298.15-298.15	1.01325-1.01325	9.8300-54.8800	0.0501-0.9500	-	-	19	0	0	382
1a6-224m5	298.15-298.15	1.01325-1.01325	10.0600-55.9000	0.0501-0.9500	-	-	19	0	0	382
224m5-1a12	298.15-298.15	1.01325-1.01325	154.5000-154.5000	0.5700-0.5700	-	-	1	0	0	380
1a6-B	298.15-363.13	1.01325-24.12000	74.7540-591.5000	0.0364-0.9499	-	-	58	0	0	188, 248, 383-384
15a6-B	298.15-298.15	1.01000-1.01000	95.0000-308.0000	0.1116-0.9004	-	-	9	0	0	385
B-1a7	298.15-298.15	1.01325-1.01325	137.8000-614.6000	0.0932-0.9550	-	-	17	0	0	373, 383
B-1a8	298.15-323.15	1.01325-1.01325	152.8000-680.0000	0.1013-0.9587	-	-	27	0	0	45, 383, 386
B-t3a8	298.20-298.20	1.01325-1.01325	578.0000-674.0000	0.3960-0.7560	-	-	5	0	0	386
B-1a10	298.15-298.15	1.01000-1.01000	224.0000-704.0000	0.1174-0.8646	-	-	9	0	0	385
1a6-mB	298.15-298.15	1.01325-1.01325	48.1800-268.0800	0.0500-0.9500	-	-	19	0	0	384
mB-1a8	298.65-298.65	1.01325-1.01325	124.0000-316.0000	0.1740-0.9040	-	-	12	0	0	386
mB-t3a8	298.65-298.65	1.01325-1.01325	233.0000-294.0000	0.3100-0.8160	-	-	4	0	0	386
mB-t4a8	298.20-298.20	1.01325-1.01325	296.0000-344.0000	0.5250-0.6760	-	-	2	0	0	386
1a7-eB	298.15-298.15	1.01325-1.01325	92.3000-264.7000	0.0901-0.8959	-	-	9	0	0	383
1a8-eB	298.15-298.15	1.01325-1.01325	60.0000-302.3000	0.0615-0.9382	-	-	28	0	0	383, 387
eB-Ba2	293.15-293.15	1.01325-1.01325	8.8760-12.1420	0.2490-0.7510	-	-	3	0	0	388
1a6-C6	298.15-413.21	1.01325-13.78000	26.6540-233.5800	0.0500-0.9500	-	-	42	0	0	178, 188, 384
t2a6-C6	298.15-298.15	1.01325-1.01325	97.0000-208.6000	0.0988-0.7761	-	-	6	0	0	371
c2a6-C6	298.15-298.15	1.01325-1.01325	87.1000-193.0000	0.0993-0.7710	-	-	6	0	0	371
t3a6-C6	298.15-298.15	1.01325-1.01325	61.7000-165.2000	0.0986-0.8400	-	-	6	0	0	371

Table V−5. (continued-11)

Binary system (1st compound-2nd compound)	Temperature rage (K)	Pressure range (bar)	Excess enthalpy range (J/mol)	x_1 range (1st compound liquid mole fraction)	y_1 range (1st compound gas mole fraction)	z_1 range (1st compound mole fraction)	Number of points (T,P,h^E,x)	Number of points (T,P,h^E,y)	Number of points (T,P,h^E,z)	References
C6-1a7	298.15-298.15	1.01325-1.01325	173.9000-241.4000	0.3440-0.8101	-	-	9	0	0	[373]
C6-1a8	298.15-323.15	1.01325-1.01325	81.7000-257.4000	0.1079-0.8970	-	-	21	0	0	[45, 371]
C6-c4a8	298.15-298.15	1.01325-1.01325	89.0000-174.0000	0.2440-0.8540	-	-	13	0	0	[387]
C6-1a10	298.15-298.15	1.00000-1.00000	54.7000-293.5000	0.0718-0.9036	-	-	18	0	0	[214]
1a6-tet	298.15-298.15	1.01325-1.01325	105.0000-223.1000	0.1399-0.7005	-	-	9	0	0	[389]
1a7-tet	298.15-298.15	1.01325-1.01325	90.7000-235.6000	0.1048-0.6735	-	-	8	0	0	[389]
1a6-mC6	298.15-298.15	1.01325-1.01325	10.0900-56.4100	0.0500-0.9500	-	-	19	0	0	[384]
1a6-bcy	298.15-298.15	1.01325-1.01325	26.8000-67.0000	0.1463-0.7601	-	-	10	0	0	[389]
1a7-bcy	298.15-298.15	1.01325-1.01325	32.9000-64.0000	0.1553-0.7395	-	-	8	0	0	[389]
a3-H2O	363.20-393.20	1.01000-1.01000	41.0000-64.1000	-	0.3690-0.5960	-	0	42	0	[346]
a3-13a4	273.15-333.15	49.78000-49.78000	-79.9900-15.7100	0.0211-0.9810	-	-	69	0	0	[390]
1a6-t2a6	298.15-298.15	1.01325-1.01325	3.4000-9.2000	0.1033-0.8711	-	-	9	0	0	[391]
1a6-t3a6	298.15-298.15	1.01325-1.01325	4.1000-11.4000	0.1047-0.9102	-	-	9	0	0	[391]
tt24a6-1a6	298.15-298.15	1.01325-1.01325	21.6000-73.7000	0.1104-0.8911	-	-	9	0	0	[391]
15a6-1a6	298.15-298.15	1.01325-1.01325	25.0000-72.3000	0.1018-0.8941	-	-	9	0	0	[391]
15a6-t2a6	298.15-298.15	1.01325-1.01325	42.4000-177.9000	0.1048-0.8966	-	-	10	0	0	[391]
15a6-t3a6	298.15-298.15	1.01325-1.01325	18.4000-72.0000	0.1205-0.9101	-	-	9	0	0	[391]
t3a6-t2a	298.15-298.15	1.01325-1.01325	-2.7000-0.0000	0.1002-0.9129	-	-	10	0	0	[391]
2m13a4-5	293.15-298.15	1.01325-1.01325	150.0000-190.0000	0.5000-0.5000	-	-	2	0	0	[14]
2m13a4-6	293.15-303.15	1.01325-1.01325	5.3000-214.1000	0.0075-0.9545	-	-	25	0	0	[14, 392]
2m13a4-7	293.15-298.15	1.01325-1.01325	210.0000-210.0000	0.5000-0.5000	-	-	2	0	0	[14]
2m1a5-12	283.15-303.15	1.01325-1.01325	38.1000-141.4000	0.2194-0.8933	-	-	34	0	0	[27]
2m3-2ma3	298.15-323.15	50.00000-150.00000	5.4000-100.5000	0.0151-0.9634	-	-	151	0	0	[393]
2m13a4-B	293.15-303.15	1.01325-1.01325	26.0000-263.2000	0.0382-0.9709	-	-	25	0	0	[14, 392]
2m13a4-C6	293.15-298.15	1.01325-1.01325	305.0000-330.0000	0.5000-0.5000	-	-	2	0	0	[14]
6-aC6	293.15-298.16	1.01325-1.01325	45.0000-235.3000	0.0433-0.8898	-	-	36	0	0	[14, 188, 394]
6-13aC6	298.15-298.15	1.01325-1.01325	229.7000-436.9000	0.1347-0.8024	-	-	9	0	0	[395]
6-14aC6	298.15-298.15	1.01325-1.01325	100.9000-443.3000	0.1837-0.9328	-	-	10	0	0	[395]
aC6-8	298.16-298.16	1.01325-1.01325	58.0000-247.0000	0.1618-0.9476	-	-	22	0	0	[394]
aC6-10	298.16-298.16	1.01325-1.01325	24.0000-293.0000	0.0757-0.9864	-	-	23	0	0	[394]
aC6-12	298.16-298.16	1.01325-1.01325	55.0000-323.0000	0.1376-0.9662	-	-	27	0	0	[394]
aC6-14	298.16-298.16	1.01325-1.01325	107.0000-408.0000	0.0957-0.9489	-	-	20	0	0	[394]
aC6-16	298.16-298.16	1.01325-1.01325	54.0000-427.0000	0.0962-0.9623	-	-	27	0	0	[394]
B-aC6	293.15-298.15	1.01000-1.01325	153.0000-389.3000	0.1247-0.8724	-	-	21	0	0	[14, 188, 385]
B-13aC6	298.15-298.15	1.01325-1.01325	42.4000-129.0000	0.0927-0.8643	-	-	11	0	0	[395]
B-14aC6	298.15-298.15	1.01325-1.01325	33.3000-86.7000	0.2030-0.8661	-	-	11	0	0	[395]
C6-aC6	293.15-308.15	1.01325-1.01325	0.9400-116.7000	0.0451-0.9980	-	-	36	0	0	[14, 188, 372, 375, 396]
13aC6-C6	298.15-308.15	1.01325-1.01325	96.9000-358.3000	0.0714-0.9241	-	-	24	0	0	[372, 395, 397]
C6-14aC6	298.15-308.15	1.01325-1.01325	115.0000-415.5000	0.0779-0.8970	-	-	22	0	0	[372, 395, 397]
aC6-tet	298.15-298.15	1.01325-1.01325	76.1000-150.8000	0.1755-0.7462	-	-	10	0	0	[398]

Table V−5. (continued-12)

Binary system (1st compound-2nd compound)	Temperature rage (K)	Pressure range (bar)	Excess enthalpy range (J/mol)	x_1 range (1st compound liquid mole fraction)	y_1 range (1st compound gas mole fraction)	z_1 range (1st compound mole fraction)	Number of points (T,P,h^E,x)	Number of points (T,P,h^E,y)	Number of points (T,P,h^E,z)	References
13aC6-tet	298.15-298.15	1.01325-1.01325	19.8000-48.4000	0.1251-0.7507	-	-	9	0	0	398
14aC6-tet	298.15-298.15	1.01325-1.01325	6.7000-24.8000	0.1135-0.7707	-	-	9	0	0	398
aC6-bcy	298.15-298.15	1.01325-1.01325	17.9000-37.2000	0.1717-0.6685	-	-	9	0	0	398
13aC6-bcy	298.15-298.15	1.01325-1.01325	98.1000-292.6000	0.1329-0.6842	-	-	12	0	0	398
14aC6-bcy	298.15-298.15	1.01325-1.01325	90.2000-282.1000	0.1209-0.7105	-	-	9	0	0	398
1a6-aC6	298.15-298.15	1.01325-1.01325	52.6000-116.1000	0.1208-0.8632	-	-	10	0	0	188
1a6-3maC5	348.15-348.15	8.00000-8.00000	5.9980-26.2400	0.0879-0.8864	-	-	9	0	0	381
2m13a4-aC6	293.15-298.15	1.01325-1.01325	60.0000-80.0000	0.5000-0.5000	-	-	2	0	0	14
ap-bp	298.15-318.15	1.01325-1.01325	7.0000-13.2000	0.2000-0.7998	-	-	21	0	0	399
H2-1	183.00-298.00	11.1000-102.3000	28.0000-3296.0000	-	0.0850-0.7480	0.0800-0.7280	0	85	24	334, 336
H2-N2	147.00-298.00	5.6700-135.7800	11.0000-793.0000	-	0.0860-0.7940	-	0	323	0	336, 400
H2-H2O	373.20-699.20	1.0100-112.0000	29.4000-2084.000	-	0.2630-0.7380	-	0	126	0	352-353, 401
Total number of points:							**18254**	**5224**	**5456**	

Table V−6. Binary systems database (c_P^E)

Binary system (1st compound-2nd compound)	Temperature rage (K)	Pressure range (bar)	Excess heat capacity range (J/mol/K)	x_1 range (1st compound liquid mole fraction)	Number of points (T,P,c_P^E,x)	References
6-7	298.15-298.15	1.01325-1.01325	-0.0980-0.0000	0.1246-0.9081	19	[402-403]
6-8	298.15-298.15	1.01325-1.01325	-0.2260-0.0000	0.0480-0.9780	30	[404]
6-12	298.15-298.15	1.01325-1.01325	-1.3720-0.0000	0.0564-0.9500	29	[405]
22m4-7	298.15-298.15	1.01325-1.01325	-0.6830-0.0000	0.0263-0.9713	45	[402]
23m4-7	298.15-298.15	1.01325-1.01325	-0.4920-0.0000	0.0311-0.9762	40	[402]
2m5-7	298.15-298.15	1.01325-1.01325	-0.2750-0.0000	0.0302-0.9467	28	[402]
3m5-7	298.15-298.15	1.01325-1.01325	-0.3190-0.0000	0.0322-0.9503	20	[402]
7-224m5	298.15-298.15	1.01325-1.01325	-0.3512-0.0000	0.0391-0.9620	24	[406-407]
22m4-8	298.15-298.15	1.01325-1.01325	-1.0850-0.0000	0.0522-0.9741	20	[404]
23m4-8	298.15-298.15	1.01325-1.01325	-0.7030-0.0000	0.0532-0.9532	17	[404]
2m5-8	298.15-298.15	1.01325-1.01325	-0.4530-0.0000	0.0748-0.9524	19	[404]
3m5-8	298.15-298.15	1.01325-1.01325	-0.5760-0.0000	0.0469-0.9285	21	[404]
6-B	298.20-298.20	1.01325-1.01325	-2.9100-0.0000	0.0953-0.9161	7	[408]
B-7	293.15-303.15	1.01325-1.01325	-3.6330-0.0000	0.0487-0.9317	43	[409-410]
B-8	298.20-298.20	1.01325-1.01325	-3.3800-0.0000	0.1110-0.8959	7	[408]
B-10	298.20-298.20	1.01325-1.01325	-4.1500-0.0000	0.0977-0.8999	7	[408]
B-12	298.20-298.20	1.01325-1.01325	-5.0900-0.0000	0.0916-0.8977	7	[408]
B-14	298.20-298.20	1.01325-1.01325	-5.9590-0.0000	0.2457-0.9237	5	[411]
B-16	298.20-298.20	1.01325-1.01325	-7.2700-0.0000	0.0884-0.9006	7	[408]
23m4-B	298.15-298.15	1.01325-1.01325	-2.9190-0.0000	0.1498-0.8584	12	[412-413]
B-224m5	298.15-323.15	1.01325-1.01325	-2.9000-0.0000	0.1036-0.8990	27	[414-416]
6-mB	298.15-313.15	1.01325-1.01325	-1.6000-0.0000	0.1078-0.9041	13	[417]
7-mB	298.15-298.20	1.01325-1.01325	-1.3780-0.0000	0.1013-0.9097	13	[411, 414]
mB-8	298.20-298.20	1.01325-1.01325	-1.3200-0.0000	0.0999-0.9069	7	[408]
mB-10	298.20-298.20	1.01325-1.01325	-1.8200-0.0000	0.0989-0.8966	7	[408]
mB-12	298.20-298.20	1.01325-1.01325	-2.4700-0.0000	0.0870-0.9054	7	[408]
mB-14	298.20-298.20	1.01325-1.01325	-3.7460-0.0000	0.1955-0.8608	5	[411]
mB-16	298.20-298.20	1.01325-1.01325	-4.2400-0.0000	0.0872-0.9034	7	[408]
6-14mB	298.20-298.20	1.01325-1.01325	-0.4800-0.0000	0.1032-0.9039	7	[408]
14mB-16	298.20-298.20	1.01325-1.01325	-2.2000-0.0000	0.1002-0.9021	7	[408]
7-eB	298.20-298.20	1.01325-1.01325	-1.6500-0.0000	0.1313-0.8699	8	[411]
eB-10	298.20-298.20	1.01325-1.01325	-2.5220-0.0000	0.2053-0.8222	5	[411]
eB-12	298.20-298.20	1.01325-1.01325	-3.0560-0.0000	0.1261-0.8879	5	[411]
eB-14	298.20-298.20	1.01325-1.01325	-4.4540-0.0000	0.1836-0.8227	5	[411]
7-124mB	298.15-298.15	1.01325-1.01325	0.0750-0.3430	0.1174-0.9052	9	[120]
10-124mB	298.15-298.15	1.01325-1.01325	0.2220-0.6620	0.1142-0.9078	9	[120]
124mB-14	298.15-298.15	1.01325-1.01325	-0.1150-0.0000	0.0934-0.8734	9	[120]
7-prB	298.20-298.20	1.01325-1.01325	-1.4180-0.0000	0.1408-0.8704	6	[411]
prB-14	298.20-298.20	1.01325-1.01325	-4.0020-0.0000	0.2078-0.8525	5	[411]
7-buB	298.20-298.20	1.01325-1.01325	-1.3870-0.0000	0.1721-0.8020	5	[411]

Table V−6. (continued-1)

Binary system (1st compound-2nd compound)	Temperature rage (K)	Pressure range (bar)	Excess heat capacity range (J/mol/K)	x_1 range (1st compound liquid mole fraction)	Number of points (T,P,c_P^E,x)	References
buB-14	298.20-298.20	1.01325-1.01325	-4.4010-0.0000	0.1780-0.8388	5	411
23m4-mB	298.15-298.15	1.01325-1.01325	-1.6710-0.0000	0.1369-0.8511	12	412-413
224m5-mB	298.15-323.15	1.01325-1.01325	-1.2700-0.9000	0.1102-0.9015	30	414-416
23m4-eB	298.15-298.15	1.01325-1.01325	-2.2840-0.0000	0.1600-0.8516	6	412
23m4-buB	298.15-298.15	1.01325-1.01325	-1.5440-0.0000	0.2055-0.8384	5	412
B-mB	298.15-298.15	1.01325-1.01325	-0.3150-0.0000	0.1127-0.8930	9	418
B-12mB	298.15-298.15	1.01325-1.01325	-1.4370-0.0000	0.1006-0.8931	9	418
B-13mB	298.15-298.15	1.01325-1.01325	-1.1090-0.0000	0.1045-0.8866	9	418
B-14mB	298.15-313.15	1.01325-1.01325	-0.8800-0.0000	0.1008-0.8772	15	418-419
B-eB	298.15-298.15	1.01325-1.01325	-0.8710-0.0000	0.0962-0.8968	17	418, 420
B-prB	298.15-298.15	1.01325-1.01325	-0.9410-0.0000	0.1936-0.8677	5	420
B-buB	298.15-298.15	1.01325-1.01325	-1.4510-0.0000	0.1349-0.8752	7	420
mB-12mB	298.15-298.15	1.01325-1.01325	-0.4620-0.0000	0.1096-0.8891	9	418
mB-13mB	298.15-298.15	1.01325-1.01325	-0.2100-0.0000	0.0949-0.8963	9	418
mB-14mB	298.15-298.15	1.01325-1.01325	-0.0340-0.0020	0.1159-0.8829	9	418
mB-eB	298.15-298.15	1.01325-1.01325	0.0160-0.0560	0.0932-0.9002	9	418
13mB-12mB	298.15-321.65	1.01325-1.01325	-0.1420-0.0000	0.0504-0.9464	79	421-422
14mB-12mB	298.15-321.65	1.01325-1.01325	-0.2200-0.0000	0.0499-0.9607	79	421-422
eB-12mB	298.15-321.65	1.01325-1.01325	-0.2820-0.0000	0.0502-0.9498	79	421-422
14mB-13mB	298.15-321.65	1.01325-1.01325	0.0030-0.0260	0.0490-0.9517	79	421-422
eB-13mB	298.15-321.65	1.01325-1.01325	-0.0350-0.0000	0.0505-0.9499	86	421-422
eB-14mB	298.15-321.65	1.01325-1.01325	0.0400-0.3510	0.0526-0.9516	79	421-422
6-C6	298.15-298.20	1.01325-1.01325	-1.4190-0.0000	0.0394-0.9533	34	403, 409
C6-7	293.15-338.15	1.01325-1.01325	-2.7440-0.0000	0.0882-0.9604	49	209, 403
C6-12	298.15-323.15	1.01325-1.01325	-3.9300-0.0000	0.0473-0.9630	234	423
C6-14	288.15-308.15	1.01325-1.01325	-6.1012-0.0000	0.0500-0.9502	52	424
C6-224m5	298.15-323.15	1.01325-1.01325	-0.6000-0.0000	0.2496-0.7497	9	425
C5-B	298.15-298.15	1.01325-1.01325	-2.6640-0.0000	0.0933-0.8778	9	426
B-C6	293.15-318.15	1.01325-1.01325	-2.9810-0.0000	0.0955-0.9148	95	427-430
B-C8	298.15-298.15	1.01325-1.01325	-3.3760-0.0000	0.1235-0.9084	9	426
C6-mB	298.15-298.15	1.01325-1.01325	-1.9200-0.0000	0.0250-0.9750	21	431
C6-12mB	298.15-323.15	1.01325-1.01325	-1.1023-0.0000	0.2503-0.7498	9	432
C6-13mB	298.15-323.15	1.01325-1.01325	-1.7294-0.0000	0.2495-0.7520	9	432
C6-14mB	298.15-323.15	1.01325-1.01325	-1.1914-1.2102	0.2537-0.7415	9	432
C6-eB	298.15-298.15	1.01325-1.01325	-2.2300-0.0000	0.0250-0.9750	21	286
C6-prB	298.15-298.15	1.01325-1.01325	-2.1900-0.0000	0.0250-0.9750	21	286
C6-iprB	298.15-298.15	1.01325-1.01325	-2.0300-0.0000	0.0250-0.9750	19	286
mC5-10	293.15-293.15	1.01325-1.01325	-1.5440-0.0000	0.0862-0.8990	10	433
7-tCC6	298.15-298.15	1.01325-1.01325	-0.7650-0.0000	0.0500-0.9500	19	434
7-cCC6	298.15-298.15	1.01325-1.01325	-1.4580-0.0000	0.0500-0.9500	19	434

Table V−6. (continued-2)

Binary system (1st compound-2nd compound)	Temperature rage (K)	Pressure range (bar)	Excess heat capacity range (J/mol/K)	x_1 range (1st compound liquid mole fraction)	Number of points (T,P,c_P^E,x)	References
22m4-tCC6	298.15-298.15	1.01325-1.01325	-1.1720-0.0000	0.0500-0.9500	11	[295]
23m4-tCC6	298.15-298.15	1.01325-1.01325	-0.9530-0.0000	0.0500-0.9500	11	[295]
2m5-tCC6	298.15-298.15	1.01325-1.01325	-0.8270-0.0000	0.0500-0.9500	11	[295]
3m5-tCC6	298.15-298.15	1.01325-1.01325	-0.7660-0.0000	0.0500-0.9500	11	[295]
224m5-tCC6	298.15-298.15	1.01325-1.01325	-0.7430-0.0000	0.0500-0.9500	19	[434]
22m4-cCC6	298.15-298.15	1.01325-1.01325	-1.3340-0.0000	0.0500-0.9500	11	[295]
23m4-cCC6	298.15-298.15	1.01325-1.01325	-1.2150-0.0000	0.1000-0.9500	10	[295]
2m5-cCC6	298.15-298.15	1.01325-1.01325	-1.3980-0.0000	0.0500-0.9500	11	[295]
3m5-cCC6	298.15-298.15	1.01325-1.01325	-1.2350-0.0000	0.0500-0.9500	11	[295]
224m5-cCC6	298.15-298.15	1.01325-1.01325	-1.2610-0.0000	0.0500-0.9500	19	[434]
B-mC6	298.15-298.15	1.01325-1.01325	-2.7100-0.0000	0.0500-0.9750	29	[426, 435]
B-tCC6	298.15-298.15	1.01325-1.01325	-2.7990-0.0000	0.0500-0.9500	19	[434]
B-cCC6	298.15-298.15	1.01325-1.01325	-3.0960-0.0000	0.0500-0.9500	19	[434]
mC6-mB	298.15-298.15	1.01325-1.01325	-1.7500-0.0000	0.0250-0.9750	20	[434]
mB-tCC6	298.15-298.15	1.01325-1.01325	-1.6930-0.0000	0.0500-0.9500	19	[434]
mB-cCC6	298.15-298.15	1.01325-1.01325	-2.0460-0.0000	0.0500-0.9500	19	[434]
C5-mC5	293.15-293.15	1.01325-1.01325	-0.0270-0.0160	0.1252-0.9009	11	[433]
C5-mC6	293.15-293.15	1.01325-1.01325	0.0520-0.2900	0.0402-0.9117	12	[433]
mC5-C6	293.15-293.15	1.01325-1.01325	-0.2740-0.0000	0.0712-0.8951	14	[433]
C6-mC6	298.15-298.15	1.01325-1.01325	-0.2800-0.2800	0.0500-0.9750	20	[435]
C6-tCC6	298.15-298.15	1.01325-1.01325	-0.5290-0.3720	0.0500-0.9500	11	[307]
C6-cCC6	298.15-298.15	1.01325-1.01325	-0.5130-0.5450	0.0500-0.9500	11	[307]
C8-tCC6	298.15-298.15	1.01325-1.01325	-0.2820-0.0680	0.0500-0.9500	11	[307]
C8-cCC6	298.15-298.15	1.01325-1.01325	-0.4650-0.0000	0.0500-0.9500	11	[307]
mC5-mC6	293.15-293.15	1.01325-1.01325	0.0730-0.2400	0.0608-0.9079	11	[433]
mC6-tCC6	298.15-298.15	1.01325-1.01325	-0.5850-0.0000	0.0500-0.9500	11	[307]
mC6-cCC6	298.15-298.15	1.01325-1.01325	-0.8170-0.0000	0.0500-0.9500	11	[307]
Total number of points:					**2251**	

References

(1) Demirel, Y.; Gecegörmez, H. Simultaneous representation of excess enthalpy and vapor--liquid equilibrium data by the NRTL and UNIQUAC models. *Fluid Phase Equilib.* **1991**, *65*, 111-133.
(2) Chen, G.; Wu, Z.; Chen, Z.; Hou, Y. Correlation of excess enthalpies and prediction of vapor-liquid equilibria from excess enthalpies by means of an equation of state. *Fluid Phase Equilib.* **1991**, *65*, 145-157.
(3) Ohta, T. Representation of excess enthalpies by the PRSV equation of state with the modified Huron-Vidal first order and Wong-Sandler mixing rules. *Fluid Phase Equilib.* **1997**, *129* (1-2), 89-103.
(4) Jaubert, J.-N.; Mutelet, F. VLE predictions with the Peng-Robinson equation of state and temperature dependent kij calculated through a group contribution method. *Fluid Phase Equilib.* **2004**, *224* (2), 285-304.
(5) Jaubert, J.-N.; Vitu, S.; Mutelet, F.; Corriou, J.-P. Extension of the PPR78 model (predictive 1978, Peng-Robinson EOS with temperature dependent kij calculated through a group contribution method) to systems containing aromatic compounds. *Fluid Phase Equilib.* **2005**, *237* (1-2), 193-211.
(6) Privat, R.; Jaubert, J. N.; Mutelet, F. Addition of the nitrogen group to the PPR78 model (predictive 1978, Peng Robinson EOS with temperature-dependent kij calculated through a group contribution method. *Ind. Eng. Chem. Res.* **2008**, *47* (6), 2033-2048.
(7) Privat, R.; Jaubert, J. N.; Mutelet, F. Addition of the sulfhydryl group (-SH) to the PPR78 model (predictive 1978, Peng-Robinson EOS with temperature dependent kij calculated through a group contribution method). *Journal of Chemical Thermodynamics* **2008**, *40* (9), 1331-1341.
(8) Privat, R.; Mutelet, F.; Jaubert, J. N. Addition of the hydrogen sulfide group to the PPR 78, Model (Predictive 1978, Peng-Robinson equation of state with temperature dependent kij- calculated through a group contribution method). *Ind. Eng. Chem. Res.* **2008**, *47* (24), 10041-10052.
(9) Vitu, S.; Jaubert, J.-N.; Mutelet, F. Extension of the PPR78 model (Predictive 1978, Peng-Robinson EOS with temperature dependent kij calculated through a group contribution method) to systems containing naphtenic compounds. *Fluid Phase Equilib.* **2006**, *243* (1-2), 9-28.
(10) Vitu, S.; Privat, R.; Jaubert, J. N.; Mutelet, F. Predicting the phase equilibria of CO2 + hydrocarbon systems with the PPR78 model (PR EOS and kij calculated through a group contribution method). *Journal of Supercritical Fluids* **2008**, *45* (1), 1-26.
(11) Orbey, H.; Sandler, S. I. A comparison of various cubic equation of state mixing rules for the simultaneous description of excess enthalpies and vapor-liquid equilibria. *Fluid Phase Equilib.* **1996**, *121* (1-2), 67-83.
(12) Poling, B. E.; Prausnitz, J. M.; O'Connell, J. P. *The Properties of Gases and Liquids, 5th Ed.* **2000**, 11-18.
(13) Wormald, C. J.; Lewis, E. J.; Hutchings, D. J. Excess enthalpies of gaseous mixtures of n-alkanes. *J. Chem. Thermodyn.* **1979**, *11* (1), 1-12.
(14) Guenzel, K.; Bittrich, H. J. Mixing ethalpies of binary systems of olefins and diolefins. *Z. Phys. Chem. (Leipzig)* **1977**, *258* (6), 1073-1080.
(15) McGlashan, M. L.; Morcom, K. W. Heats of mixing of some n-alkanes. *Trans. Faraday Soc.* **1961**, *57*, 907-913.
(16) Kimura, F.; Benson, G. C.; Halpin, C. J. Excess enthalpies of binary mixtures of n-heptane with hexane isomers. *Fluid Phase Equilib.* **1983**, *11* (3), 245-250.
(17) Kireev, V. A.; Bykov, V. T.; Khodorchenko, V. V. Heat of mixing of liquids. V. Heat of mixing of benzene with dichloroethane, benzene with carbon tetrachloride and hexane with heptane. *Zh. Fiz. Khim.* **1937**, *10* (6), 807-812.
(18) Mathieson, A. R.; Thynne, J. C. J. Thermodynamics of hydrocarbon mixtures. II. The heats of mixing of the binary mixtures formed by benzene, cyclohexane, heptane, toluene, and hexane. *J. Chem. Soc.* **1956**, *720*, 3708-3713.
(19) Hamam, S. E. M.; Kumaran, M. K.; Benson, G. C. Excess enthalpies of binary mixtures of n-octane with each of the hexane isomers at 298.15 K. *Fluid Phase Equilib.* **1984**, *18* (2), 147-153.
(20) Heintz, A.; Lichtenthaler, R. N. Excess enthalpies of liquid alkane mixtures at pressures up to 500 bar. I. Experimental results. *Ber. Bunsenges. Phys. Chem.* **1980**, *84* (8), 727-732.
(21) Tancrede, P.; Patterson, D. Excess enthalpy. n-Octane-n-hexane system. *Int. DATA Ser., Sel. Data Mixtures, Ser. A* **1975**, *1974* (1), 24.
(22) Lopez, M.; Carballo, E.; Legido, J. L.; Salgado, J.; Vijande, J.; Paz, A. M. I. Excess molar enthalpies of {x1CH3CH2COCH2CH3 + x2CH3(CH2)4CH3 + (1-x1-x2)CH3(CH2)ν-2CH3} (ν = 9 and 12) at the temperature 298.15 K. *J. Chem. Thermodyn.* **1995**, *27* (8), 879-886.
(23) Hamam, S. E. M.; Benson, G. C. Excess enthalpies of binary mixtures of n-decane with hexane isomers. *J. Chem. Eng. Data* **1986**, *31* (1), 45-47.

(24) Lopez, M.; Paz, A. M. I.; Peleteiro, J.; Legido, J. L.; Romani, L.; Perez, M. E. Excess molar enthalpies of the ternary systems pentan-3-one + n-hexane + n-decane and n-tetradecane at 298.15 K. *Thermochim. Acta* **1992**, *211*, 33-42.
(25) Marsh, K. N.; Ott, J. B.; Costigan, M. J. Excess enthalpies, excess volumes, and excess Gibbs free energies for n-hexane + n-decane at 298.15 and 308.15 K. *J. Chem. Thermodyn.* **1980**, *12* (4), 343-348.
(26) Marsh, K. N.; Ott, J. B.; Richards, A. E. Excess enthalpies, excess volumes, and excess Gibbs free energies for n-hexane + n-undecane at 298.15 and 308.15 K. *J. Chem. Thermodyn.* **1980**, *12* (9), 897-902.
(27) Fernandez-Garcia, J. G.; Boissonnas, C. G. Thermodynamic properties of binary mixtures. Heats of mixing of n-alkanes and also their isomers. *Helv. Chim. Acta* **1967**, *50* (4), 1059-1068.
(28) Hamam, S. E. M.; Kumaran, M. K.; Benson, G. C. Excess enthalpies and excess volumes of each of the mixtures: (n-dodecane + an isomer of hexane) at 298.15 K. *J. Chem. Thermodyn.* **1984**, *16* (6), 537-542.
(29) Ott, J. B.; Marsh, K. N.; Stokes, R. H. Excess enthalpies, excess volumes, and excess Gibbs free energies for (n-hexane + n-dodecane) at 298.15 and 308.15 K. *J. Chem. Thermodyn.* **1981**, *13* (4), 371-376.
(30) Tancrede, P.; Patterson, D. Excess enthalpy. n-Dodecane-n-hexane system. *Int. DATA Ser., Sel. Data Mixtures, Ser. A* **1975**, *1974* (1), 25.
(31) van der Waals, J. H. Thermodynamic properties of mixtures of alkanes differing in chain length. III. System hexane-dodecane. *Recl. Trav. Chim. Pays-Bas Belg.* **1951**, *70*, 101-104.
(32) van der Waals, J. H. Thermodynamic properties of some binary alkane mixtures at constant volume. *Trans. Faraday Soc.* **1956**, *52*, 916-925.
(33) Lopez, M.; Paz, A. M. I.; Legido, J. L.; Romani, L.; Peleteiro, J.; Jimenez, E. Excess molar enthalpies for the (ethyl propanoate + n-hexane + n-tetradecane) system at the temperature 298.15 K. *Phys. Chem. Liq.* **1993**, *25* (3), 145-152.
(34) Brady, T. J.; Shen, W. G.; Williamson, A. G. Enthalpies of mixing of multicomponent alkane mixtures. *Aust. J. Chem.* **1988**, *41* (11), 1763-1767.
(35) Fernandez-Garcia, J. G.; Stoeckli, H. F.; Boissonnas, C. G. Thermodynamic properties of binary mixtures. Mixing volumes of n-alkanes. *Helv. Chim. Acta* **1966**, *49* (7), 1983-1986.
(36) Holleman, T. Heats of mixing of liquid binary normal alkane mixtures. *Physica (The Hague)* **1965**, *31* (1), 49-63.
(37) Larkin, J. A.; Fenby, D. V.; Gilman, T. S.; Scott, R. L. Heats of mixing of nonelectrolyte solutions. III. Solutions of the five hexane isomers with hexadecane. *J. Phys. Chem.* **1966**, *70* (6), 1959-1963.
(38) Marsh, K. N.; Organ, P. P. Excess molar enthalpies and excess molar volumes for three- and four-component n-alkane mixtures simulating (n-hexane + n-hexadecane). *J. Chem. Thermodyn.* **1985**, *17* (9), 835-841.
(39) McGlashan, M. L.; Morcom, K. W. Thermodynamics of mixtures of n-hexane + n-hexadecane. I. Heats of mixing. *Trans. Faraday Soc.* **1961**, *57*, 581-587.
(40) Miller, R. C.; Williamson, A. G. Excess molar enthalpies for (n-hexane + n-hexadecane) and for three- and four-component alkane mixtures simulating this binary mixture. *J. Chem. Thermodyn.* **1984**, *16* (8), 793-799.
(41) Scatchard, G.; Ticknor, L. B.; Goates, J. R.; McCartney, E. R. Heats of mixing in some nonelectrolyte solutions. *J. Am. Chem. Soc.* **1952**, *74*, 3721-3724.
(42) Wang, Z.; Horikawa, Y.; Benson, G. C.; Lu, B. C. Y. Excess enthalpies of the ternary mixtures: diisopropyl ether+n-octane+(n-heptane or n-dodecane) at 298.15 K. *Fluid Phase Equilib.* **2001**, *181* (1-2), 215-224.
(43) Wang, Z.; Horikawa, Y.; Benson, G. C.; Lu, B. C. Y. Excess enthalpies of the ternary mixtures: ethyl tert-butylether + n-heptane + (n-decane or n-dodecane) at 298.15 K. *Can. J. Chem.* **2001**, *79* (4), 388-393.
(44) Kumaran, M. K.; Benson, G. C. Excess enthalpies of n-dodecane + n-heptane, + n-octane, and + n-decane at 298.15 K. *J. Chem. Thermodyn.* **1986**, *18* (10), 993-996.
(45) Lundberg, G. W. Thermodynamics of solutions XI. Heats of mixing of hydrocarbons. *J. Chem. Eng. Data* **1964**, *9* (2), 193-198.
(46) Wang, Z.; Benson, G. C.; Lu, B. C. Y. Excess Enthalpies of the Ternary Mixtures 2-Methyltetrahydrofuran + n-Octane + (n-Decane or n-Dodecane) at 298.15 K. *J. Chem. Eng. Data* **2001**, *46* (5), 1193-1197.
(47) Grigg, R. B.; Goates, J. R.; Ott, J. B. Excess volumes and excess enthalpies for (n-dodecane + n-octane) and excess volumes for (n-dodecane + cyclohexane) at 298.15 K. *J. Chem. Thermodyn.* **1982**, *14* (1), 101-102.
(48) Mathot, V. Thermodynamic Properties of Isomeric Hydrocarbons. Influence of the Molecular Symmetry of the Constituents. *Bull. Soc. Chim. Belg.* **1950**, *59*, 111-137.
(49) Tancrede, P.; Patterson, D. Excess enthalpy. 2,2-Dimethylbutane-n-hexane system. *Int. DATA Ser., Sel. Data Mixtures, Ser. A* **1975**, *1974* (1), 26.
(50) Tancrede, P.; Patterson, D. Excess enthalpy. 2,2-Dimethylbutane-n-octane system. *Int. DATA Ser., Sel. Data Mixtures, Ser. A* **1975**, *1974* (1), 27.
(51) Tancrede, P.; Patterson, D. Excess enthalpy. 2,2-Dimethylbutane-n-dodecane system. *Int. DATA Ser., Sel. Data Mixtures, Ser. A* **1975**, *1974* (1), 29.

(52) Ott, J. B.; Grigg, R. B.; Goates, J. R. Excess enthalpies and excess volumes for n-hexane + 2-methylpentane, + 3-methylpentane and + 2,3-dimethylbutane at 283.15, 298.15 and 313.15 K. *Aust. J. Chem.* **1980**, *33* (9), 1921-1926.
(53) Ameling, W.; Siddiqi, M. A.; Lucas, K. Excess enthalpies for the binary systems n-octane with 2-methylpentane and 3-methylpentane. *J. Chem. Eng. Data* **1983**, *28* (2), 184-186.
(54) Wang, Z.; Benson, G. C.; Lu, B. C. Y. Excess enthalpies of the ternary mixtures: {tetrahydrofuran + 3-methylpentane + (octane or decane)} at the temperature 298.15 K. *J. Chem. Thermodyn.* **2003**, *35* (10), 1635-1644.
(55) Hamam, S. E. M.; Kumaran, M. K.; Zhang, D.; Benson, G. C. Excess enthalpies of binary mixtures of 2,4-dimethylpentane with n-hexane, n-heptane, n-octane and n-dodecane. *J. Chem. Eng. Data* **1985**, *30* (2), 222-224.
(56) Tancrede, P.; Patterson, D. Excess enthalpy. 2,2,4-Trimethylpentane (isooctane)-n-hexane system. *Int. DATA Ser., Sel. Data Mixtures, Ser. A* **1975**, *1974* (1), 30.
(57) Peng, D.-Y.; Horikawa, Y.; Wang, Z.; Benson, G. C.; Lu, B. C. Y. Excess Enthalpies of 2,2,4-Trimethylpentane + n-Alkane Binary Mixtures at 298.15 K. *J. Chem. Eng. Data* **2001**, *46* (2), 237-238.
(58) Mier, W.; Oswald, G.; Tusel-Langer, E.; Lichtenthaler, R. N. Excess enthalpy HE of binary mixtures containing alkanes, ethanol and ethyl-tert. butyl ether (ETBE). *Ber. Bunsen-Ges.* **1995**, *99* (9), 1123-1130.
(59) Peng, D.-Y.; Benson, G. C.; Lu, B. C. Y. Excess Enthalpies of 2,2,4-Trimethylpentane + Hexane + (Octane or Dodecane) at 298.15 K. *J. Chem. Eng. Data* **2000**, *45* (1), 48-52.
(60) Hamam, S. E.; Benson, G. C. Excess enthalpies of some binary mixtures of hexane isomers. *J. Chem. Thermodyn.* **1986**, *18* (6), 591-594.
(61) Tancrede, P.; Patterson, D. Excess enthalpy. 2,2,4-Trimethylpentane (isooctane)-2,2-dimethylbutane system. *Int. DATA Ser., Sel. Data Mixtures, Ser. A* **1975**, *1974* (1), 31.
(62) Hutchings, D. J.; Lewis, E. J.; Wormald, C. J. Excess enthalpies of mixtures of methane + each of the n-alkanes from ethane to n-octane. *J. Chem. Thermodyn.* **1978**, *10* (6), 559-566.
(63) Miller, R. C.; Staveley, L. A. K. Excess enthalpies for some binary liquid mixtures of low-molecular-weight alkanes. *Adv. Cryog. Eng.* **1976**, *21*, 493-500.
(64) Oscarson, J. L.; Coxam, J. Y.; Gillespie, S. E.; Izatt, R. M. Excess enthalpies of mixing methane with methanol, n-heptane, toluene and methylcyclohexane at 255.4 and 310.9 K and 13.8 MPa. *Fluid Phase Equilib.* **1996**, *114* (1-2), 161-174.
(65) Ott, J. B.; Brown, P. R.; Moore, J. D.; Lewellen, A. C. Excess molar enthalpies and excess molar volumes for (propane + ethane) over the temperature range from 273.15 K to 373.15 K and the pressure range from 5 MPa to 15 MPa. *J. Chem. Thermodyn.* **1997**, *29* (2), 149-178.
(66) Adams, W. R.; Gopal, P.; Zollweg, J. A.; Streett, W. B. Excess properties of (ethane + propane)(l) and (carbon monoxide + methane)(l). *J. Chem. Thermodyn.* **1987**, *19* (1), 39-46.
(67) Diaz Peña, M.; Menduiña, C. Excess enthalpies at 298.15 K of binary mixtures of benzene with n-alkanes. *The Journal of Chemical Thermodynamics* **1974**, *6* (4), 387-393.
(68) Jones, H. K. D.; Poon, D. P. L.; Lama, R. F.; Lu, B. C. Y. Heats of mixing of liquids: Application of quasilattice theory to benzene-alkane systems. *Can. J. Chem. Eng.* **1967**, *45* (1), 22-24.
(69) Baluja Santos, M. D. C. Microcalorimetry of the heats of mixing. application to binary and ternary systems. *Acta Cient. Compostelana* **1970**, *7* (1-2), 3-15.
(70) Baud, E. Thermal analysis of binary mixtures. *Bull. Soc. Chim. Fr.* **1915**, *17*, 329-345.
(71) Casas, H.; Segade, L.; Franjo, C.; Jimenez, E.; Paz, A. M. I. Excess Molar Enthalpies of Propyl Propanoate + Hexane + Benzene at 298.15 K and 308.15 K. *J. Chem. Eng. Data* **2000**, *45* (3), 445-449.
(72) Diaz Peña, M.; Menduiña, C. Excess enthalpies at 323.15 K of binary mixtures of benzene with n-alkanes. *The Journal of Chemical Thermodynamics* **1974**, *6* (11), 1097-1102.
(73) Hwang, C. A.; Elkabule, A. S.; Whitman, D. L.; Miller, R. C. Excess molar enthalpies of (benzene + cyclohexane + n-hexane). *The Journal of Chemical Thermodynamics* **1987**, *19* (10), 1031-1036.
(74) Jones, H. K. D.; Lu, B. C. Y. Heats of mixing of liquids for the system ethanol-benzene-hexane. *J. Chem. Eng. Data* **1966**, *11* (4), 488-492.
(75) Mato, M. M.; Balseiro, J.; Jimenez, E.; Legido, J. L.; Galinanes, A. V.; Paz, A. M. I. Excess Molar Enthalpies and Excess Molar Volumes of the Ternary System 1,2-Dichlorobenzene + Benzene + Hexane at 298.15 K. *J. Chem. Eng. Data* **2002**, *47* (6), 1436-1441.
(76) Pahlke, H. The Heats of Mixing of Organic Substances. *Ph.D. thesis, Christian-Albrechts-Universitaet, Kiel* **1935**, 1-45.
(77) Paz Andrade, M. I.; Regueiro, M.; Baluja, M. C.; Jimenez, E.; Hernandez, C. Heats of mixing at mean temperatures. Hexane-benzene system. *Acta Cient. Compostelana* **1970**, *7* (3-4), 147-152.
(78) Ridgway, K.; Butler, P. A. Physical properties of the ternary system benzene-cyclohexane-hexane. *Journal of Chemical & Engineering Data* **1967**, *12* (4), 509-515.

(79) Romani, L.; Paz Andrade, M. I. Thermodynamic Excess Functions at 25 C. III. Benzene + Isomers of Hexane. *An. Quim.* **1974**, *70*, 422-425.
(80) Battler, J. R.; Rowley, R. L. Excess enthalpies between 293 and 323 K for constituent binaries of ternary mixtures exhibiting partial miscibility. *J. Chem. Thermodyn.* **1985**, *17* (8), 719-732.
(81) Brown, C. P.; Mathieson, A. R.; Thynne, J. C. J. Thermodynamics of hydrocarbon mixtures. I. The heats of mixing of the binary and ternary systems formed by benzene, cyclohexane, and heptane. *J. Chem. Soc.* **1955**, 4141-4146.
(82) Hammerl, I.; Raetzsch, M. T. Enthalpies of mixing of normal paraffins with aromatics. *Wiss. Z. Tech. Hochsch. Chem. Carl Schorlemmer Leuna-Merseburg* **1973**, *15* (3), 175-178.
(83) Kuchenbecker, D. *Ph.D. thesis, Leipzig* **1980**.
(84) Letcher, T. M.; Bayles, J. W. Thermodynamics of some binary liquid mixtures containing aliphatic amines. *J. Chem. Eng. Data* **1971**, *16* (3), 266-271.
(85) Lu, B. C. Y.; Jones, H. K. D. Extrapolation of ternary excess thermodynamic properties. *Can. J. Chem. Eng.* **1966**, *44* (5), 251-254.
(86) Muensch, E. Mixing calorimetry using a displacement calorimeter, described for the systems benzene + n-heptane, 2-methylnapthalene + 1-methylnapthalene, toluene + chlorobenzene, and chlorobenzene + ethylbenzene. *Thermochim. Acta* **1978**, *22* (2), 237-255.
(87) Messow, U.; Schuetze, D.; Pfestorf, R.; Kuchenbecker, D.; Suehnel, K. Thermodynamic studies on solvent/n-paraffin systems. III. The benzene/n-heptane and benzene/n-decane system. *Z. Phys. Chem. (Leipzig)* **1977**, *258* (1), 24-32.
(88) Ogawa, H.; Murakami, S.; Takigawa, T.; Ohba, M. Thermodynamic properties of rigid polycyclic molecules. 1: Enthalpies of solution of fused ring polycyclic aromatic hydrocarbons. *Fluid Phase Equilib.* **1997**, *136* (1-2), 279-287.
(89) Palmer, D. A.; Smith, B. D. Thermodynamic excess property measurements for acetonitrile-benzene-n-heptane system at 45.deg. *J. Chem. Eng. Data* **1972**, *17* (1), 71-76.
(90) Renker, W. *Private Communication(Leipzig)* **1969**.
(91) Timofeev, V. The Heat of Formation in Non-Aqueous Solutions. *Monograph "O teplote obrazovaniya nevodnykh rastvorov",Kiev* **1904**, 91-183.
(92) Vilcu, R.; Stanciu, F. Excess Thermodynamic Functions from Calorimetric Data. *Rev. Roum. Chim.* **1966**, *11* (2), 175-182.
(93) Yadav, O. P. Excess enthalpies of binary mixtures of some hydrocarbons. *J. Indian Chem. Soc.* **1991**, *68* (11), 596-599.
(94) Sifaou, H.; Ait-kaci, A.; Benmakhlouf, H. *J. Therm. Anal. Calorim.* **2000**, *60*, 427-436.
(95) Snow, R. L.; Ott, J. B.; Goates, J. R.; Marsh, K. N.; O'Shea, S.; Stokes, R. H. (Solid + liquid) and (vapor + liquid) phase equilibria and excess enthalpies for (benzene + n-tetradecane), (benzene + n-hexadecane), (cyclohexane + n-tetradecane), and (cyclohexane + n-hexadecane) at 293.15, 298.15, and 308.15 K. Comparison of GmE calculated from (vapor + liquid) and (solid + liquid) equilibria. *J. Chem. Thermodyn.* **1986**, *18* (2), 107-130.
(96) Prengle, H. W., Jr.; Worley, F. L., Jr.; Mauk, C. E. Thermodynamics of solutions. New equipment for measuring heats of solution. Data for five systems. *J. Chem. Eng. Data* **1961**, *6*, 395-399.
(97) Wormald, C. J. A differential-flow mixing calorimeter. The excess enthalpy of methane + benzene, methane + cyclohexane, and benzene + cyclohexane. *The Journal of Chemical Thermodynamics* **1977**, *9* (9), 901-910.
(98) Faux, P. W.; Christensen, J. J.; Izatt, R. M. The excess enthalpies of (n-hexane + toluene) at 308.15, 358.15, 413.15, 470.15, and 573.15 K from 7.50 to 12.50 MPa. *J. Chem. Thermodyn.* **1987**, *19* (7), 757-764.
(99) Raal, J. D.; Naidoo, P. Excess enthalpy measurements using a novel highly refined microflow calorimeter and the prediction of vapor-liquid equilibria from such data. *Fluid Phase Equilib.* **1990**, *57* (1-2), 147-160.
(100) Bykov, V. T. Heats of mixing of liquids. *Zh. Fiz. Khim.* **1939**, *13* (7), 1013-1019.
(101) Coxam, J. Y.; Gillespie, S. E.; Oscarson, J. L.; Izatt, R. M. Excess enthalpies of (toluene + methanol or heptane or methylcyclohexane) and of (heptane + methylcyclohexane) at the temperatures 255.4 K and 310.9 K and the pressure 13.8 MPa. *J. Chem. Thermodyn.* **1995**, *27* (10), 1133-1139.
(102) Elkabule, A. S.; Whitman, D. L.; Miller, R. C. Excess molar enthalpies of (toluene + n-heptane) and (toluene + methylcyclohexane) using a new variable-volume dilution calorimeter. *J. Chem. Thermodyn.* **1988**, *20* (5), 615-620.
(103) Otsa, E. K.; Mikhkelson, V. Y.; Kudryavtseva, L. S. Heats of Mixing in n-Alkane - n-Alk-1-yne Systems. *Russ. J. Phys. Chem.* **1979**, *53* (4), 507-509.
(104) Tamura, K.; Murakami, S.; Fujishiro, R. Excess enthalpies of binary mixtures of aromatic hydrocarbons and aliphatic ketones at 298.15.deg.K. *J. Chem. Thermodyn.* **1975**, *7* (11), 1089-1095.
(105) Tsao, C. C.; Smith, J. M. Heats of mixing of liquids. *Chem. Eng. Prog., Symp. Ser.* **1953**, *49*, 107-117.

(106) Arenosa, R. L.; Menduina, C.; Tardajos, G.; Diaz, P. M. Excess enthalpies at 298.15 K for binary mixtures of toluene + an n-alkane. *J. Chem. Thermodyn.* **1979**, *11* (9), 825-828.
(107) Paz Andrade, M. I.; Castromil, S.; Baluja, M. C. Enthalpies of mixing: n-hexane + o-xylene at 25, 35, and 50.deg. *J. Chem. Thermodyn.* **1970**, *2* (6), 775-777.
(108) Picquenard, E.; Kehiaian, H.; Abello, L.; Pannetier, G. Enthalpies of mixing of aromatic hydrocarbon-n-alkane systems. *Bull. Soc. Chim. Fr.* **1972**, (1), 120-124.
(109) Siimer, E.; Kirss, H.; Kuus, M.; Kudryavtseva, L. Excess Enthalpies for the Systems o-Xylene + Cyclohexanol + Nonane at 298.15 K and 318.15 K and 3-Methylphenol + 1-Hexanol + Heptane at 298.15 K and for Constituent Binaries. *J. Chem. Eng. Data* **1997**, *42* (3), 619-622.
(110) Jain, D. V. S.; Dhar, N. S. Excess enthalpies of binary mixtures nonane + ethylbenzene, + o-xylene, + m-xylene, + p-xylene at 298.15 K. *Indian J. Technol.* **1987**, *25* (12), 591-593.
(111) Paz Andrade, M. I.; Jimenez, E.; Baluja, M. C. Enthalpies of mixing of the hexane-m-xylene system at 25.0, 35.0, and 50.0.deg. *An. Quim.* **1970**, *66* (12), 955-959.
(112) Cannas, A.; Marongiu, B.; Porcedda, S. Thermodynamic properties of n-alkylbenzene + n-alkane or cyclohexane mixtures. Comparison with DISQUAC predictions. *Thermochim. Acta* **1998**, *311* (1-2), 1-19.
(113) Kehiaian, H. V.; Sosnkowska-Kehiaian, K.; Hryniewicz, R. Enthalpy of mixing of ethers with hydrocarbons at 25.deg. and its analysis in terms of molecular surface interactions. *J. Chim. Phys. Physicochim. Biol.* **1971**, *68* (6), 922-934.
(114) Paul, H. I.; Krug, J.; Knapp, H. Measurements of vapor-liquid equilibrium, excess enthalph and excess volumes for binary mixtures of n-alkanes with n-alkylbenzenes. *Thermochim. Acta* **1986**, *108*, 9-27.
(115) Arenosa, R. L.; Rubio, R. G.; Menduina, C.; Diaz, P. M. Excess enthalpies of binary mixtures of ethylbenzene + n-alkanes. *J. Chem. Eng. Data* **1985**, *30* (1), 24-26.
(116) Murti, P. S.; Van, W. M. Vapor-liquid equilibriums and heat of mixing: octane-ethylbenzene-Cellosolve system. *AIChE J.* **1957**, *3*, 517-522.
(117) Paul, H. I. Experimental Investigation of the Vapor-Liquid Equilibria and the volumetric Properties of binary and ternary Mixtures. *VDI Forschungsh. Reihe 3 Verfahrenst.* **1987**, *135.*
(118) Arenosa, R. L.; Rubio, R. G.; Menduina, C.; Diaz, P. M. Excess enthalpies of ethylbenzene + alkane systems at 25°C. An interpretation in terms of the Prigogine-Flory-Patterson model. *J. Solution Chem.* **1985**, *14* (5), 345-354.
(119) Ghogomu, P. M.; Bouroukba, M.; Dellacherie, J.; Balesdent, D.; Dirand, M. Calorimetric measurement of molar excess enthalpies of dilute solutions of ethylbenzene + higher n-alkanes. *Thermochim. Acta* **1997**, *302* (1-2), 159-164.
(120) Wilhelm, E.; Inglese, A.; Roux, A. H.; Grolier, J. P. E. Excess enthalpy, excess heat capacity and excess volume of 1,2,4-trimethylbenzene +, and 1-methylnaphthalene + an n-alkane. *Fluid Phase Equilib.* **1987**, *34* (1), 49-67.
(121) Kovalchuk, B. A.; Olkhov, V. P.; Tsymarnaya, O. V. The Heat of Mixing of Dodecane with Aromatic Hydrocarbons. *Teplofiz. Svoistva Veshchestv Mater.* **1988**, *24*, 31-35.
(122) Aoulmi, A.; Bouroukba, M.; Solimando, R.; Rogalski, M. Thermodynamics of mixtures formed by polycyclic aromatic hydrocarbons with long chain alkanes. *Fluid Phase Equilib.* **1995**, *110* (1-2), 283-297.
(123) Gardeler, H.; Horstmann, S.; Tsuboi, A.; Toba, S.; Rarey, J.; Gmehling, J. Vapor-liquid equilibria at six temperatures from 313.15 K to 402.15 K and excess enthalpy data at 363.15 K and 1.65 MPa for the system toluene + 2,2,4-trimethylpentane (isooctane). *ELDATA: Int. Electron. J. Phys.-Chem. Data* **1998**, *4* (1), 1-9.
(124) Harsted, B. S.; Thomsen, E. S. Excess enthalpies from flow microcalorimetry. 3. Excess enthalpies for binary liquid mixtures of aliphatic and aromatic hydrocarbons, carbon tetrachloride, chlorobenzene, and carbon disulfide. *J. Chem. Thermodyn.* **1975**, *7* (4), 369-376.
(125) Canning, J.; Cheesman, G. H. Heat of mixing of liquids. *J. Chem. Soc.* **1955**, 1230-1233.
(126) Cheesman, G. H.; Ladner, W. R. The variation of the heat of mixing with temperature. *Proc. R. Soc. London, Ser. A* **1955**, *229*, 387-395.
(127) Diaz Pena, M.; Menduina, C. Semicontinuous calorimeter for measuring heats of mixing. *An. Quim.* **1973**, *69* (7-8), 857-868.
(128) Diez, D.; Ruiz, B.; Royo, F. M.; Gutierrez, L. C. Excess molar enthalpies at 298.15 K of (cyclohexane + a methylpyridine) and of (benzene + a methylpyridine). *J. Chem. Thermodyn.* **1985**, *17* (4), 371-377.
(129) Hsu, K.-Y.; Clever, H. L. Excess enthalpies of the 15 binary mixtures formed from cyclohexane, benzene, toluene, 1,4-dimethylbenzene, 1,2,4-trimethylbenzene, and 1,3,5-trimethylbenzene at 298.15.deg.K. *J. Chem. Thermodyn.* **1975**, *7* (5), 435-442.
(130) Kremann, R.; Meingast, R.; Gugl, F. The Energy Change of Binary Systems. 2nd Communication: The Volume Change and Heat Emergence during Formation of Binary Mixtures. *Monatsh. Chem.* **1914**, *35*, 1235-1322.

(131) Murakami, S.; Lam, V. T.; Benson, G. C. Thermodynamic properties of binary aromatic systems. II. Excess enthalpies and volumes of benzene + toluene and toluene + isomeric xylene mixtures at 25.deg. *J. Chem. Thermodyn.* **1969**, *1* (4), 397-407.
(132) Paz Andrade, M. I. Thermodynamic Properties of Binary Mixtures. I. Heat of Mixing. *Acta Cient. Compostelana* **1964**, *1*, 117-130.
(133) Rastogi, R. P.; Nath, J.; Misra, J. Thermodynamics of weak interactions in liquid mixtures. I. Mixtures of carbon tetrachloride, benzene, toluene, and p-xylene. *J. Phys. Chem.* **1967**, *71* (5), 1277-1286.
(134) Rastogi, R. P.; Nath, J.; Misra, J. Thermodynamics of weak interactions in liquid mixtures. II. Mixtures of carbon tetrachloride, benzene, o-xylene, and m-xylene. *J. Phys. Chem.* **1967**, *71* (8), 2524-2535.
(135) Paz Andrade, M. I.; Baluja, M. C.; Nunez, L. Microcalorimetry of heats of mixing benzene-o-xylene, benzene-m-xylene, and benzene-p-xylene systems at 25.deg. *An. Quim.* **1971**, *67* (1), 17-22.
(136) Paz-Andrade, M. I.; Hernandez, C.; Nunez, L.; Jimenez, E. Microcalorimetric study of heats of mixing. Benzene-o-, m-, and p-xylene systems at 50.deg. *J. Chim. Phys. Physicochim. Biol.* **1972**, *69* (7-8), 1132-1135.
(137) Singh, J.; Pflug, H. D.; Benson, G. C. Molar excess enthalpies and volumes of benzene-isomeric xylene systems at 25.deg. *J. Phys. Chem.* **1968**, *72* (6), 1939-1944.
(138) Sharma, S. C.; Lakhanpal, M. L.; Rumpaul, M. L. Enthalpies of mixing of p-xylene with benzene, dioxane, cyclohexane and methylcyclohexane. *Indian J. Chem., Sect. A* **1981**, *20A* (3), 225-227.
(139) Ott, J. B.; Marsh, K. N.; Stokes, R. H. Excess enthalpies, excess volumes, and excess Gibbs free energies for benzene + p-xylene at 288.15, 298.15, 308.15, and 318.15 K. *J. Chem. Thermodyn.* **1980**, *12* (5), 493-503.
(140) Ott, J. B.; Goates, J. R.; Grigg, R. B. Excess volumes, enthalpies, and Gibbs free energies for mixtures of benzene + p-xylene. *J. Chem. Thermodyn.* **1979**, *11* (12), 1167-1173.
(141) Lutskii, A. E.; Obukhova, E. M.; Petrenko, B. G. The heat of mixing and the dipole moments of the molecules of components. *Zh. Fiz. Khim.* **1958**, *32*, 720-721.
(142) Tanaka, R.; Benson, G. C. Excess enthalpies of some ethylbenzene + aromatic hydrocarbon mixtures at 298.15 K. *J. Chem. Thermodyn.* **1976**, *8* (3), 259-268.
(143) Woycicki, W. Entalpies of mixing of some binary mixtures of benzene, cyclohexane, and pyridine and their methyl and ethyl derivatives. 2. *J. Chem. Thermodyn.* **1974**, *6* (2), 141-147.
(144) Nath, J.; Yadava, R. B. Thermodynamic properties and dielectric constants for binary mixtures of carbon tetrachloride with cumene and mesitylene and of benzene with cumene and mesitylene. *Indian J. Chem.* **1971**, *9* (1), 45-47.
(145) Woycicki, W.; Sadowska, K. W. Enthalpies and volumes of mixing in the systems: n-propylbenzene with benzene, toluene and ethylbenzene and n-butylbenzene with benzene, toluene, ethylbenzene and n-propylbenzene. *Bull. Acad. Pol. Sci., Ser. Sci. Chim.* **1977**, *25* (2), 115-121.
(146) Jain, D. V. S.; Dhar, N. S. Excess enthalpies of binary mixtures of benzene with n-propylbenzene, n-butylbenzene, n-hexylbenzene at 298.15, 308.15 and 318.15 K. *Fluid Phase Equilib.* **1989**, *47* (1), 89-94.
(147) Jain, D. V. S.; Chadha, R.; Dhar, N. S. Excess molar enthalpies of (benzene or methylbenzene or ethylbenzene + 2-methylethylbenzene) at the temperatures 298.15 K, 308.18 K, and 318.15 K. *J. Chem. Thermodyn.* **1992**, *24* (10), 1027-1031.
(148) Aznar, E.; Ruiz, B.; Losa, C. G. Excess molar enthalpies at 298.15 K of (cyclohexane + a methylquinoline) and of (benzene + a methylquinoline). *J. Chem. Thermodyn.* **1985**, *17* (12), 1121-1126.
(149) Kortuem, G.; Dreesen, G.; Freier, H. J. The Thermodynamics of Mixtures of Liquids with Different Molecular Sizes. Heat of Mixing of the System Benzene - Diphenyl. *Z. Naturforsch. Sec. A* **1953**, *8*, 546-555.
(150) Kortuem, G.; Schreiber, H. Theoretical and experimental investigation of the mixing effects of benzene with its quasidimers diphenyl, o,o'-ditolyl, and diphenylmethane. *Z. Naturforsch.* **1965**, *20a*, 1030-1044.
(151) Kracht, C.; Ulbig, P.; Schulz, S. Molar excess enthalpies of binary mixtures containing chlorobenzene, o-dichlorobenzene, toluene, 4-chlorotoluene, and o-xylene. *Private Communication* **1999**, 1-21.
(152) Lewis, G.; Johnson, A. F. Heats of mixing of toluene and ethylbenzene. *J. Chem. Eng. Data* **1969**, *14* (4), 484-486.
(153) Recko, W. M.; Sadowska, K. W. Weak dipolar interaction. Heat of mixing and excess volumes of systems formed by halogen and alkyl derivatives of benzene. *Bull. Acad. Pol. Sci., Ser. Sci. Chim.* **1969**, *17* (5), 307-310.
(154) Jain, D. V. S.; Chadha, R.; Dhar, N. S. Excess enthalpies of binary mixtures toluene + propylbenzene, + butylbenzene and + hexylbenzene at 298.15, 308.15 and 318.15 K. *Fluid Phase Equilib.* **1994**, *102* (2), 205-210.
(155) Holt, D. L.; Smith, B. D. Measurement of excess enthalpies with Tronac titration calorimeter. Data for some C8 aromatic binaries. *J. Chem. Eng. Data* **1974**, *19* (2), 129-133.
(156) Lam, V. T.; Murakami, S.; Benson, G. C. Thermodynamic properties of binary aromatic systems. III. Excess enthalpies and volumes of isomeric xylene mixtures at 25.deg. *J. Chem. Thermodyn.* **1970**, *2* (1), 17-25.
(157) Rattan, V. K.; Raju, K. S. N. Heats of mixing of binaries of isopropylbenzene with o-, m-, and p-xylenes at 298.15 K. *Indian J. Technol.* **1991**, *29* (2), 77-78.

(158) Jain, D. V. S.; Dhar, N. S. Excess molar enthalpies of binary mixtures ethylbenzene + propylbenzene, + butylbenzene and + hexylbenzene at 298.15, 308.15 and 318.15 K. *Fluid Phase Equilib.* **1992**, *81*, 231-239.
(159) Letcher, T. M.; Heyward, C.; Spiteri, W. L. The excess molar enthalpies of cyclopentane + each of six n-alkanes at two temperatures. *J. Chem. Thermodyn.* **1983**, *15* (4), 395-396.
(160) Inglese, A.; Grolier, J. P. E. Excess enthalpy. Cyclopentane-n-heptane system. *Int. DATA Ser., Sel. Data Mixtures, Ser. A* **1975**, (2), 98-109.
(161) Fenby, D. V.; Khurma, J. R.; Konner, Z. S.; Block, T. E.; Knobler, C. M.; Reeder, J.; Scott, R. L. Isomer effects in mixtures of hydrocarbons: some experimental excess volumes and enthalpies. *Aust. J. Chem.* **1980**, *33* (9), 1927-1941.
(162) Trampe, D. M.; Eckert, C. A. Calorimetric measurement of partial molar excess enthalpies at infinite dilution. *J. Chem. Eng. Data* **1991**, *36* (1), 112-118.
(163) Ahmed, A. Enthalpy of Mixing of n-Hexane and Cyclohexane. *J. Chem. Soc. Faraday Trans. I* **1973**, *69*, 387-389.
(164) Alessi, P.; Kikic, I.; Longo, V. The Heats of Mixing of Paraffin - Cycloparaffin Systems. *Univ. Studi Trieste Fac. Ing. Ist. Chim. Appl.* **1974**, *49*, 1-10.
(165) Arenosa, R. L.; Menduina, C.; Tardajos, G.; Diaz, P. M. Excess enthalpies at 298.15 K of binary mixtures of cyclohexane with n-alkanes. *J. Chem. Thermodyn.* **1979**, *11* (2), 159-166.
(166) Arm, H.; Bucher, P. A Calorimeter for Determing Enthalpies of Mixing. Enthalpies of Mixing of the Binary System n-Hexane + Cyclohexane at 25 °C. *Chimia* **1973**, *27* (2), 79-81.
(167) Aufderhaar, O. Experimental determination of caloric data with a Tian-Calvet calorimeter and correlation of vapor pressure data of pure components with an extended Antoine equation. *Diplomarbeit(Universitaet Oldenburg)* **1996**, 1-96.
(168) Bao, J. D.; Muan, Q. G.; Xie, Y. Z.; Zhao, G. H. *Huadong Huagong Xueyuan Xuebao* **1983**, (2), 267-271.
(169) Christensen, J. J.; Hansen, L. D.; Eatough, D. J.; Izatt, R. M.; Hart, R. M. Isothermal high pressure flow calorimeter. *Rev. Sci. Instrum.* **1976**, *47* (6), 730-734.
(170) Christensen, J. J.; Izatt, R. M.; Eatough, D. J.; Hansen, L. D. The effect of pressure on the excess enthalpies of cyclohexane + n-hexane at 298.15 K. *J. Chem. Thermodyn.* **1978**, *10* (1), 25-34.
(171) Comelli, F. Heat of mixing for 1,3-dioxolane - methyl ethyl ketone system. *Chim. Ind. (Milan)* **1989**, *71* (9), 70-71.
(172) D'Avila, S. G.; Carioca, J. O. B. Measurement of Activity Coefficients at Infinite Dilution by Inert Gas Stripping and Gas Chromatography. *Private Communication(Campinas, Brazil)* **1996**, 1-7.
(173) Dias d'Almeida, M.; Fernandez-Garcia, J. G.; Boissonnas, C. G. Thermodynamic of liquid binary mixtures. Heats of mixing of cycloalkanes. *Helv. Chim. Acta* **1970**, *53* (6), 1389-1394.
(174) Ewing, M. B.; Marsh, K. N. Enthalpy of mixing of n-hexane+cyclohexane at 288.15 and 318.15.deg.K. *J. Chem. Thermodyn.* **1970**, *2* (2), 295-296.
(175) Fenclova, D.; Vrbka, P.; Dohnal, V.; Rehak, K.; Garcia-Miaja, G. (Vapour + liquid) equilibria and excess molar enthalpies for mixtures with strong complex formation. Trichloromethane or 1-bromo-1-chloro-2,2,2-trifluoroethane (halothane) with tetrahydropyran or piperidine. *J. Chem. Thermodyn.* **2002**, *34* (3), 361-376.
(176) Gmehling, J.; Meents, B. Excess enthalpy. Cyclohexane-hexane system. *Int. DATA Ser., Sel. Data Mixtures, Ser. A* **1992**, (3), 144-145.
(177) Gmehling, J. Excess enthalpies for 1,1,1-trichloroethane with alkanes, ketones, and esters. *J. Chem. Eng. Data* **1993**, *38* (1), 143-146.
(178) Gmehling, J.; Krentscher, B. Excess enthalpies of 12 binary liquid mixtures containing cyclohexane at elevated temperatures and pressures (up to 416 K and 1.9 MPa). *ELDATA: Int. Electron. J. Phys.-Chem. Data* **1995**, *1* (3), 181-190.
(179) Grolier, J. P. E.; Benson, G. C.; Picker, P. Enthalpies of mixing of organic liquids measured directly as a function of composition by means of scanning dynamic flow microcalorimetry. *J. Chem. Thermodyn.* **1975**, *7* (1), 89-95.
(180) Grolier, J. P. E. Determination of the enthalpies of mixing of nonelectrolytes using the Picker dynamic-flow microcalorimeter. *Thermochim. Acta* **1976**, *16* (1), 27-38.
(181) Harsted, B. S.; Thomsen, E. S. Excess enthalpies from flow microcalorimetry. 1. Experimental method and excess enthalpies for carbon tetrachloride + cyclohexane, + benzene, and + octamethylcyclotetrasiloxane, and of n-hexane + cyclohexane. *J. Chem. Thermodyn.* **1974**, *6* (6), 549-555.
(182) Heintz, A.; Lichtenthaler, R. N. Calorimetric Study of Structures of Order in Mixtures of Alkanes. *Ber. Bunsen-Ges. Phys. Chem.* **1977**, *81* (10), 921-925.
(183) Heintz, A.; Lichtenthaler, R. N. An Isothermal Flow Calorimeter for Pressures to 600 bar. *Ber. Bunsen-Ges. Phys. Chem.* **1979**, *83* (8), 853-856.
(184) Huemer, H.; Platzer, E.; Rehak, K. Test measurements and analysis of errors for a new equipment for the determination of excess-heat data. *Thermochim. Acta* **1991**, *187*, 95-112.

(185) Kedrina, N. N.; Semenov, L. V.; Gaile, A. A. Enthalpy of Mixing of Hydrocarbons with Polar Solvents. *Deposited Doc. Oniitekhim* **1981**, (600KHP-D81), 1-10.
(186) Keil, C.; Bittrich, H. J. Mixing calorimetry without vapor space. *Z. Phys. Chem. (Leipzig)* **1971**, *248* (1-2), 65-73.
(187) Krug, J. Experimental Study of Excess Enthalpies and Excess Volumes of Binary Liquid Mixtures. *Dissertation(TU Berlin)* **1985**.
(188) Letcher, T. M.; Sack, J. The excess enthalpy of mixing of some hydrocarbon mixtures. *J. S. Afr. Chem. Inst.* **1975**, *28* (3), 316-320.
(189) Marsh, K. N.; Stokes, R. H. Enthalpies of mixing of n-hexane + cyclohexane at 25.deg. *J. Chem. Thermodyn.* **1969**, *1* (2), 223-225.
(190) Marsh, K. N. Excess Enthalpy. *Int. Data Ser. Sel. Data Mixtures Ser. A* **1973**, (1), 16-16.
(191) Marsh, K. N. Excess Enthalpy. *Int. Data Ser. Sel. Data Mixtures Ser. A* **1973**, 21-23.
(192) Mattingley, B. I.; Handa, Y. P.; Fenby, D. V. Aromatic fluorocarbon mixtures. 7. Excess enthalpies of hexafluorobenzene + triethylamine, + acetone, + diethyl ether, and + dimethyl sulfoxide. *J. Chem. Thermodyn.* **1975**, *7* (2), 169-173.
(193) McGlashan, M. L.; Stoeckli, H. F. Flow calorimeter for enthalpies of mixing. Enthalpy of mixing of n-hexane + cyclohexane at 298.15.deg.K. *J. Chem. Thermodyn.* **1969**, *1* (6), 589-594.
(194) McLure, I. A.; Trejo, R. A. Excess functions for (n-alkanenitrile + n-alkane) liquid mixtures. 2. Excess enthalpies at 298.15 K for propanenitrile and n-butanenitrile with some C5 to C14 n-alkanes. *J. Chem. Thermodyn.* **1982**, *14* (5), 439-445.
(195) Meyer, R.; Giusti, G.; Vincent, E. J.; Meyer, M. The thermodynamic properties of acetals + heptane mixtures at 298.15 K. *Thermochim. Acta* **1977**, *19* (2), 153-160.
(196) Murakami, S.; Benson, G. C. Isothermal dilution calorimeter for measuring enthalpies of mixing. *J. Chem. Thermodyn.* **1969**, *1* (6), 559-572.
(197) Paz Andrade, M. I.; Lema, F.; Baluja, M. C. Enthalpies of mixing at medium temperatures: hexane-cyclohexane system. *An. Quim.* **1970**, *66* (6), 527-530.
(198) Pineiro, A.; Olvera, A.; Garcia-Miaja, G.; Costas, M. Excess Molar Enthalpies of Tetrahydrofuran or Diisopropyl Ether + 1-Alkanols at 298.15 K, Using a Newly Designed Flow Mixing Cell for an Isothermal Microcalorimeter. *J. Chem. Eng. Data* **2001**, *46* (5), 1274-1279.
(199) Pradhan, S. D.; Pathak, G. A simple calorimeter for the heats of mixing study of associated liquids: enthalpy of hydrogen bonded ethanol-butylamine complex. *Proc. - Indian Acad. Sci., [Ser.]: Chem. Sci.* **1980**, *89* (4), 341-347.
(200) Raal, J. D.; Webley, P. A. Microflow calorimeter design for heats of mixing. *AIChE J.* **1987**, *33* (4), 604-618.
(201) Siddiqi, M. A.; Lucas, K. An isothermal high-pressure flow calorimeter. The excess enthalpy of (cyclohexane + n-hexane) at different pressures at 288.15, 298.15, and 313.15 K. *J. Chem. Thermodyn.* **1982**, *14* (12), 1183-1190.
(202) Takigawa, T.; Ohba, M.; Ogawa, H.; Murakami, S. Thermodynamic properties of binary mixtures of hexane isomer and cyclohexane at 298.15 K. *Fluid Phase Equilib.* **2003**, *204* (1), 119-130.
(203) Tanaka, R.; Murakami, S.; Fujishiro, R. Isothermal displacement calorimeter for measuring enthalpies of mixing. *Bull. Chem. Soc. Jap.* **1972**, *45* (7), 2107-2110.
(204) Tanaka, R.; D'Arcy, P. J.; Benson, G. C. Application of a flow microcalorimeter to determine the excess enthalpies of binary mixtures of nonelectrolytes. *Thermochim. Acta* **1975**, *11* (2), 163-175.
(205) Vesely, F.; Pick, J. Heats of mixing of normal paraffin hydrocarbons with cyclohexane, application of the quasi-lattice theory. *Collect. Czech. Chem. Commun.* **1969**, *34*, 1792-1796.
(206) Watts, H.; Clarke, E. C. W.; Glew, D. N. New calorimeter for measurement of the enthalpy of mixing of liquids. The enthalpy of mixing of benzene with carbon tetrachloride and of n-hexane with cyclohexane. *Can. J. Chem.* **1968**, *46* (6), 815-821.
(207) Yanes, C.; Pellicer, J.; Rojas, E.; Zamora, M. Calorimetric cell for the measurement of excess enthalpy of volatile liquids. Excess enthalpy of cis-9-octadecenoic acid + cyclohexane at 298.15 K. *J. Chem. Thermodyn.* **1979**, *11* (Z), 177-182.
(208) Yan, W.; Lin, R.; Yen, W. Excess enthalpies of seven binary liquid systems. *Thermochim. Acta* **1990**, *169*, 171-184.
(209) Grosse-Wortmann, H.; Jost, W.; Wagner, H. G. Calorimetric Measurements of the System Ethanol - Cyclohexane - n-Heptane. *Z. Phys. Chem. NF* **1966**, *49*, 74-93.
(210) Tancrede, P.; Patterson, D. Excess enthalpy. Cyclohexane-n-octane system. *Int. DATA Ser., Sel. Data Mixtures, Ser. A* **1975**, *1974* (2), 114.
(211) Hill, R. J.; Mairs, T. E.; Swinton, F. L. The thermodynamic properties of binary mixtures containing an octane. III. Excess enthalpies and excess volumes. *J. Chem. Thermodyn.* **1980**, *12* (6), 581-587.

(212) Hamoudi, Z.; Belaribi, F. B.; Ait-Kaci, A.; Boukais-Belaribi, G. Experimental and predicted excess molar enthalpies for 1,4-dioxane + octane + cyclohexane at 303.15K. *Fluid Phase Equilib.* **2006**, *244* (1), 62-67.
(213) Yang, S.-K.; Gomez-Ibanez, J. D. The excess enthalpies of cyclohexane + n-dodecane and + n-nonane. *J. Chem. Thermodyn.* **1976**, *8* (3), 209-216.
(214) Wagner, H.; Lichtenthaler, R. N. Excess properties of liquid cyclohexane/hydrocarbon mixtures. I. Experimental results of the excess enthalpy. *Ber. Bunsen-Ges. Phys. Chem.* **1986**, *90* (1), 65-68.
(215) Zhu, S.; Shen, S.; Benson, G. C.; Lu, B. C. Y. Excess enthalpies of (ethanol or propan-1-ol + cyclohexane + decane) at the temperature 298.15 K. *J. Chem. Thermodyn.* **1993**, *25* (7), 909-917.
(216) Tancrede, P.; Patterson, D. Excess enthalpy. Cyclohexane-n-dodecane system. *Int. DATA Ser., Sel. Data Mixtures, Ser. A* **1975**, *1974* (2), 115.
(217) Tancrede, P.; Patterson, D. Excess enthalpy. Cyclohexane-n-hexadecane system. *Int. DATA Ser., Sel. Data Mixtures, Ser. A* **1975**, *1974* (2), 116.
(218) Spiteri, W. L.; Letcher, T. M. The excess enthalpies of cycloheptane + an n-alkane. *J. Chem. Thermodyn.* **1982**, *14* (11), 1047-1050.
(219) Wilhelm, E.; Inglese, A.; Grolier, J. P. E. Excess enthalpies of cycloheptane + n-alkane and cyclooctane + n-alkane. *J. Chem. Eng. Data* **1983**, *28* (2), 202-204.
(220) Marongiu, B.; Porcedda, S.; Lepori, L.; Matteoli, E. The effect of the molecular shape on the enthalpic behavior of liquid mixtures: cyclic hydrocarbons in heptane and tetrachloromethane. *Fluid Phase Equilib.* **1995**, *108* (1-2), 167-183.
(221) Spiteri, W. L.; Letcher, T. M. The excess enthalpies of cyclooctane + n-alkanes. *Thermochim. Acta* **1982**, *59* (1), 73-80.
(222) Letcher, T. M.; Scoones, B. W. The excess enthalpies of 1,2,3,4-tetrahydronaphthalene + each of four n-alkanes and + each of four cycloalkanes at two temperatures. *J. Chem. Thermodyn.* **1982**, *14* (9), 831-835.
(223) Porcedda, S. Excess enthalpy of cycloheptane with heptane. *Int. DATA Ser., Sel. Data Mixtures, Ser. A* **1992**, (2), 92.
(224) Ewing, M. B.; Marsh, K. N. Excess Gibbs energies, excess enthalpies, and excess volumes for mixtures of cyclopentane + 2,3-dimethylbutane. *J. Chem. Thermodyn.* **1973**, *5* (5), 659-664.
(225) Dixon, D. T.; Hewitt, F. A. Excess enthalpies and volumes for neopentane + cyclohexane and tetramethylsilane + cyclohexane at 298.15 K. *J. Chem. Thermodyn.* **1978**, *10* (5), 501-503.
(226) Tancrede, P.; Patterson, D. Excess enthalpy. Cyclohexane-2,2-dimethylbutane system. *Int. DATA Ser., Sel. Data Mixtures, Ser. A* **1975**, *1974* (2), 117.
(227) Romani, L.; Paz, A. M. I. Excess thermodynamic functions at 25.deg.. II. Cyclohexane + hexane isomers. *An. Quim.* **1975**, *71* (1), 3-6.
(228) Peng, D.-Y.; Benson, G. C.; Lu, B. C. Y. Excess enthalpies of 2,2-dimethylbutane + cyclohexane + (octane or dodecane) at 25 °C. *J. Solution Chem.* **2000**, *29* (2), 153-164.
(229) Ewing, M. B.; Marsh, K. N. Excess Gibbs free energies, excess enthalpies, excess volumes, and isothermal compressibilities of cyclohexane + 2,3-dimethylbutane. *J. Chem. Thermodyn.* **1974**, *6* (1), 35-41.
(230) Tancrede, P.; Patterson, D. Excess enthalpy. Cyclohexane-2,2,4-trimethylpentane (isoctane) system. *Int. DATA Ser., Sel. Data Mixtures, Ser. A* **1975**, *1974* (2), 118.
(231) Ewing, M. B.; Marsh, K. N. Excess Gibbs free energies, excess enthalpies, and excess volumes of cycloheptane + 2, 3-dimethylbutane. *J. Chem. Thermodyn.* **1974**, *6* (1), 43-47.
(232) Ewing, M. B.; Marsh, K. N. Excess Gibbs free energies, excess enthalpies, and excess volumes for 2,3-dimethylbutane + cyclooctane. *J. Chem. Thermodyn.* **1973**, *5* (5), 651-657.
(233) Arora, P. S.; Phutela, R. C.; Singh, P. P. Interaction of cyclopentane with benzene, carbon tetrachloride, and cyclohexane. *Thermochim. Acta* **1974**, *10* (1), 47-53.
(234) Watson, A. E. P.; McLure, I. A.; Bennett, J. E.; Benson, G. C. Excess properties of some aromatic-alicyclic systems. I. Measurements of enthalpies and volumes of mixing. *J. Phys. Chem.* **1965**, *69* (8), 2753-2758.
(235) Abello, L. Excess heats of binary systems containing benzene hydrocarbons and chloroform or methylchloroform. I. Experimental results. *J. Chim. Phys. Physicochim. Biol.* **1973**, *70* (9), 1355-1359.
(236) Ait-Kaci, A. *Ph.D. thesis, Lyon* **1982**, 30-60.
(237) Bares, D.; Soulie, M.; Metzger, J. Experimental calorimetric and ebulliometric methods for determining the excess thermodynamic functions or organic liquids. Applications to binary systems composed of azaaromatic bases and an apolar solvent. *J. Chim. Phys. Physicochim. Biol.* **1973**, *70* (10), 1531-1539.
(238) Battler, J. R.; Clark, W. M.; Rowley, R. L. Excess enthalpy and liquid-liquid equilibrium surfaces for the cyclohexane-2-propanol-water system from 293.15 to 323.15 K. *J. Chem. Eng. Data* **1985**, *30* (3), 254-259.
(239) Cabani, S.; Ceccanti, N. Thermodynamic properties of binary mixtures of cyclohexane with cyclic amines or cyclic ethers at 298.15.deg.K. *J. Chem. Thermodyn.* **1973**, *5* (1), 9-20.

(240) Casas, H.; Segade, L.; Garcia-Garabal, S.; Pineiro, M. M.; Franjo, C.; Jimenez, E.; Paz, A. M. I. Excess molar enthalpies for propyl propanoate + cyclohexane + benzene at 298.15 and 308.15 K. *Fluid Phase Equilib.* **2001**, *182* (1-2), 279-288.
(241) Coca, J. Physical-Chemical Properties of Liquid Binary Mixtures: Viscosity and Heat of Mixing. *Acta Salmant. Cienc.* **1969**, *33*, 9-39.
(242) Coomber, B. A.; Wormald, C. J. A stirred flow calorimeter. The excess enthalpies of acetone + water and of acetone + some normal alcohols. *J. Chem. Thermodyn.* **1976**, *8* (8), 793-799.
(243) Dahmani, O.; Ait-Kaci, A. Heats of mixing at 298.15 K of the ternary cyclohexane (1) + benzene (2) + 1-chlorobutane (3) system. *J. Therm. Anal.* **1994**, *42* (5), 963-971.
(244) Devika, P. D.; Ramachandran, T. P.; Ananth, M. S. Enthalpy of mixing of five binary mixtures. *Indian J. Technol.* **1992**, *30* (11-12), 612-614.
(245) Diaz Pena, M.; Fernandez Martin, F. Thermodynamics of Mixtures of Normal Alcohols. Part 1. Heat of Mixing of the System n-Butanol - Methanol at 25 °C. *An. R. Soc. Esp. Fis. Quim. Ser. B* **1963**, *59*, 323-330.
(246) Elliott, K.; Wormald, C. J. A precision differential flow calorimeter. The excess enthalpy of benzene + cyclohexane between 280.15 K and 393.15 K. *J. Chem. Thermodyn.* **1976**, *8* (9), 881-893.
(247) Fujihara, I.; Kobayashi, M.; Murakami, S. Excess enthalpies of trans-decalin + benzene, + toluene, + isooctane, and + heptane at 298.15 K. *J. Chem. Thermodyn.* **1983**, *15* (1), 1-6.
(248) Gmehling, J. *Unpublished Data* **2004**.
(249) Goates, J. R.; Sullivan, R. J.; Ott, J. B. Heats of mixing in the system carbon tetrachloride-cyclohexane-benzene. *J. Phys. Chem.* **1959**, *63*, 589-594.
(250) Gracia, M. An isothermal dilution calorimeter for positive enthalpies of mixing. *J. Chem. Thermodyn.* **1977**, *9* (1), 55-59.
(251) Hill, R. J.; Swinton, F. L. The excess enthalpies of some mixtures containing carbon disulfide. *J. Chem. Thermodyn.* **1980**, *12* (5), 489-492.
(252) Karvo, M. Thermodynamic properties of binary and ternary mixtures containing sulfolane. V. Excess enthalpies of cyclohexane + benzene, cyclohexane + toluene, benzene + sulfolane, and toluene + sulfolane. *J. Chem. Thermodyn.* **1980**, *12* (7), 635-639.
(253) Kumaran, M. K.; Halpin, C. J.; Benson, G. C. Limiting excess partial molar enthalpies of hexan-1-ol, 2-methylpentan-1-ol, and 2-ethylbutan-1-ol in n-hexane at 298.15 K. *J. Chem. Thermodyn.* **1983**, *15* (3), 249-252.
(254) Kuus, M.; Kirss, H.; Siimer, E.; Kudryavtseva, L. Excess Enthalpies for the Systems 1,3-Butanediol + Cyclohexanol + Decane and 1,2-Propanediol + 1,3-Butanediol + Cyclohexanol and for Constituent Binaries at 318.15 K. *J. Chem. Eng. Data* **1996**, *41* (5), 1206-1209.
(255) Lacher, J. R.; Buck, W. B.; Parry, W. H. Vapor-pressure studies. II. Chlorobenzene-1-nitropropane. *J. Am. Chem. Soc.* **1941**, *63*, 2422-2425.
(256) Lark, B. S.; Kaur, S.; Singh, S. Ternary heat effects in ternary mixtures. *Thermochim. Acta* **1986**, *105*, 219-229.
(257) Lohmann, J.; Boelts, R.; Gmehling, J. Excess Enthalpy Data for Seven Binary Systems at Temperatures between 50 and 140 °C. *J. Chem. Eng. Data* **2001**, *46* (2), 208-211.
(258) Mattingley, B. I.; Fenby, D. V. Thermodynamic study of the deuterium isotope effect, the molar excess enthalpies of hexadeuterobenzene + cyclohexane and benzene + cyclohexane. *Aust. J. Chem.* **1975**, *28* (1), 185-187.
(259) Mrazek, R. V. Heats of Mixing: Binary Alcohol-Aromatic Systems at 25, 35, and 45 °C. *Ph.D. thesis, Troy, NY* **1960**, 147-185.
(260) Murakami, T.; Murakami, S.; Fujishiro, R. Heat of mixing for binary mixtures: pyridine derivatives-benzene, and -cyclohexane systems. *Bull. Chem. Soc. Jap.* **1969**, *42* (1), 35-40.
(261) Murray, R. S.; Martin, M. L. Excess enthalpies of hexafluorobenzene + diethyl ether, + di-isopropyl ether, and + di-n-butyl ether at 283.15 and 298.15 K. *J. Chem. Thermodyn.* **1978**, *10* (8), 711-720.
(262) Nagata, I.; Kazuma, K. Heats of mixing for the ternary system ethanol-1-propanol-cyclohexane at 25°C. *J. Chem. Eng. Data* **1977**, *22* (1), 79-84.
(263) Nagata, I.; Tamura, K.; Ozaki, S.; Myohen, K. Ternary excess molar enthalpies of chloroform + acetone + cyclohexane mixtures at 298.15 K. *Thermochim. Acta* **1992**, *209*, 31-41.
(264) Nicholson, D. E. Heats of mixing of benzene and cyclohexane. *J. Chem. Eng. Data* **1961**, *6*, 5.
(265) Nicolaides, G. L.; Eckert, C. A. Experimental heats of mixing of some miscible and partially miscible nonelectrolyte systems. *J. Chem. Eng. Data* **1978**, *23* (2), 152-156.
(266) Obbink, J. H.; Van, M. J. C.; Van, d. B. G. J. K. An isothermal displacement calorimeter for positive excess enthalpies. *J. Chem. Thermodyn.* **1978**, *10* (7), 691-699.
(267) Orszagh, A.; Kasprzycka-Guttman, T. Thermodynamic properties of some heterocyclic base-aliphatic n-alcohols systems. I. *Bull. Acad. Pol. Sci., Ser. Sci. Chim.* **1972**, *20* (4), 349-354.

(268) Paz Andrade, M. I.; Ocon, J.; Casanova, J. Heats of mixing near the boiling point. I. Benzene-cyclohexane. *An. R. Soc. Esp. Fis. Quim., Ser. B* **1965**, *61* (5), 707-716.
(269) Ratnam, A. V.; Rao, C. V.; Murti, P. S. Thermodynamic properties of liquid mixtures: heats of mixing at 35°. Systems: benzene-cyclohexane-ethyl acetate and the three related binaries. *Chem. Eng. Sci.* **1962**, *17*, 392-396.
(270) Sabinin, V. E.; Belousov, V. P.; Morachevskii, A. G. Heat of mixing and heat of vaporization in the system benzene - cyclohexane. *Izv. Vyssh. Uchebn. Zaved. Khim. Khim. Tekhnol.* **1966**, *9* (3), 382-386.
(271) Stokes, R. H.; Marsh, K. N.; Tomlins, R. P. Isothermal displacement calorimeter for endothermic enthalpies of mixing. *J. Chem. Thermodyn.* **1969**, *1* (2), 211-221.
(272) Touhara, H.; Ikeda, M.; Nakanishi, K.; Watanabe, N. Isothermal dilution calorimeter for measuring excess enthalpies. *J. Chem. Thermodyn.* **1975**, *7* (9), 887-893.
(273) van Ness, H. C.; Abbot, M. M. Excess Enthalpy. *Int. Data Ser. Sel. Data Mixtures Ser. A* **1974**, *1974* (3), 160-161.
(274) Vesely, F.; Hynek, V.; Svoboda, V.; Holub, R. Isothermal Calorimeter for Measuring Endothermic Heats of Mixing. *Collect. Czech. Chem. Commun.* **1974**, *39* (2), 355-365.
(275) Vesely, F.; Pick, J. Heats of Mixing of Normal Alcohols with Cyclohexane. *Collect. Czech. Chem. Commun.* **1969**, *34*, 1854-1874.
(276) Woycicki, W.; Sadowska, K. W. Heat and Volume of Mixing of Pyridine or alpha-Picoline with Cyclohexane or Methylcyclohexane. *Bull. Acad. Pol. Sci. Ser. Sci. Chim.* **1968**, *16* (3), 147-153.
(277) Letcher, T. M.; Perkins, D. M. Application of the flory theory of liquid mixtures to excess volumes and enthalpies of benzene + cycloalkane and + n-alkane mixtures. *Thermochim. Acta* **1984**, *77* (1-3), 267-274.
(278) Wilhelm, E.; Inglese, A.; Grolier, J. P. E. Excess enthalpies of binary mixtures of cycloheptane or cyclooctane with benzene or toluene or ethylbenzene at 298.15 K. *Thermochim. Acta* **1993**, *229* (1-2), 271-280.
(279) Letcher, T. M.; Baxter, R. C. Excess volumes and enthalpies of mixing benzene with various bicyclic compounds. *J. Solution Chem.* **1985**, *14* (1), 35-40.
(280) Amaya, K. Thermodynamic studies of binary systems consisting of polar and nonpolar liquids. II. Measurement of the heats of mixing for binary systems of polar and nonpolar liquids. *Bull. Chem. Soc. Jpn.* **1961**, *34* (9), 1278-1285.
(281) Paz-Andrade, M. I.; Amor, M. P. Heats of mixing at 25.deg. of the systems cyclohexane-o-xylene, cyclohexane-m-xylene, and cyclohexane-p-xylene. *An. Quim.* **1970**, *66* (9-10), 717-720.
(282) Murakami, S.; Fujishiro, R. Thermochemical evidence of OH-π type intermolecular hydrogen bonds. *Bull. Chem. Soc. Jpn.* **1967**, *40* (8), 1784-1789.
(283) French, H. T.; Stokes, R. H. Thermodynamics of ethanol at low concentrations in mixtures of cyclohexane and 1,4-dimethylbenzene. *J. Chem. Soc., Faraday Trans. 1* **1985**, *81* (6), 1459-1465.
(284) Nagata, I.; Ogasawara, Y. Prediction of ternary excess enthalpies from binary data. *Thermochim. Acta* **1982**, *52* (1-3), 155-168.
(285) Nissema, A.; Kaivamo, T.; Karvo, M. Thermodynamic properties of binary and ternary systems. XII. Excess enthalpies of cyclohexane + p-xylene, p-xylene + dimethyl sulfoxide, and dimethyl sulfoxide + cyclohexane + p-xylene. *J. Chem. Thermodyn.* **1983**, *15* (11), 1083-1086.
(286) Fujii, S.; Tamura, K.; Murakami, S. Thermodynamic properties of (an alkylbenzene + cyclohexane) at the temperature 298.15 K. *J. Chem. Thermodyn.* **1995**, *27* (12), 1319-1328.
(287) Ewing, M. B.; Marsh, K. N. Enthalpies of mixing of cyclohexane+carbon tetrachloride, of cyclohexane+cyclopentane, and of carbon tetrachloride+cyclopentane at various temperatures. *J. Chem. Thermodyn.* **1970**, *2* (3), 351-358.
(288) Ewing, M. B.; Marsh, K. N. Excess functions for cyclopentane + cyclohexane, cyclopentane + cycloheptane, and cyclohexane + cyclooctane. *J. Chem. Thermodyn.* **1974**, *6* (4), 395-406.
(289) Ewing, M. B.; Levien, B. J.; Marsh, K. N.; Stokes, R. H. Excess enthalpies, excess volumes, and excess Gibbs free energies for mixtures of cyclo-octane+cyclopentane at 288.15, 298.15, and 308.15K. *J. Chem. Thermodyn.* **1970**, *2* (5), 689-695.
(290) Stokes, R. H.; Marsh, K. N.; Tomlins, R. P. Enthalpies of exothermic mixing measured by the isothermal displacement calorimeter for cyclooctane + cyclopentane at 25.deg. *J. Chem. Thermodyn.* **1969**, *1* (4), 377-379.
(291) Ewing, M. B.; Marsh, K. N. Excess functions for cyclohexane + cycloheptane and cycloheptane + cyclooctane. *J. Chem. Thermodyn.* **1974**, *6* (1), 1087-1096.
(292) Vesely, F.; Mikulic, A. V.; Svoboda, V.; Pick, J. Heats of Mixing of Normal Alcohols with Methylcyclohexane. *Collect. Czech. Chem. Commun.* **1975**, *40* (9), 2551-2559.
(293) Brandt, H. Calorimeter for measuring small heats of mixture in binary liquid systems. *Z. Phys. Chem. (Muenchen, Ger.)* **1954**, *2*, 104-111.
(294) Wilhelm, E.; Inglese, A.; Grolier, J. P. E. Excess enthalpies of binary mixtures containing either methylcyclopentane or methylcyclohexane. *Thermochim. Acta* **1991**, *187*, 113-120.

(295) Ohnishi, K.; Fujihara, I.; Murakami, S. Thermodynamic properties of decalins mixed with hexane isomers at 298.15 K. I. Excess enthalpies and excess isobaric heat capacities. *Fluid Phase Equilib.* **1989**, *46* (1), 59-72.
(296) Shiohama, Y.; Ogawa, H.; Murakami, S.; Fujihara, I. Molar excess enthalpies of cis-decalin + benzene, + toluene, + isooctane and + heptane at 298.15 K. *Fluid Phase Equilib.* **1987**, *32* (3), 249-260.
(297) Letcher, T. M.; Scoones, B. W. H. The excess enthalpies of bicyclohexyl + a cycloalkane and + an n-alkane at two temperatures. *J. Chem. Thermodyn.* **1982**, *14* (8), 703-706.
(298) Jessup, R. S.; Stanley, C. L. Heats and volumes of mixing in several C12 hydrocarbon systems. *J. Chem. Eng. Data* **1961**, *6*, 368-371.
(299) Wang, Z.; Benson, G. C.; Lu, B. C. Y. Excess enthalpies of the ternary mixtures: {tetrahydrofuran + (2,2,4-trimethylpentane or heptane) + methylcyclohexane} at the temperature 298.15 K. *J. Chem. Thermodyn.* **2002**, *34* (12), 2073-2082.
(300) Nagata, I.; Asano, H.; Fujiwara, K. Excess enthalpies for systems of 2-propanol-benzene-methylcyclohexane. *Fluid Phase Equilib.* **1978**, *1* (3), 211-217.
(301) Tamura, K.; Murakami, S.; Fujishiro, R. Excess enthalpies of (cyclohexanone + aromatic hydrocarbon), (methylcyclohexane + aromatic hydrocarbon), and (methylcyclohexane + cyclohexanone) at 298.15 K. *J. Chem. Thermodyn.* **1981**, *13* (1), 47-52.
(302) Woycicki, W. Enthalpies of mixing of some binary mixtures of benzene, cyclohexane, and pyridine, and their methyl and ethyl derivatives. *J. Chem. Thermodyn.* **1972**, *4* (1), 1-8.
(303) Jones, D. E. G.; Weeks, I. A.; Benson, G. C. Excess thermodynamic properties of cyclopentane-isomeric decalin systems at 25.deg. *Can. J. Chem.* **1971**, *49* (15), 2481-2489.
(304) Ott, J. B.; Marsh, K. N.; Stokes, R. H. Excess enthalpies, excess Gibbs free energies, and excess volumes for (n-hexane + cyclohexane), and excess Gibbs free energies and excess volumes for (cyclohexane + methylcyclohexane) at 298.15 and 308.15 K. *J. Chem. Thermodyn.* **1980**, *12* (12), 1139-1148.
(305) Benson, G. C.; Murakami, S.; Lam, V. T.; Singh, J. Molar excess enthalpies and volumes of cyclohexane-isomeric decalin systems at 25.deg. *Can. J. Chem.* **1970**, *48* (2), 211-218.
(306) Letcher, T. M.; Spiteri, W. L.; Scoones, B. W. Excess enthalpies of decahydronaphthalene in cycloalkanes and in n-alkanes at two temperatures. *J. Solution Chem.* **1982**, *11* (6), 423-434.
(307) Shiohama, Y.; Ogawa, H.; Murakami, S.; Fujihara, I. Excess thermodynamic properties of (cis-decalin or trans-decalin + cyclohexane or methylcyclohexane or cyclooctane) at 298.15 K. *J. Chem. Thermodyn.* **1988**, *20* (11), 1307-1314.
(308) Smola, T.; Bittrich, H. J. Excess molar enthalpies of N-methyl-ε-caprolactam (NMC) + hydrocarbon systems at 298.15 K. III. NMC + cycloalkanes, aromatic hydrocarbons + cycloalkanes, NMC + aromatic hydrocarbons + cycloalkanes. *Z. Phys. Chem. (Leipzig)* **1989**, *270* (4), 645-657.
(309) Christensen, J. J.; Faux, P. W.; Cordray, D.; Izatt, R. M. The excess enthalpies of (carbon dioxide + pentane) at 348.15, 373.15, 413.15, 470.15, and 573.15 K from 7.58 to 12.45 MPa. *J. Chem. Thermodyn.* **1986**, *18* (11), 1053-1064.
(310) Pando, C.; Renuncio, J. A. R.; Izatt, R. M.; Christensen, J. J. The excess enthalpies of (carbon dioxide + pentane) at 308.15 and 323.15 K from 7.58 to 12.45 MPa. *J. Chem. Thermodyn.* **1983**, *15* (3), 259-266.
(311) Christensen, J. J.; Walker, T. A. C.; Schofield, R. S.; Faux, P. W.; Harding, P. R.; Izatt, R. M. The excess enthalpies of carbon dioxide + hexane at 308.15, 358.15, and 413.15 K from 7.50 to 12.50 MPa. *J. Chem. Thermodyn.* **1984**, *16* (5), 445-451.
(312) Christensen, J. J.; Zebolsky, D. M.; Izatt, R. M. The excess enthalpies of (carbon dioxide + hexane) at 470.15, 510.15, and 573.15 K from 7.50 to 12.50 MPa. *J. Chem. Thermodyn.* **1985**, *17* (2), 183-192.
(313) Tolley, W. K.; Izatt, R. M.; Oscarson, J. L. Simultaneous measurement of excess enthalpies and solution densities in a flow calorimeter. *Thermochim. Acta* **1991**, *181*, 127-141.
(314) Cordray, D. R.; Gunderson, L. D.; Christensen, J. J.; Oscarson, J. L.; Izatt, R. M. The excess molar enthalpies of carbon dioxide-hexane-dodecane mixtures at the temperatures (308.15, 323.15, 373.15, and 413.15) K and at the pressures 7.50 MPa and 12.50 MPa, and of carbon dioxide-nonane mixtures at 373.15 K and 7.50 MPa and 12.50 MPa. *J. Chem. Thermodyn.* **1991**, *23* (10), 941-949.
(315) Christensen, J. J.; Cordray, D.; Izatt, R. M. The excess enthalpies of (carbon dioxide + decane) from 293.15 to 573.15 K at 12.50 MPa. *J. Chem. Thermodyn.* **1986**, *18* (1), 53-61.
(316) Pando, C.; Renuncio, J. A. R.; McFall, T. A.; Izatt, R. M.; Christensen, J. J. The excess enthalpies of (carbon dioxide + decane) from 283.15 to 323.15 K at 7.58 MPa. *J. Chem. Thermodyn.* **1983**, *15* (2), 173-180.
(317) Gardeler, H.; Gmehling, J. In *Experimental determination of phase equilibria and comprehensive examination of the predictive capabilities of group contribution equations of state with a view to the synthesis of supercritical extraction processes*, 2004; Elsevier B.V.: 2004; pp 3-38.
(318) Rowley, R. L.; Oscarson, J. L.; Giles, N. F.; Tolley, W. K.; Izatt, R. M. Experimental and molecular-dynamics simulated excess enthalpies and solubilities of neopentane in supercritical carbon dioxide. *Fluid Phase Equilib.* **1990**, *60* (1-2), 143-156.

(319) Barry, A. O.; Kaliaguine, S. C.; Ramalho, R. S. Direct determination of enthalpy of mixing for the binary gaseous system methane-carbon dioxide by an isothermal flow calorimeter. *J. Chem. Eng. Data* **1982**, *27* (3), 258-264.
(320) Lee, J. I.; Mather, A. E. Excess enthalpy of gaseous mixtures of carbon dioxide with methane. *Can. J. Chem. Eng.* **1972**, *50* (1), 95-100.
(321) Pando, C.; Renuncio, J. A. R.; Izatt, R. M.; Christensen, J. J. The excess molar enthalpies of carbon monoxide-ethane mixtures from 293.15 to 323.15 K at 7.58 MPa. *J. Chem. Thermodyn.* **1983**, *15* (3), 231-235.
(322) Wallis, K. P.; Clancy, P.; Zollweg, J. A.; Streett, W. B. Excess thermodynamic properties for {carbon dioxide (xCO2) + ethane ((1-x)C2H6)}(l): experiment and theory. *J. Chem. Thermodyn.* **1984**, *16* (9), 811-823.
(323) Wormald, C. J.; Eyears, J. M. Excess molar enthalpies and excess molar volumes of carbon dioxide mixtures with ethane (xCO2 + (1-x)C2H6) up to 308.4 K and 11.0 MPa. *J. Chem. Thermodyn.* **1988**, *20* (3), 323-331.
(324) Wormald, C. J.; Hodgetts, R. W. Excess enthalpies and volumes for (carbon dioxide + ethane) at T = 291.6 K, close to the minimum in the critical locus. *J. Chem. Thermodyn.* **1997**, *29* (1), 75-85.
(325) Wormald, C. J.; Hodgetts, R. W.; Smith, G. R. Excess enthalpies of (carbon dioxide + cyclohexane)(g) and of (carbon dioxide + benzene)(g) at the pressure 101.3 kPa over the temperature range 354 K to 399 K. *J. Chem. Thermodyn.* **1992**, *24* (9), 943-952.
(326) Baba, M.; Dordain, L.; Coxam, J. Y.; Grolier, J. P. E. Calorimetric measurements of heat capacities and heats of mixing in the range 300-570 K and up to 30 MPa. *Indian J. Technol.* **1992**, *30* (11-12), 553-558.
(327) Cordray, D. R.; Christensen, J. J.; Izatt, R. M. The excess enthalpies of (carbon dioxide + toluene) at 308.15, 358.15, and 573.15 K from 6.98 to 16.63 MPa. *J. Chem. Thermodyn.* **1986**, *18* (7), 647-656.
(328) Cordray, D. R.; Christensen, J. J.; Izatt, R. M.; Oscarson, J. L. The excess enthalpies of (carbon dioxide + toluene) at 390.15, 413.15, 470.15, and 508.15 K from 7.60 to 17.50 MPa. *J. Chem. Thermodyn.* **1988**, *20* (7), 877-888.
(329) Pando, C.; Renuncio, J. A. R.; Schofield, R. S.; Izatt, R. M.; Christensen, J. J. The excess enthalpies of (carbon dioxide + toluene) at 308.15, 385.15, and 413.15 K from 7.60 to 12.67 MPa. *J. Chem. Thermodyn.* **1983**, *15* (8), 747-755.
(330) Wormald, C. J.; Eyears, J. M. Excess molar enthalpies and excess molar volumes of carbon dioxide-toluene mixtures at 298.15, 304.10, and 308.15 K from 7.5 to 12.6 MPa. *J. Chem. Thermodyn.* **1987**, *19* (8), 845-856.
(331) Christensen, J. J.; Christensen, S. P.; Schofield, R. S.; Faux, P. W.; Harding, P. R.; Izatt, R. M. The excess enthalpies of (carbon dioxide + cyclohexane) at 308.15, 358.15, and 413.15 K from 7.50 to 12.50 MPa. *J. Chem. Thermodyn.* **1983**, *15* (12), 1151-1157.
(332) Christensen, J. J.; Walker, T. A. C.; Cordray, D. R.; Izatt, R. M. The excess enthalpies of (carbon dioxide + cyclohexane) at 470.15, 553.15, and 573.15 K from 7.50 to 12.50 MPa. *J. Chem. Thermodyn.* **1987**, *19* (1), 47-56.
(333) Cordray, D. R.; Izatt, R. M.; Christensen, J. J. The excess enthalpies of (carbon dioxide + cyclohexane) at 390.15, 413.15, 438.15, 498.15, and 508.15 K from 7.50 to 14.39 MPa. *J. Chem. Thermodyn.* **1988**, *20* (20), 225-234.
(334) Lewis, K. L.; Mosedale, S. E.; Wormald, C. J. The enthalpies of mixing of methane + argon, methane + nitrogen, and methane + hydrogen in the gaseous and two-phase regions. *J. Chem. Thermodyn.* **1977**, *9* (2), 121-131.
(335) McClure, D. W.; Lewis, K. L.; Miller, R. C.; Staveley, L. A. K. Excess enthalpies and Gibbs free energies for nitrogen + methane at temperatures below the critical point of nitrogen. *J. Chem. Thermodyn.* **1976**, *8* (8), 785-792.
(336) Wormald, C. J.; Lewis, K. L.; Mosedale, S. The excess enthalpies of hydrogen + methane, hydrogen + nitrogen, methane + nitrogen, methane + argon, and nitrogen + argon at 298 and 201 K at pressures up to 10.2 MPa. *J. Chem. Thermodyn.* **1977**, *9* (1), 27-42.
(337) Calado, J. C. G.; Gopal, P.; Zollweg, J. A.; Thompson, W. R. Heat-of-mixing for the partially miscible system nitrogen-ethane. *Can. J. Chem.* **1988**, *66* (4), 626-627.
(338) Guedes, H. J. R.; Zollweg, J. A.; Filipe, E. J. M.; Martins, L. F. G.; Calado, J. C. G. Thermodynamics of liquid (nitrogen + ethane). *J. Chem. Thermodyn.* **2002**, *34* (5), 669-678.
(339) Wormald, C. J.; Lewis, E. J.; Terry, A. J. Second virial coefficients of benzene and cyclohexane from measurements of the excess molar enthalpy of (0.5N2 + 0.5C6H6) and (0.5N2 + 0.5C6H12) from 333.2 K to 433.2 K. *J. Chem. Thermodyn.* **1996**, *28* (1), 17-27.
(340) Wormald, C. J. A new gas phase flow mixing calorimeter: test measurements on (nitrogen + cyclohexane). *J. Chem. Thermodyn.* **1997**, *29* (6), 701-714.
(341) Hejmadi, A. V.; Katz, D. L.; Powers, J. E. Experimental determination of the enthalpy of mixing of nitrogen + carbon dioxide under pressure. *J. Chem. Thermodyn.* **1971**, *3* (4), 483-496.

(342) Lee, J. I.; Mather, A. E. Excess enthalpy of gaseous mixtures of nitrogen and carbon dioxide. *J. Chem. Eng. Data* **1972**, *17* (2), 189-192.
(343) Barry, A. O.; Kaliaguine, S. C.; Ramalho, R. S. Excess enthalpies of the binary system methane-hydrogen sulfide by flow calorimetry. *J. Chem. Eng. Data* **1982**, *27* (4), 436-439.
(344) Letcher, T. M.; Bricknell, B. C. Calorimetric Investigation of the Interactions of Some Hydrogen-Bonded Systems at 298.15 K. *J. Chem. Eng. Data* **1996**, *41* (2), 166-169.
(345) Allred, G. C.; Beets, J. W.; Parrish, W. R. Excess Properties for 1-Butanethiol + Heptane, + Cyclohexane, + Benzene, and + Toluene. 2. Excess Molar Enthalpies at 283.15, 298.15, and 333.15 K. *J. Chem. Eng. Data* **1995**, *40* (5), 1062-1066.
(346) Lancaster, N. M.; Wormald, C. J. Excess molar enthalpies for water + propene(g) + propane(g), and + butane(g). *J. Chem. Thermodyn.* **1986**, *18* (6), 545-550.
(347) Lancaster, N. M.; Wormald, C. J. Excess molar enthalpies of water-pentane(g) up to 698.2 K and 14.0 MPa. *J. Chem. Soc., Faraday Trans. 1* **1988**, *84* (9), 3159-3168.
(348) Smith, G. R.; Fahy, M. J.; Wormald, C. J. The excess molar enthalpy of {water (xH2O) + n-alkanes ((1-x)CnH2n+2)}(g) for n = 5, 6, 7, and 8. *J. Chem. Thermodyn.* **1984**, *16* (9), 825-831.
(349) Al-Bizreh, N.; Colling, C. N.; Lancaster, N. M.; Wormald, C. J. Excess molar enthalpies of steam-n-hexane and steam-n-heptane up to 698.2 K and 12.6 MPa. *J. Chem. Soc., Faraday Trans. 1* **1989**, *85* (6), 1303-1313.
(350) Richards, P.; Wormald, C. J.; Yerlett, T. K. The excess enthalpy of (water + nitrogen) vapor and (water + n-heptane) vapor. *J. Chem. Thermodyn.* **1981**, *13* (7), 623-628.
(351) Wormald, C. J.; Al-Bizreh, N. Excess molar enthalpy of steam-n-octane up to 648.2 K and 10.0 MPa. *J. Chem. Soc., Faraday Trans.* **1990**, *86* (1), 69-73.
(352) Smith, G.; Sellars, A.; Yerlett, T. K.; Wormald, C. J. The excess enthalpy of (water + hydrogen) vapor and (water + methane) vapor. *J. Chem. Thermodyn.* **1983**, *15* (1), 29-35.
(353) Wormald, C. J.; Colling, C. N. Excess Enthalpy Experimental Data Binary Systems: Water + Hydrogen, Water + Methane, Water + Nitrogen, Water + Argon. *GPA Tech. Publ.* **1982**, *7* (TP-7), 1-52.
(354) Wormald, C. J.; Lancaster, N. M. Excess molar enthalpies for (water + benzene)(g) and (water + cyclohexane)(g). *J. Chem. Thermodyn.* **1985**, *17* (10), 903-908.
(355) Wormald, C. J.; Lancaster, N. M.; Sowden, C. J. Benzene-water association. Excess molar enthalpy and second virial cross-coefficients for (benzene-water)(g) and (cyclohexane-water)(g). *J. Chem. Soc., Faraday Trans.* **1997**, *93* (10), 1921-1926.
(356) Wormald, C. J.; Slater, J. Excess enthalpies for (water+benzene) in the liquid and supercritical regions at T = 503 K to T = 592 K and p = 16.4 MPa. *J. Chem. Thermodyn.* **1996**, *28* (6), 627-636.
(357) Chen, X.; Gillespie, S. E.; Oscarson, J. L.; Izatt, R. M. Calorimetric determination of thermodynamic quantities for chemical reactions in the system carbon dioxide-sodium hydroxide-water from 225 to 325°C. *J. Solution Chem.* **1992**, *21* (8), 825-848.
(358) Koschel, D.; Coxam, J.-Y.; Rodier, L.; Majer, V. Enthalpy and solubility data of CO2 in water and NaCl(aq) at conditions of interest for geological sequestration. *Fluid Phase Equilib.* **2006**, *247* (1-2), 107-120.
(359) Perez, E.; Sanchez-Vicente, Y.; Cabanas, A.; Pando, C.; Renuncio, J. A. R. Excess molar enthalpies for mixtures of supercritical carbon dioxide and water + ethanol solutions. *J. Supercrit. Fluids* **2005**, *36* (1), 23-30.
(360) Smith, G. R.; Wormald, C. J. The excess molar enthalpies of water-carbon monoxide(g) and water-carbon dioxide(g). *J. Chem. Thermodyn.* **1984**, *16* (6), 543-550.
(361) Wormald, C. J.; Lancaster, N. M.; Sellars, A. J. The excess molar enthalpies of {x water + (1-x) carbon monoxide} (g) and {x water + (1-x carbon dioxide} (g) at high temperatures and pressures. *J. Chem. Thermodyn.* **1986**, *18* (2), 135-147.
(362) Wormald, C. J.; Colling, C. N. Excess enthalpies for (water + nitrogen)(g) up to 698.2 K and 12.6 MPa. *J. Chem. Thermodyn.* **1983**, *15* (8), 725-737.
(363) Wormald, C. J. (Water + hydrogen sulphide) association. Second virial cross coefficients for (water + hydrogen sulphide) from gas phase excess enthalpy measurements. *J. Chem. Thermodyn.* **2003**, *35* (6), 1019-1030.
(364) Brown, P. R.; Ott, J. B.; Lemon, L. R.; Moore, J. D. Excess molar enthalpies for (propane + ethene) over the temperature range from 273.15 K to 373.15 K and the pressure range from 5 MPa to 15 MPa. *J. Chem. Thermodyn.* **1996**, *28* (Copyright (C) 2011 American Chemical Society (ACS). All Rights Reserved.), 905-921.
(365) Lobo, L. Q.; Calado, J. C. G.; Staveley, L. A. K. The thermodynamics of liquid mixtures of methane + ethene. *J. Chem. Thermodyn.* **1980**, *12* (5), 419-427.
(366) Gagne, C.; Kaliaguine, S. C.; Ramalho, R. S. Experimental study of excess enthalpies for the binary gaseous system methane-ethylene by flow calorimetry. *J. Chem. Eng. Data* **1986**, *31* (3), 298-302.

(367) Gruszkiewicz, M. S.; Sipowska, J. T.; Ott, J. B.; Brown, P. R.; Moore, J. D. Excess enthalpies for (ethane + ethene) at the temperatures (273.15, 298.15, 323.15, 348.15, and 363.15) K and the pressures (5, 7.5, 10, 12.5, and 15) MPa. *J. Chem. Thermodyn.* **1995**, *27* (5), 507-524.
(368) Wormald, C. J.; Eyears, J. M. Excess molar enthalpies of (carbon dioxide + ethene) in the liquid and near-critical regions. *J. Chem. Thermodyn.* **2001**, *33* (7), 775-786.
(369) Ba, L. B.; Kaliaguine, S. C.; Ramalho, R. S. Excess enthalpies for gaseous ethylene + nitrogen by flow calorimetry. *J. Chem. Thermodyn.* **1978**, *10* (7), 603-612.
(370) Woycicki, W. Excess enthalpies of binary mixtures containing unsaturated aliphatic hydrocarbons. 1. n-Alkene + n-alkane. *J. Chem. Thermodyn.* **1975**, *7* (1), 77-81.
(371) Pittau, B.; Marongiu, B.; Porcedda, S. Thermodynamics of binary mixtures containing alkenes. 1. Excess enthalpies of some alkenes and polyenes + n-heptane or cyclohexane mixtures. *J. Chem. Eng. Data* **1992**, *37* (1), 124-126.
(372) Woycicki, W. Excess enthalpies of binary mixtures containing unsaturated hydrocarbons. 4. n-Diene + n-alkane and + cyclohexane. *J. Chem. Thermodyn.* **1980**, *12* (2), 165-171.
(373) Letcher, T. M.; Baxter, R. C. Excess enthalpies and excess volumes of (benzene or cyclohexane or n-hexane + an alkene or an alkyne) at 298.15 K. *J. Chem. Thermodyn.* **1987**, *19* (3), 321-326.
(374) Kudryavtseva, L. S.; Kuus, M.; Viit, H.; Eisen, O. Excess enthalpy. 1-Heptene - heptane system. *Int. DATA Ser., Sel. Data Mixtures, Ser. A* **1981**, *1981* (1), 13-16.
(375) Woycicka, M. K. Excess Enthalpies of Dilute Solutions of n-Propanol with Unsaturated Hydrocarbons. *Bull. Acad. Pol. Sci. Ser. Sci. Chim.* **1983**, *31* (3-7), 107-112.
(376) Siimer, E.; Kuus, M.; Kudryavtseva, L. Excess enthalpies of systems containing unsaturated hydrocarbons by UNIFAC group contribution. *Thermochim. Acta* **1992**, *209,* 103-110.
(377) Karbalai Ghassemi, M. H.; Grolier, J. P. E. Excess enthalpy. 1-Octene-n-hexane system. *Int. DATA Ser., Sel. Data Mixtures, Ser. A* **1976**, (1), 66-69.
(378) Kuus, M.; Kudryavtseva, L. S.; Eisen, O. Thermodynamic properties of mixtures of n-octane with isomers of n-octene. 1. Heats of mixing. *Eesti NSV Tead. Akad. Toim., Keem.* **1980**, *29* (1), 25-31.
(379) Kudryavtseva, L.; Siimer, E. Excess enthalpies of 1-nonene-n-nonane, 1-hexanol-2-hexyn-1-ol, 1-nonene-2-hexyn-1-ol-n-nonane, and 1-hexanol-2-hexyn-1-ol-n-nonane at 298.15 K. *Thermochim. Acta* **1994**, *237* (1), 43-47.
(380) Delmas, G.; Nguyen, T. T. Correlation of orientations in chain molecules in the liquid state: heats of mixing for dodecanol, dodecyl chloride, 1-dodecene and 1-decene with four normal and four branched alkanes. *J. Chim. Phys. Phys.-Chim. Biol.* **1975**, *72* (11-12), 1285-1290.
(381) Fischer, K.; Gmehling, J. Vapor-liquid equilibria, activity coefficients at infinite dilution and heats of mixing for mixtures of N-methyl pyrrolidone-2 with C5 or C6 hydrocarbons and for hydrocarbon mixtures. *Fluid Phase Equilib.* **1996**, *119* (1-2), 113-130.
(382) Wang, Z.; Benson, G. C.; Lu, B. C. Y. Excess enthalpies of binary mixtures of 1-hexene with some branched alkanes at the temperature 298.15 K. *J. Chem. Thermodyn.* **2004**, *36* (1), 45-47.
(383) Karbalai Ghassemi, M. H.; Grolier, J. P. E. Excess enthalpy. Benzene-1-hexene system. *Int. DATA Ser., Sel. Data Mixtures, Ser. A* **1975**, (2), 186-190.
(384) Wang, Z.; Benson, G. C.; Lu, B. C. Y. Excess molar enthalpies of binary mixtures of 1-hexene with some cyclic and aromatic hydrocarbons at 298.15 K. *Thermochim. Acta* **2004**, *414* (1), 31-33.
(385) Marongiu, B.; Porcedda, S.; Pittau, B.; Kehiaian, H. V. Thermodynamics of binary mixtures containing linear or cyclic alkenes. II. Mixtures with benzene or tetrachloromethane. *Fluid Phase Equilib.* **1994**, *99* (1-2), 185-198.
(386) Kuus, M.; Kudryavtseva, L.; Kirss, H. Heats of mixing of n-octene isomers with some organic compounds. *Eesti NSV Tead. Akad. Toim., Keem.* **1982**, *31* (1), 54-57.
(387) Kudryavtseva, L.; Kuus, M.; Kirss, H.; Vink, I. Effect of molecular structure on the excess enthalpies of mixtures with unsaturated hydrocarbons. *Eesti NSV Tead. Akad. Toim., Keem.* **1989**, *38* (2), 84-92.
(388) Junghans, W.; Weber, U. v. The binary system, ethylbenzene-styrene; vapor-liquid equilibriums at 30, 60, 90, and 120° by a dynamic method and the heat of mixing at 20°. *J. Prakt. Chem. [4]* **1955**, *2,* 265-273.
(389) Letcher, T. M.; Baxter, R. C. Excess enthalpies and excess volumes of (a bicyclic compound + 1-hexene or 1-hexyne or 1-heptene or 1-heptyne) at 298.15 K. *J. Chem. Thermodyn.* **1988**, *20* (1), 39-47.
(390) McFall, T. A.; Post, M. E.; Christensen, J. J.; Izatt, R. M. The excess enthalpies of (1-butene + methyl tert-butyl ether), (1,3-butadiene + propene), and (carbon disulfide + methanol) as functions of temperature. *J. Chem. Thermodyn.* **1982**, *14* (6), 509-515.
(391) Woycicki, W. Excess enthalpies of binary mixtures containing unsaturated hydrocarbons. *J. Chem. Thermodyn.* **1984**, *16* (3), 219-224.

(392) Royo, F. M.; Gracia, M.; Gutierrez, C. Thermodynamic Study of Some Binary Mixtures and Energy Parameters of the Various Types of Contacts involved. III. *Rev. Acad. Cienc. Exact. Fis. Quim. Nat. Zaragoza* **1982**, *37*, 51-59.
(393) Moore, J. D.; Brown, P. R.; Ott, J. B. Excess molar enthalpies and excess molar volumes for the binary mixtures of 2-methylpropane, 2-methylpropene, and propan-2-ol at the temperatures (298.15 and 323.15) K and the pressures (5, 10, and 15) MPa. *J. Chem. Thermodyn.* **1997**, *29* (2), 179-195.
(394) Diaz Pena, M.; Espino, B.; Perez, R.; Arenosa, R. L. Excess enthalpies of cyclohexene + n-alkanes. *Bol. Soc. Quim. Peru* **1984**, *50* (1), 64-68.
(395) Letcher, T. M.; Baxter, R. C. Excess enthalpies of binary mixtures for 1,3-cyclohexadiene and 1,4-cyclohexadiene + cyclohexane, + n-hexane and + benzene. *Thermochim. Acta* **1986**, *102*, 245-248.
(396) Grolier, J. P. E.; Inglese, A.; Wilhelm, E. Excess enthalpies of binary systems of cyclic ether + cyclohexene. *J. Chem. Eng. Data* **1982**, *27* (3), 333-335.
(397) Woycicki, W. Excess enthalpies of (cyclohexylamine or aniline + cyclohexane or cyclohexene or a cyclohexadiene). *J. Chem. Thermodyn.* **1986**, *18* (4), 317-322.
(398) Letcher, T. M.; Baxter, R. C. Excess enthalpies and excess volumes of (a bicyclic compound + cyclohexene or 1,3-cyclohexadiene or 1,4-cyclohexadiene) at 298.15 K. *J. Chem. Thermodyn.* **1988**, *20* (2), 149-157.
(399) Liao, D.-K.; Meng, X.-L.; Tong, Z.-F.; Zheng, D.-X.; Peng, D.-Y.; Lu, B. C. Y. Excess Molar Enthalpies of p-Cymene + α-Pinene + β-Pinene at (298.15, 308.15, and 318.15) K and at Atmospheric Pressure. *J. Chem. Eng. Data* **2007**, *52* (3), 808-811.
(400) Knoester, M.; Taconis, K. W.; Beenakker, J. J. M. Excess enthalpies of gaseous mixtures of hydrogen, nitrogen, and argon between 150 and 293°K. and at pressures up to 130 atm. *Physica (Amsterdam)* **1967**, *33* (2), 389-409.
(401) Wormald, C. J.; Colling, C. N. Excess enthalpies of (water + hydrogen) (g) up to 698.2 K and 11.13 MPa. *J. Chem. Thermodyn.* **1985**, *17* (5), 437-445.
(402) Benson, G. C.; D'Arcy, P. J.; Kumaran, M. K. Heat capacities of binary mixtures of n-heptane with hexane isomers. *Thermochim. Acta* **1984**, *75* (3), 353-360.
(403) Saito, A.; Tanaka, R. Excess volumes and heat capacities of binary mixtures formed from cyclohexane, hexane, and heptane at 298.15 K. *J. Chem. Thermodyn.* **1988**, *20* (7), 859-865.
(404) Benson, G. C.; D'Arcy, P. J. Heat capacities of binary mixtures of n-octane with each of the hexane isomers at 298.15 K. *Can. J. Chem.* **1986**, *64* (11), 2139-2141.
(405) Kumaran, M. K.; Benson, G. C.; D'Arcy, P. J.; Halpin, C. J. Speed of sound, molar volume, and molar isobaric heat capacity for binary liquid mixtures: analysis in terms of van der Waal's one-fluid theory. *J. Chem. Thermodyn.* **1984**, *16* (12), 1181-1189.
(406) Bendiab, H.; Roux-Desgranges, G.; Roux, A. H.; Grolier, J. P. E.; Patterson, D. Excess heat capacities of ternary systems containing chlorobenzene or chloronaphthalene. *J. Solution Chem.* **1994**, *23* (2), 307-323.
(407) Mier, W.; Lichtenthaler, R. N.; Roux, A. H.; Grolier, J. P. E. Excess molar heat capacities Cp,mE and excess molar volumes VmE of {x1CH3(CH3(CH2)5CH3 + x2CH3C(CH3)2CH2CH(CH3)CH3 + x3CH3C(CH3)2OC2H5 + (1-x1-x2-x3)C2H5OH}(1) I. Binary and quaternary mixtures. *J. Chem. Thermodyn.* **1994**, *26* (12), 1323-1334.
(408) Costas, M.; Patterson, D. Excess heat capacity. Benzene-hexane system. *Int. DATA Ser., Sel. Data Mixtures, Ser. A* **1985**, (3), 212-223.
(409) Karbalai Ghassemi, M. H.; Grolier, J. P. E. Excess heat capacity. Cyclohexane-n-hexane system. *Int. DATA Ser., Sel. Data Mixtures, Ser. A* **1976**, (2), 95-96.
(410) Tanaka, R. Excess heat capacities for mixture of benzene with n-heptane at 293.15, 298.15, and 303.15 K. *J. Chem. Eng. Data* **1987**, *32* (2), 176-177.
(411) Grolier, J. P. E.; Faradjzadeh, A. Excess heat capacity. Benzene-tetradecane system. *Int. DATA Ser., Sel. Data Mixtures, Ser. A* **1979**, (2), 131-141.
(412) Grolier, J. P. E.; Faradjzadeh, A. Excess volume. Benzene - 2,3-dimethylbutane system. *Int. DATA Ser., Sel. Data Mixtures, Ser. A* **1981**, (1), 30-38.
(413) Wilhelm, E.; Faradjzadeh, A.; Grolier, J. P. E. Excess volumes and excess heat capacities of 2,3-dimethylbutane + benzene and + toluene. *J. Chem. Thermodyn.* **1982**, *14* (12), 1199-1200.
(414) Fortier, J. L.; Benson, G. C. Excess heat capacities of binary liquid mixtures determined with a Picker flow calorimeter. *J. Chem. Thermodyn.* **1976**, *8* (5), 411-423.
(415) Iguchi, A. Excess molal specific heat of nonelectrolyte solutions. *Kagaku Sochi* **1977**, *19* (3), 64-65.
(416) Rajagopal, E.; Subrahmanyam, S. V. Excess functions VE, (δVE/δp)T, and CpE of isooctane + benzene and + toluene. *J. Chem. Thermodyn.* **1974**, *6* (9), 873-876.
(417) Malakondaiah, K.; Subbarangaiah, K.; Subrahmanyam, S. V. Excess thermodynamic functions of n-hexane + toluene: Application of Flory's theory. *Phys. Chem. Liq.* **1991**, *23* (1), 49-56.

(418) Fortier, J. L.; Benson, G. C. Heat capacities of some binary aromatic hydrocarbon mixtures containing benzene or toluene. *J. Chem. Eng. Data* **1979**, *24* (1), 34-37.
(419) Hyder Khan, V.; Subrahmanyam, S. V. Excess Thermodynamic Functions of the Systems: Benzene + p-Xylene and Benzene + p-Dioxane. *Trans. Faraday Soc.* **1971**, *67*, 2282-2291.
(420) Grolier, J. P. E.; Faradjzadeh, A. Excess Volumes and Excess Heat Capacities of Monoalkylbenzenes (C8 - C10) + Benzene Mixtures. *Int. Data Ser. Sel. Data Mixtures Ser. A* **1983**, (3), 247-252.
(421) Fortier, J.-L.; Benson, G. C. Heat capacities of binary C8 alkylbenzene mixtures. *Journal of Chemical & Engineering Data* **1980**, *25* (1), 47-49.
(422) Jain, D. V. S.; Chadha, R.; Sehgal, S. K. Excess molar heat capacities of binary mixtures of the isomeric xylenes at 303.65-321.65 K. *Fluid Phase Equilib.* **1994**, *96*, 195-202.
(423) Cerdeirina, C. A.; Tovar, C. A.; Gonzalez-Salgado, D.; Carballo, E.; Romani, L. Isobaric thermal expansivity and thermophysical characterization of liquids and liquid mixtures. *Phys. Chem. Chem. Phys.* **2001**, *3* (23), 5230-5236.
(424) Tovar, C. A.; Cerdeiriña, C. A.; González, D.; Carballo, E.; Romaní, L. Second-order excess derivatives for liquid mixtures of non-electrolytes. *Fluid Phase Equilib.* **2000**, *169* (2), 209-221.
(425) Subrahmanyam, S. V.; Rajagopal, E. Excess Thermodynamic Functions of the Systems Isooctane + Carbon Tetrachloride and Isooctane + Cyclohexane. *Z. Phys. Chem. NF* **1973**, *85* (5-6), 256-268.
(426) Tanaka, R. Excess heat capacities for mixtures of benzene with cyclopentane, methylcyclohexane, and cyclooctane at 298.15 K. *Journal of Chemical & Engineering Data* **1985**, *30* (3), 267-269.
(427) D'Arcy, P. J.; Hazlett, J. D.; Kiyohara, O.; Benson, G. C. Excess heat capacities of mixtures of benzene with cyclohexane at 298.15 K. *Thermochim. Acta* **1977**, *21* (2), 297-300.
(428) Grolier, J. P. E.; Wilhelm, E.; Hamedi, M. H. Molar Heat Capacities and Isothermal Compressibility of Binary Liquid Mixtures: Carbon Tetrachloride + Benzene, Carbon Tetrachloride + Cyclohexane and Benzene + Cyclohexane. *Ber. Bunsen-Ges. Phys. Chem.* **1978**, *82* (12), 1282-1290.
(429) Páramo, R.; Zouine, M.; Casanova, C. New Batch Cells Adapted To Measure Saturated Heat Capacities of Liquids. *Journal of Chemical & Engineering Data* **2002**, *47* (3), 441-448.
(430) Tanaka, R. Determination of excess heat capacities of (benzene + tetrachloromethane and + cyclohexane) between 293.15 and 303.15 K by use of a Picker flow calorimeter. *The Journal of Chemical Thermodynamics* **1982**, *14* (3), 259-268.
(431) Fujii, S.; Tamura, K.; Murakami, S. Thermodynamic properties of mixtures containing 1,3-diphenyl-propane at 298.15 K. *Thermochim. Acta* **1995**, *257*, 1-12.
(432) Rajagopal, E.; Subrahmanyam, S. V. Excess Thermodynamic Functions of the Systems Cyclohexane + Isomeric Xylenes. *Bull. Chem. Soc. Jpn.* **1981**, *54* (1), 282-284.
(433) Siddiqi, M. A.; Svejda, P.; Kohler, F. A Generalized van der Waals Equation of State. II. Excess Heat Capacities of Mixtures Containing Cycloalkanes (C5, C6), Methylcycloalkanes (C5, C6) and n-Decane. *Ber. Bunsen-Ges. Phys. Chem.* **1983**, *87* (12), 1176-1181.
(434) Shiohama, Y.; Ogawa, H.; Murakami, S.; Fujihara, I. Excess molar isobaric heat capacities and isentropic compressibilities of (cis- or trans-decalin + benzene or toluene or iso-octane or n-heptane) at 298.15 K. *The Journal of Chemical Thermodynamics* **1988**, *20* (10), 1183-1189.
(435) Tamura, K. Excess heat capacities of the mixtures containing methylcyclohexane at 298.15 K. *Fluid Phase Equilib.* **2001**, *182* (1-2), 303-312.

Conclusions et perspectives

Au cours de cette étude, nous avons développé une méthode de contributions de groupes permettant la prédiction du coefficient d'interactions binaires, k_{ij}, de l'équation d'état de Peng-Robinson dans sa version de 1978. Un des points clé de notre approche est que le coefficient k_{ij} ainsi obtenu dépend de la température du mélange traité, de la structure chimique des molécules étudiées ainsi que de la température critique, de la pression critique et du facteur acentrique des constituants i et j. En d'autres termes, aucune information supplémentaire, autre que celle nécessaire à la résolution de l'équation d'état n'est requise.

La majorité des diverses publications relatives au modèle PPR78 sont restées plusieurs années (et sont encore) parmi les dix publications les plus consultées des journaux *Fluid Phase Equilibria* et *Journal of Supercritical Fluids*, et ont reçu plus de deux cent cinquante citations ce qui prouve incontestablement que ce modèle a suscité jusqu'à présent, un vif intérêt.

La première partie de ce travail de thèse a consisté à étendre le domaine d'application du modèle PPR78 en définissant six nouveaux groupes. Le premier est le groupe H_2O qui va enfin permettre de modéliser les systèmes aqueux, extrêmement importants dans l'industrie pétrolière. Les quatre groupes suivants (CH_2=CH_2, $CH_{2,\text{alcène}}$ ou $CH_{\text{alcène}}$, $C_{\text{alcène}}$, et $CH_{\text{cycloalcène}}$ ou $C_{\text{cycloalcène}}$) permettent de modéliser l'ensemble des molécules comportant une double liaison éthylénique. Finalement, le groupe H_2, a été rajouté car l'industrie de l'hydrogène est en plein essor. A l'heure actuelle, vingt et un groupes, permettant de couvrir l'ensemble des molécules rencontrées dans l'industrie pétrolières (paraffines, naphtènes, aromatiques, N_2, CO_2, H_2S, mercaptans, eau, hydrogène) sont disponibles dans le modèle PPR78. Les résultats obtenus dans cette première partie indiquent sans ambigüité que ce modèle est capable de prédire avec précision les équilibres de phases pour des systèmes présentant des diagrammes de Type I et de Type II. En revanche, des difficultés persistent pour certains diagrammes de Type III et plus particulièrement lorsque le lieu des points critiques passe par un maximum puis par un minimum en pression avant de croître rapidement vers une pression infinie. De même, le minimum en température que nous rencontrons dans divers systèmes de Type III est difficilement corrélable avec précision.

Dans une deuxième partie, la précision du modèle PPR78 pour prédire les enthalpies et les capacités caloriques d'excès a été testée sur de multiples données expérimentales. Les résultats obtenus, sans être catastrophiques, ont été jugés décevants. C’est la raison pour laquelle, dans la dernière partie de ce mémoire l’ensemble des 420 paramètres de groupes ont été réajustés, non seulement sur des données d’équilibre entre phases mais également sur des milliers de données de grandeurs de mélange. Cette nouvelle version du modèle PPR78 a été baptisée *E*-PPR78 (où la lettre *E* signifie *enhanced*, c'est-à-dire amélioré). L’immense avantage de ce modèle est que les paramètres de groupes ainsi obtenus permettent de restituer les équilibres entre phases avec une précision équivalente au modèle PPR78 original et qu’ils conduisent, en outre, à une très nette amélioration de la prédiction des enthalpies et des capacités calorifiques d’excès.

A l’issue de ce travail de thèse, nous disposons donc d’un modèle entièrement prédictif capable de restituer les équilibres liquide-vapeur, les équilibres liquide-liquide, les équilibres liquide-liquide-vapeur ainsi que les grandeurs d’excès avec une très bonne précision. N’importe quel mélange complexe d’intérêt pétrolier peut être modélisé par notre approche. Le caractère prédictif du modèle *E*-PPR78 (aucun ajustement de paramètres sur des données expérimentales n’est nécessaire) va sans nul doute fortement contribuer à son implantation dans des simulateurs de procédés commerciaux comme ce fut le cas pour le modèle original.

Les perspectives concernant le modèle *E*-PPR78 sont nombreuses. En l’état actuel, il permet de prédire un coefficient d’interactions binaires, k_{ij}, dépendant uniquement de la température. C’est la raison essentielle pour laquelle il n’est pas capable de prendre en compte de manière très satisfaisante des molécules polaires comme l’eau ou les alcools. Afin de pouvoir l’étendre à de tels systèmes, il sera nécessaire d’introduire un coefficient d’interactions binaires qui soit non seulement une fonction mathématique de la variable température mais également des variables fractions molaires. La forme d’un tel modèle pourra être déduite de l’incorporation d’un modèle de coefficient d’activité à l’équation d’état.

Développement du modèle *E*-PPR78 pour prédire les équilibres de phases et les grandeurs de mélange de systèmes complexes d'intérêt pétrolier sur de larges gammes de températures et de pressions

Nous avons développé un modèle prédictif, utilisant le principe de contribution de groupes, pour prédire avec précision, le comportement des fluides pétroliers. Ce modèle baptisé PPR78 utilise l'équation d'état de Peng et Robinson et des règles de mélange de type Van der Waals avec un coefficient d'interaction binaire k_{ij}, dépendant de la température. De telles règles de mélange sont équivalentes à celles obtenues en combinant à compacité constante une fonction d'excès de type Van Laar et une équation d'état cubique.

La première partie de cette étude a consisté à étendre le domaine d'application du modèle PPR78 aux systèmes contenant de l'eau, des alcènes et de l'hydrogène, en définissant six nouveaux groupes élémentaires. Une bonne précision du modèle est obtenue pour décrire les équilibres de phases de systèmes binaires impliquant ces constituants, notamment pour les systèmes présentant des diagrammes de phases de Type I et de Type II.

Dans la deuxième partie l'ensemble des paramètres de groupes ont été réajustés, non seulement sur des données d'équilibres de phases mais également sur des données de grandeur de mélange. L'avantage de ce nouveau modèle *E*-PPR78 est qu'il permet de restituer les équilibres de phases avec une précision équivalente au modèle original et qu'il conduit à une très nette amélioration de la prédiction des enthalpies d'excès et des capacités calorifiques d'excès.

Mots-clés : équation d'état, modèle prédictif, méthode de contributions de groupes, coefficient d'interaction binaire, équilibre de phases, enthalpie d'excès, capacité calorifique d'excès.

****

Development of the *E*-PPR78 model in order to predict the phase equilibria and the mixing properties of complex systems of petroleum interest over wide ranges of temperature and pressure

We have developed a predictive model, by means of a group contribution method, in order to predict with accuracy, the behavior of petroleum fluids. The model called PPR78 uses the Peng-Robinson equation of state and Van der Waals-type mixing rules with a temperature dependent binary interaction parameter k_{ij}. Such mixing rules are identical to those obtained by combining at constant packing fraction a Van Laar-type excess function and a cubic equation of state.

The first part of this study consisted in extending the application of the model PPR78 to systems containing water, alkenes and hydrogen, by defining six new elementary groups. The phase equilibria of binary systems involving these components are accurately described by the model, especially for the phase diagrams of Type I and Type II.

In the second part, all the group parameters of the original model were re-fitted by using the phase equilibrium data, as well as the mixing property data. The advantage of this new model *E*-PPR78 is that it is capable to correlate the phase equilibria with an accuracy which is equivalent to the original model and it produces a very clear improvement in the prediction of excess enthalpies and excess heat capacities.

Keywords: equation of state, predictive model, group contribution method, binary interaction parameter, phase equilibrium, excess enthalpy, excess heat capacity.

Nancy-Université
INPL

AUTORISATION DE SOUTENANCE DE THESE
DU DOCTORAT DE L'INSTITUT NATIONAL
POLYTECHNIQUE DE LORRAINE

o0o

VU LES RAPPORTS ETABLIS PAR :
Monsieur Jérôme PAULY, Maître de Conférences, Université de Pau

Monsieur Jean-Charles DE HEMPTINNE, Professeur, IFP Energies nouvelles, Rueil-Malmaison

Le Président de l'Institut National Polytechnique de Lorraine, autorise :

Monsieur QIAN Junwei

à soutenir devant un jury de l'INSTITUT NATIONAL POLYTECHNIQUE DE LORRAINE,
une thèse intitulée :

"Développement du modèle *E*-PPR78 pour prédire les équilibres de phases et les grandeurs de mélange de systèmes complexes d'intérêt pétrolier sur de larges gammes de températures et de pressions."

en vue de l'obtention du titre de :

DOCTEUR DE L'INSTITUT NATIONAL POLYTECHNIQUE DE LORRAINE

Intitulé du doctorat : **"Génie des Procédés et des Produits"**

Fait à Vandoeuvre, le 5 Décembre 2011
Le Président de l'I.N.P.L.,
F. LAURENT

Institut National Polytechnique de Lorraine
inpl@inpl-nancy.fr | www.inpl-nancy.fr

2 av. de la Forêt de Haye | BP 3
54501 Vandœuvre-lès-Nancy Cedex
FRANCE
Tél. : +33(0)3 83 59 59 59
Fax : +33(0)3 83 59 59 55